



HAL
open science

Caractérisation moléculaire et biochimique des carbapénèmases les plus répandues chez les Entérobactéries associées à des infections sévères en vue de développer de nouveaux inhibiteurs

Saoussen Oueslati

► **To cite this version:**

Saoussen Oueslati. Caractérisation moléculaire et biochimique des carbapénèmases les plus répandues chez les Entérobactéries associées à des infections sévères en vue de développer de nouveaux inhibiteurs. Bactériologie. Université Paris Saclay (COMUE), 2019. Français. NNT : 2019SACLS483 . tel-03092328

HAL Id: tel-03092328

<https://theses.hal.science/tel-03092328>

Submitted on 2 Jan 2021

HAL is a multi-disciplinary open access archive for the deposit and dissemination of scientific research documents, whether they are published or not. The documents may come from teaching and research institutions in France or abroad, or from public or private research centers.

L'archive ouverte pluridisciplinaire **HAL**, est destinée au dépôt et à la diffusion de documents scientifiques de niveau recherche, publiés ou non, émanant des établissements d'enseignement et de recherche français ou étrangers, des laboratoires publics ou privés.

Caractérisation moléculaire et biochimique des carbapénèmases les plus répandues chez les Entérobactéries associées à des infections sévères en vue de développer de nouveaux inhibiteurs

Thèse de doctorat de l'Université Paris-Saclay
préparée à l'Université Paris Sud

École doctorale n°569
Innovation thérapeutique : du fondamental à l'appliqué (ITFA)
Spécialité de doctorat: Microbiologie

Unité EA7361
« Structure, dynamique, fonction et expression de
 β -lactamase à large spectre »

Thèse présentée et soutenue au Kremlin-Bicêtre, le 2 Décembre 2019, par

Saoussen Oueslati

Composition du Jury :

Sandrine Onger Professeur des Universités, Université Paris Sud	Présidente
Richard Bonnet Professeur des Universités-Praticien Hospitalier, Université Clermont Auvergne	Rapporteur
Jean-Yves Madec Directeur de Recherche, Unité antibiorésistance et virulence Anses Lyon	Rapporteur
Samuel Bellais Chargé de Recherche, Bioaster, Institut Pasteur	Rapporteur VAE
Anaïs Potron Maître de Conférence Universitaire-Praticien Hospitalier, Université Franche-Comté	Examinatrice
Sandra Da Re Chargée de Recherche 1, UMR INSERM 1092, Université de Limoges	Examinatrice
Fanny Roussi Directrice de Recherche, ICSN, CNRS	Examinatrice VAE
Thierry Naas Maître de Conférence Universitaire-Praticien Hospitalier, Université Paris Sud	Directeur de thèse
Laurent Dortet Maître de Conférence Universitaire-Praticien Hospitalier, Université Paris Sud	Co-Encadrant

*A mon Père et ma Sœur Anne Le Gall
qui nous ont quitté cette année 2019
Reposez en Paix...*

Remerciements

Ces travaux de thèse ont été réalisés au sein de l'Unité EA7361 Structure, dynamique, fonction et expression de β -lactamase à large spectre (Université Paris-Saclay), anciennement unité INSERM U914 Résistances Émergentes aux Antibiotiques.

En premier lieu, je tiens à remercier les membres du jury, Madame le **Professeur Sandrine Ongeri** qui m'a fait l'honneur de présider mon jury de thèse et de m'avoir aidé dans ce long et périlleux parcours qu'est la VAE. Je tiens aussi à exprimer mes plus profonds remerciements à Monsieur le **Professeur Richard Bonnet**, ainsi qu'à Monsieur le **Docteur Jean-Yves Madec**, pour avoir accepté d'être les rapporteurs de cette thèse et pour le temps consacré à son amélioration. Je remercie également Madame le **Docteur Anaïs Potron** et Madame le **Docteur Sandra Da Re** pour leur participation. Enfin, je remercie Monsieur le **Docteur Samuel Bellais** et Madame le **Docteur Fanny Roussi** pour avoir accepté d'être les membres de mon jury VAE.

Maintenant est venu le moment de remercier l'équipe EA7361, experte en carbapénèmes, avec qui j'ai partagé beaucoup de moments de joie.

Je tiens à remercier en premier mon directeur de thèse, mon collaborateur Monsieur le **Docteur Thierry Naas**, pour m'avoir fait confiance lors de la réalisation de tous ces travaux, pour m'avoir permise d'être totalement autonome et de m'avoir intégrée à de multiples projets très variés. Je le remercie également pour ses conseils, son aide et sa remarquable expertise. Cette collaboration a forgé mon esprit et m'a permis d'acquérir une richesse intellectuelle et humaine.

Je remercie Monsieur le **Docteur Laurent Dortet**, mon co-encadrant de thèse, et Monsieur le **Docteur Rémy Bonnin** pour leur aide et leur disponibilité au quotidien. Je remercie ma plus belle Star et amie **Delphine Girlich**, mon efficace **Sandrine Bernabeu**, la discrète **Gaëlle Cuzon** pour m'avoir aiguillée à mes débuts et pour leur soutien. Notre secrétaire préférée **Florence Bussy** qui tape sur son clavier plus vite que son ombre. A ma très chère et tendre amie **Garance Cotellon** qui, depuis le début, a été à mes côtés, à ma copine à moi **Elodie Creton** et à **Aimie Sauvadet** pour sa présence et son écoute, parfois une amitié sincère peut se créer en très peu de temps. Merci à toutes les trois d'avoir toujours été là. A ma petite **Agnès Jousset**, ma coloc' de congrès, merci pour ton aide à la rédaction du manuscrit et ta joie de vivre ; sans

oublier Mme OXA-48 **Laura Dabos, Lauraine Gauthier, Julie Takissian, Cécile Emeraud, Thibaud Boulant, Agustin Zavala, Jean-Baptiste Ronat** et toute l'équipe du **MiniLab** et celle de bactériologie de l'hôpital Bicêtre pour vos encouragements. Merci à mes deux fidèles acolytes **Linda Tlili** et **Cynthia Exilie**, ensemble, nous avons formé la « Dream Team » et relevé tous les challenges. Une pensée pour les étudiants ayant quittés le laboratoire et avec qui j'ai également passé de bons moments Ingrid, Ludivine, Emilie R, Emilie L, Elisabet, Karama, Victor, Yannick, Camille, Morgane, Clément, Charlotte, Aziza, Jasmine, Anaïs, Anne, Yves-Marie, Baptiste, Aurélie, Marion, Guillaume, Samia, Anne-Laure ...

Parmi les nombreux collaborateurs avec qui j'ai pu travailler, je tenais à remercier Monsieur le **Docteur Bogdan Iorga** qui m'a initié à son art : la modélisation moléculaire et avec qui j'ai pu avoir de longs échanges scientifiques enrichissants. Je remercie également mon ami le **Docteur Pierre Bogearts** pour ses nombreux conseils et son éternel soutien, mon camarade chimiste le **Docteur Kevin Cariou**, Monsieur le **Docteur Pascal Retailleau** pour tous les beaux cristaux qu'il a pu nous fournir. Je remercie le **Professeur Patrice Nordmann** qui m'a permis d'obtenir mon premier papier, mais surtout de croiser la route de cette belle équipe !

Je tenais à remercier Monsieur le **Professeur Christian Poüs**, qui d'une rencontre inattendue, a été à l'origine de mon inscription à mon doctorat. Monsieur le **Professeur Imad Kansau**, mon encadrant VAE, Monsieur le **Professeur Giles Ponchel** et Mme **Patricia Fonteneau** pour leur aide indispensable dans le dédale administratif de la VAE.

Enfin, je voulais rendre hommage à toutes ces femmes pionnières dans les sciences et qui sont pour moi des modèles. C'est grâce à leur ténacité, leur courage qu'elles nous ont permis de pouvoir vivre cette passion. Soyons à notre tour le phare pour quelqu'un/e.

Table des matières

Liste des figures et des tableaux.....	7
Abréviations.....	12
Étude bibliographique.....	13
I. Les Entérobactéries.....	13
1. Généralités.....	13
2. Habitat et pouvoir pathogène.....	13
3. Structure de la paroi des entérobactéries.....	14
a. La membrane externe.....	14
b. Le peptidoglycane.....	16
c. Les DD-peptidases ou Protéines liant les pénicillines (« Penicillin-Binding Proteins »).....	17
II. Les Antibiotiques.....	19
1. Historique.....	19
2. Généralités.....	21
3. Les β -lactamines.....	22
a. Les sous-classes.....	23
i. Les pénicillines.....	23
ii. Les céphalosporines.....	23
iii. Les monobactames.....	23
iv. Les carbapénèmes.....	24
b. Mode d'action des β -lactamines.....	24
III. Résistance aux β -lactamines.....	26
1. Modification de la cible des β -lactamines.....	27
2. Diminution de la perméabilité.....	28
3. Excrétion des β -lactamines : système d'efflux.....	28
4. Inactivation enzymatique des β -lactamines : les β -lactamases.....	29
IV. Les β -lactamases.....	30
1. Généralités.....	31
a. Les β -lactamases de classe A :.....	31
b. Les β -lactamases de classe B ou métallo- β -lactamases :.....	31
c. Les β -lactamases de classe C ou céphalosporinases :.....	32
d. Les β -lactamases de classe D ou oxacillinases :.....	32
2. Les β -lactamases à sérine active.....	33
a. Structure.....	33
b. Mécanisme catalytique.....	35
3. Les Métallo- β -lactamases.....	36
a. Structure.....	36
b. Mécanisme catalytique.....	38
V. Les carbapénémases.....	40
1. Carbapénémases de classe A.....	41
a. Généralités.....	41
b. Carbapénémases de type KPC.....	43
i. Épidémiologie.....	44
ii. Support génétique de <i>bla_{KPC}</i>	45
iii. Spectre d'hydrolyse des enzymes de type KPC.....	46
iv. Structure de KPC-2.....	47
v. Données cliniques et traitements.....	48
2. Carbapénémases de classe B.....	49
a. Généralités.....	49
b. Carbapénémases de type NDM.....	51
i. Epidémiologie.....	51
ii. Environnement génétique.....	52
iii. Spectre d'hydrolyse.....	53
iv. Structure de NDM-1.....	54

v.	Données cliniques et traitements.....	56
3.	Carbapénèmases de classe D.....	56
a.	Généralités.....	56
b.	Carbapénèmases de type OXA-48.....	57
i.	Epidémiologie.....	57
ii.	Spectre d'hydrolyse.....	61
iii.	Environnement génétique / support génétique.....	62
iv.	Structure.....	65
4.	Détection des Entérobactéries Productrices de Carbapénèmase (EPC).....	67
a.	Méthodes de détection basées sur le phénotype.....	68
i.	Antibiogramme et concentration minimale inhibitrice (CMI).....	68
ii.	Disques combinés avec inhibiteurs.....	69
iii.	Le test de Hodge modifié.....	69
iv.	Méthode d'inactivation des carbapénèmes.....	70
b.	Tests d'hydrolyse des carbapénèmes.....	72
i.	Spectrophotomètre UV.....	72
ii.	Spectrométries de masse.....	72
iii.	Tests colorimétriques.....	73
iv.	Méthodes de détection moléculaire.....	75
v.	Tests immunochromatographiques.....	75
vi.	Détection directe de la carbapénèmase par spectrométrie de masse.....	77
5.	Aspects cliniques.....	77
a.	Facteurs de risque d'acquisition des EPC.....	77
b.	Infections dues aux EPC.....	78
c.	Traitement des infections dues à des EPC.....	78
d.	Contrôle et prévention des infections.....	80
VI.	Les inhibiteurs des β-lactamases.....	82
1.	Généralité sur les inhibiteurs.....	82
a.	Les inhibiteurs irréversibles.....	82
b.	Les inhibiteurs réversibles.....	83
2.	Les premiers inhibiteurs.....	85
a.	L'acide clavulanique.....	86
b.	Le sulbactam.....	89
c.	Le tazobactam.....	90
3.	Les nouveaux inhibiteurs.....	92
a.	Les diazabicyclooctanones (DBO).....	92
i.	L'avibactam.....	93
ii.	Le relebactam.....	98
iii.	Autres DBOs.....	99
b.	Composé boronique : le vaborbactam.....	100
c.	Les inhibiteurs de Métallo- β -lactamases.....	103
i.	Inhibition par fixation aux ions Zinc.....	105
ii.	Inhibition par chélation des ions zinc.....	107
iii.	Inhibition par fixation covalente.....	108
d.	Nouveau composé non inhibiteur : le céfidérocol.....	109
	Objectifs Scientifiques.....	115
	Résultats.....	117
	Chapitre I. Études moléculaires, biochimiques et structurales des carbapénèmases majeures et de leurs variants.....	118
A.	OXA-48 : Importance de la boucle β5-β6 et du résidu Arg 214 dans l'hydrolyse des carbapénèmes.....	120
B.	KPC-2 : Rôle de la boucle 238-243 et du résidu 179 sur le profil hydrolytique de l'enzyme et de son inhibition par l'avibactam.....	165
C.	NDM-1 : Étude des relations structure-activité du site actif par mutagenèse.....	177
1.	Étude de l'impact de substitution par alanine scanning de 10 résidus d'acides aminés dans le site actif de NDM-1.....	178

2. Construction d'une banque de mutants par mutagenèse aléatoire	181
Chapitre II. Lutte active contre l'antibiorésistance : Détection des carbapénèmases et développement de nouveaux outils thérapeutiques.....	184
A. Développement de tests rapides de détection des carbapénèmases	184
B. Développement de nouveaux inhibiteurs de carbapénèmases.....	230 230
Discussion	285
Conclusion.....	294
Références bibliographiques	295
Annexes	318

Liste des articles

- Article 1. Heterogeneous hydrolytic features for OXA-48-like β -lactamases.** Oueslati *et al.*p120
- Article 2. Genetic and Biochemical Characterization of OXA-405, an OXA-48-Type Extended-Spectrum β -Lactamase without Significant Carbapenemase Activity** Dortet *et al.*p125
- Article 3. Biochemical and structural characterization of OXA-405, an OXA-48 variant with Extended-Spectrum β -Lactamase activity** Oueslati *et al.*p131
- Article 4. Role of the Arginine 214 in the substrate specificity of OXA-48** Oueslati *et al.*p143
- Article 5. Unravelling ceftazidime/avibactam resistance of KPC-28, a KPC-2 variant lacking carbapenemase activity** Oueslati *et al.*.....p166
- Letter 1. Different phenotypic expressions of KPC β -lactamases and challenges in their detection** Oueslati *et al.*.....p174
- Article 6. Development and Validation of a Lateral Flow Immunoassay for Rapid Detection of NDM-Producing Enterobacteriaceae** Boutal *et al.*.....p186
- Article 7. A multiplex lateral flow immunoassay for the rapid identification of NDM-, KPC-, IMP- and VIM-type and OXA-48-like carbapenemase-producing Enterobacteriaceae** Boutal *et al.*.....p198
- Article 8. Improvement of the immunochromatographic NG-Test CARBA5 assay for the detection of IMP-variants previously undetected** Volland *et al.*.....p205
- Article 9. Evaluation of the Amplidiag CarbaR+VRE Kit for Accurate Detection of Carbapenemase-Producing Bacteria** Oueslati *et al.*.....p213
- Article 10. Multicentre evaluation of the BYG Carba v2.0 test, a simplified electrochemical assay for the rapid laboratory detection of carbapenemase-producing Enterobacteriaceae** Bogaerts *et al.*.....p222
- Brevet 1. 3-Imidazoline carbapénèmases inhibitors**.....p232
- Brevet 1b. 2- or 3-Imidazoline as carbapénèmases inhibitors**.....p233
- Article 11. [3+2] Annulation between 1 ketenimines and azaallyl anions to access potent non-covalent carbapenemases inhibitors.** D'Hollander *et al.*.....p234
- Article 12. NMR characterization of the Zn(II) ions influence on the New-Delhi Metallo- β -lactamase-1 and its interaction with flavonols.** Rivière *et al.*.....p249

Liste des figures et des tableaux

FIGURES

- Figure 1. Représentation schématique de la paroi des bactéries à Gram négatif.** D'après Tommasi et al.⁵ 15
- Figure 2 .A. Composition d'une sous-unité du peptidoglycane ;B. Représentation schématique de la synthèse du peptidoglycane (PG).** Elle est initié par la synthèse du pentapeptide disaccharide (précurseurs) dans le cytosol (GlcNAc-MurNAc-L-Ala-DGlu-DAP-D-Ala-D-Ala), qui est ensuite transféré au niveau de l'espace périplasmique via la formation d'un complexe lipidique avec le bactoprenyl. Les précurseurs monomères sont complexés entre eux via les PLPs permettant la transglycosylation et la transpeptidation. D'après Cava et al.¹⁰ 17
- Figure 3. Schéma représentatif de la réaction de transpeptidation (A) et de la carboxypeptidation (B) catalysées pas les PLPs. Réaction chimique de ces deux réactions (C).** 18
- Figure 4. Chronologie de la découverte d'antibiotiques.** D'après Procopio et al.¹³ 20
- Figure 5. A. Homologie structurale entre le substrat naturel D-Ala-D-Ala des PLPs et la pénicilline. B. Inhibition des PLPs par la pénicilline** 25
- Figure 6 Mécanisme de résistance aux β -lactamines chez les Entérobactéries:** (i) Modification de la cible (PLPs), (ii) Diminution de la perméabilité (modification des porines), (iii) Efflux de l'antibiotique via des pompes spécialisées, (iv) Inactivation enzymatique par les β -lactamases.. Réadaptation de l'image VectorStock.com/10499529 27
- Figure 7. Représentation schématique des cinq familles de pompe d'efflux avec leurs substrats antibiotiques connus.** Famille SMR « Small Multidrug Resistance » family, famille MFS « Major Facilitator Superfamily », Famille ABC « ATP-binding cassette », Famille MATE « Multidrug and Toxic compound Extrusion », Famille RND « Resistance-Nodulation-Division. OMP (outer membrane protein) : protéine de membrane externe. D'après Yilmaz et Özcengiz²⁹ 29
- Figure 8. Schéma du mode d'action des β -lactamines et des β -lactamases.** Les antibiotiques diffusent à travers la membrane externe et inactivent les PLPs, qui sont impliqués dans la biosynthèse du peptidoglycane. L'action des β -lactamases provoque l'ouverture du noyau β -lactame de l'antibiotique, le rendant inactif. Les substitutions à chacune des trois positions (indiquées par des lignes ondulées) donnent lieu à une famille de composés bioactifs, dont beaucoup sont clivés par les β -lactamases. D'après Wang et al.³⁰ .. 30
- Figure 9. Représentation simplifiée du spectre d'hydrolyse des β -lactamases** 33
- Figure 10. Comparaison des structures tridimensionnelles des β -lactamases à sérine active avec celle d'une PLP.** A. β -lactamase de classe A : KPC-2 - Cefotaxime (réf. Pdb 5UJ3) ; B. β -lactamase de classe C : CMY-2 couplée à une molécule de citrate (réf. Pdb1CC2) ; C. : β -lactamase de classe D : OXA-10 couplée à l'avibactam (réf. Pdb4S2O) ; D. R61 DD-peptidase de Streptomyces (réf. Pdb1CEF). Le cercle noir délimite le site actif et le cercle bleu la boucle Oméga. 34
- Figure 11. A. Modèle catalytique des β -lactamases à sérine active.** E : enzyme, S : substrat, P : produit, ES : complexe de Michaelis de pré-acylation, E-S : l'acyl-enzyme. Les constantes de vitesse pour chaque étape sont représentées par k_1 (constante de vitesse d'association), k_{-1} (constante de vitesse de dissociation), k_2 (constante de vitesse d'acylation) et k_3 (constante de vitesse de désacylation). **B. Schéma de la réaction d'acylation et de désacylation.** Dans la première demi-réaction, le résidu Ser nucléophile attaque le carbone du

carbonyle du cycle β -lactame, ce qui entraîne la coupure du cycle et la formation d'un acylate d'enzyme stable. Dans la seconde étape, une molécule d'eau attaque le même carbone, la liaison se rompt et le ligand inactivé est libéré du site actif. D'après Szarecka et al. ³⁸	36
Figure 12. Comparaison de la structure tertiaire de métallo-β-lactamases provenant de <i>B. fragilis</i> : CcrA (sous classe B1), <i>B. cereus</i> : BcII (sous classe B1) et de <i>S. maltophilia</i> :L1 (sous classe B3). Les ions zinc sont représentés par des sphères vertes. D'après Wang et al. ³⁰	37
Figure 13. Site actif des métallo-β-lactamases. : A. NDM- bi-Zn^{2+} (B1, PDB 3SPU), B. Sfh-I- mono-Zn^{2+} (B2, PDB 3SD9) et C. GOB-18- mono-Zn^{2+} (B3, PDB 5K0W). Les atomes de zinc sont représentés par des sphères grise et les molécules d'eau en rouge. D'après Lisa et a.l ⁴⁴	38
Figure 14. Mécanisme réactionnel d'hydrolyse d'un carbapénème par une métallo-β-lactamase du sous-groupe B2 mono-zinc. W1 et W2 représente les molécules d'eau. D'après Meini et al. ⁴⁵	39
Figure 15. Mécanisme réactionnel d'hydrolyse de la pénicilline par les enzymes di-Zn^{2+}B1 et B3. W1 représente Wat1 et W2 représente Wat2. D'après Meini et al. ⁴⁵	39
Figure 16. Distribution géographique des bactéries productrices de KPC. D'après Munoz-price et al. ⁸⁹	46
Figure 17. A. Structure de KPC-2 (pdb 2OV1) Les régions actives sont identifiées par les couleurs suivantes: orange, motif SXXK (résidus 70 à 73), vert, boucle SDN (130 à 132), bleu, boucle oméga (164 à 179), rouge, β 3-cordon (234 à 242) B. Alignement de la séquence de la boucle oméga de KPC-2 avec d'autres β-lactamases de classe A (carbapénémase en bleu, des pénicillinases en rouge et des BLSEs en vert) avec une conservation de l'Arg-164 et l'Asp-179 C. superposition des boucles oméga de TEM-1 (rouge) et KPC-2 (bleu), montrant la liaison hydrogène entre Arg-164 et Asp-179. D'après Levitt et al ⁹⁶	48
Figure 18. Distribution mondiale des MBLs : IMP, VIM et NDM. D'après Mojica et al. ¹⁴⁸	51
Figure 19. Environnement génétique du gène bla_{NDM-1} chez <i>A. baumannii</i> et chez les Entérobactéries. D'après Bonnin et al. ¹⁵⁶	53
Figure 20. A. Alignement des séquences peptidiques de VIM-1, NDM-1 et IMP-1 (numérotation BBL). Les régions soulignées sont celles qui interagissent avec les substrats. Les résidus coordonnés aux atomes de zinc sont indiqués en bleu et rouge. B. Représentation schématique du site actif de NDM-1, avec les régions les plus importantes colorées comme suit : boucle 1 en vert (L1), boucle 2 en turquoise (L2), boucle 3 en vert olive (L3), boucle 4 en violet (L4), boucle 5 en magenta (L5). Les 2 ions zinc sont indiqués par des sphères rouges.	55
Figure 21. Distribution des entérobactéries produisant une carbapénémase de type OXA-48 D'après Nordmann et al. ¹⁸⁴	58
Figure 22. Arbre phylogénétique des variants d'OXA-48. Les séquences sont dérivées de la BLDB ¹⁹⁰ et l'arbre réalisé avec le logiciel MEGA7 ¹⁸⁸	60
Figure 23. Environnement génétique du gène bla_{OXA-48}. D'après Poirel et al. ²⁰²	63
Figure 24. Environnement génétique des transposons Tn1999-like portant le gène bla_{OXA-48} chez les entérobactéries. D'après Mairi et al. ²⁰⁸	64
Figure 25. A. Structure tertiaire de la carbapénémase OXA-48. Les hélices α sont indiquées en rouge, les feuillet β en jaune et gris, la boucle β 5- β 6 en orange. Les trois motifs DBL sont représentés avec les résidus respectifs sous forme de sticks: motif I (contenant les résidus catalytiques Ser-70, Thr-71, Phe-72 et Lys-73 carbamoylé), cyan; motif II (Ser-118, Val-119 et Val-120), magenta; motif III (Lys-208, Thr-209 et Gly-210), blanc. B. Structure du site actif. Une molécule de mérépénème est représentée au niveau du site actif, Les résidus pertinents du site actif sont affichés dans différentes couleurs. Sont représentés sous	

forme de stick : le groupe carbamoyle de Lys-73 (cyan, étiquette 1) ; la molécule d'eau impliquée dans l'étape de désacylation (étiquette 2, près de la Lys-73) et le groupe substrat acyl lié à Ser-70 (jaune, l'étiquette 3). D'après Docquier et al.....	66
Figure 26 Superposition des membres représentatifs de la famille DBL. Les cercles délimitent les parties pour lesquelles il y a des différences structurales dont la boucle β -5/ β -6. La légende des couleurs et les codes PDB sont les suivants: OXA-48 (3HBR), rouge; OXA-1 (1M6K), bleu; OXA-2 (1K38), jaune; OXA-10 (1K55), vert; OXA-24 (2JC7), magenta. D'après Docquier et al. ¹⁹²	67
Figure 27. Algorithme phénotypique de criblage des souches d'entérobactéries productrices de carbapénèmases au sein des souches non-sensibles aux carbapénèmes. Recommandations du CASFM 2019 v1 https://www.sfm-microbiologie.org/wpcontent/uploads/2019/02/CASFM2019_V1.0.pdf	68
Figure 28. Résultats obtenus avec un Hodge test modifié. Réadaptation de Pasteran et al. ²¹⁶	70
Figure 29. A. Protocole pour la réalisation du CIM-test D'après Van der Zwaluw et al. ²¹⁸ ; B. Protocole pour la réalisation du rCIM.	72
Figure 30. Analyse par MALDI-TOF, A. Imipénème et son produit ; B. Spectre de masse de l'imipénème et de son produit de dégradation , déterminé à l'aide du spectromètre de masse Ultraflex. Kempf et al. ^{227,228}	73
Figure 31. A. Principe des tests colorimétriques ; B. Résultats du Carba NP test D'après Nordmann et al. ²²⁹ ; C. Résultats du Blue carba. D'après Pire et al. ²³³	74
Figure 32. NG-Test CARBA 5 : A. Protocole ; B. Principe et résultat. D'après Boutal et al. ²⁴² et https://ngbiotech.com/carbapenemases/	76
Figure 33. Représentation graphique des différents niveaux de mesures à appliquer	81
Figure 34. Chronologie de l'apparition des premiers inhibiteurs de β-lactamases et leurs structures.	86
Figure 35. Mécanisme simplifié de l'inhibition des sérine-β-lactamases par l'acide clavulanique. Adapté de Drawz et al. ²⁸⁷	88
Figure 36. Atomes des acides aminés du site actif d'une β-lactamase de classe A et des molécules d'eau (w) impliqués dans les liaisons hydrogènes avec les atomes de l'acide clavulanique. A. Forme pré-acylée ; B. Complexe acyle avec le cycle β-lactame ouvert. D'après Imitiaz et al. ²⁹³	89
Figure 37. Structures des inhibiteurs réversibles de la famille des diazabicyclooctanones (DBOs). D'après Docquier et al. ³⁰⁷	93
Figure 38. Mécanisme simplifié de l'inhibition des sérine-β-lactamases par l'avibactam. Adapté depuis Ehmann et al. ³⁰⁸	95
Figure 39. Interaction de l'avibactam avec différentes β-lactamases. A. superposition de la β-lactamase de classe A CTX-M-15 (vert) et de classe C AmpC (orange) inhibée par l'avibactam. B. Interaction de de l'avibactam lié à la carbapénèmase de classe D, OXA-48 (magenta); la position des résidus du site actif dans l'enzyme native (blanc, PDB: 3HBR) est également montrée. L'inhibiteur (représenté sous forme de sphère et de bâtonnet) est lié de manière covalente à la sérine catalytique enzymatique et interagit avec de nombreux résidus conservés sur le plan fonctionnel, fournissant une base structurelle à la fois pour son large spectre d'inhibition et son mécanisme réversible. D'après Docquier et al. ³⁰⁷	97
Figure 40. Structure tridimensionnelle des carbapénèmases de type KPC, indiquant la position des résidus impliqués dans la résistance à la combinaison de ceftazidime et d'avibactam. Les sphères bleues représentent les positions de substitutions naturelles ; et les sphères rouges les positions des substitutions ou insertions de variants identifiés in vitro.	98
Figure 41. Structure chimique du Vaborbactam (RPX7009).	101
Figure 42. Structure chimique de boronates bicycliques. D'après Brem et al. ³⁴⁹	102

Figure 43. Mode d'action des boronates cycliques. A. Description du mode d'action sur les SBLs ; B. Description du mode d'action sur les MBLs. D'après Brem et al.³⁴⁹	102
Figure 44. Représentation des différents mécanismes d'action des inhibiteurs de MBLs. A. Inhibition par fixation aux ions zinc (NDM-1/captopril) ; B. inhibition par chélation des ions zinc ; C. Inhibition par fixation covalente (IMP-1/ dérivé de l'acide propionique). D'après Ju et al.³⁵⁶	105
Figure 45. Structure chimique du Thiorphane, Captopril et de Mercaptoacétamide substitués.	106
Figure 46. Analyse Cristallographique révélant le mode de liaison du Bismuth (Bi) dans le site actif de NDM-1. A. Site actif de NDM-1 avec 2 ions zinc (sphères grises) et l'hydroxyle (sphère rouge). B. Superposition d'images comparant la position des ions zinc à celle du bismuth (sphère violette) qui est légèrement plus proche de l'ion Zn1. D'après Wang et al.³⁷¹	107
Figure 47. A. Structure du céfidérol ; B. Mécanisme d'action. D'après shionogi and Co	111
Figure 48 Structure 3D de NDM-1 contenant les positions mutées. Sont indiquées en vert-bleu L1, cyan L3, violet L4, en orange les résidus impliqués dans la coordination des ions zinc, les AA substitués sont représentés sous forme de bâtonnets.	191

TABLEAUX

Tableau 1. Classification des antibiotiques en fonction de leur mode d'action	21
Tableau 2 Classification et structures des bêta-lactamines	22
Tableau 3. Motifs conservés au niveau du site actif des enzymes à sérines active (S)	34
Tableau 4. Phénotypes de résistance aux β-lactamines associés à la production des principales carbapénèmases	40
Tableau 5. Substitutions ponctuelles d'acides aminés ponctuelles responsables de la modification de spectre des différents variants de l'enzyme GES. Certaines substitutions sont associées à l'extension du spectre d'hydrolyse des enzymes de type GES à l'aztréonam, à la céfoxitine et/ou aux carbapénèmes. D'après Naas et al.⁷⁰	43
Tableau 6. Substitutions d'acides aminés ponctuelles responsables de la modification du spectre d'hydrolyse des variants de l'enzyme KPC-2. Adapté de Mehta et al.⁹³	47
Tableau 7. Comparaison des constantes enzymatiques des MBLs : NDM-1, IMP-1 et VIM-2 D'après Young et al.¹⁴⁸	54
Tableau 8. Comparaison des séquences et des phénotypes des différentes OXA-48-like . Selon la numérotation des β -lactamases de classe D (DBL). Le rectangle violet délimite la boucle β 5- β 6. NC : Non caractérisé Les profils d'hydrolyse ont été extraits des résultats de Poirel et al. 2004 ; Docquier et al 2009 ; Kasap et al. 2013, Poirel et al. 2011 ; Potron et al. 2011, Potron et al. 2013 ; Oteo et al. 2013 ; Gomez et al. 2013, Dortet et al. 2015 et Dabos et al. 2018 ^{174,190-197} Les résultats pour OXA-535 sont issus de Dabos. et al. ¹⁹⁸	61
Tableau 9. Constantes enzymatiques d'OXA-48 pour différents substrats. D'après Docquier et al.¹⁹¹	62
Tableau 10. Concentrations critiques, valeurs de CMI et valeurs seuil de dépistage des carbapénèmes pour les entérobactéries. EUCAST 2019 V9	69
Tableau 11. Sources des infections contractées en fonction du type de carbapénèmases. Établit à partir de Nordmann et al.²⁵⁴	78
Tableau 12. Propriétés cinétiques de différentes β-lactamases. D'après Drawz et al.²⁸⁶ ...	87
Tableau 13. Sensibilité des bacilles à Gram négatif face au Cefotolozane-Tazobactam. D'après Cluck et al.²⁹⁹	91
Tableau 14. Nouveaux inhibiteurs dirigés contre des β-lactamases produites par les bacilles à Gram négatif. D'après Karaiskos et al.³¹⁸	95
Tableau 15. Comparaison des concentrations inhibitrices à 50% de différents inhibiteurs sur différentes β-lactamases. D'après Stachyra et al.³¹⁹	96
Tableau 16. Listes des inhibiteurs de MBLs en fonction des mécanismes d'actions. Adapté de JU et al.³⁵⁵	104
Tableau 17. Valeurs des CI50 du dérivé de l'acide dipicoliniques obtenues avec NDM-1, VIM-2 et IMP-1. D'après Chen et al.³⁷²	108
Tableau 18. Spectre d'efficacité des combinaisons Inhibiteurs-Antibiotiques	112

Abréviations

AA acides amines

BLDB β -lactamase data base

BLSE β -lactamase à Spectre Etendu

CHDL *Carbapenem-Hydrolyzing class D β -Lactamase*

EUCAST *European Committee on Antimicrobial Susceptibility Testing*

C3G Céphalosporine de 3^e Génération

CIM *Carbapenem Inactivation Method*

CLSI *Clinical & Laboratory Standards*

CMI Concentration Minimale Inhibitrice

CNR Centre national de référence

EPC Entérobactérie Productrice de Carbapénèmase

IRL *Inverted Repeat Left*

IRR *Inverted Repeat Right*

IS *Insertion Sequence*

kb kilobase

kDa kilodalton

LPS lipopolysaccharide

MBL Métallo- β -lactamase

MLST multi locus sequence typing

NAG N-acetyl glucosamine

NAM N-acetyl muramique

pb paire de bases

PLP Protéine de Liaison aux Pénicillines

PCR *Polymerase Chain Reaction*

ST *Sequence-Type*

Étude bibliographique

I. Les Entérobactéries

1. Généralités

Les entérobactéries, ou Enterobacterales, constituent l'un des plus importants ordres bactériens et regroupent 9 familles (<http://www.bacterio.net/-classifphyla.html>). Ces micro-organismes présentent des caractéristiques biochimiques et morphologiques communes telles qu'une coloration de Gram négative, la capacité à croître à la fois en aérobiose et en anaérobiose. Ces bactéries métabolisent les sucres par fermentation avec production de gaz. Elles sont également capables de réduire les nitrates en nitrites. La plupart sont mobiles grâce à une ciliature péritriche, et d'autres, moins nombreuses, sont immobiles (*Klebsiella*, *Shigella*, *Yersinia pestis*). On distingue, chez les entérobactéries des espèces commensales (*Escherichia coli*, *Proteus mirabilis*, *Klebsiella sp.*), saprophytes (*Serratia sp.*, *Enterobacter sp.*), ou encore pathogènes (*Shigella*, *Y. pestis*).^{1,2} La majorité des espèces pathogènes pour l'homme est munie de *fimbriae* ou pili qui sont des facteurs d'adhésion.

2. Habitat et pouvoir pathogène

La famille des entérobactéries est très hétérogène, tant au niveau des pathologies qu'elles génèrent que des biotopes qu'elles colonisent. En effet, ces bactéries sont retrouvées dans l'environnement au niveau des sols, de l'eau et des plantes, mais aussi dans le tube digestif de l'homme et des animaux où elles font partie intégrante de la flore intestinale. Concernant le pouvoir pathogène, on distingue deux catégories en fonction de la capacité à provoquer une infection : on parle de pathogènes opportunistes ou stricts.

Les espèces pathogènes opportunistes appartiennent aux espèces de la flore commensale mais aussi aux espèces environnementales. Leur pouvoir pathogène est insuffisant pour permettre le développement spontané d'une pathologie chez un individu sain, mais elles

peuvent induire différentes pathologies chez des individus immunodéprimés ou lorsque certaines barrières naturelles sont rompues (ex : brèche cutanée, antibiothérapie entraînant un déséquilibre de la flore « barrière »).

Les espèces pathogènes strictes possèdent des facteurs de virulence spécifiques responsables de la sévérité de la pathologie, c'est par exemple le cas de *Salmonella enterica subsp. Enterica serovar Typhi* et *Paratyphi* ou de *Shigella dysenteriae*. Le cas de l'espèce *Escherichia coli* est typique puisque cette bactérie fait partie des micro-organismes commensaux de la flore intestinale, mais c'est aussi la première espèce responsable d'infections communautaires chez l'homme (notamment infections urinaires). Des souches pathogènes strictes de *E. coli* produisent des facteurs de virulences spécifiques comme, par exemple, des *Shiga* toxines responsables de diarrhées sanglantes³ ou des adhésines lui permettant de coloniser l'arbre urinaire.⁴ Il est important de noter que les entérobactéries sont la cause d'un grand nombre d'infections nosocomiales du fait de leur capacité à coloniser le matériel médical comme les sondes urinaires et les cathéters provoquant diverses pathologies : infections urinaires, bactériémies, chocs endotoxiques, infections abdominales, méningites, syndromes diarrhéiques. Les espèces les plus communément isolées en bactériologie clinique appartiennent aux genres *Citrobacter*, *Enterobacter*, *Escherichia*, *Hafnia*, *Klebsiella*, *Morganella*, *Proteus*, *Providencia*, *Salmonella*, *Serratia*, *Shigella*, *Yersinia*.

3. Structure de la paroi des entérobactéries

La paroi des bactéries Gram négatif se différencie de celle des bactéries à Gram positif par la présence d'une membrane externe. Entre cette membrane et la membrane interne (cytoplasmique) se trouve l'espace périplasmique, qui contient un polymère structurel : le peptidoglycane qui confère sa forme à la bactérie.

a. La membrane externe

Cette membrane se présente sous forme d'une bicouche phospholipidique. On y trouve majoritairement, dans sa partie interne, une lipoprotéine appelée lipoprotéine de Braun. Celle-ci est attachée de façon covalente au peptidoglycane sous-jacent ainsi elle

permet un ancrage de la membrane externe au peptidoglycane. Dans sa partie externe sont présentes des glycolipides, principalement le lipopolysaccharide (LPS, Figure 1). Le LPS est une endotoxine responsable du choc toxique dans les bactériémies à Gram négatif. Le LPS constitue une véritable barrière pour les bactéries à Gram négatif puisqu'il les protège des substances délétères hydrophobes (sels biliaires) et de masse moléculaire élevée (protéases, lipases). Le transport de molécules hydrophiles de faible masse moléculaire comme les sucres, les acides aminés mais également les antibiotiques (tels que les β -lactamines hydrophiles), est assuré par des protéines transmembranaires appelées les porines.

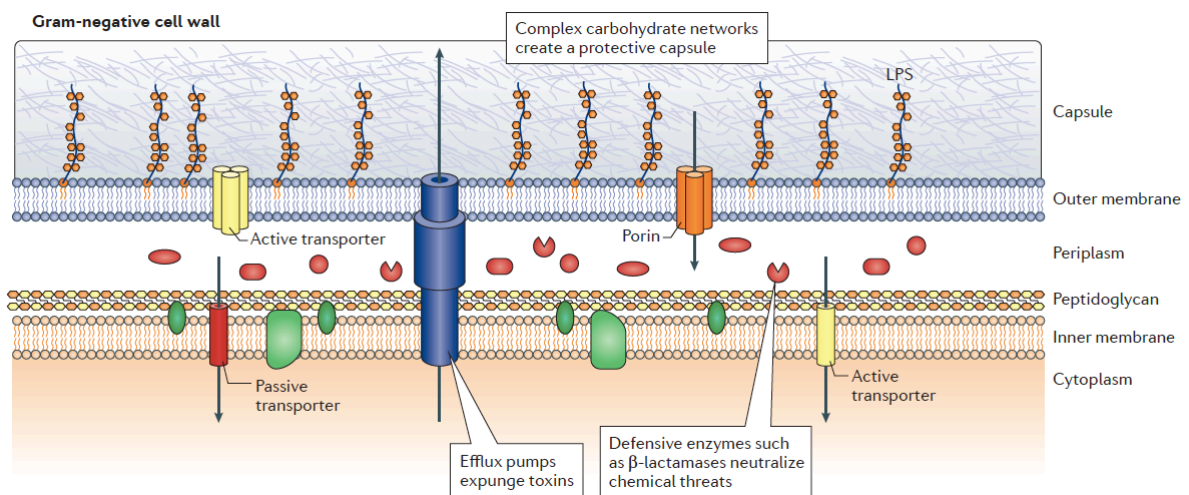


Figure 1. Représentation schématique de la paroi des bactéries à Gram négatif. D'après Tommasi et al⁵

Ces porines sont constituées de trois sous-unités qui forment des canaux étroits empêchant ainsi l'entrée de grosses molécules. Le transport passif de ces molécules dépend donc de leurs masses moléculaires mais également de leurs formes et de leurs charges.^{6,7} Il existe plusieurs porines telles que OprF (qui facilite le transport de grandes molécules comme les tri- et les tetra-saccharides), OprB (qui prend en charge le transport de sucres et saccharides), et OprD (assurant le passage d'acides aminés basiques et de peptides). De plus, ces porines constituent le point d'entrée pour les antibiotiques de la famille des β -lactamines.⁷ Quant au passage des molécules plus grosses, elles sont prises en charge par des transporteurs spécifiques et nécessitent de l'énergie.

b. Le peptidoglycane

Le peptidoglycane est une structure tridimensionnelle en réseau. Il est composé de chaînes polysaccharidiques formées de dimères (Figure 2. A) de N-acétyl-glucosamine (NAG) et d'acide N-acétyl-muramique (NAM) qui sont reliés entre eux *via* des liaisons osidiques de type $\beta(1-4)$. La synthèse du peptidoglycane se fait en plusieurs étapes : dans un premier temps, dans le cytoplasme bactérien, chaque unité de NAM est liée à un pentapeptide (NAM-PP) composé en général du L-Ala-D-Glu-DAP-D-Ala-D-Ala, où DAP représente l'acide diaminopimélique. Le NAM-PP est ensuite expédié vers la membrane plasmidique, où le NAG y est fixé (NAG-NAM-PP). Ce complexe traverse alors la membrane cytoplasmique. Enfin, dans l'espace inter-membranaire (ou périplasma), il y a polymérisation des précurseurs entre eux pour former les chaînes glucidiques, qui seront reliées entre elles par des ponts peptidiques.⁸ La réaction de pontage entre deux chaînes de glycanes est catalysée par des enzymes les DD-peptidases, aussi appelées protéines, liant les pénicillines (PLPs) (ou « Penicillin Binding Proteins » (PBPs) en anglais) qui sont des transpeptidases⁹ ou des carboxypeptidases et des transglycosylases (figure 2. B).

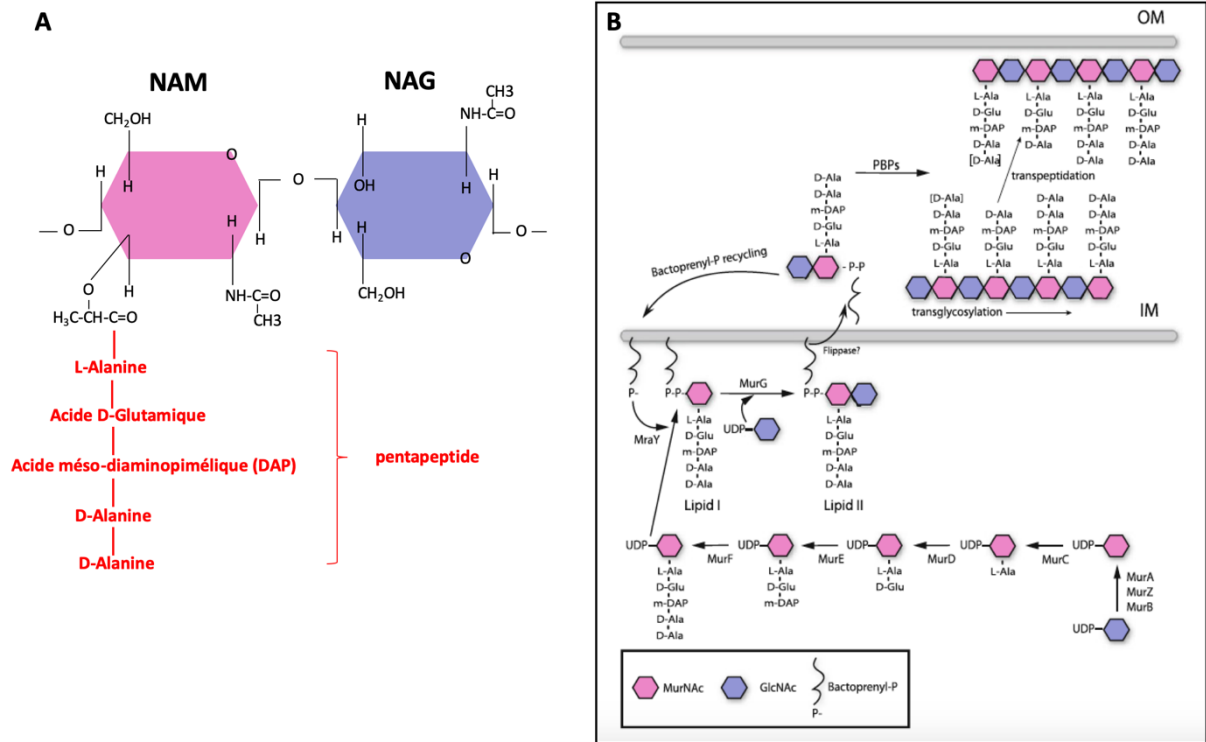


Figure 2 .A. Composition d'une sous-unité du peptidoglycane ;B. Représentation schématique de la synthèse du peptidoglycane (PG). Elle est initiée par la synthèse du pentapeptide disaccharide (précurseurs) dans le cytosol (GlcNAc-MurNAc-L-Ala-DGlu-DAP-D-Ala-D-Ala), qui est ensuite transféré au niveau de l'espace périplasmique via la formation d'un complexe lipidique avec le bactoprenyl.. Les précurseurs monomères sont complexés entre eux via les PLPs permettant la transglycosylation et la transpeptidation. D'après Cava et al.¹⁰

c. Les DD-peptidases ou Protéines liant les pénicillines (« Penicillin-Binding Proteins »)

Les PLPs sont des enzymes très importantes car elles sont responsables de l'assemblage du peptidoglycane, ce dernier assurant la rigidité de la paroi et la protection de la bactérie contre le milieu extérieur. Le nombre et la nature des PLPs varient selon les espèces bactériennes, on distingue deux grands groupes en fonction de leur poids moléculaire : celles à haut poids moléculaire qui ont une activité transpeptidase et transglycosidase et celles de faible poids moléculaire pourvues d'une activité carboxypeptidase. Toutes les PLPs sont des enzymes à sérine active, à l'exception de la DD-peptidase de *Streptomyces albus* qui est une enzyme faisant intervenir des ion zinc (Zn^{2+}) au niveau de son site actif.¹¹ Les PLPs sont ancrées dans la membrane cytoplasmique avec leur site actif dirigé vers l'espace périplasmique.

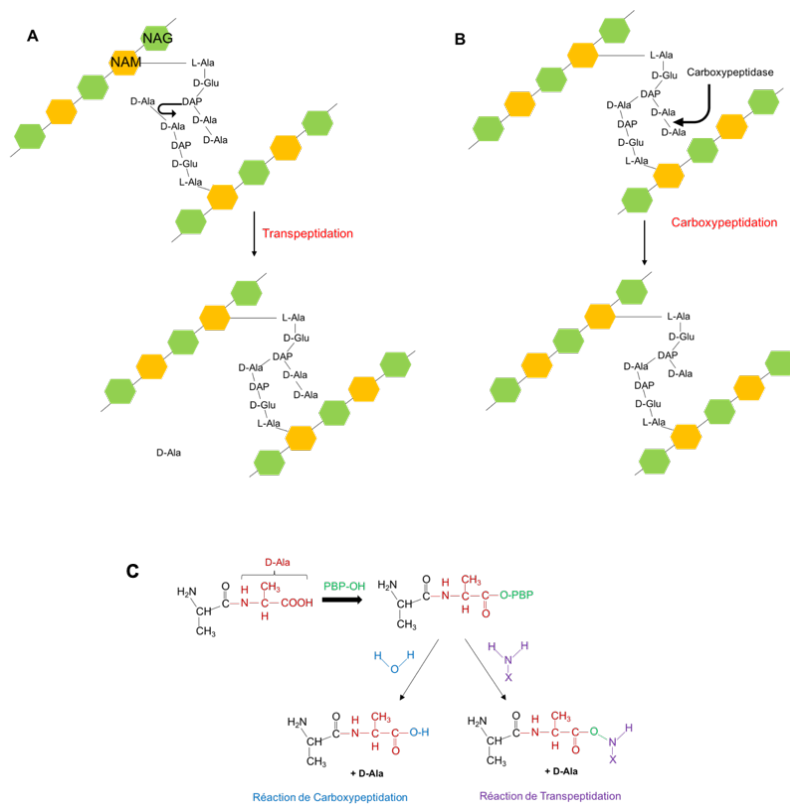


Figure 3. Schéma représentatif de la réaction de transpeptidation (A) et de la carboxypeptidation (B) catalysées par les PLPs. Réaction chimique de ces deux réactions (C).

La réticulation du peptidoglycane se fait *via* deux réactions : la transpeptidation et la carboxypeptidation (Figure 3). La transpeptidation conduit à la formation d'une liaison peptidique entre une D-Alanine d'un peptide et la fonction NH₂ libre de l'acide diaminopimélique (DAP) du peptide adjacent¹² avec l'élimination d'un résidu D-Alanine. Cette réaction est catalysée par une transpeptidase qui se fixe à l'extrémité D-Alanyl-D-Alanine formant un acyl-enzyme instable, l'attaque nucléophile par la fonction NH₂ libre du DAP permet la libération de l'enzyme et la formation de la liaison peptidique. La réaction de carboxylation permet l'élimination d'un résidu D-Alanine terminal. La carboxypeptidase se fixant également à l'extrémité D-Alanyl-D-Alanine engendrant la formation d'un acyl-enzyme instable qui est hydrolysé en présence d'une molécule d'eau.

II. Les Antibiotiques

1. Historique

La découverte du premier antibiotique a lieu en 1929 par Sir Alexander Fleming, qui constate qu'une culture de staphylocoques sur boîte de Pétri peut être inhibée par la présence d'un champignon du genre *Penicillium*. Il émet alors l'hypothèse que ce champignon secrète une substance bactéricide qu'il appellera pénicilline et tentera durant plusieurs années de purifier. C'est seulement en 1939, que Florey et Chain parviennent à purifier partiellement cette molécule et démontrent l'efficacité de son activité antibactérienne et l'absence de toxicité chez la souris. En 1945, le prix Nobel de physiologie et médecine a été décerné à ces trois scientifiques pour la découverte de la pénicilline et de ses effets curatifs dans plusieurs maladies infectieuses. En parallèle, le bactériologiste Gerhard Domagk, découvre, en 1931, une autre substance antibactérienne : le Prontosil qui permettra de traiter efficacement les infections liées à des streptocoques. La pénicilline et le Prontosil durant la Seconde Guerre mondiale seront largement utilisés afin de prévenir de nombreuses épidémies et d'éviter des septicémies.

La notion d'antibiotique apparaît en 1943 avec le microbiologiste Waksman, qui définira les antibiotiques comme « toutes substances chimiques produites par des microorganismes capables d'inhiber le développement et de détruire les bactéries et d'autres microorganismes ». En 1957, cette définition est complétée par Turpin et Velu, ils définissent les antibiotiques comme « tout composé chimique, élaboré par un organisme vivant ou produit par synthèse, à coefficient chimiothérapeutique élevé dont l'activité thérapeutique se manifeste à très faible dose d'une manière spécifique, par l'inhibition de certains processus vitaux, à l'égard des virus, des microorganismes ou même de certains êtres pluricellulaires ». Suite à la découverte de ces premiers antibiotiques, il se met en place une véritable course pour la découverte de nouvelles molécules (naturelles, synthétiques ou semi-synthétiques) entre les années 1940 et 1970. Un grand nombre de molécules est isolé à partir des bactéries du genre *Streptomyces* (Figure 4). Ce sont des bactéries à Gram positives strictement aérobie, et qui ont pour habitat naturel le sol où elles jouent un rôle important dans la décomposition et la minéralisation des matières organiques. Elles sont à l'origine de 80% de tous les antibiotiques connus.¹³

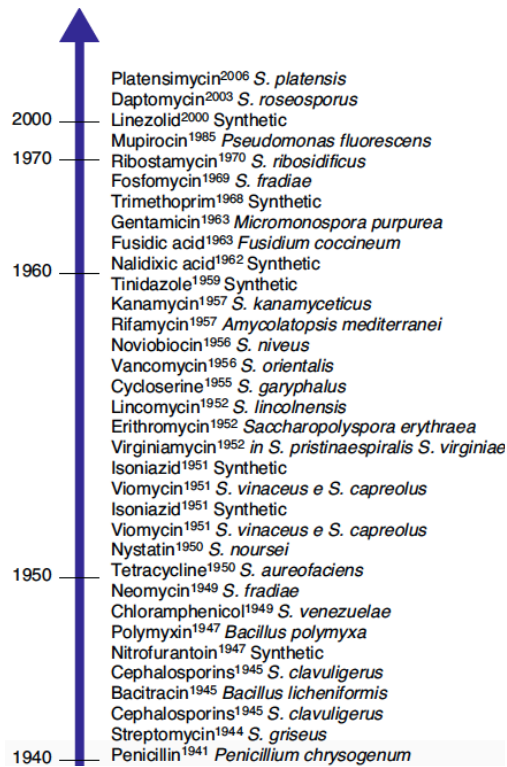


Figure 4. Chronologie de la découverte d'antibiotiques. D'après Procopio et al.¹³

L'antibiothérapie a ainsi permis une diminution importante du taux de décès liés aux maladies infectieuses (principale cause de mortalité) passant d'environ 33% à 4% entre la fin du XIX^{ème} et du XX^{ème} siècle¹⁴, et conduisant à une augmentation de l'espérance de vie de huit ans entre 1944 et 1972. De façon plus générale, l'utilisation des antibiotiques a également eu un impact en médecine en diminuant les risques d'infection au cours d'opérations complexes telles que des transplantations d'organes, progrès de la médecine qui n'aurait pas pu avoir lieu sans l'utilisation d'agents antibactériens efficaces. Cependant, malgré le succès de la découverte d'antibiotiques et les progrès majeurs dans les processus de production, les maladies infectieuses restent toujours la deuxième cause de décès dans le monde, et les infections bactériennes sont responsables d'environ 17 millions de décès chaque année, affectant principalement les enfants et les personnes âgées.

2. Généralités

La majorité des antibiotiques sont des molécules naturelles, produites par des bactéries ou des champignons capables de tuer des bactéries sensibles (effet bactéricide) ou d'inhiber leur croissance (effet bactériostatique). Il existe, également, des antibiotiques semi-synthétiques qui sont des antibiotiques naturels modifiés par l'addition de groupements chimiques dans le but de les rendre moins sensibles à l'inactivation par les micro-organismes et enfin, les antibiotiques synthétiques qui sont des analogues ou des dérivés d'antibiotiques naturels.

Les antibiotiques sont classés en fonction de leur mode d'action qui dépend de la cible de l'antibiotique (Tableau 1). Les antibiotiques peuvent agir (i) sur la paroi bactérienne *via* l'inhibition de la synthèse du peptidoglycane, (ii) sur la membrane plasmidique en perturbant la perméabilité membranaire, (iii) sur l'ADN en inhibant la réplication et la transcription, (iv) sur la synthèse des protéines (actions sur les ribosomes), et enfin, (v) sur des voies métaboliques essentielles (antimétabolites).

Tableau 1. Classification des antibiotiques en fonction de leur mode d'action

Modes d'action	Antibiotiques
Inhibition de la synthèse de la paroi	β -lactamines Vancomycine Éthionamide et isoniazide
Altération de la fonction de la membrane plasmidique	Polymyxines
Inhibition de la synthèse nucléique	Rifampicine Quinolones
Inhibition de la synthèse protéique	Aminoglycosides ou aminosides Cyclines Phénicolés Macrolides Oxazolidinones
Inhibition des voies métaboliques	Sulfamides Triméthoprim

À ce jour, il existe des milliers de molécules d'antibiotiques naturelles ou synthétiques. Toutefois, la toxicité de certaines molécules empêche leur utilisation en médecine humaine.

Globalement, une centaine d'antibiotiques peut être administrée afin de maîtriser les maladies infectieuses causées par des agents bactériens.

3. Les β -lactamines

Les β -lactamines représentent la famille d'antibiotiques la plus utilisée en antibioprofylaxie et en antibiothérapie. L'importance de leur utilisation résulte de leur large spectre d'action, de leur faible toxicité, de leur efficacité thérapeutique et de leur faible coût.

Les β -lactamines, comme leur nom l'indique, sont caractérisées par la présence d'un noyau β -lactame accolé, ou non, d'un hétérocycle de 5 à 6 atomes. Ainsi, suivant la nature de l'hétérocycle on distingue quatre sous-familles : les pénicillines, les céphalosporines, les monobactames et les carbapénèmes (Tableau 2).

Tableau 2 Classification et structures des bêta-lactamines

Sous classe des Bêta-lactames	Exemples	Structure
Pénicillines (noyau pénème)	Pénicillines Ampicilline Pipéracilline Témocilline	<p>Cycle thiazolidine</p>
Céphalosporines (noyau céphème)	Céfaloine (1 ^{er} G) Céfoxime (2 ^{ème} G) Céfuroxime (2 ^{ème} G) Céfotaxime (3 ^{ème} G) Ceftazidime (3 ^{ème} G) Ceftriaxone (3 ^{ème} G) Céfixime (3 ^{ème} G) Céfépime (4 ^{ème} G) Cefpirome (4 ^{ème} G)	<p>Cycle dihydrothiazine</p>
Carbapénèmes	Imipénème Méropénème Ertapénème Doripénème	<p>Cycle dihydropyrrrole</p>
Monobactames	Aztréonam	<p>Groupement sulfonate</p>

Le développement des différentes familles de β -lactamines depuis les pénicillines jusqu'aux carbapénèmes a été dicté par la nécessité d'élargir le spectre d'activité de ces molécules vers

les bactéries à Gram négatif, ainsi que la volonté d'améliorer la biodisponibilité de ces antibiotiques.¹⁵

a. Les sous-classes

i. Les pénicillines

Les pénicillines sont des β -lactamines à noyau pénème, c'est à dire que le cycle β -lactame est associé à un cycle thiazolidine. Au sein de cette famille, on distingue des molécules qui possèdent des spectres d'action : moyen (pénicilline G et V essentiellement actifs sur les bactéries à Gram positif), étroit (pénicilline M active sur les staphylocoques devenus résistants à la pénicilline G), ou plus large (action sur les bactéries à Gram négatif notamment) comme les aminopénicillines (amoxicilline, ampicilline), les uréidopénicillines (pipéracilline), et les carboxypénicillines (ticarcilline).

ii. Les céphalosporines

Ce sont des β -lactamines à noyau céphème. Ce noyau se compose du cycle β -lactame et d'un cycle dihydrothiazine. Depuis la découverte dans les années 1940 de la céphalosporine C produite par *Cephalosporium acremonium*, plusieurs générations de céphalosporines (1^{ère}, 2^{ème}, 3^{ème}, 4^{ème}, 5^{ème}) ont été commercialisées. Ainsi, le spectre d'activité est devenu de plus en plus large. Les céphalosporines de 3^{ème} et 4^{ème} génération (C3G et C4G) possèdent le plus large spectre d'action vis-à-vis des bactéries à Gram négatif. Leur utilisation est spécifique à certaines situations cliniques particulières. Elles sont notamment utilisées pour le traitement des infections nosocomiales sévères.

iii. Les monobactames

Ces molécules sont caractérisées par la seule présence du cycle β -lactame. Leur spectre est étroit, ils sont inactifs sur les bactéries à Gram positif et les germes anaérobies mais très actif sur les entérobactéries et *P. aeruginosa*. La seule molécule commercialisée est l'aztréonam son spectre d'activité est relativement comparable à celui des céphalosporines de 3^{ème} génération.

iv. Les carbapénèmes

Les carbapénèmes se différencient des pénicillines par la présence d'un atome de carbone au lieu d'un soufre en position 1 et d'une liaison insaturée en C2-C3, qui est également présente chez les céphalosporines. Ils ont été développés à partir de la thiénamycine naturellement produite chez *Streptomyces cattleya*¹⁶. Cette molécule naturelle étant instable, un dérivé plus stable a été développé : la N-formimidoyl thiénamycine ou imipénème. Cependant, l'imipénème est dégradé par une enzyme humaine présente au niveau des tubules rénaux, la déhydropeptidase-1 (DHP-1), par conséquent, l'imipénème est administré avec un inhibiteur de cette enzyme, la cilastatine. Les autres carbapénèmes (l'ertapénème, le méropénème et le doripénème) restent insensibles à l'activité de la DHP-1.¹⁷ Les carbapénèmes ont le spectre d'activité le plus large comprenant des bactéries à Gram positif (tel que *Staphylococcus aureus*) et les bactéries à Gram négatif aérobies et anaérobies¹⁸. Du fait de leur fort pouvoir antimicrobien, ils sont devenus des outils thérapeutiques cruciaux pour le traitement empirique des infections nosocomiales sévères.¹⁹ Les carbapénèmes sont utilisées pour le traitement des infections documentées à bactéries à Gram négatif résistantes aux C3G. Du fait de leur demi-vie courte, l'imipénème et le méropénème sont administrés plusieurs fois dans la journée. L'ertapénème, quant à lui, ayant une demi-vie plus longue (4h au lieu de 1h pour les autres molécules) n'est administré qu'une seule fois par jour. L'utilisation des carbapénèmes est considérée comme l'un des traitements de derniers recours pour les infections à germes résistants aux antibiotiques. Ainsi, l'émergence de la résistance aux carbapénèmes est inquiétante car elle limite encore les rares possibilités de traitements et peut mener à de véritables impasses thérapeutiques.

b. Mode d'action des β -lactamines

Les β -lactamines ont pour cible les DD-peptidases ou PLPs qui jouent un rôle crucial dans la dernière étape de la synthèse du peptidoglycane. Celui-ci est un élément essentiel pour la cellule car il empêche, notamment, que la cellule explose du fait de la forte pression osmotique interne (5 à 20 atmosphères). Son intégrité est donc essentielle à la survie de la bactérie, et elle doit donc être maintenue au cours de la croissance bactérienne. Toute altération du peptidoglycane conduira plus ou moins rapidement à la lyse bactérienne.

Pour pouvoir accéder à leurs cibles (les PLPs présentes dans l'espace périplasmique), les β -lactamines doivent, tout d'abord, traverser la membrane externe. Cette membrane constitue une double barrière de perméabilité. En effet, elle présente à sa surface les lipopolysaccharides qui s'opposent à l'entrée des substances lipophiles et la bicouche lipidique qui s'oppose à l'entrée de substances hydrophiles. La pénétration des β -lactamines se fait *via* des porines (canaux aqueux formés par des protéines transmembranaires) par un transport passif. Ce transport est d'autant plus facilité si les molécules sont de petites tailles, hydrophiles et chargées positivement. Par conséquent, seules les β -lactamines hydrophiles peuvent traverser la membrane externe. Une fois dans l'espace périplasmique, les β -lactamines agissent comme substrats suicides des PLPs. En effet, elles présentent une homologie structurale avec le peptide D-Alanine-D-Alanine, substrat naturel des PLPs (Figure 5). L'antibiotique se fixe de façon covalente au site actif des PLPs pour former un acyl-enzyme stable. L'inhibition des PLPs a pour conséquence l'arrêt de la synthèse du peptidoglycane, ce qui engendre, dans un premier temps, un arrêt de la croissance bactérienne (effet bactériostatique). La lyse cellulaire (effet bactéricide) intervient secondairement *via* la sécrétion d'autolysines.

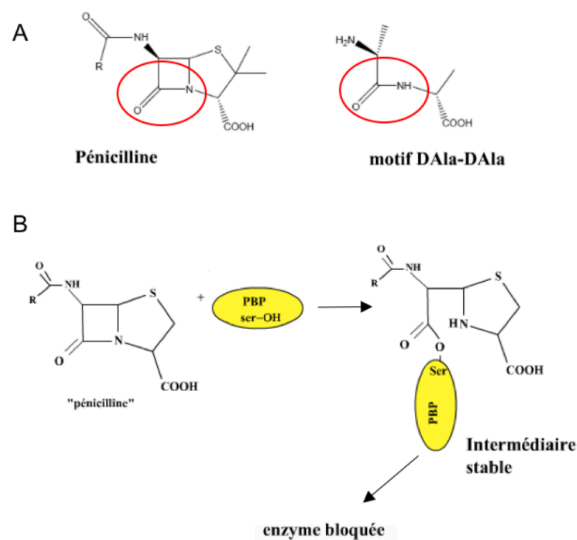


Figure 5. A. Homologie structurale entre le substrat naturel D-Ala-D-Ala des PLPs et la pénicilline. B. Inhibition des PLPs par la pénicilline

III. Résistance aux β -lactamines

Les premiers cas de souches bactériennes résistantes aux β -lactamines ont été constatés en 1941, où moins de 1% des staphylocoques étaient résistants à la pénicilline. En 1947, soit trois ans après la mise sur le marché de la pénicilline, le nombre de cas augmente passant de 1% à 38%.²⁰ L'utilisation intensive et peu contrôlée de ces antibiotiques a mené à un déclin, prémédité par Fleming, de ce remède miracle *via* l'apparition rapide de souches bactériennes résistantes.

“ It is not difficult to make microbes resistant to penicillin in the laboratory by exposing them to concentrations not sufficient to kill them, and the same thing has occasionally happened in the body. The time may come when penicillin can be bought by anyone in the shops. Then there is the danger that the ignorant man may easily underdose himself and by exposing his microbes to non-lethal quantities of the drug make them resistant.”

Alexander Fleming, Nobel Lecture, December 11, 1945

La résistance aux β -lactamines peut être naturelle ou acquise. L'acquisition de cette résistance est la conséquence (i) de mutations dans des systèmes pré-existants ou (ii) de l'acquisition de gènes. La résistance aux β -lactamines résulte de quatre types de mécanismes possibles : (i) modification de la cible ; (ii) diminution de la perméabilité membranaire ; (iii) excrétion de l'antibiotique et ; (iv) inactivation enzymatique des β -lactamines (Figure 6).

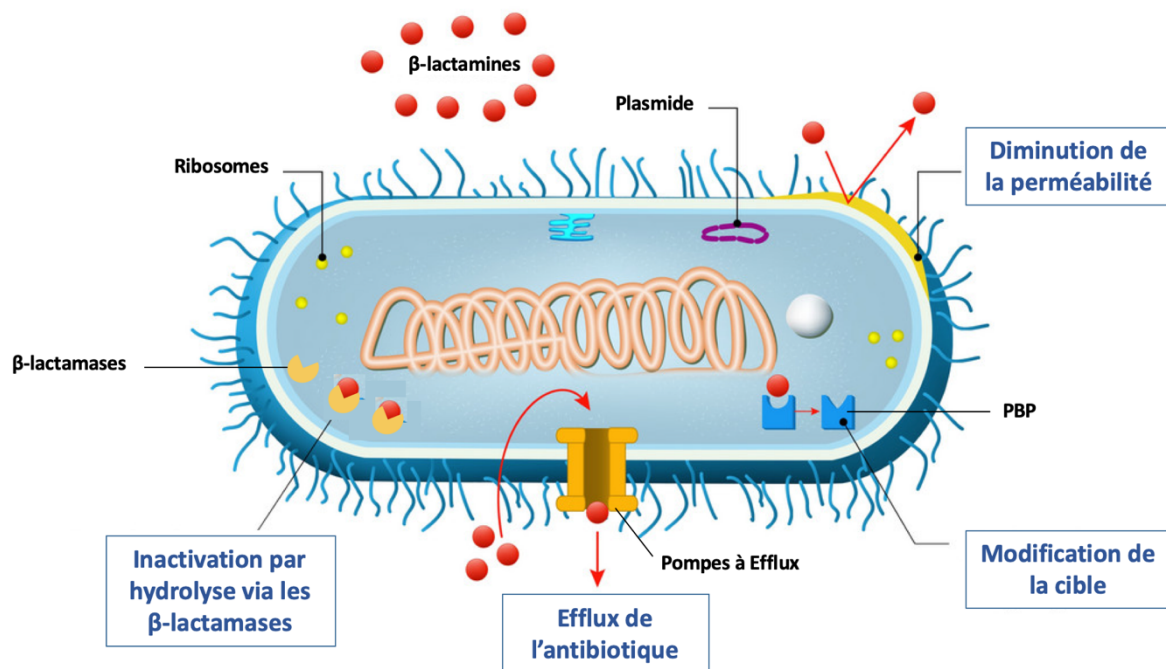


Figure 6 Mécanisme de résistance aux β -lactamines chez les Entérobactéries: (i) Modification de la cible (PLPs), (ii) Diminution de la perméabilité (modification des porines), (iii) Efflux de l'antibiotique via des pompes spécialisées, (iv) Inactivation enzymatique par les β -lactamases.. Réadaptation de l'image VectorStock.com/10499529

1. Modification de la cible des β -lactamines

La modification de la cible a pour conséquence une diminution de l'affinité des PLPs vis-à-vis des β -lactamines. Cette perte d'affinité peut résulter de mutations qui peuvent induire : une modification de la conformation des PLPs, une diminution de production d'une PLPs de forte affinité ou encore une hyperproduction d'une PLP de faible affinité. Par exemple, chez certaines souches de *Enterococcus faecium*, la PLP5fm²¹⁻²³ est surexprimée. Cette PLP possède une très faible affinité pour les β -lactamines et permet ainsi de remplacer la fonction d'autres PLPs plus affines pour les β -lactamines. On observe également cette modification de cible chez les souches de *Staphylococcus* résistantes à la méticilline. Ces souches produisent une PLP alternative, la PBP2a, encodée par un gène acquis, *mecA*.^{21,24} La PLP2a n'a pas, ou très peu, d'affinité vis-à-vis de l'ensemble des β -lactamines. Ce type de mécanisme de résistance reste rare chez les entérobactéries, il a été décrit chez des souches de *P. mirabilis* dont la résistance

à l'imipénème est médiée par une perte de l'affinité de la PLP2 et une diminution quantitative de la PLP1a.²⁵

2. Diminution de la perméabilité

L'entrée passive des β -lactamines dans la bactérie se fait *via* les porines. Une mutation au niveau de l'un des gènes codant pour ces protéines, ou la délétion de l'un d'entre eux, permet de modifier qualitativement ces porines empêchant ainsi l'entrée des β -lactamines. Une diminution de l'expression de ces porines (modification quantitative) peut être également à l'origine de ce phénomène. De nombreux cas d'acquisition de la résistance par diminution de la perméabilité ont été décrits chez *E. coli*, *Proteus sp.*, *Salmonella sp.*, *Shigella sp.*, *Klebsiella sp.*, *Enterobacter sp.* et *Serratia sp.* Ce mécanisme s'exprime généralement à bas niveau et est souvent associé à d'autres mécanismes de résistance comme la production d'enzyme inactivant les β -lactamines. Chez *E. coli*, l'altération des porines OmpA, OmpC et OmpF est fréquemment décrite dans des isolats multirésistants. Chez *K. pneumoniae*, les porines OmpK35 et OmpK36 sont impliquées dans la résistance aux carbapénèmes.^{26,27}

3. Excrétion des β -lactamines : système d'efflux

Les pompes d'efflux sont des transporteurs transmembranaires qui excrètent activement des molécules toxiques, dont les antibiotiques, en-dehors de la bactérie (Figure 7). Il existe cinq familles de pompes d'efflux, associées à une résistance aux antibiotiques : la famille ABC (ATP-Binding Casette) transporteurs, la famille des pompes SMR (Small Multidrug Resistance), la famille pompes MATE (Multidrug and Toxic Compound Extrusion), la famille des pompes MFS (Major Facilitator Superfamily) et la famille des pompes RND (Resistance Nodulation cell Division).²⁸ L'hyperproduction de ces systèmes conduit à une résistance de bas niveau croisée à différentes familles d'antibiotiques. Cette surexpression peut être due à des mutations au niveau des gènes qui régulent l'expression de ces systèmes d'efflux. Chez les bactéries à Gram négatif, les pompes les plus fréquemment observées sont de type RND. C'est un système à trois composants : le transporteur, une protéine périplasmique (Membrane Fusion Protein, MFP) et une porine (Outer Membrane Factor, OMF).²⁸

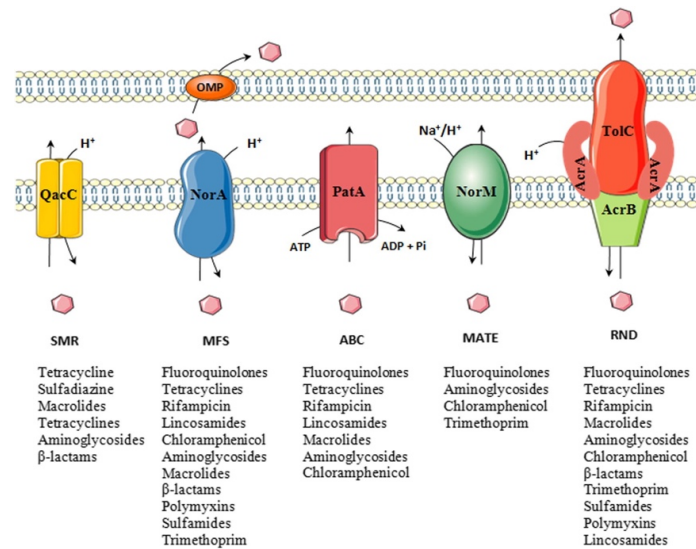


Figure 7. Représentation schématique des cinq familles de pompe d'efflux avec leurs substrats antibiotiques connus. Famille SMR « Small Multidrug Resistance » family, famille MFS « Major Facilitator Superfamily », Famille ABC « ATP-binding cassette », Famille MATE « Multidrug and Toxic compound Extrusion », Famille RND « Resistance-Nodulation-Division. OMP (outer membrane protein) : protéine de membrane externe. D'après Yilmaz et Özcengiz²⁹

4. Inactivation enzymatique des β -lactamines : les β -lactamases

C'est le principal mécanisme de résistance aux β -lactamines chez les entérobactéries. Celui-ci consiste à la dégradation des β -lactamines par des enzymes spécialisées appelées les β -lactamases (Figure 8). De nombreuses espèces bactériennes sont naturellement résistantes aux aminopénicillines et aux céphalosporines de première génération par production de β -lactamases dites naturelles, c'est à dire dont les gènes codant pour ces enzymes sont localisés sur le chromosome bactérien. Ce type de résistance peut également être acquis grâce à des transferts génétiques faisant intervenir des plasmides. L'expression de ces gènes peut être constitutive (comme la pénicillinase SHV chez *K. pneumoniae*) ou inductible *via* des gènes de régulation situés en amont du gène codant pour la β -lactamase (comme la céphalosporinase naturelle de *Serratia* sp., *Enterobacter* sp. ou *Morganella* sp.).

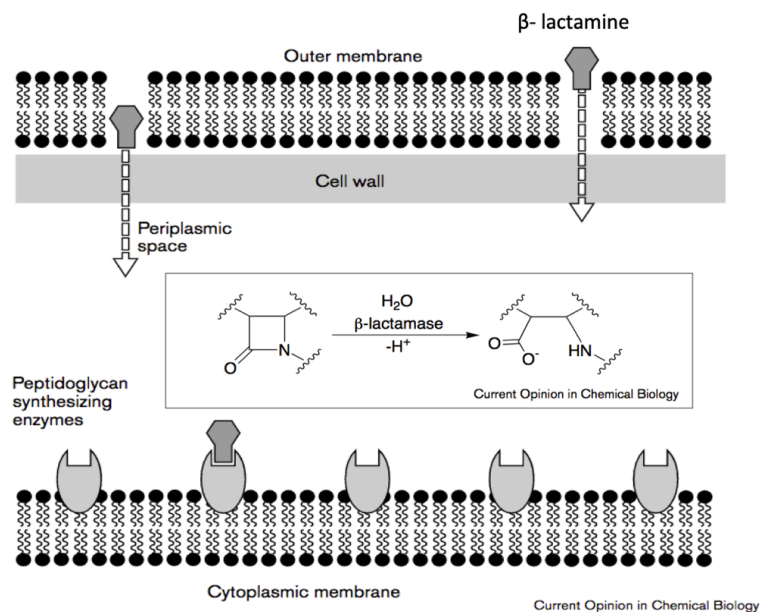


Figure 8. Schéma du mode d'action des β -lactamines et des β -lactamases. Les antibiotiques diffusent à travers la membrane externe et inactivent les PLPs, qui sont impliqués dans la biosynthèse du peptidoglycane. L'action des β -lactamases provoque l'ouverture du noyau β -lactame de l'antibiotique, le rendant inactif. Les substitutions à chacune des trois positions (indiquées par des lignes ondulées) donnent lieu à une famille de composés bioactifs, dont beaucoup sont clivés par les β -lactamases. D'après Wang et al.³⁰

IV. Les β -lactamases

Les β -lactamases sont des enzymes capables d'inactiver les β -lactamines en hydrolysant la liaison amide du cycle β -lactame (Figure 8). Cette action est irréversible, ce qui entraîne la perte complète de l'activité de l'antibiotique. Chez les bactéries à Gram négatif, les β -lactamases sont sécrétées dans l'espace périplasmique, lieu d'action des β -lactamines sur les PLPs. Les β -lactamases possèdent une vitesse d'hydrolyse des β -lactamines beaucoup plus efficace (1000 cycles β -lactame par seconde), que celles des PLPs (1 cycle β -lactame par heure).^{11,31,32} Ainsi, les β -lactamases peuvent dégrader les β -lactamines avant même qu'elles ne puissent interagir avec les PLPs.

1. Généralités

En 1940, soit douze ans après les travaux de Fleming, Abraham et Chain décrivent une enzyme bactérienne capable d'inactiver la pénicilline,³³ ils l'appelleront pénicillinase. Depuis, plusieurs milliers de β -lactamases ont été décrites et répertoriées (<http://www.lahey.org/Studies/>). Cette famille d'enzymes présente une grande diversité de structures et de propriétés catalytiques (Figure 9). Par conséquent il existe plusieurs classifications telles que la classification structurale de Ambler³⁴ et la classification fonctionnelle de Bush-Jacoby-Medeiros. La plus utilisée est celle de Ambler.

La classification de Ambler, proposée dans les années 1975, est basée sur les analogies de séquence peptidique. Elle comprenait initialement trois classes de β -lactamases (la classes A, B, C) mais une 4^{ème} a été rajoutée dans un second temps (la classe D).

a. Les β -lactamases de classe A :

Elles constituent le groupe le plus important. Elles hydrolysent préférentiellement les pénicillines et sont sensibles aux inhibiteurs de β -lactamases utilisables en clinique (acide clavulanique, tazobactam et sulbactam). Au sein de cette classe, on distingue selon leur spectre d'hydrolyse, trois grandes sous familles : les pénicillinases, les β -lactamases à spectre étendu (BLSEs) qui sont des pénicillinases ayant acquis une activité vis-à-vis de certaines céphalosporines à large spectre (ou céphalosporines de 3^{ème} génération [C3G]) et les carbapénèmases de classe A (principalement de type GES et type KPC) qui, en plus d'hydrolyser les pénicillines et les céphalosporines, hydrolysent les carbapénèmes.

b. Les β -lactamases de classe B ou métallo- β -lactamases :

Elles possèdent un large spectre d'action comprenant les pénicillines, les céphalosporines et les carbapénèmes. En effet, toutes les métallo- β -lactamases sont des carbapénèmases. Cependant, elles sont incapables d'hydrolyser les monobactames (aztréonam). Leur activité nécessite la présence d'ions Zn^{2+} au niveau du site actif et n'est pas affectée par les inhibiteurs classiques de β -lactamases. En revanche, des agents chélateurs

d'ion divalents, tel que l'EDTA (Acide éthylène diamine tetra-acétique), sont des inhibiteurs efficaces des métallo- β -lactamases.³⁵

c. Les β -lactamases de classe C ou céphalosporinases :

Leur spectre d'hydrolyse comprend les pénicillines (pénicillines G, A et V) et les céphalosporines de première génération (et pour certaines de deuxième génération). L'hydrolyse des carboxypénicillines (ticarcillines), des uréidopénicillines (pipéracilline), de l'aztréonam et des C3G est observée en cas d'hyperproduction de ces enzymes. On parle alors de « céphalosporinases de haut niveau ». Les céphalosporines de quatrième génération (céfépime, cefpirome) et les carbapénèmes ne sont pas, ou très peu, hydrolysées. Les céphalosporinases restent insensibles aux inhibiteurs classiques de β -lactamases. En revanche, ces céphalosporinases sont inhibées par la cloxacilline et l'oxacilline.

d. Les β -lactamases de classe D ou oxacillinases :

Il s'agit de la classe de β -lactamases la plus hétérogène d'un point de vue structure et spectre d'hydrolyse.³⁶ Ces enzymes ont été appelées initialement oxacillinases car elles hydrolysaient bien plus rapidement l'oxacilline que la pénicilline G. Au sein de cette famille, on distingue des oxacillinases à spectre étroit (hydrolyse des pénicillines et des céphalosporines de première génération), des oxacillinases à spectre élargi aux céphalosporines (2^{ème}, 3^{ème} et 4^{ème} génération) et des oxacillinases ayant une activité carbapénémases (tel que type OXA-48 chez les entérobactéries). L'activité de ces enzymes n'est, en général pas, affectée par les inhibiteurs classiques de β -lactamases. Pour certaines oxacillinases, une activité inhibitrice du chlorure de sodium a été identifiée *in vitro*.³⁶

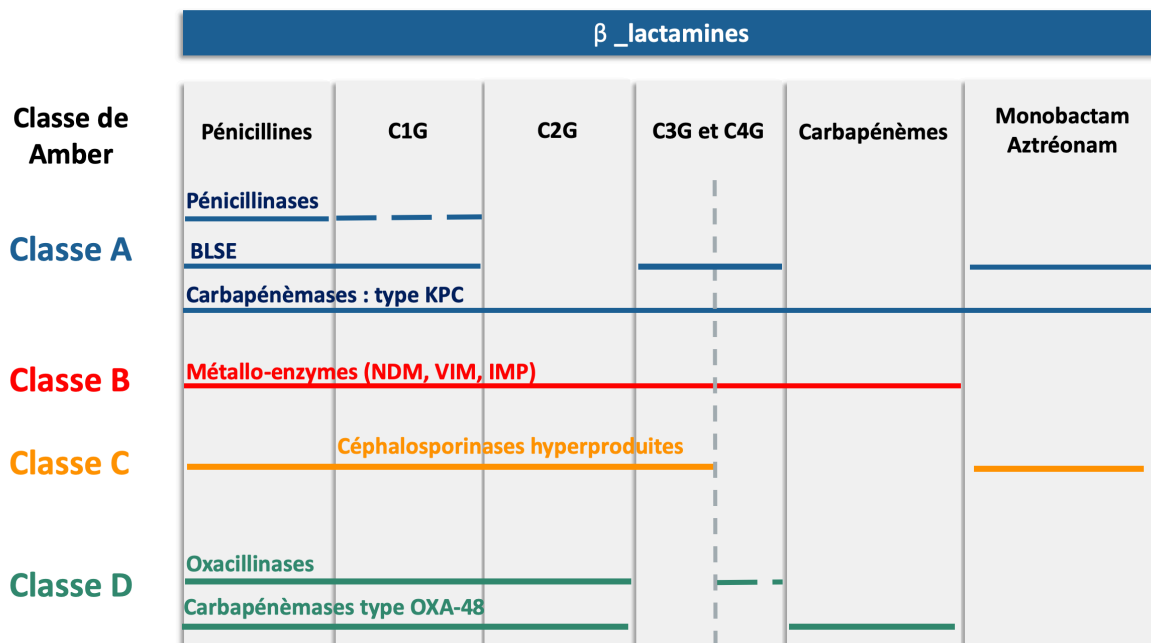


Figure 9. Représentation simplifiée du spectre d'hydrolyse des β-lactamases

Les β-lactamases peuvent être également classées en fonction du mode de fonctionnement de leur site actif. Ainsi, deux classes de β-lactamases peuvent être identifiées: les enzymes à sérine active (classe A, C et D de Ambler) et les métallo-enzymes (classe B de Ambler) qui nécessitent des ions zinc (Zn^{2+}).

2. Les β-lactamases à sérine active

a. Structure

Les β-lactamases des classe A, C et D de Ambler, ainsi que les PLPs³⁷, sont des enzymes à sérine active. Elles sont toutes constituées de deux domaines : le domaine α qui est constitué uniquement d'hélices α et le domaine α/β formé d'hélices α et de feuillet β antiparallèles. L'intersection entre ces deux domaines définit le site actif de ces protéines. De plus, elles présentent une boucle appelée boucle oméga qui interagit avec le site actif (Figure 10).

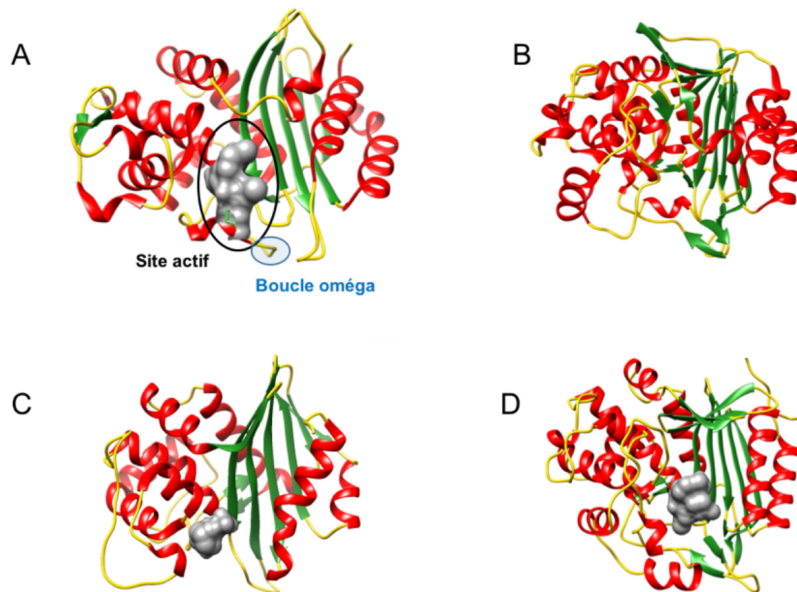


Figure 10. Comparaison des structures tridimensionnelles des β -lactamases à sérine active avec celle d'une PLP. *A.* β -lactamase de classe A : KPC-2 - Cefotaxime (réf. Pdb 5UJ3) ; *B.* β -lactamase de classe C : CMY-2 couplée à une molécule de citrate (réf. Pdb1CC2) ; *C.* β -lactamase de classe D : OXA-10 couplée à l'avibactam (réf. Pdb4S2O) ; *D.* R61 DD-peptidase de *Streptomyces* (réf. Pdb1CEF). Le cercle noir délimite le site actif et le cercle bleu la boucle Oméga.

Les β -lactamases à sérine active présentent toutes trois motifs communs très conservés.³⁷ Les motifs 1 et 3 sont identiques chez les trois classes de Amber tandis que le motif 2 varie et il est caractéristique de la classe de l'enzyme (Tableau 3).

Le premier motif : SXXK se localise au fond du site actif et plus particulièrement situé au niveau N-terminal de l'hélice $\alpha 2$. Le troisième motif KTG, présent sur le feuillet $\beta 3$, délimite le côté droit du site actif. Enfin, le deuxième motif SXN présent entre l'hélice $\alpha 4$ et l'hélice $\alpha 5$, définit le côté gauche du site actif.

Tableau 3. Motifs conservés au niveau du site actif des enzymes à sérines active (S).

Motifs	Classe A	Classe C	Classe D	DD-peptidase
1	SXXK	SXXK	STFK	S(T/S)FK
2	SDN	YAN	SXV	(Y/S)X(N/C)
3	(K/R)(S/T)G	KTG	K(T/S)G	(H/K)(T/S)G

b. Mécanisme catalytique

Le modèle cinétique de ces enzymes repose sur trois étapes caractérisées par les différentes interactions entre l'enzyme et le substrat (Figure 11). La première étape est la fixation de l'enzyme au substrat *via* une liaison non covalente formant un complexe appelé le complexe de Michaelis (ES). Ce complexe est caractérisé par deux constantes : la constante d'association (k_1) et la constante de dissociation (k_{-1}). Dans un second temps, ce complexe se transforme en un complexe covalent (appelé complexe acyl-enzyme : ES^*) *via* la formation d'une liaison ester entre la sérine active et la fonction carbonyle du noyau β -lactame. Enfin, la dernière étape correspond à l'hydrolyse de l'acyl-enzyme.³⁸

D'un point de vue moléculaire la sérine, une fois activée, réalise une attaque nucléophile au niveau du carbone de la fonction carbonyle du noyau β -lactame. Cela a pour conséquence la rupture de la liaison amide (C-N) du noyau β -lactame. Cette réaction appelée réaction d'acylation (caractérisée par la constante d'acylation k_2) permet la formation du complexe covalent stable : l'acyl-enzyme. Dans un deuxième temps, une molécule d'eau attaque ce même carbone ce qui provoque la rupture de la liaison covalente enzyme-substrat et libère le substrat devenu inactif, c'est la réaction de désacylation qui est caractérisée par la constante de désacylation k_3 .

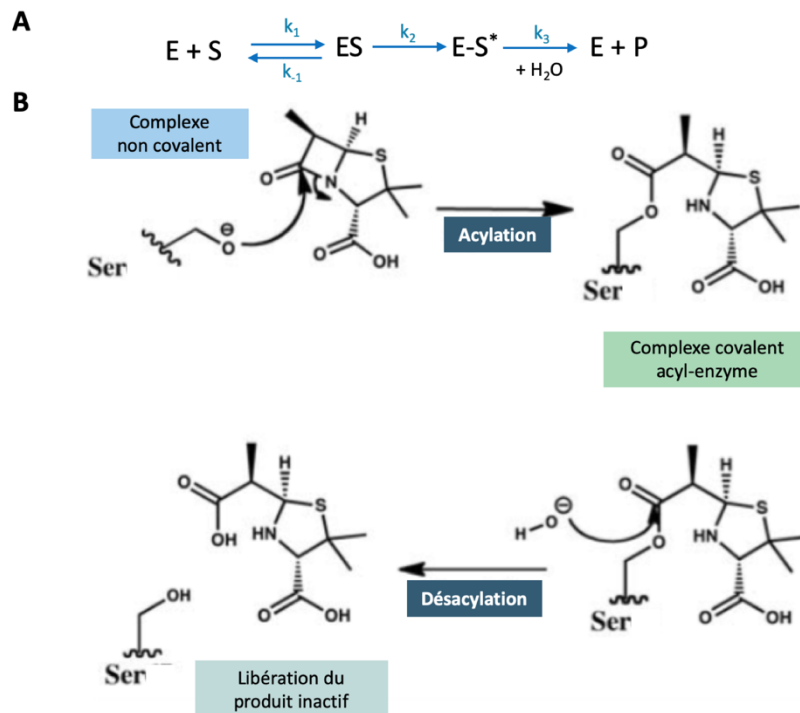


Figure 11. A. Modèle catalytique des β -lactamases à sérine active. *E* : enzyme, *S* : substrat, *P* : produit, *ES* : complexe de Michaelis de pré-acylation, *E-S* : l'acyl-enzyme. Les constantes de vitesse pour chaque étape sont représentées par k_1 (constante de vitesse d'association), k_{-1} (constante de vitesse de dissociation), k_2 (constante de vitesse d'acylation) et k_3 (constante de vitesse de désacylation). **B. Schéma de la réaction d'acylation et de désacylation.** Dans la première demi-réaction, le résidu Ser nucléophile attaque le carbone du carbonyle du cycle β -lactame, ce qui entraîne la coupure du cycle et la formation d'un acylate d'enzyme stable. Dans la seconde étape, une molécule d'eau attaque le même carbone, la liaison se rompt et le ligand inactif est libéré du site actif. D'après Szarecka et al.³⁸

3. Les Métallo- β -lactamases

a. Structure

Au sein de cette famille, on distingue trois sous-groupes déterminés selon leurs séquences en acide aminé : les sous-groupes B1, B2 et B3. Bien qu'il y ait une faible homologie de séquence entre ces différents sous-groupes, ces enzymes présentent un repliement très similaire : elles possèdent une structure de type sandwich $\alpha\beta/\beta\alpha$ composée de feuillets β au centre et d'hélices α sur les faces externes (Figure 12).

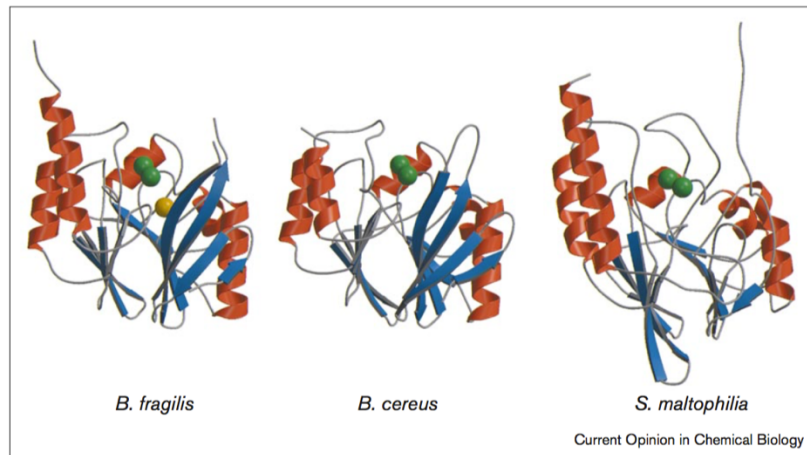


Figure 12. Comparaison de la structure tertiaire de métallob- β -lactamases provenant de *B. fragilis* : CcrA (sous classe B1), *B. cereus* : BcII (sous classe B1) et de *S. maltophilia* : L1 (sous classe B3). Les ions zinc sont représentés par des sphères vertes. D'après Wang et al.³⁰

La sous classe B1 regroupe toutes les enzymes similaires à la métallob- β -lactamase BCII de *B. cereus* telles que les enzymes VIM, NDM et IMP. Toutes les enzymes de cette sous famille sont monomériques et sont caractérisées par un site à haute affinité pour le zinc (site 1 ; $K_D=1,8\text{nM}$) et un site de faible affinité (site 2 ; $K_D=1,8\ \mu\text{M}$).³⁹ Ainsi, en fonction de la concentration en zinc dans le milieu, ces enzymes peuvent se retrouver sous forme mono ou di-zinc (Figure 13).

Les enzymes de la sous classe B2 sont toutes produites par des espèces de *Aeromonas* sp. avec, pour exemple, CphA chez *A. hydrophylia*.⁴⁰ Elles se présentent toutes sous forme de mono-zinc avec un site de haute affinité pour l'ion zinc ($K_D<10\ \text{nM}$).⁴¹ La fixation d'un second ion zinc inhibe leur activité enzymatique.

Les enzymes de la sous classe B3 sont majoritairement monomériques comme GOB-1 de *Chryseobacterium meningoseptium*⁴² et FEZ-1 de *Fluoribacter gormanii*.⁴³ La métallob- β -lactamase naturelle L1 de *Stenotrophomonas maltophilia* forme un homotétramère. Les deux sites de fixation ont de hautes affinités pour le zinc ($K_{D1}=K_{D2}=6\ \text{nM}$). C'est pour cette raison que les enzymes de cette sous-classe se présentent essentiellement sous forme di-zinc.

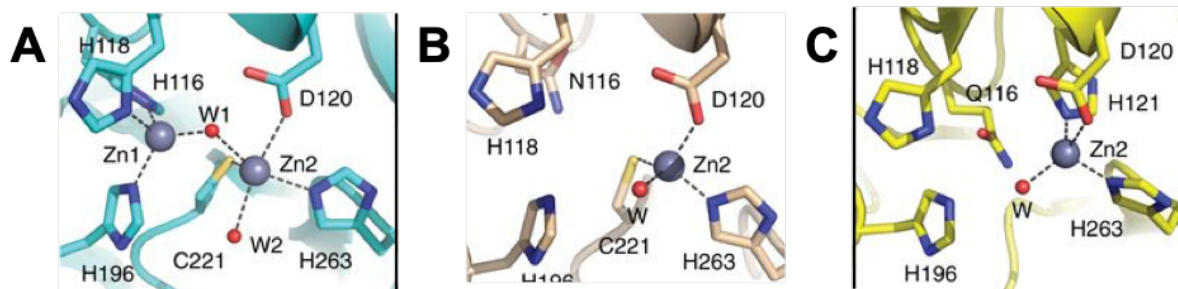


Figure 13. Site actif des métallo- β -lactamases. : A. NDM- bi- Zn^{2+} (B1, PDB 3SPU), B. Sfh-I- mono- Zn^{2+} (B2, PDB 3SD9) et C. GOB-18- mono- Zn^{2+} (B3, PDB 5K0W). Les atomes de zinc sont représentés par des sphères grise et les molécules d'eau en rouge. D'après Lisa et al.⁴⁴

b. Mécanisme catalytique

Contrairement aux enzymes à serine active, l'hydrolyse des β -lactamines par les métallo- β -lactamases serait régie par une série d'intermédiaires non covalents. De nos jours, deux modèles ont été proposés pour expliquer le mécanisme d'action des formes mono- et di-zinc des métallo- β -lactamases (figure 14 et 15).

Modèle catalytique des métallo- β -lactamases sous forme mono-zinc

Dans ce modèle, le zinc se comporterait comme un acide favorisant la formation d'un ion hydroxyle à partir d'une molécule d'eau. L'aspartate 120 jouerait le rôle de base générale et permettrait l'attaque nucléophile de l'ion hydroxyle sur la fonction carbonyle de la liaison amide du β -lactame. Il en résulterait un intermédiaire tétraédrique non covalent stabilisé par des interactions ioniques entre les deux oxygènes du carbone et l'ion zinc. Dans un second temps, ce premier intermédiaire réactionnel se réorganiserait par transfert de proton du groupement hydroxyle vers l'aspartate 120. On obtient ainsi un intermédiaire réactionnel chargé deux fois négativement. Finalement, une réorganisation moléculaire du dernier intermédiaire permet la rupture de la liaison amide et le transfert du proton directement de l'aspartate 120 vers l'azote du noyau β -lactame (Figure 14).⁴⁵

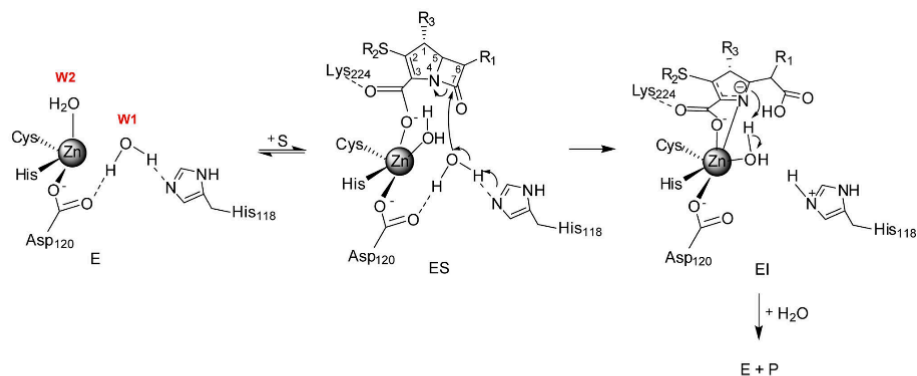


Figure 14. Mécanisme réactionnel d'hydrolyse d'un carbapénème par une métallo- β -lactamase du sous-groupe B2 mono-zinc. W1 et W2 représente les molécules d'eau. D'après Meini et al.⁴⁵

Modèle catalytique des métallo- β -lactamases sous formes di-zinc

Ce modèle propose la stabilisation d'un ion hydroxyle par les deux ions zinc du site actif. Ce dernier serait activé et réaliserait une attaque nucléophile au niveau de la fonction carbonyle du β -lactame. Il en résulterait la formation d'un intermédiaire tétraédrique stabilisé par les deux ions zinc. Une seconde molécule d'eau, ligand du zinc, céderait son proton à l'azote du noyau β -lactame. L'ion hydroxyle ainsi formé capterait le proton de la liaison carboxylique du produit et assurerait sa libération (Figure 15).⁴⁵

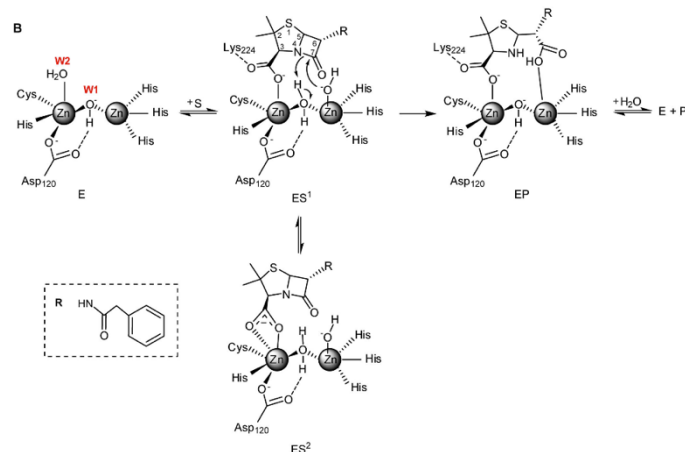


Figure 15. Mécanisme réactionnel d'hydrolyse de la pénicilline par les enzymes di-Zn²⁺B1 et B3. W1 représente Wat1 et W2 représente Wat2. D'après Meini et al.⁴⁵

V. Les carbapénèmases

Les carbapénèmases constituent une famille de β -lactamases hétérogènes capables d'hydrolyser les carbapénèmes,⁴⁶ leur spectre d'action est, en général, assez large et peut s'étendre, en plus des carbapénèmes, aux pénicillines, aux céphalosporines et aux monobactames (Tableau 4). Les différentes carbapénèmases appartiennent aux classes A, B et D de Ambler.

Les premières carbapénèmases naturelles, c'est à dire celles dont le gène est porté par le chromosome, appartenant à la classe B de Ambler, ont été identifiées chez *S. maltophilia*, *Aeromonas* sp., *B. cereus* et *Bacteroides fragilis*.⁴⁷ C'est au début des années 1980 que les premières carbapénèmases chromosomiques sont décrites chez les Entérobactéries. On recense alors : SME-1 chez *Serratia marcescens* à Londres en 1982^{48,49}, IMI-1 chez *Enterobacter* du complexe *cloacae* aux États-Unis en 1984⁵⁰, NMC-A chez *Enterobacter* du complexe *cloacae* en France en 1994. Mais des enzymes codées par des plasmides ont également été décrites principalement en Chine et au Japon. Depuis les années 2000, on constate une augmentation considérable du nombre d'entérobactéries résistantes aux carbapénèmes dans le monde entier, principalement en raison de l'acquisition généralisée de gènes codant pour des carbapénèmases. Les carbapénèmases plasmidiques les plus répandues dans le monde entier ainsi que dans de nombreuses espèces d'entérobactéries sont principalement : KPC (classe A), NDM, VIM et IMP (classe B), et OXA-48 (classe D).

Tableau 4. Phénotypes de résistance aux β -lactamines associés à la production des principales carbapénèmases.

Profil de résistance aux β -lactamines conféré par les carbapénèmases							
Enzymes	Classe de Ambler	Pénicillines	Monobactames	C1G et C2G	C3G et C4G	Inhibiteurs de β -lactamases	Carbapénèmes
KPC	A	R	R	R	R	S	R
IMP/NDM/VIM	B	R	S	R	R	R	R
OXA-48 type	C	R	R	R/S	S/I*	R	R

*Sensible à la ceftazidime, intermédiaire à la céfotaxime.

1. Carbapénèmases de classe A

a. Généralités

Les premières enzymes appartenant à cette classe ont été décrites dans les années 80 chez des souches cliniques de *E. cloacae* et de *S. marcescens* isolées de l'environnement. Ces bactéries étaient capables d'hydrolyser l'imipénème et l'ampicilline mais pas les C3G, et l'ajout d'acide clavulanique restaurait partiellement l'activité de ces molécules. Les enzymes responsables de cette résistance étaient NMC-A (non-métallo carbapenemase), SME (*Serratia marcescens* enzyme) et IMI (imipenem-hydrolyzing β -lactamase).⁵¹ Ces carbapénèmases se caractérisent toutes par un spectre d'hydrolyse large incluant les pénicillines, les céphalosporines uniquement de première génération, l'aztréonam et les carbapénèmes. Les gènes codant pour ces enzymes sont chromosomiques mais également plasmidiques tel que le gène *bla*_{IMI-2}.^{52,53}

Les quatre principales enzymes identifiées (SME, NMC-A, IMI et SFC-1) étaient codées par des gènes localisés au niveau du chromosome bactérien. Elles se caractérisent toutes par un spectre d'hydrolyse large, ces enzymes sont également inductibles par la céfoxitine (céphalosporine de 2^{ème} génération) et l'imipénème. NMC-A et IMI partagent 97% d'identité en acides aminés ; la première a été décrite en 1993 dans une souche de *Enterobacter asburiae* (NOR-1)⁵⁴, tout comme IMI-1 en 1996.⁵⁵ SME, qui partage 70% d'identité avec les deux enzymes précédentes, a été décrite dans deux souches de *S. marcescens* isolées en 1982.⁵⁶ Enfin, SFC-1 n'a été rapportée, à ce jour, que dans une seule souche de *Serratia fonticola* décrite en 2003 au Portugal.⁵⁷ L'analyse cristallographique des enzymes NMC-A et SME n'a pas permis la mise en évidence d'une modification unique responsable de l'activité carbapénèmase par rapport aux autres enzymes de classe A. Dans le cas de NMC-A, la position modifiée du résidu N132 pourrait faciliter l'hydrolyse des carbapénèmes⁵⁸, alors que la structure des SME-1 met en avant deux cystéines en position 69 et 238, formant un pont disulfure qui pourrait jouer un rôle dans l'inactivation des carbapénèmes.^{59,60} Cependant, l'activité carbapénèmase résulterait de l'association de plusieurs mutations ayant un impact sur la conformation tridimensionnelle de ces enzymes.^{59,61} Ces carbapénèmases restent rares

car elles ne sont généralement pas associées à des structures génétiques mobiles (plasmides) pouvant faciliter leur diffusion.

Plus récemment, des β -lactamases de type GES (Guiana extended-spectrum β -lactamases) ont été identifiées chez *K. pneumoniae* et *E. coli*.^{51,62} Les gènes *bla*_{GES} codant pour ces β -lactamases de type GES sont portés par des intégrons eux-mêmes insérés dans des plasmides et sont donc plus aptes à se transmettre horizontalement.^{51,62} Ces enzymes dérivent de la BLSE GES-1 et certains variants (incluant GES-2/-4/-5/-6) possèdent une activité hydrolytique plus ou moins forte sur les carbapénèmes.⁶³ En 2001, un variant possédant une activité carbapénémase, GES-2, a cependant été isolé dans une souche de *P. aeruginosa* en Afrique du Sud.⁶⁴ GES-1 et GES-2 diffèrent par la substitution d'un seul acide aminé au niveau du site actif, en position 170 (glycine remplacée par une asparagine). Ce fut le premier cas décrit d'extension du spectre d'une BLSE aux carbapénèmes par mutation ponctuelle. Depuis, 41 variants de GES ont été décrits (www.bldb.eu) dont 11 (GES-2, GES-4, GES-5, GES-6 et GES-14, GES-18, GES-20, GES-21 et GES-24) possèdent une activité carbapénémase résultant de cette mutation en position 170 (Tableau 5). Les variants possédant la mutation Gly170Ser, ne possèdent plus d'activité d'hydrolyse de la cefoxitine. Le variant GES-13 possède, lui aussi, la mutation 170 (Gly170Asn) mais une autre mutation à la position 104 (Glu104Lys) semble réduire la capacité de cette enzyme à hydrolyser l'imipénème.⁶⁵ Le variant GES-11, décrit chez *A. baumannii*, confère également une diminution de sensibilité vis-à-vis des carbapénèmes.⁶⁶ En revanche, il conserve une glycine en position 170 alors qu'une alanine est trouvée en position 243 à la place d'une glycine. La position 243 est impliquée dans l'extension du spectre vis-à-vis de l'aztréonam comme décrit avec GES-9 (Gly243Ser).⁶⁷ Le variant GES-14, quant à lui, possède la double mutation Gly170Ser et Gly243Ala. GES-14 est le premier variant de GES hydrolysant l'intégralité des β -lactamines.⁶⁸ Les gènes *bla*_{GES} possèdent la particularité d'être portés par des structures de types intégron. Tous les intégrons porteurs des gènes *bla*_{GES} sont localisés sur des plasmides, à l'exception de celui contenant le gène *bla*_{GES-13}.

Parmi les autres carbapénémases de classe A pouvant être codées par des gènes localisés sur un support plasmidique, on retrouve les enzymes IMI-2 et IMI-3 (imipenem-hydrolyzing β -lactamase). Initialement rapportés chez *E. cloacae*, les gènes *bla*_{IMI-2} et *bla*_{IMI-3}, ont également

été décrits sur des plasmides identifiés dans des souches de *E. coli* et de *Raoultella ornithinolytica* respectivement.⁶⁹

Tableau 5. Substitutions ponctuelles d'acides aminés ponctuelles responsables de la modification de spectre des différents variants de l'enzyme GES. Certaines substitutions sont associées à l'extension du spectre d'hydrolyse des enzymes de type GES à l'aztréonam, à la céfoxitine et/ou aux carbapénèmes. D'après Naas et al.⁷⁰

GES	Position selon Ambler								Hydrolyse			
	17	62	104	126	167	170	238	243	CAZ	FOX	ATM	IPM
GES-1	Gly	Met	Glu	Ala	Pro	Gly	Thr	Gly	+	-	-	-
GES-2						Asn			+	-	-	+
GES-3		Thr	Lys						+	-	-	-
GES-4		Thr	Lys			Ser			+	+	-	+
GES-5						Ser			+	+	-	+
GES-6			Lys			Ser			+	+	-	+
GES-7			Lys						+	-	-	-
GES-8				Leu					+	-	-	-
GES-9								Ser	+	-	+	-
GES-10	Thr	Thr							+	nd	nd	-
GES-11								Ala	+	-	+	-
GES-12							Ala	Ala	+	-	+	-
GES-13			Lys			Asn			+	-	+	-
GES-14						Ser		Ala	+	+	-	+
GES-15					Ser	Ser			+	nd	nd	nd
GES-16						Ser			+	nd	nd	nd
GES-17			Lys					Ala	+	nd	nd	nd

CAZ: Ceftazidime; FOX : Céfoxitine; ATM: Aztreonam; IMP: Imipénème; nd: non déterminé

A l'heure actuelle, les carbapénémases de classe A les plus répandues correspondent à des enzymes de type KPC (*Klebsiella pneumoniae* Carbapenemase).^{46,71,72}

b. Carbapénémases de type KPC

Cette famille de carbapénémase de la classe A de Ambler a été décrite pour la première fois en 1996 aux Etats-Unis.⁷³ Ces enzymes hydrolysent toutes les β -lactamines mais confèrent une résistance variable aux carbapénèmes. Les enzymes de type KPC sont peu inhibées par les inhibiteurs classiques de β -lactamases (acide clavulanique et tazobactam), le tazobactam

étant le plus efficace.^{46,74} Les gènes *bla*_{KPC} ont largement été caractérisés avec une localisation plasmidique (plasmides de différents types). En revanche, les gènes *bla*_{KPC} sont largement associés au transposon Tn4401 (de type Tn3) et sont accompagnés par d'autres mécanismes de résistance aux antibiotiques notamment aux aminosides et/ou aux fluoroquinolones, et souvent à d'autres β-lactamases comme CTX-M-15.^{72,75,76}

i. Épidémiologie

Après la première identification de KPC-1 en 1996, un nouveau variant a été identifié, KPC-2 en 2003 également aux États-Unis. Un meilleur séquençage du gène de *bla*_{KPC-1} a permis de montrer une parfaite homologie avec *bla*_{KPC-2}, par conséquent, seul le nom de KPC-2 a été retenu. De nos jours, plus de 40 variants, se différenciant par au moins une substitution en acide aminé, ont été rapportés (www.bldb.eu).

Après la première description de KPC-2⁷³ l'incidence des souches de *K. pneumoniae* productrices de cette carbapénèmase a augmenté régulièrement dans la région de New-York.⁷⁷ Une étude menée en 2004 dans les hôpitaux de Brooklyn, New-York, a montré qu'aucune souche de *E. coli* ou *E. cloacae* ne possédait le gène *bla*_{KPC}, alors que 24% des *K. pneumoniae* étaient KPC positives.⁷⁷ Parallèlement à l'émergence de KPC-2, le variant KPC-3 était également décrit dans une souche de *K. pneumoniae* et de *E. cloacae* épidémique.^{78,79} La première épidémie de KPC en dehors des États-Unis a eu lieu en Israël en 2004, les souches retrouvées avaient une relation génétique avec les souches des États-Unis, ce qui suggère une importation de souches par des voyageurs (patients rapatriés, touristes).^{3,14,15} A partir de 2007, KPC a été retrouvée en Grèce. Les données les plus récentes semblent indiquer que la situation y est endémique, avec environ 40% des souches de *K. pneumoniae* produisant une carbapénèmase de type KPC (et jusqu'à 70% dans des *K. pneumoniae* isolées de bactériemies).⁸⁰ L'Italie est un autre pays européen fortement impacté par ces souches de *K. pneumoniae* productrices d'une carbapénèmase de type KPC. Comme la Grèce, ce pays est actuellement considéré comme endémique pour cette carbapénèmase (30% des *K. pneumoniae* isolées de bactériemies sont KPC positives). Dans le reste de l'Europe, excepté l'Espagne et le Portugal qui sont en passe de devenir endémiques, des cas sporadiques/épidémiques ont été décrits dans de nombreux pays. L'analyse des cas montrait souvent que les patients avaient été soignés dans un pays considéré comme

endémique.^{2,14,15,17} A ce jour, KPC est considéré comme endémique dans plusieurs pays dont l'Amérique du Nord, le Brésil, la Colombie, l'Argentine, l'Asie de Sud-Est, l'Italie, Israël, la Grèce, la Pologne et Porto Rico (Figure 17).⁸¹

Il semblerait que la dissémination mondiale de KPC soit liée à la diffusion d'un seul clone de *K. pneumoniae* appartenant au séquence-type (ST) 258.⁸¹ Bien que la β -lactamase KPC soit fortement associée à *K. pneumoniae*, elle a été également identifiée dans de nombreuses espèces (*E. coli*, *Citrobacter* sp., *Enterobacter* sp., *S. marcescens*, *P. mirabilis*, *M. morgani*), ainsi que dans des souches de bacilles à Gram négatif non fermentant, comme *P. aeruginosa* en Amérique du Sud et *A. baumannii* à Porto Rico principalement.⁸²

ii. Support génétique de *bla*_{KPC}

Le gène *bla*_{KPC} est porté par des plasmides, appartenant à différents groupes d'incompatibilité : IncFII, FIA, I2, A/C, N, X, R, P, U, W, L/M et ColE.⁸³⁻⁸⁸ Ces plasmides portent de nombreux gènes de résistance aux β -lactamines et à d'autres familles d'antibiotiques comme les aminosides, les quinolones, les tétracyclines, les sulfamides.⁸⁶ La majorité des plasmides portant le gène *bla*_{KPC} possède un opéron de transfert, codant la machinerie nécessaire au processus de conjugaison, facilitant ainsi la diffusion de ces plasmides multi-résistants à d'autres souches et d'autres espèces. Le plasmide pKpQIL fut le premier plasmide de type IncFII_{K2} portant *bla*_{KPC-3} et provenant d'une souche de *K. pneumoniae* ST258 israélienne, à être entièrement séquencé en 2006.⁸⁷ Il a été ensuite décrit dans plusieurs pays tels que la Pologne, l'Italie, la Colombie et le Royaume-Uni.⁸⁵ Le 2^e plasmide prédominant est pBK15692, présent principalement aux USA. Il s'agit d'un plasmide de type IncI2 portant le gène *bla*_{KPC-3}.⁸¹

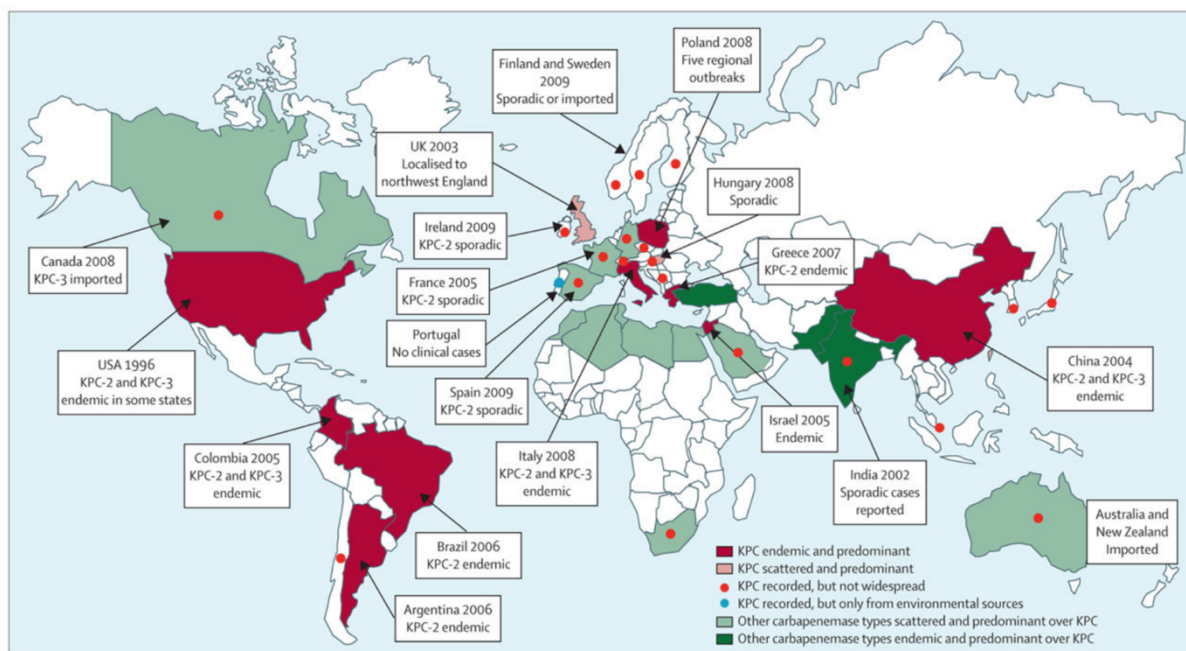


Figure 16. Distribution géographique des bactéries productrices de KPC. D'après Munoz-price et al.⁸⁹

iii. Spectre d'hydrolyse des enzymes de type KPC

Les données biochimiques révèlent que les enzymes de type KPC sont capables d'hydrolyser toutes les β -lactamines : pénicillines, céphalosporines, carbapénèmes et monobactames.⁷³ Malgré son appartenance à la classe A de Ambler, l'acide clavulanique et le tazobactam inhibent faiblement l'activité hydrolytique des β -lactamases de type KPC.⁷³ Quelques différences dans le spectre d'hydrolyse ont été mises en évidence parmi les différents variants. Ainsi, les variants KPC-3 à KPC-11 hydrolysent plus la ceftazidime que KPC-2.⁹⁰ Plusieurs substitutions ont été identifiées, à savoir M49I, P104R, P104L, V240G, V240A, et H274Y (Tableau 6). Les substitutions P104R et H274Y confèrent la plus forte augmentation de l'activité d'hydrolyse vis-à-vis de la ceftazidime, en augmentant chacune la valeur *kcat*/*Km* d'un facteur 10 par rapport à KPC-2. Par ailleurs, une substitution à la position de l'Arginine en position 164 dans la boucle Ω de KPC-2, position conservée entre les β -lactamases de classe A, est également associée à une augmentation de l'activité vis-à-vis de la ceftazidime (Figure 17.B).^{91,92} KPC-25, KPC-29 et KPC-34 possèdent respectivement une insertion de 2 (+L169 +E170), 3 (+275D, +276D, +277K) et 7 (HSEAKDDK aux positions 271 à 278) acides aminés.

Tableau 6. Substitutions d'acides aminés ponctuelles responsables de la modification du spectre d'hydrolyse des variants de l'enzyme KPC-2. Adapté de Mehta et al.⁹³

	Position selon Ambler				CMI (mg/L)		Ratio kcat/Km	
	49	104	240	274	CAZ	IMP	CAZ	IMP
KPC-2	M	P	V	H	0.38	1	8. 10 ⁻⁴	0,19
KPC-3				Y	1.5	1	7. 10 ⁻³	0,32
KPC-4		R	G		12	1	4. 10 ⁻²	0,14
KPC-5		R			2.0	0,75	9. 10 ⁻³	0,12
KPC-6			G		1.5	1	4. 10 ⁻³	0,16
KPC-7	I			Y	1.5	1	6. 10 ⁻³	0,26
KPC-8			G	Y	32	2	3. 10 ⁻²	0,22
KPC-9			G	Y	4	1	2. 10 ⁻²	0,24
KPC-10		R		Y	16	1	6. 10 ⁻²	0,15
KPC-11		L			0,5	0,75	2. 10 ⁻³	0,22

CAZ: Ceftazidime; IMP: Imipénème

iv. Structure de KPC-2

Le gène *bla*_{KPC-2} code pour une protéine de 293 acides aminés (32kDa). KPC-2 contient les motifs S-X-X-K, S-D-N et K-T-G, caractéristiques des β-lactamases à sérine active de classe A (Figure 17). L'analyse des séquences des acides aminés des différentes carbapénémases de classe A rapprochent le plus KPC de SFC-1. Ces deux enzymes partagent 62% d'identité de séquence en AA.⁵⁷ SME-1, NMC-A et IMI-1 partagent respectivement 45%, 44% et 43% d'identité avec KPC.⁷³ La détermination de la structure de KPC-2 a mis en évidence certaines particularités propres aux carbapénémases de classe A, comme la diminution de la taille de la poche contenant les deux molécules d'eau nécessaires au mécanisme enzymatique et aussi la position particulière du résidu S70, situé plus en surface du site catalytique.⁹⁴ De plus, la chaîne latérale du résidu S70 bloque partiellement le site actif et ne permet la présence que d'une seule molécule d'eau à ce niveau. Des études de mutagénèses dirigées ont également montré le rôle du résidu T237 dans la polyvalence de l'enzyme KPC.⁹⁵

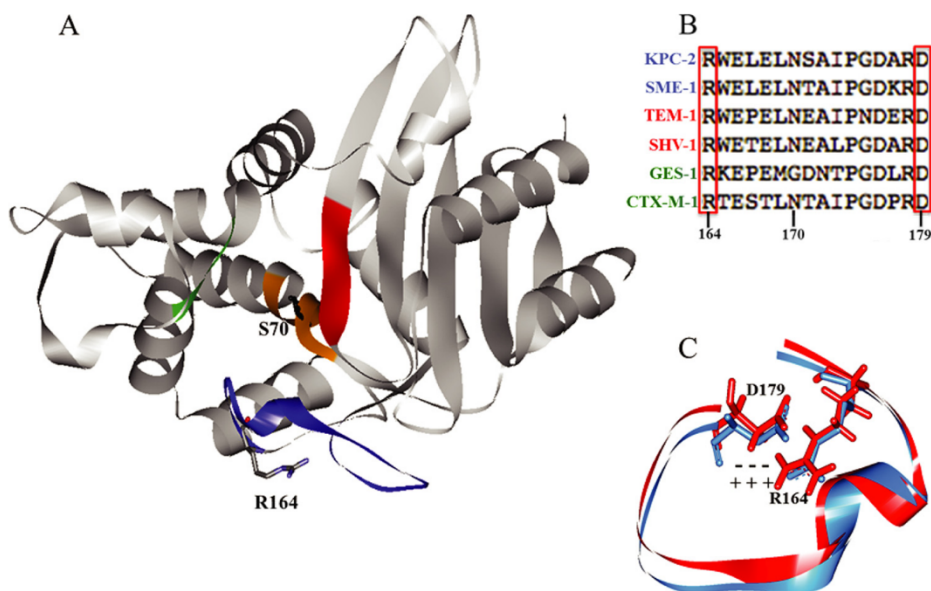


Figure 17. A. Structure de KPC-2 (pdb 2OV1) Les régions actives sont identifiées par les couleurs suivantes: orange, motif SXXK (résidus 70 à 73), vert, boucle SDN (130 à 132), bleu, boucle oméga (164 à 179), rouge, β -cordon (234 à 242) **B. Alignement de la séquence de la boucle oméga de KPC-2 avec d'autres β -lactamases de classe A** (carbapénèmase en bleu, des pénicillinases en rouge et des BLSEs en vert) avec une conservation de l'Arg-164 et l'Asp-179 **C. superposition des boucles oméga de TEM-1 (rouge) et KPC-2 (bleu), montrant la liaison hydrogène entre Arg-164 et Asp-179.** D'après Levitt et al ⁹⁶

v. Données cliniques et traitements

Les infections associées aux souches productrices de KPC ne sont pas spécifiques. Elles correspondent à tous les types d'infections causées par des entérobactéries et plus particulièrement *K. pneumoniae*, hôte privilégié du gène de *bla*_{KPC}. Ainsi, la plupart de ces infections correspondent à des infections nosocomiales survenant chez des patients fragilisés. Les facteurs de risques sont les hospitalisations prolongées, l'admission dans un service de soins aigus, la mise en place de matériel étranger, une immunodépression et la prise antérieure d'antibiotiques.^{72,77,97} La mortalité associée aux bactériémies dues à des souches *K. pneumoniae* productrices de KPC a été évaluée à 47% à 14 jours dans une étude américaine.⁷³ Les entérobactéries productrices de KPC ont été décrites dans les services de soins aigus, mais également dans les structures d'hospitalisation de longue durée.^{98,99} Les patients récemment transplantés ou greffés représenteraient également une population particulièrement à risque de développer une infection due à une *K. pneumoniae* résistante aux carbapénèmes.¹⁰⁰ Le choix pour le traitement des infections sévères est limité. Il y a moins de cinq ans, aucune β -lactamine, seule ou associée, à un inhibiteur de β -lactamases n'était

efficace. De plus, ces bactéries productrices de KPC sont souvent résistantes à d'autres familles d'antibiotiques, comme les aminosides et les fluoroquinolones mais la plupart restent sensibles à un aminoside (l'amikacine ou la gentamicine) ainsi qu'à la colistine plus ou moins la tigecycline. Cependant, des échecs thérapeutiques ont été rapportés avec cette dernière molécule, notamment du fait d'une faible diffusion urinaire et d'une pénétration tissulaire rapide (inutilisable pour le traitement des bactériémies).¹⁰¹

2. Carbapénèmases de classe B

a. Généralités

Les carbapénèmases de classe B sont caractérisées par leur résistance aux inhibiteurs de β -lactamases classiques (acide clavulanique et tazobactam), et par une inhibition de leur activité par l'EDTA (acide éthylènediamine tétra-acétique), chélateur des ions Zn^{2+} (et autres cations divalents) nécessaires à l'interaction entre les β -lactamines et le site actif de l'enzyme. Elles possèdent également un spectre d'hydrolyse large puisque les pénicillines et toutes les céphalosporines sont hydrolysées à l'exception de l'aztréonam. Au sein de ce groupe, les carbapénèmases de type VIM, IMP et NDM sont les plus répandues.

IMP-1 (pour « active on Imipenem ») fut la première enzyme décrite capable de conférer une résistance transférable aux carbapénèmes. La première bactérie exprimant cette carbapénémase a été décrite au début des années 90 au Japon ; il s'agissait d'une souche de *P. aeruginosa*.¹⁰² Cette enzyme a ensuite été décrite dans de nombreuses espèces d'entérobactéries, comme *S. marcescens*,^{103,104} *K. pneumoniae*,^{105,106} *P. rettgeri*,¹⁰⁷ et *E. aerogenes*.¹⁰⁸ IMP-2 a été décrite également chez *A. baumannii* (première espèce isolée en Europe)^{109,110} et, plus récemment, dans des souches de *Achromobacter xylosoxidans*.¹¹¹ A ce jour, soixante-quinze variants du gène *bla*_{IMP} ont été identifiés (www.bldb.eu). Les carbapénèmases de type IMP sont endémiques au Japon et à Taiwan et ont disséminé en Chine¹¹² et en Corée.¹¹³ Des cas sporadiques ont été décrits en Europe,^{114–116} en Amérique du Sud,¹¹⁷ au Canada,¹¹⁸ aux Etats-Unis,¹¹⁹ en Australie,¹²⁰ et en Afrique (Figure 18).¹²¹ De nombreuses épidémies impliquant des bactéries productrices de IMP ont été rapportées

comme IMP-13 en Italie,¹²² ou IMP-7 au Canada.¹¹⁸ *A. baumannii* et *P. aeruginosa* restent les espèces bactériennes dans lesquelles IMP a été le plus souvent décrite.¹¹³

VIM-1 (pour « Verona Integron-encoded Métallo- β -lactamase) a été décrite pour la première fois en 1997 dans une souche de *P. aeruginosa* isolée à Vérone, Italie.¹²³ Rapidement, un autre variant VIM-2 a été rapporté en France.¹²⁴ À ce jour, 66 variants ont été décrits, principalement chez *P. aeruginosa*, mais également chez *A. baumannii*,¹²⁵ et certaines espèces d'entérobactéries comme *Klebsiella* sp., *E. coli*, *Enterobacter* sp., *P. mirabilis*,^{126–128} *Providencia stuartii*,¹²⁹ et *S. marcescens*.¹³⁰ La carbapénèmase VIM-2 a particulièrement diffusée chez *P. aeruginosa* à travers le monde et a été décrite sur tous les continents (Figure 18).¹³¹ De nombreuses épidémies dues à des souches productrices de VIM ont été décrites.^{130,132–134} L'enzyme VIM est maintenant répandue de manière endémique en Grèce et en Italie (entérobactéries) ainsi qu'en Russie (*P. aeruginosa*).¹¹³

Les autres métallo- β -lactamases, à l'exception de NDM, sont d'importance moindre puisqu'elles ont très peu diffusé ou ont été rapportées sporadiquement. C'est le cas pour SPM-1 (pour « Sao Paulo Métallo- β -lactamase ») qui a été rapportée pour la première fois au Brésil dans une souche de *P. aeruginosa* en 2002,¹³⁵ et qui a été responsable de plusieurs épidémies dans ce pays.^{136,137} Elle est devenue la métallo- β -lactamase la plus répandue au Brésil.¹¹⁷ GIM-1 (pour « German Imipenemase ») et AIM-1 (pour « Adelaïde Imipenemase ») ont été décrites chez *P. aeruginosa* en Allemagne¹³⁸ et en Australie¹³⁹ respectivement. DIM-1 (pour « Dutch Imipenemase ») a été caractérisée chez *Pseudomonas stutzeri* en Hollande.¹⁴⁰ Plus récemment, 6 nouvelles carbapénèmases ont été identifiées : SMB-1 dans une souche de *S. marcescens* isolée au Japon,¹⁴¹ FIM-1 dans une souche de *P. aeruginosa* isolée en Italie,¹⁴² LMB-1 en Autriche¹⁴³ et Argentine,¹⁴³ TMB-1 dans une souche de *Achromobacter xylosoxidans* isolée en Libye,¹⁴⁵ KHM-1 au Japon¹⁴⁶ et CAM-1 au Canada.¹⁴⁵

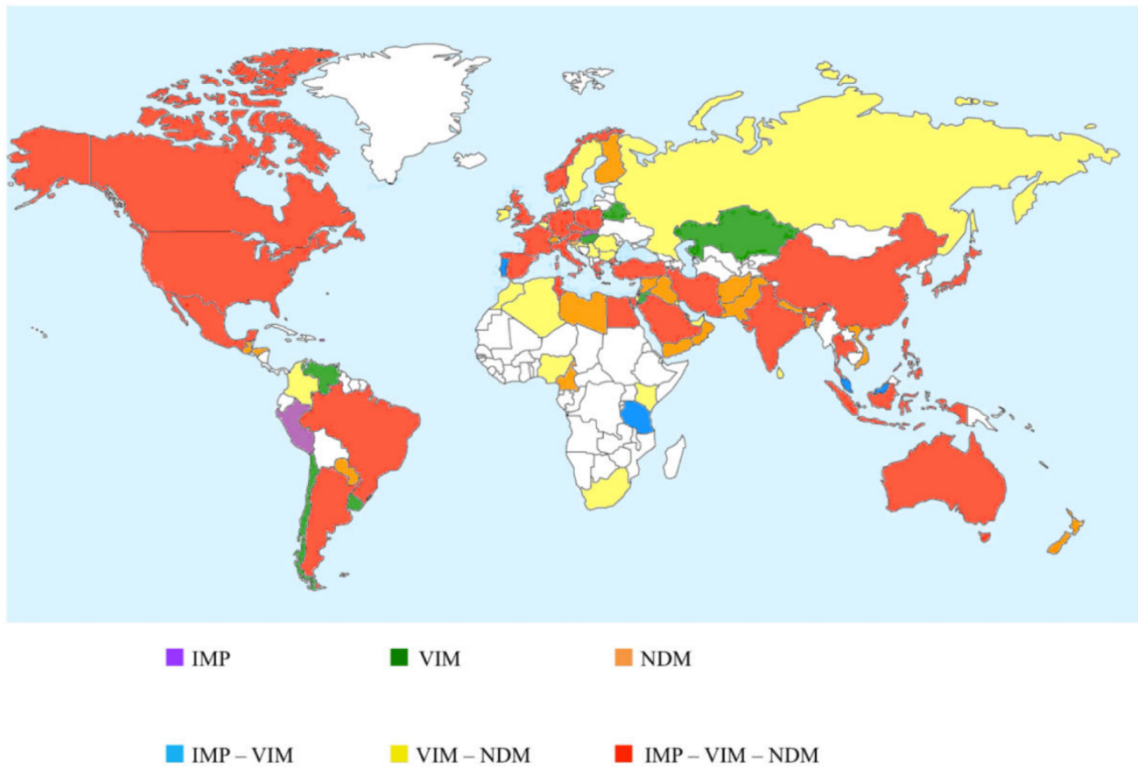


Figure 18. Distribution mondiale des MBLs : IMP, VIM et NDM. D'après Mojica et al.¹⁴⁸

b. Carbapénèmases de type NDM

i. Epidémiologie

La métallo- β -lactamase NDM-1 (New Delhi Métallo- β -lactamase) a été décrite pour la première fois en Suède, en 2009, chez une souche de *K. pneumoniae* isolée chez un patient rapatrié sanitaire d'un hôpital indien.¹⁴⁹ Depuis, elle a fait l'objet d'une attention particulière du fait de sa dissémination rapide chez les entérobactéries mais également chez *Acinetobacter* sp., et *P. aeruginosa* (Figure 18). Une étude parue en 2010 a montré la forte prévalence de souches d'entérobactéries productrices de la carbapénèmase NDM-1 en Grande-Bretagne, en Inde et au Pakistan.¹⁵⁰ Dans la plupart des cas, un voyage en Inde ou des liens avec l'Inde, le Pakistan et le Bangladesh ont été retrouvés. Il a donc pu être mis en évidence que le sous-continent indien était un réservoir du gène *bla*_{NDM-1}. De plus, la présence de ce gène dans des espèces de bacilles à Gram négatif isolés à partir de prélèvements d'eau réalisés à New

Delhi,¹⁵¹ et chez des germes responsables d'infections purement « communautaires » liées au péril fécal, comme *Salmonella* sp.¹⁵² et *Vibrio cholerae*,¹⁵³ suggère que cette carbapénèmase est fortement présente dans l'environnement. Le taux de souches productrices de NDM-1 en Inde et en Chine représente 58,15% du nombre total de bactéries productrices de NDM-1 dans le monde. 16,8% de la totalité des bactéries productrices de NDM sont retrouvées en Europe, avec une répartition essentiellement au niveau des pays Balkans constituant ainsi un réservoir secondaire.¹⁵⁴ La variant NDM-4 est présent dans le sud de l'Europe tel que l'Italie, alors que NDM-5 et NDM-7 sont plus prévalent au Danemark et en France. Sur le continent américain on recense 10,8% du nombre total de souches productrices de NDM-1,¹⁵⁵ avec comme réservoir primaire le Brésil. En Afrique, on retrouve également environ 10% des souches productrices de NDM, avec l'Algérie comme réservoir primaire.

ii. Environnement génétique

Les gènes codant pour NDM-1 et ses variants sont portés par différents plasmides (IncFII, IncL/M, IncN, IncR, IncHIB-M/FIB-M), IncFI étant le plus prévalent (Figure 19). Des études sur l'environnement génétique du gène *bla*_{NDM} ont révélé la présence systématique de la séquence d'insertion IS*Aba125*, initialement décrite chez *A. baumannii*, en amont du gène.¹⁵⁵ Il a été démontré que le transposon composite Tn125, délimité par 2 séquences IS*Aba125*, est responsable de la dissémination de *bla*_{NDM} depuis *A. baumannii* vers les entérobactéries,¹⁵⁵ qui possèdent toujours une version tronquée de Tn125.¹⁵⁶ Le gène *bla*_{NDM} est également associé, au sein d'un même opéron, avec le gène *ble*_{MBL} codant pour une protéine conférant la résistance à la bléomycine.¹⁵⁷

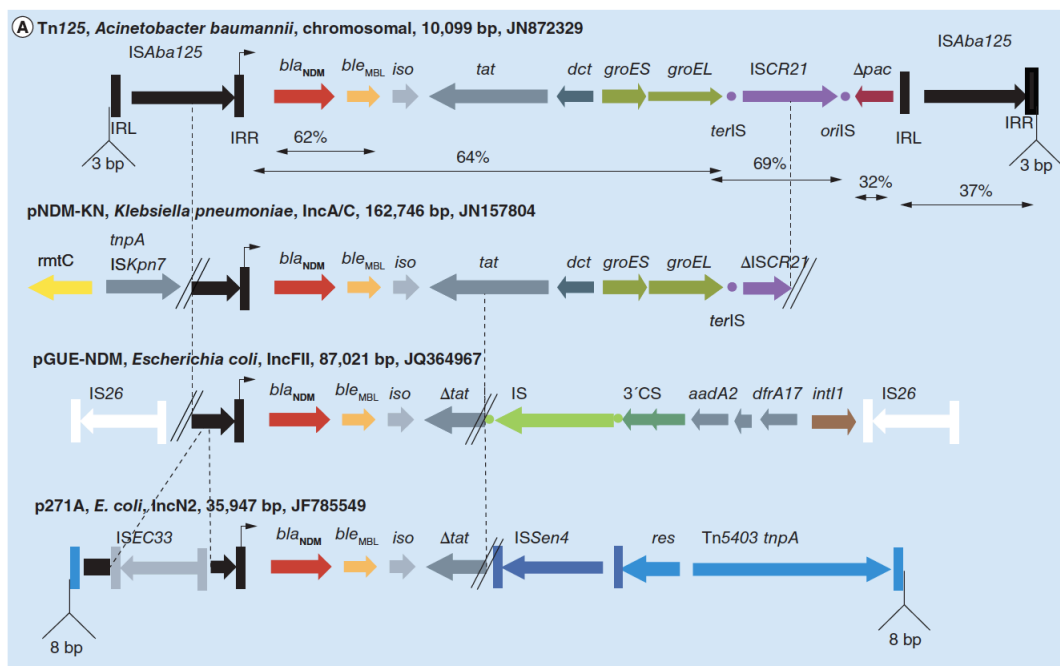


Figure 19. Environnement génétique du gène bla_{NDM-1} chez *A. baumannii* et chez les Entérobactéries. D'après Bonnin et al.¹⁵⁶

iii. Spectre d'hydrolyse

Tout comme les autres MBLs (IMP et VIM), NDM hydrolyse toutes les β -lactamines à l'exception de l'aztréonam. L'activité enzymatique de NDM n'est pas inhibée par les inhibiteurs de β -lactamases tel que l'acide clavulanique ou le tazobactam. Seuls les chélateurs d'ions divalents comme l'EDTA inhibent les MBLs.

Une comparaison des constantes enzymatiques entre les principales MBLs VIM-2, IMP-1 et NDM-1)¹⁴⁹ a permis de révéler que NDM-1 présente une efficacité catalytique (k_{cat}/K_m) pour la céfoxitine, la ceftazidime et l'imipénème, inférieure aux efficacités catalytique de VIM-2 et IMP-1 (Tableau 7).¹⁵⁸

Tableau 7. Comparaison des constantes enzymatiques des MBLs : NDM-1, IMP-1 et VIM-2 D'après Young et al.¹⁴⁹

Antibiotiques	NDM-1			IMP-1			VIM-2		
	Km (μM)	kcat (s ⁻¹)	kcat/Km (s ⁻¹ /μM)	Km (μM)	kcat (s ⁻¹)	kcat/Km (s ⁻¹ /μM)	Km (μM)	Kcat (s ⁻¹)	kcat/Km (s ⁻¹ /μM)
Penicilline G	16	11	0.68	520	320	0.62	49	56	1.14
Ampicilline	22	15	0.66	200	950	4.8	DNA		
Piperacilline	12	14	1.17	ND	ND	ND	72	33	0.45
Céphalothine	10	4	0.40	21	48	2.4	44	57	1.28
Céfoxitine	49	1	0.02	8	16	2	24	3	0.12
Céfotaxime	10	6	0.58	4	1.3	0.35	32	28	0.86
Céfuroxime	8	5	0.61	37	8	0.22	22	12	0.55
Ceftazidime	181	5	0.03	44	8	0.18	98	89	0.90
Aztreonam	ND			>1,000	>0.01	<0.0001	ND	<0.5	ND
Céfépime	77	13	0.17	11	7	0.66	184	5	0.03
Imipénème	94	20	0.21	39	46	1.2	10	10	0.99
Méropénème	49	12	0.25	10	50	0.12	5	1	0.28
Acide Clavulanique	ND			NR			NR		

ND : non déterminée, NR : non reportée

Depuis l'identification de NDM-1 en 2008, 28 variants naturels ont été identifiés, dont 16 variants ont été caractérisés. Récemment, une étude comparative de l'activité hydrolytique des variants NDM-1 à NDM-17 a été réalisée.¹⁵⁹ Pour cela, le clonage a été effectué dans le même vecteur d'expression (pHSG298). L'étude de sensibilité aux β-lactamines n'a pas révélé de différence majeure entre les différents variants, hormis pour NDM-10 dont les CMI pour l'ampicilline, l'imipénème et le méropénème sont diminuées de plus de 2 dilutions par rapport à NDM-1.

iv. Structure de NDM-1

NDM-1 est une protéine constituée d'une chaîne polypeptidique contenant 270 acides aminés, et dont le peptide signal, situé dans la partie N-terminale, est constitué de 28 acides aminés.¹⁶⁰ En termes de séquence, les enzymes les plus proches dans le groupe B1, sont VIM-2 et IMP-1, avec environ 32% de similitudes dans la séquence en acides aminés. Malgré ce faible pourcentage d'homologie de séquence, la structure générale du site actif est relativement conservée au sein des MBLs du groupe B1. De plus, les séquences qui

comportent les acides aminés impliqués dans la coordination des ions zincs (H116, H118, D120, H196, C221 et H263), sont très conservées.

C'est sous sa forme monomérique que NDM est active. Son repliement dans l'espace respecte la structure $\alpha\beta/\beta\alpha$ des MBLs. Elle est composée de 5 boucles qui ont une fonction importante pour l'activité de l'enzyme (Figure 20). Les boucles L1 et L3¹⁶¹ seraient impliquées dans la reconnaissance et la spécificité des substrats, tandis que les boucles L4 et L5 permettraient la stabilité du site actif.¹⁶² La boucle L5 contient les résidus H116, H118, et D120 qui fixent les atomes de zinc. Ils sont donc essentiels à l'activité enzymatique. Le résidu Y244, situé à l'extérieur du site actif, établit une liaison hydrogène et une interaction hydrophobe avec le résidu L221 de la boucle L3, qui délimite l'entrée du site actif. Ces interactions stabiliseraient et orienteraient la boucle L3 avec un impact probable sur les mécanismes de fixation des substrats. Le résidu W87, conservé au sein des enzymes du groupe B1, participe également aux interactions hydrophobes qui stabilisent la boucle L1 avec le centre métallique pour la reconnaissance des substrats.

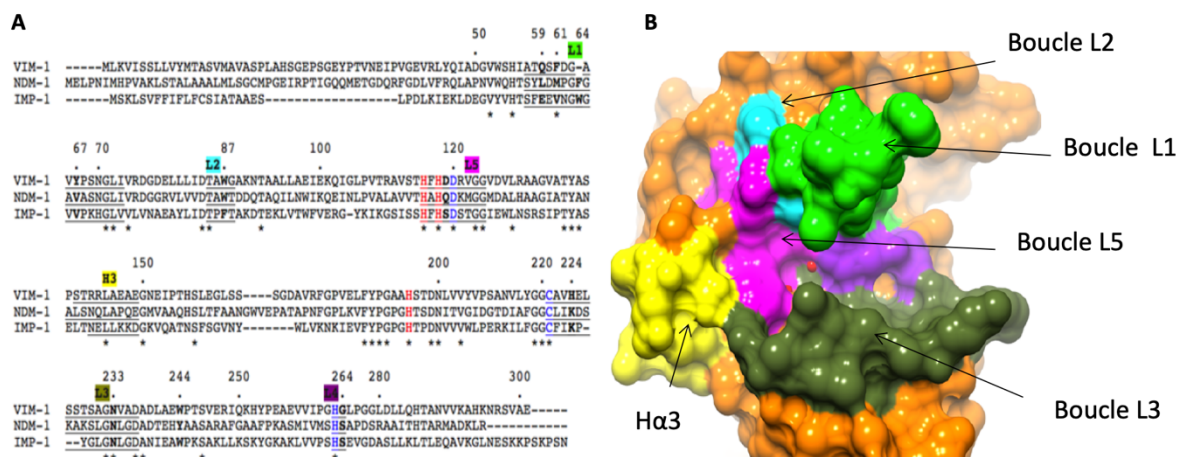


Figure 20. A. Alignement des séquences peptidiques de VIM-1, NDM-1 et IMP-1 (numérotation BBL). Les régions soulignées sont celles qui interagissent avec les substrats. Les résidus coordonnés aux atomes de zinc sont indiqués en bleu et rouge. B. Représentation schématique du site actif de NDM-1, avec les régions les plus importantes colorées comme suit : boucle 1 en vert (L1), boucle 2 en turquoise (L2), boucle 3 en vert olive (L3), boucle 4 en violet (L4), boucle 5 en magenta (L5). Les 2 ions zinc sont indiqués par des sphères rouges.

v. Données cliniques et traitements

La plupart des souches productrices de carbapénèmases de type NDM, possèdent d'autres mécanismes de résistance à d'autres grandes classes d'antibiotiques. Elles peuvent exprimer : des céphalosporinases de type AmpC, des β -lactamases à spectre étendu, d'autres carbapénèmases (OXA-48, VIM), des résistances aux aminosides médiées par des ARN16S méthylases, des résistances aux fluoroquinolones de type Qnr, au chloramphénicol, au sulfaméthoxazol.¹⁶³⁻¹⁶⁶ L'apparition de ces phénotypes de multirésistances dans des souches responsables d'infections aboutit à un nombre croissant d'impasses thérapeutiques. Le plus souvent, seules la colistine et la fosfomycine restent actifs parmi les antibiotiques bactéricides. La tigécycline constitue parfois un recours mais reste bactériostatique et non utilisable dans certains types d'infections (infections urinaires et bactériémies). Certaines études d'activité *in vitro* avec des souches productrices de NDM-1 ont montré une synergie entre la colistine et la fosfomycine et, dans de rares cas, entre colistine et tigécycline, la plupart des autres associations testées restant neutres.¹⁶⁷

3. Carbapénèmases de classe D

a. Généralités

Les β -lactamases de la classe D sont des enzymes à sérine active appelées des oxacillinases. Elles ont été initialement nommées ainsi car elles hydrolysaient plus rapidement l'oxacilline et la cloxacilline que la benzylpénicilline.¹⁶⁸ Cependant, cette définition n'est plus valable car certaines oxacillinases ont été décrites comme hydrolysant peu ou pas la cloxacilline ou l'oxacilline. En revanche, toutes les oxacillinases hydrolysent les aminopénicillines et les carboxypénicillines. Contrairement aux β -lactamases de la classe A, les oxacillinases ne sont généralement pas inhibées par l'acide clavulanique, le tazobactam et le sulbactam, mais peuvent être inhibées *in vitro* par le chlorure de sodium (NaCl).

Actuellement on recense plus de 800 oxacillinases. Il s'agit d'une famille de β -lactamases très hétérogène sur le plan génétique et biochimique.³⁶ Elles peuvent avoir un spectre d'hydrolyse étroit ou étendu. Certaines hydrolysent uniquement les pénicillines, d'autres peuvent également hydrolyser les céphalosporines à large spectre et, enfin, un petit nombre est capable d'hydrolyser les carbapénèmes.³⁶ Les β -lactamases de la classe D possédant une

activité carbapénémase sont peu nombreuses et sont nommées CHDLs (*Carbapenem-Hydrolyzing class D β -Lactamases*). L'hydrolyse des carbapénèmes par ces enzymes reste néanmoins faible par rapport à d'autres carbapénémases telles que KPC-2 ou encore NDM-1. L'autre particularité de ces CHDLs correspond à une faible hydrolyse, voire aucune hydrolyse, des céphalosporines de troisième génération (C3G).

La première CHDL, OXA-23, fut isolée dans une souche de *A. baumannii* dans les années 90.¹⁶⁹ Depuis, ces souches ont diffusé dans le monde entier.¹⁷⁰ Elles sont responsables d'un grand nombre d'épidémies.¹⁷¹⁻¹⁷³ Au sein du genre *Acinetobacter*, OXA-23 est la carbapénémase la plus fréquente. En revanche, sa présence chez les entérobactéries reste rare et uniquement reliée aux souches de *P. mirabilis* dans lesquelles le gène *bla*_{OXA-23} est chromosomique.¹⁷⁴ On distingue 12 groupes au sein des CHDLs en fonction de leur séquence en acide aminé : OXA-23, OXA-24/40, OXA-48, OXA-51, OXA-58, OXA-134a, OXA-143, OXA-211, OXA-213, OXA-214, OXA-229, et OXA-235. La majorité de ces carbapénémases est associée au genre *Acinetobacter*. Les CHDLs retrouvées chez les entérobactéries dérivent toutes de la carbapénémase OXA-48. En outre, les enzymes de type OXA-48 semblent être restreintes aux entérobactéries car ne sont pas retrouvées chez les genres *Acinetobacter* et *Pseudomonas*. Le groupe des OXA-48 regroupe actuellement 30 variants (<http://www.bldb.eu/>).

b. Carbapénémases de type OXA-48

i. Epidémiologie

La carbapénémase OXA-48 fut identifiée pour la première fois chez une souche de *K. pneumoniae* isolée en Turquie en 2001.¹⁷⁵ Cette souche clinique présentait un profil de résistance de haut niveau aux antibiotiques, hydrolysant des céphalosporines à spectre large, des céphamycines, des carbapénèmes ainsi que l'aztréonam. Cette résistance était liée à l'expression de plusieurs β -lactamases (la BLSE SHV-2a et les β -lactamases à spectre étroit TEM-1 et OXA-47) ainsi qu'à des modifications de plusieurs protéines de membrane externe.¹⁷⁵ La caractérisation de cette souche a montré que le gène *bla*_{OXA-48} était localisé sur un plasmide et qu'il codait pour une β -lactamase faiblement apparentée aux autres β -lactamases de la classe D. En effet, elle partage 46%, 36%, 32% et 21% de similarité en acides aminés avec OXA-10, OXA-23, OXA-40 et OXA-1, respectivement.¹⁷⁵ Quelques années plus

tard, le réservoir naturel de ce gène de résistance a été déterminé comme étant *Shewanella* sp., (bacille Gram négatif non fermentaire et ubiquitaire), ce qui suggère un transfert environnemental en milieu aqueux de ce gène de résistance.^{176–178}

Durant plusieurs années, la majorité des bactéries productrices d'OXA-48 était isolée chez des patients hospitalisés en Turquie ou ayant un lien avec la Turquie.¹⁷⁹ Cependant, quelques rares cas sporadiques ont été décrits dans différents pays tels que la Belgique¹⁸⁰, la Tunisie¹⁸¹, la France et l'Égypte.¹⁸² Depuis, cette carbapénèmase est devenue endémique en Turquie et les bactéries productrices d'OXA-48 ont diffusé en Afrique du Nord et au Moyen-Orient. A l'heure actuelle, tous ces pays sont considérés comme étant d'importants réservoirs de bactéries productrices d'OXA-48 (Figure 21).¹⁸³ En Europe, plusieurs épidémies hospitalières ont été décrites comme en France, en Allemagne, en Espagne, aux Pays-Bas et en Angleterre.¹⁸⁴ En Afrique sub-saharienne, des souches productrices d'OXA-48 ont été rapportées dans différents pays d'Afrique centrale et en Afrique du Sud. Enfin, plus récemment, des cas ont été décrits en Europe de l'Est,¹⁸⁵ en Russie,¹⁸⁶ au Canada et aux États-Unis.⁸²

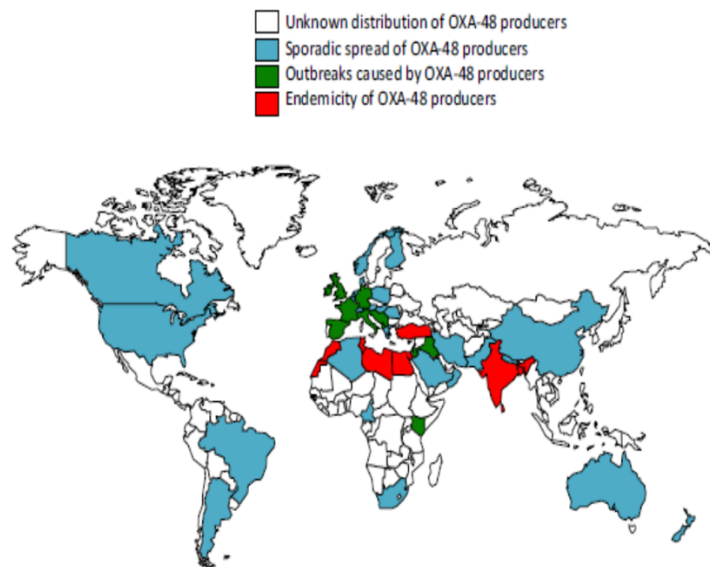


Figure 21. Distribution des entérobactéries produisant une carbapénèmase de type OXA-48
D'après Nordmann et al.¹⁸⁴

En 2018, le rapport établi par le Centre National de Référence Français aux Antibiotiques (Entérobactéries productrices de carbapénèmase, <https://www.santepubliquefrance.fr>) révèle que OXA-48 est la 1^{ère} carbapénèmase en France (71% des carbapénèmases identifiées) et que les souches de *K. pneumoniae* exprimant OXA-48 représentent la première enterobactérie productrice de carbapénèmase (EPC) en France. La propagation rapide du gène *bla*_{OXA-48} au sein de la grande famille des entérobactéries correspond à une efficacité particulièrement élevée des capacités de conjugaison du plasmide contenant le gène *bla*_{OXA-48}. En effet, il a été montré que ce plasmide, qui ne présente pas d'autres gènes de résistance, conjugait 100 fois mieux que les principaux plasmides responsables de la diffusion d'autres carbapénèmases.¹⁸⁷

Depuis la première identification d'OXA-48, de nombreux variants ont été décrits. De nos jours, il existe une vingtaine de variants chez les entérobactéries. Tous ces variants diffèrent d'OXA-48 par des substitutions ou des délétions d'acides aminés, leurs pourcentages de similarité restent néanmoins supérieurs à 90 %. La comparaison génétique de ces variants, *via* le software MEGA7,¹⁸⁸ révèle que malgré les légères différences en acides aminés, trois grands clusters sont identifiables (Figure 22). Les principales différences entre ces variants se situent dans la boucle qui relie le feuillet β 5 au feuillet β 6. Cependant, la majorité de ces variants présente un phénotype plus ou moins similaire à celui d'OXA-48, à savoir une hydrolyse des pénicillines et des carbapénèmes (bien qu'elle reste faible comparée aux autres enzymes tels que KPC et NDM) et une activité très faible, ou presque nulle, vis-à-vis des C3G. Néanmoins, il existe des exceptions comme les enzymes OXA-163, 247, 405 et 438 qui ont un phénotype opposé : une hydrolyse des céphalosporines de 3^{ème} génération et une perte quasi totale de l'hydrolyse des carbapénèmes (Tableau 8). Enfin, OXA-517 présentant une délétion de 2 AA seulement dans la boucle β 5- β 6 est capable d'hydrolyser les C3G et les carbapénèmes.¹⁸⁹

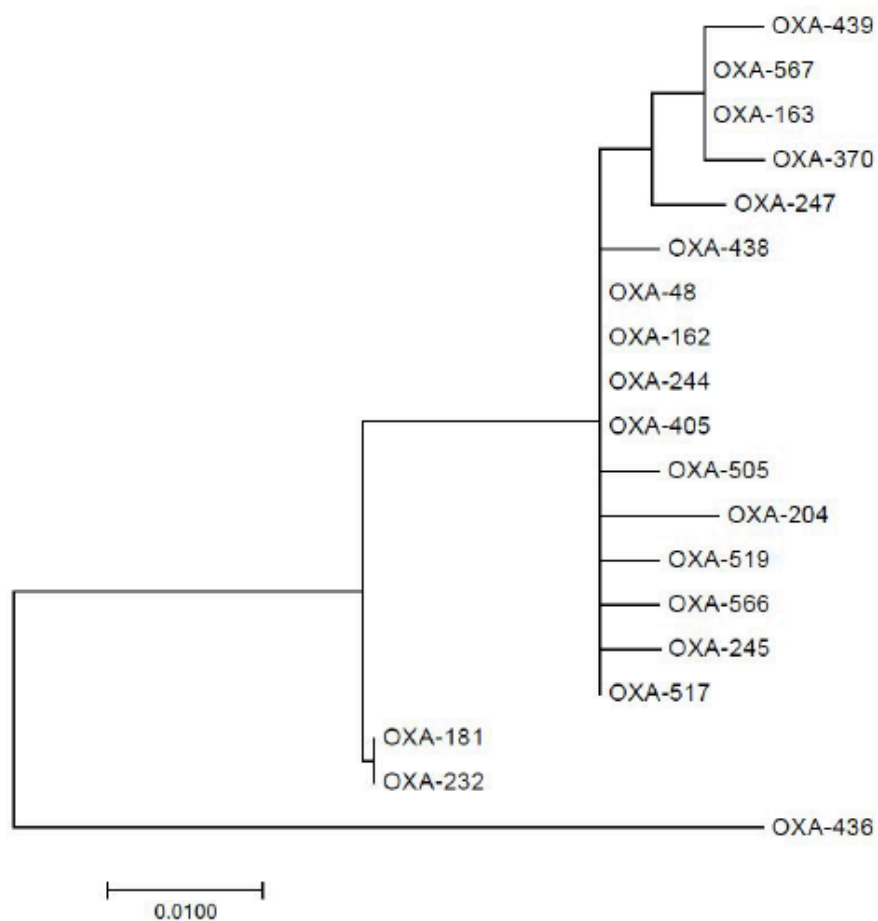


Figure 22. *Arbre phylogénétique des variants d’OXA-48. Les séquences sont dérivées de la BLDB¹⁹⁰ et l’arbre réalisé avec le logiciel MEGA7¹⁸⁸*

Parmi les différents variants d’OXA-48, OXA-181 (qui diffère par quatre substitutions en AA) est le plus répandue. La première souche décrite fut isolée chez un patient transféré d’Inde en 2011.¹⁹¹ Ce variant a été identifié dans plusieurs pays mais un lien avec l’Inde est systématiquement retrouvé.^{36,176,191} En l’espace de peu de temps, la répartition de la carbapénèmase OXA-48 et de ses variants est devenue mondiale.¹¹³

Tableau 8. Comparaison des séquences et des phénotypes des différentes OXA-48-like .

Selon la numérotation des β -lactamases de classe D (DBL). Le rectangle violet délimite la boucle β 5- β 6. NC : Non caractérisé Les profils d'hydrolyse ont été extraits des résultats de Poirel et al. 2004 ; Docquier et al 2009 ; Kasap et al. 2013, Poirel et al. 2011 ; Potron et al. 2011, Potron et al. 2013 ; Oteo et al. 2013 ; Gomez et al. 2013, Dortet et al. 2015 et Dabos et al. 2018^{175,191-198} Les résultats pour OXA-535 sont issus de Dabos. et al.¹⁹⁹

Variants	Position selon numérotation DBL															Hydrolyse	
	98	99	104	110	120	125	175	179	219	220	221	222	223	224	225	IMP	CAZ
OXA-48	Q	T	T	N	V	E	E	S	Y	S	T	R	I	E	P	+	-
OXA-162											A					++	-
OXA-244												Q				+/-	-
OXA-245						T										+	-
OXA-204	H	R														+	-
OXA-181			A	D			Q	A								+	-
OXA-232			A	D			Q	A				S				+/-	-
OXA-519					L											+/-	-
OXA-517												K	*	*		+/-	+
OXA-163										D		*	*	*	*	-	+
OXA-247									S	N		*	*	*	*	-	+
OXA-405											*	*	*	*		-	+
OXA-438										G	Y	D	*	T	*	NC	NC
OXA-439									*	*	Y	D	*	T	*	NC	NC
OXA-567										D		K		G	*	NC	NC

Boucle β 5- β 6

ii. Spectre d'hydrolyse

La β -lactamase OXA-48 a la particularité d'hydrolyser fortement toutes les pénicillines et les céphalosporines de 1^{er} génération. Cependant, les C3G sont très peu, ou pas, hydrolysées. En effet, OXA-48 hydrolyse très faiblement le céfotaxime ainsi que le céfépime et elle n'a aucune activité vis-à-vis de la ceftazidime.^{175,192} Enfin, elle présente une activité contre les carbapénèmes, qui reste néanmoins inférieure à celle des autres carbapénémases telles que KPC et NDM. L'étude des caractéristiques enzymatiques montre une efficacité catalytique 100 fois plus importante pour l'imipénème par rapport à l'ertapénème et au méropénème (Tableau 9).¹⁹² Cette différence résulte en partie d'une augmentation de la constante catalytique k_{cat} , mais également d'une augmentation de la constante d'affinité qui est 100 fois plus forte par rapport à celle de l'ertapénème. Les inhibiteurs des β -lactamases de classe A sont inefficaces vis-à-vis de OXA-48. Les CI_{50} de l'acide clavulanique, du sulbactam et du tazobactam sont de 16 μ M, 50 μ M et 1,7 μ M respectivement.¹⁷⁵ D'un point de vue clinique, les niveaux de résistance aux carbapénèmes observés dans différentes souches étudiées sont variables et, en conséquence, les valeurs de CMI peuvent fluctuer entre les intervalles de sensibilité et de résistance. Cette variabilité est notamment liée à l'association

d'autres mécanismes de résistance, tels que la perte de porines,^{175,200} et la production d'autres β-lactamases de type BLSE.

Tableau 9. Constantes enzymatiques d'OXA-48 pour différents substrats. D'après Docquier et al.¹⁹²

Substrat	k_{cat} (s ⁻¹)	K _m (μM)	k_{cat}/K_m (M ⁻¹ ·s ⁻¹)
Oxacilline	130	95	1.4 × 10 ⁶
Ampicilline	955	395	2.4 × 10 ⁶
Témocilline	0.3	45	6.6 × 10 ³
Nitrocefine	940	120	7.7 × 10 ⁶
Céphalothine	44	195	2.3 × 10 ⁵
Céfoxitine	>0.05	>200	2.6 × 10 ²
Céfotaxime	>9	>900	1.0 × 10 ⁴
Ceftazidime	N.H.	-	-
Céfépime	>0.6	>550	1.1 × 10 ³
Imipénème	4.8	13	3.7 × 10 ⁵
Méropénème	0.07	11	6.2 × 10 ³
Ertapénème	0.13	100	1.3 × 10 ³
Panipénème	1.4	14	1.0 × 10 ⁵
Faropénème	0.038	13	2.9 × 10 ³

iii. Environnement génétique / support génétique

Le gène *bla*_{OXA-48} a été identifié sur un plasmide de 62-Kb transférable ne possédant pas d'autres gènes impliqués dans une résistance associée.²⁰¹ L'analyse génotypique a révélé qu'il s'agissait d'un plasmide appartenant à la famille IncI et que le transposon Tn1999 avait été inséré (Figure 23).²⁰² Les plasmides IncI/M sont des plasmides très répandus chez les entérobactéries. Ils sont responsables de l'acquisition de nombreux gènes de résistance aux antibiotiques. La diffusion rapide de ce plasmide IncI portant le gène *bla*_{OXA-48} au sein de nombreuses espèces d'entérobactéries²⁰³ résulterait de l'inactivation, *via* l'insertion du transposon Tn1999, du gène *tir* codant pour un inhibiteur de transfert du plasmide. Ceci engendre une augmentation du taux de conjugaison d'un facteur 100.¹⁸⁷ Le plasmide pOXA-48a a été identifié dans toutes les souches productrices d'OXA-48 issues de différents pays.²⁰²

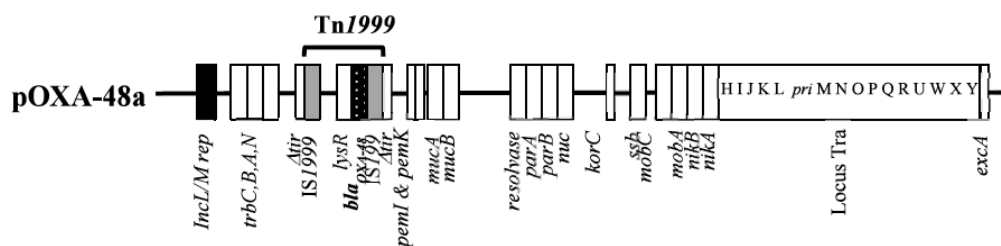


Figure 23. Environnement génétique du gène *bla*_{OXA-48}. D'après Poirel et al.²⁰²

Initialement, le gène *bla*_{OXA-48} a été identifié en association avec la séquence d'insertion IS1999 chez *K. pneumoniae* (Figure 24) apportant ainsi une séquence promotrice au gène, permettant ainsi son expression.¹⁷⁵ L'étude de l'environnement génétique du gène *bla*_{OXA-48} a démontré qu'il est porté par un transposon composite, Tn1999 de 4,5 Kb et qu'il est encadré par deux IS1999.²⁰⁴ La présence de duplications de séquences de 9 paires de bases de part et d'autre du transposon signe un événement de transposition.²⁰⁴ On recense actuellement cinq structures dérivées de Tn1999 chez les entérobactéries. L'isoforme Tn1999.2, identifiée chez une souche *K. pneumoniae*, diffère par une insertion de la séquence IS1R.¹⁸² Parmi les souches OXA-48, l'isoforme Tn1999.2 est plus fréquemment identifié par rapport à Tn1999.1. Il a été montré que la séquence IS1R en amont du gène *bla*_{OXA-48} augmente son expression.¹⁸² L'isoforme Tn1999.3 identifié chez *E. coli* en Italie possède 2 séquences IS1R.²⁰⁵ Le transposon Tn1999.4 identifié chez une souche de *E. coli* et de *E. cloacae* résulte de l'intégration au niveau du gène *lysR* du transposon Tn2015. Ce dernier comprend le gène codant pour une autre β -lactamase de type BLSE : CTX-M-15.²⁰⁶ Enfin, dernièrement, un nouvel isoforme a été décrit, Tn1999.5. Il s'agit d'un variant du Tn1999.2 dans lequel est inséré l'élément ISKpn19.²⁰⁷

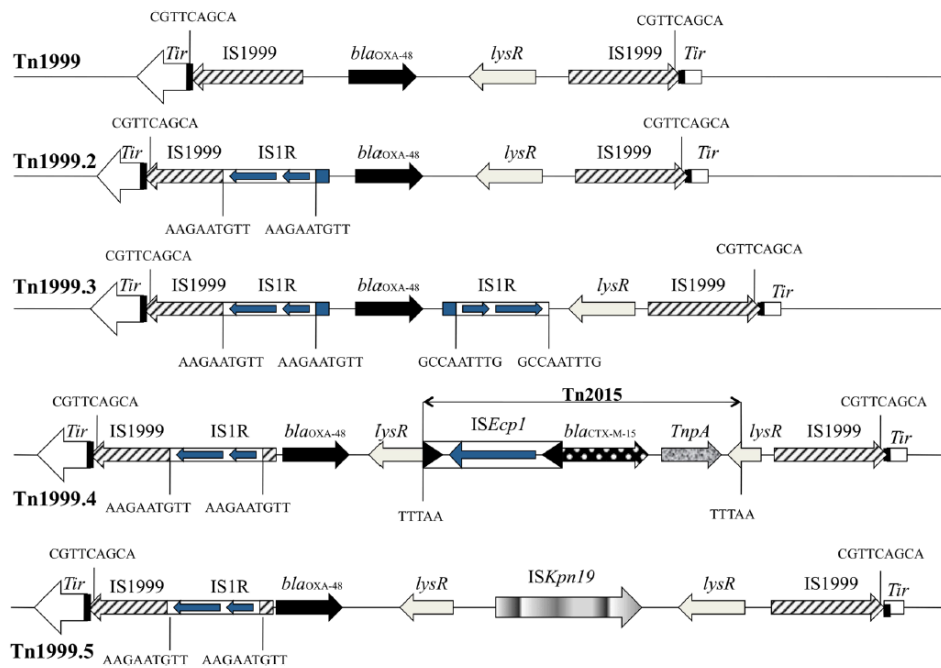


Figure 24. Environnement génétique des transposons Tn1999-like portant le gène *bla*_{OXA-48} chez les entérobactéries. D'après Mairi et al²⁰⁸

La présence du gène *bla*_{OXA-48} a également été retrouvé dans le chromosome de deux souches de *E. coli*.²⁰⁹ L'acquisition d'une séquence d'insertion *IS1R* en amont du gène *bla*_{OXA-48} (formant le Tn1999.2) a généré la formation d'un transposon composite, grâce à une autre copie d'*IS1R* située environ 21 kb en aval. Ce transposon appelé Tn6237 est capable de s'insérer à différents endroits du chromosome de *E. coli*.^{209,210}

Contrairement au gène *bla*_{OXA-48}, le gène codant pour OXA-181 (un variant d'OXA-48) est associé à des plasmides conjugatifs de type type IncT et IncX3, mais également à des plasmides non conjugatifs de type ColE. Les gènes *bla*_{OXA-204} et *bla*_{OXA-370} sont localisés sur des plasmides de type IncA/C et IncF respectivement.^{19,211} De plus, le gène *bla*_{OXA-181} n'est pas associé au transposon Tn1999, mais à la séquence d'insertion *ISEcp1*¹⁷⁶ qui est impliquée dans la diffusion mondiale des gènes *bla*_{CTX-M} ainsi que des gènes codant pour certains variants de céphalosporinase de type CMY.^{212,213}

La présence de gènes codant pour des oxacillines possédant une activité carbapénèmase, ont été identifiés au niveau du chromosome des bactéries du genre *Shewanella* sp. suggérant qu'elles puissent constituer un réservoir de gènes. En effet, *Shewanella oneidensis* MR-1

possède au niveau chromosomique le gène *bla*_{OXA-54}, un variant de *bla*_{OXA-48}.¹⁷⁷ de la même manière, *Shewanella xiamenensis* a été décrite comme progéniteur potentiel du gène *bla*_{OXA-181}.¹⁷⁶ Plus récemment, la carbapénèmase OXA-535 a été identifiée chez une souche de *Shewanella bicestria* qui serait le progéniteur du variant OXA-436.¹⁷⁸

iv. Structure

L'analyse cristallographique de la carbapénèmase OXA-48 a révélé que la protéine était formée de deux dimères indépendants.¹⁹² Sa structure tertiaire est très proche de celles des autres oxacillinasés (bien que la structure primaire soit très éloignée, Figure 25. A). Les différences structurales observées se localisent essentiellement au niveau des boucles associant les différents domaines de cette structure.

Le site actif se localise dans une crevasse délimitée par deux domaines. Celle-ci est refermée d'un côté par une arginine en position 214 (boucle β 5- β 6) et une glutamine en position 124, et de l'autre côté, par une isoleucine en position 102 et une sérine en position 244 (Figure 25. B). Le site actif est caractérisé par la présence des 3 motifs conservés typiques des oxacillinasés de classe D (le motif I : Ser-70, Thr-71, la Phe-72 et la Lys-73; le motif II : Ser-118, Val-119 et de la Val-120 ; le motif III : Lys-208, la Thr-209 et de la Gly-210) ainsi qu'une lysine carbamoylée, Lys-73 (motif I). L'activité carbapénèmase de OXA-48 pourrait être le résultat de légères modifications dans la région du site actif par rapport aux autres β -lactamasés de classe D. En effet, par rapport à d'autres oxacillinasés cristallisés comme OXA-10, les feuillets β 5 et β 6 de OXA-48 émergent hors de la crevasse modifiant ainsi sa charge et sa largeur. Cette conformation particulière serait assurée par une interaction entre l'arginine en position 214 et le résidu acide aspartique en position 159. De plus, une analyse comparative de la composition en acides aminés des sites actifs de OXA-48 et de OXA-10/13 suggère un rôle fonctionnel de l'arginine 214.

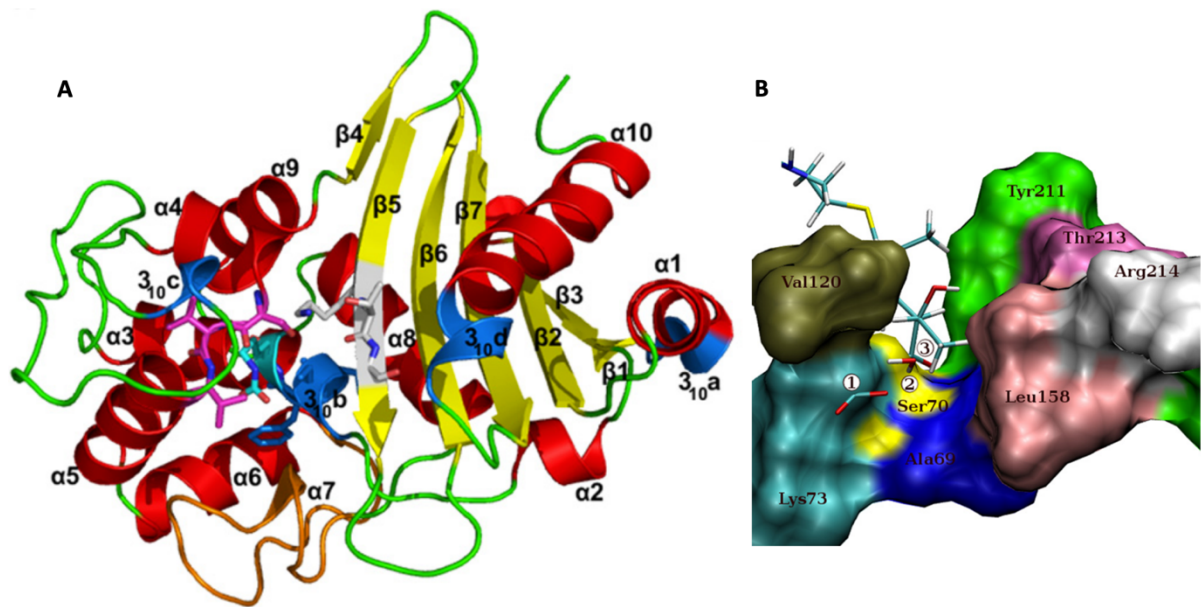


Figure 25. A. Structure tertiaire de la carbapénèmase OXA-48. Les hélices α sont indiquées en rouge, les feuillet β en jaune et gris, la boucle β 5- β 6 en orange. Les trois motifs DBL sont représentés avec les résidus respectifs sous forme de sticks: motif I (contenant les résidus catalytiques Ser-70, Thr-71, Phe-72 et Lys-73 carbamoylé), cyan; motif II (Ser-118, Val-119 et Val-120), magenta; motif III (Lys-208, Thr-209 et Gly-210), blanc. **B. Structure du site actif.** Une molécule de mérépénème est représentée au niveau du site actif, Les résidus pertinents du site actif sont affichés dans différentes couleurs. Sont représentés sous forme de stick : le groupe carbamoylé de Lys-73 (cyan, étiquette 1) ; la molécule d'eau impliquée dans l'étape de désacylation (étiquette 2, près de la Lys-73) et le groupe substrat acyl lié à Ser-70 (jaune, l'étiquette 3). D'après Docquier et al.

La comparaison du site actif d'OXA-48 à celui d'OXA-24 (carbapénèmase identifiée dans le genre *Acinetobacter*)¹⁹² révèle que les deux cavités diffèrent par leur forme, leur taille et leur charge (Figure 26). L'une des différences entre les deux sites actifs, est la présence de deux résidus (Tyr-112 et Met-223) dans le site actif d'OXA-24 qui forment une barrière hydrophobe. La boucle β 5- β 6 de ces deux carbapénèmases est très similaire, ce qui laisse fortement suggérer son implication dans l'hydrolyse des carbapénèmes.

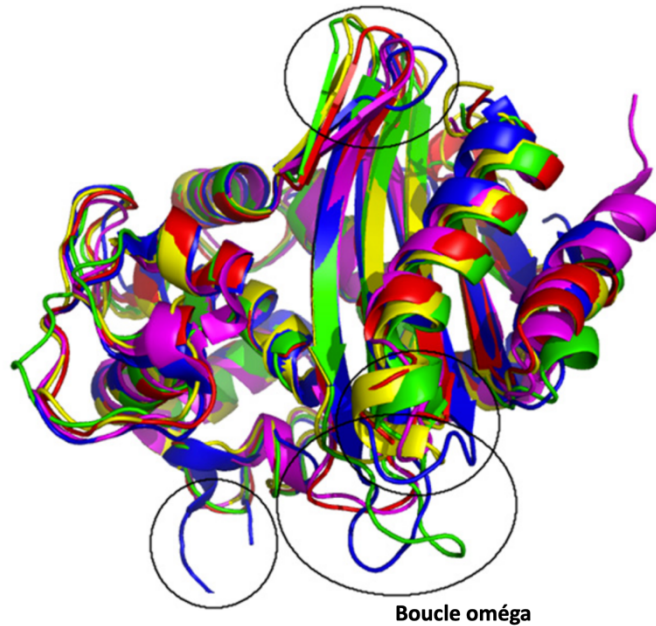


Figure 26 Superposition des membres représentatifs de la famille DBL. Les cercles délimitent les parties pour lesquelles il y a des différences structurales dont la boucle β -5/ β -6. La légende des couleurs et les codes PDB sont les suivants: OXA-48 (3HBR), rouge; OXA-1 (1M6K), bleu; OXA-2 (1K38), jaune; OXA-10 (1K55), vert; OXA-24 (2JC7), magenta. D'après Docquier et al.¹⁹²

4. Détection des Entérobactéries Productrices de Carbapénèmase (EPC)

La détection précoce des EPC a pour but (i) d'adapter au plus vite l'antibiothérapie en cas d'infection par une bactérie multi-résistante et (ii) de pouvoir mettre rapidement en place des mesures de contrôle visant à limiter la dissémination de ces germes multi-résistants d'un patient à l'autre (isolement des patients, personnel dédié ...). Ainsi, toutes les souches d'entérobactéries qui présentent une diminution de sensibilité à au moins une des carbapénèmes doivent faire l'objet de tests de confirmation. Le niveau de résistance aux carbapénèmes varie d'une souche à l'autre, en fonction de la carbapénèmase exprimée mais également en fonction des autres β -lactamases associées (BLSE, céphalosporinases...) et de l'association de mécanismes non enzymatiques (impermeabilité...).

a. Méthodes de détection basées sur le phénotype

i. Antibiogramme et concentration minimale inhibitrice (CMI)

Depuis 2015, le Comité de l'Antibiogramme de la Société Française de Microbiologie (CA-SFM) a établi des recommandations nationales pour aider à la détection des EPC. Ces recommandations se traduisent par un algorithme de dépistage débutant par l'analyse de la sensibilité vis-à-vis de l'ertapénème (Figure 27).²¹⁴ Si cette sensibilité est réduite (CMI > 0,5 mg/L ou un diamètre d'inhibition < 25 mm) la souche est suspectée comme EPC et sa caractérisation doit être réalisée.

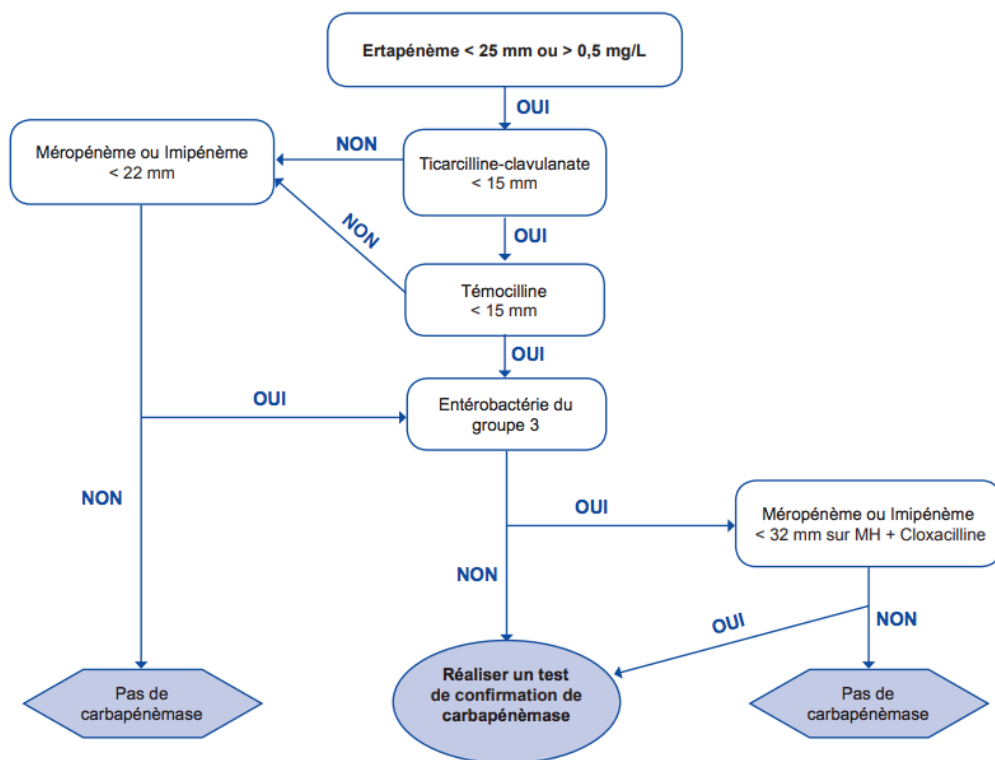


Figure 27. Algorithme phénotypique de criblage des souches d'entérobactéries productrices de carbapénémases au sein des souches non-sensibles aux carbapénèmes. Recommandations du CASFM 2019 v1 https://www.sfm-microbiologie.org/wpcontent/uploads/2019/02/CASFM2019_V1.0.pdf

Les recommandations européennes mises en place par l'EUCAST (Tableau 10) font mention de *cut-offs* épidémiologiques (*screening cut-offs* ou encore *seuil de dépistage*) qui ne sont pas des concentrations critiques cliniques utilisées pour conseiller un traitement antibiotique. Ces *cut-offs* présentent des valeurs basses permettant ainsi l'amélioration de la détection des EPC.

Cependant, la spécificité est faible car les CMI des souches associant des BLSE et/ou des céphalosporinases et/ou imperméabilité dépassent souvent ces *cut-offs*.

Tableau 10. Concentrations critiques, valeurs de CMI et valeurs seuil de dépistage des carbapénèmes pour les entérobactéries. EUCAST 2019 V9

	EUCAST CONCENTRATION CRITIQUES (mg/L)		SEUIL DE DEPISTAGE
	R>	S ≤	
Imipénème	4	2	
Méropénème	8	2	>0,125
Ertapénème	0,5	0,5	>0,125

ii. Disques combinés avec inhibiteurs

La caractérisation de la carbapénémase produite peut se faire à l'aide de l'utilisation d'inhibiteurs spécifiques aux différentes classes. Ainsi, les MBLs, par exemple, sont inhibées par l'acide dipicolinique ou EDTA alors que les carbapénémases de type KPC sont inhibées, partiellement, par l'acide boronique. L'acide boronique inhibe également les céphalosporinases (Classe C de Ambler). L'avibactam est, quant à lui, un nouvel inhibiteur capable d'inhiber les β -lactamases de classe A (BLSE et carbapénémases), les carbapénémases de type OXA-48 ainsi que les céphalosporinases. La détection de ces carbapénémases de type OXA-48 fait également intervenir l'utilisation d'un disque contenant de la témocilline. En effet, 90% des EPC exprimant OXA-48 sont très résistantes à cet antibiotique (diamètre d'inhibition inférieur à 12 mm pour des disques chargés à 30 μ g, soit une CMI > 256 mg/L).²¹⁵

iii. Le test de Hodge modifié

Ce test permet la mise en évidence d'une synergie d'activité enzymatique entre souches productrices de carbapénémases (souche à tester) et une souche sauvage de référence sensible aux carbapénèmes. Pour cela, un disque contenant un carbapénème est déposé sur une gélose de Mueller-Hintonensemencée avec une souche sauvage *E. coli* ATCC25922 sensible aux carbapénèmes. Quelques colonies de la souche à tester sont prélevées et déposées sur la gélose de manière rectiligne depuis le disque contenant le carbapénème vers

la périphérie de la boîte. Un contrôle positif est également réalisé de la même façon. La boîte est ensuite incubée de 16 à 24 heures à 37°C (Figure 28).

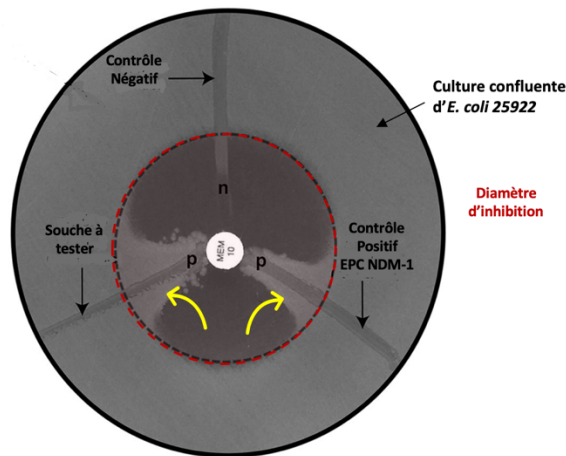


Figure 28. Résultats obtenus avec un Hodge test modifié. Réadaptation de Pasteran et al.²¹⁶

La production d'une carbapénèmase est détectée si la souche à tester permet la croissance de la souche sauvage dans le diamètre d'inhibition (en direction du disque). On parle alors d'un profil « clover leaf-like ». ²¹⁷ En effet, la production d'une carbapénèmase par la souche à tester dégradera l'antibiotique ce qui permettra à la souche de *E.coli* sauvage de croître au plus près du disque contenant le carbapénème. Ce test présente de nombreux faux positifs avec notamment des *E. cloacae* hyperproduisant l'AMPC et des faux négatifs avec notamment des metallo- β -lactamases.

iv. Méthode d'inactivation des carbapénèmes

Cette méthode (également appelée CIM test pour *Carbapenem-Inactivation Method*) est un dérivé du test de Hodge, reposant sur l'hydrolyse du méropénème contenu dans un disque chargé (10 μ g) pendant 2h par la souche à tester, puis l'étude de la sensibilité de la souche de *E. coli* sensible ATCC 25922 à ce même disque. ²¹⁸ Si la souche à tester produit une carbapénèmase, le méropénème est hydrolysé pendant l'incubation, et la souche de *E. coli* ATCC 25922 poussera au contact du disque. A l'inverse, si la souche à tester ne produit pas de

carbapénèmase, le méropénème restera actif et une zone d'inhibition sera visible (Figure 29.A).

Une version améliorée de ce test, le modified-CIM (mCIM), permet la détection des carbapénèmases de type OXA-48 en augmentant tout simplement le temps d'incubation (4h) entre le disque de méropénème et la souche d'intérêt.²¹⁹

Enfin, un dérivé de cette méthode, le rapid CIM (rCIM), permet la détection des EPC sans passer par une croissance sur un milieu gélosé permettant ainsi un gain de temps considérable. En effet, le délai de réponse passe d'une durée de 16h/24h à 2h30. Ce test repose sur l'hydrolyse de méropénème contenu dans deux disques (10 µg).²²⁰ Après incubation, le surnageant est récupéré puis mis en présence d'une suspension à 1 MacFarland de la souche *E. coli* sensible ATCC 25922 (Figure 29. B). On suit la culture de la souche de *E. coli* au néphélomètre pendant au maximum deux heures. Si la bactérie testée produit une carbapénèmase, le méropénème a été hydrolysé et on observera une croissance normale de la souche ATCC en présence du disque de méropénème ayant été incubé avec la souche à tester (ΔDO en 2h > 1 MacFarland). A l'inverse, si la bactérie testée ne produit pas de carbapénèmase, le méropénème présent dans le surnageant reste actif et inhibe la croissance de la souche ATCC (ΔDO en 2h < 0,5 McF).

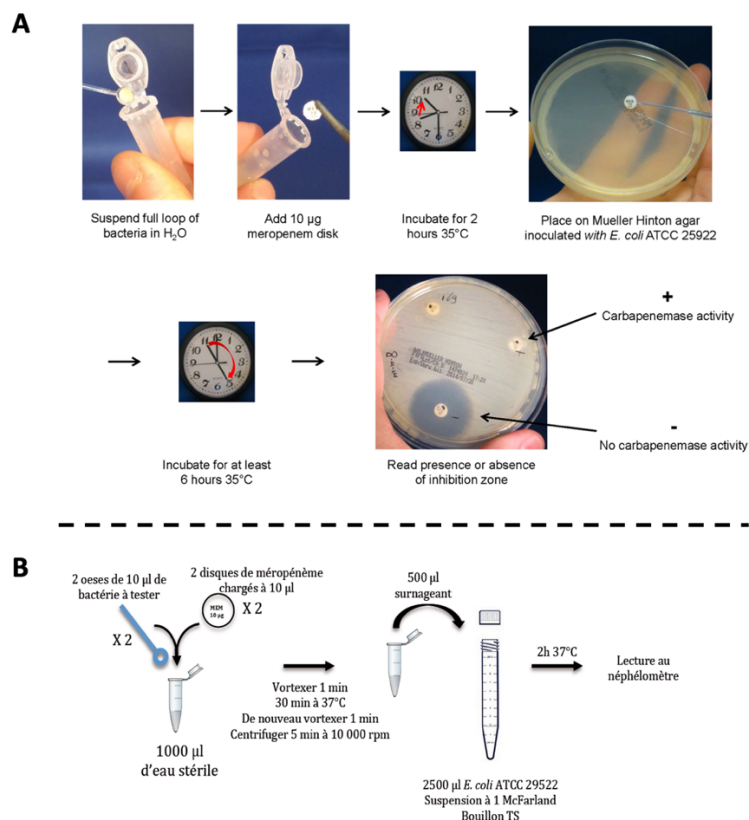


Figure 29. A. Protocole pour la réalisation du CIM-test D'après Van der Zwaluw et al²¹⁸ ; B. Protocole pour la réalisation du rCIM.

b. Tests d'hydrolyse des carbapénèmes

i. Spectrophotomètre UV

La dégradation des carbapénèmes est mise en évidence par une diminution de l'absorbance du carbapénème testé qui reflète l'ouverture du cycle β -lactame et donc l'inactivation de l'antibiotique. Pour cela, une cinétique est réalisée en utilisant un carbapénème et l'extrait brut de la souche à tester. Ce test présente une très bonne sensibilité (100%) et spécificité (98,5%) de détection des carbapénèmases mais présente l'inconvénient d'être long, de nécessité du matériel spécifique et du personnel très qualifié.²²¹

ii. Spectrométrie de masse

Cette technique repose sur la détection du produit de dégradation de l'imipénème par spectrométrie de masse de type MALDI-TOF. Le kit de détection des EPC commercialisé est le MBT STAR®-Carba IVD Kit (Bruker Daltonics)²²²⁻²²⁴, il présente une très bonne sensibilité et

spécificité. La souche d'intérêt est incubée en présence d'imipénème pendant 30 minutes puis le surnageant est analysé en spectrométrie de masse. Si la souche a dégradé l'imipénème on constate alors la disparition du pic correspondant à l'imipénème natif et l'apparition d'un pic qui correspond aux produits de dégradation de cet antibiotique (Figure 30).^{223,225,226} Cette technique présente une bonne sensibilité (100%) ainsi qu'une bonne spécificité (98%).

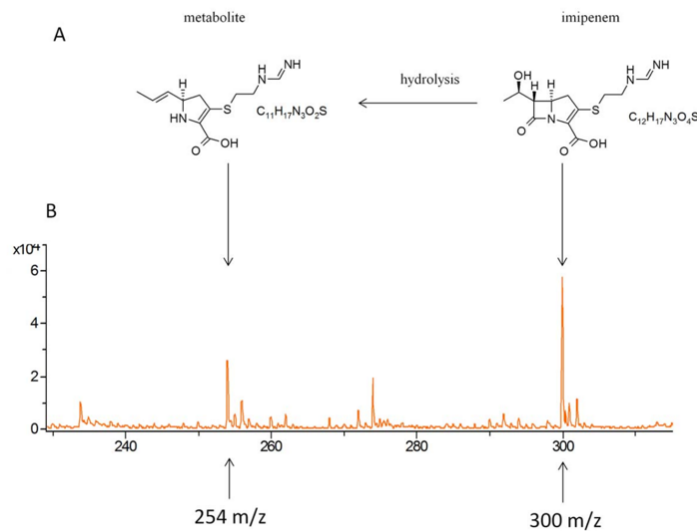


Figure 30. Analyse par MALDI-TOF, A. Imipénème et son produit ; B. Spectre de masse de l'imipénème et de son produit de dégradation, déterminé à l'aide du spectromètre de masse Ultraflex. Kempf et al.^{227,228}

iii. Tests colorimétriques

Le CarbaNP test est une technique biochimique colorimétrique de diagnostic rapide visant à détecter une activité carbapénèmase.²²⁹ Pour cela, cette méthode met en évidence l'acidification d'un milieu contenant un indicateur de pH (rouge phénol) qui vire du rouge au jaune (Figure 31. A et B). Cette acidification a lieu lors de l'hydrolyse de l'imipénème par une carbapénèmase.

Les bactéries sont lysées à l'aide d'un tampon de lyse dans deux tubes séparés. Après homogénéisation, le milieu réactionnel seul est ajouté dans un premier tube, puis le même milieu additionné d'imipénème dans le deuxième. Les tubes sont incubés à 37°C pendant 2 heures, puis une lecture visuelle est faite pour évaluer le changement de couleur du milieu. Ce test est capable de détecter l'ensemble des enzymes possédant une activité carbapénèmase sans restriction de classe. Il possède une excellente spécificité. Sa sensibilité

varie de 90% à 100% selon les études ; un défaut de sensibilité a été rapporté pour certains variants de type OXA-48 et certains variants GES pour lesquels l'activité carbapénèmase est faible.²³⁰⁻²³²

Il existe un test de détection des EPC pratiquement identique qui est le test Blue Carba. La seule différence est l'indicateur coloré qui est le bleu de bromothymol (Figure 31. C). Ce test a montré une sensibilité et spécificité de 100% pour la détection des MBLs, KPC et OXA-48.²³³

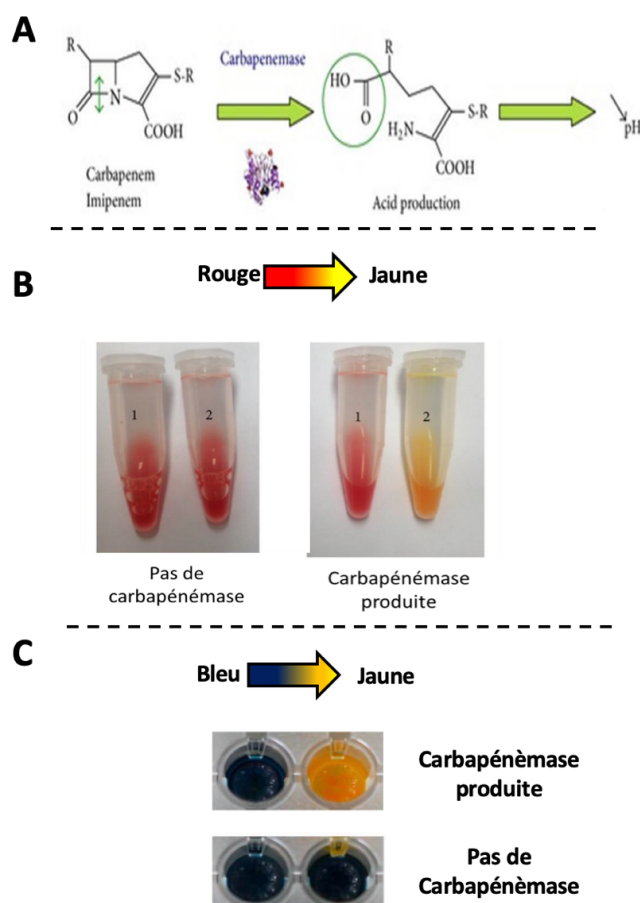


Figure 31. A. Principe des tests colorimétriques ; B. Résultats du Carba NP test D'après Nordmann et al.²²⁹ ; C. Résultats du Blue carba. D'après Pire et al.²³³

Le β -CARBA[®] test est également un test colorimétrique (commercialisé par la société BioRad) basé sur l'hydrolyse d'un substrat, une β -lactamine chromogénique dont l'identité reste inconnue. Les avantages de ce test sont sa grande facilité d'utilisation et d'interprétation, tout

comme le CarbaNP test. En revanche, on note l'absence de détection de certaines enzymes de classe A non-KPC, comme IMI, SME et FRI, très minoritaires en France, et de certains variants d'OXA-48.²³¹ Ce kit présente une sensibilité de 84,9% et une spécificité de 95,6%.²³¹

iv. Méthodes de détection moléculaire

Ces méthodes permettent de révéler la présence des gènes codant pour les carbapénèmases. Pour cela, les gènes d'intérêt sont amplifiés par PCR. L'analyse de la PCR en point final se fait par visualisation du ou des produits de l'amplification s'il s'agit du mono-test ou d'un multi-tests respectivement.²³⁴ Il faut compter en moyenne 4h pour avoir les résultats. Il existe également une autre méthode : la PCR en temps réel, ici, l'amplification du gène recherché est mise en évidence par une émission de fluorescence qui est mesurée au cours de la réaction. De nombreux kits sont commercialisés, et s'utilisent à partir de colonies ou directement à partir d'échantillons cliniques tels que des écouvillons ou encore des hémocultures positives. La plupart de ces kits se présente sous forme de PCR multiplex permettant ainsi l'identification de plusieurs gènes sur un même échantillon. La sensibilité ainsi que la spécificité de ces outils de diagnostic sont très bonnes.²³⁵⁻²³⁸ L'inconvénient majeur de ces techniques moléculaires réside dans le fait qu'ils ne détectent que les gènes recherchés et donnent un résultat positif même si ces gènes ne sont pas exprimés. De plus, une mutation survenant au niveau du site d'hybridation des amorces peut conduire à de faux négatifs.²³⁹

v. Tests immunochromatographiques

Récemment, plusieurs tests immunochromatographiques ont été commercialisés pour la détection des EPC. Ces tests détectent directement la production de l'enzyme responsable de la résistance. De plus, contrairement aux tests phénotypiques et biochimiques, ils ne sont pas influencés par l'activité enzymatique même faible de l'enzyme. La limitation de ces tests est l'émergence de variants conduisant à une modification de la structure tertiaire empêchant ainsi la reconnaissance de la carbapénémase par les anticorps. Cela induit donc des résultats faussement négatifs. Pour réaliser ce test, les bactéries sont mises en contact avec un tampon de lyse puis l'extrait est déposé sur la cassette. Les résultats sont généralement obtenus dans un délai de 15 minutes.

Les premiers tests étaient unitaires et permettaient la détection des carbapénèmases de type OXA-48 ou KPC.^{230,240} Rapidement, des tests multiplexés ont été commercialisés pour la détection de 3 types de carbapénèmase (RESIST-3 O.K.N (CORIS Bioconcept) pour la détection d'OXA-48-like/KPC/NDM, puis de 4 carbapénèmases avec RESIST-4 O.K.N.V (CORIS Bioconcept) permettant la détection de VIM en plus.²⁴¹ Enfin, le kit NG-Test CARBA 5 (NG Biotech, Figure 32) est capable de détecter les enzymes de type OXA-48-like/KPC/NDM/VIM et IMP.^{242,243}

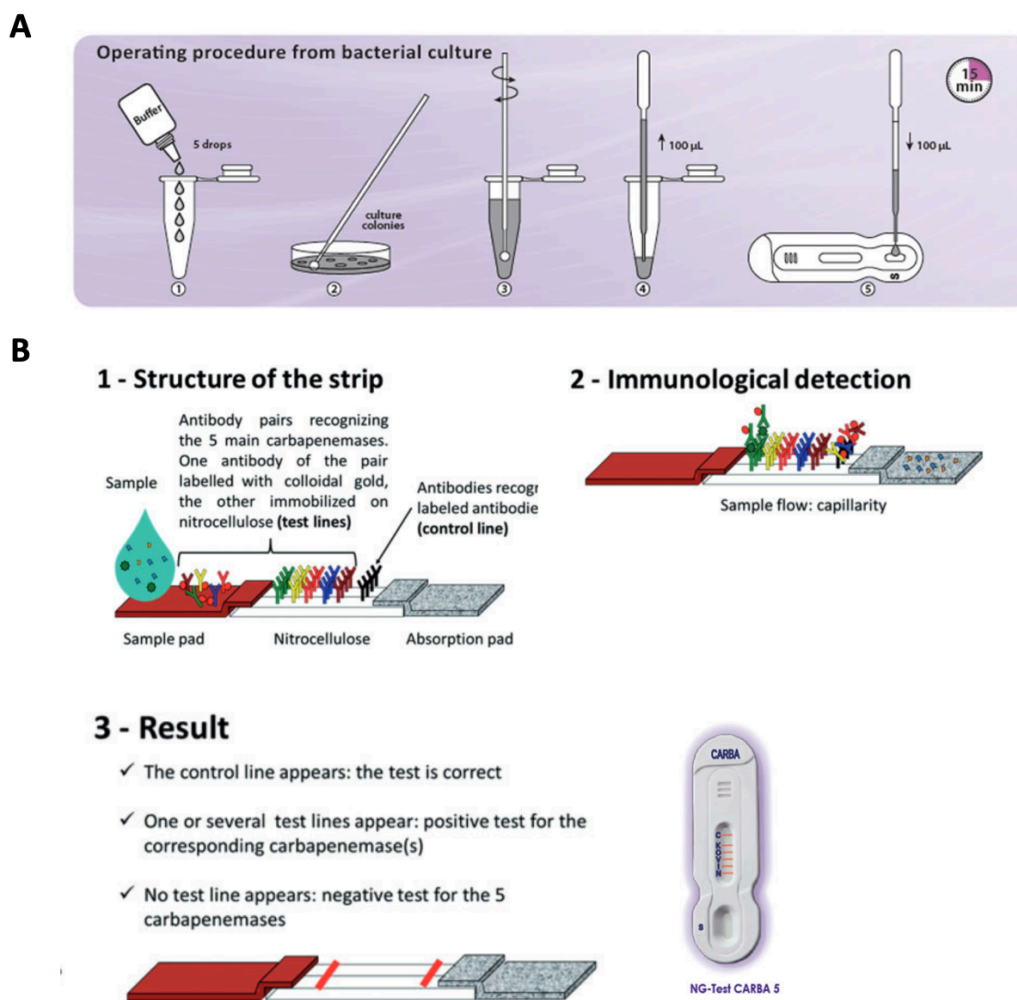


Figure 32. NG-Test CARBA 5 : A. Protocole ; B. Principe et résultat. D'après Boutal et al.²⁴² et <https://ngbiotech.com/carbapenemases/>

vi. Détection directe de la carbapénèmase par spectrométrie de masse

La spectrométrie de masse a également été utilisée pour détecter les souches produisant spécifiquement la carbapénèmase KPC.²⁴⁴ En effet, sur les spectres utilisés pour l'identification de ces bactéries, un pic situé à 11 kDa est présent uniquement chez les souches produisant cette carbapénèmase.^{244,245} Ce pic correspond à une protéine hypothétique appelée p019, dont le gène est localisé sur le plasmide pKpQIL, en aval du site d'insertion du Tn4401a. Il est cependant nécessaire d'indiquer que le gène codant pour cette protéine p019 est absent des plasmides portant les autres isoformes du Tn4401 ou les structures de type NTE_{KPC}. La protéine p019 est présente dans 97,8% des génomes possédant Tn4401a.²⁴⁵ Par son manque de sensibilité vis-à-vis de l'ensemble des structures génétiques portant *bla*_{KPC}, cette technique ne peut donc pas être utilisée pour le diagnostic des EPC dans des zones à faible prévalence en KPC, mais son intérêt réside principalement dans le suivi d'épidémies après caractérisation génétique de la souche incriminée.²⁴⁶

5. Aspects cliniques

a. Facteurs de risque d'acquisition des EPC

Les infections associées aux EPC ne sont pas spécifiques et sont majoritairement associées aux soins. Dans la majorité des cas, une étape de colonisation digestive précède l'infection. Une étude a montré que dans une cohorte de 1806 patients colonisés par une EPC, 16,5% d'entre eux s'infectaient avec cette EPC.²⁴⁷ En France, dès qu'un patient est considéré comme potentiellement porteur d'une EPC, des mesures drastiques d'hygiène sont mises en place. En effet, ce sont des porteurs asymptomatiques qui contribuent à la diffusion des bactéries hautement résistantes. Les facteurs de risque d'acquisition d'une EPC sont principalement l'usage préalable d'antibiotiques, la prise en charge dans une structure de soins, et la présence de matériel invasif comme les cathéters.^{248,249} L'équilibre du microbiote digestif joue également un rôle très important dans l'implantation des EPC.²⁴⁸ Par ailleurs, les voyages dans un pays où les EPC sont endémiques est également un facteur important d'acquisition et de diffusion des EPC au niveau mondial.²⁵⁰⁻²⁵² Le rapatriement sanitaire d'un patient provenant d'un hôpital étranger doit conduire à la mise en place de mesures d'hygiène avant même l'obtention des résultats des dépistages rectaux.

b. Infections dues aux EPC

Parmi les infections causées par des souches d'entérobactéries résistantes aux carbapénèmes, on retrouve les infections classiquement provoquées par les entérobactéries : l'infection des voies urinaires, la péritonite, la septicémie, les infections pulmonaires, les infections des tissus mous ainsi que les infections associées aux dispositifs médicaux.^{253,254} Les infections urinaires sont largement majoritaires. Aucune manifestation clinique spécifique n'a été associée aux bactéries productrices de carbapénèmases par rapport aux souches sauvages sensibles.^{253,254} Tous les types d'espèces de EPC sont impliqués dans les infections, cependant, *K. pneumoniae* et *E. coli* sont les principales sources d'infections contractées respectivement en milieu hospitalier et en milieu communautaire (Tableau 11).

Tableau 11. Sources des infections contractées en fonction du type de carbapénèmases.
Établit à partir de Nordmann et al.²⁵⁵

SOURCES DES INFECTIONS CONTRACTÉES EN MILIEU HOSPITALIER ET EN MILIEU COMMUNAUTAIRE	
KPC, IMP, VIM	Infections contractées en milieu hospitalier
OXA-48, NDM	Infections contractées en milieu hospitalier et en milieu communautaire

Il a été montré que des souches d'entérobactéries résistantes aux carbapénèmes mais ne produisant pas de carbapénèmases (principalement *K. pneumoniae* et *Enterobacter* sp.) étaient plus prévalentes en milieu hospitalier qu'en communautaire.²⁵⁵ Une étude a montré que la probabilité de décès était 4 fois supérieure chez les patients infectés par une EPC comparés aux patients infectés par des entérobactéries résistantes aux carbapénèmes par un autre mécanisme.²⁵⁶

c. Traitement des infections dues à des EPC

La plupart des bacilles à Gram négatif résistants aux carbapénèmes est aussi multirésistante à d'autres classes d'antibiotiques, à l'exception des souches de *P. aeruginosa* résistants à l'imipénème (modification de la porine OprD2) qui peuvent rester sensibles à plusieurs antibiotiques à large spectre. Les patients infectés doivent être traités, mais pas les patients uniquement colonisés. Plusieurs études décrivent l'impact de l'emploi intensif de carbapénèmes et d'autres antibiotiques à large spectre, tels que les céphalosporines et les

fluoroquinolones, comme facteurs de sélection des bacilles à Gram négatif résistants aux carbapénèmes.^{254,257}

Le choix d'une antibiothérapie optimale repose essentiellement sur l'analyse détaillée des résultats de l'antibiogramme. Dans bien des cas, le choix des antibiotiques reste limité à la colistine, la fosfomycine parentérale, la gentamicine, l'amikacine et la tigécycline.^{257–260} Le site de l'infection et la diffusion des antibiotiques au site infecté sont également des facteurs à prendre en considération dans le choix de l'antibiotique le mieux adapté. Les antibiotiques ne doivent généralement pas être administrés en monothérapie pour traiter les bactéries productrices de carbapénémases afin de ne pas renforcer la résistance aux antibiotiques et, théoriquement, d'améliorer l'efficacité clinique.

La grande majorité des études évaluant les traitements des infections causées par des EPC concerne des infections par des souches produisant KPC. Elles ont évalué l'efficacité de quelques molécules antibiotiques actives, souvent en association les unes avec les autres : (i) colistine + carbapénème, (ii) colistine + tigécycline, (iii) colistine + fosfomycine, (iv) association de 2 carbapénèmes, ou encore (v) association de 3 molécules parmi cette liste. Les associations de 2 molécules actives ou plus (notamment celles comprenant un carbapénème) sont associées à une meilleure survie dans plusieurs études.^{113,259,261} L'association de 2 carbapénèmes a pour principe d'utiliser l'ertapénème comme substrat « suicide » vis-à-vis de la carbapénémase, permettant ainsi, à l'imipénème ou au méropénème d'interagir avec leur cible bactérienne.^{262–264}

Le traitement des bactériémies se fait, en général, en administrant un carbapénème avec la colistine.²⁶⁵ Cependant, l'utilisation accrue de la colistine, surtout en Grèce et en Italie, a conduit à l'émergence de souches résistantes à cet antibiotique. Cette résistance à la colistine correspond majoritairement à l'apparition d'altérations (mutation, disruption) dans des gènes chromosomiques impliqués dans la cascade de synthèse du LPS bactérien. En 2017, en Grèce, 14% des souches des souches de *K. pneumoniae* produisant KPC étaient résistantes à la colistine.²⁶⁶

L'efficacité des carbapénèmes pour le traitement des infections impliquant des souches OXA-48, pour lesquelles les CMI des carbapénèmes sont basses, reste controversée. En effet, Maherault *et al.* ont rapporté un cas de bactériémie impliquant une souche de *K. pneumoniae*

OXA-48 (sensible aux carbapénèmes) efficacement traitée par imipénème.²⁶⁷ Cependant, l'efficacité des carbapénèmes est contestée puisque plusieurs échecs thérapeutiques ont aussi été rapportés.^{182,257}

Les céphalosporines de 3^{ème} génération, et en particulier la ceftazidime, peuvent être utilisées dans le traitement des infections dues à des souches productrices de OXA-48 mais ne produisant pas de BLSE. En effet, la ceftazidime n'est pas du tout hydrolysée par OXA-48.²⁶⁸ Cependant, de nombreuses souches productrices d'une carbapénémase de type OXA-48 produisent également une enzyme capable d'hydrolyser les céphalosporines de 3^{ème} génération (BLSE, céphalosporinase plasmidique, céphalosporinase chromosomique déréprimée). En France, environ 75% à 85% des souches de *K. pneumoniae* productrices d'une carbapénémase de type OXA-48 co-produisent une BLSE.

De la même façon, l'aztréonam pourrait être utilisé dans le traitement des infections dues à des MBL. Cependant, il est fréquent qu'une BLSE et/ou une céphalosporinase soit également produite par ces souches, rendant l'aztréonam inutilisable. Les situations d'impasses thérapeutiques sont fréquentes face à des souches produisant des MBLs.

d. Contrôle et prévention des infections

La mise en œuvre des mesures de dépistage et d'isolement est d'autant plus efficace que le diagnostic de colonisation par une EPC est effectué rapidement. Les Précautions d'hygiène Standard (PS) constituent le premier, et parfois le seul, rempart contre la diffusion des micro-organismes. Leur application rigoureuse pour tout patient, quel que soit le lieu de prise en charge, est d'une importance capitale pour la maîtrise de la diffusion de la résistance. Les PS permettent de limiter la transmission croisée, d'assurer une protection systématique des autres patients, des personnels de santé et de l'environnement du soin.

Par ailleurs, des mesures d'hygiène appropriées doivent être appliquées pour tout patient porteur ou infecté par une bactérie multi-résistante aux antibiotiques (modèle SARM ou entérobactérie productrice d'une BLSE), entrant ou séjournant dans une structure de soins.²⁶⁹ L'indication médicale de précautions complémentaires d'hygiène ainsi que l'indication de précautions spécifiques pour la prise en charge de patients porteurs/infectés par des EPC sont

des mesures graduées, pouvant aller jusqu'à la mise en place d'équipes dédiées (Figure 33). Ces mesures sont détaillées dans les recommandations du Haut Conseil de Santé Publique (HSCP) pour la prévention de la transmission croisée des « Bactéries Hautement Résistantes aux antibiotiques émergentes » (BHRé), publiées en juillet 2013.

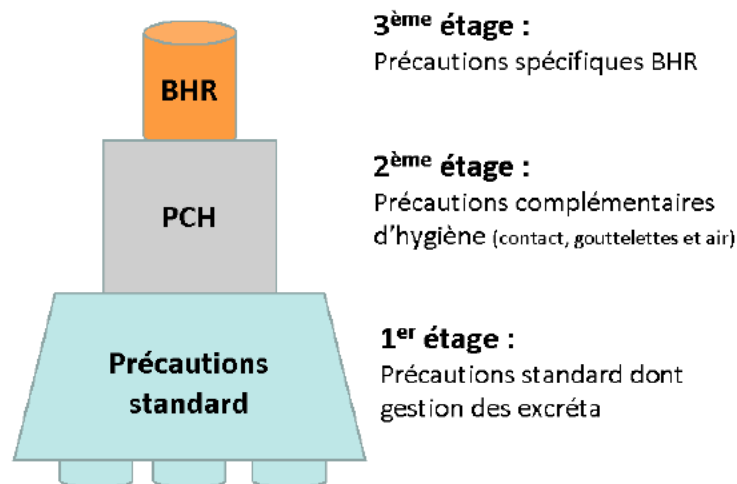


Figure 33. Représentation graphique des différents niveaux de mesures à appliquer Afin de maîtriser la diffusion de la transmission croisée. D'après le rapport du HCSP pour la prévention de la transmission croisée des « Bactéries Hautement Résistantes aux antibiotiques émergentes »

Le respect des précautions particulières BHRé requiert notamment : (i) l'utilisation appropriée d'une blouse et de gants à usage unique par le personnel de santé pour toutes les interactions impliquant un contact avec le patient ou l'environnement du patient ; (ii) l'isolement des patients porteurs dans des chambres individuelles ; (iii) le regroupement cohorting des patients en trois secteurs distincts (patients indemnes, patients dont le statut n'est pas connu et patients infectés ou colonisés avec la BHRé), chaque secteur de soins doit idéalement avoir du personnel dédié nuit et jour et (iv) un usage unique de l'équipement médical non critique ou du matériel médical jetable (par exemple brassards de tensiomètre, stéthoscopes jetables).

Afin de faciliter la mise en œuvre rapide des précautions complémentaires BHRé, seule barrière efficace pour limiter la diffusion des EPC, une surveillance informatisée doit être mise en place pour identifier (i) les patients qui possèdent un historique de colonisation ou d'infection par une BHRé ou (ii) les patients ayant été en contact avec un patient colonisé ou

infecté par une BHRe (patients dits « contacts ») lors de leur réadmission.

D'autres précautions telles que la limitation de l'utilisation de pratiques invasives ou encore la promotion de la politique de bon usage des antibiotiques, sont également très importantes dans la prévention de la dissémination des EPC.

VI. Les inhibiteurs des β -lactamases

Suite à l'émergence exponentielle de β -lactamases, le monde assiste à une nécessité urgente et continue de nouveaux outils thérapeutiques. La première des deux stratégies pour contrer l'action des β -lactamases a abouti à l'impressionnant éventail d'antibiotiques de la famille des β -lactamines décrit ci-dessus. La deuxième stratégie implique la co-administration d'un inhibiteur de β -lactamase (BLI) capable de neutraliser leurs activités.

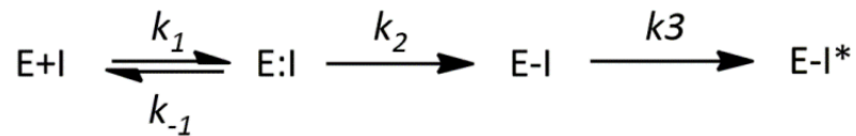
1. Généralité sur les inhibiteurs

Les inhibiteurs peuvent être classés en deux groupes en fonction du type d'inhibition exercée : on parlera d'inhibiteur irréversible ou réversible.

a. Les inhibiteurs irréversibles

Les inhibiteurs irréversibles établissent des fixations covalentes au niveau du site actif de l'enzyme conduisant à son inactivation. Parmi les inhibiteurs irréversibles, on distingue trois groupes : (i) le groupe des inhibiteurs spécifiques qui ciblent des groupements chimiques spécifiques du site actif, (ii) le groupe des inhibiteurs marqueurs du site actif qui ont une structure identique au substrat, (iii) le groupe des inhibiteurs basés sur le mécanisme appelé aussi « substrats suicides ». Ces derniers ont généralement la même structure que le substrat mais contrairement aux inhibiteurs marqueur du site actif, ils doivent être activés par l'enzyme. L'enzyme réagit donc avec l'inhibiteur comme s'il s'agissait du substrat, la réaction catalytique de l'enzyme débute mais se voit inhibée par la formation d'un intermédiaire covalent non dissociable conduisant à l'inactivation de l'enzyme. Les « substrats suicides » de β -lactamases possèdent tout un noyau β -lactame ce qui leur permet d'établir la réaction catalytique et de former une fixation covalente et irréversible au niveau du site actif.

L'équation suivante représente le mécanisme général d'inhibiteurs irréversibles de type « substrats suicides » (I) conduisant à une enzyme inactive (E-I*):



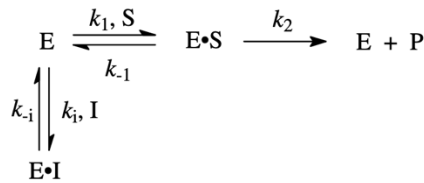
Les inhibiteurs irréversibles sont caractérisés par deux constantes : la constante d'inhibition $K_i (= k_{-1}/k_1)$ qui représente l'affinité de l'enzyme pour l'inhibiteur et la constante d'inactivation $k_{inact} (=k_3)$ qui représente le taux d'inactivation obtenue avec une concentration « infinie » d'inactivateur. Ici, k_2 représente la constante catalytique de l'enzyme.^{270,271} En plus des deux constantes, l'activité d'un inhibiteur peut être aussi évaluée par le turnover de l'enzyme (tn) (équivalent au ratio $[k_{cat}/k_{inact}]$) qui correspond au nombre de molécules inhibitrices hydrolysées par unité de temps avant qu'une molécule d'enzyme soit inactivée de manière irréversible.

La concentration inhibitrice à 50% (CI50) mesure la quantité d'inhibiteur nécessaire pour diminuer l'activité de l'enzyme de 50%. La CI50 ne constitue aucunement un indicateur direct de l'affinité mais peut refléter l'affinité d'un inhibiteur ou le rapport k_{cat}/k_{inact} .

b. Les inhibiteurs réversibles

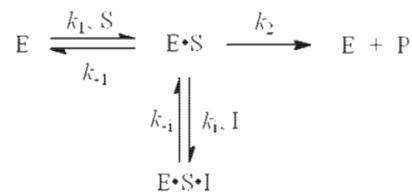
Les inhibiteurs réversibles ne se fixent non pas de façon covalente, comme les inhibiteurs irréversibles, mais établissent des liaisons faibles de type hydrogène, hydrophobes ou ioniques. Ces composés sont impliqués dans un équilibre dynamique et une réduction de leur effet inhibiteur est possible par une simple dilution de l'inhibiteur. Contrairement aux inhibiteurs irréversibles, ces inhibiteurs sont caractérisés uniquement par la constante d'inhibition $K_i (=k_i/k_i)$. Au sein de cette famille, on distingue trois groupes d'inhibiteurs : compétitifs, incompétitifs et non-compétitifs.²⁷²

- Les inhibiteurs compétitifs ont une structure identique au substrat ce qui leur permet de se fixer dans le site actif et, par conséquent, d'entrer en compétition avec le substrat. Le mécanisme de ce type d'inhibiteur est représenté par cette équation :



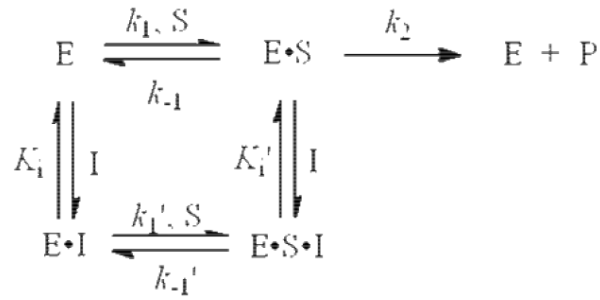
En présence d'un inhibiteur, l'affinité du substrat pour l'enzyme est diminuée, en revanche la vitesse maximale (V_{\max}) reste inchangée. Dans ce type d'inhibition, la CI50 est strictement supérieure au K_i .

- Les inhibiteurs incompétitifs se fixent uniquement sur le complexe enzyme-substrat et forment ainsi un complexe E-S-I. L'inhibiteur, ici, inhibe la formation du produit.



La présence de l'inhibiteur tend à la formation du complexe E-S-I ce qui conduit à une diminution du K_m et de la V_{\max} . Dans ce modèle, la CI50 est également strictement supérieure au K_i .

- Les inhibiteurs non-compétitifs peuvent se lier sur l'enzyme, tout comme le complexe enzyme-substrat. Sa fixation peut provoquer une modification de la structure de l'enzyme empêchant la formation du produit. L'affinité du substrat reste inchangée. En revanche, la vitesse maximale diminue. Ici, la CI50 est égale à la constante d'inhibition.



2. Les premiers inhibiteurs

Les premiers inhibiteurs de β -lactamases à avoir été décrits et utilisés en clinique dans les années 1970 furent l'acide clavulanique et le sulbactam. Le dernier inhibiteur mis sur le marché appartenant à cette classe est le tazobactam décrit au début des années 1980 et approuvé en 1993 (Figure 34).^{273,274} Ces inhibiteurs précoces ont été développés de façon à avoir une structure proche des β -lactamines. La différence avec les β -lactamines est la présence d'un groupement sur l'atome 1 (O ou S) du cycle à cinq atomes : le sulbactam et le tazobactam sont des sulfones, alors que l'acide clavulanique possède un oxygène d'éther d'énol à cette position (Figure 34). Le cycle β -lactame leur permet d'agir comme des « substrats suicides » en formant des intermédiaires stables *via* des fixations covalentes avec l'enzyme. Leurs constante d'inhibition K_i est faible car ils ont la capacité de rester dans le site actif "plus longtemps" que les β -lactamines. C'est pour cela que leur taux d'acylation est élevé tandis que leur taux de désacylation est bas.²⁷⁵ Ces inhibiteurs sont efficaces vis-à-vis de nombreuses β -lactamases de classe A de Ambler telles que les familles CTX-M, TEM, et SHV mais n'ont pas, ou peu, d'effet sur les carbapénèmases de type KPC-2 et aucune activité sur les β -lactamases des classes B, C et D.^{273,276-278}

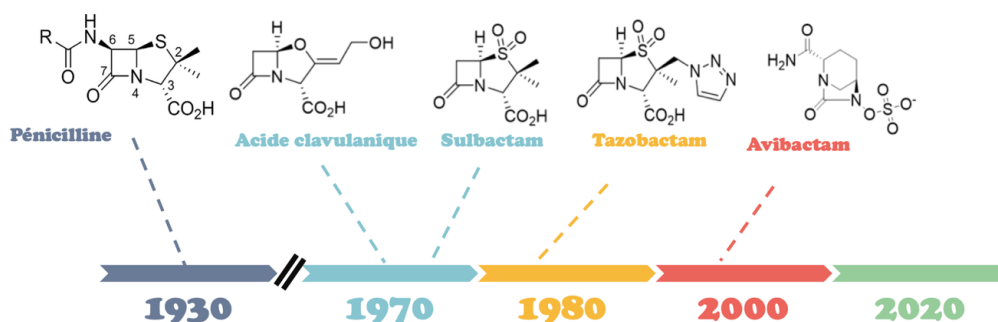


Figure 34. Chronologie de l'apparition des premiers inhibiteurs de β -lactamases et leurs structures

Il est important de souligner, qu'en règle générale, les inhibiteurs n'inactivent pas les PLPs. Cependant, il y existe des exceptions telles que : (i) l'activité du sulbactam contre *Bacteroides* sp., *Acinetobacter* sp. et *N. gonorrhoeae*; (ii) l'activité du clavulanate contre *H. influenza* et *N. gonorrhoeae*; et (iii) l'inhibition des PLPs par le tazobactam chez *B. burgdorferi*.^{273,274,279-284} Néanmoins, comme ces effets d'inhibition directe des PLPs restent négligeables leur utilisation hors combinaison avec une β -lactamine reste inenvisageable en clinique. Ces trois inhibiteurs sont toujours co-administrés avec un antibiotique et sont connus sous les dénominations commerciales suivantes : Augmentin™ (amoxicilline + clavulanate), Timentin™ (ticarcilline + clavulanate), Unasyn™ (ampicilline + sulbactam), Tazocilline™ (pipéracilline + tazobactam), Sulpérazone™ (Céfopérazone +sulbactam) et Zerbaxa™ (ceftolozane + tazobactam). Ces associations permettent donc une inactivation de la β -lactamase par l'inhibiteur en parallèle d'une inactivation de la PLP par la β -lactamine.

a. L'acide clavulanique

L'acide clavulanique, isolé en 1976 à partir de *Streptomyces clavuligeris*,²⁸⁵ possède un cycle oxapénème avec un oxygène en position 1 et une double liaison exocyclique en position 2.²⁸⁵ Cette molécule présente une activité antimicrobienne médiocre mais une excellente activité inhibitrice contre les pénicillinases (β -lactamases de classe A de Ambler).²⁸⁴ Peu de temps après, il a été formulé en association avec l'amoxicilline et commercialisé sous

le nom de Augmentin™. Ce fut un succès pour la prise en charge des patients et il continue d'ailleurs à être largement utilisé dans le traitement d'un grand nombre d'infections.²⁸⁶

Ce composé, qui est un «inhibiteur suicide»,²⁸⁷ agit en synergie avec l'amoxicilline. Il inactive de manière permanente la β -lactamase dans l'espace périplasmique par le biais de différentes réactions chimiques dans le site actif de l'enzyme, permettant ainsi à l'antibiotique associé d'atteindre sa cible.

L'acide clavulanique est efficace contre de nombreux types de β -lactamases de classe A y compris des BLSEs (Tableau 12).²⁸⁷ Les premières études sur la compréhension du mécanisme d'inactivation ont été réalisées sur les β -lactamases de *Staphylococcus aureus* PC1,²⁸⁸ TEM-2,^{289,290} la pénicillinase de *Bacillus cereus*,²⁹¹ et la pénicillinase K1 de *K. oxytoca*. Il a pu être montré que son action était bien plus efficace sur l'enzyme PC1 que TEM-1. En effet, l'inhibition de la β -lactamase TEM-1 survient après une consommation de 160 molécules d'acide clavulanique (Tableau 12), ce qui veut dire qu'il faut au minimum un excès de 100 fois plus d'acide clavulanique pour qu'une inhibition significative soit observée alors que pour la β -lactamase PC1 de *S. aureus* un simple ratio de 1:1 (inhibiteur/enzyme) est suffisant pour inactiver totalement l'enzyme.

Tableau 12. Propriétés cinétiques de différentes β -lactamases. D'après Drawz et al.²⁸⁷

β -lactamase	Classe de Ambler	Acide clavulanique			Subalctam			Tazobactam		
		Ki (μ M)	CI50 (nM)	tn	Ki (μ M)	CI50 (nM)	tn	Ki (μ M)	CI50 (nM)	tn
TEM-1	A	0.1	60	160	1.6	900	10	0.01	97	140
SHV-1	A	1	12	60	8.6	12	13	0.07	150	5
SHV-5	A		20			1,8			80	
PC1	A		30	1		80			27	1
CTX-M-2	A		200			2,1			20	
CcrA	B		>500,000	>500,000		>500,000			400	4
P99	C		>100,000	>500,000		5,6			8.5	50
CMY-2	C	4,365			101			50		
OXA-1	D		1800			4,7		380	1400	
OXA-2	D		1400		0.1	140			10	

L'analyse des structures tridimensionnelles des β -lactamases obtenues à haute résolution a permis de voir les différentes interactions qui pouvaient exister entre une β -lactamase et ces trois inhibiteurs suicides, ce qui a permis d'élucider des mécanismes d'inhibition potentiels. La formation des intermédiaires avec un inhibiteur suicide que ce soit avec le tazobactam, le sulbactam ou l'acide clavulanique dans le site actif, implique les mêmes mécanismes de protonation et de déprotonation pour effectuer les attaques nucléophiles que ceux utilisés avec les β -lactamines. Comme pour les β -lactamines, il y a d'abord formation du premier intermédiaire tétraédrique non-covalent, suivie de la seconde étape qui consiste en la formation d'un acylenzyme où le cycle β -lactame est ouvert. La divergence au niveau des mécanismes d'inactivation et d'hydrolyse des β -lactamines s'effectue à partir de l'acyl-enzyme. La différence majeure qui caractérise ces inhibiteurs est l'ouverture du cycle adjacent au cycle β -lactame à l'intérieur du site actif. L'ouverture de ce cycle empêche l'étape de la déacylation (Figure 35).²⁹²

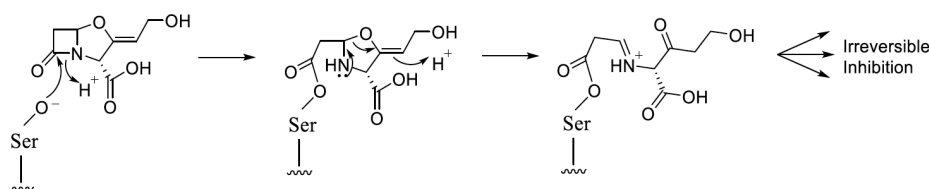


Figure 35. Mécanisme simplifié de l'inhibition des sérine- β -lactamases par l'acide clavulanique. Adapté de Drawz et al.²⁸⁷

Plusieurs acides aminés du site actif contribuent à la fixation de l'inhibiteur.²⁹³ Une des liaisons (C5-C6) de l'acide clavulanique avec l'enzyme subit une rotation d'environ 45° après l'acylation de la part de la sérine 70. Cette rotation cause un changement au niveau d'une liaison entre le substrat et l'inhibiteur. Dans le complexe pré-acyl, la sérine 130 est liée au groupement carboxylate par une liaison de coordination, alors que dans le complexe acylé, la sérine 130 donne une liaison hydrogène au doublet d'électrons libres à l'azote du cycle β -lactame (Figure 36). Ce changement de liaison abaisse l'énergie d'activation du complexe enzyme-inhibiteur au lieu de favoriser l'affinité de l'enzyme envers l'inhibiteur. Malgré cette légère rotation, la proximité qui peut exister entre d'autres atomes de l'inhibiteur et de l'enzyme n'est pas

affectée entre le complexe pré-acyle et acyl. Le groupement carboxylate qui était lié avec la sérine 130 est encore lié à la sérine 235 à l'arginine 244 et à la molécule d'eau 673. La chaîne latérale de l'arginine 244 et le groupement carbonyl de la chaîne principale de la valine 216 chélatent la molécule d'eau 673 qui peut par la suite effectuer une liaison hydrogène avec l'inhibiteur. Suite à la stabilisation de l'inhibiteur dans le site actif, des transferts d'électrons au niveau du cycle clavame s'effectuent, ce qui permet son ouverture et l'inactivation de la β -lactamase.²⁹⁴

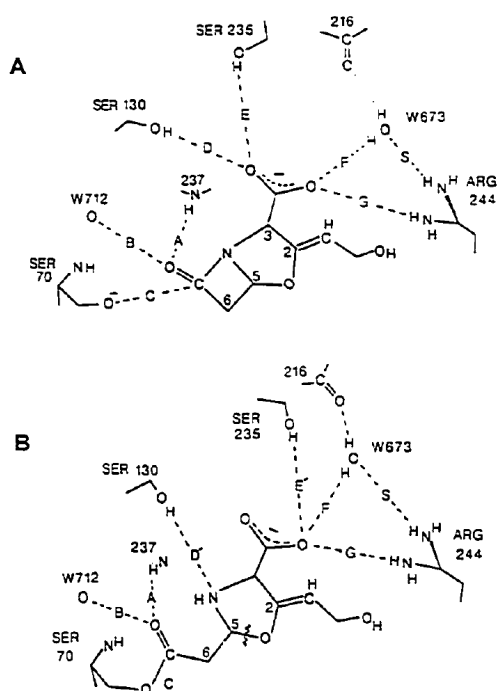


Figure 36. Atomes des acides aminés du site actif d'une β -lactamase de classe A et des molécules d'eau (w) impliqués dans les liaisons hydrogènes avec les atomes de l'acide clavulanique. A. Forme pré-acylée ; B. Complexe acyle avec le cycle β -lactame ouvert. D'après Imitiaz et al.²⁹³

b. Le sulbactam

Le sulbactam, un acide pénicillanique sulfone, est un inhibiteur semi-synthétique et possède un atome de soufre en position 1 au lieu d'un oxygène comme l'acide clavulanique. Son mécanisme d'action est similaire à celui de l'acide clavulanique. Cependant, il inhibe moins bien certaines β -lactamases comme TEM-1 (avec un turn over (tn)) de 10 000 alors que celui de l'acide clavulanique est de 160), SHV-1 et CTX-M-2 (Tableau 12). Il présente, à l'inverse de l'acide clavulanique, une très légère activité contre les céphalosporinases (Classe C de

Ambler). Une étude sur la β -lactamase TEM-2 avait montré que le groupement sulfoné du sulbactam formait un complexe inhibant de manière transitoire l'enzyme.²⁹⁵ Plus récemment, une étude a décrit des efficacités catalytiques relativement élevées pour l'hydrolyse du sulbactam par SHV-5 et TEM-1.²⁹⁶ Ces observations indiquent que le sulbactam est à la fois un inhibiteur et un vrai substrat pour certaines enzymes.

c. *Le tazobactam*

Le tazobactam dérive du sulbactam. La différence entre ces deux composés se situe au niveau de la chaîne latérale 2 (R2) où on retrouve deux groupements méthyles pour le sulbactam et un cycle triazolé pour le tazobactam (Figure 34). Le cycle triazolé contient trois atomes d'azotes qui sont plus réactifs chimiquement que les deux groupements méthyles du sulbactam ce qui permettrait de favoriser certaines interactions avec d'autres atomes du site actif.²⁹⁷ Cette modification conduit à l'amélioration de la CI50 du tazobactam, et à une diminution des valeurs de CMI pour les β -lactamases de classe A mais également de celles de classe C telles que les enzymes P99 et CMY-2 (Tableau 12).^{276,298,299}

Depuis sa découverte, il a toujours été associé avec la pipéraciline, mais depuis 2014 un nouveau médicament le Zerbaxa™ a vu le jour. Ce médicament résulte de l'association d'une nouvelle céphalosporine, le ceftolozane, structurellement similaire à la ceftazidime, avec le tazobactam. Il a été approuvé pour le traitement d'infections intra-abdominales et urinaires compliquées et des infections des voies respiratoires. Le ceftolozane – tazobactam (C-T) est sensible à l'hydrolyse par les enzymes de type carbapénémases mais n'est pas affecté par d'autres mécanismes de résistance tels que les pompes à efflux et la perte de porines. Le Zerbaxa™ possède une activité *in vitro* significative contre les espèces de *Streptococcus*; cependant, comme la ceftazidime, le C-T a une activité réduite vis-à-vis de *S. aureus*.^{300,301} Ce composé présente une activité contre les entérobactéries productrices de BLSEs (essentiellement *E. coli* BLSE), mais sa particularité est son action significative contre les souches de *P. aeruginosa* multirésistantes (Tableau 13).³⁰²

Tableau 13. Sensibilité des bacilles à Gram négatif face au Ceftolozane-Tazobactam. D'après Cluck et al.³⁰⁰

Organismes	MIC90 (µg/mL)			
	Ceftolozane–Tazobactam	Ceftazidime	Céfépime	Méropénème
<i>Enterobacter cloacae</i>	8.00	>32.00	2 à 8	≤0.06
<i>Enterobacter cloacae</i> Ceftazidime-résistant	>16.00	>64.00	>16.00	0.25
<i>Escherichia coli</i>	0.50	8.00	4.00 à >16.00	≤0.06
<i>Escherichia coli</i> phénotype BLSE	4.00	>32.00	>16.00	≤0.12 à >8.00
<i>Klebsiella pneumoniae</i>	8 à >32	≥32.00	>16.00	≤0.06 à 2
<i>Klebsiella pneumoniae</i> phénotype BLSE	>16 à >32	>32 à >64	>16.00	≤0.12 à >8
<i>Klebsiella pneumoniae</i> KPC	>16	>64	>16	>8
<i>Proteus mirabilis</i>	0.50	32.00	≤0.50	≤0.06
<i>Proteus mirabilis</i> phénotype de BLSE	8.00	>64.00	>16.00	≤0.12
<i>Pseudomonas aeruginosa</i>	1 à >32	32	16	8
<i>Pseudomonas aeruginosa</i> Ceftazidime-résistant	4–16	256	64	32
<i>Pseudomonas aeruginosa</i> Méropénème-resistant	4–8	>32	>16	32

MIC90 : Concentration inhibitrice pour une mort de 90% des isolats,

Comme décrit précédemment, l'efficacité de ces trois inhibiteurs (acide clavulanique, subactam et tazobactam) peut varier selon l'enzyme (Tableau 12). Par exemple, SHV-1 est plus résistant à l'inactivation par le sulbactam que TEM-1 mais plus sensible à l'inactivation par le clavulanate.³⁰³ Les études comparatives de TEM et des enzymes dérivées de SHV, y compris les BLSE, ont montré que les CI50 du clavulanate étaient 60 et 580 fois plus basses que celles pour le sulbactam contre TEM-1 et SHV-1, respectivement.³⁰³ Les différences d'inactivation peuvent s'expliquer par une structure différente des sites actifs des enzymes. En effet, une étude structurale de TEM-1 et SHV1 a révélé que la distance entre la Val216 et Arg244 (résidus responsables du positionnement de la molécule d'eau important dans le mécanisme d'inactivation du clavulanate) était deux fois plus grande pour l'enzyme SHV-1.³⁰⁴ Cette distance peut être trop grande pour la coordination d'une molécule d'eau, ce qui suggère que la molécule d'eau devrait être positionnée ailleurs dans SHV-1 et plus précisément au niveau du site actif. Cette variation souligne donc l'idée que le mécanisme de ces inhibiteurs peut avoir une inactivation différente même avec des enzymes très similaires.^{304,305}

Ces agents constituaient un progrès révolutionnaire permettant de revigorer et d'élargir à la fois le spectre et la longévité des antimicrobiens disponibles, et il a été longtemps considéré que ces inhibiteurs constituaient une approche thérapeutique idéale en raison de leur efficacité (qui reste néanmoins limitée à un sous ensemble de la classe A) et de leur bonne tolérance. Cependant, l'enthousiasme de la communauté scientifique a diminué en raison de l'émergence et de la propagation mondiale de gènes codant pour des β -lactamases ayant un spectre d'hydrolyse de plus en plus large. C'est dans ce contexte que de nombreuses études ont été entreprises afin de développer de nouveaux inhibiteurs.

3. Les nouveaux inhibiteurs

Le développement de nouveaux inhibiteurs est une tâche complexe car, comme décrit précédemment, un même inhibiteur n'a pas forcément le même effet sur différentes β -lactamases même issues de la même classe. De plus, la plupart des bactéries à Gram négatifs MDR possède plusieurs β -lactamases. Les MBLs et les CHDLs constituent le défi le plus difficile. En effet, les MBLs possèdent un mécanisme non covalent dépendant d'ions Zn^{2+} , alors que la classe des OXA est extrêmement hétérogène avec plus de 800 variants. De plus, le mécanisme hydrolytique des OXAs est différent des autres mécanismes à sérine active. Il en découle que le développement de pan-inhibiteurs de carbapénèmases, c'est à dire capable d'inhiber les carbapénèmases des trois classes (A, B et D), s'avère encore plus complexe. Cependant, depuis la découverte de l'acide clavulanique, de nouveaux inhibiteurs ont vu le jour dont le plus connu est l'avibactam (NXL-104). Il appartient à la famille des diazabicyclooctanones (DBO).

a. Les diazabicyclooctanones (DBO)

Les DBO sont des inhibiteurs synthétiques des β -lactamases découverts au début des années 2000. Ce sont de petites molécules (Figure 37) mimant la structure du cycle β -lactame. Cependant, ils sont structurellement différents des β -lactamines, ce qui leur permet d'échapper au mécanisme de résistance des inhibiteurs de β -lactamase.³⁰⁶ Les DBO sont des inhibiteurs réversibles qui possèdent une activité contre les enzymes de classe A et C ainsi que certaines de classe D, mais dans une moindre mesure. Cette classe de composés s'est fortement développée ces dernières années. La plupart des modifications se produisant au

niveau de la chaîne latérale C2 (Figure 37), permettant la sélection de plusieurs composés prometteurs : l'avibactam, le relebactam et le zidébactam.

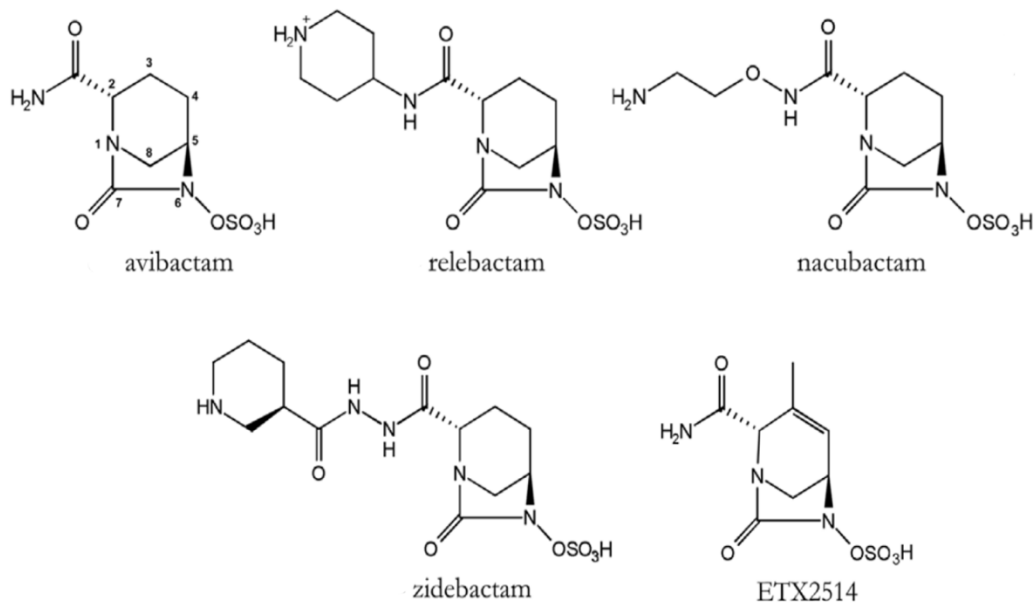


Figure 37. Structures des inhibiteurs réversibles de la famille des diazabicyclooctanones (DBOs). D'après Docquier et al³⁰⁷.

i. L'avibactam

L'avibactam (anciennement NXL104) est le premier inhibiteur novateur à recevoir l'approbation de la Food and Drug Administration (FDA) en combinaison avec la ceftazidime. L'association ceftazidime-avibactam CAZ-AVI (Avycaz™ aux Etats-Unis et Zavicefta™ en Europe) a été approuvée en février 2015 pour le traitement des infections compliquées des voies urinaires et intra-abdominales. L'avibactam s'est avéré être un puissant inhibiteur des β -lactamases, dont le spectre d'inhibition est bien plus vaste que celui de l'acide clavulanique. En effet, l'avibactam inhibe efficacement la plupart des β -lactamases de classe A (y compris les BLSEs), les enzymes de classe C (AmpC) aussi bien chromosomiques que plasmidiques, et plusieurs β -lactamases de classe D. La grande révolution vient du fait que l'avibactam est capable d'inhiber des carbapénémases de la classe A (type KPC) et D (OXA-48 like à l'exception des OXA carbapénémase de *Acinetobacter* comme OXA-23, -40 ou -58).^{306,308-312}

L'association CAZ-AVI possède un large spectre d'activité (Tableau 14). Le seuil clinique de sensibilité a été fixé par le CLSI et l'EUCAST à 8 mg/L avec une concentration fixe d'avibactam de 4 mg/L pour les entérobactéries et *P. aeruginosa*. Une étude *in vivo* menée aux États-Unis sur 20 000 souches cliniques, a montré que seuls 11 isolats présentaient une CMI de CAZ-AVI supérieure à 8 mg/L. Sur les 11 souches résistantes, deux exprimaient une MBL, intrinsèquement résistantes à l'inhibition de l'avibactam.³¹³ Cela met en évidence une limitation essentielle de l'avibactam en ce sens qu'il n'est pas actif contre les métallo- β -lactamases. Pour pallier ce problème, l'association de l'avibactam avec l'aztréonam a été envisagée car l'aztréonam n'est pas hydrolysée par les MBLs. A l'heure actuelle, ce composé fait l'objet de nombreuses études cliniques. Une étude rétrospective chez l'homme a été réalisée chez 14 patients atteints de diverses infections graves causées par *K. pneumoniae* (12), *E. cloacae* (1) et *P. aeruginosa* (1) productrices de NDM-1 et OXA-48.³¹⁴⁻³¹⁶ L'administration de la CAZ-AVI plus de l'aztréonam a conduit à la guérison de 10 patients, à 3 décès dus à un échec thérapeutique et à 1 récurrence.

Il existe une autre association : avibactam plus la ceftaroline fosamil, une céphalosporine de 5^{ème} génération. L'ajout d'avibactam à cette β -lactamine étend son spectre d'activité antimicrobien contre les infections causées par les entérobactéries, y compris celles productrices de BLSE, de KPC et d'AmpC.^{317,318} Une étude a montré l'efficacité de cette association sur des souches de *E. coli* exprimant des gènes codant pour des β -lactamases. Dans cette étude, 29 souches sur 34 étaient résistantes à la ceftaroline (avec des CMI comprises entre 2 et > 64 mg/L), l'ajout d'avibactam a permis une diminution importante des CMIs (comprises entre 0,06 et 0,5 mg/L).³¹⁷

Tableau 14. Nouveaux inhibiteurs dirigés contre des β -lactamases produites par les bacilles à Gram négatif. D'après Karaïskos et al.³¹⁹

Antibiotic	Spectrum	Clinical Development program (since 2018)	Dosage
Ceftazidime-Avibactam	Activity against: Enterobacteriaceae and <i>P. aeruginosa</i> producing ESBL, KPC, AmpC and some class D enzymes (OXA-10, OXA-48) No active against MBL, <i>Acinetobacter</i> spp, and less activity against anaerobes	Approved in 2015 in U.S.A and in 2016 in Europe	CrCl >50: 2.5g q8h CrCl: 31–50: 1.25g q8h CrCl: 10–30: 0.94 g q12h CrCl <10: 0.94g q48h Hemodialysis: 0.94 g q48h (administer after hemodialysis session) CVVH: 1.25g q8h All doses administered over 2 hours
Meropenem-Vaborbactam	Activity against: Enterobacteriaceae producing ESBL, KPC, AmpC. No active against OXA-48-like, or MBL. As active as meropenem alone against <i>P. aeruginosa</i> , <i>Acinetobacter</i> spp., and <i>S. maltophilia</i>	Approved in 2017 in U.S.A	CrCl >50: 2g q8h CrCl: 30–49: 2g q8h CrCl: 15–29: 2g q12h CrCl <15: 1g q12h Hemodialysis: 1g q12h (administer after hemodialysis session) All doses administered over 3 hours
Aztreonam-Avibactam	Activity against: Enterobacteriaceae producing ESBL, KPC, AmpC, OXA-48 and MBL. As active as Aztreonam alone against <i>P. aeruginosa</i> and <i>A. baumannii</i> , including MBL-producing isolates	Phase 3	CrCl > 50: ATM 6g/AVI 2g CrCl: 31–50: ATM 3g/AVI 1 g CrCl: 16–30: ATM 2025 mg/AVI 675 mg
Imipenem/cilastatin-Relebactam	Activity against: Enterobacteriaceae and <i>P. aeruginosa</i> producing ESBL, KPC, AmpC and porin mutations. Diminished inhibitor activity against OXA-48. No activity against MBL and <i>A. baumannii</i>	Phase 3	IMI-REL 200/100 mg to 500/250 mg, depending on renal function, q6h All doses administered as a 30-minute infusion
Ceftaroline fosamil-Avibactam	Activity against: Enterobacteriaceae producing ESBL, KPC, Amp C and some class D enzymes (OXA-like). No activity against MBL. No activity against <i>A. baumannii</i> or <i>P. aeruginosa</i> .	Phase 2	CPT 600 mg/AVI 600 mg q8h or q12h is under investigation
Cefepime-Zidebactam	Activity against Enterobacteriaceae and <i>P. aeruginosa</i> producing ESBL, KPC, AmpC and MBL	Phase 2	N/A
Meropenem-Nacubactam	Activity against class A and class C β -lactamases	Phase 1	N/A

ATM, aztreonam; AVI, avibactam; CAZ-AVI, ceftazidime-avibactam; CPT, ceftaroline fosamil; CrCl, creatinine clearance (ml/min); CVVH, continuous veno-venous hemofiltration; ESBL, extended-spectrum beta-lactamases; IMI-REL, imipenem/cilastatin/relebactam; KPC, Klebsiella pneumoniae carbapenemase; MBL, metallo- β -lactamase; N/A, non-applicable; OXA, oxacillinase; q6h, every 6 h; q8h, every 8 h; q12h, every 12 h; q48h, every 48 h.

Des études de biophysique et de cristallographie ont permis de comprendre le mode d'action de l'avibactam. Il a été démontré que l'avibactam exerce ses propriétés d'inhibition selon un processus en deux étapes. Il existe une fixation initiale non covalente, suivie d'une acylation covalente au niveau de la sérine active de la β -lactamase (Figure 38).^{320,321}

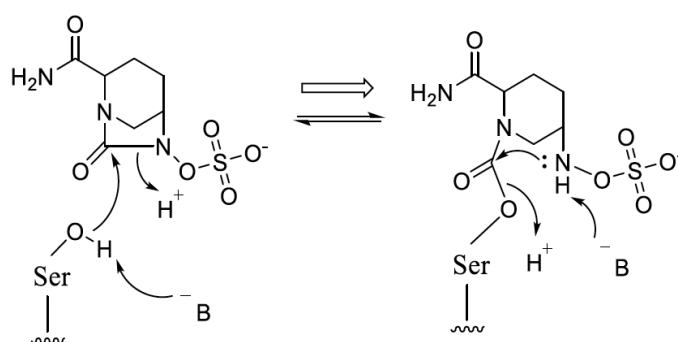


Figure 38. Mécanisme simplifié de l'inhibition des sérine- β -lactamases par l'avibactam. Adapté depuis Ehmann et al.³⁰⁸

La caractéristique de l'avibactam, par rapport aux anciens inhibiteurs, est qu'il se lie de manière réversible aux β -lactamases, permettant ainsi la régénération lente de l'avibactam par recyclisation et donc l'inhibition de β -lactamases supplémentaires. Ce mécanisme a été validé sur un grand panel de β -lactamases telles que TEM-1, CTX-M-15, KPC-2 (classe A), l'AmpC de *Enterobacter cloacae* P99, l'AmpC de *P.aeruginosa* PAO1 (classe C), OXA-10 et OXA-48 (classe D). Il est considéré comme un mécanisme général d'inhibition par l'avibactam.³⁰⁸ Cependant, dans le cas d'une inhibition de KPC-2, il a été constaté une légère hydrolyse de l'avibactam.³⁰⁸ La détermination des CI50 a révélé que l'avibactam est bien plus efficace contre TEM-1, SHV-4 et CTX-M-15 (Tableau 15) que sur KPC-2.³²⁰

Tableau 15. Comparaison des concentrations inhibitrices à 50% de différents inhibiteurs sur différentes β -lactamases. D'après Stachyra et al.³²⁰

Enzymes	CI 50 (μ M)			
	Ac clavulanique	Tazobactam	Subalctam	NXL104
Classe A				
TEM-1	0.058	0.032	1.56	0.008
CTX-M-15	0.012	0.006	0.23	0.005
KPC-2	>100	50	57	0.170
SHV-4	0.004	0.055	0.26	0.003
Classe C				
P99	>100	1.3	21.1	0.1
AmpC	>100	4.6	27	0.128

Les études cristallographiques de différentes β -lactamases couplées à l'avibactam ont montré que la molécule d'avibactam liée à la sérine catalytique, dans laquelle l'oxygène carbonyle est situé dans le trou oxyanion, crée un réseau d'interactions très semblables à celui de la β -lactamine.^{308,322,323} Le fragment sulfonate interagit avec les résidus du motif KTG conservé, tandis que la chaîne latérale du carboxamide est stabilisée par des interactions avec les résidus Asn / Gln qui se trouvent essentiellement dans le motif conservé SxN présent dans la boucle oméga Ω (Figure 39). La présence de deux atomes d'azote dans l'inhibiteur permet à ces atomes d'interagir avec des résidus indispensables pour la catalyse. L'atome d'azote (N6) interagit avec les résidus conservés de la sérine 130 (classe A) ou de la tyrosine 150 (classe C).

Un réseau d'interaction similaire est partiellement trouvé dans les enzymes de classe D, bien que la nature globalement plus hydrophobe des résidus définissant la poche du site actif empêche la chaîne latérale du carboxamide d'être stabilisée par des interactions polaires (figure 39. B). En outre, il a été montré que la liaison de l'avibactam dans la carbapénèmase OXA-48 induisait le déplacement de certains résidus, notamment des résidus isoleucine 102, valine 120 et thréonine 213.

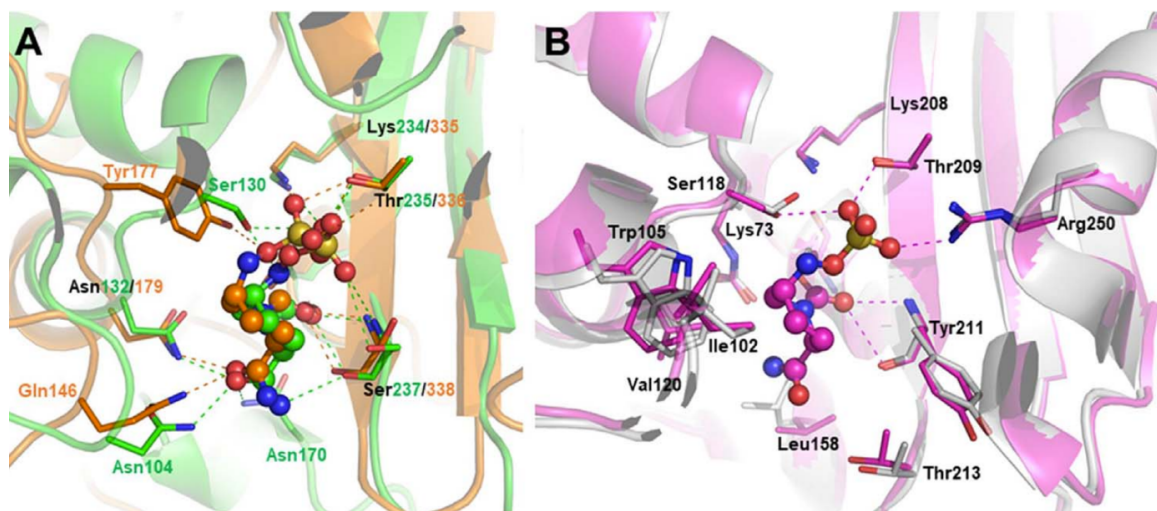


Figure 39. Interaction de l'avibactam avec différentes β -lactamases. A. superposition de la β -lactamase de classe A CTX-M-15 (vert) et de classe C AmpC (orange) inhibée par l'avibactam. B. Interaction de de l'avibactam lié à la carbapénèmase de classe D, OXA-48 (magenta); la position des résidus du site actif dans l'enzyme native (blanc, PDB: 3HBR) est également montrée. L'inhibiteur (représenté sous forme de sphère et de bâtonnet) est lié de manière covalente à la sérine catalytique enzymatique et interagit avec de nombreux résidus conservés sur le plan fonctionnel, fournissant une base structurale à la fois pour son large spectre d'inhibition et son mécanisme réversible. D'après Docquier et al.³⁰⁷

Depuis l'utilisation en clinique de l'avibactam, on commence à observer l'émergence d'entérobactéries productrices de β -lactamases résistantes à ce composé tels que certains variants de SHV-1, CTX-M-15 et KPC-2.^{324,325} Concernant la carbapénèmase KPC-2, il semblerait que les résidus 164 et 179, situés au niveau de la boucle oméga, et ceux proches du motif KTG (Val240Gly, Thr243Met, Figure 40) jouent un rôle crucial car leur substitution conduit à une augmentation des CMI de CAZ-AVI.³²⁶ Cependant, il semblerait que la perte de sensibilité au CAZ-AVI serait due à une augmentation de l'efficacité catalytique de la ceftazidime, l'avibactam inhiberait toujours mais son action deviendrait négligeable.

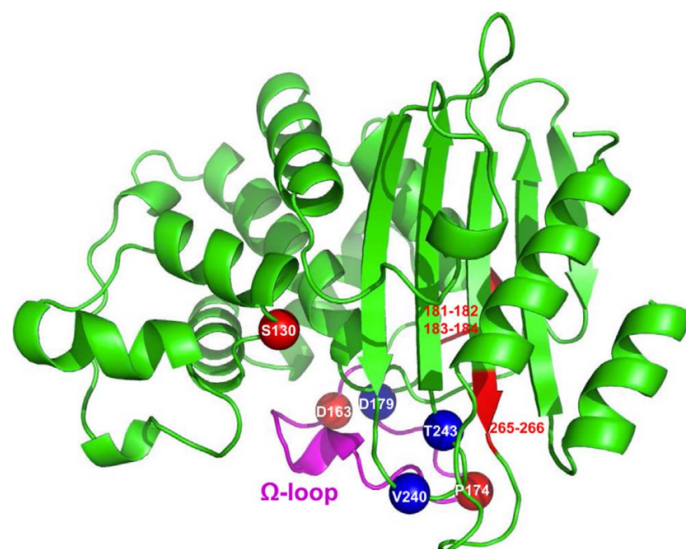


Figure 40. Structure tridimensionnelle des carbapénémases de type KPC, indiquant la position des résidus impliqués dans la résistance à la combinaison de ceftazidime et d'avibactam. Les sphères bleues représentent les positions de substitutions naturelles ; et les sphères rouges les positions des substitutions ou insertions de variants identifiés *in vitro*.

ii. Le relebactam

Relebactam (MK-7655) est structurellement proche de l'avibactam, il diffère par l'ajout d'un cycle pipéridine sur le groupe carbonyle en position 2 (Figure 37).^{327,328} Le mécanisme d'action, ainsi que le spectre d'inhibition, semblent être similaires à celui de l'avibactam. Il inhibe, tout comme l'avibactam, les β -lactamases de classe A et C mais semble avoir un effet moindre contre les enzymes de classe D.³²⁹ Une étude *in vitro* a permis de montrer que le relebactam améliore significativement l'activité de l'imipénème contre les entérobactéries productrices de BLSEs (réduction de la CMI de 2 à 16 fois) et celles produisant une carbapénémase de type KPC (réduction de la CMI de 32 à 128 fois).³²⁹ L'ajout de relebactam a montré un bénéfice significatif en améliorant l'activité de l'imipénème contre *P. aeruginosa* résistant à l'imipénème due à une hyper production de l'AmpC associée à la perte de la porine OprD.³³⁰⁻³³² Cependant, aucun avantage n'a été constaté contre *A. baumannii*.^{331,333,334} Enfin, une activité inhibitrice diminuée a été observée contre les isolats à Gram négatif produisant OXA-48,^{327,332} et aucune activité contre les souches exprimant des MBLs.³³⁰

Il est actuellement en cours d'évaluation (phase III d'essais cliniques) pour une utilisation avec imipenem-cilastatin pour le traitement des infections bactériennes à Gram négatif.^{330,331} Il s'avère que l'imipénème est un excellent partenaire pour le relebactam contre *P. aeruginosa* dans la mesure où, contrairement aux autres β -lactamines, il échappe à l'efflux particulièrement présent chez cette espèce bactérienne.³³⁰

iii. Autres DBOs

Au sein de la grande famille des DBOs, d'autres molécules sont en cours de développement comme potentiels outils thérapeutiques.

Le nacubactam (OP0595, Figure 37) présente un groupe 2-aminoéthoxy sur le carboxamide. Des tests enzymatiques ont permis de montrer qu'il inhibe les β -lactamases de type TEM, CTX-M, KPC-2 (classe A), AmpC et CMY-2 (classe C) avec des valeurs de CI50 de l'ordre du nano molaire. Cet inhibiteur a montré une activité relativement faible contre les enzymes OXA et aucune contre les MBLs. Il inhibe également la PLP2, lors de l'incubation avec une souche de *E. coli*, la formation de cellules sphériques a pu être constaté, ce qui signe une inhibition de la PLP2.³³⁵ Combiné à des β -lactamines telles que l'aztréonam, le céfépime ou encore la pipéraciline, le nacubactam serait plus efficace que le CAZ-AVI vis-à-vis des entérobactéries productrices de carbapénémases.³³⁶ A ce jour, des essais cliniques évaluent son innocuité.

Le zidébactam (Figure 37) possède une activité similaire au nacubactam, avec également une inhibition spécifique pour la PLP2 de *P. aeruginosa* PAO1.³³⁷ Il est actuellement développé en association avec le céfépime. D'après les nombreuses études menées, il semblerait que cette association soit active *in vitro* contre des souches de *K. pneumoniae* productrice de KPC, mais surtout de NDM-1 ou d'autres MBLs.³³⁸ Le céfépime-zidebactam serait également actif contre les MBLs de type IMP et VIM de *P. aeruginosa*.³³⁸

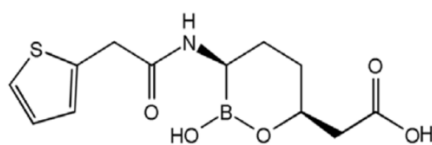
Un autre composé de la famille des DBOs, le ETX2514 (Figure 37) a démontré un très large spectre d'inhibition comprenant les β -lactamases de classe A, C et D mais également la PLP2.^{339,340} Ce composé a été conçu *via* des modifications de l'avibactam ayant pour objectif d'obtenir un panel d'inhibition plus large vis-à-vis des OXA de *Acinetobacter*. L'introduction d'une double liaison endocyclique et un groupement méthyle (en C-3) a permis d'augmenter sa réactivité chimique avec, pour conséquence, une inhibition de OXA-24 de *A. baumannii*.³³⁹

Le composé ETX2514 présente également une inhibition de la PBP2 tout en maintenant une activité inhibitrice vis-à-vis des β -lactamases, avec une activité antibactérienne intrinsèque contre les entérobactéries (MIC90, 1–8 μg / ml, sur des isolats de *E. coli* et *K. pneumoniae*).^{339,341} L'ETX2514 a été conçu de manière rationnelle pour améliorer sa réactivité vis-à-vis des β -lactamases et sa diffusion à travers la membrane externe des Gram négatif, sans affecter sa stabilité. En comparaison avec le relebactam ou le nacubactam, ETX2514 montre un effet plus rapide et plus efficace sur toutes les sérine- β -lactamases testées, avec une amélioration importante sur les β -lactamases de classe D, y compris la carbapénèmase OXA-24 de *Acinetobacter*. La combinaison sulbactam-ETX2514 a montré une bonne efficacité *in vitro* contre des souches de *A. baumannii* résistantes aux carbapénèmes, à la ceftazidime, à l'aztréonam et au sulbactam, avec des valeurs de CMI90 de 4 $\mu\text{g}/\text{ml}$. L'activité intrinsèque modérée du sulbactam sur *Acinetobacter* sp.,³⁴² associée à la double inhibition de β -lactamases et de la PBP par ETX2514, peut expliquer l'excellente activité de leur association contre *A. baumannii*, un pathogène nosocomial souvent résistant à de nombreux antibiotiques.³³⁹

b. Composé boronique : le vaborbactam

Dans les années 1970, les acides boroniques étaient décrits comme de puissants inhibiteurs des sérines protéases et ont donc suscité un intérêt clinique.^{343,344} Les boronates ont une haute affinité pour les sérines hydrolases, et se fixent de façon covalente et réversible aux β -lactamases mais ne sont pas hydrolysés.³⁴⁵ Il s'agit d'inhibiteurs compétitifs ce qui est, en soit, un nouveau mécanisme par rapport aux anciens inhibiteurs disponibles en clinique.

Le vaborbactam (RPX7009, Figure 41) est le premier inhibiteur de β -lactamase appartenant à la famille des boronates approuvé par la FDA en association avec le méropénème (Vabomere™) en 2017 pour le traitement des infections urinaires compliquées. La conception du vaborbactam est le résultat des efforts de la chimie médicinale pour développer un analogue de boronate cyclique ciblant spécifiquement les β -lactamases et non les sérines hydrolases des mammifères.



vaborbactam (RPX7009)

Figure 41. Structure chimique du Vaborbactam (RPX7009)

Les études cristallographiques et enzymatiques du vaborbactam ont montré qu'il forme un lien covalent avec la sérine catalytique de CTX-M-15 et AmpC et qu'il présente des valeurs de CI_{50} pour certaines β -lactamases de classe A et C de l'ordre du nM.³⁴⁵

L'étude *in vitro* de la combinaison vaborbactam-méropénème a été testée contre plus de 300 isolats cliniques d'entérobactéries, dont la plupart était porteuses du gène *bla*_{KPC}. L'incubation du vaborbactam (à 8 mg/L) avec du méropénème a renforcé l'effet de la β -lactamine d'au moins 64 fois.³⁴⁶ Toutefois, le vaborbactam n'a pas réduit la CMI du méropénème vis-à-vis des souches exprimant les MBLs (classe B) ou les OXA-48 (classe D).³⁴⁷ Enfin, il a pu être montré que cet inhibiteur n'a pas d'effet sur les souches de *A. baumannii* et de *P. aeruginosa*, cela serait la conséquence de mécanismes alternatifs de résistance, tels que les altérations de porines et l'efflux du médicaments.³⁴⁸

Pour identifier un composé capable d'inhiber les MBLs, un criblage important de composés boroniques a été réalisé.³⁴⁹ Ainsi, des boronates cycliques (Figure 42) présentant une activité inhibitrice contre les enzymes SBLs, les PLPs, et surtout MBLs, ont été identifiés. Parmi eux, un composé déjà breveté possède une forte inhibition envers les trois classes d'enzymes.³⁵⁰ Il permet de rétablir l'activité du méropénème vis-à-vis des bactéries à Gram négatif portant à la fois les gènes codant pour des SBLs et des MBLs.³⁴⁹

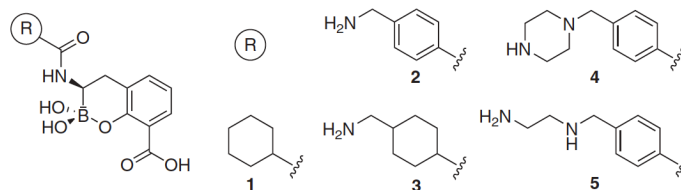


Figure 42. Structure chimique de boronates bicycliques. D'après Brem et al.³⁴⁹

De nos jours, ce sont les inhibiteurs les plus prometteurs. En effet, ils peuvent être considérés comme des pan-inhibiteurs car ils ont une action à la fois sur les SBLs les MBLs. Le spectre d'inhibition de ces composés est très vaste, il a pu être montré une action sur les β -lactamases de classe A (TEM-1, CTX-M-15, KPC-2), de classe C (AmpC), de classe D (OXA-10, OXA-23 et OXA-48) et enfin de classe B (NDM-1, VIM-2, IMP-1, BclI, CphA, et SPM-1).^{349,351} Ces inhibiteurs compétitifs ont la particularité de mimer l'intermédiaire tétraédrique durant l'hydrolyse du noyau β -lactame des substrats sans être hydrolysé (Figure 43).³⁵² Son activité contre la PLP5 lui confère également une activité antimicrobienne intrinsèque.

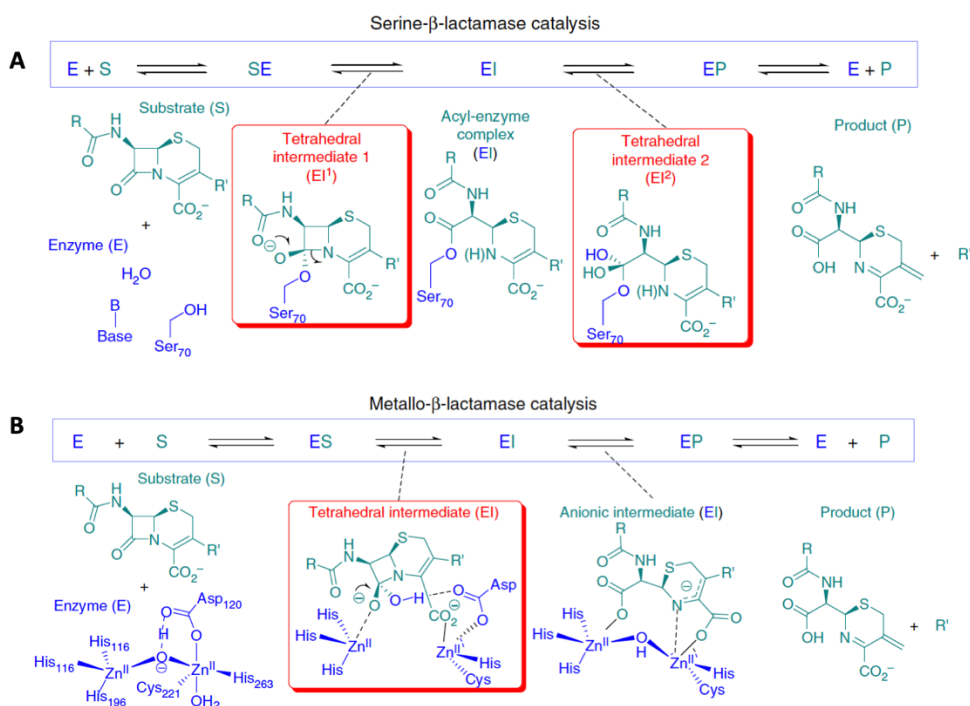


Figure 43. Mode d'action des boronates cycliques. A. Description du mode d'action sur les SBLs ; B. Description du mode d'action sur les MBLs. D'après Brem et al.³⁴⁹

Il a pu être montré que les CI50 obtenues avec des dérivés d'acides boroniques cycliques avaient un effet plus important sur TEM-1 par rapport aux autres β -lactamases de classe A mais aussi de classe C et D. Par exemple, une CI50 de 1,3nM a été retrouvée pour TEM-1 versus 13 ; 9,8 ; 250 et 160 nM pour les enzymes CTX-M-15, AmpC, OXA-23 et OXA-48.³⁵¹ Concernant les valeurs des CI50 pour les MBLs, elles sont de l'ordre du micromolaire.³⁴⁹

c. Les inhibiteurs de Métallo- β -lactamases

L'Introduction en clinique des DBOs et du vaborbactam a augmenté considérablement les options de traitement pour les infections sévères liées aux bactéries à Gram négatif. Cependant, aucun de ces composés n'est efficace contre les enzymes de classe B. Ainsi, le défi majeur actuel reste la conception de nouveaux inhibiteurs capables d'inhiber les MBLs. Car, en effet, certaines MBLs de type NDM, VIM et IMP disséminent rapidement au sein des entérobactéries, constituant un problème de santé publique considérable.

Les MBLs sont caractérisées par un spectre d'hydrolyse le plus vaste, pouvant hydrolyser toutes les β -lactamines à l'exception des monobactames (l'aztréonam).^{353,354} La difficulté à trouver un inhibiteur «universel» des MBLs provient de la structure et des mécanismes différents entre les 3 sous-classes de MBLs (classées sur la base de la similarité structurelle).^{354,355} Les MBLs contiennent 1 ou 2 ions zinc dans le site actif qui est peut être stabilisé par des histidines, une cystéine et l'aspartate (suivant la sous classe des MBLs). Toutes les MBLs partagent une structure commune de type $\alpha\beta\beta\alpha$. Ce motif protéique est largement répandu dans le domaine du vivant, aussi bien chez les bactéries que chez les eucaryotes. Ce motif est caractéristique d'une superfamille de métallo-enzymes dinucléaires catalysant une variété importante de réactions.³⁵⁴ Les inhibiteurs de MBLs peuvent être regroupés en fonction de leurs mode d'action : (i) inhibition par fixation aux ions zinc (déplacement de l'interaction enzyme/ion Zinc), (ii) inhibition par chélation des ions zinc et (iii) inhibition par fixation covalente (Tableau 16, Figure 44).

Tableau 16. Listes des inhibiteurs de MBLs en fonction des mécanismes d'actions. Adapté de JU et al.³⁵⁶

Mécanisme inhibition	Noms des inhibiteurs
Inhibition par fixation aux ions zinc (déplacement de l'interaction enzyme/ion Zinc) Fixation formant un complexe tertiaire [MBL–Zn(II)–inhibiteur]	1,2,4-Triazole-3-thiones
	Captopril et analogues
	Boronates cycliques
	Bisthiazolidines (BTZ)
	Mercaptoacetate
	Mercaptocarboxylate
	Mercaptophosphonates
	Dérivés de l'acide aminophtalique
	Dérivé d'acides succiniques
	Biphenyl tetrazoles
	Tiopronin
	Pyridine-2,4-dicarboxylic acids
	Acides thiomandéliques, autres dérivés contenant du thiol
	Produit d'hydrolyse de la rhodanine
	Analogue du triazolylthioacetamide
	Sulfonamides
	Produit naturel Tricycliques
	Benzophenone
	3-Oxoisoindoline-4-carboxylates (isoquinolines)
	Dérivés de l'acide dipicolinique
Benzyl thiol	
Analogue du cyclobutanone peneme	
Inhibition par chélation des ions zinc	EDTA
	Acide dipicolinique
	AMA
Inhibition par fixation covalente	Acide mercaptophénylacétique
	Moxalactam
	Céphamycines
	3-(3-Mercaptopropionylsulfanyl)-propionic acid pentafluorophenyl ester
	Cefaclor
	Ebselen
	Formylchromone
Inhibition non caractérisée	Azolythioacetamides
	Molécules de la classe des thionylpeptides
	Acides maléiques
	Mitoxantrone
	Triazoles
	Mercaptotriazoles
	Thiosemicarbazides substitués
	Dérivés du Pyrrole
	Thioesters
	Thiols
Alcools trifluorés et cétones	

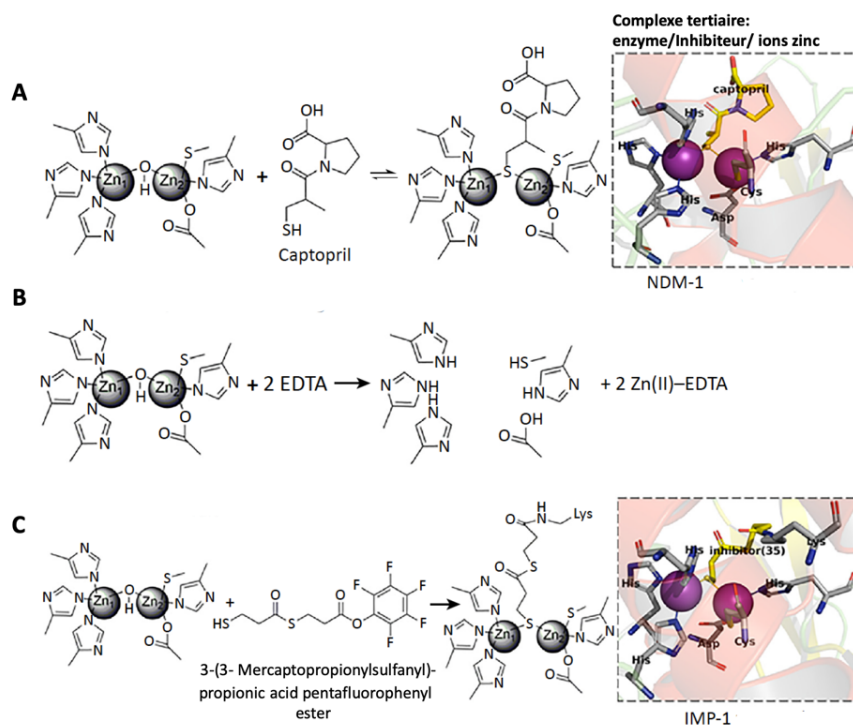


Figure 44. Représentation des différents mécanismes d'action des inhibiteurs de MBLs. A. Inhibition par fixation aux ions zinc (NDM-1/captopril) ; B. inhibition par chélation des ions zinc ; C. Inhibition par fixation covalente (IMP-1/ dérivé de l'acide propionique). D'après Ju et al.³⁵⁶

i. Inhibition par fixation aux ions Zinc

Récemment, il a été décrit que les composés possédant des groupements thiols (R-SH) libres, thioéthers (R-S-R), thioesters (R-C(=O)-S-R'), thiocétone (R-C(=S)-R') et thiourées (SC(NH₂)₂) ont une activité inhibitrice vis-à-vis des différentes classes de MBLs³⁵⁷ car ils ont la capacité de se fixer aux ions zinc. Parmi ces composés, le captopril (Figure 45), puissant inhibiteur de l'enzyme de conversion de l'angiotensine (ACE), est un médicament largement utilisé dans le traitement de l'hypertension et contient des groupes thiols et carboxylates capables d'établir une coordination avec des ions métalliques. Il a pu être montré que ces déterminants chimiques sont responsables de l'inhibition de MBLs de toutes les sous-classes (BclI, NDM-1, CphA, L1, FEZ-1).^{349,358-361} Avec une IC₅₀ pour NDM-1 de 7,9 μM.³⁶² Un autre composé le thiorphan (métabolite actif de la racécadotril antidiarrhéique) a montré un effet sur NDM-1, IMP-7 et VIM-1 avec des valeurs de CI₅₀ de l'ordre du micromolaire. Il a pu

également améliorer considérablement l'activité de l'imipénème contre des souches productrices d'une MBL.³⁶³

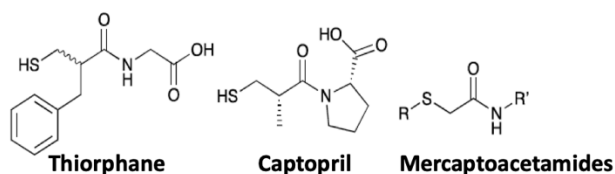


Figure 45. Structure chimique du Thiorphane, Captopril et de Mercaptoacétamide substitués.

L'acide mercaptoacétique (ou acide thioglycolique) et ses analogues structurels apparentés constituent également un inhibiteur de l'enzyme L1,³⁵⁷ une MBL de la classe B3.^{364,365} Des dérivés de ce composé : le mercaptopropionamide et le mercaptobutyramide inhiberaient IMP-1.³⁶⁶ D'autres composés thiol sont des inhibiteurs de MBLs tels que les acides thiométhylbenzoïque,³⁶⁷ et les bisthiazolidines,³⁶⁸ capables d'inhiber les 3 sous classes. Bien que les thiols constituent les plus puissants inhibiteurs des MBLs, leur tendance à s'oxyder rapidement en disulfures induit leur perte d'efficacité. Ainsi, leur stabilité constitue un sérieux défi pour le développement de nouveaux médicaments viables.

Les composés contenant des phosphonates (les 6-phosphonométhylpyridine-2-carboxylates) ont également montré *in vitro* des activités de l'ordre du nanomolaire contre les MBLs de la sous classe B1 et B3 *via* des interactions avec le centre métallique di-zinc.³⁶⁹ Une autre approche serait l'utilisation du sulfate de bismuth colloïdal, ce dernier étant capable de déplacer les ions Zn (II) du site actif NDM-1, et de générer un complexe inactif (Figure 46).³⁷⁰

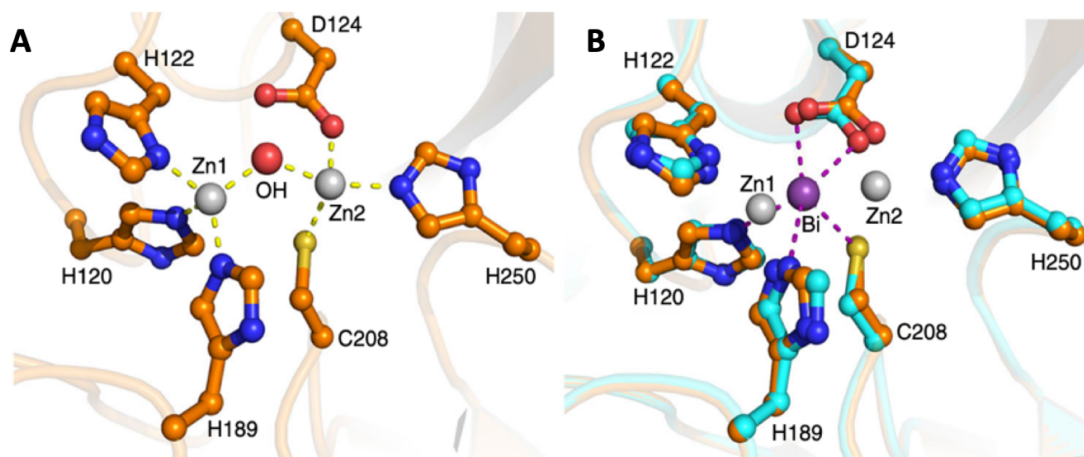


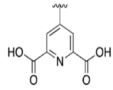
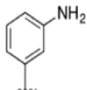
Figure 46. Analyse Cristallographique révélant le mode de liaison du Bismuth (Bi) dans le site actif de NDM-1. A. Site actif de NDM-1 avec 2 ions zinc (sphères grises) et l'hydroxyle (sphère rouge). B. Superposition d'images comparant la position des ions zinc à celle du bismuth (sphère violette) qui est légèrement plus proche de l'ion Zn1. D'après Wang et al.³⁷¹

ii. Inhibition par chélation des ions zinc

Comme décrit ci-dessus, les ions Zn^{2+} jouent un rôle vital dans l'activité catalytique des MBLs, l'inhibition de cette activité peut se faire *via* l'ajout d'agents chélateurs tels que l'EDTA. L'inconvénient est que ce composé n'est pas du tout spécifique des β -lactamases et donc s'avère toxique pour les cellules eucaryotes.

Les dérivés de l'acide 2,6-dipicolinique (DPA) sont une autre classe bien connue de chélateurs de zinc et agissent par l'intermédiaire du même mécanisme de séquestration des métaux que l'EDTA pour inhiber les MBLs.³⁷² Le criblage de dérivés d'acide picolinique a fait ressortir des composés analogues de l'acide dipicolinique inhibant de façon forte et spécifique NDM-1, par rapport à d'autres métallo-enzymes à zinc. Il a pu être montré, par des études biophysiques, que ce composé forme un complexe ternaire avec NDM-1.³⁷³ De plus, la valeur de la CI50 s'est avérée faible (80 nM, Tableau 17), et les valeurs des CMI pour l'imipénème, en présence de ce composé (100 mg/L) contre des souches cliniques *E. coli* et *K. pneumoniae* exprimant NDM-1, ont été diminuées, passant de la catégorie résistante à sensible (de 16 à 1 mg/L).³⁷³ Aucune toxicité envers les cellules eucaryotes n'a été détectée.

Tableau 17. Valeurs des CI50 du dérivé de l'acide dipicoliniques obtenues avec NDM-1, VIM-2 et IMP-1. D'après Chen et al.³⁷³

Composés	CI50 (μM)		
	NDM-1	VIM-2	IMP-1
DPA 	0.41 ± 0.02	1.66 ± 0.03	3.03 ± 0.04
36 	0.080 ± 0.002	0.21 ± 0.01	0.24 ± 0.01

Le composé naturel fongique, l'aspergillomarasmine A (AMA), s'est avéré être un bon inhibiteur de NDM-1 et VIM-2 avec des valeurs de CI50 de 4 et 10 μM respectivement.³⁷⁴ Il a également rétabli l'activité du méropénème contre des entérobactéries, des *Acinetobacter* sp. et *Pseudomonas* sp. exprimant les MBLs VIM et NDM. Il a également restauré l'activité du méropénème chez des souris infectées par *K. pneumoniae* exprimant NDM-1.

D'autres composés chélateurs capables d'inhiber les MBLs ont été décrits.^{375,376} Mais bien qu'ils n'aient pas d'effets hémolytiques et qu'ils semblent non toxiques pour les cellules de mammifères *in vitro*, leur potentiel pour passer à une application clinique doit être considéré avec prudence en raison de leur absence présumée de spécificité de cible.

iii. Inhibition par fixation covalente

Deux autres approches ont été exploitées afin d'inhiber les MBLs. La première consiste à générer une inhibition covalente irréversible avec la Lysine 224, résidu conservé chez les enzymes de la sous classe B1 (VIM, NDM et IMP) par l'intermédiaire de l'acide 3-mercaptopropionique.³⁷⁷ Cette fixation permet d'abolir l'activité de ces enzymes. La seconde approche repose sur l'utilisation de l'ebsenal, déjà soumis à des essais cliniques liés à des maladies cardio-vasculaires. Ce composé comporte un atome de sélénium capable de fixer la cystéine 221, résidu impliqué dans la coordination des ions zinc et très conservé au sein des sous classes B1 et B2.³⁷⁸

Les deux approches ont ensuite été combinées pour créer un inhibiteur double covalent, réagissant avec les deux résidus la Cys221 et la Lys224, pour avoir un spectre d'inhibition encore plus grand.³⁷⁰

d. Nouveau composé non inhibiteur : le céfidérocol

L'un des axes majeurs de la lutte contre l'antibiorésistance est le développement de nouveaux outils thérapeutiques comme les inhibiteurs de β -lactamases, mais également le développement de nouveaux antibiotiques. Récemment, un nouvel antibiotique « révolutionnaire » a vu le jour, le cefiderocol (S-649266) appelé également le cheval de Troie car sa stratégie consiste à dissimuler un antibiotique auquel une bactérie résiste, à l'aide d'une molécule familière, et même indispensable, à cette bactérie. L'antibiotique masqué par cette molécule parvient ainsi à pénétrer la bactérie alors que seul il n'y parviendrait pas. L'idée à l'origine de ce cheval de Troie est la suivante : toutes les bactéries pathogènes (à part les espèces du genre *Borrelia*) ont besoin de fer. De plus, ce besoin en fer devient important lors d'une infection (en raison d'une multiplication intense). Or, en cas d'infection, les bactéries ayant un gros besoin en fer souffrent d'une carence en fer. Pour pallier à ce problème, elles produisent des molécules spécialisées dans la captation du fer : les sidérophores. Elles libèrent des sidérophores dans leur milieu puis les reprennent lorsqu'ils sont chargés en fer. C'est à partir de cette observation que l'idée est venue pour le groupe Shionogi d'utiliser un sidérophore afin de masquer un antibiotique auquel la bactérie était résistante. La bactérie est donc trompée et accepte l'antibiotique sans le rejeter, ce qui permet à l'antibiotique de se trouver à forte concentration dans la bactérie et ainsi être moins affecté dans son action par une éventuelle enzyme inactivatrice. La voie du cheval de Troie est donc une nouvelle stratégie de lutte contre la résistance aux antibiotiques et les premiers résultats sont vraiment encourageants.

Le céfidérocol (S-649266) est une β -lactamine de type céphalosporine couplée à un sidérophore (Figure 47. A). Du point de vue structurel, il s'agit d'une oxyiminocéphalosporine dans laquelle le substituant du groupe oxyimino (2-carboxypropyle) est celui de la ceftazidime. Le substituant C3 est similaire à celui du céfépime (1-méthylpyrrolidinium) mais comprend un fragment catéchol (sidérophore). Ce dernier facilite la liaison du céfiderocol au fer ferrique,

ce qui crée un complexe avec l'ion de fer, permettant au composé de pénétrer dans l'espace périplasmique des bactéries à Gram négatif *via* un système de transporteur spécifique. Ensuite, le fer se dissocie et la composante céphalosporine du cefiderocol inhibe la synthèse de la paroi cellulaire en se liant à la PLP.³⁷⁹ Dans l'espace périplasmique la structure de ce composé augmente la stabilité de la céphalosporine inhibant ainsi son l'hydrolyse par les β -lactamases de types SBLs mais également MBLs.³⁸⁰⁻³⁸³ De plus, compte tenu de l'utilisation de la voie spécifique de transport du fer (Figure 47. B), l'action du cefiderocol n'est pas affectée par les modifications des porines. Il semblerait également que les pompes à efflux courantes présentes chez les entérobactéries n'affectent pas son action.³⁷⁹

Ce composé a démontré une activité *in vitro* puissante vis-à-vis des souches cliniques de *P. aeruginosa*,³⁸⁴ *A. baumannii*, *S. maltophilia* et des entérobactéries résistantes aux carbapénèmes (métallo- β -lactamases, KPC, NMC-A, OXA-48).^{379,383,385} Une étude a permis de démontrer que ce composé n'était pas hydrolysé par KPC-2, P99 et OXA-23. Cependant, une faible hydrolyse par IMP-1, VIM-2 et CTX-M-15 a été observée.

Les résultats des différentes études menées *in vitro* sur des bactéries à Gram négatif résistantes aux carbapénèmes mais également à la CAZ-AVI, au ceftolozane-tazobactam et à la colistine (souches d'origine mondiale dont des souches issues de notre laboratoire)³⁸⁶ ont conduit à la mise en place d'essais cliniques. Un de ces essais a évalué l'efficacité et l'innocuité du cefiderocol par rapport à l'imipénem-cilastatine dans le traitement des infections urinaires compliquées chez les patients présentant un risque d'infection à bactérie à Gram négatif multirésistante. Cette étude a montré une efficacité de 72,6% pour le cefiderocol contre 54,6% pour l'imipénème, ainsi qu'une bonne tolérance chez les patients traités.³⁸⁷

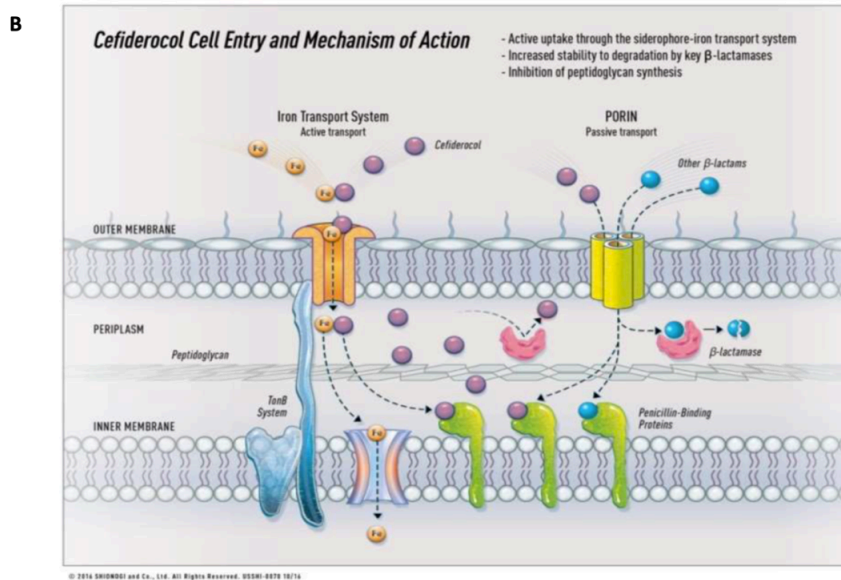
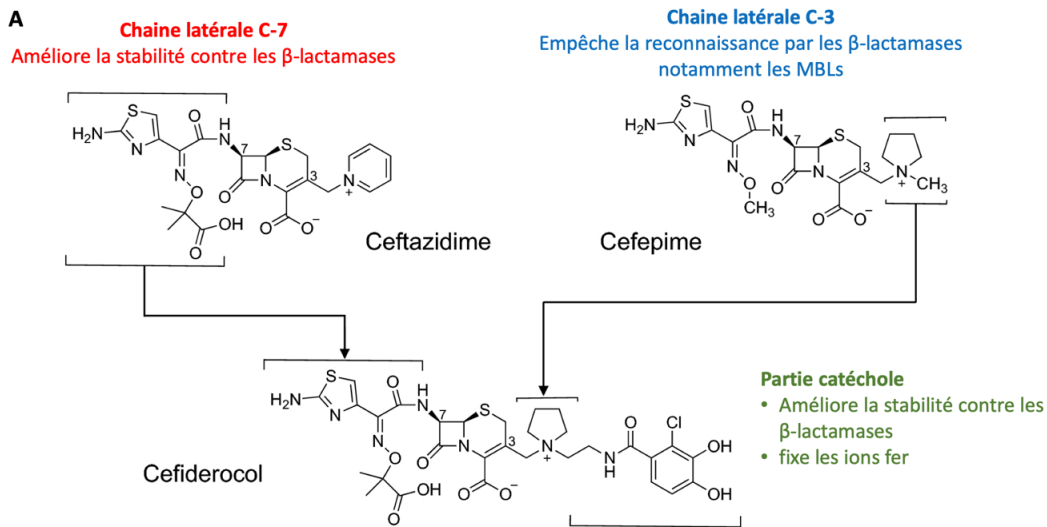


Figure 47. A. Structure du céfidérocol ; B. Mécanisme d'action. D'après shionogi and Co

Depuis la découverte des anciens inhibiteurs (c'est à dire les années 90), de nombreuses démarches ont été entreprises afin de développer de nouveaux inhibiteurs. Il existe, à l'heure actuelle, comme décrit ci-dessus, un grand nombre d'inhibiteurs déjà utilisés en clinique ou encore en cours de développement (Tableau 18). La panacée serait un inhibiteur capable d'agir sur les SBLs et les MBLs avec une très bonne efficacité.

Tableau 18. Spectre d'efficacité des combinaisons Inhibiteurs-Antibiotiques

	BLSEs	AmpC hyperproduite	KPC	OXA-48	MBLs	<i>Pseudomonas</i> spp	<i>Acinetobacter</i> spp	Phase
Ceftazidime- Avibactam	++	++	++	++	-	+	-	/
Ceftolozame- Tazobactam	++	-	-	-	-	++ (CAZ et IMP R)	-	/
Ceftaroline - Avibactam	++	++	+	-	-	-	-	/
Aztréonam - Avibactam	++	++	++	+	++	+	-	3
Imipénème - Relebactam	++	++	++	-	-	+	-	3
Méropénème - Vaborbactam	++	++	++	-	-	+/-	-	/
Céfépime - Zidebactam	++	++	++	++	++	++	-	2
Céfidérol	++	++	++	++	++	++	+	3

Objectifs Scientifiques

Depuis plusieurs années, on observe au niveau mondial une augmentation considérable de la prévalence des entérobactéries multi-résistantes. Ces germes sont capables d'inactiver des antibiotiques à large spectre d'activité et plus particulièrement ceux de la famille des β -lactamines utilisés dans le traitement des infections graves. Il s'agit, en particulier, des céphalosporines de 3^{ème} et 4^{ème} génération mais également des carbapénèmes, souvent considérés comme le traitement de dernier recours contre les infections sévères à bactéries à Gram négatif multi-résistantes en milieu hospitalier. Chez les entérobactéries, la résistance aux carbapénèmes fait intervenir deux mécanismes distincts : (i) une diminution de la perméabilité membranaire bactérienne associée à l'expression d'une β -lactamase sans activité intrinsèque vis-à-vis des carbapénèmes ou bien (ii) l'acquisition d'un gène codant pour une enzyme capable d'hydrolyser les carbapénèmes : une carbapénémase. Classiquement, les β -lactamases sont subdivisées en 4 groupes (A, B, C et D) d'après la classification de Ambler basée sur la structure de ces enzymes. Les carbapénémases décrites chez les entérobactéries appartiennent à trois de ces classes (classe A, B et D de la classification d'Ambler). Actuellement, les carbapénémases les plus répandues dans le monde sont les enzymes de type KPC (classe A de Ambler), les métallobetalactamases de type NDM, VIM et IMP (classe B de Ambler), et les oxacillinasés à activité carbapénémase de type OXA-48 (classe D de Ambler). En France, les carbapénémases de type OXA-48 sont largement majoritaires et représentent près de 75% des souches d'entérobactéries productrices de carbapénémases (EPC).

L'émergence mondiale de ces EPC constitue un problème de santé publique majeur car, en plus de leur résistance à toutes les β -lactamines dont les carbapénèmes, ces souches sont généralement résistantes à la quasi-totalité des autres familles d'antibiotiques utilisées en clinique (aminosides, fluoroquinolones, sulfamides, etc.). Pour pallier à d'éventuels impasses thérapeutiques résultant d'infections causées par ces EPC, deux stratégies sont envisageables : (i) découvrir de nouvelles familles d'antibiotiques, et/ou (ii) développer des molécules permettant d'inhiber les enzymes responsables de la résistance. En outre, le développement de ces deux stratégies doit s'accompagner par la mise en place d'outils de diagnostics rapides, sensibles, et spécifiques permettant la détection précoce des patients infectés et/ou colonisés par des EPC. A l'hôpital, la détection rapide de ces patients à risque permet la mise en place de

procédures d'hygiène spécifiques (isolement strict, personnel dédié, cohorting) ayant pour but de limiter la diffusion des EPC en milieu hospitalier.

L'objectif de cette thèse a été de répondre aux exigences d'une des deux stratégies évoquées ci-dessus, à savoir le développement d'inhibiteurs spécifiques des carbapénèmases ayant idéalement un effet sur les trois classes de carbapénèmases (classe A, B et D de Ambler) : les « pan-inhibiteurs ». Pour ce faire, nos objectifs scientifiques s'articulaient selon deux axes majeurs:

Un axe plus fondamental qui vise à une meilleure compréhension moléculaire et biochimique des carbapénèmases les plus répandues dans le monde : KPC-2 (classe A), NDM-1 (classe B) et OXA-48 (classe D). La caractérisation enzymatique et structurale de ces enzymes ainsi que des études de modélisation moléculaire ont été réalisées afin de mieux comprendre le mode d'interaction enzyme-substrat et ainsi contribuer à la conception de « pan-inhibiteurs ». Nous nous intéresserons plus particulièrement (i) à l'importance de la boucle β 5- β 6 et du résidu 214 dans l'hydrolyse des carbapénèmes par OXA-48 ; (ii) au rôle de la boucle 238–243 et du résidu 179 sur le profil hydrolytique de l'enzyme et de son inhibition par l'avibactam de KPC ; et (iii) à l'impact de substitution par des alanines de 10 résidus d'acides aminés dans le site actif de NDM-1

Le second axe a pour objectif de contribuer à la lutte contre l'antibiorésistance. D'une part en développant des « pan-inhibiteurs » (dérivés β -dicétones et imidazoline actifs et de composés analogues aux β -lactamines : les azetidimines) pouvant à terme être utilisés pour le traitement des infections à EPC et d'autre part en développant de nouveaux outils de diagnostic de détection rapide des EPC.

Résultats

Chapitre I. Études moléculaires, biochimiques et structurales des carbapénèmases majeures et de leurs variants.

Afin de mieux comprendre le mode d'action des principales carbapénèmases, il a fallu développer au sein du laboratoire une méthode rapide et efficace de surexpression et de purification de ces enzymes. Pour cela, il a fallu tenir compte du processus de synthèse des β -lactamases chez les entérobactéries.

Ces enzymes sont synthétisées dans le cytoplasme avant d'être transportées dans le périplasme, espace situé entre les deux barrières perméables sélectives que sont la membrane cytoplasmique (ou membrane interne) et la membrane externe chez les bactéries à Gram négatif. De plus, en fonction de leur mode d'action, les carbapénèmases sont divisées en deux grands groupes : (i) les enzymes dont le site catalytique possède une sérine active (ex : KPC et OXA-48) et (ii) les metallo- β -lactamases qui requièrent la coordination d'ions divalents (Zn^{2+}) au niveau de leur site actif pour l'hydrolyse des β -lactamines (ex : NDM, VIM et IMP). Bien que toutes ces enzymes appartiennent à la même famille des β -lactamases, leurs propriétés physico-chimiques sont différentes, impliquant des conditions variables d'expression et de purification. Ainsi, différentes stratégies (choix du vecteur, de l'étiquette ou « tag », de la souche bactérienne pour l'expression, conditions d'induction) ont été testées pour optimiser l'expression, la solubilité des enzymes et *in fine* augmenter le rendement de la purification.

Les premiers essais de purification avaient pour objectif d'exprimer les différentes carbapénèmases sous leur forme native (sans modification, ni ajout de « tag »). Ainsi, des clonages des gènes codant pour les différentes carbapénèmases (*bla*_{OXA-48}, *bla*_{NDM-1}, *bla*_{KPC-2}) ont été réalisés dans le vecteur d'expression pET9a. Le but premier était de s'affranchir de l'ajout d'un « tag » qui aurait pu avoir un impact négatif sur l'activité de l'enzyme (ex : problème de « repliement » ou d'encombrement stérique au niveau du site actif de l'enzyme). Malheureusement, cette stratégie s'est avérée peu concluante. En effet, les protéines étaient bien exprimées mais le processus de purification (chromatographie échangeuse d'ions) nécessitant de nombreuses étapes a abouti à un rendement de purification très faible, voire nul pour certaines enzymes (ex : NDM-1). Bien que ces rendements soient insuffisants pour la réalisation d'études cristallographiques, les quantités d'enzymes natives récupérées étaient

compatibles (sauf pour NDM-1) avec la réalisation de tests enzymatiques tels que la détermination des constantes d'affinité (K_m) et catalytique (k_{cat}).

Afin d'améliorer les rendements et de faciliter le processus de purification, une nouvelle stratégie a été mise en place. Les gènes codant pour chacune des carbapénèmases ont été clonés dans le vecteur pET41. Ce vecteur permet d'exprimer la protéine d'intérêt avec un « tag » Histidine en C-terminal (peptide de 8 histidines), et/ou un « tag » GST (Gluthathione-S-Transférase) en N-terminal facilitant la purification (chromatographie d'affinité). De plus, la séquence nucléotidique codant pour le peptide signal responsable de l'adressage de l'enzyme vers le périplasme de la bactérie a été retirée. Ainsi, les protéines exprimées se retrouvent séquestrées dans le cytoplasme, fraction dite soluble utilisable pour la purification. De plus, les conditions d'inductions (concentration d'IPTG, température, temps d'induction, milieu de culture) ont été optimisées afin d'obtenir le meilleur rendement possible. Cette stratégie a eu un impact considérable sur la solubilité et la purification des protéines OXA-48 et NDM-1. Cette méthode a permis la purification de la carbapénèmase NDM-1. L'optimisation des paramètres d'expression a secondairement permis d'augmenter les rendements de purification d'un facteur 6 et 25 pour NDM-1 et OXA-48, respectivement, permettant d'obtenir des quantités de protéines compatibles avec les besoins de la cristallographie. Concernant l'expression de KPC-2 l'ajout du « tag » a conduit à une perte totale de la solubilité de l'enzyme. KPC-2 possède deux cystéines qui forment un pont disulfure essentiel à la bonne conformation de l'enzyme. Une nouvelle stratégie a été entreprise, l'expression de cette protéine dans une souche bactérienne *E. coli* Rosetta Gami exprimant des protéines chaperonnes dont certaines sont capables de favoriser la formation des ponts disulfures. Cette stratégie a permis de purifier avec succès KPC-2-His. La comparaison des constantes enzymatiques avec ou sans queue histidine n'a pas révélé de différences majeures, suggérant que la queue histidine en C-terminale n'avait pas d'incidence sur l'activité des enzymes.

Une fois mis en place, ces protocoles ont pu être appliqués aux variants naturels ou synthétiques de ces différentes enzymes. Cette première étape de standardisation de la production des carbapénèmases a été primordiale pour les études secondaires de (i) caractérisation des propriétés enzymatiques et structurales des carbapénèmases, (ii) pour la réalisation des tests d'inhibitions ainsi que (iii) l'immunisation de souris en vue de développer d'un nouvel outil diagnostique pour la détection rapide de ces carbapénèmases par immuno-assay.

A. OXA-48 : Importance de la boucle β 5- β 6 et du résidu Arg 214 dans l'hydrolyse des carbapénèmes

OXA-48 a été la première carbapénémase de la classe D de Ambler décrite chez les entérobactéries. Elle a été retrouvée dans une souche de *K. pneumoniae* isolée en Turquie en 2004. Rapidement après la première description de cette carbapénémase, une dissémination d'entérobactéries productrices d'OXA-48 a été rapportée en Turquie puis au Moyen Orient et en Afrique du Nord. En France, depuis 2010, on observe une constante augmentation de la prévalence des entérobactéries productrices d'OXA-48 (surtout chez *E. coli* et *K. pneumoniae*). Cette carbapénémase hydrolyse fortement les pénicillines, faiblement les carbapénèmes (par rapport aux autres carbapénémases majeures de type KPC et NDM) et n'hydrolyse pas l'aztréonam et les céphalosporines à spectre élargi (dites également de 3^{ème} génération ou C3G) telles que la ceftazidime. En outre, depuis sa première identification, de nombreux variants d'OXA-48, appelés OXA-48-like, et possédant quelques substitutions ou délétions d'acides aminés par rapport à OXA-48 sont régulièrement rapportés. Cependant, la caractérisation biochimique de ces enzymes, et notamment l'impact des substitutions/délétions, reste relativement mal connue.

Pour caractériser et comparer ces différents variants d'OXA-48, les gènes *bla*_{OXA-48-like} ont été clonés dans un même vecteur d'expression constitutif (pTopo) et exprimés dans un même fond génétique (*E. coli* TOP10), permettant de réaliser des études phénotypiques (sensibilité aux antibiotiques, concentrations minimales inhibitrice CMI) comparatives. En parallèle, le protocole de purification optimisé pour OXA-48 a été utilisé pour purifier ces différents variants et entreprendre des études biochimiques plus poussées, ainsi que des études structurales tridimensionnelles pour les variants présentant des caractéristiques particulières.

Ainsi, nous avons pu démontrer que bien qu'étant assez homogènes en termes de séquence protéique ces différents variants d'OXA-48 possédaient des profils hydrolytiques assez différents. En effet, contrairement à ce qui avait été initialement suggéré, ce groupe d'enzymes n'inclut pas seulement des carbapénémases. Nous avons pu montrer que des changements d'acides aminés étaient capables de conférer des spécificités de substrats particuliers (Article 1). Afin de mieux comprendre le fonctionnement des enzymes de type OXA-48, trois variants particuliers ont été étudiés plus en détails. Tout d'abord OXA-232 possédant 5 substitutions en acide aminés (AA) par rapport à OXA-48 lui conférant une nette diminution d'activité

hydrolytique vis-à-vis des carbapénèmes, puis les variants OXA-163 et OXA-405 possédant une délétion de 4 AA dans la boucle β 5- β 6 de l'enzyme et pour lesquels nous avons pu montrer une perte d'activité carbapénémase et, à l'inverse, l'acquisition d'une activité hydrolytique vis-à-vis de céphalosporines à spectre étendu (Article 2, 3).

Ainsi, nous avons démontré que la nature de l'AA en position 214 et que la boucle β 5- β 6 jouent un rôle crucial sur l'activité des enzymes de type OXA-48. Pour confirmer cette hypothèse, mais également pour déterminer si d'autres AA pouvaient avoir un impact sur le spectre d'hydrolyse, nous avons réalisé 12 mutants ponctuels pour chacune des enzymes OXA-48 et OXA-232 (Article 4). De plus, nous avons cristallisé et résolu la structure des enzymes OXA-232 et OXA-405 (en collaboration avec Dr B. Iorga de l'ICSN, CNRS, Gif sur Yvette). Nos résultats, associés à une étude de modélisation, ont permis de mettre en exergue les changements structuraux induits par la liaison au substrat, ainsi que la distribution des molécules d'eau dans le site actif et leur rôle dans l'hydrolyse du substrat. Nous avons ainsi démontré que la boucle β 5- β 6 et l'AA 214 étaient critiques pour contrôler le profil d'hydrolyse des différents substrats et pouvaient donc représenter la base structurelle pour la conception de nouveaux inhibiteurs des carbapénémases de la classe D de Ambler.

Heterogeneous hydrolytic features for OXA-48-like β -lactamases

Saoussen Oueslati^{1,2}, Patrice Nordmann^{1–5} and Laurent Poirel^{1–4*}

¹INSERM U914 'Emerging Resistance to Antibiotics', K.-Bicêtre, France; ²LabEx LERMIT, Faculté de Médecine Paris Sud, K.-Bicêtre, France; ³Centre National Associé-Centre de Référence des Résistances aux Antibiotiques, K.-Bicêtre, France; ⁴Medical and Molecular Microbiology, Department of Medicine, Faculty of Science, University of Fribourg, Fribourg, Switzerland; ⁵HFR-Hôpital Cantonal, Fribourg, Switzerland

*Corresponding author. Medical and Molecular Microbiology Unit, Department of Medicine, Faculty of Science, University of Fribourg, 3 rue Albert Gockel, CH-1700 Fribourg, Switzerland. Tel: +41-26-300-9582; E-mail: laurent.poirel@unifr.ch

Received 8 October 2014; returned 3 November 2014; revised 14 November 2014; accepted 26 November 2014

Objectives: Carbapenem-hydrolysing class D β -lactamases of the OXA-48 type are increasingly reported from Enterobacteriaceae. β -Lactamase OXA-48 hydrolyses penicillins very efficiently, but carbapenems only weakly and spares broad-spectrum cephalosporins. Recently, diverse OXA-48-like β -lactamases have been identified worldwide (OXA-162, OXA-181, OXA-163, OXA-204 and OXA-232). They differ by few amino acid substitutions or by amino acid deletions.

Methods: *bla*_{OXA-48}, *bla*_{OXA-162}, *bla*_{OXA-163}, *bla*_{OXA-181}, *bla*_{OXA-204} and *bla*_{OXA-232} were cloned into the same expression vector and expressed in the same *Escherichia coli* background. Kinetic studies were performed with enzymes purified by ion-exchange chromatography. Determination of hydrolytic activities was performed by UV spectrophotometry. MICs were determined for all recombinant strains, using as background either the WT *E. coli* TOP10 strain or a porin-deficient *E. coli* strain.

Results: Kinetic studies showed that OXA-162 and OXA-204 shared the same hydrolytic properties as OXA-48. On the other hand, OXA-181 possessed a higher ability to hydrolyse carbapenems, while OXA-232 hydrolysed those substrates less efficiently. In contrast to the other OXA-48-like β -lactamases, OXA-163 hydrolysed broad-spectrum cephalosporins very efficiently, but did not possess significant carbapenemase activity. Although several of these OXA-48-like enzymes possess low activity against carbapenems, MICs of carbapenems were significantly elevated when determined for strains possessing permeability defects.

Conclusions: A detailed comparative analysis of the kinetic properties of the OXA-48-like β -lactamases is provided here. It clarifies the respective features of each OXA-48-like variant and their respective impacts in terms of carbapenem resistance.

Keywords: carbapenemases, class D β -lactamases, enzymatic activity

Introduction

The emerging mechanism of resistance to carbapenems in Enterobacteriaceae is related to the horizontal transfer of plasmid-mediated carbapenemase genes.^{1,2} Carbapenemases belong to the Ambler class A, B or D β -lactamases.³ OXA-48 and its derivatives are class D β -lactamases and have disseminated widely, but only in Enterobacteriaceae.^{4,5} They are widespread in particular in Europe, Africa and the Indian subcontinent.¹ β -Lactamase OXA-48 hydrolyses penicillins at a high level and carbapenems at a low level, but spares expanded-spectrum cephalosporins such as ceftazidime.⁵ Due to these properties, OXA-48 producers may be either susceptible or

resistant to broad-spectrum cephalosporins (additional production of an ESBL observed in 80% of strains^{6,7}) and to carbapenems. Indeed, additional mechanisms such as permeability defects, efflux overproduction and high-level production of expanded-spectrum β -lactamases (AmpC and ESBLs) have been shown to confer reduced susceptibility to carbapenems when combined.⁵

Since the first identification of OXA-48,⁸ different variants have been reported, differing by few amino acid substitutions or deletions.⁵ Whereas some OXA-48-related enzymes such as OXA-48, OXA-162, OXA-181, OXA-204 and OXA-232 have been reported as conferring a very similar resistance pattern, OXA-163 (with a single amino acid substitution together with a four amino acid

deletion compared with OXA-48) compromises the efficacy of broad-spectrum cephalosporins and hydrolyses carbapenems only marginally.⁹ From a biochemical point of view, these OXA-48-like β -lactamases have not been purified and analysed under the same conditions. This may create misleading interpretations when comparing the respective kinetic data, since values are known to vary under different experimental conditions (e.g. buffer content and concentration for hydrolysis assays, reaction temperature and type of UV spectrophotometer). Similarly, since expression of the different *bla*_{OXA-48}-like genes has been evaluated using different cloning vectors and different *Escherichia coli* host strains, MIC interpretations might again be misleading when comparing the susceptibility of the different recombinant strains. Therefore, and in order to gain further insights into the relative hydrolytic properties of these different variants, we designed a study aiming to clone and express in the same genetic background a series of *bla*_{OXA-48}-like genes. Here, we evaluated the susceptibility of the corresponding recombinant clones to β -lactams, including temocillin, which is reported to be a good substrate of OXA-48 and therefore used as a marker for the detection of OXA-48-like producers.¹⁰ Additionally, the relative catalytic activities of purified enzymes and the performance of the Carba NP test were tested for these OXA-48-like β -lactamases.

Materials and methods

Bacterial strains

A series of clinical *Klebsiella pneumoniae* isolates harbouring *bla*_{OXA-48}-like genes were used as templates. These isolates respectively harboured

genes encoding OXA-162 (France, 2013),⁷ OXA-163 (Argentina, 2011),⁹ OXA-181 (France 2013),¹¹ OXA-204 (France, 2013)¹² and OXA-232 (India, 2012).¹³ These variants differed from OXA-48 by a single amino acid substitution or by amino acid deletions (Figure 1). *E. coli* TOP10 was used as a recipient strain for cloning and expressing the different *bla*_{OXA-48}-like genes as described previously.¹² In addition, *E. coli* HB4 lacking the major porins OmpF and OmpC was also used as a recipient strain to evaluate the relative impact of the expression of these genes in an *E. coli* reference strain with low-level outer membrane permeability.¹⁴

Cloning and expression of the *bla*_{OXA-48}-like genes

The entire coding sequences of the β -lactamase genes (*bla*_{OXA-162}, *bla*_{OXA-163}, *bla*_{OXA-181}, *bla*_{OXA-204} and *bla*_{OXA-232}) were obtained by PCR amplification using primers OXA-48A (5'-TTGGTGGCATCGATTATCGG-3') and OXA-48B (5'-GAGCACTTCTTTGTGATGGC-3') and were then inserted into plasmid pCR[®]-Blunt II-TOPO[®] (Invitrogen, Illkirch, France) for the phenotypic studies and pET9a (Novagen, VWR International, Fontenay-sous-Bois, France) following the manufacturer's recommendations. Recombinant plasmids obtained with pCR[®]-Blunt II-TOPO[®] were transformed into either *E. coli* strain TOP10 or *E. coli* strain HB4. The orientation of the respective inserts was checked by sequencing to ensure all genes were under the control of the *P*_{lac} promoter. Recombinant plasmids constructed in plasmid pET9a (Stratagene, Amsterdam, the Netherlands) used as expression vector and then were transformed into *E. coli* strain BL21(DE3) (Novagen) following the manufacturer's recommendations.

β -Lactamase purification

An overnight culture of *E. coli* strain BL21 harbouring pET9a-derived recombinant plasmids was used to inoculate 2 L of LB medium broth containing 50 mg/L kanamycin. Bacteria were cultured at 37°C until reaching

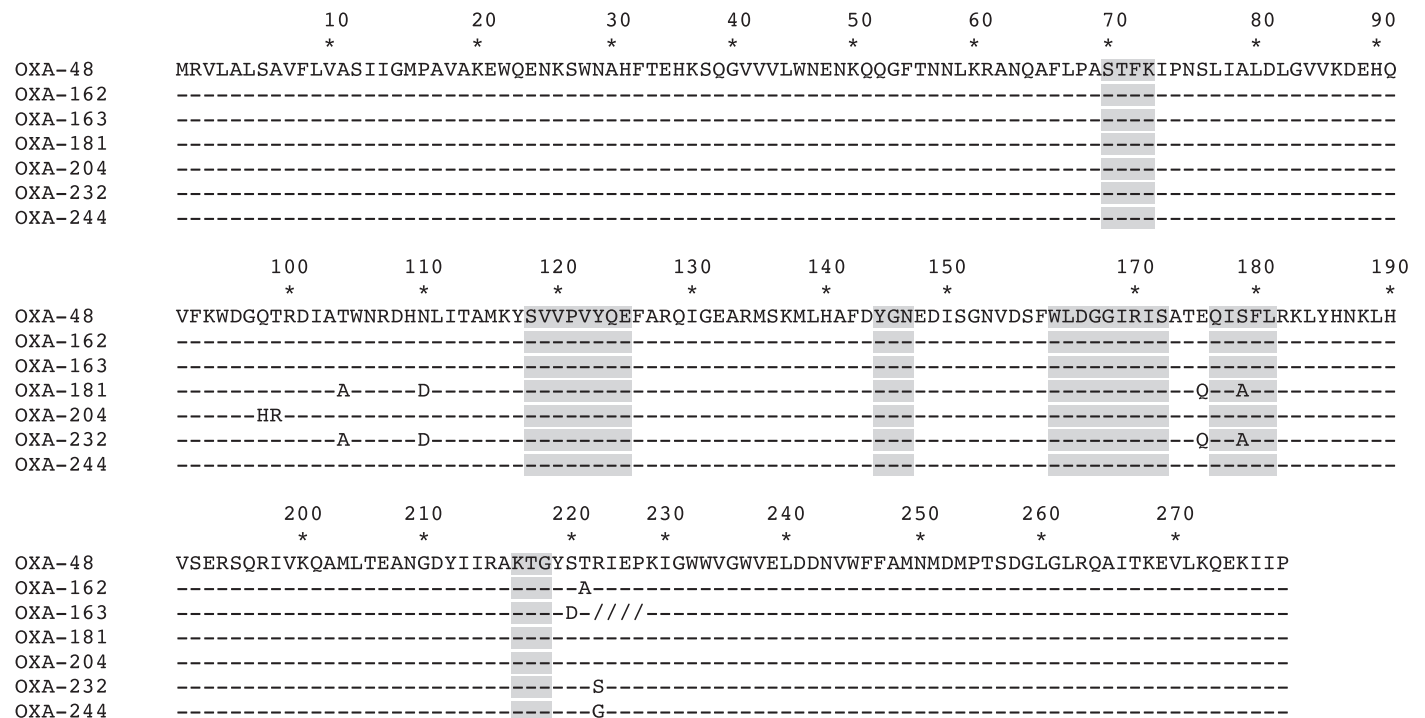


Figure 1. Amino acid alignment of OXA-48 and six other variants. Dashes indicate identical residues among all amino acid sequences. Slashes indicate the absence of amino acids. Amino acid motifs that are well conserved among class D β -lactamases are indicated by boxes. Numbering is according to class D β -lactamase (DBL nomenclature).¹⁷

an OD of 0.6 at 600 nm. Then, expression of the β -lactamase genes was carried out overnight at 25°C with 0.1 mM IPTG as inducer. Cultures were centrifuged at 6000 g for 15 min and then the pellets were resuspended with 10 mL of 20 mM triethanolamine H₂SO₄ (pH 7.2). Bacterial cells were disrupted by sonication and the bacterial pellet was removed by two consecutive centrifugation steps at 10000 g for 1 h at 4°C and then the supernatant was centrifuged at 48000 g for 1 h at 4°C. β -Lactamases were purified by using two successive steps of anion-exchange chromatography [20 mM triethanolamine H₂SO₄ (pH 7.2) and then 20 mM piperazine H₂SO₄ (pH 9.5)] using Q-Sepharose columns, followed by a gel filtration step [100 mM sodium phosphate buffer (pH 7) and 150 mM K₂SO₄]. Peaks of β -lactamase activity were concentrated by using Vivaspin® columns (GE Healthcare, Freiburg, Germany) and dialysed with 100 mM sodium phosphate buffer (pH 7). Protein purity was estimated by SDS-PAGE.

Kinetic studies

Purified β -lactamases were used for kinetic measurements, which were determined at 30°C in 100 mM Tris-H₂SO₄ and 300 mM K₂SO₄ (pH 7). The *k_{cat}* and *K_m* values were determined by analysing β -lactam hydrolysis under initial-rate conditions with an ULTROSPEC 2000 model UV spectrophotometer (Amersham Pharmacia Biotech) using the Eadie-Hoffstee linearization of the Michaelis-Menten equation. The different β -lactams were purchased from Sigma-Aldrich (Saint-Quentin-Fallavier, France).

Susceptibility testing

The susceptibility pattern was determined by the disc diffusion method and MICs by the microbroth dilution method. Results were interpreted according to CLSI guidelines.¹⁵ MICs were determined only for clones harbouring recombinant pCR®-Blunt II-TOPO® plasmids and transformed into either *E. coli* TOP10 or *E. coli* HB4 strains.

Results and discussion

Susceptibility patterns of the recombinant strains expressing the OXA-48-like β -lactamases

MIC determination for *E. coli* recombinants always showed high-level resistance to ampicillin and temocillin (Table 1). A significant decreased susceptibility to carbapenems was noticed for all clones (4- to 16-fold increase), with the exception of the clone producing OXA-163 with only a 2-fold increase in MICs of imipenem and doripenem, although the MIC of meropenem remained unchanged. Notably, the recombinant strain producing OXA-181 showed the highest MICs of carbapenems, while almost identical values were obtained for OXA-48, OXA-162 and OXA-204 producers. Lower MICs were obtained for the OXA-232 producer, suggesting lower hydrolytic activity of that variant towards carbapenems (Table 1).

Recombinant strains producing OXA-163 or OXA-232 had lower MICs of temocillin than those producing other OXA-48 derivatives. This result might have a significant impact considering that several screening techniques of OXA-48-like producing isolates now rely on this peculiar property.

As previously noted, the OXA-163 producer was the only OXA-48-like producer exhibiting elevated MICs of broad-spectrum cephalosporins such as cefotaxime and ceftazidime.

Table 1. MICs of β -lactams

β -Lactam	MIC (mg/L)											
	<i>E. coli</i> TOP10 (pTOPO-OXA-48)	<i>E. coli</i> TOP10 (pTOPO-OXA-162)	<i>E. coli</i> TOP10 (pTOPO-OXA-163)	<i>E. coli</i> TOP10 (pTOPO-OXA-181)	<i>E. coli</i> TOP10 (pTOPO-OXA-204)	<i>E. coli</i> TOP10 (pTOPO-OXA-232)	<i>E. coli</i> HB4 (pTOPO-OXA-48)	<i>E. coli</i> HB4 (pTOPO-OXA-162)	<i>E. coli</i> HB4 (pTOPO-OXA-163)	<i>E. coli</i> HB4 (pTOPO-OXA-181)	<i>E. coli</i> HB4 (pTOPO-OXA-204)	<i>E. coli</i> HB4 (pTOPO-OXA-232)
Ampicillin	>256	>256	>256	>256	>256	>256	>256	>256	>256	>256	>256	>256
Temocillin	>256	>256	32	>256	256	32	>256	>256	>256	>256	>256	>256
Cefalotin	16	32	64	32	16	64	>256	>256	>256	256	>256	>256
Cefotaxime	0.25	0.5	16	1	0.25	0.06	8	128	8	4	2	0.5
Ceftazidime	0.25	0.5	64	0.5	0.5	0.12	1	256	0.5	0.5	0.5	0.5
Imipenem	2	2	0.5	4	2	0.25	64	0.5	128	64	16	0.25
Meropenem	0.25	0.5	0.06	0.5	0.25	0.06	64	4	128	64	32	0.12
Ertapenem	0.5	0.5	0.06	1	0.5	0.01	256	32	>256	256	256	1
Doripenem	0.5	0.5	0.12	0.5	0.5	0.06	32	2	32	16	16	<0.03

Impact of the OXA-48-like β -lactamases in a porin-deficient *E. coli* background

Expression of the *bla*_{OXA-48}-like genes in *E. coli* HB4 gave rise to higher MICs of carbapenems compared with those MICs obtained for *E. coli* TOP10 (Table 1). Notably, production of OXA-163 increased the MIC of imipenem only slightly although those of other carbapenems, in particular ertapenem, increased more significantly. This result further confirms that OXA-163 is a very weak carbapenemase that does impact the activity of carbapenems only slightly in the absence of additional mechanisms of resistance.

Notably, despite conferring similar resistance patterns, discrepancies among the different OXA-48-like enzymes were highlighted here. For example, MICs of carbapenems were much higher for OXA-181 than for OXA-232 when produced in *E. coli* HB4 (128 versus 16 mg/L) (Table 1).

Hydrolytic properties of OXA-48-like β -lactamases

Kinetic studies were performed with purified OXA-48-like β -lactamases in order to compare their relative catalytic properties. The hydrolysis rates of purified OXA-162, OXA-181 and OXA-204 enzymes for all β -lactams tested were very similar to those obtained with OXA-48 (Table 2). These results are in accordance with MIC data showing very similar susceptibility patterns for the different *E. coli* clones producing OXA-48, OXA-162, OXA-181 and OXA-204, respectively (Table 2). Unlike other variants, OXA-232 had a catalytic activity for temocillin that was ~10-fold lower than that of OXA-48, while hydrolysis of temocillin by OXA-163 remained undetectable. The hydrolysis rates of carbapenems by OXA-232 were significantly lower than those obtained for OXA-48, OXA-162, OXA-181 and OXA-204 (Table 2).

Biochemical analysis of the hydrolytic properties of OXA-163 confirmed that it is an ESBL hydrolysing cefotaxime and ceftazidime efficiently, but carbapenems only marginally.

Conclusions

Several biochemical features of the different OXA-48-like β -lactamases were compared. The results showed that this group of enzymes, although being quite homogeneous in terms of protein sequence, is rather heterogeneous in terms of hydrolytic profile. Indeed, and as opposed to what was initially considered, this group of enzymes does not encompass only carbapenemases. It was shown that subtle amino acid changes may basically confer different substrate specificities, with some variants being either ESBLs or true carbapenemases. Therefore, detection of those genes encoding OXA-48-like enzymes possessing carbapenemase activities only cannot rely on PCR-based amplification of those genes only. Complete sequencing of the corresponding genes is therefore required to extrapolate the kinetic profile of the corresponding enzymes.

In addition, we showed here that additional non-enzymatic resistance mechanisms are required in order to achieve high MIC values of carbapenems for most OXA-48-like producers and that the resistance levels obtained in a porin-deficient *E. coli* background are variable depending on the nature of the OXA-48-like variant.

Additionally, we showed that high-level resistance to temocillin is not a common feature for all OXA-48-like producers.

Table 2. Kinetic parameters of OXA-48 and OXA-48-like β -lactamases

Substrate	K_m (μ M)										k_{cat} (s^{-1})										k_{cat}/K_m (mM^{-1}/s^{-1})										
	OXA-48	OXA-162	OXA-163	OXA-181	OXA-204	OXA-232	OXA-48	OXA-162	OXA-163	OXA-181	OXA-204	OXA-232	OXA-48	OXA-162	OXA-163	OXA-181	OXA-204	OXA-232	OXA-48	OXA-162	OXA-163	OXA-181	OXA-204	OXA-232	OXA-48	OXA-162	OXA-163	OXA-181	OXA-204	OXA-232	
Benzylpenicillin	ND	35	13	90	90	60	ND	123	23	444	353	125	ND	3400	1800	5000	4100	2100	ND	3400	1800	5000	4100	2100	ND	3400	1800	5000	4100	2100	
Ampicillin	400	315	315	170	450	220	955	269	23	218	389	132	955	830	70	1300	860	600	400	2400	830	70	1300	860	600	2400	830	70	1300	860	600
Oxacillin	95	75	90	80	100	130	130	3	34	90	56	156	130	40	370	1100	540	1200	1400	40	40	370	1100	540	1400	40	40	370	1100	540	1200
Temocillin	45	170	NH	60	75	60	0.3	0.7	NH	0.3	0.5	0.03	0.3	4	ND	5	7	0.5	6	6	4	ND	5	7	6	4	ND	5	7	0.5	
Cefalotin	195	180	10	250	270	125	44	12	3	13	12	13	44	70	300	50	45	105	225	10	10	230	13	12	10	10	10	230	13	12	6
Cefotaxime	>900	310	45	>1000	990	>1000	>9	3	10	>62	12	>6.5	>9	3	3	3	3	6	>6.5	10	10	10	13	12	10	10	10	10	13	12	6
Ceftazidime	NH	NH	>1000	NH	NH	>1000	NH	ND	8	ND	ND	>0.6	NH	ND	3	ND	ND	0.1	>0.6	NH	ND	3	ND	ND	3	ND	3	ND	ND	0.1	
Imipenem	13	25	520	13	9	9	5	11	0.03	7.5	4	0.2	5	420	0.06	550	420	20	370	420	0.06	550	420	20	370	420	0.06	550	420	20	
Meropenem	10	80	>2000	70	60	100	0.07	0.1	>0.1	0.1	0.05	0.03	0.07	1.3	0.03	1.5	0.8	0.3	6	1.3	0.03	1.5	0.8	0.3	6	1.3	0.03	1.5	0.8	0.3	
Ertapenem	100	30	130	100	90	110	0.13	0.3	0.05	0.2	0.1	0.04	0.13	9	0.3	2	1	0.4	1	9	0.3	2	1	0.4	1	9	0.3	2	1	0.4	
Doripenem	ND	50	NH	55	25	10	ND	0.05	NH	0.04	0.02	0.005	ND	1	NH	0.7	0.8	0.5	ND	1	NH	0.7	0.8	0.5	ND	1	NH	0.7	0.8	0.5	

ND, not determined; NH, no detectable hydrolysis was observed with 1 μ M purified enzyme and up to 500 μ M substrate. Data are the means of three independent experiments. Standard deviations were within 10% of the means. Data for OXA-48 are from Docquier et al.¹⁸

However, resistance to carbapenems correlates well with the carbapenemase activity of these different enzymes. OXA-163 (without any significant carbapenemase activity) and OXA-232 (with weaker carbapenemase activity compared with other OXA-48-like enzymes) hydrolysed temocillin weakly and corresponding producers did not exhibit high MICs of that antibiotic. This suggests that detection and screening strategies based on temocillin resistance are valid for OXA-48-like enzymes with significant carbapenemase activity only. On the other hand, the Carba NP test¹⁶ is an excellent tool for evaluating the carbapenemase activity of these OXA-48-like enzymes.

Funding

This work was funded by a grant from the INSERM (UMR914), by the University of Fribourg (Switzerland) and by a grant from ANR (ANR-10-LABX-33) as members of the Laboratory of Excellence LERMIT.

Transparency declarations

An international patent form for the Carba NP test has been deposited on behalf of INSERM Transfert (Paris, France).

References

- 1 Nordmann P, Poirel L. The difficult-to-control spread of carbapenemase producers among Enterobacteriaceae worldwide. *Clin Microbiol Infect* 2014; **20**: 821–30.
- 2 Tzouvelekis LS, Markogiannakis A, Psychogiou M *et al*. Carbapenemases in *Klebsiella pneumoniae* and other Enterobacteriaceae: an evolving crisis of global dimensions. *Clin Microbiol Rev* 2012; **25**: 682–707.
- 3 Queenan AM, Bush K. Carbapenemases: the versatile β -lactamases. *Clin Microbiol Rev* 2007; **20**: 440–58.
- 4 Poirel L, Naas T, Nordmann P. Diversity, epidemiology, and genetics of class D β -lactamases. *Antimicrob Agents Chemother* 2010; **54**: 24–38.
- 5 Poirel L, Potron A, Nordmann P. OXA-48-like carbapenemases, the phantom menace. *J Antimicrob Chemother* 2012; **67**: 1597–606.
- 6 Potron A, Poirel L, Rondinaud E *et al*. Intercontinental spread of OXA-48 β -lactamase-producing Enterobacteriaceae over a 11-year period, 2001 to 2011. *Euro Surveill* 2013; **18**: pii=20549.
- 7 Dortet L, Cuzon G, Nordmann P. Dissemination of carbapenemase-producing Enterobacteriaceae in France, 2012. *J Antimicrob Chemother* 2014; **69**: 623–7.
- 8 Poirel L, Héritier C, Tolün V *et al*. Emergence of oxacillinase-mediated resistance to imipenem in *Klebsiella pneumoniae*. *Antimicrob Agents Chemother* 2004; **48**: 15–22.
- 9 Poirel L, Castanheira M, Carrér A *et al*. OXA-163, an OXA-48-related class D β -lactamase with extended activity toward expanded-spectrum cephalosporins. *Antimicrob Agents Chemother* 2011; **55**: 2546–51.
- 10 Huang TD, Poirel L, Bogaerts P *et al*. Temocillin and piperacillin/tazobactam resistance by disc diffusion as antimicrobial surrogate markers for the detection of carbapenemase-producing Enterobacteriaceae in geographical areas with a high prevalence of OXA-48 producers. *J Antimicrob Chemother* 2014; **69**: 445–50.
- 11 Potron A, Nordmann P, Lafeuille E *et al*. Characterization of OXA-181, a carbapenem-hydrolyzing class D β -lactamase from *Klebsiella pneumoniae*. *Antimicrob Agents Chemother* 2011; **55**: 4896–9.
- 12 Potron A, Nordmann P, Poirel L. Characterization of OXA-204, a carbapenem-hydrolyzing class D β -lactamase from *Klebsiella pneumoniae*. *Antimicrob Agents Chemother* 2013; **57**: 633–6.
- 13 Potron A, Rondinaud E, Poirel L *et al*. Genetic and biochemical characterisation of OXA-232, a carbapenem-hydrolysing class D β -lactamase from Enterobacteriaceae. *Int J Antimicrob Agents* 2013; **41**: 325–9.
- 14 Mammeri H, Guillon H, Eb F *et al*. Phenotypic and biochemical comparison of the carbapenem-hydrolyzing activities of five plasmid-borne AmpC β -lactamases. *Antimicrob Agents Chemother* 2010; **54**: 4556–60.
- 15 Clinical and Laboratory Standards Institute. *Performance Standards for Antimicrobial Susceptibility Testing: Twenty-fourth Informational Supplement M100-S24*. CLSI, Wayne, PA, 2014.
- 16 Nordmann P, Poirel L, Dortet L. Rapid detection of carbapenemase-producing Enterobacteriaceae. *Emerg Infect Dis* 2012; **18**: 1503–7.
- 17 Couture F, Lachapelle J, Levesque RC. Phylogeny of LCR-1 and OXA-5 with class A and class D β -lactamases. *Mol Microbiol* 1992; **6**: 1693–705.
- 18 Docquier JD, Calderone V, De Luca F *et al*. Crystal structure of the OXA-48 β -lactamase reveals mechanistic diversity among class D carbapenemases. *Chem Biol* 2009; **16**: 540–7.

Genetic and Biochemical Characterization of OXA-405, an OXA-48-Type Extended-Spectrum β -Lactamase without Significant Carbapenemase Activity

Laurent Dortet,^{a,b,c,d} Saoussen Oueslati,^a Katy Jeannot,^{b,e} Didier Tandé,^f Thierry Naas,^{a,b,c,d} Patrice Nordmann^{a,b,g,h}

INSERM U 914, Le Kremlin-Bicêtre, France^a; Associated National Reference Center for Antibiotic Resistance, Le Kremlin-Bicêtre, France^b; Faculty of Medicine, South-Paris University, Le Kremlin-Bicêtre, France^c; Bacteriology-Hygiene Unit, Bicêtre Hospital, Assistance Publique/Hôpitaux de Paris, Le Kremlin-Bicêtre, France^d; Besançon Hospital, Microbiology Laboratory, Besançon, France^e; Brest Hospital, Microbiology Laboratory, Brest, France^f; Medical and Microbiology Unit, Department of Medicine, University Fribourg, Fribourg, Switzerland^g; HFR-Hôpital Cantonal, Fribourg, Switzerland^h

The epidemiology of carbapenemases worldwide is showing that OXA-48 variants are becoming the predominant carbapenemase type in *Enterobacteriaceae* in many countries. However, not all OXA-48 variants possess significant activity toward carbapenems (e.g., OXA-163). Two *Serratia marcescens* isolates with resistance either to carbapenems or to extended-spectrum cephalosporins were successively recovered from the same patient. A genomic comparison using pulsed-field gel electrophoresis and automated Rep-PCR typing identified a 97.8% similarity between the two isolates. Both strains were resistant to penicillins and first-generation cephalosporins. The first isolate was susceptible to expanded-spectrum cephalosporins, was resistant to carbapenems, and had a significant carbapenemase activity (positive Carba NP test) related to the expression of OXA-48. The second isolate was resistant to expanded-spectrum cephalosporins, was susceptible to carbapenems, and did not express a significant imipenemase activity, (negative for the Carba NP test) despite possessing a *bla*_{OXA-48}-type gene. Sequencing identified a novel OXA-48-type β -lactamase, OXA-405, with a four-amino-acid deletion compared to OXA-48. The *bla*_{OXA-405} gene was located on a ca. 46-kb plasmid identical to the prototype IncL/M *bla*_{OXA-48}-carrying plasmid except for a ca. 16.4-kb deletion in the *tra* operon, leading to the suppression of self-conjugation properties. Biochemical analysis showed that OXA-405 has clavulanic acid-inhibited activity toward expanded-spectrum activity without significant imipenemase activity. This is the first identification of a successive switch of catalytic activity in OXA-48-like β -lactamases, suggesting their plasticity. Therefore, this report suggests that the first-line screening of carbapenemase producers in *Enterobacteriaceae* may be based on the biochemical detection of carbapenemase activity in clinical settings.

Amblar class D β -lactamases (oxacillinases) are widely disseminated among clinically relevant Gram-negative bacteria (1). They exhibit a high degree of diversity of hydrolysis activity ranging from narrow to broad-spectrum hydrolysis activity toward β -lactams (1). Among the class D β -lactamases, several enzymes hydrolyze carbapenems. Most carbapenem-hydrolyzing class D β -lactamases (CHDLs) are from *Acinetobacter* spp. (e.g., OXA-23, OXA-40, OXA-58, OXA-143) (2, 3), whereas OXA-48-type enzymes are identified in *Enterobacteriaceae* only (4). The OXA-48-derived CHDLs have initially been identified in Turkey (5), first in *Klebsiella pneumoniae* and then in other enterobacterial species (4). The known OXA-48 variants are currently as follows: (i) OXA-162, identified from *K. pneumoniae* isolates in Turkey (6); (ii) OXA-163, identified from *K. pneumoniae* and *Enterobacter cloacae* isolates in Argentina (7, 8); (iii) OXA-181, identified from a *K. pneumoniae* isolate in India (9); (iv) OXA-204, identified from *K. pneumoniae* isolates in patients having a link with North Africa (10); (v) OXA-232, identified in France from a *K. pneumoniae* isolate recovered from a patient who had been transferred from India to Mauritius (11); (vi) OXA-244 and OXA-245, from *K. pneumoniae* isolates collected in Spain (12); (vii) OXA-247, identified from a *K. pneumoniae* isolate recovered in Argentina (13); and (viii) OXA-370, reported from an *Enterobacter hormaechei* isolate in Brazil (14). These variants differ from OXA-48 by one to five amino acid substitutions and/or by a four-amino-acid deletion which results in a modified β -lactam hydrolysis spectrum.

The epidemiology of carbapenemases worldwide shows that OXA-48 variants are becoming the predominant carbapenemase type in *Enterobacteriaceae* in many regions and countries, such as North Africa, Turkey, France, Germany, and the Middle East.

The aim of this study was to characterize the peculiar molecular mechanisms of resistance to β -lactams, involving a switch from a carbapenem resistance/expanded-spectrum cephalosporin susceptibility profile to a carbapenem susceptibility/expanded-spectrum cephalosporin resistance profile, among two successive *Serratia marcescens* isolates from the same patient.

(This work was presented in part at the 54th Interscience Conference on Antimicrobial Agents and Chemotherapy, 5 to 9 September 2014, Washington, DC.)

Received 15 December 2014 Returned for modification 8 February 2015

Accepted 5 April 2015

Accepted manuscript posted online 13 April 2015

Citation Dortet L, Oueslati S, Jeannot K, Tandé D, Naas T, Nordmann P. 2015. Genetic and biochemical characterization of OXA-405, an OXA-48-type extended-spectrum β -lactamase without significant carbapenemase activity. *Antimicrob Agents Chemother* 59:3823–3828. doi:10.1128/AAC.05058-14.

Address correspondence to Patrice Nordmann, patrice.nordmann@unifr.ch.

Copyright © 2015, American Society for Microbiology. All Rights Reserved.

doi:10.1128/AAC.05058-14

TABLE 1 Primers used for mapping of plasmids carrying *bla*_{OXA-48}-type genes

Primer name	Nucleotide data according to GenBank accession no. JN626286			Location	Amplicon size (bp)
	Start	Stop	5' to 3' sequence		
C1F	57425	57444	ATCCGGTCCCCCTGATTATC	Incl/M replicase	4531
C1R	55	74	GTCTGCGACTGACAGACGAT	<i>trbA</i>	
C2F	1208	1227	CGAAAGCCAAACCACATCAC	<i>trbA</i>	4469
OXA-48-3' external	5655	5676	TATTGTCAAACAAGCCATGCTG	<i>bla</i> _{OXA-48}	
OXA-48-5' external	6099	6119	ATTCCAGAGCACAACTACGCC	<i>bla</i> _{OXA-48}	3025
C3R	9104	9123	CCGTCGTTGTTGCTGAGAAC	<i>mucB</i>	
C4F	10248	10267	CGCAGTGAAGGATATTCCC	<i>mucB</i>	4077
C4R	15005	15024	TTCAGGGCGCTGGATTCAAG	<i>orf12</i>	
C5F	15480	15499	GCGTGACCGCCTCAAATTCT	<i>orf12</i>	4207
C5R	19667	19686	CGAGCACTTACGGTTATCAG	<i>parB</i>	
C6F	20083	20102	CATCTGTTCCCGGATGATGA	<i>parB</i>	3892
C6R	23955	23974	TCTATGCCGCCCTGTATTCC	<i>orf25</i>	
C7F	25154	25173	CAGTGAAGGACTGAGCCACT	<i>orf25</i>	4240
C7R	29374	29393	GGCGGGTTGATTCAAGTTCAG	<i>klcA</i>	
C8F	29786	29805	GATTACCGCGGATTGACT	<i>klcA</i>	3757
C8R	33523	33542	GACTTTTTGTCCCTTCGGCC	<i>mobA</i>	
C9F	35370	35389	GCAGGCGTATGCTCAAACCG	<i>mobA</i>	2913
C9R	38263	38282	ACGTGGCGATCGTCAAAGG	<i>pri</i>	
C10F	41356	41375	CAGCCTCAGCATTTACAAGC	<i>pri</i>	4613
C10R	45949	45968	TCAGCAGGCTTAGCAGACAC	<i>traP</i>	
C11F	46577	46596	CAAGTAAAGGCCTTATCCGC	<i>traP</i>	4597
C11R	51154	51173	CTGACCGTTTTGCTTTTCCG	<i>traW</i>	
C12F	52321	52340	GAGTGTGAACGCGGGAGTAT	<i>traW</i>	4144
C12R	56445	56464	ATGAACTCCGGCGAAAGACC	Incl/M replicase	

MATERIALS AND METHODS

Bacterial strains. Identification of clinical isolates was performed by using the API20E system (bioMérieux, La Balme-les-Grottes, France) and confirmed by matrix-assisted laser desorption ionization–time of flight (MALDI-TOF) mass spectrometry (MALDI Biotyper CA system, Bruker Daltonics, Billerica, MA, USA). *Escherichia coli* TOP10 (Invitrogen, Saint-Aubin, France) was used for cloning experiments, and azide-resistant *E. coli* J53 was used for conjugation assays.

Susceptibility testing. Antimicrobial susceptibilities were determined by the disk diffusion technique on Mueller-Hinton agar (Bio-Rad, Marnes-La-Coquette, France) and interpreted according to the EUCAST breakpoints, updated in 2014 (<http://www.eucast.org>). MICs were determined using the Etest technique (bioMérieux).

Detection of carbapenemase activity. The carbapenemase activity was searched for using two techniques: the updated Carba NP test (15) and UV spectrophotometry (16). The updated Carba NP test, which detects imipenemase activity, was performed after plating the culture on a Trypticase soy agar medium supplemented with ZnSO₄, as previously described (17). The UV spectrophotometry technique used has been detailed elsewhere (16).

PCR, cloning experiments, and DNA sequencing. Whole-cell DNAs of the two *S. marcescens* isolates and of OXA-48-producing and OXA-163-producing *K. pneumoniae* isolates (8) were extracted using the QIAamp DNA minikit (Qiagen, Courtabouef, France) and were then used as a template to amplify the *bla*_{OXA-48}-like genes. The PCR, using the primers preOXA-48A (5'-TATATTGCATTAAGCAAGGG-3') and preOXA-48B (5'-CACACAAATACGCGCTAACCC-3'), was able to amplify *bla*_{OXA-48}, *bla*_{OXA-163}, and *bla*_{OXA-405} genes. The amplicons obtained were then cloned into the pCR-Blunt II-Topo plasmid (Invitrogen) downstream from the pLac promoter, in the same orientation. The recombinant pTOPO-OXA plasmids were electroporated into the *E. coli* TOP10 strain. Plasmid DNAs extraction was performed using the Qiagen miniprep kit. Both strands of the inserts of the recombinant plasmids were sequenced using a T7 promoter and M13 reverse primers with an automated se-

quencer (ABI Prism 3100; Applied Biosystems). The nucleotide sequences were analyzed using software available at the National Center for Biotechnology Information website (<http://www.ncbi.nlm.nih.gov>).

Plasmid characterization and mating-out assay. Plasmid DNAs of both clinical *S. marcescens* isolates and OXA-163-producing *K. pneumoniae* 6299 were extracted using the Kieser method (18). Plasmids of ca. 154, 66, 48, and 7 kb of *Escherichia coli* NCTC 5019 were used as plasmid size markers. Plasmid DNA was analyzed by agarose gel electrophoresis. Transfer of the β-lactam resistance markers was attempted by liquid mating-out assays at 37°C using *E. coli* J53 as the recipient strain and by electroporation of the plasmid DNA suspension of clinical isolates into *E. coli* TOP10. Selection of transconjugants was performed on agar-supplemented plates with ticarcillin (100 mg/liter) and with azide (100 mg/liter). Plasmids were typed using the PCR-based replicon typing (PBRT) scheme, as described previously (19), and using the specific primers RepA-A (5'-GACATTGAGTCAGTAGAAGG-3') and RepA-B (5'-CGTG CAGTTCGCTTTTCGGC-3') designed for the detection of the Incl/M OXA-48 plasmid replicase (20).

The *bla*_{OXA-405}-carrying plasmid was characterized by PCR mapping followed by DNA sequencing. Fourteen primer pairs were used for the mapping of the 61,881-bp Incl/M plasmid carrying the *bla*_{OXA-48} gene (Table 1). The *bla*_{OXA-48}-carrying plasmid sequence (GenBank accession number JN626286) was used as a positive control for PCR mapping (20).

Hydrolysis analysis. The specific activities of the β-lactamases OXA-48, OXA-163, and OXA-405 were determined using the supernatant of a whole-cell crude extract obtained from an overnight culture of *E. coli* clones expressing those β-lactamases (pTOPO-OXA-48, pTOPO-OXA-163, and pTOPO-OXA-405 in *E. coli* TOP 10) with the UV spectrophotometer Ultrospec 2000 (Amersham Pharmacia Biotech), as previously described (10).

Nucleotide sequence accession number. The nucleotide sequence of the *bla*_{OXA-405} gene has been submitted to the EMBL/GenBank nucleotide sequence database under the accession number KM589641.

TABLE 2 MICs of β -lactams for *S. marcescens* OXA-48 (Sm1), *S. marcescens* OXA-405 (Sm2), *E. coli* pTOPO-OXA-48, *E. coli* pTOPO-OXA-405, *E. coli* pTOPO-OXA-163, and *E. coli* TOP10

β -Lactams	MIC (mg/liter) of:					
	<i>S. marcescens</i> OXA-48 (Sm1)	<i>S. marcescens</i> OXA-405 (Sm2)	<i>E. coli</i> TOP10 (pTOPO-OXA-48)	<i>E. coli</i> TOP10 (pTOPO-OXA-405)	<i>E. coli</i> TOP10 (pTOPO-OXA-163)	<i>E. coli</i> TOP10
Amoxicillin	>256	>256	>256	>256	>256	2
Amoxicillin + CLA ^a	>256	>256	192	>256	96	2
Piperacillin	>256	>256	128	>256	>256	1.5
Piperacillin + TZB ^b	96	>256	12	24	32	1
Temocillin	>256	8	>256	32	32	4
Ticarcillin	>256	>256	>256	>256	>256	2
Cefalotin	>256	>256	8	32	64	2
Cefepime	0.25	3	0.032	0.5	0.5	0.023
Cefepime + TZB ^b	0.25	2	0.032	0.19	0.19	0.023
Cefotaxime	1.5	6	0.19	0.5	3	0.06
Cefotaxime + TZB ^b	1.5	4	0.19	0.19	1	0.06
Ceftazidime	0.25	4	0.25	3	16	0.12
Ceftazidime + TZB ^b	0.25	2	0.25	1	3	0.12
Imipenem	4	0.5	0.5	0.25	0.25	0.19
Meropenem	4	0.19	0.094	0.023	0.023	0.01
Ertapenem	>32	0.75	0.25	0.032	0.032	0.06
Doripenem	3	0.125	0.064	0.023	0.023	0.023
Aztreonam	0.125	4	0.064	1	2	0.047

^a CLA, clavulanic acid at a fixed concentration of 4 mg/liter.

^b TZB, tazobactam at a fixed concentration of 4 mg/liter.

RESULTS

Patient features and characteristics of the *S. marcescens* clinical isolates.

In January 2011, a 26-year-old woman was admitted at the emergency unit of the University Hospital of Besançon (eastern part of France) for an acute pulmonary infection. After 2 days of hospitalization, blood cultures and a tracheal aspirate identified *S. marcescens* isolates with identical antibiotic susceptibility profiles (these isolates were denoted Sm1). They were resistant to ticarcillin, ticarcillin-clavulanic acid, piperacillin-tazobactam, and temocillin (MIC, >256 mg/liter), had decreased susceptibility to carbapenems (imipenem, meropenem, ertapenem, and doripenem), and remained susceptible to expanded-spectrum cephalosporins (Table 2). A positive Carba NP test indicated the expression of a carbapenemase, and PCR experiments were carried out on purified DNA of Sm1 with primers specific to common carbapenemase genes (*bla*_{KPC}, *bla*_{IMP}, *bla*_{VIM}, *bla*_{NDM}, and *bla*_{OXA-48}). A *bla*_{OXA-48}-like gene was amplified and was later identified as *bla*_{OXA-48} according to sequencing results. The patient was successfully treated with cefepime and amikacin for 15 days. Furthermore, due to the irradiation of the nasopharynx for a carcinoma at the age of 14, the patient presented with important locoregional sequelae composed of sclerosis of the thorax and cervical regions and the persistence of a right laryngeal-cervical fistula. More than 18 months later (October 2012), another *S. marcescens* strain (Sm2) was isolated from a breast hematoma. This *S. marcescens* isolate was resistant to ticarcillin, ticarcillin-clavulanic acid, and piperacillin-tazobactam, had a decreased susceptibility to ertapenem, but remained susceptible to the other tested carbapenem molecules (imipenem, meropenem, and doripenem). The Carba NP test did not reveal carbapenemase activity. Unlike isolate Sm1, isolate Sm2 was resistant to expanded-spectrum cephalosporins (cefotaxime, ceftazidime, cefepime) and aztreonam (Table 2) and recovered susceptibility to temocillin (MIC, 8 mg/liter). PCR using whole-cell DNA of Sm2 as the template was positive for a

*bla*_{OXA-48}-like gene. Sequencing results identified a novel *bla*_{OXA-405}-like gene, designated the *bla*_{OXA-405} gene.

Genomic comparison using a Rep-PCR-based technique (Diversi-Lab, bioMérieux) identified a 97.8% genomic similarity between the *S. marcescens* Sm1 and Sm2 isolates (Fig. 1A). Therefore, these strains were considered to be clonally related. This clonality has been confirmed by pulsed-field gel electrophoresis (Fig. 1B).

Characterization of the β -lactamase OXA-405. This *bla*_{OXA-405} gene differs from the *bla*_{OXA-48} gene by a 12-bp deletion leading to a four-amino-acid deletion in the OXA-405 protein sequence from residues Thr213 to Glu216 compared to the OXA-48 sequence (Fig. 2). The comparison of the hydrolysis spectra of OXA-405, OXA-48, and OXA-163 was done by cloning *bla*_{OXA-405}, *bla*_{OXA-48}, and *bla*_{OXA-163} genes in the pCR-Blunt II-Topo kit (Invitrogen) and expressing them in *E. coli* TOP10. OXA-405 and OXA-163 conferred similar resistance profiles, consisting of a decreased susceptibility to expanded-spectrum cephalosporins and aztreonam compared to that conferred by OXA-48 (Table 2). As opposed to OXA-48, OXA-405, like the OXA-163 enzyme, once expressed in a reference *E. coli* strain was not associated with a decreased susceptibility to carbapenems (Table 2). Both the Carba NP test and the UV spectrophotometry analysis showed that OXA-405 and OXA-163 did not express significant imipenemase activity (Table 3). In addition, OXA-405 producers and also OXA-163 producers were 8-fold more susceptible to temocillin than OXA-48 producers (Table 2).

The specific activities of OXA-405 and of OXA-163 were very similar for penicillins, broad-spectrum cephalosporins, and carbapenems. However, OXA-405 hydrolyzed less ceftazidime (6-fold less) than OXA-163 (Table 3). Both OXA-405 and OXA-163 had barely detectable activity against carbapenems compared to OXA-48 (~25-fold less for imipenem) (Table 3). On the other hand, OXA-405 and OXA-163 hydrolyzed expanded-spectrum cephalosporins and aztreonam at high rates, while OXA-48 did

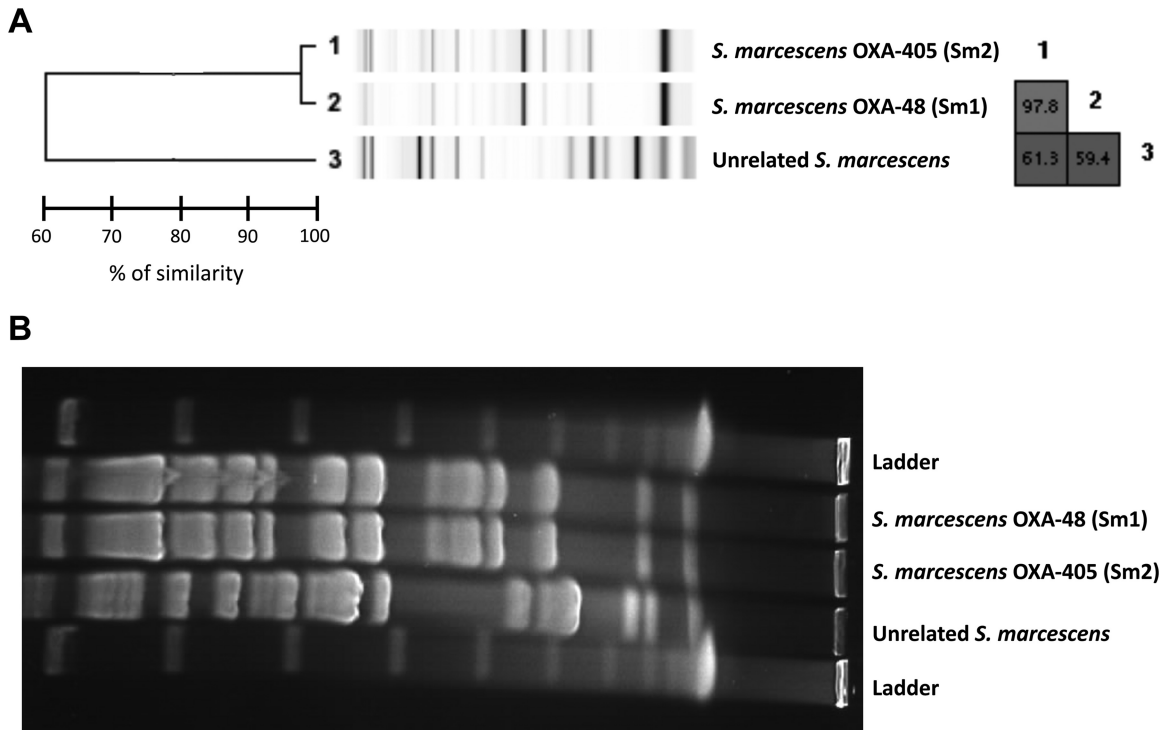


FIG 1 (A) Rep-PCR analysis using the Diversilab technique. Dendrogram and computer-generated image of Rep-PCR banding patterns of OXA-48-producing *S. marcescens*, OXA-405-producing *S. marcescens*, and an unrelated strain of *S. marcescens*. (B) Pulsed-field gel electrophoresis of OXA-48-producing *S. marcescens*, OXA-405-producing *S. marcescens*, and an unrelated strain of *S. marcescens*.

not (Table 3). This activity against expanded-spectrum cephalosporins of OXA-405 was inhibited by the addition of tazobactam (Table 2).

Genetic environment of the *bla*_{OXA-405} gene. The *bla*_{OXA-405} gene was located on transposon Tn1999, as the *bla*_{OXA-48} gene usually is (4, 20). Plasmid DNAs of *S. marcescens* Sm1 (pOXA-48) and Sm2 (pOXA-405) were extracted and compared. A single plasmid was identified from each strain, of ca. 62 kb and ca. 46 kb for Sm1 and Sm2, respectively. A PCR-based replicon typing method revealed that these plasmids belonged to the same IncL/M incompatibility group. Whereas transformants in *E. coli* were obtained

by using both plasmids, transconjugants were obtained with the pOXA-48 plasmid only. PCR mapping of plasmids pOXA-48 and pOXA-405 showed that pOXA-48 was structurally identical to the prototype IncL/M OXA-48-positive plasmid. Plasmid pOXA-405 had a backbone similar to that of pOXA-48 but had a 16,382-bp deletion from nucleotides 24210 to 40587 according to the reference *bla*_{OXA-48} plasmid (number JN626286, GenBank nucleotide database) (20). This deletion included the *ssb* gene, the *mobC* and *mobA* genes, the *nikB* and *nikA* genes, and a part of locus *tra* (*traH*, *traI*, *traJ*, *traK*, *traL*, and primase genes). This deleted DNA section was replaced by an insertion sequence, IS1R (Fig. 3B).

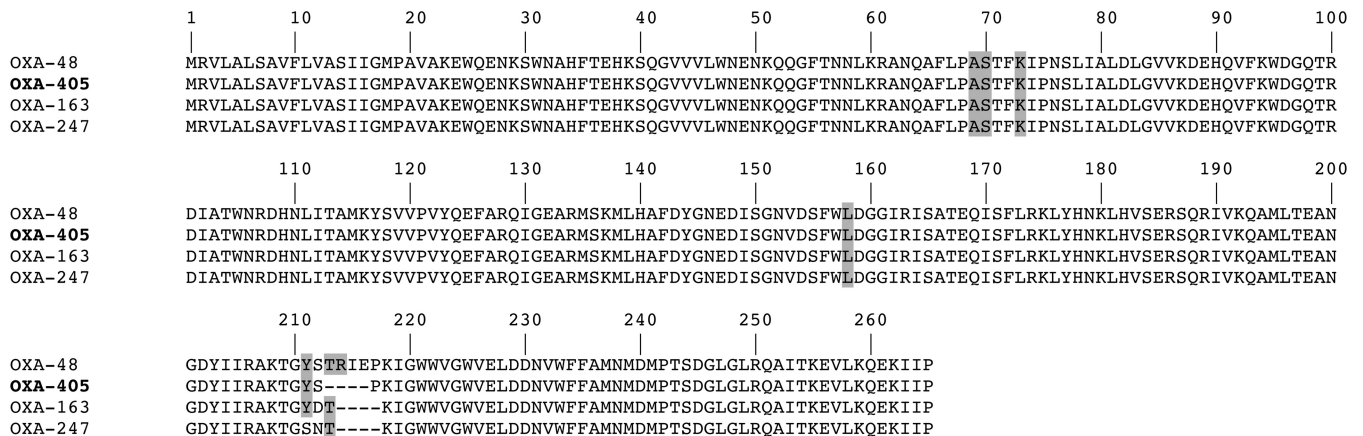


FIG 2 Alignment of the amino acid sequences of OXA-48, OXA-405, OXA-163, and OXA-247. Possible conserved residues of the active site of the OXA-48-type β -lactamases are highlighted in gray.

TABLE 3 Specific activities of β -lactamases OXA-48, OXA-405, and OXA-163

β -Lactams	Specific activity (mean mU/mg of protein \pm SD) of:		
	OXA-48	OXA-405	OXA-163
Amoxicillin	981 \pm 62	485 \pm 35	795 \pm 81
Piperacillin	450 \pm 5	436 \pm 4	214 \pm 2
Temocillin	11 \pm 2	5 \pm 0.5	5 \pm 0.4
Ticarcillin	647 \pm 59	63 \pm 6	80 \pm 7
Cefepime	5 \pm 0.5	27 \pm 2	30 \pm 3
Cefotaxime	60 \pm 6	117 \pm 10	167 \pm 15
Cefoxitin	2 \pm 0.2	1 \pm 0.1	1 \pm 0.1
Ceftazidime	2 \pm 0.2	9 \pm 0.8	53 \pm 5
Cefalotin	75 \pm 8	140 \pm 12	130 \pm 10
Imipenem	57 \pm 4	3 \pm 0.2	2 \pm 0.2
Meropenem	3 \pm 0.1	2 \pm 0.2	2 \pm 0.1
Ertapenem	2 \pm 0.2	1 \pm 0.1	1 \pm 0.1
Doripenem	2 \pm 0.2	1 \pm 0.1	1 \pm 0.1
Aztreonam	5 \pm 0.5	14 \pm 1	18 \pm 2

DISCUSSION

A novel OXA-48-type β -lactamase, OXA-405, has been identified here. OXA-405, like the other OXA-48-type β -lactamases OXA-163 and OXA-247, has a significant activity toward expand-

ed-spectrum cephalosporins but barely any activity toward carbapenems. Therefore, it should be underlined that OXA-48-like β -lactamases, as opposed to all known KPC, NDM, VIM, or IMP β -lactamases, are not all significant carbapenemases. In addition, it has been shown that OXA-48-type producers with carbapenemase activity are mostly resistant to temocillin. Here, we confirm that this temocillin resistance trait would be a good criterion for differentiating OXA-48-type producers with and without carbapenemase activity.

Structural protein analysis of OXA-405, OXA-163, and OXA-247 showed that they possess at least the same four-amino-acid deletion in a specific region, from Thr213 to Glu216 (8, 13). This result agrees with crystal structure analysis of OXA-48 showing that Arg 214 (which is part of a β 5 strand) is critical for carbapenemase activity (21). In addition, recent studies point out the crucial role of this short loop connecting β 5 and β 6 strands in conferring carbapenemase activity of Ambler class D β -lactamases (22, 23).

Genetic analysis of the *S. marcescens* clinical isolates Sm1 and Sm2 producing OXA-48 and OXA-405, respectively, indicates that they are clonally related. This result suggests that the *bla*_{OXA-405} gene may derive from the same ancestor, a *bla*_{OXA-48} gene. This hypothesis is reinforced by the common genetic environment of those two genes. Actually, the *bla*_{OXA-48} and *bla*_{OXA-405} genes were

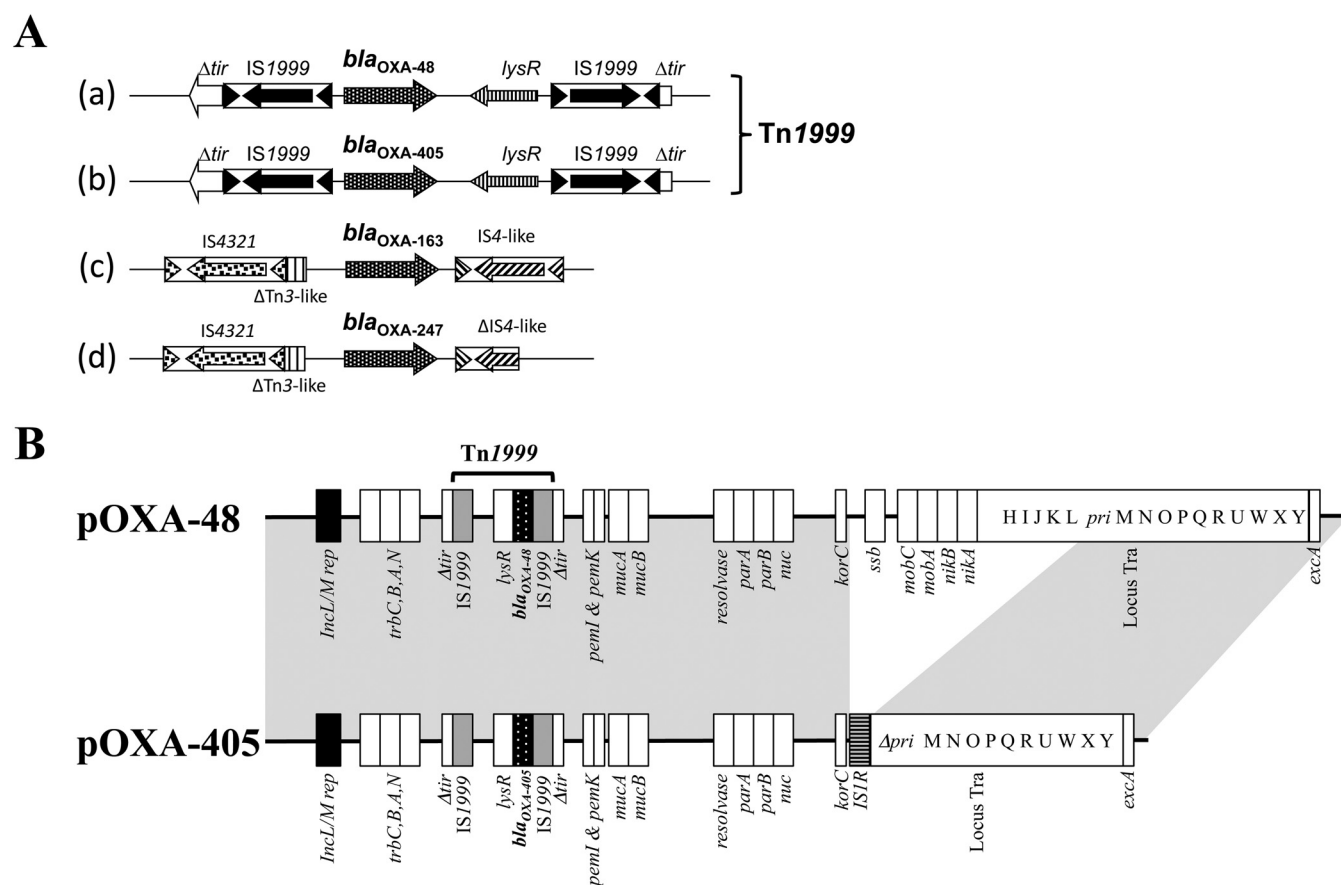


FIG 3 (A) Schematic representation of the genetic environment of the *bla*_{OXA-48} (a), *bla*_{OXA-405} (b), *bla*_{OXA-163} (c), and *bla*_{OXA-247} (d) genes. The Tn1999 composite transposon is made of two copies of insertion sequence IS1999, bracketing a fragment containing the *bla*_{OXA-48} and *bla*_{OXA-405} genes. (B) Major structural features of the plasmid pOXA-405 from *S. marcescens* Sm2 in comparison with the prototype IncL/M *bla*_{OXA-48} plasmid (pOXA-48) (GenBank accession number JN626286). Common structures are highlighted in gray.

bracketed by two copies of an identical IS element, IS1999, forming a composite transposon Tn1999. This genetic environment was completely different from the mosaic structures made of insertion sequences and the truncated mobile element that surrounds the *bla*_{OXA-163} gene and its derivative, *bla*_{OXA-247} (Fig. 3) (8, 13). In addition, the *bla*_{OXA-405} gene was identified on the plasmid pOXA-405, which possessed a backbone similar to that of the IncL/M *bla*_{OXA-48}-bearing plasmid (pOXA-48) (20), except for a deletion of ca. 16 kb replaced by the insertion sequence IS1R. This deletion/insertion led to the loss of conjugative genes and the related self-conjugative property of pOXA-405 (20). The selection pressure of a cephalosporin-containing treatment (here, cefepime) remains to be determined for selecting an OXA-48-type β -lactamase with activity against expanded-spectrum cephalosporins from an OXA-48-type β -lactamase with carbapenemase activity.

In conclusion, this report underlines that OXA-48-type β -lactamases are more diverse than expected. As exemplified by OXA-405, the OXA-48-type β -lactamases are not all true carbapenemases. The same statement is valid for another group of serine β -lactamases, the GES group of enzymes, in which GES-1 is an extended-spectrum β -lactamase, while GES-2 is a carbapenemase (24). Therefore, the first-line screening of carbapenemase producers in *Enterobacteriaceae* may be best based on the biochemical detection of carbapenemase activity in clinical settings. The molecular biology techniques, although useful, may overreport OXA-48-like producers as being all carbapenemases and, conversely, may fail to detect carbapenemase producers related to totally novel or slightly structurally modified carbapenemase genes.

ACKNOWLEDGMENTS

We thank Christophe De Champs, who let us work on the OXA-405-producing *S. marcescens* isolate.

This work was partially funded by a grant from the INSERM (U 914).

REFERENCES

- Poirel L, Naas T, Nordmann P. 2010. Diversity, epidemiology, and genetics of class D β -lactamases. *Antimicrob Agents Chemother* 54:24–38. <http://dx.doi.org/10.1128/AAC.01512-08>.
- Higgins PG, Poirel L, Lehmann M, Nordmann P, Seifert H. 2009. OXA-143, a novel carbapenem-hydrolyzing class D β -lactamase in *Acinetobacter baumannii*. *Antimicrob Agents Chemother* 53:5035–5038. <http://dx.doi.org/10.1128/AAC.00856-09>.
- Poirel L, Nordmann P. 2006. Carbapenem resistance in *Acinetobacter baumannii*: mechanisms and epidemiology. *Clin Microbiol Infect* 12: 826–836. <http://dx.doi.org/10.1111/j.1469-0691.2006.01456.x>.
- Poirel L, Potron A, Nordmann P. 2012. OXA-48-like carbapenemases: the phantom menace. *J Antimicrob Chemother* 67:1597–1606. <http://dx.doi.org/10.1093/jac/dks121>.
- Poirel L, Heritier C, Tolun V, Nordmann P. 2004. Emergence of oxacillinase-mediated resistance to imipenem in *Klebsiella pneumoniae*. *Antimicrob Agents Chemother* 48:15–22. <http://dx.doi.org/10.1128/AAC.48.1.15-22.2004>.
- Kasap M, Torol S, Kolayli F, Dundar D, Vahaboglu H. 2013. OXA-162, a novel variant of OXA-48, displays extended hydrolytic activity towards imipenem, meropenem and doripenem. *J Enzyme Inhib Med Chem* 28: 990–996. <http://dx.doi.org/10.3109/14756366.2012.702343>.
- Abdelaziz MO, Bonura C, Aleo A, El-Domany RA, Fasciana T, Mamina C. 2012. OXA-163-producing *Klebsiella pneumoniae* in Cairo, Egypt, in 2009 and 2010. *J Clin Microbiol* 50:2489–2491. <http://dx.doi.org/10.1128/JCM.06710-11>.
- Poirel L, Castanheira M, Carrer A, Rodriguez CP, Jones RN, Smayevsky J, Nordmann P. 2011. OXA-163, an OXA-48-related class D β -lactamase with extended activity toward expanded-spectrum cephalosporins. *Antimicrob Agents Chemother* 55:2546–2551. <http://dx.doi.org/10.1128/AAC.00022-11>.
- Potron A, Nordmann P, Lafeuille E, Al Maskari Z, Al Rashdi F, Poirel L. 2011. Characterization of OXA-181, a carbapenem-hydrolyzing class D β -lactamase from *Klebsiella pneumoniae*. *Antimicrob Agents Chemother* 55:4896–4899. <http://dx.doi.org/10.1128/AAC.00481-11>.
- Potron A, Nordmann P, Poirel L. 2013. Characterization of OXA-204, a carbapenem-hydrolyzing class D β -lactamase from *Klebsiella pneumoniae*. *Antimicrob Agents Chemother* 57:633–636. <http://dx.doi.org/10.1128/AAC.01034-12>.
- Potron A, Rondinaud E, Poirel L, Belmonte O, Boyer S, Camiade S, Nordmann P. 2013. Genetic and biochemical characterisation of OXA-232, a carbapenem-hydrolyzing class D β -lactamase from *Enterobacteriaceae*. *Int J Antimicrob Agents* 41:325–329. <http://dx.doi.org/10.1016/j.ijantimicag.2012.11.007>.
- Oteo J, Hernandez JM, Espasa M, Fleites A, Saez D, Bautista V, Perez-Vazquez M, Fernandez-Garcia MD, Delgado-Iribarren A, Sanchez-Romero I, Garcia-Picazo L, Miguel MD, Solis S, Aznar E, Trujillo G, Mediavilla C, Fontanals D, Rojo S, Vindel A, Campos J. 2013. Emergence of OXA-48-producing *Klebsiella pneumoniae* and the novel carbapenemases OXA-244 and OXA-245 in Spain. *J Antimicrob Chemother* 68:317–321. <http://dx.doi.org/10.1093/jac/dks383>.
- Gomez S, Pasteran F, Faccione D, Bettiol M, Veliz O, De Belder D, Rapoport M, Gatti B, Petroni A, Corso A. 2013. Inpatient emergence of OXA-247: a novel carbapenemase found in a patient previously infected with OXA-163-producing *Klebsiella pneumoniae*. *Clin Microbiol Infect* 19:E233–E235. <http://dx.doi.org/10.1111/1469-0691.12142>.
- Sampaio JL, Ribeiro VB, Campos JC, Rozales FP, Magagnin CM, Falci DR, da Silva RC, Dalarosa MG, Luz DI, Vieira FJ, Antochevis LC, Barth AL, Zavascki AP. 2014. Detection of OXA-370, an OXA-48-related class D β -lactamase, in *Enterobacter hormaechei* from Brazil. *Antimicrob Agents Chemother* 58:3566–3567. <http://dx.doi.org/10.1128/AAC.02510-13>.
- Nordmann P, Poirel L, Dortet L. 2012. Rapid detection of carbapenemase-producing *Enterobacteriaceae*. *Emerg Infect Dis* 18:1503–1507. <http://dx.doi.org/10.3201/eid1809.120355>.
- Bernabeu S, Poirel L, Nordmann P. 2012. Spectrophotometry-based detection of carbapenemase producers among *Enterobacteriaceae*. *Diagn Microbiol Infect Dis* 74:88–90. <http://dx.doi.org/10.1016/j.diagmicrobio.2012.05.021>.
- Dortet L, Brechard L, Poirel L, Nordmann P. 2014. Impact of the isolation medium for detection of carbapenemase-producing *Enterobacteriaceae* using an updated version of the Carba NP test. *J Med Microbiol* 63:772–776. <http://dx.doi.org/10.1099/jmm.0.071340-0>.
- Kieser T. 1984. Factors affecting the isolation of CCC DNA from *Streptomyces lividans* and *Escherichia coli*. *Plasmid* 12:19–36. [http://dx.doi.org/10.1016/0147-619X\(84\)90063-5](http://dx.doi.org/10.1016/0147-619X(84)90063-5).
- Carattoli A, Bertini A, Villa L, Falbo V, Hopkins KL, Threlfall EJ. 2005. Identification of plasmids by PCR-based replicon typing. *J Microbiol Methods* 63:219–228. <http://dx.doi.org/10.1016/j.mimet.2005.03.018>.
- Poirel L, Bonnin RA, Nordmann P. 2012. Genetic features of the widespread plasmid coding for the carbapenemase OXA-48. *Antimicrob Agents Chemother* 56:559–562. <http://dx.doi.org/10.1128/AAC.05289-11>.
- Docquier JD, Calderone V, De Luca F, Benvenuti M, Giuliani F, Bellucci L, Tafi A, Nordmann P, Botta M, Rossolini GM, Mangani S. 2009. Crystal structure of the OXA-48 β -lactamase reveals mechanistic diversity among class D carbapenemases. *Chem Biol* 16:540–547. <http://dx.doi.org/10.1016/j.chembiol.2009.04.010>.
- De Luca F, Benvenuti M, Carboni F, Pozzi C, Rossolini GM, Mangani S, Docquier JD. 2011. Evolution to carbapenem-hydrolyzing activity in noncarbapenemase class D β -lactamase OXA-10 by rational protein design. *Proc Natl Acad Sci U S A* 108:18424–18429. <http://dx.doi.org/10.1073/pnas.1110530108>.
- Mitchell JM, Clasman JR, June CM, Kaitany KC, LaFleur JR, Taracila MA, Klinger NV, Bonomo RA, Wymore T, Szarecka A, Powers RA, Leonard DA. 2015. Structural basis of activity against aztreonam and extended-spectrum cephalosporins for two carbapenem-hydrolyzing class D β -lactamases from *Acinetobacter baumannii*. *Biochemistry* 54: 1976–1987. <http://dx.doi.org/10.1021/bi501547k>.
- Poirel L, Weldhagen GF, Naas T, De Champs C, Dove MG, Nordmann P. 2001. GES-2, a class A β -lactamase from *Pseudomonas aeruginosa* with increased hydrolysis of imipenem. *Antimicrob Agents Chemother* 45: 2598–2603. <http://dx.doi.org/10.1128/AAC.45.9.2598-2603.2001>.



Article

Biochemical and Structural Characterization of OXA-405, an OXA-48 Variant with Extended-Spectrum β -Lactamase Activity

Saoussen Oueslati ¹, Pascal Retailleau ², Ludovic Marchini ², Laurent Dortet ^{1,3,4}, Rémy A. Bonnin ^{1,3} , Bogdan I. Iorga ² and Thierry Naas ^{1,3,4,*}

¹ EA7361 “Structure, dynamic, function and expression of broad spectrum β -lactamases”, Faculty of Medicine of Paris-Sud University, Labex LERMIT, University Paris-Saclay, 94270 Le Kremlin-Bicêtre, France; oueslati.saoussen@gmail.com (S.O.); laurent.dortet@aphp.fr (L.D.); remy.bonnin@u-psud.fr (R.A.B.)

² Institut de Chimie des Substances Naturelles, CNRS UPR 2301, Labex LERMIT, 91198 Gif-sur-Yvette, France; pascal.retailleau@cnrs.fr (P.R.); ludovic.Marchini@vinci.fr (L.M.); bogdan.iorga@cnrs.fr (B.I.I.)

³ French National Reference Center for Antibiotic Resistance: Carbapenemase-producing Enterobacteriaceae, 94270 Le Kremlin-Bicêtre, France

⁴ Bacteriology-Hygiene unit, Bicêtre Hospital, Assistance Publique/Hôpitaux de Paris, 94270 Le Kremlin-Bicêtre, France

* Correspondence: thierry.naas@aphp.fr; Tel.: +33-1-45-21-20-19; Fax: +33-1-45-21-63-40

Received: 21 November 2019; Accepted: 18 December 2019; Published: 21 December 2019



Abstract: OXA-48-producing Enterobacterales have now widely disseminated globally. A sign of their extensive spread is the identification of an increasing number of OXA-48 variants. Among them, three are particularly interesting, OXA-163, OXA-247 and OXA-405, since they have lost carbapenem activities and gained expanded-spectrum cephalosporin hydrolytic activity subsequent to a four amino-acid (AA) deletion in the β 5– β 6 loop. We investigated the mechanisms responsible for substrate specificity of OXA-405. Kinetic parameters confirmed that OXA-405 has a hydrolytic profile compatible with an ESBL (hydrolysis of expanded spectrum cephalosporins and susceptibility to class A inhibitors). Molecular modeling techniques and 3D structure determination show that the overall dimeric structure of OXA-405 is very similar to that of OXA-48, except for the β 5– β 6 loop, which is shorter for OXA-405, suggesting that the length of the β 5– β 6 loop is critical for substrate specificity. Covalent docking with selected substrates and molecular dynamics simulations evidenced the structural changes induced by substrate binding, as well as the distribution of water molecules in the active site and their role in substrate hydrolysis. All this data may represent the structural basis for the design of new and efficient class D inhibitors.

Keywords: oxacillinase; OXA-ESBL; carbapenemase; substrate selectivity; beta-lactamase; crystal structure; docking; antibiotic resistance

1. Introduction

The widespread use of antibiotics led to the emergence of carbapenem resistance in Gram-negative bacteria and became a real clinical concern. This resistance is mostly due to the production of carbapenem-hydrolyzing β -lactamases, carbapenemases that belong to Amber class A (KPC), B (NDM, VIM, and IMP), or D (OXA-48 and its variants) [1]. One of the main carbapenemases is the class D β -lactamase OXA-48, which represents a major public health threat because of its rapid spread worldwide [2–4]. Although OXA-48 hydrolyzes penicillins at high level, it hydrolyzes carbapenems at a low level and shows very weak activity against expanded-spectrum cephalosporins. However, when associated to impaired outer-membrane permeability and an ESBL, OXA-48-producers may turn

into deadly bacteria, as only limited antibiotic choices are left for treating serious infections with these bacteria [5].

The OXA-48 β -lactamase was initially identified from a *Klebsiella pneumoniae* isolate in Istanbul (2004) [4]; it then rapidly spread throughout the Mediterranean area, the Middle East, and Europe [6] and became an increasing threat. Since OXA-48's first identification, several OXA-48 variants have been reported worldwide [7,8]. All these enzymes, except OXA-163, OXA-247, and OXA-405, have similar hydrolytic profiles as OXA-48: a high level of hydrolysis of penicillin, a low level of carbapenem hydrolysis, but no significant hydrolysis of broad-spectrum cephalosporins, such as ceftazidime [9]. OXA-163 (identified from *K. pneumoniae* and *Enterobacter cloacae* isolates in Argentina and in Egypt) [10,11], OXA-247, a point mutant derivative of OXA-163 from Argentina [12], OXA-439, another point mutant derivative of OXA-163 (unpublished, KP727573.1), and OXA-405 (identified from *S. marcescens* in France) [13] differ by a four amino-acid deletion (213-TRIE-217 for OXA-405; 214-RIEP-217, plus a substitution S212D for OXA-163, Y124H, and S212D for OXA-439, and YS211-212SN for OXA-247), located in the β 5– β 6 loop, which results in a modified β -lactam spectrum of hydrolysis (Figure 1). Indeed, analysis of the hydrolytic properties of OXA-163 and OXA-405 showed an ESBL-type profile, that they hydrolyze cefotaxime and cephalothin efficiently, are partially inhibited by clavulanate, and lack significant carbapenem hydrolysis [13]. The aim of this study was to investigate the mechanisms responsible for this peculiar substrate specificity of OXA-405, using biochemical and structural tools, and to compare the resulting structure and the hydrolytic profile with those of OXA-163 and OXA-48.

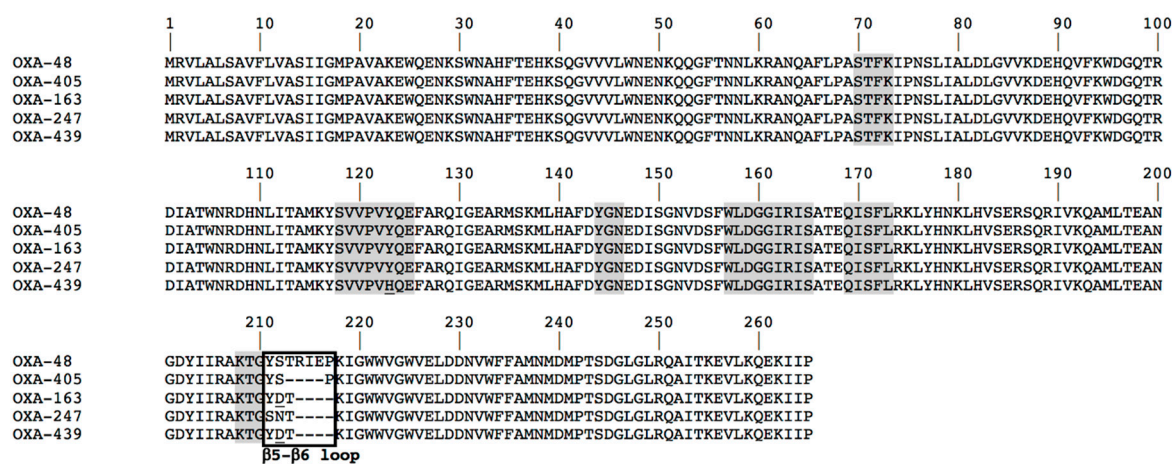


Figure 1. Amino acid sequence alignment of OXA-48 variants. Amino acid motifs that are well conserved among class D lactamases are indicated by gray shading, and the black frame corresponds to the β 5– β 6 loop. Numbering is according to OXA-48 sequence.

2. Materials and Methods

2.1. Bacterial Strains

The clinical strain *S. marcescens* expressing the OXA-405 β -lactamase was used for the cloning of the *bla*_{OXA-405} gene [13]. *E. coli* TOP10 (Invitrogen, Saint-Aubin, France) was used for cloning, and *E. coli* BL21 (DE3) (Novagen, Fontenay-sous-Bois, France) was used for overexpression experiments.

2.2. PCR, Cloning, Expression, and DNA Sequencing

Whole-cell DNA of *S. marcescens* [13] isolates producing OXA-405 was extracted, using the QIAamp DNA mini kit (Qiagen, Courtaboeuf, France) and used as a template to amplify the *bla*_{OXA-405} gene. The sequences without the peptide signal (predicted by SignalIP 4.1 Server) of *bla*_{OXA-405} gene, encoding for the mature protein from amino acid K23 to P261, were obtained by PCR amplification,

using primers OXA₂₃₋₂₅₆NdeI (5'-aaaaaCATATGaaggaatggcaagaaaacaaa-3'), which included an *NdeI* restriction site and the reverse primer OXAXhoI- Δ stop (5'-aaaaaCTCGAGggggaataatcttctgtttgag-3'), which included an *XhoI* restriction site and a deletion of the stop codon of the gene to allow the expression of an C_Term His tag. Then, PCR product was cloned into pET41b vector (Invitrogen[®], Life Technologies, Cergy-Pontoise, France), using *NdeI* and *XhoI* restriction enzymes, to obtain a C-Term His₈-tag. The accuracy of the recombinant plasmid was verified by sequencing, using a T7 promoter and T7 terminator with an ABI Prism 3100 automated sequencer (Applied Biosystems, Thermo Fisher Scientific, Les Ulis, France). The nucleotide sequences were analyzed by using software available at the National Center for Biotechnology Information website (<http://www.ncbi.nlm.nih.gov>).

2.3. Protein Purification

The recombinant plasmid pET41b-OXA-405₂₃₋₂₆₅HIS was transformed into *E. coli* BL21 (DE3), and an overnight culture was used to inoculate 2 L of Luria Bertani medium broth containing 50 μ g/mL of kanamycin. Bacteria were cultured at 37 °C, until an OD of 0.6 at 600 nm was reached. The expression of the β -lactamase genes was carried out at 37 °C for 3 h, with 1 mM of IPTG as an inducer. Cells were pelleted by centrifugation, at 6000 \times g for 15 min, then resuspended with 25 mM of phosphate sodium pH 7.4, 300 mM of K₂SO₄, and 10 mM of imidazole. Bacterial cells were disrupted by sonication, and the bacteria debris was removed by 2 centrifugations: first at 10,000 \times g for 1 h at 4 °C, and then the supernatants obtained were centrifuged at 96,000 \times g for 1 h at 4 °C. The soluble fraction was filtered and then passed through a HisTrap[™]HP column (GE Healthcare[®], Velizy-Villacoublay, France). The OXA-405_{HIS8} protein was eluted, using elution buffer (25 mM of phosphate sodium pH 7.4, 300 mM of K₂SO₄, and 500 mM of imidazole). The eluted protein was concentrated by using Vivaspin 20 (10 000 MWCOPES Sartorius[®], Aubagne, France) and then dialyzed against 0.1 M of HEPES (pH 7.5) buffer. The protein purity, estimated by SDS-PAGE, was more than 99%, and the pooled fractions were dialyzed against 10 mM of Tris-HCl pH 7.6 and concentrated, using Vivaspin columns. Protein concentration was determined by Bradford Protein assay (Bio-Rad, Marnes-La-Coquette, France).

2.4. Steady State Kinetic Determinations

Purified β -lactamase was used for kinetic measurements, which were determined in 100 mM of Tris-H₂SO₄ and 300 mM of K₂SO₄ (pH 7), and antibiotics were purchased from Sigma-Aldrich (Saint-Quentin Fallavier, France) [9]. The k_{cat} and K_m values were determined by analyzing β -lactam hydrolysis under initial-rate conditions, with an ULTROSPEC[®] 2000 model UV spectrophotometer (GE Healthcare, Velizy-Villacoublay, France) and SWIFT II software (GE Healthcare, Velizy-Villacoublay, France), using the Eadie-Hofstee linearization of the Michaelis-Menten equation. The concentration that reduced the level of hydrolysis by 50% (IC₅₀) was determined in a buffer comprising 100 mM of Tris-H₂SO₄ and 300 mM of K₂SO₄ (pH 7), with 100 μ M of benzylpenicillin as a reporter substrate. The enzymes were incubated with different concentrations of inhibitors, for 3 min, before the kinetic parameter determination [9].

2.5. Protein Crystallization and X-Ray Crystallography

Crystallization conditions using commercial kits (Classics, PEGs I and II, and AmSO4 suites from Qiagen, Courtaboeuf, France) were screened in sitting-drop vapor diffusion experiments, using a Cartesian nanodrop robot (Genomic Solutions, Ann Harbor, MI, USA) on the I2BC Crystallization Platform (CNRS, Gif-sur-Yvette, France). OXA-405 at 33 mg/mL concentration was crystallized over a reservoir containing 2.2 M of ammonium sulfate and 0.2 M of sodium fluoride. Crystals were transferred to a cryoprotectant solution (mother liquor supplemented with 20% glycerol) and flash-frozen in liquid nitrogen. Diffraction data were collected at 100 K, to a resolution of 2.26 Å, using a RIGAKU MicroMax[™] 007 HF rotating copper anode with OSMIC VariMaxHF mirrors and an MAR345 image plate detector, at the Institut de Chimie des Substances Naturelles (CNRS, Gif-sur-Yvette, France). Diffraction intensities were integrated with the program XDS [14].

The dimer structure of OXA-405 was solved by molecular replacement with Molrep [15], using the monomer moiety of the OXA-48 structure (Protein Data Bank code 3HBR [16]) as a search model. Model refinement was performed with BUSTER-TNT [17]. Electron density maps were evaluated, using COOT [18] for manual refinement. The maps revealed clear density for the carboxylated lysine-73 residues. In contrast, the side chain of the N-ter Met-22 residues, as well as the C-ter 6xHis-tag, was unseen. Refinement details of the structure are shown in Table 3. Molecular graphics images were generated using UCSF Chimera version 1.10.2 (<https://www.cgl.ucsf.edu/chimera/>) [19].

2.6. Structure Analysis, Docking, Molecular Dynamics, and Water Network Analysis

OXA-405 structural analysis and comparison with other crystal structures were performed with UCSF Chimera package [19]. Covalent docking calculations were performed, using the GOLD software, version 5.2 (CCDC suite) [20]. Ligand structures were generated with 3D Structure Generator CORINA Classic (Molecular Networks GmbH, Nuremberg, Germany). Molecular dynamics simulations of OXA-405 were performed with Gromacs version 4.6 [21], using the OPLS-AA force field [22]. HOP software version 0.4.0 alpha 2 (<https://github.com/Becksteinlab/hop>) [23] was used for water molecule dynamics analysis.

2.7. PDB Deposition

The crystallographic structure of OXA-405 was deposited into the Protein Data Bank (PDB) [24], accession code 5FDH.

3. Results

3.1. Biochemical Properties of OXA-405

To confirm previous findings based only on specific activities [13], and to understand the structural features explaining the differences observed with OXA-48, we purified OXA-405, determined the 3D structure, and determined the steady-state kinetic parameters for several clinically relevant substrates (penicillin, cephalosporins, and carbapenems) and compared them to those of OXA-163 and OXA-48 (Table 1). For OXA-48, the highest catalytic efficiency was observed for amoxicillin hydrolysis ($2400 \text{ mM}^{-1} \text{ s}^{-1}$) (Table 2). As observed by others, carbapenems are among the preferred OXA-48 substrates, with the highest catalytic efficiency ($k_{\text{cat}}/K_{\text{m}}$) observed for the hydrolysis of imipenem ($370 \text{ mM}^{-1} \text{ s}^{-1}$) [9,16]. Compared to imipenem, the OXA-48 $k_{\text{cat}}/K_{\text{m}}$ value is 59-fold smaller for meropenem and 284-fold smaller for ertapenem hydrolysis because of a reduction in the turnover number (k_{cat}). In addition, the early cephalosporin, cephalothin, is hydrolyzed with a $k_{\text{cat}}/K_{\text{m}}$ slightly higher than that of the oxyimino cephalosporin cefotaxime mainly because of a lower K_{m} value. Finally, the steady-state kinetic analysis indicates OXA-48 does not hydrolyze the bulky oxyimino-cephalosporin ceftazidime, as previously suggested. The substrate profile of OXA-405 is substantially different from that of OXA-48, but quite similar to that of OXA-163. Unlike OXA-48, OXA-405 hydrolysis preferentially cephalosporins (Table 1). The highest $k_{\text{cat}}/K_{\text{m}}$ values were observed for benzylpenicillin ($667 \text{ mM}^{-1} \text{ s}^{-1}$), ampicillin ($137 \text{ mM}^{-1} \text{ s}^{-1}$), cephalothin ($444 \text{ mM}^{-1} \text{ s}^{-1}$), and cefotaxime ($26 \text{ mM}^{-1} \text{ s}^{-1}$). Ceftazidime was hydrolyzed with the lowest $k_{\text{cat}}/K_{\text{m}}$ ($0.7 \text{ mM}^{-1} \text{ s}^{-1}$) among the cephalosporins tested because of a high K_{m} value. Nevertheless, OXA-405 does hydrolyze ceftazidime. The carbapenemase activity of OXA-405 is attenuated largely because of a reduction in the turnover number and of the affinity for carbapenems, except for ertapenem; the carbapenemase activity was nevertheless higher for OXA-405 as compared to OXA-163.

Table 1. Steady-state kinetic parameters ^a for hydrolysis of β -lactam substrates by OXA-405, OXA-163, and OXA-48 β -lactamases.

Substrate	K_m (μM) ^a			k_{cat} (s^{-1})			k_{cat}/K_m ($\text{mM}^{-1} \text{s}^{-1}$)		
	OXA-405	OXA-163	OXA-48	OXA-405	OXA-163	OXA-48	OXA-405	OXA-163	OXA-48
Benzylpenicillin	18	13	ND ^b	12	23	ND	667	1800	ND
Ampicillin	212	315	395	29	23	955	137	70	2400
Oxacillin	69	90	95	19	34	130	275	370	1400
Temocillin	NH ^c	NH	45	NH	NH	0.3	ND	ND	6.6
Cephalothin	18	10	195	8	3	44	444	300	225
Cefotaxime	369	45	>900	9.7	10	>9	26	230	10
Ceftazidime	>1000	>1000	NH	0.7	8	NH	0.7	3	NH
Imipenem	532	520	13	0.1	0.03	4.8	0.2	0.06	370
Meropenem	>2000	>2000	11	0.1	>0.1	0.07	0.09	0.03	6.2
Ertapenem	88	130	100	0.04	0.05	0.13	0.4	0.3	1.3

^a: data are the mean of three independent experiments; standard deviations were within 10% of the mean; ^b: ND, not determined; ^c: NH, no detectable hydrolysis was observed with 1 mM of purified enzyme and 500 μM of substrate. Data for OXA-163 are from Oueslati et al. [9] and OXA-48 from Docquier et al. [16].

This leads to a decrease of 1850-fold in the catalytic efficiency of OXA-405 for imipenem in comparison to that of OXA-48, while, for OXA-163, a 6166-fold decrease was observed. However, it is noteworthy that the catalytic efficiencies of OXA-405 are higher for ertapenem and imipenem as compared to meropenem. Although the reason for this cannot be known without further structural data, it is possible that the smaller size of imipenem in comparison to meropenem and ertapenem allows it to fit better into the active site of OXA-48, leading to a higher rate of turnover of imipenem by OXA-48, which is then lost due to the active-site expansion that occurs in OXA-405, as described below.

In summary, the results confirm the ability of the OXA-48 active site to accommodate carbapenem substrates, particularly imipenem, while it is unable to hydrolyze ceftazidime, a bulkier oxymino-cephalosporin. Our results confirm, that the four AA deletion in the $\beta 5$ – $\beta 6$ loop observed in OXA-405 is responsible for a drastic loss of carbapenemase activity, particularly for imipenem, and a gain of cephalosporinase activity with the ability to hydrolyze cefotaxime and ceftazidime. The hydrolytic properties of OXA-405 make it more similar to an Amber class A extended-spectrum β -lactamase. Therefore, the 213-TRIE-217 alters the substrate specificity of OXA-405. This finding is consistent with previously published kinetic data showing a significant increase in the level of ceftazidime hydrolysis compared to that of OXA-48. Additionally, two other members of the OXA-48-like β -lactamases, OXA-247 and OXA-163, which differ from OXA-48 by a four amino acid deletion, 214-RIEP-218 and 214-RIEP-217 deletion and S212D substitution, respectively, have significantly lowered activity toward carbapenem substrates as compared to that of OXA-48 [16]. Determination of IC_{50} (Table 2) showed that OXA-405, as OXA-163 and OXA-48, can be inhibited by clavulanic acid (6 μM), tazobactam (1.8 μM), and NaCl (40×10^3 μM).

Table 2. Fifty percent inhibitory concentration (IC_{50}) of clavulanic acid and tazobactam for β -lactamases OXA-405, OXA-163, and OXA-48 ^a.

Inhibitor	IC_{50} (μM)		
	OXA-405	OXA-163	OXA-48
Clavulanic acid	6	13.4	28.5
Tazobactam	1.8	0.75	20
NaCl	40×10^3	97×10^3	35×10^3

Note: ^a data are the mean of three independent experiments; standard deviations were within 10% of the mean. Data for OXA-163 from Stojanoski et al. [25].

In a general way, OXA-405 and OXA-163 have similar catalytic efficiency values for penicillin, which are lower than those of OXA-48. Concerning cephalosporins, the three enzymes have nearly the same catalytic efficiency for cephalothin, however, there is a difference for the hydrolysis of cefotaxime:

value of OXA-405 ($26 \text{ mM}^{-1} \text{ s}^{-1}$) is two-fold higher than OXA-48 ($10 \text{ mM}^{-1} \text{ s}^{-1}$) but nine-fold lower than that of OXA-163 ($230 \text{ mM}^{-1} \text{ s}^{-1}$). The $k_{\text{cat}}/K_{\text{m}}$ values for ceftazidime of OXA-405 ($0.7 \text{ mM}^{-1} \text{ s}^{-1}$) and OXA-163 ($1.3 \text{ mM}^{-1} \text{ s}^{-1}$) are low, but significant to confer ceftazidime resistance in bacteria expressing these enzymes, which is not the case for OXA-48. The fact that OXA-163 hydrolyses better cefotaxime and ceftazidime as compared to OXA-405 is likely related to the two-point mutations between these two enzymes.

3.2. X-Ray Crystallography

The crystal structure of OXA-405 refined at 2.26 \AA presents the typical class D fold with an α -helical region and a mixed α -helix/ β -sheet region, with 96% of all residues inside the favored regions of the Ramachandran plot, 4% in the allowed regions, and no outliers (Table 3).

Table 3. X-ray data collection and refinement statistics.

	OXA-405
Protein Data Bank code	5FDH
wavelength (\AA)	1.54187
Space group	P4 ₃ 2 ₁ 2
Asymmetric unit	1 dimer
Unit cell (\AA)	
<i>A</i>	90.40
<i>B</i>	90.40
<i>C</i>	172.63
α (deg)	90.0
β (deg)	90.0
γ (deg)	90.0
Resolution (\AA)	13.12–2.26
Observed reflections	35,642 (4116) ^a
Unique reflections	10,205 (1346)
Completeness (%)	98.0 (90.3)
<i>I</i> / σ (<i>I</i>)	18.9 (4.6)
<i>R</i> _{sym} (%)	9.7 (46.8)
<i>R</i> _{cryst} (%)	17.5
<i>R</i> _{free} (%)	21.3
no. of nonhydrogen atoms	4482
Protein	3952
heterogen	530
Waters	434
no. of protein residues	484
no. of ligands	8 SO4, 3 GOL
Root mean square deviation	

Table 3. Cont.

OXA-405	
Bond lengths (Å)	0.010
Bond angles (deg)	1.10
Ramachandran	
favored (%)	96
outliers (%)	0
Mean B value (Å ²)	
Protein	38.2 (chain A), 39.1 (chain B)
Solvent	46.1 (SO4) 55.2 (GOL), 45.9 (HOH)

^a Numbers in parentheses represent values in the highest resolution shell: 2.26–2.40 Å (OXA-405).

The asymmetric unit contains two protein chains, A and B, modeled with 246 residues each. The OXA-405 structure has a C α RMSD of 0.52 Å on 236 residues compared to the OXA-48 structure (PDB code 3HBR [16]) and 0.37 Å on 237 residues compared to OXA-163 (PDB code 4S2L [25]). The conformations of residues from active sites are very similar (Figure 2A), and the only difference between these three structures is the shorter β 5– β 6 loop in OXA-405 and OXA-163, due to the four-residue deletion in this loop (Figure 2A), which induces important changes in the corresponding active sites (Figure 2B). Clear electron density is observed for both backbones and side chains, including the active site and the β 5– β 6 loop, with the exception of side chains of Lys218 (OXA-48 numbering) from the β 5– β 6 loop (Figure 2C) and of Met22 (not shown).

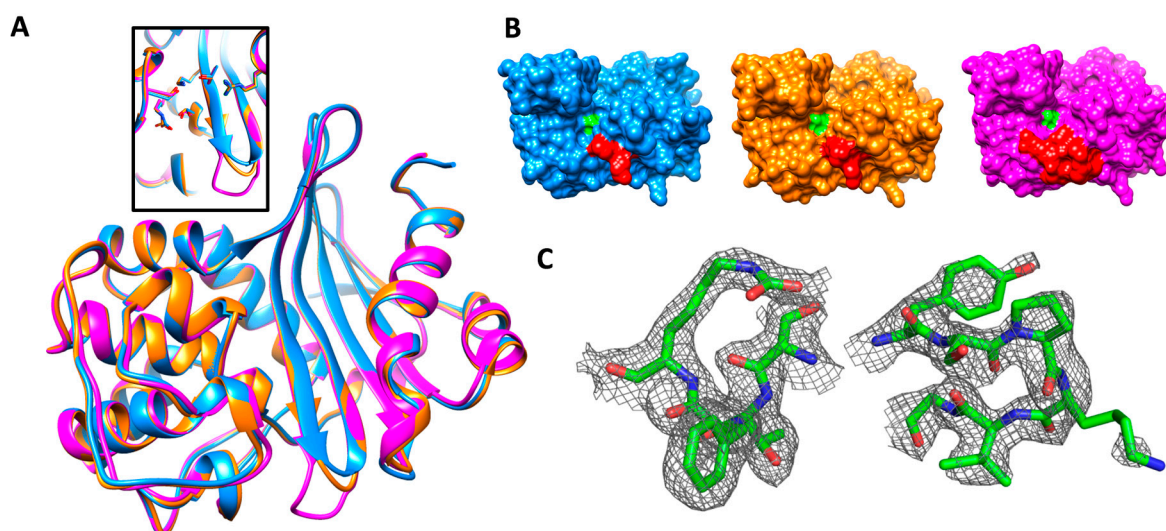


Figure 2. (A) Superposition of crystal structures of OXA-405 (blue, PDB 5FDH), OXA-163 (orange, PDB 4S2L) and OXA-48 (magenta, PDB 3HBR), with an insert showing the almost perfect superposition of key binding site residues of the three enzymes. (B) Surface representation of the three enzymes with the same color scheme as above. Ser70 and the β 5– β 6 loop are colored in green and red, respectively. (C) Residues from the STFK motif (left) and the β 5– β 6 loop (right) in stick representation, with a 2Fo-Fc map contoured at 0.8 σ .

3.3. Structural Analysis of Covalent Protein-Ligand Complexes

A molecular modelling study was performed to identify the structural determinants that could explain the differences between the hydrolytic profiles of OXA-405 and OXA-48. Covalent docking calculations were performed with β -lactam antibiotics belonging to the penicillin (oxacillin),

cephalosporin (cefotaxime, ceftazidime, and cephalothin), and carbapenem (ertapenem, imipenem, and meropenem) families into the active site of OXA-405 (Figure 3).

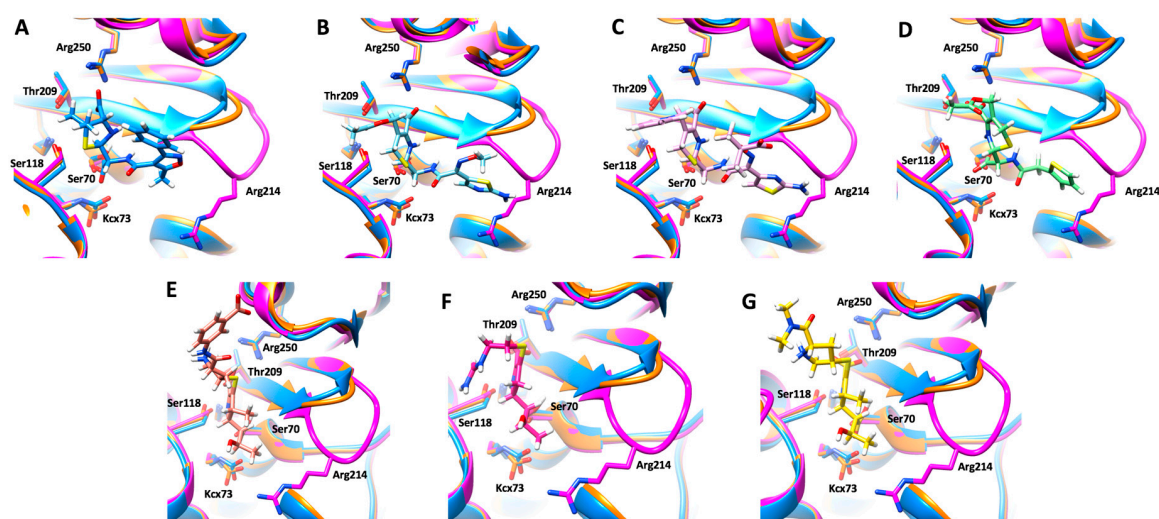


Figure 3. Covalent docking poses of oxacillin ((A), blue sticks), cefotaxime ((B), cyan sticks), ceftazidime ((C), pink sticks), cephalothin ((D), green sticks), ertapenem ((E), orange sticks), imipenem ((F), red sticks) and meropenem ((G), yellow sticks), in the active site of OXA-405 (blue). Superposed OXA-163 (orange) and OXA-48 (magenta) are also shown for comparison. Key residues of the active sites are represented as sticks and labelled using the OXA-48 numbering.

The binding mode of oxacillin is not influenced by the four-residues' deletion in the $\beta 5$ – $\beta 6$ loop due to the relatively small size of the R2 substituent in the penicillin family (Figure 3A), which is in agreement with similar K_m values determined for OXA-405 and OXA-48 (Table 1). In contrast, the R2 substituent of cephalosporins has unfavorable steric clashes with Arg214 in OXA-48 that are not observed in OXA-405, where this residue is absent and the $\beta 5$ – $\beta 6$ loop is shorter (Figure 3B–D). These structural differences explain the systematically lower K_m values of cephalosporins in the complex with OXA-405 compared with those of OXA-48 (Table 1). On the other hand, the R2 substituent in carbapenems is quite small compared to other β -lactams, and, in this case, the protein-ligand complexes obtained by covalent docking (Figure 3E–G) cannot fully explain the higher K_m values determined with imipenem and meropenem, but not with ertapenem, in the complex with OXA-405 as compared with OXA-48 (Table 1). These differences would likely come from contrasting levels of flexibility of the $\beta 5$ – $\beta 6$ loop in OXA-405 and OXA-48, due to the absence in the former case of the stabilizing interaction between Arg214 (which is part of the four-residues deleted in the $\beta 5$ – $\beta 6$ loop) and Asp159 from the Ω loop.

3.4. Molecular Dynamics and Water Network Analysis

Molecular dynamics (MD) simulations of OXA-405 and OXA-48 dimers (50 ns each) that were carried out by using Gromacs [21], with the OPLS-AA force field [22], confirmed the stability of these systems (RMSD values of 2 Å or less for the entire length of the simulation) and constituted the input data for the water network analysis, using the HOP software [23]. The stabilized water molecules identified in this way on the protein surfaces of OXA-405 and OXA-48 are shown in Figure 4.

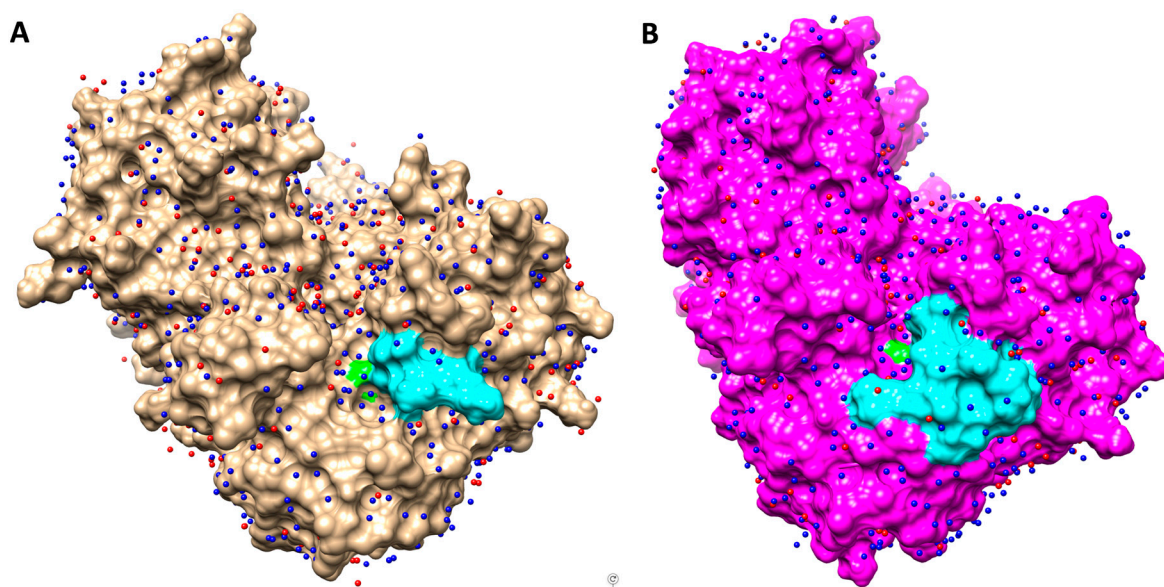


Figure 4. Crystallographic water molecules (red) and stabilized water molecules computed with HOP (blue) represented on the surfaces of OXA-405 ((A), brown) and OXA-48 ((B), magenta). Ser70 and β 5- β 6 loop are colored in green and cyan, respectively.

These stabilized waters are more numerous than the crystallographic waters determined for these two proteins, highlighting the superiority of the in-silico approach, which is not dependent on the crystal structure resolution and takes into account the protein flexibility. In some cases, the positions of waters determined using these two approaches were quite similar, emphasizing the convergence of these two methods and the possible use of MD simulations to improve the refinement of crystallographic structures [26].

4. Discussion

OXA-48-producing Enterobacteriaceae are now endemic in the Middle East, North Africa, and India [7]. Since its first description, many variants have been identified [8]. Three of them are interesting—OXA-405, OXA-163 [10], and OXA-247 [12]—because they have a significant activity toward expanded-spectrum cephalosporins but a very weak activity toward carbapenems. In this study, we characterized the biochemical and structural properties of OXA-405, which has a four amino-acid deletion 213-TRIE-217 compared to OXA-48. The steady-state kinetics of OXA-405 revealed that the deletion conferred a decrease of the catalytic efficiency for carbapenems, particularly imipenem (with a decrease of 1850-fold), but gains the ability to hydrolyze ceftazidime as compared to OXA-48. This data show that the 213-TRIE-217 deletion alter the substrate specificity of the enzyme. This finding is in agreement with previously published kinetics data of OXA-163, which has approximately the same deletion 214-RIEP-217, plus a substitution S212D [9]. Additionally, another member of the OXA-48-like β -lactamases, OXA-247 [12,27], which differs from OXA-48 by another four amino-acid deletion 214-RIEP-218, has significantly lowered activity toward carbapenem substrates as compared to OXA-48. The IC₅₀ values show that OXA-405, similarly to OXA-163, is susceptible to the inhibition by class A inhibitors (tazobactam and clavulanic acid).

The crystal structure of OXA-405 showed that the 213-TRIE-217 deletion did not modify the overall structure of the protein (Figure 2A) but resulted in an important decrease of the size of the β 5- β 6 loop, with important consequences on the overall shape of the binding site (Figure 2B). The Lys218 is flexible, as shown by the reduced electron density observed on this side chain (Figure 2C). The covalent docking calculations showed that Arg214 plays a key role in defining the hydrolysis profile. In OXA-48, this residue blocks the binding of cephalosporins through unfavored steric clashes with their bulky R2

substituents, whereas the carbapenems are accommodated into a specific conformation of the active site stabilized by the ionic interaction between Arg214 and Asp159 [27]. OXA-405 features a more open conformation of the active site due to the absence of Arg214 and its stabilizing interaction with Asp159, as well as the smaller size of the $\beta 5$ – $\beta 6$ loop. This leads to an increased affinity for cephalosporins and a decreased stabilization of carbapenems in the active site, thus explaining the important differences in affinity for these substrates observed between OXA-48 and OXA-405. Overall, all these observations may constitute the basis for the development of efficient new inhibitors targeting all OXA-48-like β -lactamases, and even the false carbapenemases like OXA-163, OXA-247, and OXA-405.

5. Conclusions

OXA-405 is a peculiar OXA-48-like enzyme, as it has lost carbapenem activities and gained expanded-spectrum cephalosporin hydrolytic activity subsequent to a 4 amino-acid (AA) deletion in the $\beta 5$ – $\beta 6$ loop. Kinetic parameters confirmed that OXA-405 behaves more like an ESBL β -lactamase, rather than a carbapenemase. Molecular modeling techniques and 3D structure determination show that the overall dimeric structure of OXA-405 is very similar to that of OXA-48, except for the $\beta 5$ – $\beta 6$ loop, which is shorter for OXA-405, suggesting that the length of the $\beta 5$ – $\beta 6$ loop is critical for substrate specificity. Covalent docking with selected substrates and molecular dynamics simulations evidenced the structural changes induced by substrate binding, as well as the distribution of water molecules in the active site and their role in substrate hydrolysis. All this data may represent the structural basis for the design of new and efficient class D inhibitors. Our findings provide a molecular basis for the hydrolysis of ceftazidime by OXA-405 and, more broadly, illustrate further how minor sequence changes can profoundly alter the structure of the active site and thereby affect the substrate profile of an enzyme. Furthermore, our results should allow us to better understand the potential of class D carbapenemases, to extend their spectrum, and thus evaluate the potential threat to public health.

Author Contributions: B.I.I. and T.N. designed the experiments; S.O., R.A.B., and L.D. performed the cloning, expression, and purification and determined the kinetic parameters; S.O., P.R., and L.M. prepared and solved the crystal structures; S.O. and B.I.I. performed the docking and molecular dynamics studies; S.O., B.I.I., and T.N. analyzed the data and wrote the paper. All authors have read and agreed to the published version of the manuscript.

Funding: This work was supported by the Assistance Publique-Hôpitaux de Paris, the University Paris-Sud, the Laboratory of Excellence in Research on Medication and Innovative Therapeutics (LERMIT) through a grant from the French National research Agency (ANR-10-LABX-33), and by the JPIAMR transnational project DesInMBL (ANR-14-JAMR-0002).

Acknowledgments: We acknowledge SOLEIL for provision of synchrotron radiation facilities (proposal ID BAG20150780) in using PROXIMA beamlines.

Conflicts of Interest: The authors declare that they have no conflicts of interest with the content of this article.

References

1. Queenan, A.M.; Bush, K. Carbapenemases: The Versatile β -Lactamases. *Clin. Microbiol. Rev.* **2007**, *20*, 440–458. [[CrossRef](#)] [[PubMed](#)]
2. Poirel, L.; Naas, T.; Nordmann, P. Diversity, epidemiology and genetics of class D beta-lactamases. *Antimicrob. Agents Chemother.* **2010**, *54*, 24–38. [[CrossRef](#)] [[PubMed](#)]
3. Van Duin, D.; Doi, Y. The global epidemiology of carbapenemase-producing Enterobacteriaceae. *Virulence* **2017**, *8*, 460–469. [[CrossRef](#)]
4. Poirel, L.; Héritier, C.; Tolün, V.; Nordmann, P. Emergence of Oxacillinase-Mediated Resistance to Imipenem in *Klebsiella pneumoniae*. *Antimicrob. Agents Chemother.* **2004**, *48*, 15–22. [[CrossRef](#)] [[PubMed](#)]
5. Dabos, L.; Bogaerts, P.; Bonnin, R.A.; Zavala, A.; Sacré, P.; Iorga, B.I.; Huang, D.T.; Glupczynski, Y.; Naas, T. Genetic and Biochemical Characterization of OXA-519, a Novel OXA-48-Like β -Lactamase. *Antimicrob. Agents Chemother.* **2018**, *62*, e00469-18. [[CrossRef](#)]

6. Potron, A.; Poirel, L.; Rondinaud, E.; Nordmann, P. Intercontinental spread of OXA-48 beta-lactamase-producing Enterobacteriaceae over a 11-year period, 2001 to 2011. *Eurosurveillance* **2013**, *18*, 20549. [[CrossRef](#)]
7. Poirel, L.; Potron, A.; Nordmann, P. OXA-48-like carbapenemases: The phantom menace. *J. Antimicrob. Chemother.* **2012**, *67*, 1597–1606. [[CrossRef](#)]
8. Naas, T.; Oueslati, S.; Bonnin, R.A.; Dabos, M.L.; Zavala, A.; Dortet, L.; Retailleau, P.; Iorga, B.I. Beta-lactamase database (BLDB)—structure and function. *J. Enzym. Inhib. Med. Chem.* **2017**, *32*, 917–919. [[CrossRef](#)]
9. Oueslati, S.; Nordmann, P.; Poirel, L. Heterogeneous hydrolytic features for OXA-48-like β -lactamases. *J. Antimicrob. Chemother.* **2015**, *70*, 1059–1063. [[CrossRef](#)]
10. Poirel, L.; Castanheira, M.; Carrère, A.; Rodriguez, C.P.; Jones, R.N.; Smayevsky, J.; Nordmann, P. OXA-163, an OXA-48-related class D β -lactamase with extended activity toward expanded-spectrum cephalosporins. *Antimicrob. Agents Chemother.* **2011**, *55*, 2546–2551. [[CrossRef](#)]
11. Abdelaziz, M.O.; Bonura, C.; Aleo, A.; El-Domany, R.A.; Fasciana, T.; Mammina, C. OXA-163-producing *Klebsiella pneumoniae* in Cairo, Egypt, in 2009 and 2010. *J. Clin. Microbiol.* **2012**, *50*, 2489–2491. [[CrossRef](#)] [[PubMed](#)]
12. Gomez, S.; Pasteran, F.; Faccone, D.; Bettiol, M.; Veliz, O.; De Belder, D.; Rapoport, M.; Gatti, B.; Petroni, A.; Corso, A. Inpatient emergence of OXA-247: A novel carbapenemase found in a patient previously infected with OXA-163-producing *Klebsiella pneumoniae*. *Clin. Microbiol. Infect.* **2013**, *19*, E233–E235. [[CrossRef](#)] [[PubMed](#)]
13. Dortet, L.; Oueslati, S.; Jeannot, K.; Tandé, D.; Naas, T.; Nordmann, P. Genetic and Biochemical Characterization of OXA-405, an OXA-48-Type Extended-Spectrum β -Lactamase without Significant Carbapenemase Activity. *Antimicrob. Agents Chemother.* **2015**, *59*, 3823–3828. [[CrossRef](#)] [[PubMed](#)]
14. Kabsch, W. XDS. *Acta Crystallogr. D Biol. Crystallogr.* **2010**, *66*, 125–132. [[CrossRef](#)]
15. Vagin, A.; Teplyakov, A. MOLREP: An Automated Program for Molecular Replacement. *J. Appl. Crystallogr.* **1997**, *30*, 1022–1025. [[CrossRef](#)]
16. Docquier, J.D.; Calderone, V.; De Luca, F.; Benvenuti, M.; Giuliani, F.; Bellucci, L.; Tafi, A.; Nordmann, P.; Botta, M.; Rossolini, G.M.; et al. Crystal structure of the OXA-48 beta-lactamase reveals mechanistic diversity among class D carbapenemases. *Chem. Biol.* **2009**, *16*, 540–547. [[CrossRef](#)]
17. Blanc, E.; Roversi, P.; Vornrhein, C.; Flensburg, C.; Lea, S.M.; Bricogne, G. Refinement of severely incomplete structures with maximum likelihood in BUSTER-TNT. *Acta Crystallogr. D Biol. Crystallogr.* **2004**, *60*, 2210–2221. [[CrossRef](#)]
18. Emsley, P.; Cowtan, K. Coot: Model-building tools for molecular graphics. *Acta Crystallogr. D Biol. Crystallogr.* **2004**, *60*, 2126–2132. [[CrossRef](#)]
19. Pettersen, E.F.; Goddard, T.D.; Huang, C.C.; Couch, G.S.; Greenblatt, D.M.; Meng, E.C.; Ferrin, T.E. UCSF Chimera—A visualization system for exploratory research and analysis. *J. Comput. Chem.* **2004**, *25*, 1605–1612. [[CrossRef](#)]
20. Verdonk, M.L.; Cole, J.C.; Hartshorn, M.J.; Murray, C.W.; Taylor, R.D. Improved protein–ligand docking using GOLD. *Proteins* **2003**, *52*, 609–623. [[CrossRef](#)]
21. Pronk, S.; Páll, S.; Schulz, R.; Larsson, P.; Bjelkmar, P.; Apostolov, R.; Shirts, M.R.; Smith, J.C.; Kasson, P.M.; van der Spoel, D.; et al. GROMACS 4.5: A high-throughput and highly parallel open source molecular simulation toolkit. *Bioinformatics* **2013**, *29*, 845–854. [[CrossRef](#)] [[PubMed](#)]
22. Kaminski, G.A.; Friesner, R.A.; Tirado-Rives, J.; Jorgensen, W.L. Evaluation and Reparametrization of the OPLS-AA Force Field for Proteins via Comparison with Accurate Quantum Chemical Calculations on Peptides. *J. Phys. Chem. B* **2001**, *105*, 6474–6487. [[CrossRef](#)]
23. Beckstein, O.; Michaud-Agrawal, N.; Woolf, T.B. Quantitative Analysis of Water Dynamics in and near Proteins. *Biophys. J.* **2009**, *96*, 601a. [[CrossRef](#)]
24. Berman, H.M.; Westbrook, J.; Feng, Z.; Gilliland, G.; Bhat, T.N.; Weissig, H.; Shindyalov, I.N.; Bourne, P.E. The Protein Data Bank. *Nucleic Acids Res.* **2000**, *28*, 235–242. [[CrossRef](#)]
25. Stojanoski, V.; Chow, D.C.; Fryszczyn, B.; Hu, L.; Nordmann, P.; Poirel, L.; Sankaran, B.; Prasad, B.V.V.; Palzkill, T. Structural Basis for Different Substrate Profiles of Two Closely Related Class D β -Lactamases and Their Inhibition by Halogens. *Biochemistry* **2015**, *54*, 3370–3380. [[CrossRef](#)]

26. Wall, M.E.; Calabró, G.; Bayly, C.I.; Mobley, D.L.; Warren, G.L. Biomolecular Solvation Structure Revealed by Molecular Dynamics Simulations. *J. Am. Chem. Soc.* **2019**, *141*, 4711–4720. [[CrossRef](#)]
27. Lund, B.A.; Thomassen, A.M.; Carlsen, T.J.O.; Leiros, H.K.S. Structure, activity and thermostability investigations of OXA-163, OXA-181 and OXA-245 using biochemical analysis, crystal structures and differential scanning calorimetry analysis. *Acta Crystallogr. F Struct. Biol. Commun.* **2017**, *73*, 579–587. [[CrossRef](#)]



© 2019 by the authors. Licensee MDPI, Basel, Switzerland. This article is an open access article distributed under the terms and conditions of the Creative Commons Attribution (CC BY) license (<http://creativecommons.org/licenses/by/4.0/>).

1 **Article 4: Role of the Arginine 214 in the substrate specificity of**
2 **OXA-48**

3
4 Saoussen Oueslati¹, Pascal Retailleau⁴, Ludovic Marchini,⁴ Camille Berthault¹, Laurent
5 Dortet^{1,2,3}, Rémy A. Bonnin^{1,2,3}, Bogdan I. Iorga⁴, and Thierry Naas^{1,2,3*}

6
7 ¹ EA7361 “Structure, dynamic, function and expression of broad spectrum β -lactamases”, Faculty of Medicine
8 Université Paris-Sud, LabEx LERMIT, Université Paris-Saclay, Le Kremlin-Bicêtre, France

9 ² Institut de Chimie des Substances Naturelles, CNRS UPR 2301, Labex LERMIT, Université Paris-Saclay, Gif-sur-
10 Yvette, France.

11 ³ Associated French National Reference Center for Antibiotic Resistance: Carbapenemase-producing
12 *Enterobacteriaceae*, Le Kremlin-Bicêtre, France

13 ⁴ Bacteriology-Hygiene unit, Assistance Publique/Hôpitaux de Paris, Bicêtre Hospital, Le Kremlin-Bicêtre, France
14

15 *Corresponding author: Service de Bactériologie-Hygiène, Hôpital de Bicêtre 78 rue du Général Leclerc, 94275
16 Le Kremlin-Bicêtre, France

17 Tel : +33 1 45 21 20 19

18 Fax : +33 1 45 21 63 40

19 thierry.naas@bct.aphp.fr

20 **KEYWORDS** oxacillinase, carbapenemase, OXA-232, antibiotic resistance, beta-lactamase, OXA-48

21
22 Abstract : 163/250max

23 **Carbapenem-hydrolyzing class D β -lactamase OXA-48 is now widely disseminated in**
24 **Enterobacterales. A sign of their extensive spread is the identification of increasing number**
25 **of OXA-48 variants. Among them, OXA-181 and OXA-232 are of particular interest. Indeed,**
26 **these two variants, differing only by a single amino acid substitution at position 214 (Arg to**
27 **ser), exhibit different hydrolytic properties towards carbapenems. Unlike OXA-181 and**
28 **OXA-48, OXA-232 displays low carbapenemase activity. Here, the X-ray structure of OXA-**
29 **232 was determined and six mutants of OXA-48 and OXA-232 were generated using site-**
30 **directed mutagenesis to evaluate the role of the residue at position 214. These mutants**
31 **were characterized phenotypically, and three mutants of OXA-232 were purified to study**
32 **their biochemical properties. A molecular modeling study was performed to understand the**
33 **role of the Arg214. Overall, our study demonstrates the key role of the residue Arg214 in**
34 **the substrate specificity of OXA-48.**

35

36 Introduction

37 The intensive use of β -lactams to treat infections leads to the emergence of multidrug
38 pathogens especially in Gram-negative bacteria. Among β -lactams, carbapenems is
39 considered as last resort antibiotics to treat severe caused by Gram-negative rods. The major
40 mechanism of carbapenem resistance in Enterobacterales is (i) the association of an extended-
41 spectrum β -lactamase and decrease of membrane permeability or (ii) inactivation of
42 carbapenems by β -lactamases able to hydrolyze those compounds, carbapenemases. Genes
43 encoding for these enzymes are mostly harbored by plasmid explaining their rapid spread. β -
44 lactamases can be classified into 4 groups (Amber's classes A to D) based upon sequence
45 homology (1). The most prevalent carbapenemases are members of the class A (KPC-type), B
46 (NDM, VIM, IMP) and D (OXA-48-like). OXA-48 was first identified in Turkey (2) and then has
47 rapidly spread in the Mediterranean area, middle East, Europe, India and became a worrisome
48 threat (3). OXA-48 hydrolyzes penicillins including temocillin, narrow spectrum
49 cephalosporins, and also carbapenems at low rate, but do not hydrolyze ceftazidime and
50 cefepime (4). Since the first description of OXA-48, several variants have been described (5).
51 These variants are either point mutant derivatives and deletion mutants in the β 5- β 6 loop.
52 Amino-acid (AA) sequence analysis of Two OXA-48 variants, OXA-181 that differs from OXA-
53 48 by 4 amino-acid substitutions: T103A, N110D, E169Q and S171A) and OXA-232 that differs
54 from OXA-181 by an additional substitution R214S, are of particular interest. Indeed,
55 enzymatic activity studies revealed that OXA-181 displays the same hydrolytic profile as OXA-
56 48, whereas OXA-232 has a significant decrease of the carbapenem-hydrolyzing activity (6).
57 These results suggested that the Arg214 plays a crucial role in the hydrolysis of carbapenems.
58 To further explore the role of Arg214 in the hydrolytic profile of OXA-48-like carbapenemases,
59 we determined the X-ray structure of OXA-232, and determined the kinetic parameters of
60 OXA-232 mutants of that we generated at position 214.

61

62 Materials and methods

63 Bacterial strains

64 The clinical strain *Escherichia coli* LIEU (7) expressing the OXA-232 β -lactamase was
65 used to clone the *bla*_{OXA-232} gene. *E. coli* TOP10 (Invitrogen, Saint-Aubin, France) was used for

66 cloning and mutagenesis experiments and *E. coli* BL21 DE3 was used for overexpression
67 experiments (Novagen, Fontenay-sous-Bois, France)

68

69 **Antimicrobial agents, susceptibility testing and microbiological techniques**

70 Antimicrobial susceptibilities were determined by the disc diffusion technique on
71 Mueller–Hinton agar (Bio-Rad, Marnes-La-Coquette, France) and interpreted according to the
72 EUCAST breakpoints, updated in May 2018 (<http://www.eucast.org>). MICs were determined
73 using the Etest technique (bioMérieux, La Balme les Grottes, France). Antibiotics were
74 purchased from Sigma (Saint-Quentin-Fallavier, France) except temocillin (Eumedica,
75 Brussels, Belgium)

76

77 **PCR, cloning, site-directed mutagenesis and DNA sequencing**

78 The recombinant plasmids pTOPO-*bla*_{OXA-232} and pTOPO-*bla*_{OXA-48}, obtained from a
79 previous study (6), were used as a template for the site-directed mutagenesis assays and
80 specific primers were designed for the different mutations, using the program QuickChange
81 Primer Design (Agilent Technologies). QuikChange II Site-Directed Mutagenesis Kit (Agilent
82 Technologies) was used, following the manufacturer's recommendations, in order to
83 substitute the residue 214 into a Glycine (G), a Lysine (K), a Leucine (L), an Aspartic acid (D), a
84 Glutamic acid (E), a Serine (S) and an Arginine (R). Mutagenesis reaction products were
85 transformed in *E. coli* TOP10 (Invitrogen, Saint-Aubin, France) and selection was performed
86 on TSA plate containing Kanamycin (50µg/ml). For the production of OXA-232, genes were
87 amplified by PCR using the forward primer OXA_{23-256NdeI} (5'-
88 aaaaCATATGaaggaatggcaagaaaacaaa-3') and the reverse primer OXA_{XhoI-Δstop} (5'-
89 aaaaCTCGAGggggaataattttcctgttgag-3') to increase the purification yield. For the mutants
90 OXA-232 S214E, OXA-232 S214G and OXA-232 S214K the forward primers OXA_{NdeI} (5'-
91 aaaaCATATGTTGGTGGCATCGATTATCGG-3') and reverse primer OXA_{XhoI-Δstop} (5-
92 aaaaCTCGAGGAGCACTTCTTTGTGATGGC-3') were used. Recombinant plasmids were cloned
93 into pET41b (for OXA-232 *wt*) allowing the expression of the enzyme with an His-tag and pET9a
94 (for OXA-232 mutants) vector (Invitrogen®, Life Technologies, Cergy-Pontoise, France), then
95 transformed into *E. coli* BL21 DE3 (Novagen). All the recombinant plasmids were extracted
96 using the Qiagen miniprep Kit and sequenced using a T7 promoter and M13 reverse primers
97 or T7 terminator (depending on the plasmid) with an automated sequencer (ABI Prism3100;

98 Applied Biosystems). The nucleotide sequences were analyzed using software available at the
99 National Center for Biotechnology Information website (<http://www.ncbi.nlm.nih.gov>).

100

101 **Protein purification**

102 Overnight culture of *E. coli* BL21 DE3 harboring recombinant pET41b-OXA-232 or
103 pET9a-OXA-232-mutants plasmids were used to inoculate 2 L of LB medium broth containing
104 50 mg/L kanamycin. Bacteria were cultured at 37°C until an OD of 0.6 at 600 nm was reached.
105 The β -lactamase was induced overnight with 0.2 mM IPTG as inducer and cultures were
106 centrifuged at 6000 g for 15min. The pellets were resuspended with the binding buffer 25mM
107 phosphate sodium pH 7.4, 300 mM K₂SO₄, 10 mM imidazole for OXA-232 *wt* and with the
108 buffer 20 mM Bis-Tris H₂SO₄ (pH 7.2) for mutants of OXA-232. Bacterial cells were disrupted
109 by sonication and the bacterial pellet was removed by two consecutive centrifugation steps
110 at 10 000 g for 1 h at 4°C; the supernatant was then centrifuged at 96 000 g for 1 h at 4°C.
111 OXA-232 *wt* was purified with a NTA-Nickel column (GE Healthcare, Freiburg, Germany) by
112 using the elution buffer 25 mM phosphate sodium pH 7.4, 300 mM K₂SO₄, 500 mM imidazole.
113 Mutants of OXA-232 were purified by using 2 anion-exchange chromatography HiTrap™ QHP
114 GE Healthcare (20 mM Bis-Tris H₂SO₄ pH 7.2, then 20 mM piperazine H₂SO₄ pH 9.5) (6). Finally,
115 a gel filtration step was performed for the purifications of all β -lactamases with 100mM
116 sodium phosphate buffer pH 7 and 150 mM NaCl with a Superdex 75 column (GE Healthcare,
117 Freiburg, Germany). The protein purity was estimated by SDS–PAGE and the pooled fractions
118 were dialyzed against 10 mM Tris-HCl pH 7 for the mutants and against 0.1 M Hepes (pH 7.5)
119 for OXA-232 *wt* and concentrated using vivaspin 20 (10 000 MWCO PES Sartorius®) columns.
120 Protein concentration was determined by Bradford Protein using the Bio-Rad protein assay
121 standard II kit (Bio-Rad, Marnes-la-Coquette, France) with bovine serum albumin (BSA) as a
122 standard.

123

124 **Kinetics assays**

125 Steady-state kinetic parameters were determined using a spectrophotometer
126 ULTROSPEC 2000 (Amersham Pharmacia Biotech) and performed at 30°C in 100 mM
127 phosphate buffer (pH 7) during 10 minutes.

128 The disappearance of substrate (β -lactam antibiotics) was monitored at the specific
129 wavelengths and converted to initial velocities using the specific extinction coefficients. The

130 k_{cat} and K_m values were determined by analysing β -lactam hydrolysis under initial-rate
131 conditions using the Eadie-Hoffstee linearization of the Michaelis-Menten equation with
132 SFWIFT II software.

133

134 **Crystallization and data collection**

135 Crystal conditions were screened with 10 mg/mL of concentrated protein using a range
136 of commercially available screens. OXA-232 crystals grew in 0.2 M Lithium sulfate, 0.1M Tris
137 pH 8.5 and 30% w/v PEG 3000. Crystals were dipped briefly in cryoprotectant (20% v/v glycerol
138 in the reservoir solution) and flash-frozen in liquid nitrogen prior to be transferred in a stream
139 of nitrogen at 100K (delivered by a Rigaku X-tream cryosystem). A 2.21-Å resolution data set
140 was collected on a Rigaku MicroMax-007-HF rotating-anode generator with Cu K α radiation,
141 Varimax HF mirror focusing optics (Rigaku) and MAR345 image-plate detector (MAR
142 Research).

143

144 **Structure determination and refinement**

145 X-ray diffraction data sets were processed using *XDS* (8) and *AIMLESS* (9); the crystals
146 diffracted to 2.2 Å resolution (Table 4). Initial phases were obtained by molecular replacement
147 with MOLREP (10) using OXA-48 (PDB ID 3HBR) as a search probe. Refinement was performed
148 by successive and alternate rounds of refinement with *BUSTER* (11) and model improvement
149 using *Coot* (12). The final model was evaluated using *MolProbity* (13). Data collection and
150 refinement statistics are provided in Table 4.

151

152 **Molecular modelling**

153 Molecular modelling was performed to evaluate the effects of the mutations on OXA-232 β -
154 lactamase. Substitution of amino acid was performed by mutating the OXA-232 structure (PDB
155 code 5HFO) *in silico* using the Dunbrack rotamer library (*swapaa* command) as a part of the
156 UCSF Chimera software (14, 15). The Dunbrack rotamer library predicts the conformation of
157 the amino acid side-chain based on the global energy minimum of the protein. The
158 identification of interatomic clashes based on VDW radii (16) was performed with UCSF
159 Chimera software (14, 15).

160 Three-dimensional structures of the β -lactam ligands were generated using Corina 3.60
161 (Molecular Networks GmbH, Erlangen, Germany).

162 Molecular docking calculations were performed using Gold (Cambridge Crystallographic Data
163 Centre, Cambridge, UK)(17) and the GoldScore scoring function. The binding site, defined as a
164 20 Å radius sphere, was centered on the OG oxygen atom of Ser70. All other parameters had
165 default values.

166 The receptor-ligand complex images were produced using UCSF Chimera (14, 15).

167

168 **PDB accession codes**

169 The OXA-232 structure atomic coordinates were deposited in the Protein Data Bank with the
170 accession code 5HFO.

171

172 **Results**

173 **Susceptibility testing**

174 To determine the effect of the substitution at the position 214 on the hydrolysis of imipenem
175 and temocillin, MIC values of *E. coli* expressing OXA-48 and OXA-232 and their respective point
176 mutant derivatives were determined. The substitution OXA-48-S214R led to a phenotype
177 profile similar of OXA-232, with a decrease of the hydrolysis of temocillin and imipenem (Table
178 1). Conversely, OXA-232-R214S re-stored the hydrolysis rate for temocillin and imipenem of
179 OXA-48/181. When the residue 214 is substituted with an uncharged amino acid, such as
180 Glycine and Leucine, the MIC values are similar to those of the OXA-232. The most interesting
181 results were obtained with a substitution by negatively charged amino acids at pH7 such as
182 aspartic acid (D) and glutamic acid (E). Indeed, MIC values for imipenem and temocillin were
183 remarkably affected, leading to a loss of hydrolysis of these β -lactams. In a second step, we
184 focused on the analysis of mutants of OXA-232: OXA-232-S214G; OXA-232-S214E and OXA-
185 232-S214K, which are representative for each amino acid group: polar positively charged (K),
186 polar charged negatively (E) and uncharged (G). MIC values for other β -lactams were
187 performed and compared to those of OXA-232, OXA-181 (OXA-232-S214R) and OXA-48 (Table
188 2). Overall, MIC values for benzylpenicillin and cephalothin were not affected and MIC values
189 of the mutants for the other carbapenems (meropenem and ertapenem) vary in the same way
190 as for imipenem.

191

192 **Biochemical properties determination**

193 To further characterize the impact of the nature of the residue at position 214 on the
194 hydrolytic profile, steady-state kinetic parameters of the 3 mutants (OXA-232-S214G; OXA-
195 232-S214E and OXA-232-S214K) were determined and compared to those of OXA-48, OXA-
196 181 and OXA-232 (4, 6). Overall, the kinetic studies revealed three patterns (Table 3). OXA-
197 232-S214G exhibited hydrolytic activity towards all the β -lactams similar to those of OXA-232.
198 The mutant OXA-232-S214K possessed a higher catalytic efficiency for imipenem of ~ 4 fold
199 than the one for OXA-232, due to a weak increase of the turnover of the enzyme (k_{cat}). The
200 most interesting result was observed with the OXA-232-S214E mutant. Indeed, the
201 substitution by a negatively charged amino acid led to a drastic increase of the K_m of at least
202 ~ 200 fold compared to OXA-232, decreasing the catalytic efficiency. Moreover, this mutant
203 totally lost its hydrolysis properties for temocillin. All these results were concordant with the
204 observed MIC values. Taken together, our results confirm that the hydrolysis of imipenem
205 depends on the nature of the residue in position 214. It appears in the light of these results
206 that a long amino acid positively charged improves the hydrolysis of imipenem.

207

208 **Crystal Structure of OXA-232**

209 The crystals of OXA-232 were obtained at basic pH in 30% w/v PEG3000 and in the
210 presence of 0.2 M Li_2SO_4 (Figure 2). Glycerol was added to the mother liquor to cryoprotect
211 the crystals before flash-annealing for data collection. They belonged to hexagonal space
212 group, $P 6_2$, with 43.8 % solvent as calculated from the Matthews coefficient of $2.19 \text{ \AA}^3 \text{ Da}^{-1}$
213 (18, 19). At that time, the best available OXA-48 model in the PDB was 3HBR (1.9 \AA) (4)
214 obtained from crystals grown at lower pH (7.5 vs 8.5), in PEG 4000 then dipped into
215 cryoprotectant ethyleneglycol, and which belonged to the monoclinic space group $P 2_1$ with
216 48.3% solvent (Matthews coefficient, $2.38 \text{ \AA}^3 \text{ Da}^{-1}$). After deletion of 22 N-ter amino acids, one
217 half of R214S-3HBR coordinates were used as quasi-homologous model for phasing the
218 hexagonal crystal to 2.2 \AA resolution. The refined electron density appeared neat throughout
219 the entire backbone and most of side chains of the biological dimer per asymmetric unit of
220 the crystal. Alternate positions for Q41 and Q53 were observed as well for D230, whose one
221 position permitted a salt bridge with R107 at the dimer interface. The average Real-space
222 correlation factor calculated by Sfcheck (20) is 0.932. Compared to 3HBR, up to three
223 additional C-ter amino acids could be displayed in chain B of OXA-232 (only one in chain A)
224 but not the 9-His-tag chain, disordered in the surrounding solvent. Additionally, some minor

225 discontinuities observed in some parts of 3HBR main chains could be fixed in 5HFO
226 (N50D/K51D, T99C, S150A h-bonding D148A). The rmsd values with the two 3HBR dimers
227 range between 0.3452 and 0.4197 Å (Superpose, (21)). Obviously, the OXA-232 tertiary
228 structure of each monomer features the usual class D β -lactamase fold, with an α -helical
229 region (α 3: 73–82; α 4: 110–115; α 5: 120–130; α 6: 132–142; α 9: 185–194) and a mixed α -
230 helix/ β -sheet region (β 1: 26–28; α 1: 31–35; β 2: 42–48; β 3: 53–56; α 2: 59–62; β 4: 196–199;
231 β 5: 204–212; β 6: 219–227; β 7: 232–240). 98.2% of all residues were inside the favored regions
232 of the Ramachandran plot, and 1.8% in the allowed regions. The quaternary structure of OXA-
233 232 is dimeric as observed for OXA-48 around a non-crystallographic two-fold axis, in
234 compliance with our data of size-exclusion chromatography. It was already shown that less
235 monomer surface (200\AA^2) was buried in that dimer formation compared to OXA-10 and it was
236 built upon an intermolecular β sheet involving β 4 from each subunit linked by reciprocal H-
237 bonds between the A199 NH and the A199 carbonyl O of one chain with the corresponding
238 one related by the ncs two-fold axis. Several other H-bonds and salt bridges also participated
239 in the dimeric interface stabilization, and among these interactions, an anionic binding site
240 lying on the ncs two-fold axis is tweezed by two facing R206 from ncs related β 5 sheets. This
241 contrasts with the cation-binding site described at the interface of OXA-10, involving other
242 residues replaced in OXA-48. In the original 3HBR structure, a water molecule was placed but
243 on the faith of spherical electron density shape, low B-factor and recurrent presence of
244 halogens in other class D beta-lactamase structures (but not upon anomalous signal), it was
245 substituted by a residual chloride coming from previous purification steps. The same
246 misinterpretation was also done in the structure 4S2K (22), where chlorine was also reported
247 in the crystallizing medium composition. If sulfate ions have also been seen making that salt
248 bridge in class D structures grown in the presence of large amount of sulfate salts (e.g.
249 structures 6NLW and 5FDH), here six such anions have been spotted essentially at the
250 molecule surface as well as five opportune glycerol molecules. Carbamylated lysines (KCX 73)
251 can be described in a similar environment in both structures. Regarding the mutation of R214S
252 (the R214 residue was shown in water-mediated interaction with the avibactam drug in the
253 active site in the structure 4S2K (22), this has not structurally disturbed the β 5- β 6 hairpin and
254 its direct environment, just adding few solvent molecules in the created void (2-3 waters, and
255 one glycerol molecule in chain A) and modifying the L158B and I215B side chain conformers.
256 Deeper into both active sites, respective carbamylated lysine (KCX 73) can be described in a

257 similar environment in both structures OXA-232 and OXA-48. We notify however the presence
258 of a sulfate ion in interaction with the same residues that recognize the sulfate moiety of the
259 avibactam (Figure 3). More recently the structure of another variant, OXA-181; which differs
260 from OXA-232 by five substitutions T103A, N110D, E169Q, S171A and R214S, has been
261 released (PDB code 5OE0(23)) at a similar resolution (2.05 Å). The rmsd with OXA-232 is even
262 lower than the former overlay (0.224 and 0.252Å) in relation to the fact that structure
263 crystallized in the same unit cell dimensions and space group P6₂ than OXA-232. However five
264 residue mutations are on the protein surface that could potentially modulate the contacts
265 leading to the crystal growth and crystallization conditions were slightly different with a
266 neutral pH and PEG-mme 5000 instead of PEG 3000 or PEG 4000 for 3HBR. Like OXA-232,
267 sulfate has been used in low quantity in the crystallization drop and one anion was reported
268 in the final 5HFO model bound to the amide N of R186A as for OXA-232. Variability in β-
269 lactamase crystal forms remains tenuous to explain or even predict, since crystals of OXA-48
270 in complex with inhibitors grew in the same unit cell dimensions (the choice of P32 space
271 group instead of P62 could be interpreted by the author's intention to refine two more
272 monomers and active sites independently) in different crystallizing solution conditions (MPD
273 was the major component) and in absence of sulfate.

274 **Molecular modelling**

275 *An in silico* study was performed to identify the structural determinants that could
276 explain the experimentally determined differences between the hydrolytic profiles of OXA-
277 232 and its variants in comparison with OXA-48. The OXA-232 structure was used as a starting
278 point and the mutations S214G, S214K and S214E were modeled based on predicted low
279 energy conformations (14). The resulting models showed that lateral chains of serine and
280 lysine mutants are positioned in the same axis and direction as the lateral chain of arginine,
281 without any clashes. The glutamate mutant would be positioned differently, oriented towards
282 the active site, establishing hydrogen bonds with the backbone nitrogen and with the
283 sidechain hydroxyl of Thr213. This is the only conformation that avoids clashes of this
284 glutamate mutant with the neighboring residues Ile215 and Asp159, the latter being known
285 to interact with R214 in OXA-48 by salt bridge (4).

286 Molecular docking calculations of imipenem and temocillin on the R214E mutant of
287 OXA-48 provided explanations for the different hydrolytic parameters that were observed
288 experimentally. Imipenem showed two alternative binding modes, one that was known, with

289 a single ionic interaction between the imipenem carboxylate and the sidechain of Arg250,
290 compatible with a nucleophilic attack by Ser70 (Figure 4 B), and a second one, presumably
291 more stable, with two ionic interactions, one between the imipenem carboxylate and the
292 sidechain of Arg250 as in the previous binding mode, and a second between the positively
293 charged R2 substituent of imipenem and the mutated residue Glu214 (Figure 4 A). This latter
294 binding mode is not compatible with a nucleophilic attack by Ser70 and in this case the
295 imipenem acts like an inhibitor. On the other hand, temocillin is the only β -lactam tested
296 possessing a negative charge on the R1 substituent. Our docking calculations showed that this
297 negative charge would establish strong unfavorable ionic interactions with the mutated
298 residue Glu214, thus precluding the binding in a conformation compatible with a nucleophilic
299 attack by Ser70 (Figure 5).

300

301 Discussion

302 OXA-48-producing Enterobacterales are now endemic in many countries, such as
303 Turkey, Middle East, North Africa, India and have widely spread across Europe. Since the first
304 description of OXA-48, several variants have been described (5). These variants can be
305 classified into 3 groups according to their hydrolysis profile. Most of them, including such OXA-
306 181 (6) or OXA-162 (6), have an enzymatic activity similar to OXA-48 (4). The second group,
307 represented by OXA-163 (6), OXA-247 (24) and OXA-405 (25), exhibited a loss of their
308 carbapenemase activity, but being able to hydrolyze broad-spectrum cephalosporins such as
309 ESBLs. Finally, OXA-244 (26) and OXA-232 (6) exhibit an OXA-48-like profile with decreased
310 carbapenemase activity. The comparison of amino acid sequences of all OXA-48-like enzymes
311 shows that there is a link between the primary structure and the function of these enzymes.
312 Indeed, all β -lactamases that can be assimilated to ESBLs because of their loss of carbapenem
313 hydrolysis and the gain of activity toward expanded-spectrum cephalosporins have an amino
314 acid deletion in the β 5- β 6 loop (Figure 1). This observation suggests that this loop plays a role
315 in the substrate specificity. The phenotypic study of OXA-244 (which differs from OXA-48 by
316 only one substitution R214Q) (26) and the enzymatic study of OXA-232 (which differs from
317 OXA-181 by a single substitution R214S) underline that the residue 214 is crucial for the
318 carbapenems hydrolysis. To confirm this hypothesis, we generated mutants of OXA-48 and
319 OXA-232 at the position 214, and analyzed their hydrolytic profiles including OXA-232-S214R

320 and OXA-48-R214S. Thus, it has been observed that the substitution of Serine by an Arginine
321 (for OXA-232) allowed re-establishing hydrolytic properties toward temocillin and imipenem.
322 In parallel, the substitution of an Arginine into a Serine for OXA-48, led to a drastic decrease
323 of imipenem and temocillin hydrolysis. In order to better understand this phenomenon, 5
324 mutants for each enzyme OXA-48 and OXA-232 were generated. The substitution of the
325 residue 214 was performed with a representative amino acid of each group: polar positively
326 charged (214K), polar negatively charged (214E and 214D), non-polar (214L) and glycine
327 (214G). Overall, the substitutions with aspartate, glutamate, leucine and glycine led to a
328 decrease in resistance to imipenem and temocillin. The substitution with lysine for OXA-232
329 has allowed the increase of the MIC values, which remain nevertheless lower than OXA-48.
330 The biochemical study of OXA-232 mutants S214G and S214K showed that these 2
331 substitutions did not affect the affinity toward β -lactams (K_m values were similar to those of
332 OXA-232 and OXA-48) but have an effect on the acylation or deacylation step of the substrate
333 catalysis (k_{cat} values were similar to OXA-232 but smaller than OXA-48 values). The catalytic
334 efficiencies (k_{cat}/K_m) of these two mutants were in agreement with MIC values. The most
335 significant differences were observed with OXA-232-S214E, with a drastic decrease of the
336 affinity for imipenem (K_m was at least ~ 200 fold higher compared to OXA-232 and OXA-48)
337 and a loss of temocillin hydrolysis. The glutamate substitution seems to have a direct effect
338 on the affinity of imipenem. Analysis of the 3D structure of OXA-48 showed that R214 interacts
339 with D159 *via* a salt bridge (4), which maintains the shape and the water molecules network
340 within the binding site. Our molecular modeling study revealed that in the 214G or 214S
341 mutants this interaction with D159 is lacking, which presumably increases the flexibility of this
342 part of the binding site. In contrast, lysine is a positively charged polar amino acid which
343 appears to maintain the interaction with D159, even with a lateral chain shorter than arginine.
344 In the mutant 214E, we evidenced an alternative binding conformation of imipenem which is
345 not compatible with a nucleophilic attack of Ser70. In this case, imipenem acts as an inhibitor,
346 which explains the significantly higher K_m values determined experimentally for this substrate.
347 We also showed that, in the same 214E mutant, the unfavorable interaction between the
348 negatively charged R1 substituent of temocillin with the mutated Glu214 residue precludes
349 the binding of this antibiotic, revealing the structural details responsible for the absence of
350 hydrolysis observed experimentally.

351 Overall, we demonstrate that the position 214 in OXA-48-like β -lactamases is critical
352 for the carbapenemase activity and therefore this could represent the structural basis for the
353 design of novel carbapenemases inhibitors of the Ambler class D β -lactamases.

354

355 **ACKNOWLEDGMENTS**

356 This work was supported by Université Paris Sud and by the Laboratory of Excellence in
357 Research on Medication and Innovative Therapeutics (LERMIT), through a grant from the
358 French National Research Agency (ANR-10-LABX-33). We have no competing interests to
359 declare.

360

REFERENCES

1. Bush K. 2013. The ABCD's of β -lactamase nomenclature. *J Infect Chemother Off J Jpn Soc Chemother* 19:549–559.
2. Poirel L, Héritier C, Tolün V, Nordmann P. 2004. Emergence of oxacillinase-mediated resistance to imipenem in *Klebsiella pneumoniae*. *Antimicrob Agents Chemother* 48:15–22.
3. Poirel L, Potron A, Nordmann P. 2012. OXA-48-like carbapenemases: the phantom menace. *J Antimicrob Chemother* 67:1597–1606.
4. Docquier J-D, Calderone V, De Luca F, Benvenuti M, Giuliani F, Bellucci L, Tafi A, Nordmann P, Botta M, Rossolini GM, Mangani S. 2009. Crystal structure of the OXA-48 beta-lactamase reveals mechanistic diversity among class D carbapenemases. *Chem Biol* 16:540–547.
5. Naas T, Oueslati S, Bonnin RA, Dabos ML, Zavala A, Dortet L, Retailleau P, Iorga BI. 2017. Beta-lactamase database (BLDB) – structure and function. *J Enzyme Inhib Med Chem* 32:917–919.
6. Oueslati S, Nordmann P, Poirel L. 2015. Heterogeneous hydrolytic features for OXA-48-like β -lactamases. *J Antimicrob Chemother* 70:1059–1063.
7. Potron A, Rondinaud E, Poirel L, Belmonte O, Boyer S, Camiade S, Nordmann P. 2013. Genetic and biochemical characterisation of OXA-232, a carbapenem-hydrolysing class D β -lactamase from Enterobacteriaceae. *Int J Antimicrob Agents* 41:325–329.
8. Kabsch W. 2010. XDS. *Acta Crystallogr D Biol Crystallogr* 66:125–132.
9. Evans PR, Murshudov GN. 2013. How good are my data and what is the resolution? *Acta Crystallogr D Biol Crystallogr* 69:1204–1214.
10. Vagin A, Teplyakov A. 2010. Molecular replacement with MOLREP. *Acta Crystallogr D Biol Crystallogr* 66:22–25.
11. Bricogne, G., Blanc, E., Brandl, M., Flensburg, C., Keller, P., Paciorek, W., Roversi, P., Sharff, A., Smart, O. S., Vornrhein, C. & Womack, T. O. BUSTER. Global Phasing Ltd., Cambridge, England 2017.
12. Emsley P, Lohkamp B, Scott WG, Cowtan K. 2010. Features and development of Coot. *Acta Crystallogr D Biol Crystallogr* 66:486–501.
13. Williams CJ, Headd JJ, Moriarty NW, Prisant MG, Videau LL, Deis LN, Verma V, Keedy DA, Hintze BJ, Chen VB, Jain S, Lewis SM, Arendall WB, Snoeyink J, Adams PD, Lovell SC, Richardson JS, Richardson DC. 2018. MolProbity: More and better reference data for improved all-atom structure validation. *Protein Sci Publ Protein Soc* 27:293–315.

14. Dunbrack RL. 2002. Rotamer libraries in the 21st century. *Curr Opin Struct Biol* 12:431–440.
15. Pettersen EF, Goddard TD, Huang CC, Couch GS, Greenblatt DM, Meng EC, Ferrin TE. 2004. UCSF Chimera--a visualization system for exploratory research and analysis. *J Comput Chem* 25:1605–1612.
16. Tsai J, Taylor R, Chothia C, Gerstein M. 1999. The packing density in proteins: standard radii and volumes. *J Mol Biol* 290:253–266.
17. Verdonk ML, Cole JC, Hartshorn MJ, Murray CW, Taylor RD. 2003. Improved protein–ligand docking using GOLD. *Proteins Struct Funct Bioinforma* 52:609–623.
18. Matthews BW. 1968. Solvent content of protein crystals. *J Mol Biol* 33:491–497.
19. Winn MD, Ballard CC, Cowtan KD, Dodson EJ, Emsley P, Evans PR, Keegan RM, Krissinel EB, Leslie AGW, McCoy A, McNicholas SJ, Murshudov GN, Pannu NS, Potterton EA, Powell HR, Read RJ, Vagin A, Wilson KS. 2011. Overview of the CCP4 suite and current developments. *Acta Crystallogr D Biol Crystallogr* 67:235–242.
20. Vaguine AA, Richelle J, Wodak SJ. 1999. SFCHECK: a unified set of procedures for evaluating the quality of macromolecular structure-factor data and their agreement with the atomic model. *Acta Crystallogr D Biol Crystallogr* 55:191–205.
21. Krissinel E, Henrick K. 2004. Secondary-structure matching (SSM), a new tool for fast protein structure alignment in three dimensions. *Acta Crystallogr D Biol Crystallogr* 60:2256–2268.
22. King DT, King AM, Lal SM, Wright GD, Strynadka NCJ. 2015. Molecular Mechanism of Avibactam-Mediated β -Lactamase Inhibition. *ACS Infect Dis* 1:175–184.
23. Lund BA, Thomassen AM, Carlsen TJO, Leiros H-KS. 2017. Structure, activity and thermostability investigations of OXA-163, OXA-181 and OXA-245 using biochemical analysis, crystal structures and differential scanning calorimetry analysis. *Acta Crystallogr Sect F Struct Biol Commun* 73:579–587.
24. Gomez S, Pasteran F, Faccone D, Bettiol M, Veliz O, De Belder D, Rapoport M, Gatti B, Petroni A, Corso A. 2013. Inpatient emergence of OXA-247: a novel carbapenemase found in a patient previously infected with OXA-163-producing *Klebsiella pneumoniae*. *Clin Microbiol Infect Off Publ Eur Soc Clin Microbiol Infect Dis* 19:E233-235.
25. Dortet L, Oueslati S, Jeannot K, Tandé D, Naas T, Nordmann P. 2015. Genetic and Biochemical Characterization of OXA-405, an OXA-48-Type Extended-Spectrum β -Lactamase without Significant Carbapenemase Activity. *Antimicrob Agents Chemother* 59:3823–3828.

26. Potron A, Poirel L, Dortet L, Nordmann P. 2016. Characterisation of OXA-244, a chromosomally-encoded OXA-48-like β -lactamase from *Escherichia coli*. *Int J Antimicrob Agents* 47:102–103.

Table 1: Minimum inhibitory concentrations (MICs) of β -lactams for *E. coli* (pTOPO-OXA-48), *E. coli* (pTOPO-OXA-232) and their variants.

β -lactams	MIC (mg/L)														
	<i>E. coli</i> pTOPO-OXA-48							<i>E. coli</i> pTOPO-OXA-232							<i>E. coli</i>
	<i>wt</i>	R214S	R214G	R214L	R214K	R214D	R214E	<i>wt</i>	S214R	S214G	S214L	S214K	S214D	S214E	Top 10
Temocillin	>256	32	32	64	128	8	8	32	256	32	64	128	8	8	8
Imipenem	0.75	0.25	0.25	0.25	0.38	0.25	0.25	0.38	0.75	0.25	0.25	0.5	0.25	0.25	0.25

Table 2: Minimum inhibitory concentrations (MICs) of β -lactams for *E. coli* (pTOPO-OXA-48), *E. coli* (pTOPO-OXA-181), *E. coli* (pTOPO-OXA-232 and its variants), and *E. coli* TOP10.

β -lactams	MIC (mg/L)						
	<i>E. coli</i> TOP10 (pTOPO-OXA-)						
	OXA-232 S214G	OXA-232 S214E	OXA-232 S214K	OXA-232	OXA-181	OXA-48	Top10
Benzypenicillin	>256	>256	>256	>256	>256	>256	64
Temocillin	32	8	128	32	>256	>256	8
Cephalothin	16	16	16	16	16	16	4
Imipenem	0.25	0.25	0.5	0.38	0.75	0.75	0.25
Meropenem	0.047	0.032	0.094	0.047	0.125	0.094	0.016
Ertapenem	0.012	0.012	0.094	0.012	0.19	0.094	0.004

Table 3 : Kinetic parameters for β -lactamases OXA-48, OXA-181, OXA-232 and its mutants

Substrate	K_m (μM)						k_{cat} (s^{-1})						k_{cat}/K_m ($\text{mM}^{-1}\cdot\text{s}^{-1}$)					
	OXA-232 S214E	OXA-232 S214G	OXA-232 S214K	OXA- 232	OXA- 181	OXA- 48	OXA-232 S214E	OXA-232 S214G	OXA-232 S214K	OXA- 232	OXA- 181	OXA- 48	OXA-232 S214E	OXA-232 S214G	OXA-232 S214K	OXA- 232	OXA- 181	OXA- 48
Benzylpenicillin	140	95	95	60	90	ND	235	130	115	125	444	ND	1678	1369	1189	2090	5000	ND
Temocillin	NH	63	28	62	60	45	NH	0.01	0.03	0.03	0.3	0.3	NH	0.15	1	0.5	5	6
Cephalothin	100	133	160	124	250	195	8	4	5	13	13	44	81	30	31	105	50	225
Imipenem	>2000	5	6	9	13	13	>64	0.1	0.5	0.3	7.5	5	<32	20	83	23	550	370

NH, no detectable hydrolysis was observed with 1 μM of purified enzyme and 500 μM of substrate; ND, not determined. a Data are the mean of three independent experiments; standard deviations were within 10% of the mean. Data for OXA-181 and OXA-232 are from Oueslati *et al.* (6) and OXA-48 from Docquier *et al.* (4)

Table 4: X-ray crystallography and refinement statistics.

Data collection	
Diffractometer	Rigaku RA mm007HF - mar345
Wavelength (Å)	1.5418
Temperature (K)	100
Crystal-to-detector distance (mm)	200
Rotation range per image (°)	1°
Total rotation range (°)	205
Exposure time per image (min)	5
Space group	P 6 ₂
Cell dimensions	
a, b, c (Å)	144.08, 144.08, 53.13
α, β, γ (°)	90.00, 90.00, 120.00
Resolution (Å)	17.2-2.21
R _{merge}	0.134 (0.527)
I/σ(I)	13.8 (4.1)
Completeness (%)	97.6 (90.5)
Multiplicity	7.0 (5.7)
Refinement	
Resolution range (Å)	17.2-2.21
No. unique reflections	30389
No. of reflections, working set	30389 (2284)
No. of reflections, test set	1534 (102)
R _{work} /R _{free}	0.172/0.208 (0.343/0.404)
Overall B factor from Wilson plot Wilson B factor (Å ²)	24.3
Cruickshank's DPI for coordinate error (Å)	0.179
No. non-hydrogen atoms	
Protein	4014
Water	471
Ligand/Ions	66
Average B, all atoms (Å²)	
Protein	33.63 <i>31.01 (m.c) / 36.11 (s.c)</i>
Water	42.85
Ligand/Ions	46.37
Root mean squared deviations	
Bond lengths (Å)	0.01
Bond angles (°)	1.03
Ramachandran plot	
Most favoured (%)	98.2
Allowed (%)	1.8

Values in parentheses are for the outer shell (2.21-2.36Å)

Figure 1. Amino acid sequence alignment of OXA-48 variants. Asterisks indicate identical residues in all the three sequences, colon indicate a substitution with an other amino acid but with the same proprieties. Amino acid motif that are well conserved among class D lactamases are indicated by grey boxes, and the black-outlined box corresponds to the β 5- β 6 loop. The black arrow indicates position 214. CLUSTAL O(1.2.4) multiple sequence alignment

```

OXA-48      mrvlalsavflvasiigmpavakewqenkswnahftehksqgvvvlwnenkqggftnnlk      60
OXA-181    mrvlalsavflvasiigmpavakewqenkswnahftehksqgvvvlwnenkqggftnnlk      60
OXA-232    mrvlalsavflvasiigmpavakewqenkswnahftehksqgvvvlwnenkqggftnnlk      60
*****

OXA-48      rangaflpastfkipnslialdlgvkvkdehqvfkwddgqtrdiatwnrdhnlitamkysv      120
OXA-181    rangaflpastfkipnslialdlgvkvkdehqvfkwddgqtrdiaawnrdhnlitamkysv      120
OXA-232    rangaflpastfkipnslialdlgvkvkdehqvfkwddgqtrdiaawnrdhnlitamkysv      120
*****

OXA-48      pvyqefarqigearmskmlhafdygnedisgnvdsfwldggirisateqisflrklyhnk      180
OXA-181    pvyqefarqigearmskmlhafdygnedisgnvdsfwldggirisatqgiaflrklyhnk      180
OXA-232    pvyqefarqigearmskmlhafdygnedisgnvdsfwldggirisatqgiaflrklyhnk      180
*****
                                 $\beta$ 5- $\beta$ 6
OXA-48      lhvsersqrivkqamlteangdyiraktgystriepkigwvvgwvlddnvffamnm      240
OXA-181    lhvsersqrivkqamlteangdyiraktgystriepkigwvvgwvlddnvffamnm      240
OXA-232    lhvsersqrivkqamlteangdyiraktgystsiepkigwvvgwvlddnvffamnm      240
*****

OXA-48      mptsdglglrqaitkevlkqekiip      265
OXA-181    mptsdglglrqaitkevlkqekiip      265
OXA-232    mptsdglglrqaitkevlkqekiip      265
*****

```

Figure 2. Superposition of crystal structures and of OXA-48 (yellow, PDB: 3HBR) and OXA-232 (grey; PDB: 5HFO). The β 5- β 6 loop is delimited by the circle.



Figure 3. Partial active-site close-up of sulfate 302A-bound OXA-232 . Atoms are colored by type (C, white;N, blue; O, red; S, yellow). Hydrogen bonding and electrostatic interactions are depicted as blue dashes.

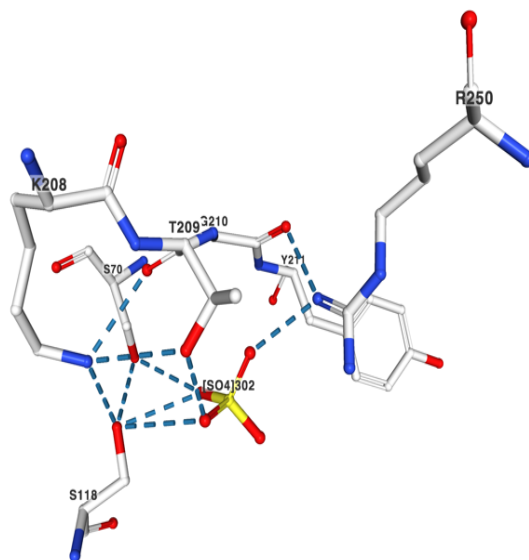


Figure 4. Alternative docking conformations of imipenem (colored in magenta (A) and yellow (B), closed form of the β -lactam ring) as non-covalent (Michaelis) complexes with the OXA-48 R214E mutant (colored in cyan, generated from structure 6P97). Hydrogen bonds and favorable ionic interactions are shown as orange springs. Protein hydrogens are hidden for clarity.

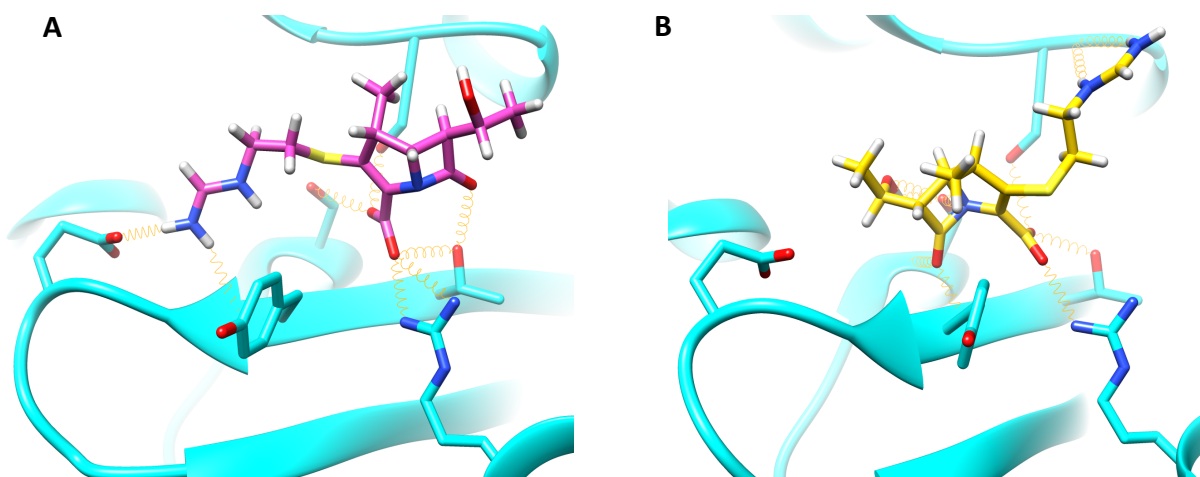
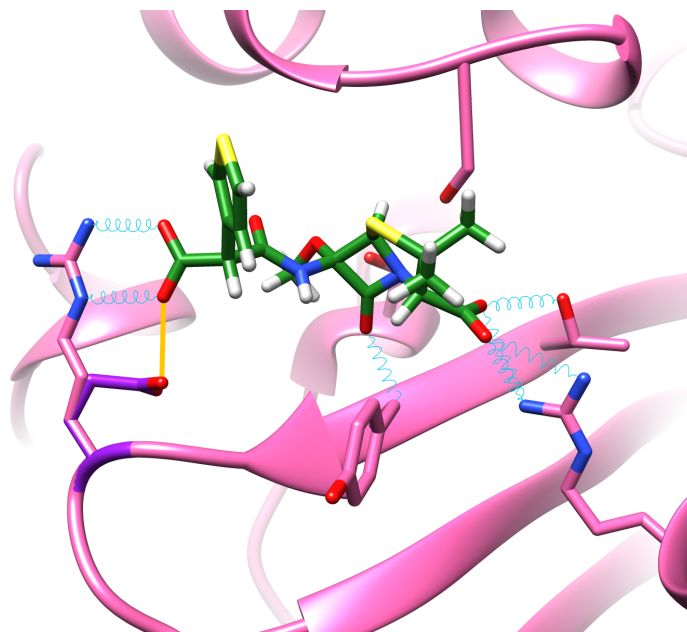





Figure 5. Docking conformation of temocillin (colored in green, closed form of the β -lactam ring) as non-covalent (Michaelis) complex with OXA-48 (colored in pink, PDB 6P97), superposed with the OXA-48 R214E mutant (colored in purple, generated from structure 6P97, only Glu214 residue shown). Hydrogen bonds and favorable ionic interactions are represented as blue springs, and unfavorable ionic interactions are represented as orange thick lines. Protein hydrogens are hidden for clarity.




B. KPC-2 : Rôle de la boucle 238–243 et du résidu 179 sur le profil hydrolytique de l'enzyme et de son inhibition par l'avibactam

La première entérobactérie productrice d'une carbapénémase de type KPC a été décrite en 2001. Il s'agissait d'une souche de *K. pneumoniae* isolée aux États-Unis. Rapidement, les souches productrices de KPC-2 sont devenues endémiques dans ce pays et en Amérique latine puis en Israël, en Chine, en Grèce et plus récemment en Italie (2009-2010). C'est en 2004 que fut décrite la première souche française productrice de KPC, isolée chez un patient de retour de New-York. Les carbapénémases de type KPC sont capables d'hydrolyser toutes les β -lactamines y compris les carbapénèmes et ne sont que très peu inhibées par les inhibiteurs de β -lactamases tels que l'acide clavulanique et le tazobactam. En 2016, la découverte au sein de notre laboratoire d'un nouveau variant de KPC ayant perdu toute activité carbapénémase, KPC-28 (Article 5), nous a incité à étudier l'impact de quelques substitutions d'AA particulières sur l'activité hydrolytique des enzymes de type KPC. Nous avons généré 14 mutants de KPC-2 par mutagenèse dirigée (dont 7 correspondent à des mutants naturels : KPC-5, KPC-6, KPC-11, KPC-12, et KPC-14, KPC-31 et KPC-33, Lettre 1). L'étude des profils hydrolytiques de ces variants a permis de démontrer que la substitution d'un unique AA était capable de modifier drastiquement le profil hydrolytique de l'enzyme. Ainsi nous avons démontré qu'une substitution en position 104 et 240 induisait un gain d'activité vis-à-vis des C3G sans impact sur l'hydrolyse des carbapénèmes. A l'inverse, nous avons identifié le rôle crucial des AA 179, 241 et 242 pour l'hydrolyse des carbapénèmes (notamment perte totale d'activité carbapénémase pour KPC-28, KPC-31 et KPC-33). En outre, ces mutants dépourvus d'activité carbapénémase ne sont plus inhibés efficacement par l'avibactam. Il en résulte une résistance à l'association ceftazidime-avibactam pourtant considérée comme le traitement de référence pour le traitement des infections souches d'entérobactéries productrices d'une carbapénémase de type KPC. Afin d'appuyer cette hypothèse, une étude de modélisation a été réalisée. La meilleure compréhension des liens structure-activité émanant de nos travaux a également servi de base structurelle à la modélisation de nouveaux pan-inhibiteurs des carbapénémases.

Unravelling ceftazidime/avibactam resistance of KPC-28, a KPC-2 variant lacking carbapenemase activity

Saoussen Oueslati¹, Bogdan I. Iorga ², Linda Tlili¹, Cynthia Exilie¹, Agustin Zavala², Laurent Dortet^{1,3,4}, Agnès B. Jousset^{1,3,4}, Sandrine Bernabeu^{1,3}, Rémy A. Bonnin ^{1,4} and Thierry Naas ^{1,3,4*}

¹EA7361 'Structure, Dynamic, Function and Expression of Broad Spectrum β -Lactamases', Faculty of Medicine, Université Paris-Sud, LabEx Lermite, Université Paris-Saclay, Le Kremlin-Bicêtre, France; ²Institut de Chimie des Substances Naturelles, CNRS UPR 2301, Université Paris-Saclay, LabEx LERMIT, Gif-sur-Yvette, France; ³Bacteriology-Hygiene Unit, Assistance Publique/Hôpitaux de Paris, Bicêtre Hospital, Le Kremlin-Bicêtre, France; ⁴Associated French National Reference Centre for Antibiotic Resistance: Carbapenemase-Producing Enterobacteriaceae, Le Kremlin-Bicêtre, France

*Corresponding author. Service de Bactériologie-Hygiène, Hôpital de Bicêtre 78 rue du Général Leclerc, 94275 Le Kremlin-Bicêtre, France. Tel: +33-1-45-21-20-19; Fax: +33-1-45-21-63-40; E-mail: thierry.naas@bct.aphp.fr  orcid.org/0000-0001-9937-9572

Received 9 November 2018; returned 25 January 2019; revised 9 April 2019; accepted 18 April 2019

Background: KPC-like carbapenemases have spread worldwide with more than 30 variants identified that differ by single or double amino-acid substitutions.

Objectives: To describe the steady-state kinetic parameters of KPC-28, which differs from KPC-2 by a H274Y substitution and the deletion of two amino acids (Δ 242-GT-243).

Methods: The *bla*_{KPC-2}, *bla*_{KPC-3}, *bla*_{KPC-14} and *bla*_{KPC-28} genes were cloned into a pTOPO vector for susceptibility testing or into pET41b for overexpression, purification and subsequent kinetic parameter (K_m , k_{cat}) determination. Molecular docking experiments were performed to explore the role of the amino-acid changes in the carbapenemase activity.

Results: Susceptibility testing revealed that *Escherichia coli* producing KPC-28 displayed MICs that were lower for carbapenems and higher for ceftazidime and ceftazidime/avibactam as compared with KPC-2. The catalytic efficiencies of KPC-28 and KPC-14 for imipenem were 700-fold and 200-fold lower, respectively, than those of KPC-2, suggesting that Δ 242-GT-243 in KPC-28 and KPC-14 is responsible for reduced carbapenem hydrolysis. Similarly, the H274Y substitution resulted in KPC-28 in a 50-fold increase in ceftazidime hydrolysis that was strongly reversed by clavulanate.

Conclusions: We have shown that KPC-28 lacks carbapenemase activity, has increased ceftazidime hydrolytic activity and is strongly inhibited by clavulanate. KPC-28-producing *E. coli* isolates display an avibactam-resistant ESBL profile, which may be wrongly identified by molecular and immunochromatographic assays as the presence of a carbapenemase. Accordingly, confirmation of carbapenem hydrolysis will be mandatory with assays based solely on *bla*_{KPC} gene or gene product detection.

Introduction

In Gram-negative bacteria, acquired resistance to β -lactams may be mediated by various non-enzymatic mechanisms, such as decreased permeability of the outer membrane, or active efflux, but enzymatic inactivation by β -lactamases is the main mechanism. These enzymes, which are able to hydrolyse β -lactams, are divided into four molecular classes based on structural homologies (Ambler classification). Ambler's classes A, C and D are β -lactamases possessing a serine in their active site, whereas the class B enzymes are MBLs that use divalent Zn^{2+} ion(s) for their hydrolytic activity. It has been suggested that the rising use of carbapenems

(imipenem and meropenem) for the treatment of infections caused by MDR Gram-negative pathogens during the last decade has contributed to the emergence of carbapenem-resistant bacteria that may be the result of outer membrane permeability alteration associated with overproduction of a cephalosporinase and/or production of an ESBL or of carbapenem-hydrolysing β -lactamases called carbapenemases.¹ These enzymes belong to Ambler's classes A, B and D.² Within class A, several enzymes have been described in Enterobacteriaceae (NMC-A, IMI-1, SME-1, GES-2 and FRI-1), but *Klebsiella pneumoniae* carbapenemase (KPC) is the most prevalent across the globe. KPC is regarded as the most

worrying class A carbapenemase because of its location on self-conjugative plasmids and its frequent association with a highly successful *K. pneumoniae* clone, the clonal complex (CC) 258.³ Until 2005, the geographical distribution of KPC-producing Enterobacteriaceae remained limited to the eastern USA.⁴ Today, KPC producers have disseminated worldwide and are endemic in the USA, South America, Greece, Italy, Poland, China and Israel. Since its initial description in a *K. pneumoniae* clinical isolate from North Carolina,⁵ 39 KPC variants have been reported (www.bldb.eu).⁶ Among these variants, a mono-substitution (KPC 3–6 and 9–11) resulted in increased ceftazidime hydrolysis, with carbapenem hydrolysis being unaffected.^{7–12} Recently, *in vitro* selection of ceftazidime/avibactam resistance in Enterobacteriaceae with KPC-3 carbapenemase revealed modifications in the Ω loop that are also responsible for carbapenem susceptibility. The most prevalent modification occurs at position 179 of the KPC enzyme,^{13,14} but a few other substitutions at different positions were also involved, such as V240G and T243A.¹³ Ceftazidime/avibactam resistance also occurred *in vivo*, usually following ceftazidime/avibactam treatment for prolonged periods (>2 weeks).^{15–18} The D179 modification is always reported in cases of *in vivo* selection of ceftazidime/avibactam-resistant KPC-producing isolates.^{15,17} Recently, KPC-28, a new variant of KPC-2 with a two-amino-acid deletion (Δ 242-GT-243, according to the ABL numbering scheme)¹⁹ and a substitution, H274Y, was reported.²⁰ In that study, a KPC-28-producing clone was found to be more resistant to ceftazidime as compared with KPC-2 or KPC-3 producers, but was fully susceptible to carbapenems, suggesting a complete loss of carbapenemase activity. Here, we report the susceptibility profile and the steady-state kinetic characterization of the KPC-28 β -lactamase (a variant of KPC-3 with a two-amino-acid deletion, Δ 242-GT-243) compared with KPC-2, KPC-3 and KPC-14.

Materials and methods

Bacterial strains

The clinical strain *Escherichia coli* WI2 expressing the KPC-28 β -lactamase was used for cloning of the *bla*_{KPC-28} gene.²⁰ *E. coli* TOP10 (Invitrogen, Saint-Aubin, France) was used for cloning and mutagenesis experiments and *E. coli* BL21 Rosetta-gamiTM DE3 (Novagen, Fontenay-sous-Bois, France) was used for overexpression experiments.

Susceptibility testing

Antimicrobial susceptibilities were determined by the disc diffusion technique on Mueller–Hinton agar (Bio-Rad, Marnes-La-Coquette, France) and interpreted according to the EUCAST breakpoints, updated in May 2018 (<http://www.eucast.org>). MICs were determined using the Etest technique (bioMérieux, La Balme les Grottes, France).

PCR, cloning experiments, site-directed mutagenesis and DNA sequencing

Whole-cell DNA of *E. coli* isolates producing KPC-2, KPC-3 and KPC-28 were extracted using the QIAamp DNA minikit (Qiagen, Courtaboeuf, France) and were then used as a template to amplify the *bla*_{KPC-2}-like genes. The gene encoding KPC-14 was obtained by site-directed mutagenesis (QuikChange II Site-Directed Mutagenesis Kit, Agilent Technologies), using the primer KPC-Y274H (5'-CTAACAAGGATGACAAGCACAGCGAGGCGGCATC-3') and the plasmid pTOPO-*bla*_{KPC-28} as a template. The PCR, using the

primers Kpc-rbs (5'-CTCCACCTCAAACAAGGAAT-3') and Kpc-rev (5'-ATCTGCAGAATTCGCCCTTCGCATCGTACAGTCTCTAC-3'), was able to amplify *bla*_{KPC-3} and *bla*_{KPC-28} genes. The amplicons obtained were then cloned into the pCR-Blunt II-Topo plasmid (Invitrogen) downstream from the pLac promoter, in the same orientation as for the phenotypic studies. The recombinant pTOPO-KPC plasmids were electroporated into the *E. coli* TOP10 strain. For protein production, the sequences without the peptide signal of the *bla*_{KPC-2}, *bla*_{KPC-3}, *bla*_{KPC-14} and *bla*_{KPC-28} genes were obtained by PCR amplification using primers NdeI-KPC-2_{30–293} (5'-CATATGGCGAACCATTTCGCTAAC-3') and KPC-2 Δ STOP (5'-CTCGAGCTGCCGTTGACGCCAAT-3') and were then inserted into plasmid pET41b (Novagen). The recombinant plasmids were transformed into *E. coli* BL21 Rosetta-gamiTM DE3 (Novagen). All the recombinant plasmids were sequenced using a T7 promoter and M13 reverse primers or T7 terminator (depending on the plasmid) with an automated sequencer (ABI Prism 3100; Applied Biosystems). The nucleotide sequences were analysed using software available at the National Center for Biotechnology Information website (<http://www.ncbi.nlm.nih.gov>).

Detection of KPC producers and carbapenemase activity

The detection of the KPC variants was performed with *E. coli* TOP10 harbouring the recombinant vector pTOPO-KPC. The carbapenemase activity was detected using six techniques: the Carba NP test as previously described,²¹ the CIM test,²² the modified Hodge test²³ and the β CARBATM test (Bio-Rad),²⁴ the RAPIDEC[®] CARBA NP (bioMérieux)²⁵ and the MBT STAR[®]-Carba IVD Kit (Bruker Daltonics, Bremen, Germany)²⁶ in accordance with the manufacturers' recommendations. Molecular tests were performed with the Xpert[®] Carba-R kit (Cepheid, Sunnyvale, USA)²⁷ and by standard in-house PCR using the primers KPC-A (5'-CTGTCTGTCTCTCATGGCC-3') and KPC-B (5'-CTCGCTGTGCTTGT-CATCC-3'). Immunoenzymatic tests were carried out using two techniques: NG-Test CARBA 5 (NG Biotech, Guipry, France)²⁸ and the Resist-4 O.K.N.V. K-Set (CORIS BioConcept, Gembloux, Belgium).²⁹

Protein purification

An overnight culture of *E. coli* BL21 Rosetta-gamiTM DE3 harbouring recombinant pET41b-KPC plasmids was used to inoculate 2 L of LB medium broth containing 50 mg/L kanamycin and 30 mg/L chloramphenicol. Bacteria were cultured at 37°C until an OD of 0.6 at 600 nm was reached. The expression of the β -lactamase genes was carried out overnight at 22°C with 1 mM IPTG as inducer. Cultures were centrifuged at 6000 g for 15 min and then the pellets were resuspended with the binding buffer (10 mM imidazole, 25 mM sodium phosphate pH 7.4 and 300 mM NaCl). Bacterial cells were disrupted by sonication and the bacterial pellet was removed by two consecutive centrifugation steps at 10000 g for 1 h at 4°C; the supernatant was then centrifuged at 96000 g for 1 h at 4°C. The soluble fractions were filtered and then passed through a HisTrapTM HP column (GE Healthcare) and proteins were eluted with the elution buffer (500 mM imidazole, 25 mM sodium phosphate pH 7.4 and 300 mM NaCl). Finally, a gel filtration step was performed with 100 mM sodium phosphate buffer pH 7 and 150 mM NaCl with a Superdex 75 column (GE Healthcare). The protein purity was estimated by SDS-PAGE and the pooled fractions were dialysed against 10 mM Tris-HCl pH 7.6 and concentrated using Vivaspinn columns. The concentrations were determined by measuring the OD at 280 nm and with the extinction coefficients obtained from the ProtParam tool (Swiss Institute of Bioinformatics online resource portal).³⁰

Steady-state kinetic parameters

Kinetic parameters were determined using purified KPC-2, KPC-3, KPC-14 and KPC-28 β -lactamases in 100 mM sodium phosphate buffer (pH 7). The k_{cat} and K_m values were determined by analysing β -lactam hydrolysis under initial-rate conditions with an ULTROSPEC 2000 UV spectrophotometer and the SWIFT II software (GE Healthcare, Velizy-Villacoublay, France)

using the Eadie–Hoffstee linearization of the Michaelis–Menten equation. The different β -lactams were purchased from Sigma–Aldrich (Saint-Quentin-Fallavier, France). For some cephalosporins, saturation could not be reached. Thus, the values for the catalytic efficiency (k_{cat}/K_m) of the enzymes KPC-2 and KPC-3 against these substrates were evaluated with the lower limits for the k_{cat} and K_m determined. The IC_{50} of the β -lactamase inhibitors clavulanate and avibactam was determined in 100 mM sodium phosphate buffer (pH 7) and with 100 μ M piperacillin and 100 μ M ceftazidime (respectively) as a reporter substrate.

Molecular modelling

Molecular models of KPC-3, KPC-14 and KPC-28 were generated by comparative modelling using MODELLER version 9.16³¹ with the KPC-2 structure³² (PDB code 5UJ3) as template. Three-dimensional structures of the ligands were generated using CORINA version 3.60 (Molecular Networks GmbH, Erlangen, Germany; <http://www.molecular-networks.com>). Covalent docking calculations were carried out using GOLD version 5.2³³ and the GoldScore scoring function. The binding site was defined as a sphere with a 20 Å radius around the OG atom of the Ser70 residue. The covalent connection was made between the OG atom of the Ser70 residue and the open form of the β -lactam ring in order to generate the acyl-enzyme complex. Molecular modelling images were generated using UCSF CHIMERA.³⁴

Results

Clinical isolate

E. coli WI2 was recovered from a faecal sample from a Portuguese patient upon admission to a French hospital subsequent to a

medical repatriation. This isolate was resistant to broad-spectrum cephalosporins, aminoglycosides and colistin and of reduced susceptibility to carbapenems.²⁰ As previously described, this isolate possessed the bla_{OXA-48} and bla_{KPC-28} genes and the acquired colistin resistance determinant $mcr-1$.²⁰ KPC-28 is a variant of KPC-3 with a deletion of two amino acids ($\Delta 242$ -GT-243) and KPC-14 is a variant of KPC-2 with the same deletion of these two amino acids (Figure 1).

Antimicrobial susceptibilities of transformants with KPC-2, KPC-3, KPC-14 and KPC-28

To evaluate and compare the antimicrobial susceptibility profiles conferred by KPC-28, the bla_{KPC-2} , bla_{KPC-3} , bla_{KPC-14} and bla_{KPC-28} genes were cloned into pTOPO vector and expressed in *E. coli* TOP10 (Table 1). Although the different KPC variants exhibited similar MICs of amoxicillin, temocillin, cefixime and cefepime, KPC-28- and KPC-14-producing *E. coli* TOP10 possessed lower MICs of cefotaxime and carbapenems (being fully susceptible), but exhibited higher MICs of ceftazidime as compared with KPC-2-producing *E. coli* TOP10 (Table 1). The highest MICs of cefotaxime and aztreonam were found for the KPC-3-producing *E. coli* TOP10 clones. The addition of clavulanate restored susceptibility to amoxicillin for KPC-28- and KPC-14-producing *E. coli* clones, while inhibition by avibactam seemed to be less efficient, as both KPC-28- and KPC-14-producing *E. coli* isolates were resistant to the combination ceftazidime/avibactam. Thus, MIC values suggested that $\Delta 242$ -GT-243 (in KPC-14 and KPC-28) resulted in the loss of carbapenemase activity, but in increased hydrolytic activity

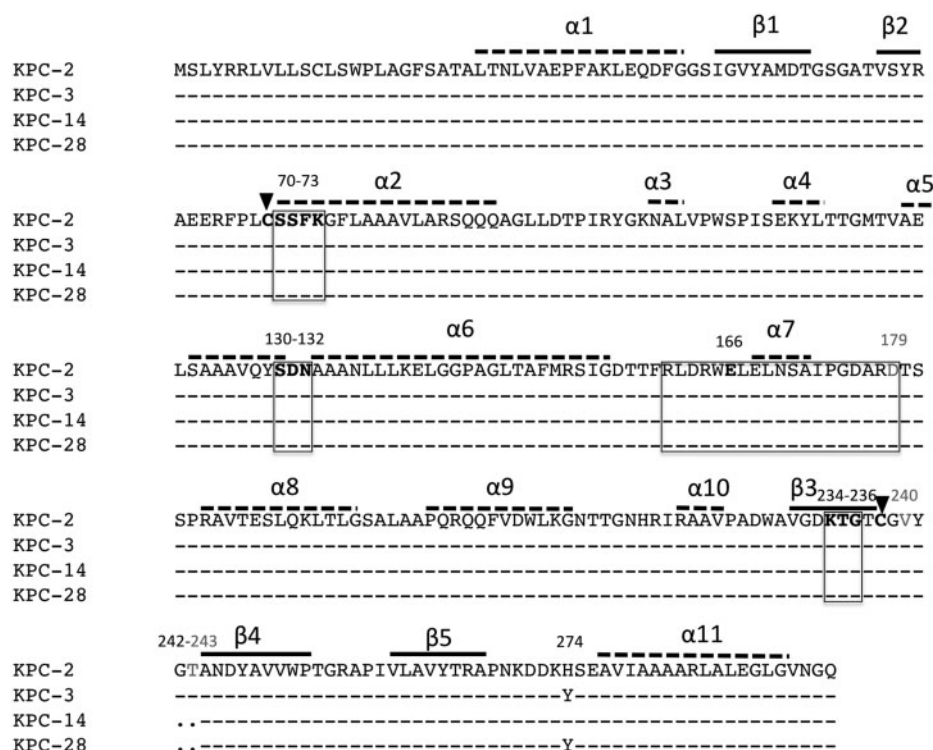


Figure 1. Sequence alignment of KPC variants. Alpha helices are indicated by dashed lines and β strands by continuous black lines. Cysteines involved in disulphide bonds are indicated by inverted black triangles. Key residues known to be implicated in ceftazidime/avibactam resistance are indicated in grey. Conserved residues among class A β -lactamases are indicated by boxes.

Table 1. MIC profile of *E. coli* TOP10 expressing KPC-2, KPC-3, KPC-14 and KPC-28 β -lactamases determined by Etests

Antimicrobial agent	MIC (mg/L)				
	<i>E. coli</i> TOP10 pTOPO KPC-2	<i>E. coli</i> TOP10 pTOPO KPC-3	<i>E. coli</i> TOP10 pTOPO KPC-14	<i>E. coli</i> TOP10 pTOPO KPC-28	<i>E. coli</i> TOP10
Amoxicillin	>256	>256	>256	>256	6
Amoxicillin/clavulanate ^a	24	48	6	6	6
Temocillin	12	16	16	16	6
Ceftriaxone	12	48	6	4	0.032
Cefotaxime	8	>32	6	4	0.064
Ceftazidime	4	>256	>256	>256	0.125
Ceftazidime/avibactam ^b	0.38	0.75	24	12	0.125
Cefixime	3	12	12	8	0.38
Cefepime	2	6	4	4	0.0064
Aztreonam	24	>256	32	24	0.047
Imipenem	8	8	0.25	0.25	0.25
Meropenem	3	3	0.032	0.032	0.032
Ertapenem	1	1	0.006	0.008	0.004

^aClavulanate at a fixed concentration of 4 mg/L.

^bAvibactam at a fixed concentration of 4 mg/L.

Table 2. Steady-state kinetic parameters^a for hydrolysis of β -lactam substrates by KPC-2 and KPC-2-like β -lactamases

Substrate	K_m (μ M)				k_{cat} (s^{-1})				k_{cat}/K_m ($mM^{-1} s^{-1}$)			
	KPC-2	KPC-3	KPC-14	KPC-28	KPC-2	KPC-3	KPC-14	KPC-28	KPC-2	KPC-3	KPC-14	KPC-28
Piperacillin	137	255	6	11	59	38	0.8	0.95	434	150	127	86
Cefoxitin	>1000	>1000	NH	NH	>12	>4	ND	ND	2	1.6	ND	ND
Cefotaxime	>1000	335	77	75	>163	403	4	5	95	1202	52	67
Ceftazidime	>1000	656	41	125	>16	9	1	4	0.6	14	24	32
Cefepime	>1000	491	34	30	>48	14	1.7	2.5	13	29	50	83
Imipenem	198	235	5	18	47	31	0.006	0.006	237	131	1.2	0.34
Meropenem	45	18	7	NH	3	2	0.003	ND	67	103	0.4	ND
Ertapenem	30	25	5	9	4	3	0.002	0.004	133	114	0.47	0.42

ND, not determined; NH, no detectable hydrolysis.

^aData are the mean of three independent experiments. Standard deviations were within 10% of the mean value.

towards ceftazidime. This increased ceftazidime hydrolytic activity was potentiated by the H274Y substitution in KPC-28, as already shown for KPC-3, but, in the latter case, carbapenem resistance was not affected.¹²

Biochemical properties of KPC-28

To characterize and compare kinetic parameters of KPC-28, the four variants were purified and kinetic studies were performed (Table 2). KPC-2 was used as a control for comparison. Overall, the steady-state kinetics revealed three patterns. KPC-3 exhibited a higher hydrolytic activity towards extended-spectrum cephalosporins (cefotaxime, ceftazidime and cefepime), but a similar hydrolysis rate for carbapenems to KPC-2. KPC-14 and KPC-28 possessed a higher affinity for ceftazidime, which increased their catalytic efficiencies 40-fold and 50-fold, respectively. However,

their carbapenemase activities were reduced. Imipenem catalytic efficiencies were reduced 200-fold and 700-fold, respectively, compared with KPC-2. Thus, the reduced carbapenem hydrolysis can be linked to Δ 242-GT-243 that results in a 10-fold increase in affinity, but also a 1000-fold decrease in k_{cat} values. Similarly, KPC-14 and KPC-28 completely lost hydrolytic activity for cefoxitin. IC_{50} values of clavulanate for KPC-2, KPC-3, KPC-14 and KPC-28 were 47, 16, 0.1 and 0.09 μ M, respectively. Taken together, our results suggest that KPC-28 has a clavulanate-inhibited ESBL profile and no longer displays that of a carbapenemase. Finally, our data suggest that the increased ceftazidime hydrolysis of KPC-28 is due to the H274Y substitution (Table 2) confirming previous results,¹² but is potentiated by the two-amino-acid deletion Δ 242-GT-243. The H274Y substitution does not affect carbapenem hydrolysis, unlike the Δ 242-GT-243 deletion (Table 2). The activity of avibactam against the different KPCs was determined by IC_{50} measurements.

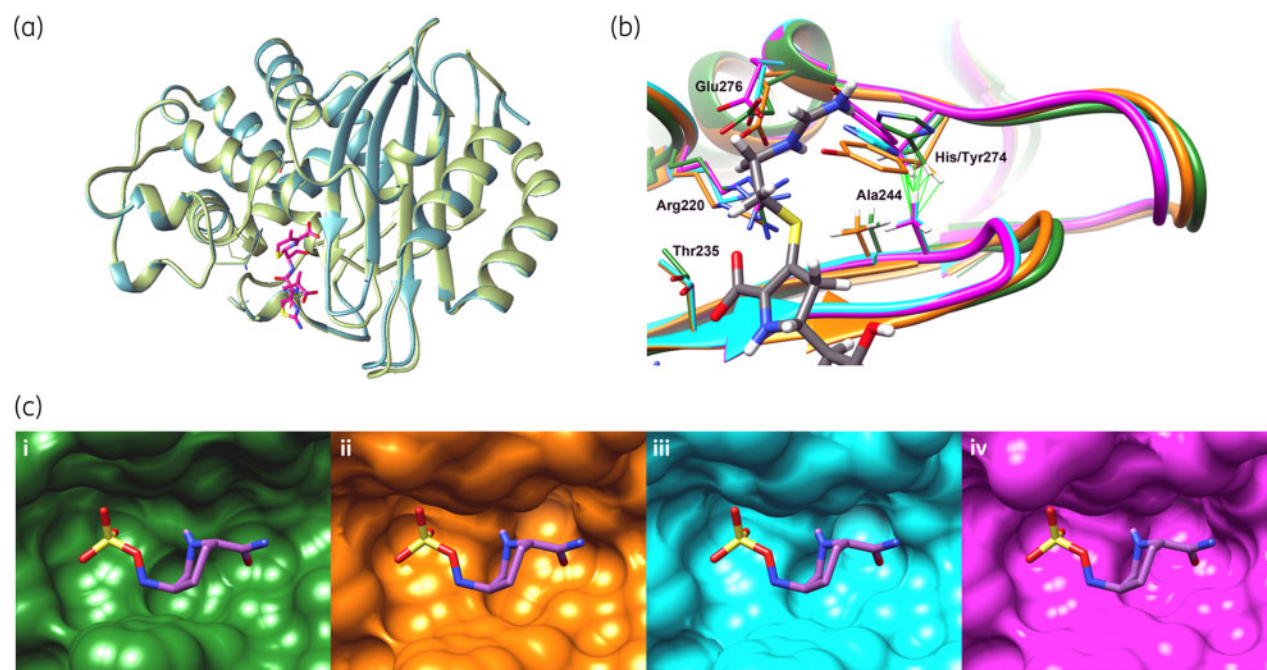


Figure 2. Models of interaction of KPC-3 variant (KPC-14 and KPC-28) with ceftazidime and imipenem. (a) Superposition of the molecular model of KPC-3 and KPC-28 with ceftazidime. KPC-3 is in light green, KPC-28 in dark green and ceftazidime in magenta. (b) Crystal structure of KPC-2 (PDB code 5UJ3, green) superposed with homology models of KPC-3 (orange), KPC-14 (cyan) and KPC-28 (magenta). The imipenem conformation obtained by covalent docking on KPC-2 is shown as grey sticks. The steric clashes between the side chains of A244 and of the residue at position 274 are highlighted in light green. (c) Crystal structure of KPC-2 in complex with avibactam (i, PDB code 4ZBE, green) superposed with the KPC-3 (ii, orange), KPC-14 (iii, cyan) and KPC-28 (iv, magenta) homology models, showing no significant clashes between the protein and the ligand.

The IC_{50} values for KPC-2, KPC-3, KPC-14 and KPC-28 were 230, 350, 107 and 586 nM, respectively. These values are very similar, which suggests that the two-amino-acid deletion $\Delta 242$ -GT-243 has no impact on the inhibition properties of avibactam.

Molecular modelling

We performed a molecular modelling study to identify the structural determinants that could explain the experimentally determined differences between the hydrolytic profiles of KPC-2, KPC-3, KPC-14 and KPC-28. In the absence of structural data for the KPC-2 variants, we generated molecular models of KPC-3, KPC-14 and KPC-28 by comparative modelling using MODELLER version 9.16³¹ with the KPC-2 structure (PDB code 5UJ3) as template (Figure 2a and b).³² The resulting models showed that the $\Delta 242$ -GT-243 deletion did not modify the overall structure of the protein, but resulted in a shorter 238–243 loop, giving rise to a 2.4 Å shift of A244 in KPC-14 and KPC-28 (Figure 2a). This new position of A244 led to a clash between the side chains of A244 and of the residue at position 274 (H and T for KPC-14 and KPC-28, respectively) that may expand the active site and allow better access for the substrates. In addition, the covalent complex of KPC-2 with imipenem obtained by docking showed a stabilizing interaction between H274 and the positively charged R2 substituent of imipenem (Figure 2b). In the case of KPC-14 and KPC-28, the above-mentioned clash may prevent this stabilizing interaction with imipenem. Under these conditions, the substrate may interact with the binding site in a slightly different way and therefore

explain the 10-fold increase in K_m and the 1000-fold decrease in k_{cat} , which ultimately lead to the loss of the carbapenemase activity in these mutants. Additional theoretical calculations, and especially molecular dynamics simulations, will be needed to understand these details.

Detection methods for KPC variants

Four carbapenemase detection tests based on imipenem hydrolysis were evaluated with respect to their ability to detect these four variants when expressed in *E. coli* TOP10 (Table 3). Thus, the Carba NP test,²¹ the RAPIDEC® CARBA NP, the MBT STAR®-Carba IVD Kit, the β CARBA™ test, the CIM test and the modified Hodge test were able to detect KPC-2 and KPC-3, but failed to detect KPC-14 and KPC-28.^{21–26} These results are in line with the kinetic studies, which showed a loss of carbapenemase activity for KPC-14 and KPC-28. On the other hand, the immunochromatographic assays Resist-4 O.K.N.V. K-Set (CORIS BioConcept) and the NG-Test CARBA 5 (NG Biotech) and molecular Xpert® Carba-R test (Cepheid) and in-house PCR were positive for all four enzymes.^{27–29,35} The positive results of the immunochromatographic assays for KPC-14 and KPC-28 confirmed our molecular modelling results, suggesting that $\Delta 242$ -GT-243 did not affect the overall conformation of these proteins.

Discussion

KPC-producing Enterobacteriaceae are now endemic in the USA and have spread worldwide. So far, 39 variants of KPC have been

Table 3. Diagnostic tests performed on *E. coli* TOP10 harbouring the vector pTOPO expressing KPC-2, KPC-3, KPC-14 and KPC-28

	Biochemical tests					Molecular tests		Immunoenzymatic tests		
	Carba NP test	RAPIDEC [®] CARBA NP	CIM test	modified Hodge test	β CARBA [™] test	MBT STAR [®] -Carba IVD Kit	standard <i>bla</i> _{KPC} PCR	Xpert [®] Carba-R	NG-Test CARBA 5	CORIS BioConcept Resist-4 O.K.N.V. K-Set
KPC-2	+	+	+	+	+	+	+	+	+	+
KPC-3	+	+	+	+	+	+	+	+	+	+
KPC-14	–	–	–	–	–	–	+	+	+	+
KPC-28	–	–	–	–	–	–	+	+	+	+

Key: +, positive test result; –, negative test result.

reported,⁶ with KPC-2 and KPC-3 appearing to be the most prevalent.³⁶ In this study, we have characterized the biochemical properties of KPC-28, which has the same H274Y substitution as KPC-3 and possesses in addition a Δ242-GT-243 deletion previously identified in KPC-14. Steady-state kinetics of KPC-2, KPC-3, KPC-14 and KPC-28 β-lactamases revealed that the unique substitution of KPC-3 (H274Y) conferred an ~20-fold increase in the catalytic efficiency towards ceftazidime as compared with KPC-2. This substitution has also been identified in other variants, such as KPC-7 (M49I; H274Y), KPC-8 (V240G; H274Y), KPC-9 (V240A; H274Y) and KPC-10 (P104R; H274Y), which are associated with increased ceftazidime resistance.⁹ The study of KPC-5 showed that substitution of residue 104 can also confer increased ceftazidime hydrolysis.¹¹ These studies highlighted that a single or a double substitution can affect the hydrolysis rate of cephalosporins, but do not significantly change the carbapenemase activity. More recently, Shields *et al.*¹³ reported that the T243A substitution increased ceftazidime hydrolysis of the KPC-3 enzyme with little impact on carbapenemase activity. Here, we demonstrated that the Δ242-GT-243 deletion also leads to an increase in ceftazidime hydrolysis, but, unlike the T243A substitution, has a drastic impact on carbapenemase activity. For example, compared with KPC-2, the catalytic efficiencies (k_{cat}/K_m) towards imipenem were 700-fold and 200-fold lower for KPC-28 and KPC-14, respectively. This deletion is linked with a 10-fold higher affinity (lower K_m) but a 1000-fold decrease in k_{cat} for carbapenems. The loss of the carbapenemase activity can be explained by the loss of the interaction between the residue H274 in KPC-14 and Y274 in KPC-28 and carbapenems due to a 2 Å shift of the A244. Additionally, the IC₅₀ of clavulanate was 500-fold lower for KPC-28 as compared with KPC-2. The most worrying result is that this two-amino-acid deletion also has an impact on ceftazidime/avibactam susceptibility. Indeed, while KPC-2- and KPC-3-producing *E. coli* isolates remain susceptible to ceftazidime/avibactam, *E. coli* isolates producing KPC-14 (and those producing KPC-28) are resistant. Several mutations in KPC enzymes have been shown to yield ceftazidime/avibactam resistance. The most common *in vivo* mutation described is D179Y, especially when associated with the H279Y mutation that yields increased ceftazidime hydrolysis.^{14,37} Other mutations with minor phenotypic expressions have also been identified, such as S130G, T243A or T243M.³⁸ In KPC-28, T243 has been deleted and may thus play an additional role in avibactam resistance. It is very likely that avibactam resistance in KPC-28 is the result of the increase in the catalytic efficiency for ceftazidime, since no clashes were evidenced between avibactam

and the homology models of the KPC-3, KPC-14 and KPC-28 variants (Figure 2c). This hypothesis is reinforced by the fact that the IC₅₀ values of avibactam for the different KPC variants are very similar.

Conclusions

This study underlines that KPC-type β-lactamases are more complex and diverse than expected. As exemplified by KPC-28 and KPC-14, they are not all true carbapenemases, a scenario well known for OXA-48-like enzymes.³⁹ Unfortunately, molecular detection assays and immunochromatographic tests are not able to distinguish KPC variants with carbapenem hydrolytic capacities from those lacking any carbapenemase activity. Therefore, the first-line screening of carbapenemase producers in Enterobacteriaceae must include a test able to detect any carbapenemase activity, such as biochemical tests (e.g. Carba NP test and derivatives, β CARBA[™] test), or MALDI-TOF-based assays (e.g. MBT STAR[®]-Carba IVD Kit, Bruker Daltonics). Finally, as KPC-producing organisms cause infections with a high morbidity and mortality, avibactam was designed as a powerful inhibitor of KPC enzymes.^{40–43} However, several studies now report the resistance of KPC-producing isolates to ceftazidime/avibactam as a consequence of the selection of point-mutation derivatives.⁴³ KPC-28-producing bacterial isolates are resistant to ceftazidime/avibactam as a consequence of increased ceftazidime hydrolysis, rather than intrinsic avibactam resistance. Finally, as KPC-28 lacks carbapenemase activity, has increased ceftazidime hydrolytic activity and is strongly inhibited by clavulanate, KPC-28-producing bacterial isolates may be identified as ESBL producers.

Funding

This work was supported by the Assistance Publique – Hôpitaux de Paris, by a grant from the Université Paris-Sud (EA 7361), and by the LabEx LERMIT with a grant from the French National Research Agency (ANR-10-LABX-33). This work was also funded in part by a grant from the Joint Programming Initiative on Antimicrobial Resistance (ANR-14-JAMR-0002).

Transparency declarations

L. D. is co-inventor of the Carba NP test, the patent for which has been licensed to bioMérieux (La Balme les Grottes, France). All other authors: none to declare.

References

- 1 Hawkey PM. Resistance to carbapenems. *J Med Microbiol* 1997; **46**: 451–4.
- 2 Queenan AM, Bush K. Carbapenemases: the versatile β -lactamases. *Clin Microbiol Rev* 2007; **20**: 440–58.
- 3 Peirano G, Bradford PA, Kazmierczak KM *et al.* Importance of clonal complex 258 and IncFK2-like plasmids among a global collection of *Klebsiella pneumoniae* with bla_{KPC} . *Antimicrob Agents Chemother* 2017; **61**: e02610-16.
- 4 Bratu S, Landman D, Haag R *et al.* Rapid spread of carbapenem-resistant *Klebsiella pneumoniae* in New York City: a new threat to our antibiotic armamentarium. *Arch Intern Med* 2005; **165**: 1430–5.
- 5 Yigit H, Queenan AM, Anderson GJ *et al.* Novel carbapenem-hydrolyzing β -lactamase, KPC-1, from a carbapenem-resistant strain of *Klebsiella pneumoniae*. *Antimicrob Agents Chemother* 2001; **45**: 1151–61.
- 6 Naas T, Oueslati S, Bonnin RA *et al.* Beta-lactamase database (BLDB)—structure and function. *J Enzyme Inhib Med Chem* 2017; **32**: 917–9.
- 7 Naas T, Dortet L, Iorga BI. Structural and functional aspects of class A carbapenemases. *Curr Drug Targets* 2016; **17**: 1006–28.
- 8 Alba J, Ishii Y, Thomson K *et al.* Kinetics study of KPC-3, a plasmid-encoded Class A carbapenem-hydrolyzing β -lactamase. *Antimicrob Agents Chemother* 2005; **49**: 4760–2.
- 9 Hidalgo-Grass C, Warburg G, Temper V *et al.* KPC-9, a novel carbapenemase from clinical specimens in Israel. *Antimicrob Agents Chemother* 2012; **56**: 6057–9.
- 10 Lamoureux TL, Frase H, Antunes NT *et al.* Antibiotic resistance and substrate profiles of the Class A carbapenemase KPC-6. *Antimicrob Agents Chemother* 2012; **56**: 6006–8.
- 11 Wolter DJ, Kurpiel PM, Woodford N *et al.* Phenotypic and enzymatic comparative analysis of the novel KPC variant KPC-5 and its evolutionary variants, KPC-2 and KPC-4. *Antimicrob Agents Chemother* 2009; **53**: 557–62.
- 12 Mehta SC, Rice K, Palzkill T. Natural variants of the KPC-2 carbapenemase have evolved increased catalytic efficiency for ceftazidime hydrolysis at the cost of enzyme stability. *PLoS Pathog* 2015; **11**: e1004949.
- 13 Shields RK, Nguyen MH, Press EG *et al.* In vitro selection of meropenem resistance among ceftazidime-avibactam-resistant, meropenem-susceptible *Klebsiella pneumoniae* isolates with variant KPC-3 carbapenemases. *Antimicrob Agents Chemother* 2017; **61**: e00079-17.
- 14 Livermore DM, Warner M, Jamroz D *et al.* In vitro selection of ceftazidime-avibactam resistance in Enterobacteriaceae with KPC-3 carbapenemase. *Antimicrob Agents Chemother* 2015; **59**: 5324–30.
- 15 Giddins MJ, Macesic N, Annavajhala MK *et al.* Successive emergence of ceftazidime-avibactam resistance through distinct genomic adaptations in bla_{KPC-2} -harboring *Klebsiella pneumoniae* sequence type 307 isolates. *Antimicrob Agents Chemother* 2018; **62**: e02101-17.
- 16 Humphries RM, Yang S, Hemarajata P *et al.* First report of ceftazidime-avibactam resistance in a KPC-3-expressing *Klebsiella pneumoniae* isolate. *Antimicrob Agents Chemother* 2015; **59**: 6605–7.
- 17 Gaibani P, Campoli C, Lewis RE *et al.* In vivo evolution of resistant subpopulations of KPC-producing *Klebsiella pneumoniae* during ceftazidime/avibactam treatment. *J Antimicrob Chemother* 2018; **73**: 1525–9.
- 18 Shields RK, Potoski BA, Haidar G *et al.* Clinical outcomes, drug toxicity, and emergence of ceftazidime-avibactam resistance among patients treated for carbapenem-resistant Enterobacteriaceae infections. *Clin Infect Dis* 2016; **63**: 1615–8.
- 19 Ambler RP, Coulson AFW, Frère JM *et al.* A standard numbering scheme for the class A β -lactamases. *Biochem J* 1991; **276**: 269–70.
- 20 Beyrouthy R, Robin F, Lessene A *et al.* MCR-1 and OXA-48 in vivo acquisition in KPC-producing *Escherichia coli* after colistin treatment. *Antimicrob Agents Chemother* 2017; **61**: e02540-16.
- 21 Nordmann P, Poirel L, Dortet L. Rapid detection of carbapenemase-producing Enterobacteriaceae. *Emerg Infect Dis* 2012; **18**: 1503–7.
- 22 Gauthier L, Bonnin RA, Dortet L *et al.* Retrospective and prospective evaluation of the Carbapenem inactivation method for the detection of carbapenemase-producing Enterobacteriaceae. *PLoS One* 2017; **12**: e0170769.
- 23 Anderson KF, Lonsway DR, Rasheed JK *et al.* Evaluation of methods to identify the *Klebsiella pneumoniae* carbapenemase in Enterobacteriaceae. *J Clin Microbiol* 2007; **45**: 2723–5.
- 24 Bernabeu S, Dortet L, Naas T. Evaluation of the β -CARBATM test, a colorimetric test for the rapid detection of carbapenemase activity in Gram-negative bacilli. *J Antimicrob Chemother* 2017; **72**: 1646–58.
- 25 Dortet L, Agathine A, Naas T *et al.* Evaluation of the RAPIDEC[®] CARBA NP, the Rapid CARB Screen[®] and the Carba NP test for biochemical detection of carbapenemase-producing Enterobacteriaceae. *J Antimicrob Chemother* 2015; **70**: 3014–22.
- 26 Dortet L, Tandé D, de Briel D *et al.* MALDI-TOF for the rapid detection of carbapenemase-producing Enterobacteriaceae: comparison of the commercialized MBT STAR[®]-Carba IVD Kit with two in-house MALDI-TOF techniques and the RAPIDEC[®] CARBA NP. *J Antimicrob Chemother* 2018; **73**: 2352–9.
- 27 Dortet L, Fusaro M, Naas T. Improvement of the Xpert Carba-R Kit for the detection of carbapenemase-producing Enterobacteriaceae. *Antimicrob Agents Chemother* 2016; **60**: 3832–7.
- 28 Boutal H, Vogel A, Bernabeu S *et al.* A multiplex lateral flow immunoassay for the rapid identification of NDM-, KPC-, IMP- and VIM-type and OXA-48-like carbapenemase-producing Enterobacteriaceae. *J Antimicrob Chemother* 2018; **73**: 909–15.
- 29 Glupczynski Y, Jousset A, Evrard S *et al.* Prospective evaluation of the OKN K-SeT assay, a new multiplex immunochromatographic test for the rapid detection of OXA-48-like KPC and NDM carbapenemases. *J Antimicrob Chemother* 2017; **72**: 1955–60.
- 30 Artimo P, Jonnalagedda M, Arnold K *et al.* ExPASy: SIB bioinformatics resource portal. *Nucleic Acids Res* 2012; **40**: W597–603.
- 31 Šali A, Blundell TL. Comparative protein modelling by satisfaction of spatial restraints. *J Mol Biol* 1993; **234**: 779–815.
- 32 Pemberton OA, Zhang X, Chen Y. Molecular basis of substrate recognition and product release by the *Klebsiella pneumoniae* carbapenemase (KPC-2). *J Med Chem* 2017; **60**: 3525–30.
- 33 Verdonk ML, Cole JC, Hartshorn MJ *et al.* Improved protein–ligand docking using GOLD. *Proteins* 2003; **52**: 609–23.
- 34 Pettersen EF, Goddard TD, Huang CC *et al.* UCSF Chimera—a visualization system for exploratory research and analysis. *J Comput Chem* **25**: 1605–12.
- 35 Sağıroğlu P, Hasdemir U, Altinkanat Gelmez G *et al.* Performance of “RESIST-3 O.K.N. K-SeT” immunochromatographic assay for the detection of OXA-48 like, KPC, and NDM carbapenemases in *Klebsiella pneumoniae* in Turkey. *Braz J Microbiol* 2018; **49**: 885–90.
- 36 Stoesser N, Sheppard AE, Peirano G *et al.* Genomic epidemiology of global *Klebsiella pneumoniae* carbapenemase (KPC)-producing *Escherichia coli*. *Sci Rep* 2017; **7**: 5917.
- 37 Barnes MD, Winkler ML, Taracila MA *et al.* *Klebsiella pneumoniae* carbapenemase-2 (KPC-2), substitutions at Ambler position Asp179, and resistance to ceftazidime-avibactam: unique antibiotic-resistant phenotypes emerge from β -lactamase protein engineering. *Mbio* 2017; **8**: e00528-17.
- 38 Papp-Wallace KM, Winkler ML, Taracila MA *et al.* Variants of β -lactamase KPC-2 that are resistant to inhibition by avibactam. *Antimicrob Agents Chemother* 2015; **59**: 3710–7.
- 39 Dortet L, Oueslati S, Jeannot K *et al.* Genetic and biochemical characterization of OXA-405, an OXA-48-type extended-spectrum β -lactamase

without significant carbapenemase activity. *Antimicrob Agents Chemother* 2015; **59**: 3823–8.

40 Nordmann P, Cuzon G, Naas T. The real threat of *Klebsiella pneumoniae* carbapenemase-producing bacteria. *Lancet Infect Dis* 2009; **9**: 228–36.

41 Ben-David D, Kordevani R, Keller N *et al.* Outcome of carbapenem-resistant *Klebsiella pneumoniae* bloodstream infections. *Clin Microbiol Infect* 2012; **18**: 54–60.

42 Patel G, Huprikar S, Factor SH *et al.* Outcomes of carbapenem-resistant *Klebsiella pneumoniae* infection and the impact of antimicrobial and adjunctive therapies. *Infect Control Hosp Epidemiol* 2008; **29**: 1099–106.

43 Stachyra T, Levasseur P, Pêchereau M-C *et al.* *In vitro* activity of the β -lactamase inhibitor NXL104 against KPC-2 carbapenemase and Enterobacteriaceae expressing KPC carbapenemases. *J Antimicrob Chemother* 2009; **64**: 326–9.

J Antimicrob Chemother
doi:10.1093/jac/dkz508

Different phenotypic expression of KPC β -lactamase variants and challenges in their detection

Saoussen Oueslati¹, Linda Tlili¹, Cynthia Exilie¹,
Sandrine Bernabeu^{1,2}, Bogdan Iorga³,
Rémy A. Bonnin^{1,4}, Laurent Dortet^{1,2,4} and
Thierry Naas^{1,2,4*}

¹EA7361 'Structure, dynamic, function and expression of broad spectrum β -lactamases', Faculty of Medicine Université Paris-Sud, LabEx LERMIT, Université Paris-Saclay, Le Kremlin-Bicêtre, France; ²Bacteriology-Hygiene unit, Assistance Publique/Hôpitaux de Paris, Bicêtre Hospital, Le Kremlin-Bicêtre, France; ³Institut de Chimie des Substances Naturelles, CNRS UPR 2301, Université Paris-Saclay, LabEx LERMIT, Gif-sur-Yvette, France; ⁴Associated French National Reference Center for Antibiotic Resistance: Carbapenemase-producing Enterobacteriaceae, Le Kremlin-Bicêtre, France

*Corresponding author. E-mail: thierry.naas@aphp.fr

Sir,
Carbapenem resistance among Enterobacteriaceae has become a major public health issue owing to their rapid worldwide spread.¹ In Enterobacteriaceae this resistance is largely due to the production of carbapenemases, with the most prevalent throughout the world being KPC-, VIM-, IMP-, NDM- and OXA-48-type variants. KPC-2, initially described in the USA in 2001,² went global in less than a decade. This was probably a result of KPC-2 being located on a transposon, Tn4401, capable of high frequency transposition, itself inserted in self-conjugative plasmids, and its frequent association with the highly successful *Klebsiella pneumoniae* clonal group 258.³ To date, more than 44 natural KPC variants have been described, but only a few of them have been characterized in terms of β -lactam hydrolytic properties.⁴ It is crucial to understand the impact of single amino acid changes on the hydrolytic profile of KPC variants and the ability of commercially available diagnostic tests to detect them efficiently.

In this work, we have compared the phenotypic expression of 14 KPC variants (either natural or generated by site-directed mutagenesis) and evaluated the performance of several diagnostic tests to detect them. *bla*_{KPC-2} and *bla*_{KPC-3} alleles were cloned into the pTOPO vector along with its natural ribosomal binding site (RBS) upstream, and electroporated into electrocompetent *Escherichia coli* TOP10 as previously described.⁵ The resulting plasmids were used to construct 11 *bla*_{KPC-2} single mutants and 1 *bla*_{KPC-3} single mutant using the QuikChange II Site-Directed

Mutagenesis Kit (Agilent Technologies, Les Ulis, France) (Table 1). Thus, among the 12 generated mutants (Figure S1A, available as Supplementary data at JAC Online), 4 were natural variants of KPC-2 [KPC-5 (P104R),⁶ KPC-6 (V240G),⁷ KPC-12 (L168M) and KPC-33 (D179Y)] and 1 of KPC-3 [KPC-31 (D179Y)]. Six substitutions correspond to natural substitutions that occurred in KPC-2, but that were not reported alone: V240A, G147K, A120L, D92G, W105A and W105G. Finally, the last mutant has the substitution C238S, which is a conserved residue that establishes a disulphide bridge with C68. MICs were determined using the Etest (bioMérieux, Marcy-l'Étoile, France) and detection tests were performed according to the manufacturers' recommendations. Phenotypic profiles and diagnostic testing results are summarized in Table 1. Increased MICs of aztreonam and cephalosporins with unaltered/similar MICs of imipenem were observed for mutations at position 240. In contrast, substitutions at positions 168 and 92 led to low carbapenem MICs, but carbapenem hydrolysis was still detectable (as evidenced using biochemical tests; see Table 1). The mutations P104R and G147K led to increased MICs of aztreonam and cephalosporins, with slightly decreased MICs of carbapenems. The mutations at residues 105 and 238 resulted in a global decrease in MICs of all β -lactams except amoxicillin, with a stronger impact observed for the C238S mutant. With all of these mutants (including those with highly increased MICs of ceftazidime, such as P104R, V240G and V240A), avibactam was able to restore ceftazidime susceptibility. Interestingly, KPC-31 and KPC-33, with a D179Y substitution, exhibit reduced MICs of all β -lactams, including aztreonam and amoxicillin, except for ceftazidime (for which increased MICs were observed) and cefixime (for which unaltered and increased MICs were observed, respectively). In addition, these two mutants had increased MICs of the combination of ceftazidime/avibactam being even in the range of resistance for KPC-31 according to EUCAST. These results suggest that avibactam is not capable of inhibiting KPC-31 and KPC-33 efficiently. In order to confirm this hypothesis, IC₅₀s were measured with purified proteins.⁵ The IC₅₀ values for KPC-31 (20 μ M) and KPC-33 (42 μ M) were ~100-fold higher than those of KPC-2 (230 nM) and KPC-3 (350 nM), further supporting that the residue D179 is important in the binding of avibactam.^{5,8,9}

Overall, all tested residues, except A120, have a direct impact on the phenotypic expression profile of KPC enzymes. Residues 168 and 179 are located on the Ω loop, which is known to play a crucial role in the substrate selectivity of the enzyme.⁹ Residues 105, 104 and 240 delimit the cavity of the active site. Accordingly, the hydrolysis spectrum is influenced by the nature of the residues at these positions. Since the two cysteines C238 and C68 (adjacent to S70) form a disulphide bridge that stabilizes the folding of KPC, we expected to identify a dramatic impact of the C238S substitution on the catalytic activity of the enzyme, as shown for other class A carbapenemases such as SME and GES-5.^{10,11} Finally, although located on the opposite of the active site, residues 92 and 147 also have a crucial impact on KPC activity. Molecular modelling of the G147K mutant, performed with UCSF Chimera software,¹² shows a clash with G143 located on

Table 1. MIC profiles for *E. coli* TOP10 expressing single KPC mutants and performances of various diagnostic tests

AA changes	MIC (mg/L) ^a													Carbapenem hydrolysis assays ^b					PCR ^b		LFIA ^b	
	Variant	AMX	ATM	CRO	CAZ	CAZ/AVI	CFM	CTX	FEP	IPM	MEM	ETP	Carba NP Test	RAPIDEC CARBA NP	β-CARBA	MBT STAR-Carba IVD	in-house bla _{KPC} PCR	Xpert Carba-R	NG-Test CARBA 5	RESIST-4 O.K.N.V. K-Set		
-	KPC-2	>256	32	16	4	0.38	4	8	2	8	3	1	+	+	+	+	+	+	+	+	+	
H272Y	KPC-3	>256	>256	48	>256	0.75	12	>32	6	8	3	1	+	+	+	+	+	+	+	+	+	
P104R	KPC-5	>256	>256	>256	>256	0.5	>256	8	2	1	0.25	0.19	+	+	+	+	+	+	+	+	+	
V240G	KPC-6	>256	>256	48	32	0.75	16	>32	4	4	3	1	+	+	+	+	+	+	+	+	+	
L168M	KPC-12	>256	12	6	4	0.38	3	4	1	0.75	0.25	0.125	+	+	+	+	+	+	+	+	+	
D179Y	KPC-33	12	0.75	1	>256	8	6	1.5	1	0.25	0.032	0.008	-	-	-	+	+	+	-	-	-	
H272Y, D179Y	KPC-31	6	0.75	2	>256	12	4	1.5	1	0.25	0.032	0.008	-	-	-	+	+	+	-	-	-	
D92G		>256	64	12	4	0.25	4	4	2	1.5	0.5	0.38	+	+	+	+	+	+	+	+	+	
W105A		>256	32	1	1	0.25	3	1.5	0.75	0.75	0.125	0.094	+	+	+	+	+	+	+	+	+	
W105G		>256	24	1	1	0.25	2	0.75	0.25	1	0.19	0.125	+	+	+	+	+	+	+	+	+	
A120L		>256	32	16	3	0.38	3	6	2	6	1.5	1.5	+	+	+	+	+	+	+	+	+	
G147K		>256	64	32	6	0.38	6	24	6	6	1	0.75	+	+	+	+	+	+	+	+	+	
C238S		>256	2	0.25	2	0.38	1	0.25	0.19	0.25	0.047	0.008	-	-	-	+	+	+	+	+	+	
V240A		>256	>256	64	12	0.38	12	>32	4	8	2	1.5	+	+	+	+	+	+	+	+	+	
<i>E. coli</i> TOP10		6	0.047	0.032	0.012	0.012	0.38	0.064	0.064	0.25	0.032	0.004	-	-	-	-	-	-	-	-	-	

AA, amino acid; AMX, amoxicillin; ATM, aztreonam; CRO, ceftazidime; CAZ, ceftazidime; AVI, avibactam; CFM, cefixime; CTX, cefotaxime; FEP, cefepime; IPM, imipenem; MEM, meropenem; ETP, ertapenem.

^aDark grey, light grey and white cells represent MICs in the resistant, intermediate and susceptible range, respectively. Breakpoints were those of EUCAST: Breakpoint tables for interpretation of MICs and zone diameters Version 9.0, valid from 01/01/2019 (http://www.eucast.org/fileadmin/src/media/PDFs/EUCAST_files/Breakpoint_tables/v_9.0_Breakpoint_Tables.pdf; last accessed September 2019).

^bGrey cells represent negative test results.

helix $\alpha 6$, which is in the vicinity of the active site (Figure S1B). This clash might lead to a switch of this helix that subsequently impacts on the shape of the active site.

Several diagnostic tests based on imipenem hydrolysis (biochemical and MALDI-TOF MS based), lateral flow immunoassays (LFIA) and molecular techniques (PCR) were evaluated with these different mutants. Unlike molecular tests that were able to detect all mutants, biochemical tests based on imipenem hydrolysis [Carba NP test,¹³ RAPIDEC CARBA NP¹³ (bioMérieux) and β -CARBA¹⁴ (Bio-Rad, Marnes la Coquette, France)] and MALDI-TOF MS-based MBT STAR-Carba IVD¹⁵ (Bruker, Illkirch-Graffenstaden, France) were able to distinguish between KPC variants with carbapenem hydrolytic capacities and those lacking any carbapenemase activity (Table 1). Molecular assays, in this case an in-house KPC-specific PCR or a commercially available PCR (Xpert Carba-R; Cepheid, Maurens-Scopont, France), detected all variants accurately. NG-Test CARBA 5 (NG Biotech, Guipry, France) and RESIST-4 O.K.N.V. K-Set (Coris, Gembloux, Belgium) LFIA¹⁶ were also able to detect all KPC variants except KPC-31 and KPC-33.⁴ As the two latter variants lack carbapenemase activity, their non-detection does not lead to false-negative results in terms of true carbapenemase detection. As these two variants lead to avibactam resistance, it would nevertheless be important that they are detected, but not classified as carbapenemases. Whether carbapenems might be used to treat infections with KPC-31 or KPC-33 producers is still debatable, but according to EUCAST guidelines the answer is 'yes', as the MICs of imipenem are in the susceptible range.

Overall, our results demonstrate that KPC variants are not equal, probably selected by different antibiotic usages. This is the case for KPC-5, which leads to high-level cefixime resistance. Some KPC variants can no longer be considered as carbapenemases. This is the case for KPC-31 and KPC-33, which have lost their carbapenemase activity in a similar manner to KPC-14 and KPC-28 variants.⁵ These peculiar variants are challenging to detect, and will require complementary approaches combining molecular assays or LFIA together with carbapenem hydrolysis detection systems.

Funding

This work was supported by the Assistance Publique – Hôpitaux de Paris, by a grant from the Université Paris-Sud (EA 7361) and by grants from the French National Research Agency (ANR-10-LABX-33 and ANR-17-ASTR-0018). All authors are members of LabEx LERMIT.

Transparency declarations

L.D. is co-inventor of the Carba NP test, whose patent has been licensed to bioMérieux (La Balmes les Grottes, France). All other authors: none to declare.

Supplementary data

Figure S1 is available as [Supplementary data](#) at JAC Online.

References

- Eichenberger EM, Thaden JT. Epidemiology and mechanisms of resistance of extensively drug resistant Gram-negative bacteria. *Antibiotics (Basel)* 2019; **8**: E37.
- Yigit H, Queenan AM, Anderson GJ *et al.* Novel carbapenem-hydrolyzing β -lactamase, KPC-1, from a carbapenem-resistant strain of *Klebsiella pneumoniae*. *Antimicrob Agents Chemother* 2001; **45**: 1151–61.
- Peirano G, Bradford PA, Kazmierczak KM *et al.* Importance of clonal complex 258 and IncF_{K2-like} plasmids among a global collection of *Klebsiella pneumoniae* with *bla*_{KPC}. *Antimicrob Agents Chemother* 2017; **61**: e02610-16.
- Naas T, Oueslati S, Bonnin RA *et al.* Beta-Lactamase Database (BLDB) – structure and function. *J Enzyme Inhibit Med Chem* 2017; **32**: 917–9.
- Wolter DJ, Kurpiel PM, Woodford N *et al.* Phenotypic and enzymatic comparative analysis of the novel KPC variant KPC-5 and its evolutionary variants, KPC-2 and KPC-4. *Antimicrob Agents Chemother* 2009; **53**: 557–62.
- Lamoureaux TL, Frase H, Antunes NT *et al.* Antibiotic resistance and substrate profiles of the class A carbapenemase KPC-6. *Antimicrob Agents Chemother* 2012; **56**: 6006–8.
- Oueslati S, Iorga BI, Tlili L *et al.* Unravelling ceftazidime/avibactam resistance of KPC-28, a KPC-2 variant lacking carbapenemase activity. *J Antimicrob Chemother* 2019; **74**: 2239–46.
- Livermore DM, Warner M, Jamrozny D *et al.* *In vitro* selection of ceftazidime-avibactam resistance in Enterobacteriaceae with KPC-3 carbapenemase. *Antimicrob Agents Chemother* 2015; **59**: 5324–30.
- Barnes MD, Winkler ML, Taracila MA *et al.* *Klebsiella pneumoniae* carbapenemase-2 (KPC-2), substitutions at Ambler position Asp179, and resistance to ceftazidime-avibactam: unique antibiotic-resistant phenotypes emerge from β -lactamase protein engineering. *mBio* 2017; **8**: e00528-17.
- Sougakoff W, L'Hermite G, Pernot L *et al.* Structure of the imipenem-hydrolyzing class A β -lactamase SME-1 from *Serratia marcescens*. *Acta Crystallogr D Biol Crystallogr* 2002; **58**: 267–74.
- Smith CA, Nossoni Z, Toth M *et al.* Role of the conserved disulfide bridge in class A carbapenemases. *J Biol Chem* 2016; **291**: 22196–206.
- Petersen EF, Goddard TD, Huang CC *et al.* UCSF Chimera—a visualization system for exploratory research and analysis. *J Comput Chem* 2004; **25**: 1605–12.
- Dortet L, Agathine A, Naas T *et al.* Evaluation of the RAPIDEC[®] CARBA NP, the Rapid CARB Screen[®] and the Carba NP test for biochemical detection of carbapenemase-producing Enterobacteriaceae. *J Antimicrob Chemother* 2015; **70**: 3014–22.
- Bernabeu S, Dortet L, Naas T. Evaluation of the β -CARBA[™] test, a colorimetric test for the rapid detection of carbapenemase activity in Gram-negative bacilli. *J Antimicrob Chemother* 2017; **72**: 1646–58.
- Dortet L, Tandé D, de Briel D *et al.* MALDI-TOF for the rapid detection of carbapenemase-producing Enterobacteriaceae: comparison of the commercialized MBT STAR[®]-Carba IVD Kit with two in-house MALDI-TOF techniques and the RAPIDEC[®] CARBA NP. *J Antimicrob Chemother* 2018; **73**: 2352–9.
- Boutal H, Vogel A, Bernabeu S *et al.* A multiplex lateral flow immunoassay for the rapid identification of NDM-, KPC-, IMP- and VIM-type and OXA-48-like carbapenemase-producing Enterobacteriaceae. *J Antimicrob Chemother* 2018; **73**: 909–15.

C. NDM-1 : Étude des relations structure-activité du site actif par mutagenèse.

Les enzymes de classe B de Ambler, également appelées métallo- β -lactamases (ou MBLs), ont la capacité d'hydrolyser l'ensemble des β -lactamines y compris les carbapénèmes, à l'exception de l'aztréonam. Leur activité enzymatique est dépendante de la présence d'ions Zn^{2+} au niveau du site actif d'où leur nom de métallo-enzymes. Cette propriété implique que ces enzymes sont inhibées en présence de chélateurs d'ions métalliques divalents comme l'EDTA. Elles restent cependant insensibles aux inhibiteurs classiques de β -lactamases disponibles en clinique (acide clavulanique et tazobactam). Les MBLs les plus prévalentes sont de type VIM (Verona imipénèmase), IMP (Imipénèmase) et plus récemment NDM (New Delhi métallo- β -lactamase). NDM-1 a été décrite pour la première fois en Suède, en 2009, chez une souche de *K. pneumoniae* isolée chez un patient rapatrié d'Inde. Depuis, cette carbapénèmase a fait l'objet d'une attention particulière suite à une dissémination mondiale extrêmement rapide chez les entérobactéries.

Une des particularités des MBLs est le faible pourcentage d'homologie de séquence entre les différentes familles (VIM, IMP et NDM), avec parfois moins de 25% d'identité de séquence AA. Cependant, elles partagent toutes une structure secondaire et tertiaire commune, notamment au niveau du site actif de l'enzyme. Le repliement spatial de la protéine aboutit à la formation d'une structure de type $\alpha\beta/\beta\alpha$, dont le site actif se situe au fond d'une large « crevasse », peu profonde et dont l'entrée est délimitée par 5 boucles : L1 et L3, toutes deux impliquées dans la reconnaissance et la spécificité de liaison aux substrats ; L4 et L5 qui stabilisent le site actif et la boucle L2 hydrophobe dont le rôle n'est pas clairement défini. Il existe 2 sites de fixation aux ions Zn^{2+} , respectivement nommés Zn1 et Zn2. Les résidus impliqués dans la fixation du 1^{er} ion de Zinc (Zn1) correspondent à 3 histidines (site 3H). Concernant le site Zn2, les liaisons impliquent un aspartate, une cystéine et un résidu histidine (DCH) en position 120, 221 et 263 (numérotation BBL métallo- β -lactamase). Les connaissances relatives au fonctionnement du site actif de NDM-1 sont encore partielles. Nous avons entrepris d'étudier les spécificités du site actif de cette enzyme pour approfondir les connaissances relatives aux mécanismes de reconnaissance des substrats ; avec pour but ultime le développement de nouveaux d'inhibiteurs utilisables en clinique. Il est à noter qu'il n'existe à l'heure actuelle aucun inhibiteur de MBL utilisable en clinique. Afin de pouvoir étudier en détail les spécificités structurales de NDM, différents mutants ont été générés : (i) par

mutagénèse dirigée, le but a été de vérifier le rôle de certains résidus d'acides aminés préalablement identifiés comme pertinents dans la reconnaissance du substrat pour d'autres MBLs telles que IMP et VIM et (ii) par mutagénèse aléatoire avec pour objectif d'évaluer les possibilités d'extension du spectre d'hydrolyse, et éventuellement de mettre en évidence le rôle de nouveaux résidus n'ayant pas encore été étudiés.

1. Étude de l'impact de substitution par alanine scanning de 10 résidus d'acides aminés dans le site actif de NDM-1

Dans cette étude, nous avons réalisé 10 substitutions d'acides aminés, par une technique de mutagénèse dirigée par « alanine scanning », pour lesquels des travaux antérieurs avaient montré un rôle critique dans le fonctionnement du site actif d'autres MBLs.^{161,388,389} La technique de « l'alanine scanning » consiste à réaliser une substitution systématique d'un résidu par une alanine, permettant d'étudier les fonctions des acides aminés dans une protéine donnée. Elle permet d'éliminer les interactions dues à la chaîne latérale, sans modifier la conformation de la chaîne principale. Elle permet aussi d'éviter l'introduction d'interactions électrostatiques ou stériques. Les boucles L1 et L3 seraient impliquées dans la reconnaissance des substrats. Afin de vérifier cette hypothèse, nous avons réalisé des mutations aux niveaux de ces boucles L1 (M61, G65, V67) et L3 (K224, N233, D236). De plus, 4 mutants possédant une substitution d'AA à proximité des boucles (L4, L5, H196) délimitant le cœur du site actif ont été générés (K121, D199 et F218, S262, Figure1).

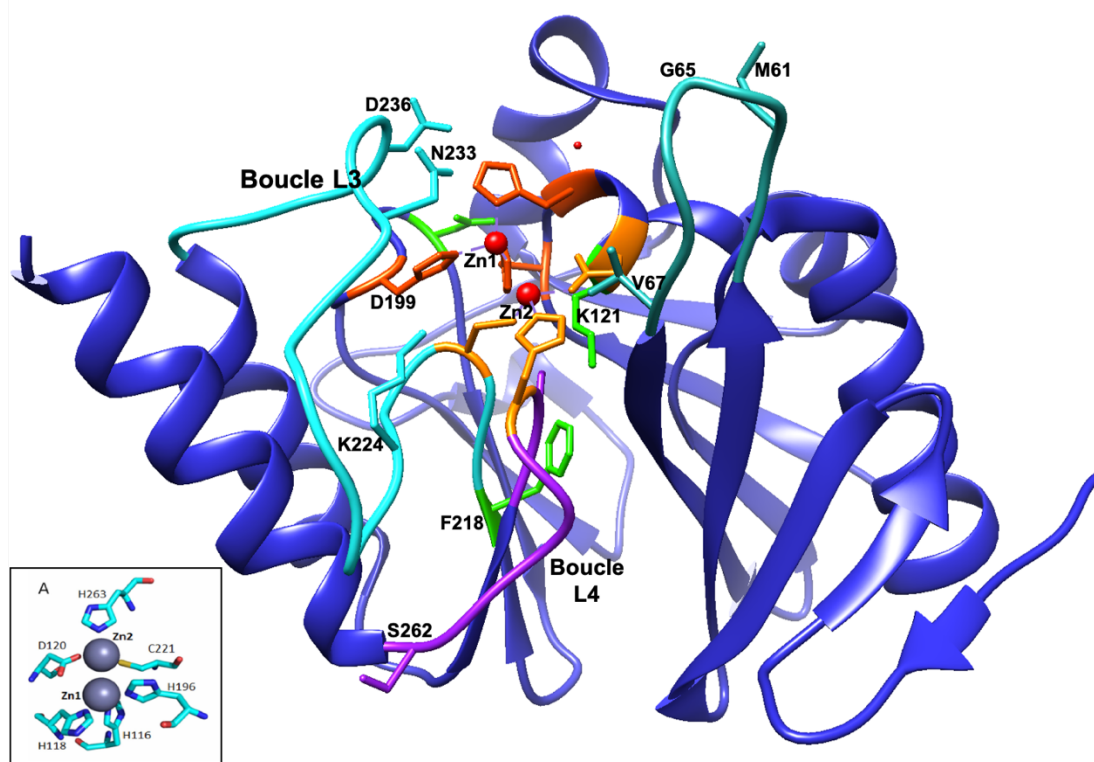


Figure 48 Structure 3D de NDM-1 contenant les positions mutées. Sont indiquées en vert-bleu L1, cyan L3, violet L4, en orange les résidus impliqués dans la coordination des ions zinc, les AA substitués sont représentés sous forme de bâtonnets.

Pour chaque variant, la sensibilité aux β -lactamines (CMI, Tableau 19) et l'activité spécifique (résultats non montrés) ont été comparés aux résultats obtenus avec l'enzyme princeps, NDM-1. Les 3 mutants (M61, G65, V67) générés au niveau de la boucle L1 présentaient tous un phénotype relativement similaire au phénotype sauvage. La même conclusion a été obtenue avec l'étude menée sur VIM.³⁸⁹ Cela nous indique qu'ils ont peu d'impact dans les mécanismes de reconnaissance des substrats liés à la boucle L1. Concernant les 3 mutants au niveau de la boucle L3 (K224, N233, D236), nous avons pu observer que le mutant K224A possédait une augmentation significative de la sensibilité vis-à-vis des carbapénèmes et des céphalosporines de 3^{ème} et 4^{ème} génération, signifiant une perte d'activité de l'enzyme. Le mutant N233A présentait une différence de sensibilité vis-à-vis des céphalosporines (ceftazidime, céfépime et céfoxitine) avec des valeurs de CMI plus basses. Les 4 mutants générés au niveau du site actif (K121, D199, F218 et S262) montraient une diminution drastique des valeurs de CMI pour l'ensemble des β -lactamines, avec une perte totale de l'activité enzymatique pour les mutants S262 et D199. Ces résidus présentent donc un rôle majeur pour l'activité hydrolytique de NDM-1.

Tableau 19 Concentrations minimales inhibitrices obtenues avec les transformants Top10 pTOPO-bla_{NDM-1}.

	N° MBL	CMI (µg/ml)						
		IMP	MEM	ETP	AMX	FEP	CAZ	FOX
<i>E. coli</i> pTopo-bla _{NDM-1}		2	0,75	0,75	32	1,5	>256	>256
	N233A	1	0,75	0,75	32	0,19	32	64
Boucle L3	K224	0,38	0,05	0,01	16	0,25	48	32
	D236A	1	0,75	0,38	32	0,75	>256	128
	G65A	2	0,5	0,5	32	0,5	>256	128
Boucle L1	M61A	2	0,5	0,5	24	0,5	>256	256
	V67A	2	0,5	0,5	24	0,5	>256	128
	D199A	0,25	0,047	0,004	6	0,032	1	2
	F218A	0,25	0,047	0,006	16	0,064	6	16
	K121A	0,25	0,047	0,012	12	0,25	6	8
	S262A	0,25	0,032	0,03	6	0,032	0,5	32
<i>E. coli</i> Top10		0,25	0,032	0,004	6	0,064	0,125	2

IMP : Imipénème, MEM : Méropénème, ETP : Ertapénème, AMX : Amoxicilline, FEP : Céfépime, CAZ : Ceftazidime, FOX : Céfoxitine

En conclusion, ce travail a permis de montrer le rôle essentiel de certains résidus dans les mécanismes de reconnaissance et d'hydrolyse de NDM-1, notamment au niveau de la boucle L3 avec le résidu K224. Ce dernier résultat est en parfait accord avec l'étude menée par Zhang et Hao qui révèle une liaison entre le résidu K224 et le groupement carboxyle de l'ampicilline.^{160,161} Nos résultats montrent également que les 4 résidus D199, F218, K121 et S262, situés à la périphérie du site actif ont un impact majeur sur l'activité enzymatique de NDM-1, comme cela avait été démontré pour IMP.¹⁶² Pour pouvoir étayer d'avantage cette observation, la production et la purification de ces mutants sont envisagées afin de déterminer les constantes enzymatiques. Ainsi, nous pourrions déterminer si ces résidus sont impliqués dans la fixation avec le substrat ou dans l'étape de catalyse.

2. Construction d'une banque de mutants par mutagenèse aléatoire

La création d'une banque de mutants de NDM a été entreprise pour pouvoir identifier de nouveaux résidus favorisant une modification du spectre d'hydrolyse et, de façon plus intéressante, une augmentation de la résistance. Pour cela, une première étape d'optimisation de la technique de mutagenèse aléatoire a été entreprise pour diminuer la fréquence de mutation et favoriser l'obtention de mono- ou bi-mutants. Ainsi, nous avons obtenu environ 600 clones. Actuellement 25 mutants ont été identifiés. Cent clones ne présentaient pas de mutation et le reste des clones obtenus est en cours d'analyse.

Cette expérience a permis d'identifier de nouvelles positions influençant le spectre d'hydrolyse de l'enzyme (Tableau 20). Parmi ces 25 mutants, 3 possédaient un phénotype semblable à celui de NDM-1 (A114E, A257V et E227V/L132M), 21 possédaient une diminution, voire une perte de l'activité vis-à-vis, des carbapénèmes et un possédait une activité carbapénémase plus importante (E152V/A174S). Parmi les mutants ayant perdu toute résistance vis-à-vis des β -lactamines, le mutant L3W est intéressant car cette mutation se trouve dans le peptide signal, indiquant que ce résidu aurait un rôle important dans l'adressage de la β -lactamase au niveau du périplasme. Les mutations conduisant à une diminution de l'activité carbapénémase ont été retrouvées sur les différentes structures fonctionnelles : (i) au niveau des sites 3H et DCH : H189Y, C208S ; (ii) dans la boucle L4 et à proximité S251P, D254E ; (iii) adjacent à la boucle L5 : T119N ; (iv) dans la boucles L2 : W93C et (v) dans la boucle L3 : L221H.

Au cours de l'étude de mutagenèse dirigée, nous avons déjà pu révéler l'importance du résidu S251 (ou S262 en N° MBL). Ce résidu muté chez IMP-1 et IMP-6¹⁶² conduit à une modification des propriétés d'hydrolyse des carbapénèmes. Ce résidu serait impliqué dans la stabilisation des ions zinc. Le résidu T119 est situé juste en amont de H116 qui constitue le site 3H. Tout comme le résidu S251 il pourrait assurer la stabilité du centre métallique de l'enzyme. Le résidu W93, très conservé au sein des MBLs, est localisé sur la boucle L2 impliquée dans la reconnaissance et la spécificité des substrats. Chez IMP, la position a été identifiée comme sans influence quelle que soit la nature de la substitution.³⁸⁸ Chez NDM-1, Chiou *et al.* ont montré que ce résidu participe aux interactions hydrophobes qui stabiliseraient la boucle L1 par rapport au centre métallique.¹⁶¹

Tableau 20 CMI des mutants aléatoires de NDM-1

Mutants N°NDM-1	Position	MICs (µg/ml)					
		IMP	MEM	ETP	CAZ	FOX	AMX
NDM-1	-	2	0,75	0,75	>256	>256	>256
L3W	Peptide signal	0.25	0,032	0.004	2	2	8
F46L	-	0,25	0,032	0,004	6	8	16
P68R	L1	0,25	0,032	0,004	3	8	8
W93C	L2	0,25	0,032	0,004	1,5	6	16
L111M	-	0.25	0,032	0.006	2	4	8
A114E	-	2	0,38	0,5	>256	>256	>256
T119N	Début L5	0.38	0,032	0.125	6	8	16
Q123H	L5	0,25	0,032	0,004	3	6	8
N142T	-	1	0.094	0.125	2	24	>256
N142S	-	0.25	0,032	0,004	3	6	8
W168R	-	0.125	0,032	0.002	32	8	8
P185A	-	0,5	0,25	0,19	4	8	16
H189Y	Site 3H	0.25	0,032	0.004	0,125	2	6
C208S	L3	0,38	0,032	0,006	1,5	8	16
L221H	L3	0,38	0,032	0,006	1,5	8	16
S251P	L4	0,25	0,032	0,004	4	4	8
D254E	L4	0,25	0,032	0,004	64	8	8
A257T	-	0,38	0,032	0,004	4	12	16
A257V	-	2	0,75	0,75	>256	>256	>256
A266T	-	0,38	0,047	0,064	2	4	16
M22T, F183I	-	0.25	0,032	0,004	12	6	16
D95Y*, A141V	L2	0.25	0,032	0,004	0,5	4	6
E152V, A174S	Hα3	3	1,5	0,25	>256	>256	>256
E227V, L132M	-	2	0,75	0,75	>256	>256	>256
A74V/G128S	-	0,25	0,032	0.004	1	8	6
E. coli TOP 10		0,25	0,032	0,004	0,125	2	6

IMP : Imipénème, MEM : Méropénème, ETP : Ertapénème, AMX : Amoxicilline, CAZ : Ceftazidime, FOX : Céfoxitine

L'analyse des séquences des variants naturels (28)¹⁹⁰ a révélé que les mutations obtenues par mutagenèse aléatoire n'avaient pas encore été décrites chez des variants naturels de NDM, à l'exception du résidu E152 retrouvé chez NDM-9 (E152K). Ce variant naturel de NDM-1 présente également une activité carbapénémase légèrement plus élevée par rapport à celle de NDM-1.³⁸⁹

Afin de confirmer les résultats des CMI obtenus pour le mutant E152V/A174S, le gène muté a été cloné dans le vecteur d'expression pET41b, dans le but de le purifier et de déterminer les

constantes enzymatiques de ce nouveau variant de NDM. Ainsi, Les données cinétiques ont été comparées à celles de NDM-1 et NDM-9. Il était intéressant de comparer également ces résultats avec le variant NDM-4 (M154L)³⁹¹ car les résidus M154 et E152 se trouvent tous deux sur l'hélice H α 3 et ces variants, tout comme NDM-9, présentent une meilleure hydrolyse vis-à-vis de l'imipénème.

Ainsi, nous avons montré que le mutant E152V/A174S possédait des valeurs de K_m plutôt similaires à celle de NDM-1, en revanche les valeurs de k_{cat} étaient bien plus élevées, expliquant l'activité catalytique plus importante. Ce mutant possède une efficacité catalytique vis-à-vis des carbapénèmes 2 fois plus grande que celle de NDM-1 et NDM-4. Cependant, cette activité catalytique reste inférieure à celle de NDM-9.

Tableau 21 Paramètres cinétiques du mutant E152V/A174S et de NDM-1 et de ces variants naturels NDM-4 et NDM-9

B-lactams	E152V/ A174S			NDM-1			NDM-4			NDM-9 (E152K)		
	K_m (μM)	K_{cat} (s^{-1})	K_{cat}/K_m ($\text{s}\cdot\mu\text{M}^{-1}$)	K_m (μM)	K_{cat} (s^{-1})	K_{cat}/K_m ($\text{s}\cdot\mu\text{M}^{-1}$)	K_m (μM)	K_{cat} (s^{-1})	K_{cat}/K_m ($\text{s}\cdot\mu\text{M}^{-1}$)	K_m (μM)	K_{cat} (s^{-1})	K_{cat}/K_m ($\text{s}\cdot\mu\text{M}^{-1}$)
Amoxicillin	606	137	0,2	NA	NA	NA	3400	1007	0,3	NA	-	-
Cefalotin	14	28	2	10	4	0,4	46	24	0,5	NA	-	-
Cefoxitin	103	15,6	0,2	49	1	0,02	NA	-	-	90	43	0,19
Cefotaxime	41	42	1	10	6	0,6	18	22	1,2	118	36	0,18
Ceftazidime	155,3	33	0,21	181	5	0,03	72	4	0,06	131	32	0,44
Céfépime	113	22	0,2	77	13	0,2	169	7	0,04	101	57	0,58
Imipeneme	101	48	0,5	94	20	0,2	86	40	0,46	58	118	1,46
Méropeneme	194	72	0,4	49	12	0,25	95	30	0,31	61	191	1,57
Ertapeneme	44	26	0,6	NA	NA	NA	74	6	0,25	NA	NA	NA

Valeurs de NDM-1 issues de Wirth T, et al, valeurs de NDM-4 issues de Nordmann *et al.*, valeurs de NDM-9 de Wang *et al.*

Ces résultats préliminaires nous ont permis d'identifier des résidus impliqués dans le spectre d'hydrolyse de NDM. La caractérisation enzymatique de ces différents mutants, ainsi que des études de modélisation moléculaire, permettront de comprendre si ces résidus interviennent dans (i) la reconnaissance du substrat, dans (ii) le mécanisme d'action de l'enzyme, ou dans (iii) la stabilité du centre métallique. Ces résultats faciliteront le développement des travaux relatifs à la mise au point d'inhibiteurs. De plus, nous avons également produit et caractérisé trois variants naturels de NDM-1 : NDM-4, NDM-7 et NDM-9 présentant tous une hydrolyse des carbapénèmes plus élevée que celle de NDM-1. Ces enzymes permettront de tester le pouvoir inhibiteur de nouveaux composés sur un panel plus exhaustif de carbapénémases de classe B.

Chapitre II. Lutte active contre l'antibiorésistance : Détection des carbapénèmases et développement de nouveaux outils thérapeutiques

A. Développement de tests rapides de détection des carbapénèmases

Un des axes majeurs de la lutte contre la dissémination de la résistance aux antibiotiques réside dans la détection rapide des mécanismes de résistance. Cette détection précoce a pour but (i) d'adapter au plus vite l'antibiothérapie en cas d'infection par une bactérie multi-résistante et (ii) de pouvoir mettre rapidement en place des mesures de contrôle visant à limiter la dissémination de ces germes multi-résistants d'un patient à l'autre (isolement des patients, personnel dédié ...).

En 2012, au début de mes travaux, aucun test de diagnostic rapide (moins de 2 heures) des carbapénèmases n'était commercialisé. Le travail de purification des carbapénèmases les plus répandues a permis de mettre au point, en collaboration avec le CEA, des tests immunochromatographiques capables de détecter et de discriminer en moins de 15 minutes les principales carbapénèmases (KPC, NDM, VIM, IMP et OXA-48-like). En effet, ces protéines purifiées ont été notamment utilisées pour l'immunisation de souris permettant la production d'anticorps monoclonaux dirigés contre ces 5 familles de carbapénèmases. A ce jour, ce test de diagnostic rapide est commercialisé dans plus de 55 pays (y compris les USA) (Articles 6,7 et 8).

Nous avons également contribué à la mise en place d'un kit de diagnostic moléculaire, le test Amplidiag CarbaR VRE, permettant la détection d'un plus grand panel de carbapénèmases incluant notamment les carbapénèmases de *Acinetobacter* (OXA-23, OXA-24/-40, OXA-58 et lorsqu'elle est surexprimée OXA-51, Article 9). Ce test est un système de diagnostic moléculaire basé sur la technique de la PCR en temps réel utilisant des amorces multiplexes. Lors de cette études, nous avons évalué sa capacité à détecter un grand nombre de gènes codant pour des carbapénèmases présents chez 100 bacilles à Gram Négatif bien caractérisés et dans 200 isolats d'entérobactéries issus du Centre National de Référence pour la résistance aux carbapénèmes. Nos résultats ont montré que ce test présentait une très bonne sensibilité (100%) ainsi qu'une très bonne spécificité (99%).

Enfin, nous avons participé à une étude multicentrique, impliquant quatre laboratoires européens de référence, visant à expertiser un nouveau type de test de diagnostic, le BYG Carba v2.0 (Article 10). Il s'agit d'un test électrochimique en temps réel hautement simplifié et précis, permettant de détecter les EPCs en moins de 30 min. Cette nouvelle procédure réduit le temps de manipulation de 5 à 1 minute et ne nécessite qu'une quantité limitée de matériel (une à trois colonies), empêchant ainsi la nécessité de sous-cultiver des isolats bactériens pour atteindre une plus grande quantité de biomasse pure. L'étude a montré que pour les 1181 isolats, testés dans les quatre centres, le BYG Carba v2.0 a produit une sensibilité et une spécificité globales de 96,3% et de 99,7% respectivement. Concernant le délai avant la positivité, 85% des EPCs détectés étaient positifs dans les dix minutes.



Development and Validation of a Lateral Flow Immunoassay for Rapid Detection of NDM-Producing *Enterobacteriaceae*

Hervé Boutal,^a Thierry Naas,^{b,c} Karine Devilliers,^a Saoussen Oueslati,^b

Laurent Dortet,^{b,c} Sandrine Bernabeu,^b Stéphanie Simon,^b Hervé Volland^b

Service de Pharmacologie et Immunoanalyse, CEA, INRA, Université Paris-Saclay, Gif-sur-Yvette, France^a; EA7361, Université Paris-Sud, Université Paris-Saclay, LabEx Lermite, Bacteriology-Hygiene Unit, APHP, Hôpital Bicêtre, Le Kremlin-Bicêtre, France^b; Associated French National Reference Center for Antibiotic Resistance: Carbapenemase-Producing Enterobacteriaceae, Le Kremlin-Bicêtre, France^c

ABSTRACT The global spread of carbapenemase-producing *Enterobacteriaceae* (CPE) that are often resistant to most, if not all, classes of antibiotics is a major public health concern. The NDM-1 carbapenemase is among the most worrisome carbapenemases given its rapid worldwide spread. We have developed and evaluated a lateral flow immunoassay (LFIA) (called the NDM LFIA) for the rapid and reliable detection of NDM-like carbapenemase-producing *Enterobacteriaceae* from culture colonies. We evaluated the NDM LFIA using 175 reference enterobacterial isolates with characterized β -lactamase gene content and 74 nonduplicate consecutive carbapenem-resistant clinical isolates referred for expertise to the French National Reference Center (NRC) for Antibiotic Resistance during a 1-week period (in June 2016). The reference collection included 55 non-carbapenemase producers and 120 carbapenemase producers, including 27 NDM producers. All 27 NDM-like carbapenemase producers of the reference collection were correctly detected in less than 15 min by the NDM LFIA, including 22 strains producing NDM-1, 2 producing NDM-4, 1 producing NDM-5, 1 producing NDM-7, and 1 producing NDM-9. All non-NDM-1 producers gave a negative result with the NDM LFIA. No cross-reaction was observed with carbapenemases (VIM, IMP, NDM, KPC, and OXA-48-like), extended-spectrum β -lactamases (ESBLs) (TEM, SHV, and CTX-M), AmpCs (CMY-2, DHA-2, and ACC-1), and oxacillinases (OXA-1, -2, -9, and -10). Similarly, among the 74 referred nonduplicate consecutive clinical isolates, all 7 NDM-like producers were identified. Overall, the sensitivity and specificity of the assay were 100% for NDM-like carbapenemase detection with strains cultured on agar. The NDM LFIA was efficient, rapid, and easy to implement in the routine workflow of a clinical microbiology laboratory for the confirmation of NDM-like carbapenemase-producing *Enterobacteriaceae*.

KEYWORDS NDM-1, lateral flow immunoassay, detection

Enterobacteriaceae have a major role as causes of nosocomial infections (and, for *Escherichia coli*, also of community-acquired infections), and expanded-spectrum cephalosporins and carbapenems are essential in the treatment of these infections (1). The dissemination of broad-spectrum β -lactamases (extended-spectrum β -lactamases [ESBLs] and carbapenemases) among *Enterobacteriaceae* is undoubtedly a matter of great public health concern. Indeed, ESBL-producing *Enterobacteriaceae* are resistant to all β -lactams up to third-generation cephalosporins (2), and this leads to the use of last-resort antibiotics such as carbapenems. Unfortunately, the emergence of carbapenemase-producing *Enterobacteriaceae* (CPE), which are often resistant to several antibiotic classes, has become a major issue, as they are often involved in nosocomial or community-acquired infections (3).

Received 14 February 2017 Returned for modification 20 March 2017 Accepted 3 April 2017

Accepted manuscript posted online 12 April 2017

Citation Boutal H, Naas T, Devilliers K, Oueslati S, Dortet L, Bernabeu S, Simon S, Volland H. 2017. Development and validation of a lateral flow immunoassay for rapid detection of NDM-producing *Enterobacteriaceae*. *J Clin Microbiol* 55:2018–2029. <https://doi.org/10.1128/JCM.00248-17>.

Editor Yi-Wei Tang, Memorial Sloan Kettering Cancer Center

Copyright © 2017 Boutal et al. This is an open-access article distributed under the terms of the [Creative Commons Attribution 4.0 International license](https://creativecommons.org/licenses/by/4.0/).

Address correspondence to Hervé Volland, herv.volland@cea.fr.

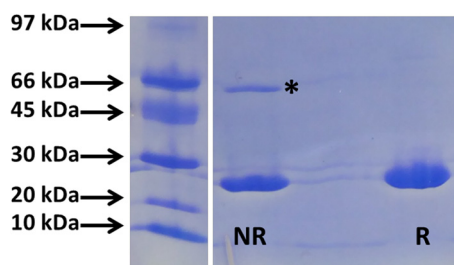


FIG 1 SDS-PAGE (Pharmacia Phast system) with purified recombinant NDM-1 (2 mg/ml) and Coomassie blue staining. NR, nonreducing conditions; R, reducing conditions. * indicates dimers.

Of the carbapenemases most commonly encountered (4), the metallo- β -lactamase (MBL) NDM-1 (Ambler class B) (5) shows the most tremendous spread (3, 6). Moreover, the *bla*_{NDM-1} gene is located on plasmids that encode other resistance determinants, conferring a broad drug resistance pattern (7). Initially isolated in India, it is now endemic in the entire Indian subcontinent and represents a major threat considering the high rate of acquisition (72.4%) of multiresistant *Enterobacteriaceae* (MRE), including NDM-1-expressing strains, while traveling in this area (8). Thus, the rapid and reliable detection of NDM-1-producing bacteria is essential to identify infected or colonized patients in order to prevent further spread and to provide proper treatments.

Tests to detect carbapenemases have already been developed. Some are based on the detection of carbapenem hydrolysis using matrix-assisted laser desorption ionization–time of flight mass spectrometry (MALDI-TOF MS) (9, 10). Others are biochemical tests (e.g., Carba NP test and derivatives [11, 12] and the carbapenem inactivation method [CIM] [13]) or phenotypic tests like the OXA-48 disk test (14, 15) and various phenotypic confirmation tests, including tests of inhibition of carbapenemase activity (15, 16). Some of these tests have proven useful albeit with turnaround times of 2 to 24 h (14, 15). These tests may be used on colonies, and some have been evaluated directly on blood cultures (17). Recently, a lateral flow immunoassay (LFIA) for the detection of OXA-48-type carbapenemases has been evaluated (18). This test yields results from cultured strains within 15 min, with 100% specificity and sensitivity. Finally, molecular methods, such as endpoint PCR and real-time PCR, can also be used in single or multiplex formats targeting the main carbapenemases, with high specificity and sensitivity (19–21). However, these methods are expensive and require a high level of expertise to obtain accurate results.

To respond to the needs optimally, antimicrobial drug resistance detection methods must be cheap (reduced costs of consumables and equipment) and easy to use (reduced technical complexity) for the end user. This led us to develop an LFIA for the detection of NDM-like carbapenemases that presents several advantages: robust technology, easily transferable in a commercialized version, stable for more than 24 months without refrigeration, user-friendly (no requirement for trained staff), high performance (sensitive and specific), low cost (around 6€ per test [22, 23], compared to more than 20€ for molecular tests), and detection results in less than 30 min without the need for highly technical equipment for the readout. We have validated this assay on 175 agar-cultured enterobacterial isolates (27 expressing NDM-like enzymes), with test results in less than 15 min, 100% sensitivity, and 100% specificity.

RESULTS

Combinatorial test and best-pair selection. Eighty milligrams of recombinant NDM was produced from 1 liter of culture. SDS-PAGE (Fig. 1) under nonreducing conditions showed a major band corresponding to the theoretical molecular mass of 26 kDa and another one close to 66 kDa. NDM-1 can exist as a monomer and dimer in solution (24), and only a band corresponding to monomers is observed under reducing conditions. The presence of dimers was also confirmed by trypsin digestion and MALDI-TOF analysis. This protein was then used to immunize mice. Twenty-two mono-

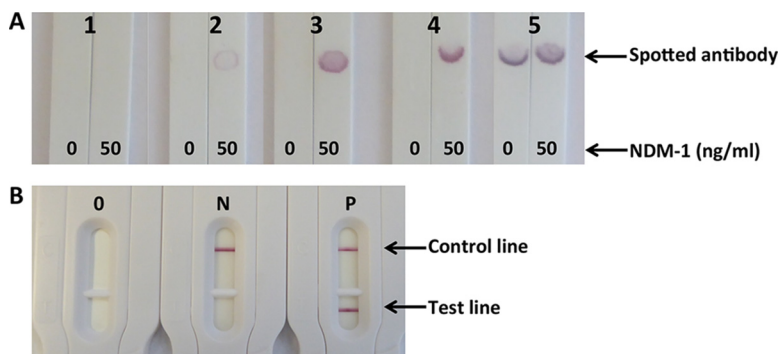


FIG 2 (A) Pair selection with handmade strips. Shown are signals obtained with 0 and 50 ng/ml of recombinant NDM-1 as a function of the pair performance. 1, no specific signal; 2, low specific signal; 3, medium specific signal; 4, high specific signal (U shape); 5, high specific and nonspecific signals. (B) Manufactured cassettes. O, cassette before use; N, negative result; P, positive result.

clonal antibodies (MAbs) were finally selected (named NDM 101 to NDM 122). A total of 484 pairs were tested during the combinatorial study done with spotted strips. The 3 pairs of antibodies displaying the strongest specific signal with a specific U-shaped signal (Fig. 2A) revealing a high-affinity capture antibody (25) and no nonspecific signals were further selected (NDM 105/NDM 103, NDM 105/NDM 106, and NDM 105/NDM 120). In order to decide between these three pairs, they were further tested with serial dilutions of NDM-expressing strains. The NDM 105/NDM 103 pair, showing the lowest limit of detection, was selected, and a batch of 1,000 tests (strip plus cassette) was produced (NG Biotech) in order to carry out assay validation (sensitivity and specificity) (Fig. 2B).

Limit of detection using the NDM LFIA. Although a positive line test was visible (by the naked eye) at 208 pg/ml (equivalent to 5×10^6 CFU/ml), it does not appear on the picture due to the camera sensitivity. Thus, limits of detection (LOD) of the NDM LFIA of between 208 and 617 pg/ml and around 5×10^6 CFU/ml were determined by eye after 15 min of migration using purified recombinant NDM protein or one NDM-1-producing *Klebsiella pneumoniae* strain (Fig. 3).

Performance of the NDM LFIA with reference isolates. As shown in Table 1, the NDM LFIA was able to detect all 27 reference strains expressing NDM-like enzymes (22 expressing NDM-1, 2 expressing NDM-4, 1 expressing NDM-5, 1 expressing NDM-7, and 1 expressing NDM-9). All the strains that did not produce an NDM carbapenemase gave negative results. This corresponded to 30 strains expressing class A carbapenemases (22 expressing KPC, 3 expressing IMI, 1 expressing NMC-A, 1 expressing SME, 1 expressing GES, and 1 expressing FRI-1), 28 strains expressing class B carbapenemases (17 expressing VIM, 11 expressing IMP, and 1 expressing GIM), 40 strains expressing class D carbap-

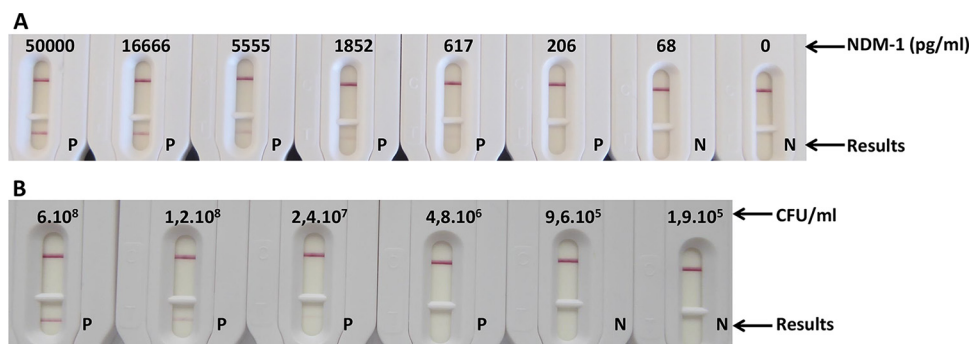


FIG 3 Limit of detection in extraction buffer. (A) Serial dilutions with recombinant NDM-1 (nanograms per milliliter). (B) Serial dilution with NDM-1-expressing *Klebsiella pneumoniae* (CFU per milliliter). P, positive result; N, negative result.

TABLE 1 Results of the NDM LFIA and the Carba NP test in a collection of strains comprising carbapenemase and non-carbapenemase producers

β -Lactam resistance mechanism	Bacterial species	No. of isolates	β -Lactamase content (PCR) ^b	Result ^a	
				NDM LFIA	Carba NP test
Ambler class B carbapenemases					
NDM type	<i>E. coli</i>	1	NDM-1 + OXA-1 + OXA-10 + CMY-16 + TEM-1	P	P
	<i>E. coli</i>	1	NDM-1 + OXA-1 + TEM-1	P	P
	<i>E. coli</i>	1	NDM-1 + CTX-M-15 + TEM-1	P	P
	<i>E. coli</i>	1	NDM-1 + OXA-1 + OXA-2 + CTX-M-15 + TEM-1	P	P
	<i>E. coli</i>	1	NDM-1 + CTX-M-15 + TEM-1	P	P
	<i>E. coli</i>	1	NDM-4 + CTX-M-15 + OXA-1	P	P
	<i>E. coli</i>	1	NDM-4 + CTX-M-15 + CMY-6	P	P
	<i>E. coli</i>	1	NDM-5 + TEM-1 + CTX-M-15	P	P
	<i>E. coli</i>	1	NDM-6 + CTX-M-15 + OXA-1	P	P
	<i>E. coli</i>	1	NDM-7 + CTX-M-15	P	P
	<i>K. pneumoniae</i>	1	NDM-1 + CTX-M-15 + SHV-11 + OXA-1	P	P
	<i>K. pneumoniae</i>	1	NDM-1 + CTX-M-15 + CMY-4 + OXA-1	P	P
	<i>K. pneumoniae</i>	1	NDM-1 + CTX-M-15 + OXA-1 + OXA-9 + TEM-1 + SHV-28 + SHV-11	P	P
	<i>K. pneumoniae</i>	1	NDM-1 + OXA-1 + SHV-11	P	P
	<i>K. pneumoniae</i>	1	NDM-1 + OXA-1 + CTX-M-15 + TEM-1 + SHV-28 + OXA-9 + CMY-6	P	P
	<i>K. pneumoniae</i>	1	NDM-1 + TEM-1 + CTX-M-15 + SHV-12 + OXA-9	P	P
	<i>K. pneumoniae</i>	1	NDM-1 + TEM-1 + CTX-M-15 + SHV-12 + OXA-9	P	P
	<i>K. pneumoniae</i>	1	NDM-1 + TEM-1 + CTX-M-15 + SHV-11 + OXA-1	P	P
	<i>P. stuartii</i>	1	NDM-1 + OXA-1 + CMY-6 + TEM-1	P	P
	<i>P. rettgeri</i>	1	NDM-1 + CTXM-15	P	P
	<i>Salmonella enterica</i>	1	NDM-1 + CTX-M-15 + TEM-1 + OXA-1 + OXA-9 + OXA-10	P	P
VIM type	<i>E. coli</i>	1	VIM-1	N	P
	<i>E. coli</i>	1	VIM-1 + CMY-13	N	P
	<i>E. coli</i>	1	VIM-4	N	P
	<i>K. pneumoniae</i>	3	VIM-1	N	P
	<i>K. pneumoniae</i>	4	VIM-1 + SHV-5	N	P
	<i>K. pneumoniae</i>	1	VIM-1 + SHV-12	N	P
	<i>K. pneumoniae</i>	1	VIM-1 + TEM-1 + SHV-5	N	P
	<i>K. pneumoniae</i>	1	VIM-19 + CTX-M-3 + TEM-1 + SHV-1	N	P
	<i>Enterobacter cloacae</i>	1	VIM-1 + SHV-70	N	P
	<i>E. cloacae</i>	1	VIM-4 + TEM-1 + SHV-31	N	P
	<i>Citrobacter freundii</i>	1	VIM-2 + TEM-1 +	N	P
	<i>C. freundii</i>	1	VIM-2 + TEM-1 + OXA-9 + OXA-10	N	P
IMP type	<i>E. coli</i>	1	IMP-1	N	P
	<i>E. coli</i>	1	IMP-8 + SHV-12	N	P
	<i>K. pneumoniae</i>	1	IMP-1	N	P
	<i>K. pneumoniae</i>	1	IMP-1 + TEM-15	N	P
	<i>K. pneumoniae</i>	1	IMP-1 + TEM-15	N	P
	<i>K. pneumoniae</i>	1	IMP-1 + SHV-5	N	P
	<i>K. pneumoniae</i>	1	IMP-8	N	P
	<i>K. pneumoniae</i>	1	IMP-8 + SHV-12	N	P
	<i>E. cloacae</i>	1	IMP-8	N	P
	<i>E. cloacae</i>	1	IMP-8 + SHV-12	N	P
	<i>Serratia marcescens</i>	1	IMP-11	N	P
GIM type	<i>E. cloacae</i>	1	GIM-1	N	P
Ambler class A carbapenemases					
KPC-2	<i>E. coli</i>	1	KPC-2	N	P
	<i>E. coli</i>	1	KPC-2 + CTXM-15	N	P
	<i>E. coli</i>	1	KPC-2 + TEM-1 + OXA-9	N	P
	<i>E. coli</i>	1	KPC-2 + CTX-M-9 + TEM-1	N	P
	<i>K. pneumoniae</i>	1	KPC-2 + SHV-11 + TEM-1 + CTX-M-2	N	P

(Continued on next page)

Downloaded from <http://jcm.asm.org/> on September 19, 2019 by guest

TABLE 1 (Continued)

β -Lactam resistance mechanism	Bacterial species	No. of isolates	β -Lactamase content (PCR) ^b	Result ^a	
				NDM LFIA	Carba NP test
	<i>K. pneumoniae</i>	1	KPC-2 + SHV-11 + TEM-1 + CTX-M-2 + OXA-9	N	P
	<i>K. pneumoniae</i>	1	KPC-2 + SHV-11	N	P
	<i>K. pneumoniae</i>	1	KPC-2 + TEM-1 + SHV-1 + CTX-M-15	N	P
	<i>K. pneumoniae</i>	1	KPC-2 + SHV-11 + TEM-1 + SHV-12 + OXA-9	N	P
	<i>K. pneumoniae</i>	1	KPC-2 + SHV-11	N	P
	<i>K. pneumoniae</i>	1	KPC-2 + SHV-11 + TEM-1	N	P
	<i>E. cloacae</i>	1	KPC-2	N	P
	<i>E. cloacae</i>	1	KPC-2 + TEM-1	N	P
	<i>E. cloacae</i>	1	KPC-2 + TEM-1 + OXA-1 + CTX-M-15	N	P
	<i>E. cloacae</i>	1	KPC-2 + TEM-1 + SHV-11	N	P
	<i>E. cloacae</i>	1	KPC-2 + TEM-3	N	P
	<i>C. freundii</i>	1	KPC-2 + TEM-1	N	P
	<i>S. marcescens</i>	1	KPC-2 + TEM-1 + SHV-12	N	P
	<i>S. marcescens</i>	1	KPC-2 + TEM-1	N	P
KPC-3	<i>K. pneumoniae</i>	1	KPC-3 + TEM-1 + SHV-1 + OXA-9	N	P
	<i>K. pneumoniae</i>	1	KPC-3 + SHV-11 + OXA-9 + TEM-1	N	P
	<i>Klebsiella ozaenae</i>	1	KPC-3 + OXA-9 + TEM-1	N	P
IMI type	<i>E. cloacae</i>	1	IMI-1	N	P
	<i>Enterobacter asburiae</i>	1	IMI-2	N	P
	<i>E. asburiae</i>	1	IMI-2	N	N
NmcA	<i>E. cloacae</i>	1	NmcA	N	P
Sme type	<i>S. marcescens</i>	1	Sme-1	N	P
	<i>S. marcescens</i>	1	Sme-2	N	P
GES type	<i>E. cloacae</i>	1	GES-5	N	N
FRI	<i>E. cloacae</i>	1	FRI-1	N	P
Ambler class D carbapenemases					
OXA-48	<i>E. coli</i>	4	OXA-48 + CTX-M-15	N	P
	<i>E. coli</i>	1	OXA-48 + CTX-M-24 + TEM-1	N	P
	<i>E. coli</i>	1	OXA-48 + TEM-1 + CTX-M-1	N	P
	<i>K. pneumoniae</i>	4	OXA-48	N	P
	<i>K. pneumoniae</i>	1	OXA-48 + CTX-M-15	N	P
	<i>K. pneumoniae</i>	1	OXA-48 + TEM-1	N	P
	<i>K. pneumoniae</i>	1	OXA-48 + SHV-11	N	P
	<i>K. pneumoniae</i>	2	OXA-48 + CTX-M-15 + TEM-1	N	P
	<i>E. cloacae</i>	2	OXA-48 + TEM-1 + CTX-M-15 + OXA-1	N	P
	<i>E. cloacae</i>	1	OXA-48 + SHV-5	N	P
	<i>Citrobacter koseri</i>	1	OXA-48	N	P
	<i>C. koseri</i>	1	OXA-48 + TEM-1	N	P
	<i>C. freundii</i>	1	OXA-48 + SHV-12 + TEM-1	N	P
OXA-162	<i>K. pneumoniae</i>	1	OXA-162 + TEM-1 + SHV-11 + CTX-M-15	N	P
OXA-181	<i>E. coli</i>	1	OXA-181	N	P
	<i>E. coli</i>	1	OXA-181	N	P
	<i>K. pneumoniae</i>	1	OXA-181 + SHV-11 + TEM-1 + CTX-M-15 + NDM-1 + OXA-1	P	P
	<i>K. pneumoniae</i>	1	OXA-181 + SHV-27 + CTX-M-15 + TEM-1 + NDM-1 + OXA-1	P	P
	<i>K. pneumoniae</i>	1	OXA-181 + SHV-11 + CTX-M-15 + NDM-1 + OXA-1	P	P
	<i>K. pneumoniae</i>	1	OXA-181 + SHV-11 + TEM-1 + CTX-M-15 + NDM-1 + OXA-9	P	P
	<i>K. pneumoniae</i>	1	OXA-181 + SHV-11 + CTX-M-15 + OXA-1	N	P
	<i>K. pneumoniae</i>	1	OXA-181 + NDM-1 + SHV-2 + CTX-M-15 + OXA-1	P	P
	<i>C. freundii</i>	1	OXA-181 + NDM-1 + OXA-1 + OXA-9 + OXA-10 + CTX-M-15 + TEM-1	P	P
OXA-204	<i>K. pneumoniae</i>	1	OXA-204 + CMY-4	N	P
	<i>E. coli</i>	1	OXA-204 + CMY-2 + CTX-M-15 + OXA-1	N	P
	<i>E. coli</i>	1	OXA-204 + CMY-4 + CTX-M-15 + OXA-1	N	P
	<i>E. coli</i>	1	OXA-204 + CMY-4 + CTX-M-15	N	P
	<i>K. pneumoniae</i>	1	OXA-204 + SHV-28 + TEM-1 + CTX-M-15	N	P

(Continued on next page)

TABLE 1 (Continued)

β -Lactam resistance mechanism	Bacterial species	No. of isolates	β -Lactamase content (PCR) ^b	Result ^a		
				NDM LFIA	Carba NP test	
OXA-232	<i>E. coli</i>	1	OXA-232 + CTX-M-15 + OXA-1	N	P	
	<i>K. pneumoniae</i>	1	OXA-232 + SHV-1 + TEM-1 + CTX-M-15 + OXA-1	N	P	
OXA-244	<i>E. coli</i>	1	OXA-244 + TEM-1 + CMY-2	N	E	
	<i>E. coli</i>	1	OXA-244 + TEM-1 + CMY-2	N	N	
Non-carbapenemase producers						
Wild type	<i>K. pneumoniae</i>	1	SHV-11	N	N	
Acquired cephalosporinase	<i>E. coli</i>	1	DHA-1	N	N	
	<i>E. coli</i>	1	ACC-1	N	N	
	<i>K. pneumoniae</i>	1	DHA-2	N	N	
	<i>Proteus mirabilis</i>	1	ACC-1	N	N	
	<i>E. coli</i>	1	CTX-M-1	N	N	
ESBL	<i>E. coli</i>	1	CTX-M-3	N	N	
	<i>K. pneumoniae</i>	1	CTX-M-3	N	N	
	<i>E. coli</i>	2	CTX-M-14	N	N	
	<i>K. pneumoniae</i>	1	CTX-M-14	N	N	
	<i>E. coli</i>	2	CTX-M-15	N	N	
	<i>K. pneumoniae</i>	3	CTX-M-15	N	N	
	<i>E. cloacae</i>	1	CTX-M-15	N	N	
	<i>E. cloacae</i>	1	VEB-1	N	N	
	Cephalosporinase + impermeability	<i>E. coli</i>	1	⚡⚡⚡ cephalosporinase	N	N
		<i>E. cloacae</i>	13	⚡⚡⚡ cephalosporinase	N	N
<i>E. cloacae</i>		1	⚡⚡⚡ cephalosporinase + CTX-M-15	N	N	
<i>Enterobacter aerogenes</i>		1	⚡⚡⚡ cephalosporinase	N	N	
<i>Morganella morganii</i>		1	⚡⚡⚡ cephalosporinase	N	N	
ESBL + impermeability	<i>E. coli</i>	1	CTX-M-15	N	N	
	<i>K. pneumoniae</i>	1	CTX-M-15 + SHV-1	N	N	
	<i>K. pneumoniae</i>	2	CTX-M-15 + TEM-1 + SHV-1	N	N	
	<i>K. pneumoniae</i>	1	CTX-M-15 + SHV-11	N	N	
	<i>K. pneumoniae</i>	1	CTX-M-15 + SHV-28 - TEM-1	N	N	
	<i>K. pneumoniae</i>	1	TEM-1 + SHV-28	N	N	
	<i>K. pneumoniae</i>	4	CTX-M-15 + TEM-1 + SHV-11	N	N	
	<i>K. pneumoniae</i>	1	CTX-M-15 + TEM-1 + SHV-12	N	N	
	<i>K. pneumoniae</i>	1	CTX-M-15 + TEM-1 + SHV-1 + OXA-1	N	N	
ESBL + cephalosporinase + impermeability	<i>E. cloacae</i>	3	⚡⚡⚡ case + CTX-M-15	N	N	
	<i>C. freundii</i>	1	⚡⚡⚡ case + TEM-3	N	N	
Extended-spectrum oxacillinases	<i>K. pneumoniae</i>	1	OXA-163	N	N	
	<i>E. cloacae</i>	1	OXA-163	N	N	
	<i>S. marcescens</i>	1	OXA-405	N	N	

^aP indicates a positive result, N indicates a negative result, and E indicates an equivocal result.

^b⚡⚡⚡ indicates a hyperproduced cephalosporinase.

enemases (21 expressing OXA-48, 1 expressing OXA-162, 9 expressing OXA-181, 5 expressing OXA-204, 2 expressing OXA-232, and 2 expressing OXA-244), and 55 non-carbapenemase producers (Table 1). Our results perfectly correlated with the β -lactamase genotype of the strains as determined by PCR analysis. Positive results showed a dark pink band (Fig. 4A) in most cases, except for *Providencia rettgeri* and *Providencia stuartii*. These two strains were detected, but the corresponding tests showed signals with a much lower intensity (Fig. 4A). This validation experiment showed that our test was able to detect NDM-producing bacteria with 100% sensitivity and 100% specificity (i.e., without any false-negative or false-positive results).

Effects of growth media on LFIA results. Ten strains (6 NDM producers and 4 non-NDM producers) from the reference collection were grown on 7 of the most common media used for bacteria growth (Table 2). Some media currently used for the identification and/or selection of carbapenemase-expressing strains generate colonies with genus-specific colors (blue, green, pink, or dark purple on Uri-4 plates, for

Downloaded from <http://jcm.asm.org/> on September 19, 2019 by guest

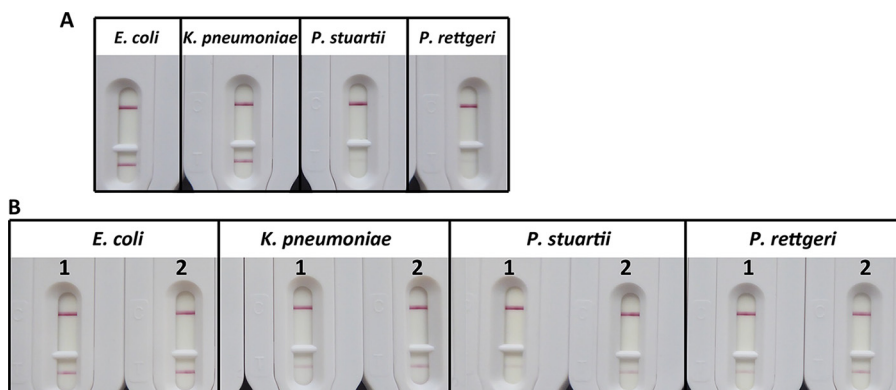


FIG 4 (A) Results obtained with different strains (colonies of equal sizes were tested). 1, NDM-4-expressing *Escherichia coli*; 2, NDM-1-expressing *Klebsiella pneumoniae*; 3, NDM-1-expressing *Providencia stuartii*; 4, NDM-1-expressing *Providencia rettgeri*. (B) Extraction buffer performance. For *Escherichia coli* and *Klebsiella pneumoniae*, 1 was colony suspended in 1 ml. For *Providencia stuartii* and *Providencia rettgeri*, 10 colonies were suspended in 300 μ l. The suspension was separated in two parts. 1, extraction buffer only; 2, extraction buffer plus 5 freeze-thaw cycles and 1 min of sonication (14 W).

example). These colored colonies, suspended in extraction buffer, stained the latter in a similar manner. This staining did not interfere with the test results, since the 6 NDM producers gave positive results and the 4 non-NDM producers gave negative results, whatever the medium used for culture. Thus, colony staining did not modify the appearance of the nitrocellulose membrane and still yielded easily interpretable results (data not shown).

Prospective evaluation of the NDM LFIA. Using PCR and Carba NP tests, a carbapenemase was detected in 44% (33/74) of the isolates. Subsequent sequencing of the positive PCR products allowed the identification of the variants of a given carbapenemase (Table 3). Concerning the 41 non-carbapenemase-producing isolates, the decreased carbapenem susceptibility might result from ESBL and/or cephalosporinase production associated with reduced outer membrane permeability (not evaluated).

The test was able to detect all isolates producing an NDM carbapenemase (7 isolates corresponding to 2 NDM-1 and 5 NDM-5 producers). All isolates that did not produce an NDM-like carbapenemase gave negative results. These isolates included 26 carbapenemase producers (23 expressing OXA-48-like enzymes, 2 expressing KPC-like enzymes, and 1 expressing a VIM-like enzyme) and the 41 non-carbapenemase-producing *Enterobacteriaceae* (Table 3).

TABLE 2 Results of the NDM LFIA with strains grown on different agar media

Bacterial species	No. of isolates	β -Lactamase content (PCR)	Result with culture medium ^a						
			MH	TSA	COH	Uri-4	DRIG	ChromID ESBL	Carba Smart
<i>E. coli</i>	1	NDM-1 + OXA-1 + OXA-2 + CTX-M-15 + TEM-1	P	P	P	P	P	P	P
<i>E. coli</i>	1	NDM-1 + CTX-M-15 + TEM-1	P	P	P	P	P	P	P
<i>K. pneumoniae</i>	1	NDM-1 + CTX-M-15 + SHV-11 + OXA-1	P	P	P	P	P	P	P
<i>K. pneumoniae</i>	1	NDM-1 + CTX-M-15 + CMY-4 + OXA-1	P	P	P	P	P	P	P
<i>K. pneumoniae</i>	1	NDM-1 + CTX-M-15 + OXA-1 + OXA-9 + TEM-1 + SHV-28 + SHV-11	P	P	P	P	P	P	P
<i>Salmonella enterica</i>	1	NDM-1 + CTX-M-15 + TEM-1 + OXA-1 + OXA-9 + OXA-10	P	P	P	P	P	P	P
<i>E. coli</i>	1	VIM-1 + CMY-13	N	N	N	N	N	N	N
<i>K. pneumoniae</i>	1	VIM-1	N	N	N	N	N	N	N
<i>E. cloacae</i>	1	VIM-4 + TEM-1 + SHV-31	N	N	N	N	N	N	N
<i>S. marcescens</i>	1	IMP-11	N	N	N	N	N	N	N

^aMH, Mueller-Hinton agar; TSA, Trypticase soya agar; COH, Columbia agar plus 5% horse blood; DRIG, Drigalski agar; Uri-4, URISelect 4 medium; Carba Smart, ChromID Carba Smart; P, positive result; N, negative result.

TABLE 3 Results of a prospective study of the NDM LFIA in comparison with PCR and the Carba NP test in enterobacterial isolates with reduced susceptibility referred to the French NRC

β -Lactam resistance mechanism	Bacterial species	No. of isolates	β -Lactamase content (PCR)	Result ^a	
				NDM LFIA	CarbaNP test
Carbapenemases producers					
NDM type	<i>E. coli</i>	1	NDM-like	P	P
	<i>K. pneumoniae</i>	1	NDM-like	P	P
	<i>E. cloacae</i>	1	NDM-like	P	P
OXA-48-like	<i>E. coli</i>	8	OXA-48-like	N	P
	<i>E. coli</i>	1	NDM-like + OXA-48-like	P	P
	<i>K. pneumoniae</i>	5	OXA-48-like	N	P
	<i>E. cloacae</i>	1	OXA-48-like	N	P
KPC	<i>K. pneumoniae</i>	2	KPC-like	N	P
VIM	<i>E. cloacae</i>	1	VIM-like	N	P
Non-carbapenemase producers					
	<i>E. coli</i>	2		N	N
	<i>K. pneumoniae</i>	8		N	N
	<i>E. cloacae</i>	7		N	N
	<i>Klebsiella oxytoca</i>	1		N	N
	<i>Hafnia alvei</i>	1		N	N
	<i>S. marcescens</i>	1		N	N
	<i>C. freundii</i>	1		N	N

^aP indicates a positive result, and N indicates a negative result.

DISCUSSION

The spread of NDM-expressing strains is a major public health concern. From an infection control standpoint, the rapid identification of such strains is essential. A fast and easy-to-use test like the NDM LFIA described here would be a valuable tool to identify such producers and stratify the carriers.

During the development of the NDM LFIA, all the screening steps until the selection of 22 MAbs were done by using an immunoenzymatic assay to test the capacity of MAbs to bind recombinant NDM-1. The assay conditions of this screening format (see Text S1 in the supplemental material) are very different from those of LFIA (duration of the assay, contact of antibodies with antigen, buffers, washing steps, etc.) and are not predictive of antibody performances in LFIAs (25). In order to select the MAbs best adapted to the LFIA, we performed a combinatorial analysis by spotting the MAb onto the membrane so as to be closer to the operating conditions used in the LFIA format. As we had previously observed that the best pair for the detection of a recombinant protein is not systematically the best for the detection of the natural protein, the final selection was performed by using serial dilutions of strains expressing NDM-like enzymes. This resulted in the selection of one pair of MAbs, NDM 105 as the capture antibody and NDM 103 as the colloidal gold reporter antibody, for the validation experiments. The LOD of this LFIA is close to those of other similar tests developed in our laboratory for *Staphylococcus enterotoxin B* (SEB) (312 pg/ml) and *Yersinia* spp. (range from 10⁵ CFU/ml to 10⁶ CFU/ml), for example (26, 27). Moreover, a commercial LFIA for OXA-48 detection (23) has a comparable LOD of 2.41 × 10⁶ CFU/ml.

The validation performed with well-characterized clinical strains showed that the NDM LFIA is able to detect NDM-1 and all its variants available at the French National Reference Center (NRC), whether or not associated with other β -lactamases. No false-positive, no false-negative, and no ambiguous results were observed with the 249 tested isolates. Our test therefore showed 100% sensitivity and 100% specificity. When grown on chromogenic plates currently used in laboratories to detect CRE (such as ChromID Carba; bioMérieux, Marcy l'Etoile, France) or simply enterobacterial species in urine samples (such as ChromID CPS [bioMérieux] and Uri-4 [Bio-Rad, Marnes la Coquette, France]), bacterial isolates may show a very strong coloration (for example, dark blue for *Klebsiella*). Nevertheless, this coloration did not lead to false-positive results in the NDM LFIA. Thus, our assay is fully compatible with most samples handled in bacteriology laboratories. Our assay is easy to use and does not require any specific

equipment or skills. The results are easy to read after 15 min of migration. However, for most positive samples, the positivity of NDM carbapenemase-producing strains could already be evidenced after 1 or 2 min. This test could be relevant in areas with a high prevalence of NDM producers in enterobacterial isolates with decreased susceptibility to carbapenems and in strains grown on CPE-screening media. *Providencia stuartii* and *P. rettgeri* showed positive results with a lower intensity. This could be due to the location of the *bla*_{NDM-1} gene. A chromosomal or plasmid location under the control of a promoter with low efficiency in these strains could result in a low expression level. Partial extraction was observed for *Providencia* strains and also for *Klebsiella* (Fig. 4B), but this inconvenience seems minor, as NDM-1 expression in *Klebsiella* was strongly detected. The fact that more bacteria were needed to obtain an equivalent signal, as with our NDM-expressing *E. coli* or *K. pneumoniae* strains (Fig. 4B), could confirm the major influence of the expression level.

Besides these good results, we have to keep in mind that any new mutation occurring in the epitope of one of the MAbs involved may give false-negative results. To face this eventuality, we have already identified 4 compatibility groups among our best MAbs using combinatorial analysis, corresponding to 4 different regions recognized mainly on the NDM-1 protein. This would allow us to develop a new test rapidly by the addition of new antibodies targeting nonmutated regions in the existing LFIA.

Interestingly, another immunochromatographic assay has been developed for the detection of IMP-type metallo-carbapenemases that are highly prevalent in Southeast Asia. This test also presented 100% sensitivity and 100% specificity for the detection of IMP-type carbapenemases in *Pseudomonas* spp. (28). Moreover, Glupczynski et al. developed a single immunochromatographic test for the detection of both OXA-48-like and KPC carbapenemases (22). Thus, in the near future, we aim to combine different antibodies targeting the five most relevant carbapenemases (OXA-48, NDM, KPC, VIM, and IMP) into a single immunochromatographic assay in order to provide a very powerful and broad-spectrum tool for the detection of CPE.

Conclusion. The NDM LFIA was efficient, rapid, and easy to implement in the routine workflow of a clinical microbiology laboratory for the confirmation of NDM-like carbapenemase-producing *Enterobacteriaceae*. It could complete the existing panel of tests available for the confirmation of NDM carbapenemases, especially in countries with low resources and/or a high NDM prevalence.

MATERIALS AND METHODS

Ethics statement. All experiments were performed in compliance with French and European regulations on the care of laboratory animals (European Community [EC] Directive 86/609, French Law 2001-486, 6 June 2001) and with agreement no. 91-416 delivered to S.S. by the French Veterinary Services and CEA agreement D-91-272-106 from the Veterinary Inspection Department of Essonne (France).

Reagents. Biozzi mice were bred at the animal care unit of the CEA (Gif sur Yvette, France). Bovine serum albumin (BSA), Tween 20, isopropyl- β -D-thiogalactoside (IPTG), biotin *N*-hydroxysuccinimide ester, streptavidin, a gold chloride solution, *N*-succinimidyl-*S*-acetyl-thioacetate (SATA), imidazole, and kanamycin (from *Streptomyces kanamyceticus*) were obtained from Sigma-Aldrich (Saint Quentin Fallavier, France). Ndel and Xhol were obtained from New England BioLabs (Evry, France). Goat anti-mouse (GAM) IgG and IgM polyclonal antibodies were obtained from Jackson ImmunoResearch (West Grove, PA, USA). Protein A-Sepharose (ProsepA) was obtained from Millipore (Guyancourt, France). A serine protease inhibitor [4-(2-aminoethyl)benzenesulfonyl fluoride hydrochloride (AEBSF)] was obtained from Interchim (Montluçon, France). Metal agarose affinity resin (Chelating Sepharose FastFlow) was obtained from GE Healthcare (Vélizy-Villacoublay, France). Enzyme immunoassays (EIAs) were performed with MaxiSorp 96-well microtiter plates (Nunc, Paris, France), and all reagents were diluted in EIA buffer (0.1 M phosphate buffer [pH 7.4] containing 0.15 M NaCl, 0.1% BSA, and 0.01% sodium azide). Plates coated with proteins were saturated in EIA buffer (18 h at 4°C) and washed with washing buffer (0.1 M potassium phosphate [pH 7.4] containing 0.05% Tween 20). Nitrocellulose strips with polystyrene backing were obtained from GE Healthcare (Prima 40). For culture media, Luria broth (LB) and LB agar were obtained from Sigma-Aldrich; tryptone soy agar (TSA) was obtained from Oxoid (Dardilly, France); Mueller-Hinton (MH) agar and URISelect 4 (Uri-4) were obtained from Bio-Rad (Marnes la Coquette, France); and Columbia agar plus 5% horse blood (COH), ChromID ESBL agar, ChromID Carba Smart, and Drigalski (DRIG) agar were obtained from bioMérieux SA (Marcy l'Etoile, France). The Vibra cell 75185 sonicator apparatus was obtained from Bioblock Scientific (Illkirch, France).

Strains tested. For the LFIA validation, 175 enterobacterial isolates with characterized β -lactamase content were used to evaluate the NDM LFIA (18). This collection included 55 non-carbapenemase

producers and 120 carbapenemase producers, including 27 NDM producers. For the prospective evaluation, 74 enterobacterial clinical isolates with decreased susceptibility to at least one carbapenem were used. These isolates were sent by clinical microbiology laboratories throughout France to the Associated French NRC for CRE.

Cloning and expression of the NDM-1(29–270) protein in *E. coli*. The gene (from *E. coli*) encoding the protein without a signal sequence from amino acids G29 to R270 (predicted by the SignalP 4.1 server) was amplified by PCR using forward primer NDM-1 29-270 NdeI (5'-aaaaCATATGggtgaaatccgc cgcagc-3'; lowercase type on the 3' side of the restriction site [uppercase] represents the gene coding sequence, and "aaaa" represents irrelevant nucleobases) and reverse primer NDM-1 XhoI-Δstop (5'-aaaCTCGAGgcgagctgtcgccat-3'). After amplification, the sequence was further cloned into the pET41b vector (Invitrogen, Life Technologies, Cergy-Pontoise, France), using NdeI and XhoI restriction enzymes, allowing the insertion of a polyhistidine tag sequence at the 3' end of the gene. The inserted gene was verified by sequencing.

E. coli BL21(DE3)/pLysS was then transformed with the recombinant gene. One positive clone was grown in 1 liter of LB with 50 μg/ml kanamycin at 30°C until the optical density at 600 nm (OD₆₀₀) reached 0.6. IPTG (100 μM) was then added to the culture, which was incubated for 4 h with shaking at 30°C. The culture was pelleted by centrifugation at 3,000 × *g* for 15 min at 4°C. The pellet was suspended in 40 ml of solubilizing buffer (50 mM Tris-HCl buffer [pH 8], 100 mM NaCl, 1 mM AEBSF) and frozen at –20°C. After melting, the bacterial suspension was sonicated (3 pulses of 15 s at 14 W) and centrifuged for 15 min at 10,000 × *g*. Imidazole (20 mM final concentration) was added to the supernatant, which was incubated for 2 h with 4 ml of Ni-nitrilotriacetic acid (NTA) agarose affinity resin with shaking at room temperature. The gel was washed with 100 ml of binding buffer (50 mM Tris-HCl buffer [pH 8], 100 mM NaCl, 20 mM imidazole). Elution of the His-tagged protein was performed by incubating the resin for 10 min with 4 ml of solubilizing buffer with 500 mM (final concentration) imidazole, and the operation was repeated 5 times.

The eluted fractions were pooled and dialyzed twice in 2 liters of 50 mM potassium phosphate buffer (pH 7.4). The protein concentration was measured by the absorbance at 280 nm, and purity was assessed by SDS-PAGE (Phast system; GE Healthcare). The recombinant NDM-1 protein was then used to immunize mice, as a standard for the selection of MAb pairs, and to determine the limit of detection.

Antibody selection for the lateral flow format. (i) Preparation of colloidal gold-labeled NDM-1 antibodies. Colloidal gold was prepared as previously described (26), 1 ml was centrifuged for 15 min at 15,000 × *g*, and the pellet was suspended in water. One hundred microliters of a 100-μg/ml solution of each MAb (previously produced and selected [see Text S1 in the supplemental material]) in 5 mM phosphate buffer (pH 7.4) was added, and the mixture was incubated for 1 h at 20°C, allowing the adsorption of the MAbs to the surface of the gold particles. One hundred microliters of a solution containing 20 mM phosphate buffer (pH 7.4) and 1% BSA was then added, and the mixture was centrifuged for 15 min at 15,000 × *g*. The supernatant was discarded, and the pellet was suspended in 1 ml of 2 mM phosphate buffer (pH 7.4) and 0.1% BSA, sonicated for a few seconds, and centrifuged for 15 min at 15,000 × *g*. The supernatant was discarded, and the pellet was suspended in 250 μl of a solution containing 2 mM phosphate buffer (pH 7.4) and 0.1% BSA and stored at 4°C in the dark.

(ii) Strip screening test. To select the best MAb pairs for the development of the two-site lateral flow immunoassay, a combinatorial analysis was carried out by using each MAb as either a capture or a gold-labeled antibody. Briefly, the strips were prepared by spotting 1 μl of MAb (100 μg/ml in 50 mM phosphate buffer [pH 7.4]) and then dried. One hundred microliters of an NDM-1 solution (50 ng/ml in EIA buffer–0.5% Tween 20) or buffer alone and 10 μl of colloidal gold-labeled MAb were mixed in microtiter plate wells (Greiner) and allowed to react for 5 min before the strip was dipped into the solution. After a 30-min migration, signals were analyzed by the naked eye. The parameters used to select the best MAb pairs were the intensity of the visual signals obtained with an NDM-1 concentration (50 ng/ml) and the absence of a signal without NDM-1 (nonspecific signal).

(iii) Selection of best pairs. For this study, we used a conventional strip format. The strips (0.5 cm wide and 4.5 cm long) were composed of 3 parts, (i) a sample pad (standard 14; Whatman) (0.5 cm long), (ii) a nitrocellulose membrane (Prima 40) (2.5 cm long), and (iii) an absorption pad (cellulose-grade 470; Whatman) (1.5 cm long), all attached to a backing card. The detection zone contained immobilized goat anti-mouse antibodies as a control line and an anti-NDM-1 MAb as a test line (1 mg/ml in 50 mM sodium phosphate buffer [pH 7.4]) dispensed at 1 μl/cm by using an automatic dispenser (Biojet XYZ 3050; BioDot, England). After drying for 1 h at 37°C in an air oven, the membrane was incubated with a blocking solution (phosphate-buffered saline [PBS] [pH 7.4] containing 0.5% BSA) for 30 min at room temperature (RT). The membrane was washed twice with deionized water, incubated for 20 min at RT in a preserving solution (PBS containing 0.1% Tween 20 and 7.5% glucose), and then dried for 20 min at 37°C in an air oven. After the absorption pad and the sample pad were fixed to the top and the bottom of the membrane, respectively, the card was cut into 5-mm-wide strips by using an automatic programmable cutter (CM4000 Guillotine cutting system; BioDot).

Each selected pair of antibodies was evaluated in the LFIA format using serial dilutions (1 × 10⁸, 2 × 10⁷, 4 × 10⁶, 8 × 10⁵, and 1.6 × 10⁵ CFU/ml) of NDM-producing bacteria in extraction buffer {100 mM Tris-HCl (pH 8), 0.15 M NaCl, 0.1% BSA, 0.5% Tween 20, 1% 3-[(3-cholamidopropyl)-dimethylammonio]-1-propanesulfonate (CHAPS)}. One hundred microliters of this solution was mixed for 5 min with 10 μl of the conjugate antibody before the strip was dipped (for each pair of antibodies).

NDM LFIA evaluation and use. The NDM LFIAs (strip plus cassette) were manufactured by NG Biotech (Guipry, France) using our MAbs. The 175 strains to be tested were grown on MH agar for 16 h at 37°C. Ten strains were also grown under the same conditions on TSA, Uri-4, COH, ChromID ESBL,

ChromID Carba Smart, and DRIG agar plates. Using a 1- μ l inoculation loop, a single colony was resuspended in 150 μ l of extraction buffer (lysis step) and vortexed for a few seconds, and subsequently, 100 μ l was dispensed onto the cassette. The results were read by eye after 15 min of migration by monitoring the appearance of a red band specific for NDM-1, along with a band corresponding to the internal control. This protocol is similar to the one recommended for the future commercial NDM LFIA.

Limit of detection with recombinant NDM-1 and NDM-1-producing enterobacterial isolates.

Serial dilutions (50,000, 16,666, 5,555, 1,852, 617, 206, 68, and 0 pg/ml) of the recombinant NDM-1 protein or of one NDM-1-producing *K. pneumoniae* strain (6×10^8 , 1.2×10^8 , 2.4×10^7 , 4.8×10^6 , 9.6×10^5 , and 1.9×10^5 CFU/ml) were performed with extraction buffer or LB medium, respectively. Bacterial dilution vials were centrifuged for 20 min at $5,000 \times g$, the supernatant was carefully discarded, and the pellet was suspended in extraction buffer (same volume as LB). Consecutively, 100 μ l of each solution was dispensed onto the cassette and allowed to migrate. Results were read by eye after 15 min.

SUPPLEMENTAL MATERIAL

Supplemental material for this article may be found at <https://doi.org/10.1128/JCM.00248-17>.

SUPPLEMENTAL FILE 1, PDF file, 0.1 MB.

ACKNOWLEDGMENTS

This work was funded by a grant from the Ministère de l'Éducation Nationale et de la Recherche (EA7361), Universit  Paris-Sud, Universit  Paris Saclay. We are members of the Laboratory of Excellence LERMIT, supported by a grant from the ANR (ANR-10-LABX-33).

For Laurent Dortet, the patent for the Carba NP test has been licensed to bioM rieux (La Balmes les Grottes, France).

REFERENCES

- Page MG, Bush K. 2014. Discovery and development of new antibacterial agents targeting Gram-negative bacteria in the era of pandrug resistance: is the future promising? *Curr Opin Pharmacol* 18:91–97. <https://doi.org/10.1016/j.coph.2014.09.008>.
- Paterson DL, Bonomo RA. 2005. Extended-spectrum β -lactamases: a clinical update. *Clin Microbiol Rev* 18:657–686. <https://doi.org/10.1128/CMR.18.4.657-686.2005>.
- Nordmann P, Dortet L, Poirel L. 2012. Carbapenem resistance in Enterobacteriaceae: here is the storm! *Trends Mol Med* 18:263–272. <https://doi.org/10.1016/j.molmed.2012.03.003>.
- Nordmann P, Naas T, Poirel L. 2011. Global spread of carbapenemase-producing Enterobacteriaceae. *Emerg Infect Dis* 17:1791–1798. <https://doi.org/10.3201/eid1710.110655>.
- Yong D, Toleman MA, Giske CG, Cho HS, Sundman K, Lee K, Walsh TR. 2009. Characterization of a new metallo- β -lactamase gene, blaNDM-1, and a novel erythromycin esterase gene carried on a unique genetic structure in *Klebsiella pneumoniae* sequence type 14 from India. *Antimicrob Agents Chemother* 53:5046–5054. <https://doi.org/10.1128/AAC.00774-09>.
- Walsh TR. 2010. Emerging carbapenemases: a global perspective. *Int J Antimicrob Agents* 36:S8–S14. [https://doi.org/10.1016/S0924-8579\(10\)70004-2](https://doi.org/10.1016/S0924-8579(10)70004-2).
- Moellering RC, Jr. 2010. NDM-1—a cause for worldwide concern. *N Engl J Med* 363:2377–2379. <https://doi.org/10.1056/NEJMp1011715>.
- Rupp  E, Armand-Lef vre L, Estellat C, Consigny P-H, Mniat AE, Boussadia Y, Goujon C, Ralaimazava P, Campa P, Girard P-M, Wyplosz B, Vittecoq D, Bouchaud O, Loup GL, Pialoux G, Perrier M, Wieder I, Moussa N, Esposito-Far se M, Hoffmann I, Coignard B, Lucet J-C, Andremont A, Matheron S. 2015. High rate of acquisition but short duration of carriage of multidrug-resistant Enterobacteriaceae after travel to the tropics. *Clin Infect Dis* 61:593–600. <https://doi.org/10.1093/cid/civ333>.
- Papagiannitsis CC,  studentov V, Izdebski R, Oikonomou O, Pfeifer Y, Petinaki E, Hrabk J. 2015. Matrix-assisted laser desorption ionization–time of flight mass spectrometry meropenem hydrolysis assay with NH_4HCO_3 , a reliable tool for direct detection of carbapenemase activity. *J Clin Microbiol* 53:1731–1735. <https://doi.org/10.1128/JCM.03094-14>.
- Lasserre C, De Saint Martin L, Cuzon G, Bogaerts P, Lamar E, Glupczynski Y, Naas T, Tand  D. 2015. Efficient detection of carbapenemase activity in Enterobacteriaceae by matrix-assisted laser desorption ionization–time of flight mass spectrometry in less than 30 minutes. *J Clin Microbiol* 53:2163–2171. <https://doi.org/10.1128/JCM.03467-14>.
- Dortet L, Brechard L, Poirel L, Nordmann P. 2014. Impact of the isolation medium for detection of carbapenemase-producing Enterobacteriaceae using an updated version of the Carba NP test. *J Med Microbiol* 63:772–776. <https://doi.org/10.1099/jmm.0.071340-0>.
- Dortet L, Agathine A, Naas T, Cuzon G, Poirel L, Nordmann P. 2015. Evaluation of the RAPIDEC CARBA NP, the Rapid CARB Screen and the Carba NP test for biochemical detection of carbapenemase-producing Enterobacteriaceae. *J Antimicrob Chemother* 70:3014–3022. <https://doi.org/10.1093/jac/dkv213>.
- Tijet N, Patel SN, Melano RG. 2016. Detection of carbapenemase activity in Enterobacteriaceae: comparison of the carbapenem inactivation method versus the Carba NP test. *J Antimicrob Chemother* 71:274–276. <https://doi.org/10.1093/jac/dkv283>.
- Dortet L, Poirel L, Nordmann P. 2012. Rapid identification of carbapenemase types in Enterobacteriaceae and *Pseudomonas* spp. by using a biochemical test. *Antimicrob Agents Chemother* 56:6437–6440. <https://doi.org/10.1128/AAC.01395-12>.
- Tsakris A, Poulou A, Bogaerts P, Dimitroulia E, Pournaras S, Glupczynski Y. 2015. Evaluation of a new phenotypic OXA-48 disk test for differentiation of OXA-48 carbapenemase-producing Enterobacteriaceae clinical isolates. *J Clin Microbiol* 53:1245–1251. <https://doi.org/10.1128/JCM.03318-14>.
- Hrabk J, Chudckov E, Papagiannitsis CC. 2014. Detection of carbapenemases in Enterobacteriaceae: a challenge for diagnostic microbiological laboratories. *Clin Microbiol Infect* 20:839–853. <https://doi.org/10.1111/1469-0691.12678>.
- Carvalhoes CG, Cayo R, Visconde MF, Barone T, Frigatto EAM, Okamoto D, Assis DM, Juliano L, Machado AMO, Gales AC. 2014. Detection of carbapenemase activity directly from blood culture vials using MALDI-TOF MS: a quick answer for the right decision. *J Antimicrob Chemother* 69:2132–2136. <https://doi.org/10.1093/jac/dku094>.
- Dortet L, Jousset A, Sainte-Rose V, Cuzon G, Naas T. 2016. Prospective evaluation of the OXA-48 K-SeT assay, an immunochromatographic test for the rapid detection of OXA-48-type carbapenemases. *J Antimicrob Chemother* 71:1834–1840. <https://doi.org/10.1093/jac/dkw058>.
- Lupo A, Papp-Wallace KM, Sendi P, Bonomo RA, Endimiani A. 2013. Non-phenotypic tests to detect and characterize antibiotic resistance

- mechanisms in Enterobacteriaceae. *Diagn Microbiol Infect Dis* 77: 179–194. <https://doi.org/10.1016/j.diagmicrobio.2013.06.001>.
20. Singh P, Pfeifer Y, Mustapha A. 2016. Multiplex real-time PCR assay for the detection of extended-spectrum β -lactamase and carbapenemase genes using melting curve analysis. *J Microbiol Methods* 124:72–78. <https://doi.org/10.1016/j.mimet.2016.03.014>.
 21. Naas T, Ergani A, Carr er A, Nordmann P. 2011. Real-time PCR for detection of NDM-1 carbapenemase genes from spiked stool samples. *Antimicrob Agents Chemother* 55:4038–4043. <https://doi.org/10.1128/AAC.01734-10>.
 22. Glupczynski Y, Evrard S, Ote I, Mertens P, Huang T-D, Leclipteux T, Bogaerts P. 2016. Evaluation of two new commercial immunochromatographic assays for the rapid detection of OXA-48 and KPC carbapenemases from cultured bacteria. *J Antimicrob Chemother* 71:1217–1222. <https://doi.org/10.1093/jac/dkv472>.
 23. Wareham DW, Shah R, Betts JW, Phee LM, Momin MHFA. 2016. Evaluation of an immunochromatographic lateral flow assay (OXA-48 K-SeT) for rapid detection of OXA-48-like carbapenemases in Enterobacteriaceae. *J Clin Microbiol* 54:471–473. <https://doi.org/10.1128/JCM.02900-15>.
 24. King D, Strynadka N. 2011. Crystal structure of New Delhi metallo- β -lactamase reveals molecular basis for antibiotic resistance. *Protein Sci* 20:1484–1491. <https://doi.org/10.1002/pro.697>.
 25. O'Farrell B. 2013. Lateral flow immunoassay systems, p 89–107. *In* Wild D, John R, Sheehan C, Binder S, He J (ed), *The immunoassay handbook*, 4th ed. Elsevier, Oxford, United Kingdom.
 26. Khreich N, Lamourette P, Boutal H, Devilliers K, Cr eminon C, Volland H. 2008. Detection of Staphylococcus enterotoxin B using fluorescent immunoliposomes as label for immunochromatographic testing. *Anal Biochem* 377:182–188. <https://doi.org/10.1016/j.ab.2008.02.032>.
 27. Laporte J, Savin C, Lamourette P, Devilliers K, Volland H, Carniel E, Cr eminon C, Simon S. 2015. Fast and sensitive detection of enteropathogenic Yersinia by immunoassays. *J Clin Microbiol* 53:146–159. <https://doi.org/10.1128/JCM.02137-14>.
 28. Kitao T, Miyoshi-Akiyama T, Tanaka M, Narahara K, Shimojima M, Kirikae T. 2011. Development of an immunochromatographic assay for diagnosing the production of IMP-type metallo- β -lactamases that mediate carbapenem resistance in Pseudomonas. *J Microbiol Methods* 87: 330–337. <https://doi.org/10.1016/j.mimet.2011.09.011>.

A multiplex lateral flow immunoassay for the rapid identification of NDM-, KPC-, IMP- and VIM-type and OXA-48-like carbapenemase-producing Enterobacteriaceae

Hervé Boutal¹, Anaïs Vogel¹, Sandrine Bernabeu², Karine Devilliers¹, Elodie Creton^{2,3}, Garence Cotellon^{2,3}, Marc Plaisance¹, Saoussen Oueslati², Laurent Dortet^{2,3}, Agnès Jousset^{2,3}, Stéphanie Simon¹, Thierry Naas^{2,3} and Hervé Volland^{1*}

¹Service de Pharmacologie et Immunoanalyse (SPI), CEA, INRA, Laboratoire d'Etudes et de Recherches en Immunanalyse, Université Paris-Saclay, F-91191, Gif-sur-Yvette, France; ²EA7361, Université Paris-Sud, Université Paris-Saclay, LabEx Lermite, Bacteriology-Hygiene unit, AP-HP, Hôpital Bicêtre, Le Kremlin-Bicêtre, France; ³Associated French National Reference Centre for Antibiotic Resistance: Carbapenemase-producing Enterobacteriaceae, Le Kremlin-Bicêtre, France

*Corresponding author. Tel: +33-1-69-08-78-98; Fax: +33-1-69-08-59-07; E-mail: herve.volland@cea.fr

Received 16 October 2017; returned 3 December 2017; revised 11 December 2017; accepted 13 December 2017

Objectives: The global spread of carbapenemase-producing Enterobacteriaceae represents a substantial challenge in clinical practice and rapid and reliable detection of these organisms is essential. The aim of this study was to develop and validate a lateral flow immunoassay (Carba5) for the detection of the five main carbapenemases (KPC-, NDM-, VIM- and IMP-type and OXA-48-like).

Methods: Carba5 was retrospectively and prospectively evaluated using 296 enterobacterial isolates from agar culture. An isolated colony was suspended in extraction buffer and then loaded on the manufactured Carba5.

Results: All 185 isolates expressing a carbapenemase related to one of the Carba5 targets were correctly and unambiguously detected in <15 min. All other isolates gave negative results except those producing OXA-163 and OXA-405, which are considered low-activity carbapenemases. No cross-reaction was observed with non-targeted carbapenemases, ESBLs, AmpCs or oxacillinases (OXA-1, -2, -9 and -10). Overall, this assay reached 100% sensitivity and 95.3% (retrospectively) to 100% (prospectively) specificity.

Conclusions: Carba5 is efficient, rapid and easy to implement in the routine workflow of a clinical microbiology laboratory for confirmation of the five main carbapenemases encountered in Enterobacteriaceae.

Introduction

The worldwide spread of carbapenemase-producing organisms is a global concern¹ and an economic threat.² Among these organisms, Enterobacteriaceae have a major role as causes of nosocomial infections (and, for *Escherichia coli*, also of community-acquired infections). The emergence and dissemination of carbapenemase-producing Enterobacteriaceae (CPE) is undoubtedly a matter of great public health concern considering CPE are often resistant to several if not all classes of antibiotics, and very few (or no) antibiotic options remain available for them.^{3,4} The rapid detection and identification of CPE is essential to help physicians quickly implement appropriate infection control measures, to adapt antibiotic treatment rapidly and to optimize care strategies and outcomes. Based on their amino acid sequence, carbapenemases are divided into different molecular

classes: A, B and D of the Ambler classification. Their susceptibility to carbapenems varies from weak activity to very efficient hydrolysis. Discrimination between these carbapenemases will provide valuable information for appropriate treatment. For instance, a β -lactamase inhibitor (ceftazidime/avibactam) is now available, but does not inhibit MBL activity.^{5,6}

Several diagnostic tests have been developed based on the detection of carbapenem-hydrolysing activity [MALDI-TOF MS^{7,8} or biochemical assay (e.g. Carba NP test and derivatives),^{9,10} the carbapenem inactivation method¹¹ and OXA-48 disc test^{12,13}]. In addition, several phenotypic confirmation tests have also been developed, but usually require 24 h.^{13,14} Although they have proven useful, it is now also crucial to identify the implicated carbapenemase. Molecular methods are undoubtedly appropriate for this purpose. End-point PCR and real-time PCR can also be used in

single or multiplex formats targeting the main carbapenemases with high specificity and sensitivity.¹⁵⁻¹⁷ However, these methods are expensive and require a high level of expertise to obtain accurate results and are not suitable for all clinical microbiology laboratories worldwide. As an alternative, antibody-based methods such as lateral flow immunoassay (LFIA) have already been validated for carbapenemase-producer detection and carbapenemase identification.¹⁸⁻²² These tests yield results from cultured strains within 15 min, with 100% sensitivity and specificity, although they do not allow the simultaneous detection of the five main carbapenemases.

To meet current needs, antimicrobial drug resistance detection methods must be cheap (reduced cost of consumables and equipment) and easy to use (reduced technical complexity) for the end user. This led us to develop an LFIA, named Carba5, for the detection of the five main carbapenemase families, NDM-, IMP-, VIM- and KPC-type and OXA-48-like. Carba5 is a robust assay, easily transferable in a commercialized version, which is stable for >24 months without refrigeration, user-friendly (no need for trained staff), high in performance (sensitive and specific) and low in cost (although pricing is not yet specified, similar LFIA tests usually cost ~10€ per test)²⁰ compared with >30-40€ for molecular tests. Moreover, the detection results are obtained in a short time without the need for highly technical equipment for the readout. Here, we validated Carba5 on 296 agar-cultured enterobacterial isolates [180 characterized isolates for their β -lactamase content and 116 consecutive carbapenem-resistant isolates referred to the Associated French National Reference Centre (F-NRC) for expertise], including 185 isolates expressing NDM-, IMP-, VIM- or KPC-type or OXA-48-like carbapenemases, which were perfectly detected in 15 min.

Methods

Ethics statement

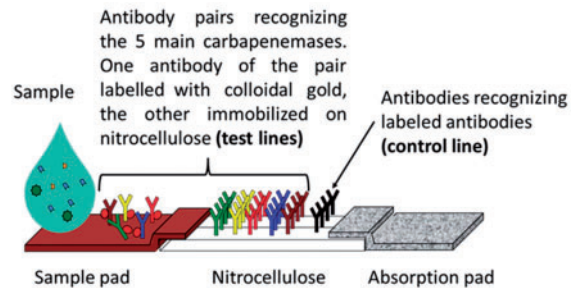
All experiments were performed in compliance with French and European regulations on the care of laboratory animals (European Community Directive 86/609, French Law 2001-486, 6 June 2001) and with the agreements of the Ethics Committee of the Commissariat à l'Énergie Atomique (CETEA 'Comité d'Éthique en Expérimentation Animale' n° 44) no. 12-026 and 15-055 delivered to S. S. by the French Veterinary Services and CEA agreement D-91-272-106 from the Veterinary Inspection Department of Essonne (France).

Strains tested

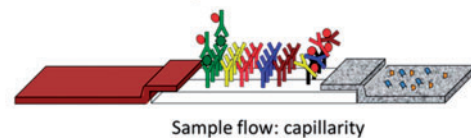
For the LFIA validation, 180 enterobacterial isolates with PCR-characterized β -lactamase content were used to evaluate Carba5. This collection represented 55 non-carbapenemase producers and 125 carbapenemase producers, including 30 Ambler class A producers (22 KPC, 3 IMI, 2 SME, 1 NMC-A, 1 FRI-1, 1 GES-5), 52 metallo- β -lactamase producers from Ambler class B (23 NDM, 17 VIM, 11 IMP, 1 GIM-1) and 38 Ambler class D producers corresponding to 37 OXA-48-like (21 OXA-48, 1 OXA-162, 3 OXA-181, 5 OXA-204, 2 OXA-232, 2 OXA-244, 1 OXA-517, 1 OXA-519, 1 OXA-535) and one OXA-372. Five isolates expressed both NDM-type and OXA-48-like carbapenemases.

For the prospective evaluation, 116 consecutive enterobacterial clinical isolates with decreased susceptibility to at least one carbapenem were used. These isolates were sent between April and May 2017 by clinical microbiology laboratories throughout France to the F-NRC for carbapenem-resistant Enterobacteriaceae.

1 - Structure of the strip



2 - Immunological detection



3 - Result

- ✓ The control line appears: the test is correct
- ✓ One or several test lines appear: positive test for the corresponding carbapenemase(s)
- ✓ No test line appears: negative test for the 5 carbapenemases



Figure 1. Carba5 principle.

Carbapenemase activity detection and PCR/sequencing experiments

Carbapenemase activity was evidenced in Enterobacteriaceae using the updated version of the Carba NP test and using an in-house PCR and sequencing approach directly on colonies.¹⁰

Monoclonal antibodies

Biozzi mice (10 weeks old) were immunized with the five recombinant carbapenemases, NDM-1 (G29-R270), OXA-48 (K23-P265), KPC-2 (A30-Q293), IMP-1 (L22-N246) and VIM-1 (A22-E266), corresponding to the full sequence without the signal sequence expressed with the hexa-histidine tag on their C terminus. Consecutively, monoclonal antibodies were obtained, characterized and selected for the LFIA format as previously described.¹⁹

Manufactured Carba5 and assay protocol

The required antibodies were produced on a large scale as previously described¹⁹ and provided to NG Biotech (Guipry, France) for the development of multiplex LFIA (see Figure 1). The strains to be tested were grown overnight at 37°C on URISelect™ 4 or Mueller-Hinton agar plates (Bio-Rad, Marnes la Coquette, France). One single isolated colony was collected from the plate with an inoculation loop and suspended in 150 μ L of extraction buffer to perform the lysis step. Subsequently, 100 μ L of this extract was

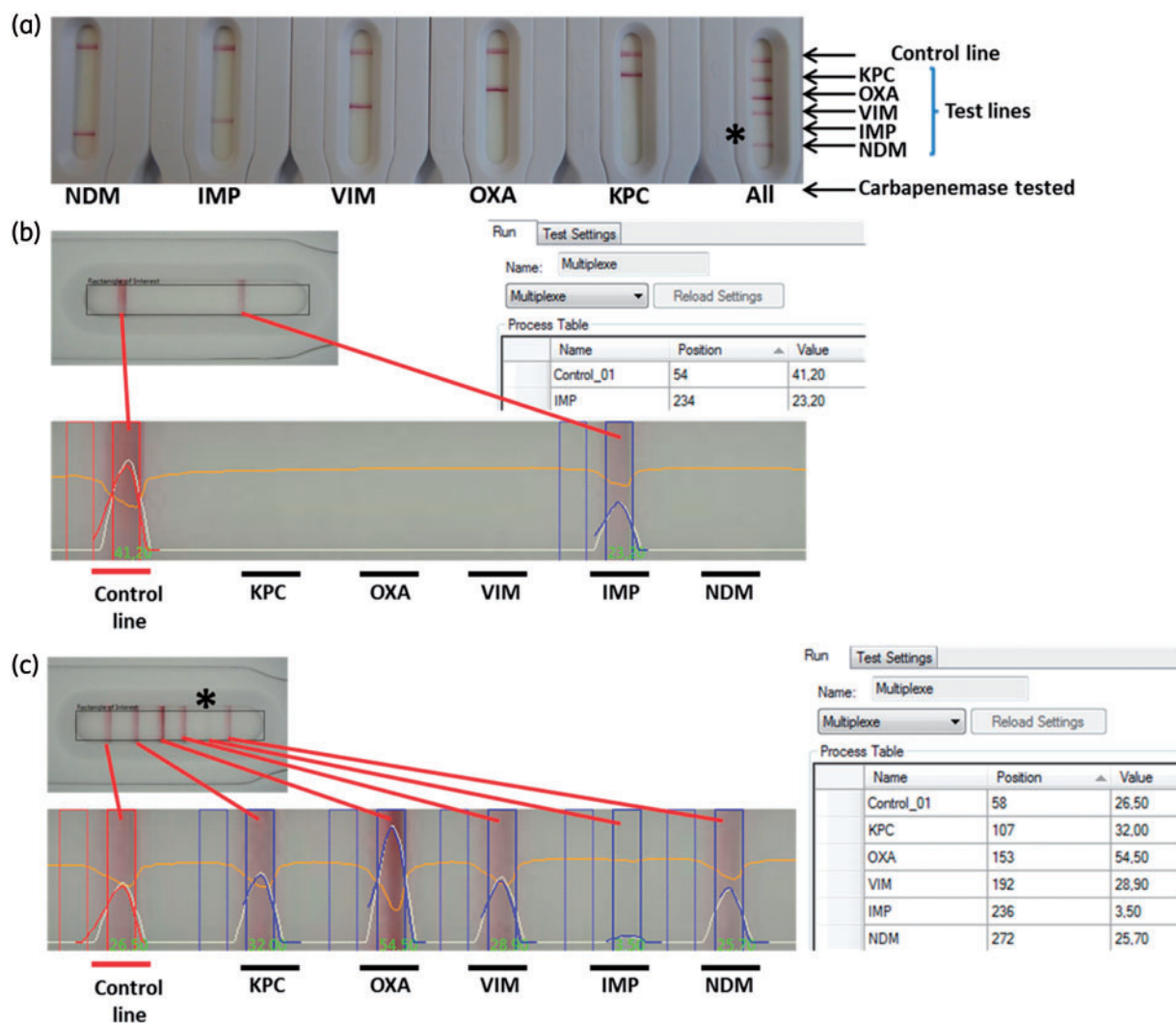


Figure 2. Data acquisition using a handheld reader. (a) Results obtained after 15 min of migration with carbapenemase-expressing strains. NDM, IMP, VIM, OXA and KPC, one colony resuspended in 150 μ L of extraction buffer and 100 μ L loaded on the cassette. For all, 25 μ L from each previous extract pooled leading to a 1 to 5 dilution and 100 μ L of this pool loaded on the cassette. (b) Previous IMP-expressing strain extract, picture of the cassette, positive test line analysis and corresponding value and carbapenemase name (table). (c) Previous pool of the five carbapenemase-expressing strain extracts, positive test line analysis and corresponding value (table). An asterisk indicates a test line not visible owing to camera sensitivity.

loaded on the cassette and allowed to migrate for 15 min. The protocol of the commercialized kit will be similar to the protocol described here.

Data acquisition

Data could be acquired in two separate ways, i.e. (i) a naked eye reading [the carbapenemase is identified by associating the positive result (positive test line) with the name of the carbapenemase written on the plastic part of the cassette], and (ii) using a computer-assisted reader that only gives results for positive test lines with the corresponding target name. An illustration of the results obtained is shown in Figure 2.

For this study, basic format cassettes were used and the carbapenemase names were not indicated, so the 'handheld reader' method was preferred.

Statistical analysis

The sensitivity, specificity, positive predictive value and negative predictive value were calculated with their respective 95% CI using the free software vassarStats: Website for Statistical Computation on <http://vassarstats.net/>. The gold standard was PCR followed by sequencing. Results were extrapolated to the global French epidemiology data obtained between 2012 and 2015.

Results

Prior to Carba5 validation, manufactured single-test LFIAs were validated with the F-NRC carbapenem-resistant Enterobacteriaceae collection (180 isolates) for the detection of NDM-type,¹⁹ IMP-type, VIM-type and OXA-48-like carbapenemases (data not

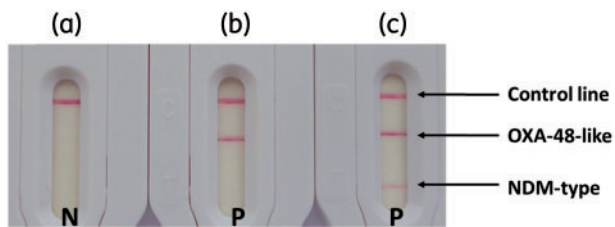


Figure 3. Results obtained with different strains. One colony suspended in extraction buffer and loaded on the cassette. (a) *Klebsiella pneumoniae* expressing CTX-M-18. (b) *K. pneumoniae* expressing OXA-162. (c) *K. pneumoniae* expressing NDM-1 and OXA-48. N, negative result; P, positive result.

shown). The manufactured single test for KPC-type carbapenemase was validated with only 60 strains from the same collection. These single tests gave 100% sensitivity and specificity according to the PCR-characterized β -lactamase content of the isolates. The manufactured Carba5 was developed with the same antibodies and tested with the F-NRC collection for validation. Routine use was successively assessed with strains showing a decreased susceptibility to at least one carbapenem.

Validation of Carba5

As described in Table S1 (available as [Supplementary data](#) at JAC Online), Carba5 was able to detect (strong signals) unambiguously all OXA-48-like-producing isolates with carbapenemase activity [$n = 37$; including OXA-48 ($n = 21$), OXA-162 ($n = 1$), OXA-181 ($n = 3$), OXA-204 ($n = 5$), OXA-232 ($n = 2$), OXA-244 ($n = 2$), OXA-517 ($n = 1$), OXA-519 ($n = 1$) and OXA-535 ($n = 1$)], as well as the KPC producers [$n = 22$; including KPC-2 ($n = 19$) and KPC-3 ($n = 3$)], NDM producers [$n = 23$; including NDM-1 ($n = 16$), NDM-4 ($n = 2$), NDM-5 ($n = 1$), NDM-6 ($n = 1$), NDM-7 ($n = 1$) and NDM-9 ($n = 2$)], IMP producers [$n = 11$; including IMP-1 ($n = 5$), IMP-8 ($n = 5$) and IMP-11 ($n = 1$)] and VIM producers [$n = 17$; including VIM-1 ($n = 12$), VIM-2 ($n = 2$), VIM-4 ($n = 2$) and VIM-19 ($n = 1$)]. Five strains simultaneously expressing NDM-1 and OXA-181 were also detected and thus show two positive test lines. The results obtained with a non-carbapenemase-producing strain, a carbapenemase-producing strain and a multiple carbapenemase-producing strain are shown in Figure 3. The three isolates expressing OXA-48-like broad-spectrum oxacillinases with very weak carbapenemase activity, OXA-163 ($n = 2$) and OXA-405 ($n = 1$), also gave positive results and were considered false positives.

All the CPE expressing a carbapenemase not related to any of the five carbapenemase families targeted gave negative results. They corresponded to eight Ambler class A [IMI ($n = 3$), GES-5 ($n = 1$), NMC-A ($n = 1$), SME ($n = 2$) and FRI-1 ($n = 1$)], one OXA-372 (an Ambler class D carbapenem-hydrolysing enzyme not related to OXA-48 β -lactamase)²³ and one Ambler class B GIM-1. In addition, no positive signal was obtained with the 51 non-carbapenemase producers.

Prospective evaluation of Carba5

For this study, 116 consecutive isolates were blindly tested and LFIA results were compared with those of the home-made Carba NP test and PCR sequencing, which are routinely performed by the

F-NRC on all isolates.¹⁰ In less than 15 min Carba5 detected 70 carbapenemase-positive isolates (Table 1) corresponding to OXA-48-like producers [$n = 57$; including OXA-48 ($n = 52$), OXA-181 ($n = 3$) and OXA-244 ($n = 2$)], NDM producers [$n = 9$; including NDM-1 ($n = 5$), NDM-5 ($n = 3$) and NDM-9 ($n = 1$)], VIM producers [$n = 2$; including VIM-1 ($n = 1$) and VIM-4 ($n = 1$)] and one KPC-3 producer. One strain was positive for both NDM and OXA-48 (NDM-5 and OXA-48). The 46 other isolates gave negative test results. Similar results were obtained with the Carba NP test, with 2 h incubation, for 45 isolates. The PCR sequencing results revealed 71 carbapenemase producers; 70 corresponded to those previously identified with Carba5 and the Carba NP test, and one corresponded to the IMI-producing *Enterobacter cloacae*, a non-targeted carbapenemase, which gave a positive result with the Carba NP test. Forty-five non-carbapenemase producers were confirmed negative by PCR.

Global performances of Carba5

Considering the results obtained with the F-NRC collection, the sensitivity and specificity of Carba5 towards the five target-related enzymes respectively reached 100% (95% CI = 95.8%–100%) and 95.3% (95% CI = 86.0%–98.8%) (misidentifying two OXA-163 and one OXA-405 as positives). This test is able to detect strains simultaneously expressing two carbapenemases (e.g. six strains with a combination of NDM-type and OXA-48-like enzymes). Importantly, no cross-reaction was observed with the non-targeted carbapenemases (IMI, SME, NMC-A, FRI, GES, GIM and OXA-372), ESBLs (TEM, SHV and CTX-M), AmpCs (CMY-2, DHA-2 and ACC-1) or oxacillinases (OXA-1, -2, -9 and -10). During the prospective study, Carba5 reached 100% (95% CI = 93.5%–100%) sensitivity, 100% (95% CI = 90.4%–100%) specificity, 100% (95% CI = 93.5%–100%) positive predictive value and 100% (95% CI = 90.4%–100%) negative predictive value for the identification of the five main carbapenemase families. Bacterial colonies were grown on two different plates and there was no interference depending on the media considered (Mueller-Hinton/URISelectTM 4).

Discussion

The spread of carbapenemase-expressing strains is a major public health concern. From an infection control point of view, the rapid identification of such strains is essential to prevent spread in hospital settings. Furthermore, with novel inhibitor/ β -lactam combinations, knowing exactly which carbapenemase is present is a prerequisite for the proper use of these novel molecules. Therefore, fast and user-friendly assays are mandatory. Carba5 fulfils all of the requirements to stratify patients.

Carba5 has been optimized to detect the KPC, NDM, VIM and IMP carbapenemase families as well as OXA-48 and its related variants. Most of the time, positive results were interpretable in less than the recommended 15 min of migration. Compared with the single-test LFIAs, no interference between the different carbapenemase detections was induced by the multiplex format. Moreover, Carba5 is able to detect and identify the simultaneous production of several of the five main carbapenemases by one strain. Overall, Carba5 detects these five carbapenemases with a sensitivity of 100% without any false negatives. It detected new variants of OXA-48, such as OXA-517, OXA-519 and OXA-535,^{24–26}

Table 1. Prospective evaluation of Carba5 on 116 consecutive isolates referred to the F-NRC for carbapenem-resistant Enterobacteriaceae

	Species	No. of isolates	Carba5 results					Carbapenemase content (PCR + sequencing)	
			NDM	IMP	VIM	OXA	KPC		
Carbapenemase producers									
NDM-type	<i>E. coli</i>	1	P	N	N	N	N	NDM-1	
	<i>E. coli</i>	3	P	N	N	N	N	NDM-5	
	<i>E. coli</i>	1	P	N	N	N	N	NDM-9	
	<i>K. pneumoniae</i>	3	P	N	N	N	N	NDM-1	
	<i>Morganella morganii</i>	1	P	N	N	N	N	NDM-1	
OXA-48-like	<i>E. coli</i>	13	N	N	N	P	N	OXA-48	
	<i>K. pneumoniae</i>	24	N	N	N	P	N	OXA-48	
	<i>Klebsiella oxytoca</i>	3	N	N	N	P	N	OXA-48	
	<i>E. cloacae</i>	3	N	N	N	P	N	OXA-48	
	<i>Citrobacter koseri</i>	2	N	N	N	P	N	OXA-48	
	<i>Citrobacter freundii</i>	6	N	N	N	P	N	OXA-48	
	<i>Enterobacter aerogenes</i>	1	N	N	N	P	N	OXA-48	
	<i>E. coli</i>	2	N	N	N	P	N	OXA-181	
	<i>K. pneumoniae</i>	1	N	N	N	P	N	OXA-181	
	<i>E. coli</i>	2	N	N	N	P	N	OXA-244	
	KPC-type	<i>K. pneumoniae</i>	1	N	N	N	N	P	KPC-3
	VIM-type	<i>K. pneumoniae</i>	1	N	N	P	N	N	VIM-1
		<i>E. cloacae</i>	1	N	N	P	N	N	VIM-4
IMI-type	<i>E. cloacae</i>	1	N	N	N	N	N	IMI-1	
multiple carbapenemases	<i>E. coli</i>	1	P	N	N	P	N	NDM-1 + OXA-48	
Non-carbapenemase producers									
	<i>E. coli</i>	4	N	N	N	N	N		
	<i>K. pneumoniae</i>	15	N	N	N	N	N		
	<i>E. cloacae</i>	17	N	N	N	N	N		
	<i>E. aerogenes</i>	3	N	N	N	N	N		
	<i>Hafnia alvei</i>	2	N	N	N	N	N		
	<i>Proteus mirabilis</i>	1	N	N	N	N	N		
	<i>C. freundii</i>	1	N	N	N	N	N		
	<i>M. morganii</i>	2	N	N	N	N	N		

N, negative result; P, positive result.

and OXA-48-related variants without significant carbapenemase activity (OXA-163 and OXA-405). As these enzymes do not confer reduced susceptibility to carbapenems, their identification requires further testing. In our testing scheme, these peculiar OXA variants were over-represented (3 of 180), while they represent only 1 of almost 10000 isolates in France over a 4 year period. Therefore, considering global French epidemiology, the specificity of Carba5 would be 99.98% (95% CI = 99.90%–99.99%).

Meanwhile, during the prospective evaluation, Carba5 detected 70 of the 71 (98.6%) carbapenemase producers. One IMI producer was not detected, but this should not be considered a major drawback considering the very low prevalence of this carbapenemase.

During the period 2012–15, 3320 carbapenemase producers of 9518 enterobacterial isolates were received at the F-NRC. 118 KPC, 13 IMI, 1 FRI-1, 366 NDM, 115 VIM, 10 IMP, 2491 OXA-48, 120 OXA-181, 35 OXA-204, 8 OXA-232, 10 OXA-244 and 33 multiple carbapenemase producers (including 30 NDM + OXA-

48-like, 1 NDM + VIM and 2 VIM + OXA-48-like) have been identified. By extrapolating the results obtained with the LFIA, we would expect that all isolates except those producing IMI, and FRI-1 (total = 14) would have been correctly identified. In addition, the unique OXA-405-producing *Serratia marcescens* would give a false-positive result. Thus, the overall performances of Carba5 for the detection of the five main carbapenemase would be 100% (95% CI = 99.86%–100%) sensitivity, 99.98% (95% CI = 99.90%–99.99%) specificity, 99.97% (95% CI = 99.80%–99.99%) positive predictive value and 100% (95% CI = 99.92%–100%) negative predictive value, respectively. More generally, the overall performance of Carba5 for the detection of all CPE (considering the 14 non-targeted carbapenemases as false-negative results) would be 99.58% (95% CI = 99.27%–99.76%) sensitivity, 99.98% (95% CI = 99.90%–99.99%) specificity, 99.97% (95% CI = 99.80%–99.99%) positive predictive value and 99.77% (95% CI = 99.61%–99.87%) negative predictive value, respectively.

So far, Carba5 can detect NDM-1/4/5/6/7/9, IMP-1/8/11, VIM-1/2/4/19, KPC-2/3 and OXA-48/162/181/204/232/244/517/519/535, and could be performed in routine laboratories, yielding unequivocal results in ~15 min. Strains with decreased susceptibility to at least one carbapenem could quickly be characterized if at least one of the main carbapenemases is expressed. Carba5 has been used at the F-NRC to confirm negative results obtained with the Carba NP test (data not shown). Some *Providencia* strains with negative Carba NP test results were actually NDM producers and were identified by Carba5 and later confirmed by PCR (data not shown). These false-negative Carba NP test results could be due to low expression levels of the carbapenemase or low permeability of the bacterial outer membrane. In addition, Carba5 is currently used with strains growing on CPE screening media (such as CarbaSMART)²⁷ and shows the same performance as with the two media used for this study, making it a reliable tool for CPE confirmation.

Compared with other LFIA tests available, Carba5 targets the five main carbapenemases. It could be used whatever the carbapenemase endemic context. Its universal use could help to report sporadic outbreaks leading to epidemiological updates. We agree that the epidemiology of carbapenemases is different between countries from different continents, but the five main carbapenemases account in each country for >99.5% of the determinants encountered. The relative percentages vary between the different countries and our test is thus suitable for most. We also agree that greater validation is now necessary in the form of multicentre validation. This validation is currently in progress in countries with high prevalences of OXA-48, KPC and MBLs.

In the near future, we aim to combine Carba5 with an LFIA already developed and dedicated to the identification of CTX-M producers to provide a very powerful and broad-spectrum tool for the detection of β -lactamases and guidance of antibiotic treatments.

Conclusions

Carba5 is efficient, rapid and easy to implement in the routine workflow of a clinical microbiology laboratory for the detection of CPE. It could complete the existing panel of tests available for the detection of carbapenemases, particularly in countries with limited resources and/or high prevalence of carbapenemases. Discrimination of OXA-48-like and KPC carbapenemases could rapidly guide treatments with ceftazidime/avibactam, and more generally prevent antibiotic misuse and provide efficient tools to contain the spread of these deadly bacteria in hospital settings.

Acknowledgements

We are thankful to Quentin Baratte for his involvement in the production of the required monoclonal antibodies.

Funding

This work was supported by the Assistance Publique—Hôpitaux de Paris (AP-HP), the University Paris-Sud, the Laboratory of Excellence in Research on Medication and Innovative Therapeutics (LERMIT) supported

by a grant from the French National Research Agency (ANR-10-LABX-33) and by the Joint Programming Initiative on Antimicrobial Resistance (JPIAMR) DesInMBL (ANR-14-JAMR-002).

Transparency declarations

L. D. is co-inventor of the Carba NP test, the patent of which has been licensed to bioMérieux (La Balme les Grottes, France). All other authors: none to declare.

Supplementary data

Table S1 is available as [Supplementary data](#) at JAC Online.

References

- WHO. *Antimicrobial Resistance: Global Report on Surveillance*. 2014. http://apps.who.int/iris/bitstream/10665/112642/1/9789241564748_eng.pdf?ua=1.
- Shriber DE, Baris E, Marquez PV et al. *Final Report*. The World Bank, 2017; 1–172. <http://documents.worldbank.org/curated/en/323311493396993758/pdf/114679-REVISED-v2-Drug-Resistant-Infections-Final-Report.pdf>.
- Poirel L, Pitout JD, Nordmann P. Carbapenemases: molecular diversity and clinical consequences. *Future Microbiol* 2007; **2**: 501–12.
- Doi Y, Paterson DL. Carbapenemase-producing Enterobacteriaceae. *Semin Respir Crit Care Med* 2015; **36**: 74–84.
- Stone GG, Bradford PA, Yates K et al. In vitro activity of ceftazidime/avibactam against urinary isolates from patients in a Phase 3 clinical trial programme for the treatment of complicated urinary tract infections. *J Antimicrob Chemother* 2017; **72**: 1396–9.
- Pfizer Launches Zavicefta™ (Ceftazidime-Avibactam) in the U.K. and Germany, a New Antibiotic to Treat Complicated Infections Caused by Gram-Negative Bacteria. 2017. <http://press.pfizer.com/press-release/pfizer-launches-zavicefta-ceftazidime-avibactam-uk-and-germany-new-antibiotic-treat-co>.
- Lasserre C, De Saint Martin L, Cuzon G et al. Efficient detection of carbapenemase activity in Enterobacteriaceae by matrix-assisted laser desorption/ionization–time of flight mass spectrometry in less than 30 minutes. *J Clin Microbiol* 2015; **53**: 2163–71.
- Papagiannitsis CC, Študentová V, Izdebski R et al. Matrix-assisted laser desorption/ionization–time of flight mass spectrometry meropenem hydrolysis assay with NH₄HCO₃, a reliable tool for direct detection of carbapenemase activity. *J Clin Microbiol* 2015; **53**: 1731–5.
- Dortet L, Brechard L, Poirel L et al. Impact of the isolation medium for detection of carbapenemase-producing Enterobacteriaceae using an updated version of the Carba NP test. *J Med Microbiol* 2014; **63**: 772–6.
- Dortet L, Agathine A, Naas T et al. Evaluation of the RAPIDEC® CARBA NP, the Rapid CARB Screen® and the Carba NP test for biochemical detection of carbapenemase-producing Enterobacteriaceae. *J Antimicrob Chemother* 2015; **70**: 3014–22.
- Tijet N, Patel SN, Melano RG. Detection of carbapenemase activity in Enterobacteriaceae: comparison of the carbapenem inactivation method versus the Carba NP test. *J Antimicrob Chemother* 2016; **71**: 274–6.
- Dortet L, Poirel L, Nordmann P. Rapid identification of carbapenemase types in Enterobacteriaceae and *Pseudomonas* spp. by using a biochemical test. *Antimicrob Agents Chemother* 2012; **56**: 6437–40.
- Tsakris A, Poulou A, Bogaerts P et al. Evaluation of a new phenotypic OXA-48 disk test for differentiation of OXA-48 carbapenemase-producing Enterobacteriaceae clinical isolates. *J Clin Microbiol* 2015; **53**: 1245–51.

- 14** Hrabák J, Chudáčková E, Papagiannitsis CC. Detection of carbapenemases in Enterobacteriaceae: a challenge for diagnostic microbiological laboratories. *Clin Microbiol Infect* 2014; **20**: 839–53.
- 15** van der Zee A, Roorda L, Bosman G *et al.* Multi-centre evaluation of real-time multiplex PCR for detection of carbapenemase genes OXA-48, VIM, IMP, NDM and KPC. *BMC Infect Dis* 2014; **14**: 27.
- 16** Tato M, Ruiz-Garbajosa P, Traczewski M *et al.* Multisite evaluation of Cepheid Xpert Carba-R assay for detection of carbapenemase-producing organisms in rectal swabs. *J Clin Microbiol* 2016; **54**: 1814–9.
- 17** Ellington MJ, Findlay J, Hopkins KL *et al.* Multicentre evaluation of a real-time PCR assay to detect genes encoding clinically relevant carbapenemases in cultured bacteria. *Int J Antimicrob Agents* 2016; **47**: 151–4.
- 18** Glupczynski Y, Evrard S, Ote I *et al.* Evaluation of two new commercial immunochromatographic assays for the rapid detection of OXA-48 and KPC carbapenemases from cultured bacteria. *J Antimicrob Chemother* 2016; **71**: 1217–22.
- 19** Boutal H, Naas T, Devilliers K *et al.* Development and validation of a lateral flow immunoassay for rapid detection of NDM-producing Enterobacteriaceae. *J Clin Microbiol* 2017; **55**: 2018–29.
- 20** Dortet L, Jousset A, Sainte-Rose V *et al.* Prospective evaluation of the OXA-48 K-SeT assay, an immunochromatographic test for the rapid detection of OXA-48-type carbapenemases. *J Antimicrob Chemother* 2016; **71**: 1834–40.
- 21** Glupczynski Y, Jousset A, Evrard S *et al.* Prospective evaluation of the OKN K-SeT assay, a new multiplex immunochromatographic test for the rapid detection of OXA-48-like, KPC and NDM carbapenemases. *J Antimicrob Chemother* 2017; **72**: 1955–60.
- 22** Notake S, Matsuda M, Tamai K *et al.* Detection of IMP metallo- β -lactamase in carbapenem-nonsusceptible Enterobacteriaceae and non-glucose-fermenting Gram-negative rods by immunochromatography assay. *J Clin Microbiol* 2013; **51**: 1762–8.
- 23** Antonelli A, D'Andrea MM, Vaggelli G *et al.* OXA-372, a novel carbapenem-hydrolysing class D β -lactamase from a *Citrobacter freundii* isolated from a hospital wastewater plant. *J Antimicrob Chemother* 2015; **70**: 2749–56.
- 24** Dabos L, Bogaerts P, Raczynska J *et al.* OXA-517, an extended-spectrum cephalosporin- and carbapenem-hydrolysing OXA-48-like variant. In: *Abstracts of the Twenty-seventh European Congress of Clinical Microbiology and Infectious Diseases, Vienna, Austria, 2017*. Abstract P0234. ESCMID, Basel, Switzerland.
- 25** Dabos L, Bogaerts P, Bonnin R *et al.* Genetic and biochemical characterization of OXA-519, a novel OXA-48-like β -lactamase. In: *Abstracts of the Twenty-seventh European Congress of Clinical Microbiology and Infectious Diseases, Vienna, Austria, 2017*. Abstract P0232. ESCMID, Basel, Switzerland.
- 26** Dabos L, Jousset A, Potron A *et al.* Genetic and biochemical characterization of OXA-535, a novel OXA-48-like enzyme progenitor of OXA-436 from *Shewanella bicestrii*. In: *Abstracts of the Twenty-seventh European Congress of Clinical Microbiology and Infectious Diseases, Vienna, Austria, 2017*. Abstract P0233. ESCMID, Basel, Switzerland.
- 27** Meunier D, Vickers A, Pike R *et al.* Evaluation of the K-SeT R.E.S.I.S.T. immunochromatographic assay for the rapid detection of KPC and OXA-48-like carbapenemases. *J Antimicrob Chemother* 2016; **71**: 2357–9.



Improvement of the Immunochromatographic NG-Test Carba 5 Assay for the Detection of IMP Variants Previously Undetected

Hervé Volland,^a Delphine Girlich,^{b,c} Marine Laguide,^{b,c} Camille Gonzalez,^{b,c} Virginie Paris,^{b,c} Maxime Laroche,^d Saoussen Oueslati,^{b,c} Laurent Dortet,^{b,c,e,f} Stéphanie Simon,^a Thierry Naas^{b,c,e,f}

^aService de Pharmacologie et Immunoanalyse (SPI), CEA, INRA, Laboratoire d'Etudes et de Recherches en Immunanalyse, Université Paris-Saclay, Gif-sur-Yvette, France

^bEA7361 "Structure, Dynamic, Function and Expression of Broad Spectrum β -Lactamases," Université Paris Sud, Université Paris Saclay, LabEx Lermite, Faculty of Medicine, Le Kremlin-Bicêtre, France

^cEvolution and Ecology of Resistance to Antibiotics Unit, Institut Pasteur-APHP, Université Paris Sud, Paris, France

^dNG Biotech, Z.A Courbouton, Guipry, France

^eAssociated French National Reference Center for Antibiotic Resistance: Carbapenemase-producing Enterobacteriaceae, Le Kremlin-Bicêtre, France

^fHygiene Unit, Assistance Publique/Hôpitaux de Paris, Bicêtre Hospital, Le Kremlin-Bicêtre, France

ABSTRACT Here, we evaluated the immunochromatographic assay NG-Test Carba 5v2 (NG-Biotech), with improved IMP variant detection on 31 IMP producers, representing the different branches of the IMP phylogeny, including 32 OXA-48, 19 KPC, 12 VIM, 14 NDM, and 13 multiple carbapenemase producers (CPs), 13 CPs that were not targeted, and 13 carbapenemase-negative isolates. All tested IMP variants were accurately detected without impairing detection of the other carbapenemases. Thus, NG-Test Carba 5v2 is now well adapted to countries with high IMP prevalence and to the epidemiology of CP-*Pseudomonas aeruginosa*, where IMPs are most frequently detected.

KEYWORDS rapid diagnostic, OXA-48, KPC, NDM, VIM, IMP, *Enterobacterales*, *Pseudomonas aeruginosa*, CPEs, detection, LFIA

Carbapenem resistance among Gram-negative bacilli (GNB) (*Enterobacterales*, *Pseudomonas*, and *Acinetobacter* species) has become a major public health issue (1). Resistance to carbapenems can stem from production of carbapenemases or other mechanisms, such as decreased permeability, overproduction of extended-spectrum β -lactamases (ESBL) or cephalosporinases, efflux pumps, or combinations of these mechanisms (2). Carbapenemase producers (CPs) are by far the most worrisome; thus, their rapid detection and identification are essential to help physicians to quickly implement appropriate infection control measures, to adapt antibiotic treatment rapidly, and to optimize care strategies and outcomes (3). Based on their amino acid sequence, carbapenemases are divided into different molecular classes, A, B, and D, of the Ambler classification. Class A (mainly KPC enzymes) and D (mostly OXA-48-like enzymes) carbapenemases are serine active-site enzymes, while class B carbapenemases, which are also called metallo- β -lactamases (MBLs) (mostly enzymes of NDM, VIM, and IMP types), require zinc ions to be active (2). The IMP family of carbapenemases is a very heterogeneous family of enzymes (sharing only 79% amino acid sequence identity), rendering their detection difficult (4–6) (Fig. 1).

Recently, the NG-Test Carba 5 immunochromatographic assay (ICA) (NG Biotech, Guipry, France) was developed to detect the five most widespread carbapenemase families in *Enterobacterales* (CPEs) (i.e., KPC, NDM, VIM, IMP, and OXA-48-like enzymes). It was demonstrated to accurately identify the claimed enzymes in culture and also from positive blood cultures growing with *Enterobacterales* (7, 8). Unlike other ICAs

Citation Volland H, Girlich D, Laguide M, Gonzalez C, Paris V, Laroche M, Oueslati S, Dortet L, Simon S, Naas T. 2020. Improvement of the immunochromatographic NG-Test Carba 5 assay for the detection of IMP variants previously undetected. *Antimicrob Agents Chemother* 64:e01940-19. <https://doi.org/10.1128/AAC.01940-19>.

Copyright © 2019 American Society for Microbiology. All Rights Reserved.
Address correspondence to Thierry Naas, thierry.naas@aphp.fr.

Received 24 September 2019

Returned for modification 22 October 2019

Accepted 28 October 2019

Accepted manuscript posted online 4 November 2019

Published 20 December 2019

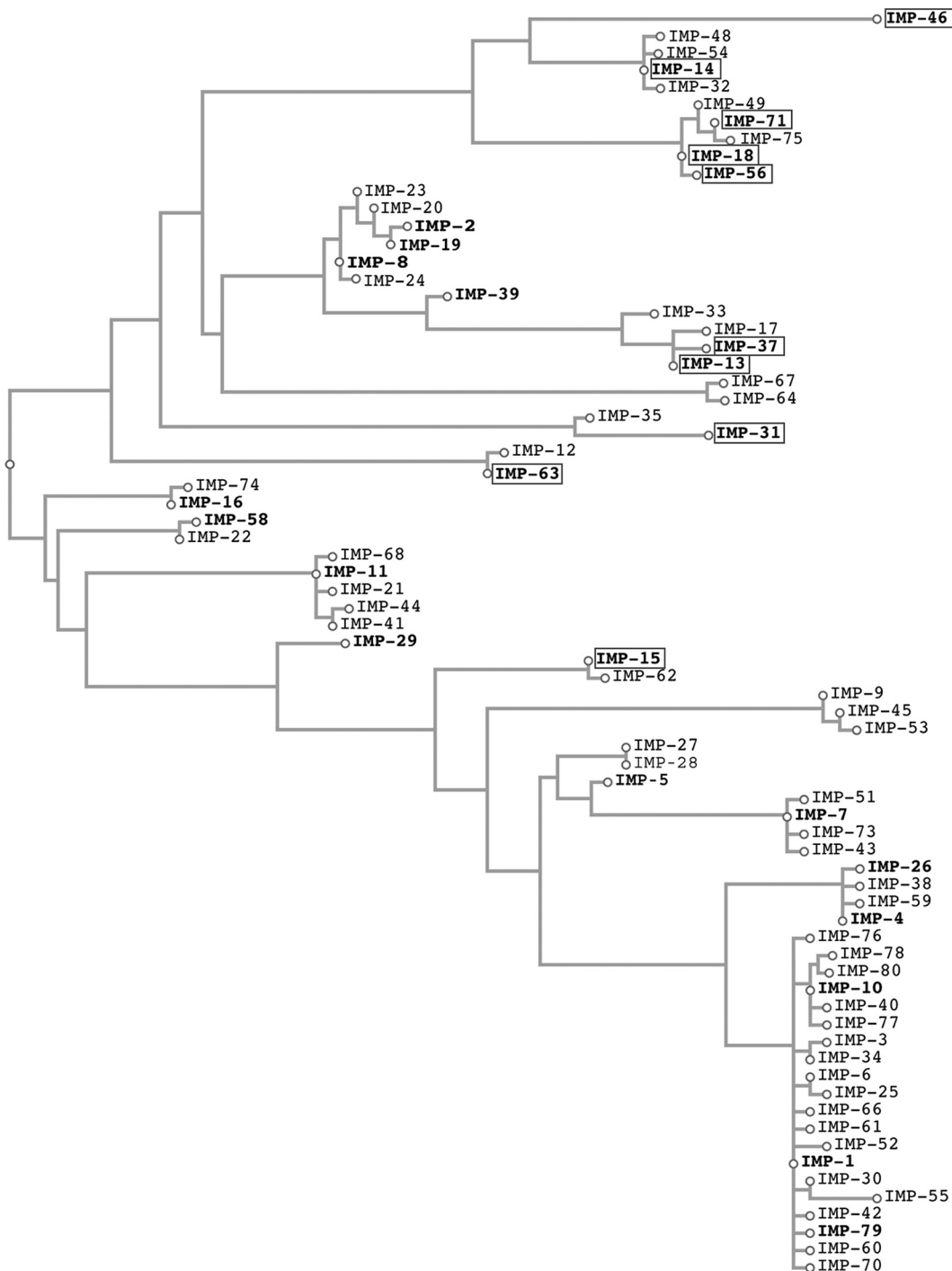


FIG 1 Phylogenetic tree of IMP variants. Amino acid sequences were from the BLDB web site (<http://www.bldb.eu/alignment.php?align=B1:IMP>). Alignment and phylogenetic reconstructions were performed using the function “build” of ETE3 v3.0.0b32 (23), as implemented on the GenomeNet (<https://www.genome.jp/tools/ete/>). A maximum-likelihood tree was inferred using PhyML v20160115 run with model JTT and parameters `-f m -pinv e -o tlr -alpha e -nclases 4 -bootstrap -2` (24). Tested isolates are in boldface, and boxed isolates are those that were not detected with version 1 of the NG-Test Carba 5.

developed to detect CPEs (RESIT-4 OKVN; Coris Bioconcept, Gembloux, Belgium), the NG-Test Carba 5 also targets the IMP type enzymes, which are more prevalent in CPEs from the Asian continent and in nonfermenters worldwide (5, 9). In a recent study, Potron et al. have evaluated the performance of the NG-Test Carba 5 test for the detection of carbapenemase-producing *Pseudomonas* spp. and *Acinetobacter* spp. en-

countered in France (6). The NG-Test Carba 5 allows the detection of 14 out of the 21 IMP variants, with the 7 false-negative results corresponding to the IMP-13 clade (IMP-13 and IMP-37), IMP-14, IMP-15, IMP-18 clade (IMP-18 and IMP-71), and IMP-63 (6). Here, we have evaluated the NG-Test Carba 5v2, a novel version of the test with additional antibodies for the detection of all IMP variants.

Monoclonal antibodies (MAb) derived from IMP-immunized mice (7) were further tested against IMP-13 enzyme. To select the best MAb pairs for the development of the two-site lateral flow immunoassay with IMP-13, a combinatorial analysis was carried out using each MAb either as a capture or gold-labeled antibody as previously described (10). Briefly, the strips were prepared by spotting 0.5 μ l of MAb (500 μ g/ml in 50 mM phosphate buffer, pH 7.4) and then dried. One hundred microliters of a crude IMP-13 extract from *P. aeruginosa* (11) or extraction buffer alone and 10 μ l of colloidal gold-labeled MAb were mixed in microtiter plate wells (Greiner, Paris, France) and allowed to react for 5 min before dipping the strip into the solution. After 30 min of migration, signals were analyzed by eye. The parameters used to select the best MAb pairs were the intensity of the visual signals obtained with IMP-13 crude extract and the absence of signal without IMP-13 (nonspecific signal). The NG-Test Carba 5v2 tests (strip plus cassette) were manufactured by NG Biotech using the additional IMP-13-selected MAbs.

In order to see whether the novel version, NG-Test Carba 5v2, is now able to detect all IMP variants without modifying the biological performances for the other targets, a collection of 147 isolates with whole genome sequence-characterized β -lactamase content were used to evaluate the NG-Test Carba 5v2 and the results compared with those obtained with the NG-Test Carba 5v1. Both assays were used as recommended by the manufacturer. Results were eye read and the time for appearance of a red band specific for a given carbapenemase was recorded. After 15 min of migration, in the absence of a band, the test was considered negative (Table 1).

This collection included 134 carbapenemase producers and 13 non-carbapenemase producers. The produced carbapenemases included 14 NDM, 12 VIM, 31 IMP, 19 KPC, 32 OXA-48, 13 multiple carbapenemases, and 13 other carbapenemases not targeted by the NG-Test Carba 5v2 (Table 1). The 31 IMP variants corresponded to very diverse enzymes, as illustrated in Fig. 1.

The NG-Test Carba 5v2 gave results similar to those of NG-Test Carba 5v1, except for IMP results. The median time for a positive signal was comparable between the two assays, indicating that the addition of novel antibodies did not interfere with the other targets. The NG-Test Carba 5v2 allows the detection of 100% of the IMP variants tested ($n = 31/31$), unlike the NG-Test Carba 5v1, which detects only 67% of the tested variants ($n = 21/31$). The NG-Test Carba 5v2 identified all VIM ($n = 12$) and NDM ($n = 14$) producers with no false-positive results. All OXA-48 carbapenemase variants were correctly identified, including difficult-to-detect variants (OXA-244 and OXA-519), using biochemical tests such as Carba NP (12, 13). It also detects very recently identified variants that have never been tested by ICA (OXA-484, -505, -517, and -793; Table 1) and the distantly related OXA-535 variant (14), which is the progenitor of OXA-436, a distantly related OXA-48 variant responsible for an outbreak associated with several enterobacterial species in Denmark (14–16). Moreover, OXA-163 and OXA-405, two OXA-48 variants that lack significant imipenemase activity (17) but with strong expanded-spectrum hydrolytic activity, were consistently detected. It is still debated whether these enzymes are or are not carbapenemases (17, 18). From the point of view of diagnostic tests based on imipenem hydrolysis, these variants are not carbapenemases (17). These results are in line with an 820-fold decrease in OXA-163 catalytic efficiency for imipenem (19). However, only a 4-fold decrease in catalytic efficiency for meropenem and doripenem compared to that of OXA-48 was observed, suggesting that OXA-163 can still be considered a meropenemase or doripenemase (19). Similarly, as the specific carbapenemase activities of OXA-405 and OXA-163 are comparable (20), it is likely that OXA-405 behaves in a similar manner with respect to meropenem activity. As it has been shown that enzymes with low carbapenem-hydrolyzing activities, such as OXA-163, may develop clinically significant carbapenem resistance when

TABLE 1 Results of the NG-Test Carba 5 v1 and v2 on the collection of *Enterobacteriales*, *Pseudomonas* spp., and *Acinetobacter* spp.

β-Lactam resistance mechanism	Species	No. of isolates	Meropenem MICs (μg/ml)	NG-Test Carba 5 test result ^a												
				v1					v2							
				β-Lactamase	NDM	IMP	VIM	OXA	KPC	Median	NDM	IMP	VIM	OXA	KPC	Median
Non-carbapenemase producers																
Acquired AmpC ESBL + impermeability	<i>Escherichia coli</i>	1	0.02													
	<i>E. coli</i> (1); <i>Klebsiella pneumoniae</i> (3)	4	1–6	ACC-1 CTX-M-15	–	–	–	–	–	–	–	–	–	–	–	
	<i>E. coli</i>	1	0.02	CTX-M-2	–	–	–	–	–	–	–	–	–	–	–	
	<i>K. pneumoniae</i>	1	0.02	CTX-M-14	–	–	–	–	–	–	–	–	–	–	–	
	<i>K. pneumoniae</i>	1	0.02	SHV-38	–	–	–	–	–	–	–	–	–	–	–	
AmpC + impermeability	<i>Enterobacter aerogenes</i>	1	0.02	TEM-24	–	–	–	–	–	–	–	–	–	–	–	
	<i>E. coli</i> (1); <i>Enterobacter cloacae</i> (2); <i>Citrobacter freundii</i> (1)	4	0.25–2	Cephalosporinase ^b	–	–	–	–	–	–	–	–	–	–	–	
	Nontargeted carbapenemases															
Class A	<i>Serratia marcescens</i> (2)	2	8	Sme-2, Sme-4	–	–	–	–	–	–	–	–	–	–	–	
	<i>E. cloacae</i> (1); <i>Enterobacter asburiae</i> (1)	2	8–>32	IMI-1, IMI-2	–	–	–	–	–	–	–	–	–	–	–	
	<i>K. pneumoniae</i> (1); <i>E. cloacae</i> (1)	2	0.19–>32	GES-5	–	–	–	–	–	–	–	–	–	–	–	
	<i>E. cloacae</i>	1	16	FRI-1	–	–	–	–	–	–	–	–	–	–	–	
	<i>Proteus mirabilis</i>	1	0.25	OXA-23	–	–	–	–	–	–	–	–	–	–	–	
Class D	<i>P. mirabilis</i>	1	0.25	OXA-58	–	–	–	–	–	–	–	–	–	–	–	
	<i>C. freundii</i>	1	0.5	OXA-372	–	–	–	–	–	–	–	–	–	–	–	
	<i>C. freundii</i>	1	0.09	LMB-1	–	–	–	–	–	–	–	–	–	–	–	
Class B	<i>E. cloacae</i>	1	8	TMB-1	–	–	–	–	–	–	–	–	–	–	–	
	<i>E. cloacae</i>	1	6	GIM-1	–	–	–	–	–	–	–	–	–	–	–	
Targeted carbapenemases																
NDM type	<i>E. coli</i> (2); <i>K. pneumoniae</i> (2); <i>Providencia rettgeri</i> (1); <i>Salmonella enterica</i> (1)	6	1–>32	NDM-1	40''–3' ^c	–	–	–	–	–	–	2'	40''–3'	–	2'	
	<i>Acinetobacter baumannii</i>	1	>32	NDM-2	2'	–	–	–	–	–	–	2'	–	–	–	
	<i>E. coli</i>	1	>32	NDM-4	2'	–	–	–	–	–	–	2'	–	–	–	
	<i>E. coli</i>	1	>32	NDM-5	45''	–	–	–	–	–	–	45''	–	–	–	
	<i>E. coli</i>	1	8	NDM-6	2'	–	–	–	–	–	–	2'	–	–	–	
	<i>E. coli</i>	1	3	NDM-7	2'	–	–	–	–	–	–	2'	–	–	–	
	<i>E. coli</i>	1	4	NDM-9	1'	–	–	–	–	–	–	1'	–	–	–	
	<i>E. coli</i>	1	8	NDM-11	1'	–	–	–	–	–	–	1'	–	–	–	
	<i>E. coli</i>	1	>32	NDM-19	45''	–	–	–	–	–	–	45''	–	–	–	
	<i>E. coli</i> (1); <i>K. pneumoniae</i> (2); <i>E. cloacae</i> (1); <i>C. freundii</i> (1)	5	1–>32	VIM-1	–	–	–	–	–	–	–	–	–	–	–	2'
VIM type	<i>C. freundii</i> (2); <i>P. aeruginosa</i> (1)	3	>32	VIM-2	–	–	–	–	–	–	–	–	–	–	–	2'30'''
	<i>E. coli</i> (1); <i>E. cloacae</i> (1)	2	4–>32	VIM-4	–	–	–	–	–	–	–	–	–	–	–	1'–2'
	<i>P. aeruginosa</i>	1	<32	VIM-5	–	–	–	–	–	–	–	–	–	–	–	1'
	<i>K. pneumoniae</i>	1	4	VIM-19	–	–	–	–	–	–	–	–	–	–	–	2'
	(Continued on next page)															

TABLE 1 (Continued)

β-Lactam resistance mechanism	NG-Test Carba 5 test result ^a																	
	Species	No. of isolates	Meropenem MICs (μg/ml)	β-Lactamase			V1			V2								
				IMP-1	IMP-2	IMP-3	NDM	IMP	VIM	OXA	KPC	Median	NDM	IMP	VIM	OXA	KPC	Median
IMP type	<i>E. coli</i> (1); <i>K. pneumoniae</i> (1)	2	0.5-8	IMP-1	IMP-2	IMP-3	—	1'-3'	—	1'-3'	—	1'-3'	—	1'-3'	—	1'-3'	—	1'
	<i>P. aeruginosa</i> (2)	2	>32	IMP-2	IMP-2	1'-2'	—	1'-2'	—	1'-2'	—	1'-2'	—	1'-2'	—	1'-2'	—	—
	<i>A. baumannii</i>	1	>32	IMP-4	IMP-4	2	—	2	—	2	—	2	—	2	—	2	—	—
	<i>P. aeruginosa</i>	1	>32	IMP-5	IMP-5	2	—	2	—	2	—	2	—	2	—	2	—	—
	<i>P. aeruginosa</i>	1	>32	IMP-7	IMP-7	1	—	1	—	1	—	1	—	1	—	1	—	—
	<i>E. coli</i> (1); <i>K. pneumoniae</i> (2); <i>E. cloacae</i> (1)	4	0.5-3	IMP-8	IMP-8	1'-2'	—	1'-2'	—	1'-2'	—	1'-2'	—	1'-2'	—	1'-2'	—	—
	<i>S. marcescens</i>	1	4	IMP-10	IMP-10	10	—	10	—	10	—	10	—	10	—	10	—	—
	<i>S. marcescens</i>	2	0.5	IMP-11	IMP-11	1'30"	—	1'30"	—	1'30"	—	1'30"	—	1'30"	—	1'30"	—	—
	<i>P. aeruginosa</i>	2	>32	IMP-13	IMP-13	—	—	—	—	—	—	—	—	—	—	—	—	—
	<i>Acinetobacter nosocomialis</i>	1	>32	IMP-14	IMP-14	—	—	—	—	—	—	—	—	—	—	—	—	—
	<i>P. aeruginosa</i>	1	>32	IMP-15	IMP-15	—	—	—	—	—	—	—	—	—	—	—	—	—
	<i>P. aeruginosa</i>	1	>32	IMP-16	IMP-16	2'	—	2'	—	2'	—	2'	—	2'	—	2'	—	—
	<i>P. aeruginosa</i>	1	>32	IMP-18	IMP-18	—	—	—	—	—	—	—	—	—	—	—	—	—
	<i>P. aeruginosa</i>	1	>32	IMP-19	IMP-19	1'	—	1'	—	1'	—	1'	—	1'	—	1'	—	—
	<i>P. aeruginosa</i>	1	>32	IMP-26	IMP-26	1'	—	1'	—	1'	—	1'	—	1'	—	1'	—	—
	<i>P. aeruginosa</i>	1	>32	IMP-29	IMP-29	45"	—	45"	—	45"	—	45"	—	45"	—	45"	—	—
	<i>P. aeruginosa</i>	1	>32	IMP-31	IMP-31	—	—	—	—	—	—	—	—	—	—	—	—	—
	<i>P. aeruginosa</i>	1	>32	IMP-37	IMP-37	—	—	—	—	—	—	—	—	—	—	—	—	—
	<i>P. aeruginosa</i>	1	>32	IMP-39	IMP-39	1'40"	—	1'40"	—	1'40"	—	1'40"	—	1'40"	—	1'40"	—	—
	<i>P. aeruginosa</i>	1	>32	IMP-46	IMP-46	—	—	—	—	—	—	—	—	—	—	—	—	—
	<i>P. aeruginosa</i>	1	>32	IMP-56	IMP-56	—	—	—	—	—	—	—	—	—	—	—	—	—
	<i>C. freundii</i>	2	>32	IMP-58	IMP-58	1'	—	1'	—	1'	—	1'	—	1'	—	1'	—	—
	<i>P. aeruginosa</i>	1	>32	IMP-63	IMP-63	—	—	—	—	—	—	—	—	—	—	—	—	—
	<i>P. aeruginosa</i>	1	>32	IMP-71	IMP-71	—	—	—	—	—	—	—	—	—	—	—	—	—
	<i>P. aeruginosa</i>	1	>32	IMP-79	IMP-79	2'	—	2'	—	2'	—	2'	—	2'	—	2'	—	—
KPC type	<i>E. coli</i> (3); <i>S. marcescens</i> (1); <i>E. cloacae</i> (2); <i>C. freundii</i> (1)	7	1->32	KPC-2	KPC-2	—	—	—	—	—	—	—	—	—	—	—	—	2'-2'30" 2'
	<i>E. coli</i> (1); <i>K. pneumoniae</i> (3)	4	2->32	KPC-3	KPC-3	—	—	—	—	—	—	—	—	—	—	—	—	1'-3'
	<i>E. coli</i>	1	0.25	KPC-5	KPC-5	—	—	—	—	—	—	—	—	—	—	—	—	1'
	<i>E. coli</i>	1	3	KPC-6	KPC-6	—	—	—	—	—	—	—	—	—	—	—	—	1'40"
	<i>E. coli</i>	1	0.25	KPC-7	KPC-7	—	—	—	—	—	—	—	—	—	—	—	—	1'40"
	<i>E. coli</i>	1	0.03	KPC-14	KPC-14	—	—	—	—	—	—	—	—	—	—	—	—	1'30"
	<i>E. coli</i>	1	0.03	KPC-28	KPC-28	—	—	—	—	—	—	—	—	—	—	—	—	2'30"
	<i>E. coli</i>	1	0.03	KPC-31	KPC-31	—	—	—	—	—	—	—	—	—	—	—	—	—
	<i>E. coli</i>	1	0.03	KPC-33	KPC-33	—	—	—	—	—	—	—	—	—	—	—	—	—
	<i>K. pneumoniae</i>	1	0.12	KPC-39	KPC-39	—	—	—	—	—	—	—	—	—	—	—	—	3'

(Continued on next page)

expressed in bacterial isolates with decreased outer membrane permeability (12, 21), it is important that these two OXA variants are efficiently detected. Among the KPC-positive isolates, 90% ($n = 17/19$) were correctly identified. The two isolates that yielded negative results after 15 min of incubation corresponded to KPC-31 and KPC-33, two rare D179Y variants of KPC-3 and KPC-2, respectively, known to be responsible for ceftazidime/avibactam resistance and for not being detected using ICA tests such as KPC K-SET (Coris BioConcept) and NG-Test Carba 5v1 (NG Biotech). Of note, this D179Y variant impaired the carbapenem hydrolytic activity of this enzyme, which cannot be considered a carbapenemase anymore, leading to negative results with biochemical tests such as the Carba NP test (22). All 13 non-carbapenemase-producing isolates and all 13 isolates producing a carbapenemase different from those targeted by the NG-Test Carba 5v2 gave negative test results, demonstrating no cross-reactivity between carbapenemases.

In summary, the NG-Test Carba 5v2 is a significant improvement, as all of the tested IMP variants were detected without impairing the detection of the other four carbapenemases. The NG-Test Carba 5v2 is now well adapted to countries where the epidemiology of IMP producers is high, especially to CP-*P. aeruginosa* isolates, where the proportion of IMP producers is higher, e.g., <1% in CPEs and 8% in *P. aeruginosa* in 2017 in France (http://www.cnr-resistance-antibiotiques.fr/ressources/pages/Rapport_CNR_2017_VF_2.pdf). Considering the French epidemiology of CP-*P. aeruginosa* in 2017, the NG-Test Carba 5v2 might have correctly detected 97.4% of them (missing 10 GES and one DIM producer).

ACKNOWLEDGMENTS

We acknowledge the NG Biotech Company for providing the NG-Test Carba 5 v1 and v2 assays.

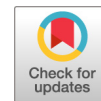
This work was partially funded by the University Paris-Sud, France. L.D., T.N., S.O., and D.G. are members of the Laboratory of Excellence in Research on Medication and Innovative Therapeutics (LERMIT), supported by a grant from the French National Research Agency (ANR-10-LABX-33).

L.D. is coinventor of the Carba NP test, a patent for which has been licensed to bioMérieux (La Balmes les Grottes, France).


REFERENCES

- Eichenberger EM, Thaden JT. 2019. Epidemiology and mechanisms of resistance of extensively drug resistant gram-negative bacteria. *Antibiotics* 8:37. <https://doi.org/10.3390/antibiotics8020037>.
- Nordmann P, Naas T, Poirel L. 2011. Global spread of carbapenemase-producing Enterobacteriaceae. *Emerg Infect Dis* 17:1791–1798. <https://doi.org/10.3201/eid1710.110655>.
- Logan LK, Weinstein RA. 2017. The epidemiology of carbapenem-resistant Enterobacteriaceae: the impact and evolution of a global menace. *J Infect Dis* 215:S28–S36. <https://doi.org/10.1093/infdis/jiw282>.
- Naas T, Oueslati S, Bonnin RA, Dabos ML, Zavala A, Dortet L, Retailliau P, Iorga BI. 2017. Beta-lactamase DataBase (BLDB)—structure and function. *J Enzyme Inhib Med Chem* 32:917–919. <https://doi.org/10.1080/14756366.2017.1344235>.
- Hopkins KL, Meunier D, Naas T, Volland H, Woodford N. 2018. Evaluation of the NG-Test Carba 5 multiplex immunochromatographic assay for the detection of KPC, OXA-48-like, NDM, VIM and IMP carbapenemases. *J Antimicrob Chemother* 73:3523–3526. <https://doi.org/10.1093/jac/dky342>.
- Potron A, Fournier D, Emeraud C, Tripoiny P, Plésiat P, Naas T, Dortet L. 2019. Evaluation of the immunochromatographic NG-Test Carba 5 for rapid identification of carbapenemase in nonfermenters. *Antimicrob Agents Chemother* 63:e00968. <https://doi.org/10.1128/AAC.00968-19>.
- Boutal H, Vogel A, Bernabeu S, Devilliers K, Creton E, Cotellon G, Plaisance M, Oueslati S, Dortet L, Jousset A, Simon S, Naas T, Volland H. 2018. A multiplex lateral flow immunoassay for the rapid identification of NDM-, KPC-, IMP- and VIM-type and OXA-48-like carbapenemase-producing Enterobacteriaceae. *J Antimicrob Chemother* 73:909–915. <https://doi.org/10.1093/jac/dkx521>.
- Takissian J, Bonnin RA, Naas T, Dortet L. 2019. NG-Test Carba 5 for rapid detection of carbapenemase-producing Enterobacteriales from positive blood cultures. *Antimicrob Agents Chemother* 63:e00011-19. <https://doi.org/10.1128/AAC.00011-19>.
- Greissl C, Saleh A, Hamprecht A. 2019. Rapid detection of OXA-48-like, KPC, NDM, and VIM carbapenemases in Enterobacteriales by a new multiplex immunochromatographic test. *Eur J Clin Microbiol Infect Dis* 38:331–335. <https://doi.org/10.1007/s10096-018-3432-2>.
- Boutal H, Naas T, Devilliers K, Oueslati S, Dortet L, Bernabeu S, Simon S, Volland H. 2017. Development and validation of a lateral flow immunoassay for rapid detection of NDM-producing Enterobacteriaceae. *J Clin Microbiol* 55:2018–2029. <https://doi.org/10.1128/JCM.00248-17>.
- Naas T, Bogaerts P, Kostyanov T, Cuzon G, Huang TD, Ozsu S, Nordmann P, Glupczynski Y. 2011. Silent spread of IMP-13-producing *Pseudomonas aeruginosa* belonging to sequence type 621 in Belgium. *J Antimicrob Chemother* 66:2178–2179. <https://doi.org/10.1093/jac/dkr252>.
- Dabos L, Bogaerts P, Bonnin RA, Zavala A, Sacré P, Iorga BI, Huang DT, Glupczynski Y, Naas T. 2018. Genetic and biochemical characterization of OXA-519, a novel OXA-48-like β -lactamase. *Antimicrob Agents Chemother* 62:e00469-18. <https://doi.org/10.1128/AAC.00469-18>.
- Hoyos-Mallemot Y, Naas T, Bonnin RA, Patino R, Glaser P, Fortineau N, Dortet L. 2017. OXA-244-producing *Escherichia coli* isolates, a challenge for clinical microbiology laboratories. *Antimicrob Agents Chemother* 61:e00818-17. <https://doi.org/10.1128/AAC.00818-17>.
- Dabos L, Jousset AB, Bonnin RA, Fortineau N, Zavala A, Retailliau P, Iorga BI, Naas T. 2018. Genetic and biochemical characterization of OXA-535, a distantly related OXA-48-like β -lactamase. *Antimicrob Agents Chemother* 62:e01198-18. <https://doi.org/10.1128/AAC.01198-18>.
- Jousset AB, Dabos L, Bonnin RA, Girlich D, Potron A, Cabanel N, Dortet

- L, Glaser P, Naas T. 2017. CTX-M-15-producing *Shewanella* species clinical isolate expressing OXA-535, a chromosome-encoded OXA-48 variant, putative progenitor of the plasmid-encoded OXA-436. *Antimicrob Agents Chemother* 62:e01879-17. <https://doi.org/10.1128/AAC.01879-17>.
16. Samuelsen Ø, Hansen F, Aasnæs B, Hasman H, Lund BA, Leiros H-K, Lilje B, Janice J, Jakobsen L, Littauer P, Søres LM, Holzknecht BJ, Andersen LP, Stegger M, Andersen PS, Hammerum AM. 2017. Dissemination and characteristics of a novel plasmid-encoded carbapenem-hydrolyzing class D β -lactamase, OXA-436, found in isolates from four patients at six different hospitals in Denmark. *Antimicrob Agents Chemother* 62:e01260-17. <https://doi.org/10.1128/AAC.01260-17>.
17. Dabos L, Oueslati S, Bernabeu S, Jousset AB, Dortet L, Naas T. 2019. Oxa-48-like enzymes: carbapenemase or not? AAR-652. *ASM Microbe*, 20–27 June 2019, San Francisco, CA, USA.
18. Arlet G, Decré D, Lavollay M, Podglajen I. 2017. Reply to “noncarbapenemase OXA-48 variants (OXA-163 and OXA-405) falsely detected as carbapenemases by the β -Carba test.” *J Clin Microbiol* 55:656–657. <https://doi.org/10.1128/JCM.02114-16>.
19. Stojanoski V, Chow DC, Fryszczyn B, Hu L, Nordmann P, Poirel L, Sankaran B, Prasad BV, Palzkill T. 2015. Structural basis for different substrate profiles of two closely related class D β -lactamases and their inhibition by halogens. *Biochemistry* 54:3370–3380. <https://doi.org/10.1021/acs.biochem.5b00298>.
20. Dortet L, Oueslati S, Jeannot K, Tandé D, Naas T, Nordmann P. 2015. Genetic and biochemical characterization of OXA-405, an OXA-48-type extended-spectrum β -lactamase without significant carbapenemase activity. *Antimicrob Agents Chemother* 59:3823–3828. <https://doi.org/10.1128/AAC.05058-14>.
21. Abdelaziz MO, Bonura C, Aleo A, El-Domany RA, Fasciana T, Mammina C. 2012. OXA-163-producing *Klebsiella pneumoniae* in Cairo, Egypt, in 2009 and 2010. *J Clin Microbiol* 50:2489–2491. <https://doi.org/10.1128/JCM.06710-11>.
22. Antonelli A, Giani T, Di Pilato V, Riccobono E, Perriello G, Mencacci A, Rossolini GM. 2019. KPC-31 expressed in a ceftazidime/avibactam-resistant *Klebsiella pneumoniae* is associated with relevant detection issues. *J Antimicrob Chemother* 74:2464–2466. <https://doi.org/10.1093/jac/dkz156>.
23. Huerta-Cepas J, Serra F, Bork P. 2016. ETE 3: reconstruction, analysis, and visualization of phylogenomic data. *Mol Biol Evol* 33:1635–1638. <https://doi.org/10.1093/molbev/msw046>.
24. Guindon S, Dufayard JF, Lefort V, Anisimova M, Hordijk W, Gascuel O. 2010. New algorithms and methods to estimate maximum-likelihood phylogenies: assessing the performance of PhyML 3.0. *Syst Biol* 59:307–321. <https://doi.org/10.1093/sysbio/syq010>.



Evaluation of the Amplidiag CarbaR+VRE Kit for Accurate Detection of Carbapenemase-Producing Bacteria

Saoussen Oueslati,^{a,b,c} Delphine Girlich,^{a,b,c} Laurent Dortet,^{a,b,c,d}  Thierry Naas^{a,b,c,d}

^aBacteriology-Hygiene Unit, Assistance Publique/Hôpitaux de Paris, Bicêtre Hospital, Le Kremlin-Bicêtre, France

^bEA7361 "Structure, dynamic, function and expression of broad spectrum β -lactamases," Université Paris-Sud, Université Paris-Saclay, LabEx Lermite, Faculty of Medicine, Le Kremlin-Bicêtre, France

^cAssociated French National Reference Center for Antibiotic Resistance: Carbapenemase-producing Enterobacteriaceae, Le Kremlin-Bicêtre, France

^dEvolution and Ecology of Resistance to Antibiotics Unit, Institut Pasteur-APHP-Université Paris-Sud, Paris, France

ABSTRACT As carbapenemase-producing Gram-negative bacilli (CP-GNB) (*Enterobacteriaceae*, *Pseudomonadaceae*, and *Acinetobacter* spp.) are becoming a major public health issue, there is an urgent need for accurate and fast diagnostic tests. The Amplidiag CarbaR+VRE assay is a multiplex nucleic acid-based *in vitro* diagnostic test intended for the detection of CP-GNB and vancomycin-resistant enterococci (VRE) from cultured colonies. We have evaluated its ability to detect carbapenemase genes in 100 well-characterized GNB and in 200 consecutive enterobacterial isolates with reduced susceptibility to carbapenems that were referred to the French National Reference Center for carbapenem resistance. The assay has been validated on purified DNA but also directly on colonies. The Amplidiag CarbaR+VRE assay could detect all KPC, NDM, VIM, IMP, and OXA-48-like variants tested and all acquired carbapenem-hydrolyzing oxacillinases from *Acinetobacter baumannii* (OXA-23, OXA-24/-40, and OXA-58) as well as the overexpressed chromosomally encoded OXA-51-like β -lactamase associated with an upstream inserted *ISAbal1*. However, as claimed by the manufacturer, other carbapenemases such as GES-like carbapenemases (GES-2, GES-5, and GES-14), GIM-1, AIM-1, SPM-1, DIM-1, OXA-198 in *Pseudomonas aeruginosa*, or OXA-143-like in *A. baumannii* were not detected. Amplidiag CarbaR+VRE's performance values were high (100% sensitivity and 99% specificity) as it could detect the five major carbapenemases—NDM, VIM, IMP, KPC, and OXA-48—as well as OXA-type carbapenemases from *Acinetobacter* spp. that are currently emerging also among *Proteus mirabilis* and other enterobacterial isolates. It can provide a result directly from colonies growing on Mueller-Hinton (MH) agar or on selective screening medium in less than 2 h. Further evaluations are now necessary to determine the performance values directly on rectal swabs.

KEYWORDS multiplex PCR, real-time detection, screening, confirmation, carbapenemase, molecular methods

Carbapenemase-producing *Enterobacteriaceae* (CPE) and nonfermenters (CPNF; *Pseudomonadaceae* and *Acinetobacter* species) have increasingly been reported worldwide (1, 2). The most clinically relevant carbapenemases belong to either Ambler class A (KPC type); Ambler class B, i.e., metallo- β -lactamases (MBLs) (such as IMP, VIM, and NDM types); or Ambler class D, such as (i) OXA-48-like in *Enterobacteriaceae*; (ii) OXA-23, OXA-24/-40, OXA-58, OXA-143, and the overexpressed intrinsic OXA-51-like enzymes in *Acinetobacter* spp.; and (iii) OXA-198 in *Pseudomonas aeruginosa* (3–6).

There is a large heterogeneity of carbapenem resistance mechanisms depending on the bacterial species and its geographical location. Concerning *Enterobacteriaceae*, KPC

Received 25 July 2017 Returned for modification 20 August 2017 Accepted 2 January 2018

Accepted manuscript posted online 5 January 2018

Citation Oueslati S, Girlich D, Dortet L, Naas T. 2018. Evaluation of the Amplidiag CarbaR+VRE kit for accurate detection of carbapenemase-producing bacteria. *J Clin Microbiol* 56:e01092-17. <https://doi.org/10.1128/JCM.01092-17>.

Editor Karen C. Carroll, Johns Hopkins University School of Medicine

Copyright © 2018 American Society for Microbiology. All Rights Reserved.

Address correspondence to Thierry Naas, thierry.naas@aphp.fr.

dominates in the United States, Greece, Italy, and Israel (1, 4). The IMP-1 enzyme is mostly prevalent in Japan, and OXA-48-like carbapenemases are of great concern in the Middle East, in most Mediterranean countries, and in many European countries such as France, where a large variety of enzymes are present (7). In *Pseudomonas* spp. and *Acinetobacter* spp., Ambler class A, B, and D carbapenemases have been detected. In addition to the acquired OXA carbapenemases (mostly OXA-23, OXA-24/-40, OXA-58, and OXA-143), the *Acinetobacter baumannii*-*Acinetobacter calcoaceticus* complex possesses a chromosomally encoded OXA-51-like enzyme with weak carbapenemase activity (6). However, transposition of an insertion sequence (IS), mostly IS*Aba1*, upstream of the *bla*_{OXA-51-like} gene can lead to overexpression of the latter, resulting in carbapenem resistance (5). Currently, in the United States and Europe, acquired OXA carbapenemase production (particularly of OXA-23) is the most prevalent mechanism among *A. baumannii* isolates. At the opposite end, mutations or the loss of expression in OprD porin, even in the absence of any carbapenemase, is the primary mechanism of resistance to imipenem among *P. aeruginosa* species (5). However, in *Pseudomonas* spp. the most prevalent carbapenemases worldwide are of the VIM and IMP types (5).

Simple, rapid, and accurate methods are needed to detect all carbapenemase producers and discriminate them among non-carbapenemase producers in order to implement proper infection control measures to prevent further spread in hospitals. Various tests (combined with algorithms) have been developed for the early detection of carbapenemase producers: (i) algorithms based on disc diffusion (8–11); (ii) combination disc diffusion assays (9); (iii) tests able to detect a carbapenem-hydrolyzing activity, such as the Carba NP test and derivatives (12), matrix-assisted laser desorption ionization–time of flight (MALDI-TOF) protocols (13), the BYG test (14), the carbapenem inactivation method (CIM) test (15), and the β -Carba test (16); (iv) immunochromatographic tests for the rapid detection of KPC, OXA-48-type, and NDM carbapenemases (17, 18); and (v) molecular biology-based techniques that all aim to detect the most widespread carbapenemase-encoding genes from bacterial colonies and/or directly from clinical samples (such as rectal swabs) (19, 20).

Molecular diagnostic assays include DNA amplification-based methods: PCR, loop-mediated isothermal amplification (LAMP), microarrays, and whole-genome sequencing (WGS) (19, 21, 22). These methods detect the presence of a carbapenemase gene likely accounting for carbapenem resistance (19). The most common commercially available molecular assays are (i) the Xpert Carba-R kit (Cepheid, Sunnyvale, CA, USA), which detects KPC, NDM, VIM, IMP-1-like, and OXA-48-like carbapenemases; (ii) Eazyplex SuperBug CRE (Amplex Biosystems GmbH, Giessen, Germany), which detects KPC, NDM, VIM, and OXA-48 carbapenemases; (iii) Eazyplex complete A (Amplex Biosystems), which detects also OXA-23, OXA-40, and OXA-58 from *Acinetobacter* spp.; and (iv) the Check-Direct CPE assay (Check-Points, Wageningen, The Netherlands), which detects KPC, NDM, VIM, and OXA-48. Most of these assays detect at least the four most prevalent carbapenemases, representing more than 95% of the carbapenemases produced by *Enterobacteriaceae* in France (19, 20, 23).

Here, we have evaluated the performance of Amplidiag CarbaR+VRE (Mobidiag Ltd., Espoo, Finland), a qualitative multiplexed nucleic acid-based *in vitro* diagnostic test intended for the detection of carbapenemase-encoding genes in *Enterobacteriaceae* and nonfermenting rods as well as vancomycin (Van) resistance related to ligase genes *vanA* and *vanB* in enterococci (VRE).

(Part of these results have been presented at ECCMID 2017, Vienna, Austria.)

MATERIALS AND METHODS

Bacterial isolates. A total of 100 collection isolates with characterized β -lactamase content were used in this study. They included 50 *Enterobacteriaceae*, 30 *Pseudomonas* species, and 20 *Acinetobacter baumannii* isolates (see Tables S1, S2, S3, S4, and S5 in the supplemental material). These isolates comprised 79 carbapenemase-producing Gram-negative bacilli (CP-GNB) and 21 non-CP-GNB. The 79 CP-GNB consisted of 41 *Enterobacteriaceae* (9 KPC, 5 NDM, 4 VIM, 3 IMP, and 15 OXA-48-like producers and 5 isolates producing multiple carbapenemases [three NDM plus OXA-48-like, one NDM-1 plus VIM-2, and one VIM-4 plus OXA-48] [Table S2]), 20 *P. aeruginosa* isolates (2 KPC-2, 2 GES-like, 7 VIM-like, 4 IMP-like, 1 GIM-1, 1 AIM-1, 1 SPM-1, 1 DIM-1, and 1 OXA-198) (Table S3), and 18 *Acinetobacter* isolates (4

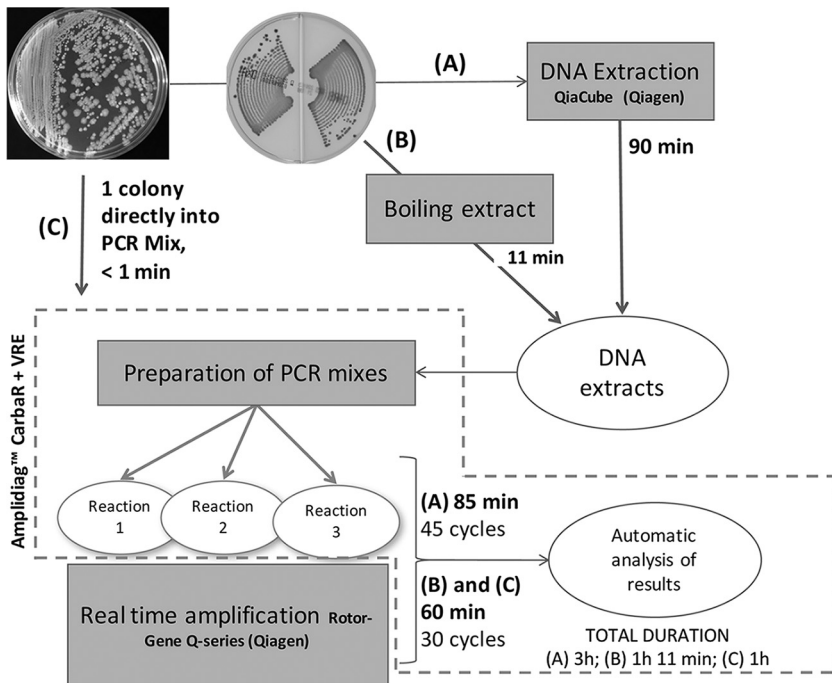


FIG 1 Experimental procedures. (A) Experimental setup as recommended by the manufacturer. As DNA extraction is open, the QIAcube automated DNA extractor was used. (B) Boiling DNA extraction. (C) One colony was picked three times in each 20- μ l PCR tube. PCR amplification results have been automatically interpreted using the manufacturer's proprietary software. The total duration of the process is also indicated.

ISAb1-OXA-51-like, 3 OXA-23, 2 OXA-24/-40, 2 OXA-58, 2 OXA-143-like, 2 NDM, 1 IMP, 1 VIM and 1 GES-14) (Table S4). Non-CP-GNB ($n = 21$) were 9 *Enterobacteriaceae*, 10 *P. aeruginosa*, and 2 *A. baumannii* isolates. Non-CP-GNB also included 2 OXA-48-like producers that are devoid of carbapenem-hydrolytic activity (OXA-163 and OXA-405) (22–24), which usually give false-positive results with molecular methods (Table S2) (15). A collection of well-characterized *Proteus mirabilis* isolates have been tested subsequently. These isolates comprised 10 carbapenemase producers (8 OXA-23 and 2 OXA-58) and 2 non-carbapenemase producers.

From 20 January to 10 February 2016, 200 consecutive enterobacterial isolates were referred to the French National Reference Center (F-NRC) for Antibiotic Resistance for evaluation. Reidentification of these 200 isolates revealed 198 *Enterobacteriaceae* and 2 *A. baumannii* isolates.

Susceptibility testing. Antimicrobial susceptibilities were determined by the disc diffusion technique on Mueller-Hinton (MH) agar (Bio-Rad, Marnes-La-Coquette, France) and interpreted according to the EUCAST breakpoints as updated in 2016 (<http://www.eucast.org>). MICs were determined using the Etest technique (bioMérieux).

Carbapenemase detection. Carbapenemase activity was evidenced in *Enterobacteriaceae* using the updated version of the Carba NP test (12), and carbapenemase genes were detected using an in-house PCR-sequencing approach directly on colonies (6, 15, 21).

Automated DNA extraction from cultured bacterial colonies. Fresh overnight bacterial cultures (on MH agar) were used for DNA extraction with a QIAamp DNA minikit (Qiagen, Les Ulis, France) and the QIAcube instrument (Qiagen, Courtaboeuf, France). A full loop of colonies was suspended in 180 μ l of tissue lysis (ATL; Qiagen) buffer and processed in the automated extractor according to the protocol suggested by the manufacturer for bacterial pellets. Total extraction time was 1 h. Five microliters of this DNA was used as sample in a 20- μ l PCR mixture.

Whole-cell DNA extracted by boiling. One colony of each bacterial strain was suspended in 100 μ l of distilled water. After 10 min at 100°C on a dry heating block (Thermo Fisher), the suspensions were centrifuged (1 min at 10,000 rpm). Total extraction time was 11 min. Five microliters of supernatant was used in a 20- μ l PCR assay mixture.

Direct amplification. One colony was pricked three times with the tip of three loops of 1 μ l each, and bacteria of each tip were dispersed directly into each PCR tube containing 20 μ l of PCR mix (see Tables 2 and S5).

Real-time PCR assay (Amplidiag CarbaR+VRE assay). The Amplidiag CarbaR+VRE multiplex amplification was performed to detect carbapenemase (and vancomycin resistance) genes using a fluorophore-labeled TaqMan probe (Fig. 1). The markers detected by the assay are listed in Table S6. Amplidiag CarbaR+VRE comprises required test reagents for PCR and analysis software. The sample material is DNA extracted from a bacterial culture. Assays are performed in 3 reactions per sample,

TABLE 1 Global performance of the Amplidiag CarbaR+VRE assay^a

Test parameter	% for isolate group (95% CI)			
	Prospective (all isolates) (n = 200)	<i>Enterobacteriaceae</i> (n = 50)	<i>Pseudomonas</i> spp. (n = 30)	<i>A. baumannii</i> (n = 20)
Sensitivity	100 (95.4–100)	100 (85.6–100)	100 (71.7–100)	100 (74.7–100)
Specificity	100 (95.3–100)	88.9 (50.7–99.4)	100 (65.6–100)	100 (19.8–100)
PPV	100 (95.4–100)	NA	NA	NA
NPV	100 (95.3–100)	NA	NA	NA

^aAbbreviations: NA, not applicable; PPV, positive predictive value; NPV, negative predictive value.

according to the fluorophores indicated in Table S6. The Amplidiag CarbaR+VRE kit obtained CE marking for *in vitro* diagnostic kits (CE-IVD) on 8 December 2015. The recommended DNA extraction method for pure culture samples to be used in conjunction with the Amplidiag CarbaR+VRE assay is the “Generic 2.0.1” protocol of NucliSENS easyMAG (bioMérieux) or the Amplidiag Easy system (provided by M-bidiag). Other extraction methods could be used with thorough validation by the users (such as for the QIAcube instrument). Concerning PCR instrumentation, the kit is validated on the Rotorgene (Qiagen), CFX96 (Bio-Rad), and ABI7500 (Applied Biosystems) systems.

The assay is divided into three multiplex PCRs, each of which amplifies a specific group of target genes: (i) *Acinetobacter* oxacillinase genes (*bla*_{OXA-23}, *bla*_{OXA-40}, *bla*_{OXA-58}, and *bla*_{OXA-51} with upstream *ISAbal*); (ii) *bla*_{OXA-48-like}, *bla*_{NDM}, *bla*_{VIM}, *bla*_{IMP}, and *bla*_{KPC}; and (iii) *vanA* and *vanB*. Each mix contained 10 μ l of 2 \times PCR master mix, 5 μ l of assay mix, and 5 μ l of DNA (or a bacterial suspension in water for direct amplification assay on one colony pricked three times). The real-time PCR Rotorgene 6000 amplification-detection system (Qiagen) was used. The total run time was 85 min, for 45 cycles of amplifications (recommended by the manufacturer), and 60 min when reducing the number of cycles to 30 (for time optimization), and analysis was available immediately after the run. Results were automatically interpreted using the proprietary analyzer software that analyzes the quantitative PCR (qPCR) raw data obtained in each experiment. To prevent cross talk, the users have to calibrate the system with a DNA calibrator as recommended. The results were represented in several ways: a plate, a graph, and a table panel. The plate panel contains positive or negative symbols and possible warnings and errors related to the analyzed well. The graph panel contains normalized fluorescence intensity and cycle numbers. The table panel contains all results (positive, negative, quantification cycle [*C*_q] values, warnings, and errors). The software considers that the sample is positive when the *C*_q is lower than 35.

Statistical analysis. The sensitivity, specificity, positive predictive value, and negative predictive value of the Amplidiag CarbaR+VRE assay were calculated with their respective 95% confidence intervals (95% CIs) using the free software vassarStats (website for statistical computation) at <http://vassarstats.net/>. The gold standard was PCR followed by sequencing.

RESULTS AND DISCUSSION

The Amplidiag CarbaR+VRE has been tested on a collection of 100 characterized isolates expressing various β -lactamases and on 200 consecutive enterobacterial isolates with reduced susceptibility to at least one carbapenem (imipenem, meropenem, or ertapenem) according to EUCAST guidelines as updated in 2016 (<http://www.eucast.org>) and referred to the Associated French National Reference Center (F-NRC) for Antimicrobial Resistance dedicated to carbapenem-resistant *Enterobacteriaceae* from 20 January to 10 February 2016. The markers detected by this assay are *bla*_{KPC-like}, *bla*_{NDM-like}, *bla*_{VIM-like}, *bla*_{IMP-like}, and *bla*_{OXA-48-like}; *Acinetobacter*-related OXA genes, including *bla*_{OXA-23}, *bla*_{OXA-24/40}, *bla*_{OXA-58}, and *bla*_{OXA-51} with upstream *ISAbal*; and *vanA* and *vanB* for enterococci. The last parameter was not evaluated here.

Retrospective evaluation of a collection of well-characterized *Enterobacteriaceae*, *P. aeruginosa*, and *A. baumannii* isolates. During this retrospective evaluation, the Amplidiag CarbaR+VRE assay was used as recommended by the manufacturer, on QIAcube-extracted DNA recovered from fresh overnight bacterial colonies.

In *Enterobacteriaceae*, the Amplidiag CarbaR+VRE assay detected all KPC, NDM, VIM, IMP, and OXA-48 producers. In addition, strains that produce an OXA-48 variant with carbapenemase activity, including OXA-162, -181, -204, -232, and -244, were also accurately detected (see Table S2 in the supplemental material). In multiple carbapenemase producers, all resistance determinants were correctly identified (Table 1). None of the non-carbapenemase producers gave positive PCR results, except one *Serratia marcescens* isolate that produced OXA-405, an OXA-48 variant that lacked carbapenemase activity but gained efficient expanded-spectrum cephalosporin hydrolytic activity due to a 4-amino-acid deletion in the active site (Table 1) (24). Consequently, and as

already observed with several other molecular assays (23), this OXA-405-producing *S. marcescens* isolate was considered a false positive. Surprisingly, as opposed to most of the other molecular assays (23), OXA-163, another OXA-48 variant with a slightly different 4-amino-acid deletion in the active site but also lacking carbapenem-hydrolytic activity, was not detected and thus, this isolate was correctly identified as a non-carbapenemase producer (Table S2). Using this strain collection ($n = 50$), the overall sensitivity and specificity were 100% (95% confidence interval [95% CI] = 85.6% to 99.9%) and 88.9% (95% CI = 50.7% to 99.4%) for the detection of carbapenemase-producing *Enterobacteriaceae* (CPE), respectively (Table 1).

Concerning *Pseudomonadaceae*, all KPC, VIM, and IMP producers were correctly detected (Table S3). As claimed by the manufacturer, other carbapenemases such as GES-like carbapenemases (GES-2 and GES-5), GIM-1, AIM-1, SPM-1, DIM-1, and OXA-198 were not detected (Table S3). All non-carbapenemase producers gave a negative result. Excluding strains producing rare carbapenemases (7/30) that are not targeted by the assay, the overall sensitivity and specificity were 100% (95% CI = 71.7% to 100%) and 100% (95% CI = 65.6% to 100%) for the detection of carbapenemase-producing *Pseudomonadaceae*, respectively (Table 1).

The F-NRC for multidrug-resistant (MDR) *P. aeruginosa* isolates showed that between 2013 and 2016 most of the carbapenem resistance was due to OprD mutations (76%) and only 24% was due to carbapenemases. VIM (72.8%), KPC (0.4%), and IMP (15.6%) enzymes would have been identified with this assay, while DIM (0.2%) and GES-carbapenemases (11%) would have been missed (http://www.cnr-resistance-antibiotiques.fr/ressources/pages/Rapport_CNR_2016.pdf). Thus, 88.8% of the currently spreading carbapenemases in *P. aeruginosa* in France would be identified with the Amplidiag CarbaR+VRE assay.

Among *A. baumannii* isolates, the Amplidiag CarbaR+VRE assay could detect all OXA-23-like, OXA-24/-40-like, and OXA-58-like enzymes as well as overexpression of the chromosomally encoded OXA-51-like β -lactamases, due to the presence of *ISAbal* upstream of the *bla*_{OXA-51-like} genes (Table S4). As claimed by the manufacturer, carbapenemases of GES type (e.g., GES-14) and of the OXA-143 group (e.g., OXA-143 and OXA-243) were not detected (Table S4). Of note, carbapenem-resistant *A. baumannii* isolates have become increasingly frequently isolated in Brazil, and those producing OXA-23 and OXA-143-like enzymes are the most prevalent (25). Excluding strains producing a rare carbapenemase (3/20) that is not targeted by the assay, the overall sensitivity and specificity were 100% (95% CI = 74.7% to 100%) and 100% (95% CI = 19.8% to 100%) for the detection of carbapenemase-producing *A. baumannii*, respectively (Table S4). During 2013 to 2016, the F-NRC for *A. baumannii* revealed that most of the carbapenem resistance was due to OXA-23 producers (84.4%), followed by producers of OXA-40 (5.4%), OXA-58 (2.2%), NDM (3.6%), and *ISAbal*-OXA-51 (4.4%) (http://www.cnr-resistance-antibiotiques.fr/ressources/pages/Rapport_CNR_2016.pdf). Thus, using the Amplidiag CarbaR+VRE assay, all the carbapenemase-producing *A. baumannii* isolates would have been identified.

One of the limitations of the Amplidiag CarbaR+VRE assay is that it gives only a "positive" or "negative" answer for *Acinetobacter* oxacillinases with carbapenemase activity (AcOXA) without any distinction between the variants OXA-23, OXA-40, OXA-58, and *ISAbal*-OXA-51. Moreover, if the *bla*_{OXA-51} gene is not located downstream of an *ISAbal* sequence, then it is not detected. However, infection control measures with imipenem-resistant *Acinetobacter* (carbapenem-resistant *A. baumannii* [CRAB]) would be the same whatever the resistance mechanism involved (26).

Prospective evaluation of enterobacterial isolates with reduced susceptibility to at least one carbapenem. From 20 January to 10 February 2016, 200 consecutive isolates with reduced susceptibility to at least one carbapenem (imipenem, meropenem, and/or ertapenem) were referred to the F-NRC for Antibiotic Resistance for evaluation. Reidentification of these 200 isolates revealed 198 *Enterobacteriaceae* and 2 *A. baumannii* isolates. They corresponded to 101 non-CP-GNB and 99 CP-GNB as revealed by the Carba NP test and subsequent in-house PCR analysis. The Amplidiag CarbaR+VRE assay performed on QIAcube-extracted whole DNA could detect all NDM

($n = 12$), VIM ($n = 2$), IMP ($n = 1$), OXA-48 ($n = 83$), and NDM plus OXA-48 ($n = 1$) isolates, including several variants of these enzymes (NDM-1, NDM-4, IMP-10, VIM-1, VIM-19, OXA-181, OXA-204, and OXA-244). In addition, both $bla_{\text{OXA-48}}$ and bla_{NDM} genes were correctly detected by the Amplidiag CarbaR+VRE assay in one *Klebsiella pneumoniae* isolate that coexpressed the two enzymes. Among the non-carbapenemase producers, 8 gave positive PCR results for OXA-48, VIM, and/or NDM with threshold cycle (C_T) values ranging from 35 to 40. These isolates were considered contaminations during DNA extraction. Indeed, C_T s of true-positive isolates were below 20. Repeated QIAcube DNA extraction and PCRs directly done on colonies of these 8 isolates grown on MH medium gave a PCR-negative result. *K. pneumoniae* was the most prevalent species ($n = 73$), including 53.4% that were carbapenemase producers (29 OXA-48, 9 NDM, and 1 VIM-19). Among *Escherichia coli* isolates, 67.5% (27/40) produced a carbapenemase. The percentage of carbapenemase producers was lower in *Enterobacter* spp., with only 21.8% (12/55) of the isolates, which is in line with the French epidemiology (6). The other isolates were 7 *Klebsiella oxytoca* (5 producing OXA-48), 1 VIM-1-producing *Raoultella ornithinolytica*, 2 *Morganella morganii* (1 producing NDM-1), 4 *Serratia marcescens* (1 producing OXA-48 and 1 producing IMP-10), and 14 *Citrobacter* (12 producing OXA-48) isolates. Noticeably, the 2 *Hafnia alvei* and the 2 *A. baumannii* isolates were non-CP-GNB. The performances of the Amplidiag CarbaR+VRE assay in the prospective study of 200 isolates referred to the F-NRC were 100% (95% CI = 95.4% to 100%) for sensitivity, 100% (95% CI = 95.3% to 100%) for specificity, 100% (95% CI = 95.4% to 100%) for positive predictive value, and 100% (95% CI = 95.3% to 100%) for negative predictive value, respectively (Table 1).

When these results were extrapolated to the global French epidemiology (6) the Amplidiag CarbaR+VRE assay would have been able to identify 99.57% (3,306/3,320) of the CPE, missing only 13 IMI producers and one FRI-1 producer (27) (Table 1) and falsely detecting the unique OXA-405-producing *S. marcescens* as a carbapenemase producer (24).

Detection of OXA carbapenemases in *P. mirabilis*. The OXA-23 and OXA-58 carbapenemases, which are highly prevalent in carbapenem-resistant *Acinetobacter* spp., are still considered to be extremely rare in *Enterobacteriaceae*. Consequently, the molecular tests that are commercially available for the detection of CPE usually do not include $bla_{\text{OXA-23}}$ and $bla_{\text{OXA-58}}$ genes in their targeted genes (19, 20). However, OXA-23- and OXA-58-producing *P. mirabilis* isolates have been recently described not only in Europe (28–31) but also in other enterobacterial isolates from different countries and continents: Turkey (32), Africa (33), and India (34). It has been suggested (30) that their prevalence might be underestimated due to detection difficulties related to (i) the very weak hydrolysis activity of these carbapenemases and (ii) the intrinsic decreased susceptibility to imipenem (but not ertapenem) of *P. mirabilis*. To assess whether the Amplidiag CarbaR+VRE assay might detect these strains, we have tested 10 OXA-producing (8 OXA-23 and 2 OXA-58) *P. mirabilis* isolates and two negative controls (Table S1). All OXA producers were correctly identified. The Amplidiag CarbaR+VRE assay is the first assay able to detect the five most common carbapenemases and the OXA carbapenemases preferentially found in *A. baumannii*. The use of this assay would allow identification of these “*Acinetobacter*-related” enzymes not only in *P. mirabilis* but also in other enterobacterial isolates (32–34), allowing evaluation of the current spread of these resistance determinants and assessment of the risk of further dissemination of these enzymes in *Enterobacteriaceae*.

Performance of the Amplidiag CarbaR+VRE assay directly on bacterial colonies. The Amplidiag CarbaR+VRE assay allowed detection of the presence of a carbapenemase within a 3-hour period, using the recommended protocol of the manufacturer (Fig. 1). To see whether this time could be reduced, the Amplidiag CarbaR+VRE PCR was directly performed on colonies grown on Muller-Hinton (MH) medium (representing bacteria from a suspicious antibiogram) and on ChromID Carba Smart medium (a medium that is now classically used to screen for CPE).

TABLE 2 Results of the Amplidiag CarbaR+VRE assay on bacterial colonies recovered from ChromID Carba Smart medium directly from colonies versus DNA extraction (QIAamp DNA extraction or boiling extract)

Species and strain	β -Lactamase content ^c	Amplidiag Carba-R+VRE result ^a		
		QIAamp DNA extraction	Direct from colonies ^b	Boiling extract
<i>Enterobacteriaceae</i>				
<i>Klebsiella ozaenae</i> N15	KPC-3 + OXA-9 + TEM-1	KPC	KPC + OXA-48 + AcOXA	KPC
<i>E. coli</i> 2 A1	OXA-48 + CTX-M-15	OXA-48	OXA-48 + AcOXA	OXA-48
<i>K. pneumoniae</i> N38	OXA-204 + CMY-4	OXA-48	NDM + OXA-48 + AcOXA	OXA-48
<i>P. mirabilis</i>				
GUI	OXA-23	AcOXA	IMP + AcOXA	AcOXA
VAC	OXA-23	AcOXA	KPC + IMP + AcOXA	AcOXA
MOR	OXA-23	AcOXA	KPC + IMP + AcOXA	AcOXA
VAG	None		KPC + IMP + OXA-48	
<i>P. aeruginosa</i>				
A1	KPC-2	KPC	KPC	KPC
C4	VIM-4	VIM	VIM	VIM
D1	IMP-1	IMP	IMP	IMP
E7	GIM-1			
N100	OXA-198			

^aAcOXA, *Acinetobacter* oxacillinases with carbapenemase activity (OXA-23-like, OXA-24/-40-like, OXA-58-like, and ISAb_a plus OXA-51-like).

^bDiscrepancies compared to the manufacturer-recommended protocol (i.e., QIAamp DNA extraction) are highlighted in gray.

^cCarbapenemases are highlighted in bold.

For bacterial colonies grown on MH medium and directly suspended in the Amplidiag CarbaR+VRE PCR mix, correct results were obtained for all tested strains (Table S5) compared to the manufacturer-recommended protocol (i.e., DNA extraction using the QIAamp DNA extraction kit), with C_T values below 20. Thus, in addition to the avoidance of DNA extraction steps, this protocol optimization also allowed the reduction of the total number of cycles to 30 (instead of 45 in the original protocol), leading to a time-to-result of less than 1 h 10 min instead of 3 h (Fig. 1).

When applied on bacterial colonies grown on ChromID Carba Smart medium, the Amplidiag CarbaR+VRE yielded variable results (Table 2). Although *P. aeruginosa* isolates gave correct results, several false-positive results were obtained with *Enterobacteriaceae* (Table 2). Assuming that the pigmentation of enterobacterial isolates on ChromID Carba Smart medium might interfere with direct PCR, a fast (11-min) and cheap whole-DNA boiling extraction was performed. By directly applying 5 μ l of this boiling extracted DNA to the Amplidiag CarbaR+VRE PCR mix, correct results were then obtained for all tested *Enterobacteriaceae* (Table 2). Thus, the time-to-result was slightly increased to 1 h 11 min, which is still compatible with a short time-to-result. In addition, this low-cost DNA extraction technique leads to a drastic decrease in the global cost of the test. However, the presence of vancomycin (Van) primers in the present PCR mix is not appropriate for a study on colonies, because carbapenemase genes will be searched for in Gram-negative bacteria and vancomycin resistance genes will be searched for in Gram-positive bacteria. This PCR mix has been developed for an application to complex clinical samples such as rectal swabs or blood cultures.

Conclusion. Our study demonstrated that the Amplidiag CarbaR+VRE assay is well adapted to the French epidemiology of CP-GNB, which reflects the epidemiology of many European countries. Overall, and when excluding the nontargeted less-prevalent carbapenemases in CP-GNB (10/100), the Amplidiag CarbaR+VRE performances reached 100% (95% CI = 91.1% to 99.9%) and 99% (95% CI = 74.1% to 99.8%) sensitivity and specificity, respectively. The main advantage of this test is that it contains a large panel of targeted resistance determinants. Indeed, it detects the main carbapenemases encountered in *Enterobacteriaceae* (KPC, NDM, VIM, IMP, and OXA-48-like), but it also identifies the most widespread OXA carbapenemases usually identified in *A. baumannii* (OXA-23-like, OXA-24/-40-like, and OXA-58-like). This last panel might be increasingly important in the future with the recent reports of OXA-23- and OXA-58-producing *P. mirabilis* and *E. coli* (28–33).

As for most molecular assays, mutation and/or polymorphisms in the primer/probe binding region of the targeted gene may lead to false-negative results, and thus, new emerging variants may not be detected. Regular testing of novel variants is required to assess sensitivity and specificity of this assay in a constantly evolving carbapenemase field. The main drawback of this assay compared to other molecular techniques (23) is that it requires pure cultures and DNA extraction steps before analysis. The DNA extraction step significantly increases the global cost of the test since ready-to-use kits are recommended by the manufacturer. However, we demonstrated that a rapid and very cheap DNA extraction by boiling might be accurate enough to recover DNA extract and obtain adequate results. In addition, we also showed that the Amplidag CarbaR+VRE assay might be directly performed on bacterial colonies grown on MH agar, avoiding any additional DNA extraction step. Of note, our results suggested that at least the boiling DNA extraction step is crucial for bacterial colonies recovered from chromogenic media. Other limitations of the current test are that it is not validated directly on stool samples and that it lacks random access. Thus, the use of the Amplidag CarbaR+VRE assay for the investigation of an outbreak will require at least 24 or 48 h for the culture, and the global cost of this assay will be approximately 15 euros, but the assay might efficiently confirm the presence of carbapenemase production and identify its determinant if targeted.

SUPPLEMENTAL MATERIAL

Supplemental material for this article may be found at <https://doi.org/10.1128/JCM.01092-17>.

SUPPLEMENTAL FILE 1, PDF file, 0.2 MB.

ACKNOWLEDGMENTS

We are thankful to Elodie Creton and Garance Cotellon from the French National Reference Center for Antibiotic Resistance.

This work was supported by the Assistance Publique-Hôpitaux de Paris (AP-HP), the University Paris-Sud, and the Laboratory of Excellence in Research on Medication and Innovative Therapeutics (LERMIT) supported by a grant from the French National Research Agency (ANR-10-LABX-33) and by the Joint Programming Initiative on Antimicrobial Resistance (JPIAMR) DesInMBL (ANR-14-JAMR-002).


L.D. is coinventor of the Carba NP test, the patent for which has been licensed to bioMérieux (La Balmes les Grottes, France).

REFERENCES

- Logan LK, Weinstein RA. 2017. The epidemiology of carbapenem-resistant Enterobacteriaceae: the impact and evolution of a global menace. *J Infect Dis* 215:528–536. <https://doi.org/10.1093/infdis/jiw282>.
- Gniadek TJ, Carroll KC, Simner PJ. 2016. Carbapenem-resistant non-glucose-fermenting Gram-negative bacilli: the missing piece to the puzzle. *J Clin Microbiol* 54:1700–1710. <https://doi.org/10.1128/JCM.03264-15>.
- Queenan AM, Bush K. 2007. Carbapenemases: the versatile beta-lactamases. *Clin Microbiol Rev* 20:440–458. <https://doi.org/10.1128/CMR.00001-07>.
- Albiger B, Glasner C, Struelens MJ, Grundmann H, Monnet DL, European Survey of Carbapenemase-Producing Enterobacteriaceae (EuSCAPE) Working Group. 2015. Carbapenemase-producing Enterobacteriaceae in Europe: assessment by national experts from 38 countries. *Euro Surveill* 20(45). <https://doi.org/10.2807/1560-7917.ES.2015.20.45.30062>.
- Potron A, Poirel L, Nordmann P. 2015. Emerging broad-spectrum resistance in *Pseudomonas aeruginosa* and *Acinetobacter baumannii*: mechanisms and epidemiology. *Int J Antimicrob Agents* 45:568–585. <https://doi.org/10.1016/j.ijantimicag.2015.03.001>.
- Bonnin RA, Nordmann P, Poirel L. 2013. Screening and deciphering antibiotic resistance in *Acinetobacter baumannii*: a state of the art. *Expert Rev Anti Infect Ther* 11:571–583. <https://doi.org/10.1586/eri.13.38>.
- Dortet L, Cuzon G, Ponties V, Nordmann P. 2017. Trends in carbapenemase-producing Enterobacteriaceae, France, 2012 to 2014. *Euro Surveill* 22(6):30461. <https://doi.org/10.2807/1560-7917.ES.2017.22.6.30461>.
- Lutgring JD, Limbago BM. 2016. The problem of carbapenemase-producing-carbapenem-resistant-Enterobacteriaceae detection. *J Clin Microbiol* 54:529–534. <https://doi.org/10.1128/JCM.02771-15>.
- Maurer FP, Castelberg C, Quiblier C, Bloemberg GV, Hombach M. 2015. Evaluation of carbapenemase screening and confirmation tests with *Enterobacteriaceae* and development of a practical diagnostic algorithm. *J Clin Microbiol* 53:95–104. <https://doi.org/10.1128/JCM.01692-14>.
- Dortet L, Cuzon G, Plesiat P, Naas T. 2016. Prospective evaluation of an algorithm for the phenotypic screening of carbapenemase-producing *Enterobacteriaceae*. *J Antimicrob Chemother* 71:135–140. <https://doi.org/10.1093/jac/dkv308>.
- Dortet L, Bernabeu S, Gonzalez C, Naas T. 2017. Comparison of two phenotypic algorithms to detect carbapenemase-producing *Enterobacteriaceae*. *Antimicrob Agents Chemother* 61:e00796-17. <https://doi.org/10.1128/AAC.00796-17>.
- Dortet L, Agathine A, Naas T, Cuzon G, Poirel L, Nordmann P. 2015. Evaluation of the RAPIDEC CARBA NP, the Rapid CARB Screen and the Carba NP test for biochemical detection of carbapenemase-producing *Enterobacteriaceae*. *J Antimicrob Chemother* 70:3014–3022. <https://doi.org/10.1093/jac/dkv213>.
- Lasserre C, De Saint Martin L, Cuzon G, Bogaerts P, Lamar E, Glupczynski Y, Naas T, Tande D. 2015. Efficient detection of carbapenemase activity

- in *Enterobacteriaceae* by matrix-assisted laser desorption/ionization-time of flight mass spectrometry in less than 30 minutes. *J Clin Microbiol* 53:2163–2171. <https://doi.org/10.1128/JCM.03467-14>.
14. Bogaerts P, Yunus S, Massart M, Huang TD, Glupczynski Y. 2016. Evaluation of the BYG Carba test, a new electrochemical assay for rapid laboratory detection of carbapenemase-producing *Enterobacteriaceae*. *J Clin Microbiol* 54:349–358. <https://doi.org/10.1128/JCM.02404-15>.
 15. Gauthier L, Bonnin RA, Dortet L, Naas T. 2017. Retrospective and prospective evaluation of the carbapenem inactivation method for the detection of carbapenemase-producing *Enterobacteriaceae*. *PLoS One* 12:e0170769. <https://doi.org/10.1371/journal.pone.0170769>.
 16. Bernabeu S, Dortet L, Naas T. 2017. Evaluation of the β -CARBA test, a colorimetric test for the rapid detection of carbapenemase activity in Gram-negative bacilli. *J Antimicrob Chemother* 72:1646–1658. <https://doi.org/10.1093/jac/dkx061>.
 17. Boutal H, Naas T, Devilliers K, Oueslati S, Dortet L, Bernabeu S, Simon S, Volland H. 2017. Development and validation of a lateral flow immunoassay for the rapid detection of NDM-producing *Enterobacteriaceae*. *J Clin Microbiol* 55:2018–2029. <https://doi.org/10.1128/JCM.00248-17>.
 18. Glupczynski Y, Jousset A, Evrard S, Bonnin RA, Huang TD, Dortet L, Bogaerts P, Naas T. 2017. Prospective evaluation of the OKN K-SeT assay, a new multiplex immunochromatographic test for the rapid detection of OXA-48-like, KPC and NDM carbapenemases. *J Antimicrob Chemother* 72:1955–1960. <https://doi.org/10.1093/jac/dkx089>.
 19. Findlay J, Hopkins KL, Meunier D, Woodford N. 2015. Evaluation of three commercial assays for rapid detection of genes encoding clinically relevant carbapenemases in cultured bacteria. *J Antimicrob Chemother* 70:1338–1342. <https://doi.org/10.1093/jac/dku571>.
 20. Hoyos-Mallecot Y, Ouzani S, Dortet L, Fortineau N, Naas T. 2017. Performance of the Xpert Carba-R v2 in the daily workflow of a hygiene unit in a country with a low prevalence of carbapenemase-producing *Enterobacteriaceae*. *Int J Antimicrob Agents* 49:774–777. <https://doi.org/10.1016/j.ijantimicag.2017.01.025>.
 21. Naas T, Cuzon G, Bogaerts P, Glupczynski Y, Nordmann P. 2011. Evaluation of a DNA microarray (Check-MDR CT102) for rapid detection of TEM, SHV, and CTX-M extended-spectrum β -lactamases and of KPC, OXA-48, VIM, IMP, and NDM-1 carbapenemases. *J Clin Microbiol* 49:1608–1613. <https://doi.org/10.1128/JCM.02607-10>.
 22. Ellington MJ, Ekelund O, Aarestrup FM, Canton R, Doumith M, Giske C, Grundman H, Hasman H, Holden MT, Hopkins KL, Iredell J, Kahlmeter G, Köser CU, MacGowan A, Mevius D, Mulvey M, Naas T, Peto T, Rolain JM, Samuelsen Ø, Woodford N. 2017. The role of whole genome sequencing in antimicrobial susceptibility testing of bacteria: report from the EUCAST Subcommittee. *Clin Microbiol Infect* 23:2–22. <https://doi.org/10.1016/j.cmi.2016.11.012>.
 23. Dortet L, Fusaro M, Naas T. 2016. Improvement of the Xpert Carba-R kit for the detection of carbapenemase-producing *Enterobacteriaceae*. *Antimicrob Agents Chemother* 60:3832–3837. <https://doi.org/10.1128/AAC.00517-16>.
 24. Dortet L, Oueslati S, Jeannot K, Tandé D, Naas T, Nordmann P. 2015. Genetic and biochemical characterization of OXA-405, an OXA-48-type extended-spectrum β -lactamase without significant carbapenemase activity. *Antimicrob Agents Chemother* 59:3823–3828. <https://doi.org/10.1128/AAC.05058-14>.
 25. Mostachio AK, Levin AS, Rizek C, Rossi F, Zerbini J, Costa SF. 2012. High prevalence of OXA-143 and alteration of outer membrane proteins in carbapenem-resistant *Acinetobacter* spp. isolates in Brazil. *Int J Antimicrob Agents* 39:396–401. <https://doi.org/10.1016/j.ijantimicag.2012.01.021>.
 26. Munoz-Price LS, Weinstein RA. 2008. *Acinetobacter* infection. *N Engl J Med* 358:1271–1281. <https://doi.org/10.1056/NEJMra070741>.
 27. Naas T, Dortet L, Iorga BI. 2016. Structural and functional aspects of class A carbapenemases. *Curr Drug Targets* 17:1006–1028. <https://doi.org/10.2174/1389450117666160310144501>.
 28. Bonnet R, Marchandin H, Chanal C, Sirot D, Labia R, De Champs C, Jumas-Bilak E, Sirot J. 2002. Chromosome-encoded class D β -lactamase OXA-23 in *Proteus mirabilis*. *Antimicrob Agents Chemother* 46:2004–2006. <https://doi.org/10.1128/AAC.46.6.2004-2006.2002>.
 29. Österblad M, Karah N, Halkilahti J, Sarkkinen H, Uhlin BE, Jalava J. 2016. Rare detection of the *Acinetobacter* class D carbapenemase blaOXA-23 gene in *Proteus mirabilis*. *Antimicrob Agents Chemother* 60:3243–3245. <https://doi.org/10.1128/AAC.03119-15>.
 30. Girlich D, Bonnin RA, Bogaerts P, De Laveleye M, Huang DT, Dortet L, Glaser P, Glupczynski Y, Naas T. 2017. Chromosomal amplification of the blaOXA-58 carbapenemase gene in a *Proteus mirabilis* clinical isolate. *Antimicrob Agents Chemother* 61:e01697-16. <https://doi.org/10.1128/AAC.01697-16>.
 31. Lange F, Pfenningwerth N, Gerigk S, Gohlke F, Oberdorfer K, Purr I, Wohanka N, Roggenkamp A, Gatermann SG, Kaase M. 2017. Dissemination of blaOXA-58 in *Proteus mirabilis* isolates from Germany. *J Antimicrob Chemother* 72:1334–1339. <https://doi.org/10.1093/jac/dkw566>.
 32. Budak S, Aktas Z, Oncul O, Acar A, Ozyurt M, Turhan V, Gorenek L. 2012. Detection of *Acinetobacter baumannii* derived OXA-51 and OXA-58 carbapenemase genes in enteric bacteria: a new dimension on carbapenemase resistance. *Clin Microbiol Infect* 18(Suppl):311.
 33. Leski TA, Bangura U, Jimmy DH, Ansumana R, Lizewski SE, Li RW, Stenger DA, Taitt CR, Vora GJ. 2013. Identification of bla_{OXA-51}-like, bla_{OXA-58}, bla_{DIM-1}, and bla_{VIM} carbapenemase genes in hospital *Enterobacteriaceae* isolates from Sierra Leone. *J Clin Microbiol* 51:2435–2438. <https://doi.org/10.1128/JCM.00832-13>.
 34. Paul D, Ingti B, Bhattacharjee D, Maurya AP, Dhar D, Chakravarty A, Bhattacharjee A. 2017. An unusual occurrence of plasmid-mediated bla_{OXA-23} carbapenemase in clinical isolates of *Escherichia coli* from India. *Int J Antimicrob Agents* 49:642–645. <https://doi.org/10.1016/j.ijantimicag.2017.01.012>.

SCIENTIFIC REPORTS



OPEN

Multicentre evaluation of the BYG Carba v2.0 test, a simplified electrochemical assay for the rapid laboratory detection of carbapenemase-producing Enterobacteriaceae

Pierre Bogaerts¹, Saoussen Oueslati^{2,3,4}, Danièle Meunier ⁵, Claire Nonhoff⁶, Sami Yunus⁷, Marion Massart¹, Olivier Denis⁶, Neil Woodford⁵, Katie L. Hopkins⁵, Thierry Naas^{2,3,4}, Laurent Dortet^{2,3,4}, Te-Din Huang¹ & Youri Glupczynski¹

Rapid detection of carbapenemase-producing Enterobacteriaceae (CPE) represents a major challenge for microbiology laboratories. We evaluated the BYG Carba v2.0 using a simplified protocol, which detects CPE in less than 30 minutes. This new procedure reduces the hands-on-time from 5 to one minute and only requires a limited amount of material (one to three colonies) thereby preventing the need for subculturing bacterial isolates to reach a larger amount of pure biomass. This multicentre study involved four European reference laboratories. For the 1181 isolates tested across four centres, BYG Carba v2.0 yielded overall sensitivity and specificity of 96.3% (CI95: 94.5–97.5) and 99.7% (CI95: 98.6–100) respectively. Considering only the 670 consecutive isolates tested prospectively, the BYG Carba v2.0 displayed overall positive and negative predictive values of 99.7% (CI95: 95.4–98.9) and 97.5% (CI95: 94.9–98.8). Regarding time to positivity, 85% of CPE detected were positive within ten minutes. The BYG Carba v2.0 is a new highly simplified, rapid and accurate electrochemical assay discriminating between CPE and non-CPE in less than 30 min. The real-time quantified signal allows objective and traceable interpretation of the results.

The emergence and worldwide spread of carbapenemase-producing Enterobacteriaceae (CPE) represents a major public health concern. Accurate and timely detection of CPE is essential for patient management and for rapid implementation of infection control measures^{1,2}.

Various confirmatory tests for the non-molecular detection of CPE have been proposed³. The most rapid methods rely on the detection of carbapenem hydrolysis by colorimetric assay or by mass spectrometry³. We recently evaluated three colorimetric assays, the RAPIDEC® CARBA NP test (BioMérieux, Marcy l'Étoile,

¹Laboratory of clinical microbiology, National reference center for monitoring antimicrobial resistance in Gram-negative bacteria, CHU UCL Namur, Yvoir, Belgium. ²Bacteriology-Hygiene unit, Assistance Publique/Hôpitaux de Paris, Bicêtre Hospital, Le Kremlin-Bicêtre, France. ³EA7361 "Structure, dynamic, function and expression of broad spectrum β -lactamases", Université Paris Sud, Université Paris Saclay, LabEx Lermite, Faculty of Medicine, Le Kremlin-Bicêtre, France. ⁴Associated French National Reference Center for Antibiotic Resistance: Carbapenemase-producing Enterobacteriaceae, Le Kremlin-Bicêtre, France. ⁵Antimicrobial Resistance and Healthcare Associated Infections (AMRHAI) Reference Unit, National Infection Service, Public Health England, London, NW9 5EQ, UK. ⁶Department of Microbiology, Associated national reference center, Hôpital Erasme, Université Libre de Bruxelles, Route de Lennik 808, 1070, Brussels, Belgium. ⁷Bio and Soft Matter, Institute of Condensed Matter and Nanosciences, Université catholique de Louvain, Louvain-La-Neuve, Belgium. Saoussen Oueslati, Danièle Meunier and Claire Nonhoff contributed equally to this work. Correspondence and requests for materials should be addressed to P.B. (email: pierre.bogaerts@uclouvain.be)

France), the Neo-Rapid CARB kit (Rosco Diagnostica, Taastrup, Denmark) and the β -CARBA™ test (Bio-Rad, Marnes-la-Coquette, France) and found that overall all these tests showed satisfactory results for the detection of CPE despite differences in performance between the tests⁴. Nevertheless, all the colorimetric assays are based on a subjective visual observation of colour change, which can be sometimes challenging to interpret, especially for some carbapenemase families (e.g. OXA-48 like, GES-like) with lower hydrolytic activity. Furthermore, the format of the colorimetric assays does not lend itself to automated traceability in a laboratory information system.

We recently developed and evaluated the BYG Carba test, an electrochemical assay that allows the rapid (within 30 minutes) and objective confirmation of carbapenemase activity in Enterobacteriaceae⁵. The BYG Carba test detects variations of conductivity of an electrode coated with polyaniline, an electrochemical sensing polymer. The polyaniline is highly sensitive to the modifications of pH and redox activity, which occur during the hydrolysis of imipenem by a carbapenemase. These modifications, which can be measured and monitored in real-time by the BYG Carba test, are indicative of the presence of an enzyme having carbapenem hydrolytic activity including the five major carbapenemase families (VIM, NDM, IMP, KPC, OXA-48)⁵. The major drawback of this method was that in its original format (BYG v1.0) a heavy bacterial suspension (McFarland 4 corresponding to $\pm 10^9$ CFU/ml) was required like for the other colorimetric assays. For the present study, we adapted and modified the BYG assay to use a smaller inoculum corresponding to only one to three colonies (i.e. corresponding approximately to 10^6 CFU/ml) directly deposited on the electrode (hands-on-time of about one minute). This reduced bacterial load still permits the use of the primary culture plate and avoids the need for additional subculture. The BYG Carba test using this new protocol (v2.0) (supplemental video) was validated in a multicentre survey that was conducted in four laboratories with recognized expertise in the characterization of the mechanisms of antimicrobial resistance (two laboratories in Belgium, one in France and one in the United Kingdom).

Results

Preliminary assessment of BYG Carba v2.0 compared to BYG Carba v1.0. A signal cut-off of 3.5 and of 11.5 (arbitrary units [AU]) was defined as the threshold for discrimination between carbapenemase and non-carbapenemase producers for the BYG v1.0 and BYG v2.0, respectively and were established previously using ROC curve^{4,5}.

The comparison of the results obtained with BYG v1.0 and BYG v2.0 are presented in Fig. 1. All CPE isolates except one *Citrobacter braakii* isolate producing GES-6, a very weak and rarely reported class A carbapenemase⁶, were correctly identified by the BYG Carba v2.0. GES-6 was also not detected by the BYG Carba v1.0. The maximum value obtained with BYG Carba v2.0 for the non-CPE was 3.5 AU while the minimum value obtained for the CPE detected (GES-6 excluded) was 29.4 AU. The signal intensity of the positive strains when tested in triplicate was significantly higher ($p < 0.00001$) with BYG Carba v2.0 (Mean = 97.8 AU, CI 95 = 87.9–107.7; Median = 98.5) than with BYG Carba v1.0 (Mean = 44.0 AU, CI 95 = 40.0–48.0; Median = 48.0) with accuracy of CPE detection remaining unchanged for this isolate panel. For the negative results, the mean and median values were not significantly different between BYG Carba v1.0 (Mean = -0.9 ; Median = -0.1) and BYG Carba v2.0 (Mean = -0.2 ; median = -0.1).

BYG Carba v2.0 results on retrospective and prospective clinical isolates. A total of 1181 clinical Enterobacteriaceae isolates were included in this evaluation (511 clinical isolates retrieved from local archives with previously characterized β -lactam resistance mechanisms and 670 consecutive Enterobacteriaceae clinical isolates collected prospectively at the four laboratories; Table 1). According to the reference methods used in each laboratory, this study included 704 CPE (OXA-48-like [n = 359], KPC [n = 114], NDM [n = 107], VIM [n = 78], IMP [n = 17], NDM + OXA-48-like [n = 14] and other miscellaneous carbapenemase-producing Enterobacteriaceae (IMI, SME, NMC-A, GES, FRI and GIM carbapenemases; [n = 15]) as well as 477 non-CPE isolates (Table 2). Among the 1181 tested isolates the species distribution was as following: *Klebsiella pneumoniae* (n = 507), *Escherichia coli* (n = 228), *Enterobacter cloacae* complex (n = 228), *Citrobacter freundii* (n = 59), *Klebsiella oxytoca* (n = 57), *Enterobacter aerogenes* (n = 49), *Serratia marcescens* (n = 20), and miscellaneous others (n = 33). The performance of the BYG Carba v2.0 assay for CPE detection did not differ by bacterial species and was not related to the MICs to carbapenems as had already been observed for BYG Carba assay v1.0⁵.

When analyzing separately the subset of archived isolates with known carbapenem resistance mechanisms, the BYG Carba v2.0 correctly identified 330/348 (94.8%) CPE isolates and 163/163 non-CPE isolates including OXA-163 (n = 2) and OXA-405 (n = 1)-producing isolates, two OXA-48 variants lacking any carbapenemase activity (sensitivity of 94.8%, specificity of 100%). When considering the performance of the test for detecting individual carbapenemase families, the BYG Carba v2.0 detected isolates belonging to the five major carbapenemase families with a sensitivity ranging from 86.7% for IMP to 100% for KPC (Table 3). Notably, 122/127 (96.1%) OXA-48-like producing organisms were correctly detected by the BYG Carba v2.0 as were also less common carbapenemase types such as SME, NMC-A, FRI-1 and GIM-1. None of the four GES-5-producing isolates were detected by the BYG Carba v2.0 (Table 2).

In the prospective part of this evaluation (670 consecutive isolates), the BYG Carba v2.0 detected 348/356 (97.8%) of the CPE while 313/314 (99.7%) (Table 2) of the non-CPE were correctly identified. Across the four centres the performance of the BYG Carba v2.0 was 97.7% (CI95 = 95.4–98.9) sensitivity, 99.7% (CI95 = 97.9–100) specificity, 99.7% (CI95 = 98.2–100) positive predictive value (PPV) and 97.5% (CI95 = 94.9–98.8) negative predictive value (NPV) (Table 3).

Across the four centres out of the total of 1181 isolates, the test showed 96.3% sensitivity and 99.7% specificity (Tables 2 and 4). Overall, only 27 discrepant results were observed (2.3% of the 1181 tested isolates). Fourteen discrepant results were observed in centre D, nine in centre C, two in centre A and two in centre B. Among these, 26 strains yielded a false-negative result (18/511 [3.5%] from the archived isolates and 8/670 [1.2%] from the prospective evaluation) and one false-positive result was observed during the prospective evaluation. The BYG Carba

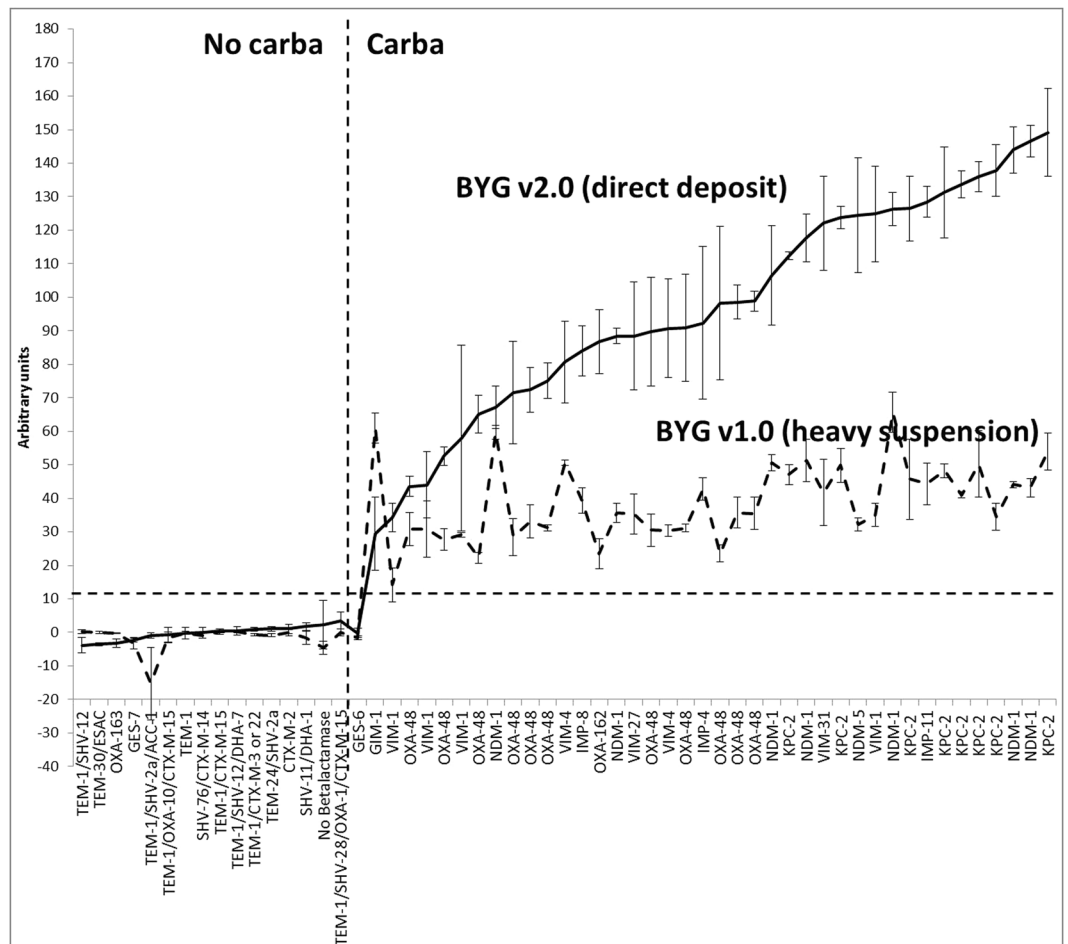


Figure 1. Comparison of polyaniline conductance signals by BYG Carba v1.0 and BYG Carba v2.0 assays. Intensity of the signal is expressed in arbitrary units and reflects the conductance of the sensor (Y axis). Main resistance mechanisms are indicated on the X axis. No carba/Carba vertical dotted line represents the boundary between the non-carbapenemase producers and the carbapenemase producers. Horizontal dotted line is the cut-off of positivity of the test (11.5 AU); Vertical bars on the curves represent standard deviation of 3 independent measures. The mean value for all positive values is 44.0 (CI95: 40.0–48.0) and 97.8 (CI95: 88.0–107.7) for BYG Carba v1.0 and BYG Carba v2.0 respectively and are significantly different ($p < 0.00001$ by independent two-sample Student's t-test).

	Retrospective collection (n = 511)	Prospective collection (n = 670)
Centre A	150	258
Centre B	87	111
Centre C	175	201
Centre D	99	100

Table 1. Number of clinical isolates analyzed in each centre.

v2.0 failed to detect ten OXA-48-like (OXA-244 [n = 4], OXA-48 [n = 4], OXA-232 and OXA-181 [n = 1, each]), NDM (n = 5), GES carbapenemase variants (n = 4), VIM (n = 3), IMP and IMI-producing Enterobacteriaceae (n = 2, each). The observed false negative values ranged between 5 AU for an IMI-1-producing *E. cloacae* to 11 AU for an IMI-2-producing *E. cloacae*. The false-positive result was detected for a SHV-12-expressing *E. cloacae* with a value of 15 AU (Table 4).

The 27 strains that did not yield matching results were reevaluated in centre A for possible resolution of the discrepancies and repeat screening with the BYG test. False-negative results were confirmed for 17 strains while for 10 strains, the repeated results were in agreement with the results of the molecular tests obtained in centre A, therefore suggesting a loss of plasmid or a technical problem in the original testing centre (Table 5). In particular, the false-positive *E. cloacae* was repeatedly negative when tested 3 times (true-negative), one NDM-1 and one OXA-48-producing strains were phenotypically fully susceptible when received in center A (suggesting

	Retrospective collection (n = 511)		Prospective collection (n = 670)	
	Reference method	Detected by BYG Carba (% of correct results)	Reference method	Detected by BYG Carba (% of correct results)
Total CPE	348	330 (94.8)	356	348 (97.8)
OXA-48-like	127	122 (96.1)	232	227 (97.8)
KPC	71	71 (100)	43	43 (100)
NDM	60	56 (93.3)	47	46 (97.9)
VIM	52	51 (98.1)	26	24 (92.3)
IMP	15	13 (86.7)	2	2 (100)
OXA-48-like + NDM	8	8 (100)	6	6 (100)
IMI	6	4 (66.7)	0	NA
SME	2	2 (100)	0	NA
NMC-A	1	1 (100)	0	NA
GES-5	4	0 (0)	0	NA
FRI-1	1	1 (100)	0	NA
GIM-1	1	1 (100)	0	NA
Total of Non-CPE	163*	0 (100)	314	1 (99.7)

Table 2. BYG Carba v2.0 results for the 1181 clinical isolates analyzed in this study. *Including 3 isolates expressing an OXA-48 variant devoid of carbapenemase activity (OXA-163 [n = 2] and OXA-405 [n = 1]). NA: not applicable.

	Retrospectively (n = 511) Spec: 100% (CI95: 97.1–100)	Prospectively (n = 670) Spec: 99.7% (CI95: 97.9–100)			Total (n = 1181) Spec: 99.7% (CI95: 98.6–100)
	Sens (%) (CI95)	Sens (%) (CI95)	PPV (%) (CI95)	NPV (%) (CI95)	Sens (%) (CI95)
CPE	94.8 (91.8–96.8)	97.7 (95.4–98.9)	99.7 (98.2–100)	97.5 (94.9–98.8)	96.3 (94.5–97.5)
OXA-48-like	96.1 (90.6–98.5)	97.8 (94.8–99.2)	99.6 (97.2–100)	98.4 (96.1–99.4)	97.2 (94.8–98.6)
KPC	100 (93.6–100)	100 (89.8–100)	97.7 (86.5–99.9)	100 (98.5–100)	100 (95.9–100)
NDM	93.3 (83.0–97.8)	97.9 (87.3–99.9)	97.9 (87.3–99.9)	99.7 (97.9–100)	95.3 (88.9–98.2)
VIM	98.1 (88.4–99.9)	92.3 (73.4–98.6)	96.0 (77.7–99.8)	99.4 (97.4–100)	96.1 (88.4–99.0)
IMP	86.7 (58.4–97.6)	100 (19.8–100)	66.7 (12.5–98.2)	100 (98.5–100)	88.2 (62.2–97.9)
OXA-48-like + NDM	100 (59.8–100)	100 (51.7–100)	85.7 (42.0–99.2)	100 (98.5–100)	100 (73.2–100)

Table 3. Performance of the BYG Carba v2.0 according to carbapenemase family. The values are based on the results reported by each centre without any correction of the discrepancies by the CHU UCL Namur. Sens: sensitivity; Spec: specificity; PPV: positive predictive value; NPV: negative predictive value.

loss of plasmid) and seven strains were retested positive in center A (GES-5, IMI-1, IMP-1, NDM-1, OXA-244 and OXA-48, [n = 1] each). In addition, these discrepant isolates were also tested with the Carba NP test which showed 13 positive results. This suggests that the carbapenemase activity of the 14 negative isolates is particularly low (either because of a lack of expression of the carbapenemase or because of a low carbapenemase activity of the variant [for example OXA-244]). The time to positivity was also determined along with the value of the signal at the end of the run. For the 678 out of 704 CPE (96.3%) detected by the BYG Carba v2.0, the maximum value obtained at 30 min was 171.6 AU for a KPC-producing *K. pneumoniae* and the minimum value was 11.5 for a VIM-producing *E. cloacae*. The mean of the signal values was 97.3 AU (Table 4). On the whole, 45% and 85% of CPE were detected within five minutes and 10 minutes, respectively. The results for the individual targets are presented in Table 4.

Discussion

The accurate and timely detection of CPE is of paramount importance for prevention and control of outbreaks in clinical settings and for the management of patients infected with CPE⁷. The detection of CPE can be performed by culture methods on specific media followed by confirmatory phenotypic testing or by in-house/commercial molecular testing. Molecular methods present the advantage of rapidity and can be used for non-culture based detection of carbapenemases directly from screening samples⁸. However, a major limitation is that only the genes and allelic variants targeted by the assays can be detected. These methods are also usually expensive, necessitating specific costly instruments, or are not accessible on a routine daily basis for general clinical laboratories that lack specifically trained personnel and dedicated rooms.

Here we present the results of a multicentre evaluation of the performance of a simplified version of the recently published⁵ BYG Carba test in four laboratories in Europe. Overall, only 2.3% of discrepant results were observed in comparison to the reference molecular methods. Contrarily to molecular methods, as it is the case

Type	Total detected	Mean of signal in AU (CI95)	% detected in ≤ 5 min (CI95)	% detected in ≤ 10 min (CI95)
CPE	678	97.3 (94.9–99.8)	45.1 (41.4–48.9)	85.2 (82.6–87.9)
OXA-48-like	349	85.3 (82.3–88.3)	43.8 (38.6–49.0)	89.1 (85.8–92.4)
KPC	114	122.2 (117.4–127.1)	75.4 (67.5–83.3)	94.7 (90.6–98.8)
NDM	102	114.7 (109.1–120.2)	54.9 (45.2–64.6)	90.2 (84.4–96.0)
VIM	75	99.3 (92.0–106.6)	8 (3.7–17.7)	54.7 (43.4–65.9)
IMP	15	72.5 (54.9–90.0)	0	53.3 (28.1–78.5)

Table 4. Signal value obtained with the BYG Carba v2.0 and time to detection for the ‘big five’ carbapenemases. AU: Arbitrary units. CI: confidence interval.

with colorimetric assays, the BYG carba test would be able to detect even unknown (novel) carbapenemases. One definite advantage of the BYG Carba test over the colorimetric assays^{9–18} relates to the fact that once a cut-off limit is set, the interpretation becomes objective by reporting a number (arbitrary value expressing the polyaniline conductance) and indicating the positivity in real-time.

Some metallo- β -lactamases such as IMP were detected with a lower efficiency by the BYG Carba v2.0 (86.7% sensitivity in the retrospective survey). In the prospective phase of this evaluation, only two IMP-producers were collected during the study period, confirming the extremely low prevalence of this carbapenemase in the UK, France and Belgium as already observed in Europe¹⁹. The performance of the BYG Carba v2.0 test against this particular carbapenemase should be further evaluated in countries with higher endemic settings, such as Japan, Korea or Taiwan. On the other hand, the BYG Carba v2.0 detected 349/359 (97.2%) of the OXA-48 like producing isolates, 90% of these (311/349) being detected in 10 minutes or less. Nevertheless, some OXA-48 variants such as OXA-244, a weak and rare carbapenemase²⁰, were less well detected than other OXA-48-like allelic variants (four false negative results among five OXA-244-producers). The latter results match with those previously observed with the RAPIDEC[®] CARBA NP⁹. Accordingly, microbiologists should be alerted to this fact and any suspicion of an OXA-48-like carbapenemase based on *in vitro* resistance to temocillin and to piperacillin/tazobactam could be confirmed directly by nucleic acid amplification methods or by the immunochromatographic OXA-48 K-SeT assay (Coris BioConcept, Gembloux, Belgium)^{21,22}. Interestingly, Meunier *et al.* reported that two GES-5-producing strains that failed to be detected with the BYG Carba assay were correctly detected by the RAPIDEC[®] CARBA NP²³. Again, GES-type carbapenemases very rarely occurred as shown by the fact that no GES-positive isolate was identified during the prospective evaluation.

The procedure used with BYG Carba v2.0 is very simple (supplementary video). Among commercial tests only the β -CARBA[™] Test from Bio-Rad offers similar advantages with minimal hands-on time and low bacterial inoculum but detection remains based on visual detection of a colour change⁴. In the laboratory, the cost for a BYG Carba test prototype seems affordable. The home-made reader, adaptable to any computer, is built at a cost of 100 euros and all materials/reagents needed for the electrodes including the different coatings cost less than 1 euro per strain. It opens the possibility of industrialisation, commercialisation or even open accessibility at a price allowing its broad usage for the detection of carbapenemases. Based on the measurement of the modification of pH and redox potential by several electrodes connected in parallel, it would also permit analysis of the effect of several antimicrobials on a single isolate. Finally, after disinfection with non alcoholic chlorhexidine, we experimented that the electrodes could be reusable. But this should be further investigated.

In conclusion, the BYG Carba v2.0 is a fast and accurate test for the detection of CPE. It allows the objective detection of CPE from 1–3 colonies in less than 30 minutes and could represent a major additional tool in the laboratory armamentarium for detection of CPE. In addition the technology is very adaptable for miniaturisation and further multiplexing, permitting the testing of several antimicrobials in parallel.

Methods

Electrochemical instrumentation and the electrodes. The principle and technology was described in details in previous publications^{24,25}. Briefly, the system is composed of a small homemade electronic device (potentiostat), and of disposable electrodes coated with polyaniline as a sensor⁵. Up to five potentiostats can be connected at the same time to a computer through a USB Hub (serial port) allowing the simultaneous analysis of 20 isolates.

The results of the BYG Carba test are displayed as curves visualized in real-time. One curve corresponds to the signal (conductance) detected with imipenem and another curve to the signal without imipenem (background curve). The software then subtracts the background signal from the conductance signal obtained with imipenem. For non-carbapenemase-producing isolates, the resulting signal may be negative when the conductance signal obtained at 30 min with imipenem is lower than the background signal without imipenem. An isolate is reported as positive when the resulting curve crosses the cut-off. At the end of the run, the software generates a report.

BYG Carba test v1.0 and v2.0. For the BYG Carba v1.0, the bacterial suspensions were prepared as previously described⁵.

The BYG Carba test v2.0 was recently developed and validated in order to simplify the procedure by avoiding multiple pipetting steps and by allowing the test to be performed directly from a smaller amount of bacterial growth (4, Supplementary video).

N°	Species	Carbapenemase	First testing			Confirmation in centre A			Additional hydrolysis testing
			BYG value at 30 min (AU)	Result	Time to pos (min)	BYG value at 30 min (AU) repeat	Time to pos (min) repeat	Result repeat	Carba NP test
1	<i>Enterobacter cloacae</i>	GES-5	0.4	FN	—	4.6	—	FN	POS
2	<i>Enterobacter cloacae</i>	GES-5	2.9	FN	—	−4.3	—	FN	POS
3	<i>Klebsiella oxytoca</i>	GES-5	−1.3	FN	—	0.8	—	FN	NEG
4	<u><i>Klebsiella oxytoca</i></u>	<u>GES-5</u>	<u>−0.5</u>	<u>FN</u>	—	<u>12.3</u>	<u>28</u>	<u>TP</u>	<u>POS</u>
5	<u><i>Enterobacter cloacae</i></u>	<u>IMI-1</u>	<u>−5.0</u>	<u>FN</u>	—	<u>94.0</u>	<u>6</u>	<u>TP</u>	<u>POS</u>
6	<i>Enterobacter cloacae</i>	IMI-2	11.0	FN	—	0.4	—	FN	NEG
7	<i>Escherichia coli</i>	IMP-1	2.0	FN	—	−0.2	—	FN	POS
8	<u><i>Enterobacter cloacae</i></u>	<u>IMP-1</u>	<u>6.1</u>	<u>FN</u>	—	<u>12.1</u>	<u>27</u>	<u>TP</u>	<u>NEG</u>
9	<i>Providencia stuartii</i>	NDM-1	1.9	FN	—	−1.6	—	FN	NEG
10	<i>Providencia rettgeri</i>	NDM-1	9.3	FN	—	11.4	—	FN	NEG
11	<i>Klebsiella oxytoca</i>	NDM-1 *	8.4	FN	—	0.9	—	TN	NEG
12	<u><i>Proteus mirabilis</i></u>	<u>NDM-1</u>	<u>3.9</u>	<u>FN</u>	—	<u>14.9</u>	<u>24</u>	<u>TP</u>	<u>POS</u>
13	<i>Klebsiella pneumoniae</i>	OXA-181	3.1	FN	—	3.5	—	FN	NEG
14	<i>Escherichia coli</i>	OXA-244	0.9	FN	—	2.2	—	FN	NEG
15	<i>Escherichia coli</i>	OXA-244	1.2	FN	—	3.1	—	FN	NEG
16	<u><i>Escherichia coli</i></u>	<u>OXA-244</u>	<u>3.7</u>	<u>FN</u>	—	<u>16.3</u>	<u>24</u>	<u>TP</u>	<u>POS</u>
17	<i>Escherichia coli</i>	OXA-48	9.4	FN	—	8.8	—	FN	POS
18	<i>Enterobacter cloacae</i>	VIM-1	6.8	FN	—	6.0	—	FN	NEG
19	<u><i>Providencia stuartii</i></u>	<u>NDM</u>	<u>−0.1</u>	<u>FN</u>	—	<u>32.5</u>	<u>16</u>	<u>TP</u>	<u>NEG</u>
20	<i>Klebsiella oxytoca</i>	OXA-232	−4.1	FN	—	1.2	—	FN	POS
21	<i>Escherichia coli</i>	OXA-244	1.1	FN	—	0.8	—	FN	POS
22	<u><i>Escherichia coli</i></u>	<u>OXA-48</u>	<u>3.6</u>	<u>FN</u>	—	<u>71.4</u>	<u>6</u>	<u>TP</u>	<u>POS</u>
23	<i>Escherichia coli</i>	OXA-48 *	0.2	FN	—	−1.1	—	TN	NEG
24	<i>Klebsiella pneumoniae</i>	OXA-48	10.3	FN	—	10.0	—	FN	NEG
25	<i>Enterobacter cloacae</i>	VIM-1	8.0	FN	—	9.1	—	FN	POS
26	<i>Escherichia coli</i>	VIM-4	1.1	FN	—	8.2	—	FN	POS
27	<u><i>Enterobacter cloacae</i></u>	<u>No Carba (SHV-12)</u>	<u>15.8</u>	<u>FP</u>	<u>20</u>	<u>1.1 and 4.1</u>	—	<u>TN</u>	<u>NEG</u>

Table 5. Discrepant results between the BYG Carba v2.0 test and the reference method. Isolates 1 to 18 were retrospectively collected and the isolates 19 to 27 are prospectively collected. The Carba NP imipenem hydrolysis test was performed to confirm the imipenem hydrolysis in these isolates. FN: False negative; TP: True positive; TN: True negative; POS: positive; NEG: negative. *These isolates have probably lost their plasmid. Correct results obtained in centre A are in bold and underlined.

In this new protocol, the bacterial inoculum consists of one to three colonies ($+/-10^6$ CFU/ml) directly smeared onto two adjacent probes of the BYG Carba test in such a way that the sensor is completely covered by the colonies. The electrode is then overlaid with 50 μ l of a 4 M NaCl; 0.3 mM ZnSO₄ solution with or without imipenem (same concentration as in BYG Carba v1.0). The BYG Carba test measures the conductivity of the polyaniline sensor during the hydrolysis of imipenem. This signal is transformed into an objective value calculated in real-time. Once the threshold is reached, the software automatically reports the CPE positivity status of the isolate (Supplementary video). A cut-off of 11.5 (arbitrary units [AU]) was defined previously as the threshold for discrimination between carbapenemase and non-carbapenemase producers⁴.

Bacterial isolates and characterisation. The BYG Carba v2.0 was initially validated retrospectively against a collection of 57 reference strains of Enterobacteriaceae including 41 CPE isolates (OXA-48-like [n = 12], KPC [n = 8], NDM [n = 8], VIM [n = 8], IMP [n = 3], GIM [n = 1] and GES-6 [n = 1]) and 16 non-CPE isolates also used for the validation of the BYG Carba test v1.0 in order to compare the signals obtained with both protocols⁵. All 57 isolates were analyzed in triplicate with both methods run in parallel.

The evaluation of the BYG Carba v2.0 was performed in each laboratory both retrospectively, on a collection of strains reflecting the local epidemiology of carbapenemases in different geographical areas in Europe, and prospectively on consecutive non-duplicate isolates referred on a voluntary basis to the national reference centres for investigation of the mechanism(s) of carbapenem resistance. Non-susceptibility to carbapenems was assessed by the reference laboratories following the European Committee on Antimicrobial Susceptibility Testing (EUCAST) guidelines (<http://www.eucast.org>, latest accessed August 23rd 2016). Molecular testing for the detection of carbapenemases was considered as the gold standard and was performed in each laboratory as follows:

In the CHU UCL NAMUR (Yvoir, Belgium) (centre A), the BYG Carba v2.0 was initially challenged retrospectively against 150 clinical consecutive non-duplicate isolates received between January and March 2014. Subsequently, the BYG Carba v2.0 was evaluated against 258 consecutive non-duplicate Enterobacteriaceae isolates referred between August and November 2015. The isolates were characterized as previously described⁵.

Carbapenemases were sought by two in-house ISO15189-certified multiplexed PCRs targeting *bla*_{OXA-48-like}, *bla*_{NDM}, *bla*_{KPC}, *bla*_{VIM} and *bla*_{IMP}²⁶, and the amplicons were sequenced using external Sanger sequencing services (Macrogen, Seoul, Korea) for allele identification.

In the ULB Erasme hospital associated national reference centre (Brussels, Belgium) (centre B), 86 clinical retrospective isolates representative of the hospital epidemiology received between January 2014 and October 2015, and 112 prospective isolates received between November 2015 and April 2016 were analyzed. These isolates were characterised according to the same procedures as in centre A.

In France (centre C), the BYG Carba v2.0 was challenged retrospectively against a collection of 175 Enterobacteriaceae already used for the validation of other carbapenemase diagnostic tests⁹ and prospectively against consecutive 201 non-duplicate clinical enterobacterial isolates received at the French National Reference Centre for Antibiotic Resistance between 15th February and 15th March 2015 for carbapenemase identification. These isolates were analyzed according to the procedure published previously²⁷.

In Public Health England's Antimicrobial Resistance and Healthcare Associated Infections (AMRHA) Reference Unit (London, UK) (centre D), the BYG Carba v2.0 was retrospectively evaluated on 99 Enterobacteriaceae representative of the UK epidemiology and received between January 2013 and December 2015 and prospectively on 100 consecutive Enterobacteriaceae isolates received between April and July 2015. Carbapenemase genes were sought using in-house multiplex PCRs^{28, 29} and confirmed by WGS using a HiSeq sequencer (Illumina) for the retrospective isolates. The resulting WGS data were analyzed using an in-house bioinformatics pipeline with resistance genes identified by mapping reads to an in-house library curated from publicly-available databases³⁰.

Any discrepancies between the BYG Carba v2.0 and molecular assay results obtained in centres B, C, D, were reanalyzed in centre A following its own procedure for bacterial identification, antibiotic susceptibility testing by disc diffusion and PCR for carbapenemase genes. The isolates were also retested with the BYG test v2.0 in centre A. The results subsequently obtained in centre A, were not used for the calculation of the performance of the test but only to investigate the potential sources of discrepancies. Sensitivity, specificity, positive and negative predictive values were calculated using the free software vassarStats: Website for statistical Computation on <http://vassarstats.net/>.

References

- Nordmann, P. & Poirel, L. The difficult-to-control spread of carbapenemase producers in Enterobacteriaceae worldwide. *Clin. Microbiol. Infect.* **20**, 821–830 (2014).
- Patel, G. & Bonomo, R. A. “Stormy waters ahead”: global emergence of carbapenemases. *Front. Microbiol.* **4**, 48 (2013).
- Aguirre-Quinonero, A. & Martínez-Martínez, L. Non-molecular detection of carbapenemases in Enterobacteriaceae clinical isolates. *J. Infect. Chemother.* **23**, 1–11 (2016).
- Noel, A. *et al.* Comparative evaluation of four phenotypic tests for the detection of carbapenemase-producing Gram-negative bacteria. *J. Clin. Microbiol.* **55**, 510–518 (2017).
- Bogaerts, P., Yunus, S., Massart, M., Huang, T. D. & Glupczynski, Y. Evaluation of the BYG Carba Test, a New Electrochemical Assay for Rapid Laboratory Detection of Carbapenemase-Producing Enterobacteriaceae. *J. Clin. Microbiol.* **54**, 349–358 (2016).
- Vourli, S. *et al.* Novel GES/IBC extended-spectrum beta-lactamase variants with carbapenemase activity in clinical Enterobacteria. *FEMS Microbiol. Lett.* **234**, 209–213 (2004).
- Schwaber, M. J. & Carmeli, Y. An ongoing national intervention to contain the spread of carbapenem-resistant Enterobacteriaceae. *Clin. Infect. Dis.* **58**, 697–703 (2014).
- Tato, M. *et al.* Multisite Evaluation of Cepheid Xpert Carba-R Assay for Detection of Carbapenemase-Producing Organisms in Rectal Swabs. *J. Clin. Microbiol.* **54**, 1814–1819 (2016).
- Dortet, L. *et al.* Evaluation of the RAPIDEC® CARBA NP, the Rapid CARB Screen® and the Carba NP test for biochemical detection of carbapenemase-producing Enterobacteriaceae. *J. Antimicrob. Chemother.* **70**, 3014–3022 (2015).
- Lee, C. R. *et al.* Global Dissemination of Carbapenemase-Producing *Klebsiella pneumoniae*: Epidemiology, Genetic Context, Treatment Options, and Detection Methods. *Front. Microbiol.* **7**, 895 (2016).
- Lutgring J. D. & Limbago B. M. 2016. The problem of carbapenemase-producing-carbapenem-resistant-Enterobacteriaceae detection. *J. Clin. Microbiol.* **54**, 529–534 (2016).
- Tijet, N., Boyd, D., Patel, S. N., Mulvey, M. R. & Melano, R. G. Evaluation of the Carba NP test for rapid detection of carbapenemase-producing Enterobacteriaceae and *Pseudomonas aeruginosa*. *Antimicrob. Agents Chemother.* **57**, 4578–4580 (2013).
- Osterblad, M., Hakanen, A. J. & Jalava, J. Evaluation of the Carba NP test for carbapenemase detection. *Antimicrob. Agents Chemother.* **58**, 7553–7556 (2014).
- Chong, P. M. *et al.* MALDI-TOF MS detection of carbapenemase activity in clinical isolates of Enterobacteriaceae spp., *Pseudomonas aeruginosa*, and *Acinetobacter baumannii* compared against the Carba-NP assay. *J. Microbiol. Methods.* **111**, 21–23 (2015).
- Maurer, F. P., Castelberg, C., Quiblier, C., Bloemberg, G. V. & Hombach, M. Evaluation of carbapenemase screening and confirmation tests with Enterobacteriaceae and development of a practical diagnostic algorithm. *Clin. Microbiol.* **53**, 95–104 (2015).
- Dortet, L., Bréchar, L., Poirel, L. & Nordmann, P. Impact of the isolation medium for detection of carbapenemase-producing Enterobacteriaceae using an updated version of the Carba NP test. *J. Med. Microbiol.* **63**, 772–776 (2014).
- Pires, J., Tinguely, R., Thomas, B., Luzzaro, F. & Endimiani, A. Comparison of the in-house made Carba-NP and Blue-Carba tests: Considerations for better detection of carbapenemase-producing Enterobacteriaceae. *J. Microbiol. Methods.* **122**, 33–37 (2016).
- Hombach, M., von Gunten, B., Castelberg, C. & Bloemberg, G. V. Evaluation of the Rapidec Carba NP Test for Detection of Carbapenemases in Enterobacteriaceae. *J. Clin. Microbiol.* **53**, 3828–3833 (2015).
- Albiger, B. *et al.* Carbapenemase-producing Enterobacteriaceae in Europe: assessment by national experts from 38 countries, May 2015. *Euro. Surveill.* **20** (2015).
- Potron, A., Poirel, L., Dortet, L. & Nordmann, P. Characterisation of OXA-244, a chromosomally-encoded OXA-48-like β-lactamase from *Escherichia coli*. *Int. J. Antimicrob. Agents.* **47**, 102–103 (2016).
- Glupczynski, Y. *et al.* Evaluation of two new commercial immunochromatographic assays for the rapid detection of OXA-48 and KPC carbapenemases from cultured bacteria. *J. Antimicrob. Chemother.* **71**, 1217–1222 (2016).
- Meunier, D. *et al.* 2016. Evaluation of the K-SeT R.E.S.I.S.T. immunochromatographic assay for the rapid detection of KPC and OXA-48-like carbapenemases. *J. Antimicrob. Chemother.* **71**, 2357–2359 (2016).

23. Kabir, M. H., Meunier, D., Hopkins, K. L., Giske, C. G. & Woodford, N. A two-centre evaluation of RAPIDEC® CARBA NP for carbapenemase detection in Enterobacteriaceae, *Pseudomonas aeruginosa* and *Acinetobacter* spp. *J. Antimicrob. Chemother.* **71**, 1213–1216 (2016).
24. Yunus, S. *et al.* A method to probe electrochemically active material state in portable sensor applications. *Sensors and Actuators B: Chemical.* **156**, 35–42 (2011).
25. Yunus, S. *et al.* Smart sensor system using an electroactive polymer. WO Patent 2011082837 (2011).
26. Bogaerts, P. *et al.* Validation of carbapenemase and extended-spectrum β -lactamase multiplex endpoint PCR assays according to ISO 15189. *J. Antimicrob. Chemother.* **68**, 1576–1582 (2013).
27. Dortet, L., Cuzon, G., Plésiat, P. & Naas, T. Prospective evaluation of an algorithm for the phenotypic screening of carbapenemase-producing Enterobacteriaceae. *J. Antimicrob. Chemother.* **71**, 135–140 (2016).
28. Ellington, M. J. *et al.* Multicentre evaluation of a real-time PCR assay to detect genes encoding clinically relevant carbapenemases in cultured bacteria. *Int. J. Antimicrob. Agents.* **47**, 151–154 (2016).
29. Ellington, M. J., Kistler, J., Livermore, D. M. & Woodford, N. Multiplex PCR for rapid detection of genes encoding acquired metallo-beta-lactamases. *J. Antimicrob. Chemother.* **59**, 321–322 (2007).
30. Doumith, M. *et al.* Rapid identification of major *Escherichia coli* sequence types causing urinary tract and bloodstream infections. *J. Clin. Microbiol.* **53**, 160–6 (2015).

Acknowledgements

This work was partially supported by the Belgian Walloon region (POC project VALBYG and First Spin off E-Sens Convention 1117301). The funders had no role in study design, data collection and interpretation, or in the decision to submit the work for publication.

Author Contributions

P.B. wrote the manuscript, organized the study and trained the technicians on the field. He validated the molecular results in center A.S.O., D.M., C.N., M.M. performed the evaluation in each laboratory. S.Y. provided the electrodes, the reader and the software and provided electrochemical and informatic support. He realized the video with M.M. O.D., N.W., K.L.H., T.N., L.D., T.-D.H. supervised the study at each center, collected and validated the results of comparative methods at each center. Y.G. designed the study, wrote the manuscript and supervised the whole study. All authors revised the manuscript.

Additional Information

Supplementary information accompanies this paper at doi:[10.1038/s41598-017-09820-y](https://doi.org/10.1038/s41598-017-09820-y)

Competing Interests: PHE's AMRHAI Reference Unit (Daniele Meunier, Katie L Hopkins and Neil Woodford) has received financial support for conference attendance, lectures, research projects or contracted evaluations from numerous sources, including: Accelerate Diagnostics, Achaogen Inc, Allegra Therapeutics, Amplex, AstraZeneca UK Ltd, Basilea Pharmaceutica, Becton Dickinson Diagnostics, bioMérieux, Bio-Rad Laboratories, The BSAC, Cepheid, Check-Points B.V., Cubist Pharmaceuticals, Department of Health, Enigma Diagnostics, Food Standards Agency, GlaxoSmithKline Services Ltd, Henry Stewart Talks, IHMA Ltd, Kalidex Pharmaceuticals, Melinta Therapeutics, Merck Sharpe & Dohme Corp, Meiji Seika Pharm Co., Ltd, Mobidiag, Momentum Biosciences Ltd, Nordic Pharma Ltd, Norgine Pharmaceuticals, Rempex Pharmaceuticals Ltd, Roche, Rokitan Ltd, Smith & Nephew UK Ltd, Trius Therapeutics, VenatoRx Pharmaceuticals and Wockhard Ltd.

Publisher's note: Springer Nature remains neutral with regard to jurisdictional claims in published maps and institutional affiliations.



Open Access This article is licensed under a Creative Commons Attribution 4.0 International License, which permits use, sharing, adaptation, distribution and reproduction in any medium or format, as long as you give appropriate credit to the original author(s) and the source, provide a link to the Creative Commons license, and indicate if changes were made. The images or other third party material in this article are included in the article's Creative Commons license, unless indicated otherwise in a credit line to the material. If material is not included in the article's Creative Commons license and your intended use is not permitted by statutory regulation or exceeds the permitted use, you will need to obtain permission directly from the copyright holder. To view a copy of this license, visit <http://creativecommons.org/licenses/by/4.0/>.

© The Author(s) 2017

B. Développement de nouveaux inhibiteurs de carbapénèmases

Une des approches thérapeutiques utilisable en clinique pour le traitement des souches productrices de carbapénèmases est l'utilisation de la combinaison d'un inhibiteur de carbapénèmases avec un carbapénème. Ainsi, l'inhibiteur cible la β -lactamase en l'inactivant, de sorte que le partenaire β -lactamine peut atteindre sa cible (PLP), entraînant finalement la lyse des cellules bactériennes. Cette stratégie combinatoire est utilisée depuis les années 1980 où un réel succès avait été noté en associant l'acide clavulanique ou d'autres composés semi-synthétiques (sulbactam et tazobactam) avec une pénicilline (amoxicilline, ticarcilline ou pipéracilline) pour le traitement des infections causées par les bactéries productrices de β -lactamases à spectre restreint, les pénicillinases. Malheureusement, ces inhibiteurs spécifiques des β -lactamases de classe A ne sont pas efficaces contre les carbapénèmases des classe B (NDM, VIM, IMP) et D (OXA-48-like) de Ambler. De plus, ils ne possèdent qu'une activité minime, et donc non compatible avec la clinique, pour les carbapénèmases de la classe A d'Ambler (KPC). Afin de mettre au point des inhibiteurs plus efficaces et ayant une bonne activité sur toutes les classes de carbapénèmases (des pan-inhibiteurs), notre unité de recherche a établi une collaboration, dans le cadre du LabEx LERMIT, avec 4 équipes de chimie médicinale (Laboratoire de Chimie Bioorganique du CEA ; ICSN du CNRS; BioCIS et ICCMO de l'Université Paris-Sud) et une équipe de modélisation moléculaire et cristallographie structurale (ICSN du CNRS).

Plusieurs stratégies ont été mise en place pour concevoir ces nouveaux pan-inhibiteurs : (i) synthétiser des inhibiteurs de type chélatant de métaux sélectionnés à partir d'un criblage *in silico* (« docking »), (ii) synthétiser des dérivés de flavonoïdes et de β -dicétones qui se sont révélés être actifs après un criblage *in vitro* d'une chimiothèque, (iii) synthétiser des composés analogues aux β -lactamines : azetidimines, (iv) synthétiser des dérivés imizadolines et (v) synthétiser des β -lactamines (monobactames) fluorés.

Une étape importante du processus de mise-au-point de ces pan-inhibiteurs était de pouvoir tester leur efficacité directement sur des carbapénèmases purifiées. Notre travail a donc consisté à mettre au point un test d'inhibition à haut débit des carbapénèmases OXA-48, KPC-2 et NDM-1 pour le criblage efficace et rapide des molécules néo-synthétisées. D'autres

optimisations ont été nécessaire pour la détermination par spectrophotométrie UV des concentrations inhibitrices 50% (CI50) de ces carbapénèmases pour la β -lactamine d'intérêt clinique (l'imipénème). Ces optimisations ont notamment eu lieu au niveau des quantités d'enzymes et de substrat, ainsi que la mise en place de contrôles appropriés. En parallèle de cette étude biochimique sur enzyme purifiée, les effets de ces pan-inhibiteurs ont été testés sur des souches d'entérobactéries productrices de carbapénèmases (mesure de CMI en présence de différentes concentrations d'inhibiteurs). Les résultats obtenus ont permis une adaptation structurale en temps réel des composés chimiques les plus prometteurs afin d'augmenter leur efficacité mais également leur solubilité. En parallèle, des études de modélisation impliquant les carbapénèmases purifiées en interaction avec quelques inhibiteurs ont permis de comprendre les interactions réelles entre l'enzyme et l'inhibiteur.

Au total, plus de 450 molécules ont été testées. Nous avons pu identifier des molécules (composés flavonoïdes, inhibiteurs de type chélatant de métaux, azetidiniènes et imidazolines) possédant un effet inhibiteur sur les 3 classes de carbapénèmases et avec des valeurs de CI50 sub-micromolaires (et donc compatible avec une possible utilisation *in vivo*). Concernant les composés azetidiniènes (résultats non montrés, Brevet 1) et imidazolines (Brevet 2, Article 11), les valeurs de CI50 sont encourageantes (100 nM), cependant, la solubilité reste faible ce qui nécessitera encore des étapes d'optimisation chimique de ces molécules. Quant aux composés chélateurs, nous avons identifié pour un composé (ayant une CI50 de 50 nM pour l'enzyme NDM-1) une restauration importante de la sensibilité à l'imipénème chez des souches productrices de NDM-1. Cette dernière série de composés ne sera pas évoquée pour des raisons de confidentialité et de propriété intellectuelle. Enfin, les interactions NDM-1 / flavonoïdes (tel que le morin, la quercétine et la myricétine) ont été étudiées par RMN (Article 12). Les résultats obtenus ont permis de mettre en évidence les résidus impliqués dans la liaison avec l'inhibiteur. Nos résultats fournissent la structure RMN de NDM-1 pouvant être utilisée pour étudier les interactions NDM-1 / inhibiteur, ce qui sera très utile pour la conception rationnelle d'inhibiteurs dirigés contre NDM-1.

In fine, bien qu'il y ait encore des optimisations à apporter sur ces inhibiteurs, les résultats obtenus sont prometteurs par rapport à d'autres inhibiteurs déjà décrits dans la littérature.

Brevet 1

Europäisches
Patentamt
European
Patent Office
Office européen
des brevets

European Patent Office
80298 MUNICH
GERMANY

Questions about this communication ?
Contact Customer Services at www.epo.org/contact



OUESLATI, Saoussen
[REDACTED]
[REDACTED]
FRANCE

Date

03.05.17

Reference	Application No./Patent No. 17305257.2 - 1452
Applicant/Proprietor Centre National de la Recherche Scientifique (CNRS), et al	

Designation as inventor - communication under Rule 19(3) EPC

You have been designated as inventor in the above-mentioned European patent application. Below you will find the data contained in the designation of inventor and further data mentioned in Rule 143(1) EPC:

DATE OF FILING : 09.03.17
PRIORITY : //
TITLE : 3-IMIDAZOLINES AS CARBAPENEMASES INHIBITORS
DESIGNATED STATES : AL AT BE BG CH CY CZ DE DK EE ES FI FR GB GR HR HU IE IS IT LI LT LU LV MC MK MT NL NO PL PT RO RS SE SI SK SM TR

INVENTOR (PUBLISHED = 1, NOT PUBLISHED = 0):

1/CARIOU, Kevin/[REDACTED]
1/DODD, Robert H./[REDACTED]
1/ROMERO, Eugénie/[REDACTED]
1/BENCHEKROUN, Mohamed/[REDACTED]
1/IORGA, Bogdan/[REDACTED]
1/NAAS, Thierry/[REDACTED]
1/OUESLATI, Saoussen/[REDACTED]

DECLARATION UNDER ARTICLE 81 EPC:

The applicant(s) has (have) acquired the right to the European patent as employer(s).

Receiving Section



Brevet 1b

Europäisches
Patentamt
European
Patent Office
Office européen
des brevets

European Patent Office
80298 MUNICH
GERMANY

Questions about this communication ?
Contact Customer Services at www.epo.org/contact



QUESLATI, Saoussen

FRANCE

Date

14.10.19

Reference	Application No./Patent No. 18709593.0 - 1110
Applicant/Proprietor Centre National de la Recherche Scientifique - CNRS, et al	

Notification of the data mentioned in Rule 19(3) EPC

In the above-identified patent application you are designated as inventor/co-inventor.
Pursuant to Rule 19(3) EPC the following data are notified herewith:

DATE OF FILING : 08.03.18

PRIORITY : EP/09.03.17/ EPA 17305257

TITLE : 2- OR 3-IMIDAZOLINES AS CARBAPENEMASES INHIBITORS

DESIGNATED STATES : AL AT BE BG CH CY CZ DE DK EE ES FI FR GB GR HR HU IE
IS IT LI LT LU LV MC MK MT NL NO PL PT RO RS SE SI SK SM
TR

For the Examining Division



1 **Article 11: [3+2] Annulation between ketenimines and azaallyl**
2 **anions to access potent non-covalent carbapenemases inhibitors.**

3 Agathe C. A. D'Hollander,¹ Saoussen Oueslati,² Eugénie Romero,¹ Kamsana, Vijayakumar,¹ Camille Le
4 Houérou,¹ Cynthia Exilie,² Linda Tlili,² Pascal Retailleau,¹ Robert H. Dodd,¹ Thierry Naas,^{2,3} Bogdan I.
5 Iorga,¹ Kevin Cariou^{1,*}

6 **Introduction**

7 Due to their safety, reliable killing properties and clinical efficacy, β -lactams such as
8 penicillins, cephalosporins and carbapenems (Fig. 1a) are among the most frequently
9 prescribed antibiotics nowadays. However, their usefulness is being threatened by the
10 worldwide emergence and proliferation of bacteria exhibiting one or several mechanisms of
11 resistance.^{1,2} Unless solutions are found, global projections for 2050 lead to an estimate of 10
12 million deaths per year that would be attributable to antimicrobial resistance vs. 8.2 million due
13 to cancer.³ One prevalent mechanism consists in the enzymatic hydrolysis of the β -lactam ring
14 by β -lactamases (BLs). These enzymes belong to four classes depending on their amino-acid
15 sequence and their mode of action. ⁴ Classes A, C and D, contain an active serine residue in the
16 active site (serine- β -lactamases, SBLs) and act through a covalent inhibition mechanism. Class B
17 gathers metallo- β -lactamases (MBLs) such as New-Delhi Metallo- β -lactamase-1 (NDM-1),⁵ that
18 proceed through a hydrolysis mechanism assisted by one or two Zn^{2+} ions in the catalytic site.
19 Among BLs, carbapenemases are highly worrisome since they hydrolyze penicillins,
20 cephalosporins and even carbapenems, the most potent and last resort β -lactam antibiotics that
21 are used in intensive care units. The rapid global dissemination of BLs, and more particularly of
22 carbapenemases, in *Enterobacteriaceae* can produce community-acquired carbapenem-
23 resistant strains that are a matter of great clinical concern.⁶ Since the discovery of novel
24 antibiotics is difficult to foresee,⁷ developing strategies to inhibit β -lactamases may safeguard

¹ Institut de Chimie des Substances Naturelles, CNRS UPR 2301, Université Paris-Sud, Université Paris-Saclay, Avenue de la
Terrasse, 91198 Gif-sur-Yvette, France. ²EA7361, Université Paris-Sud, Université Paris-Saclay, LabEx Lermite, Bacteriology-
Hygiene unit, AP-HP, Hôpital Bicêtre, Le Kremlin-Bicêtre, France. ³Associated French National Reference Centre for
AntibioticResistance: Carbapenemase-producing Enterobacteriaceae, Le Kremlin-Bicêtre, France *e-mail:
kevin.cariou@cnrs.fr

25 our current antibacterial armamentarium.⁸⁻¹⁰ Since 2012, several new broad-spectrum
 26 inhibitors of class A and class C SBLs that can be used in combination with β -lactam antibiotics
 27 have emerged. Avibactam¹¹ and vaborbactam (RPX7009)¹² were recently approved by the FDA
 28 (Fig. 1b) in combination with a cephalosporine and a carbapenem respectively. Several other
 29 inhibitors¹³⁻¹⁶ are currently at different stages of preclinical or clinical development. Despite
 30 continuous efforts, there is still a need for the development of efficient MBLs,¹⁷⁻²¹ as none has
 31 been clinically approved yet. The task is becoming even more arduous as bacteria
 32 simultaneously producing two and even three different carbapenemases of different classes are
 33 more frequently isolated. This critical situation now dictates the development of β -lactamase
 34 inhibitors capable of simultaneously inhibiting SBLs and MBLs. To date, only one series of cyclic
 35 boronates has been reported of being able to simultaneously inhibit SBLs and MBLs.^{22,23} To rise
 36 to this challenge we elected the β -lactam nucleus, which is recognized by all these enzymes, as
 37 the starting point. As a mean to structurally diverge from this minimal substrate scaffold to
 38 access an inhibitor scaffold, we resorted to purely synthetic organic methodology.^{24,25} Long
 39 before the discovery of penicillin, Staudinger devised a straightforward access to the β -lactam
 40 ring by a [2+2] cycloaddition between a ketene and an imine (Fig. 1c).²⁶ This reaction, named
 41 the Staudinger Synthesis, set the template for accessing this particular heterocycle and
 42 stemmed myriads of synthetic variations.²⁷ Our group developed an imino-variant of this
 43 transformation by using an ynamide (**1a**)²⁸⁻³⁰ to generate *in situ* a highly reactive
 44 ketenimine(**2a**)³¹⁻³³ which can engage in a [2+2] cycloaddition with a diaryl imine (**3a**) to give an
 45 azetidimine (Fig. 1d).³⁴ *In vitro* evaluation of these compound confirmed that they could inhibit
 46 all classes of carbapenemases.³⁵ Exploring further this transformation, we found that when the
 47 same reaction conditions were applied to the homologous benzylimine **3b**, the formation of
 48 the expected azetidimine was not observed. Instead, 2,5-dihydro-1H-imidazole **6ab** was
 49 obtained with 39% yield (Fig. 1e). We hypothesized that this 5-membered ring arose from a
 50 [3+2] cycloaddition between the ketenimine and with semi-stabilized 2-azaallyl lithium **5'a**,
 51 which was also formed *in situ* under the basic reactions conditions.^{36,37} Overall, reports of 1,3
 52 dipolar cycloaddition with a ketenimine as the dipolarophile remain rather scarce.³⁸⁻⁴⁰
 53 Moreover, [3+2] cycloadditions with non- or semi-stabilized azallylanions^{41,42} were mostly
 54 developed with olefins as the dipolarophiles.⁴³⁻⁴⁵ This serendipitous discovery thus gave us
 55 the opportunity to explore some uncharted chemical space for the discovery of BL inhibitors.

56 Results

57 Chemical synthesis

58 When we reacted ynamide **1a** with *N*-benzylimine **3c** under the imino-Staudinger
59 synthesis reaction conditions,³⁴ 2,5-dihydro-1H-imidazole **6ac** was obtained in 42% yield,
60 along with 15% of imidazole **7ac** and 6% of 4,5-dihydro-1H-imidazole **8ac** that incorporates
61 two ketenimine fragments. The reaction conditions were optimized (see Supplementary
62 Information) by increasing the dilution (from 0.1 M to 0.2 M), lowering the temperature (from
63 100 °C to 80 °C) and using 10mol% of zinc acetate as an additive and a larger excess of base
64 (4.4 equivalents). It was also found that the formation of the oxidized **7** could be mostly
65 avoided by bubbling argon and that diminishing the amount of ynamide to 1.5 equivalents
66 reduced the formation of **8**. Having selected the best conditions, we then explored the scope
67 of this [3+2] annulation, starting with the imine partner. First, benzylic aldimines **3** leading to
68 symmetrical aza-allyl anions **5**, with various groups – H (**3d**), halogens (**3e,f,h**), MeO (**3g**) and
69 electron withdrawing groups (**3i,j**) on the *para* positions, were screened. The 1,5-dihydro-1H-
70 imidazoles were obtained in moderate to good yields with good to excellent
71 diastereoselectivities in favor of the *cis*-isomer (Fig. 2a), as confirmed single-crystal X-ray
72 diffraction analysis for **6ag** (Fig. 2b). The reaction was not operative for imines bearing strong
73 electron withdrawing groups such as CF₃ or NO₂ (**3i,j**), and the low solubility of diiodo imine
74 **3h** was found detrimental to the reaction's success. Nevertheless, imines bearing heterocycles
75 such as 2-furanyl (**3k**), 2-thiopheny (**3l**) or 2-pyridinyl (**3m**) were well tolerated. Finally, a
76 ketenimine (*N*-benzyl-1,1-diphenylmethanimine **3n**) was also subjected to the reaction
77 conditions and **6al** was formed as a single regioisomer in 72 % yield. This is in sharp contrast
78 with the reactivity of aldimines bearing two different aryl groups, such as **3b**, that lead to
79 inseparable mixtures of regioisomers.

80 The scope of the ynamide partner was then delineated (Fig. 2c). As with the imino-
81 Staudinger [2+2] cycloaddition, only ynamides bearing an aryl group on the nitrogen were
82 suitable for the generation of the ketenimine intermediate and Boc was the best leaving
83 group. *N*-Aryl ynamides bearing halogens (Cl and F, **1b,c**), electron-donating (OMe and OEt,

84 **1e,f**) or electron withdrawing (CF₃, **1g**) groups gave 1,5-dihydro-1H-imidazoles **5** as the major
 85 adducts, generally along with minor amounts of double addition compound **8**.

86 Again, the low solubility of the *p*-iodo compound was responsible for the low yield of **6dc**,
 87 while the *p*-nitro functionality (**1h**) was incompatible with the reaction conditions. The
 88 reaction was also operative if the triple bond was substituted by an alkyl (*n*-Bu, **1i**), an aryl (Ph,
 89 **1j**) or a silyl (TIPS, **1k**), albeit with a low 18 % yield in this case. When an ynamide bearing a
 90 silyl-protected primary alcohol on the triple bond (**1l**) was submitted to the reaction
 91 conditions, imidazole **9** was isolated instead of **6lc**. The latter would not come from a oxidative
 92 aromatization but rather from the isomerization of a vinylated 1,5-dihydro-1H-imidazole,
 93 resulting from a [3+2] annulation with a cumulenimine (see **2l'**, Fig. 3f).

94 In order to gain more insight on the [3+2] annulation process and the formation of side
 95 products **7** and **8**, we performed several control experiments. First, deuterated ynamide **1a-D**
 96 was synthesized and reacted with imine **3c** (Fig. 3a). All adducts **6ac**, **7ac** and **8ac** were isolated
 97 as mixtures of non- and mono-deuterated compounds, predominantly corresponding to the
 98 initial ynamide deuterium position (C1 as well as C4 for **8ac**). Yet, for **6ac-D** other deuterium
 99 incorporation sites were identified at the C2 and C3 positions of the five-membered ring. A
 100 complementary experiment was performed by reacting ynamide **1a** with the bis-deuterated
 101 imine **3c-D₂** (Fig. 3b). In this setting, the adducts were obtained as non-, mono- and di-
 102 deuterated compounds, again with several deuterium incorporation sites at C1, C2, C3 and/or
 103 C4, including a double deuteration at C4 for **8ac-D₂**. This broad distribution pattern seems to
 104 indicate that many proton exchange steps would take place during the formation of the five-
 105 membered adducts. However no deuteration was observed when the reaction was performed
 106 in deuterated DMF. To ascertain whether some elemental steps in our manifold would be
 107 reversible we resubmitted *cis*-**6ac** to the reaction conditions with 1.5 equivalents of **1a** (Fig.
 108 3c).

109 While *cis*-**6ac** was mostly recovered (67% yield), the *trans* isomer (*trans*-**6ac**, 9%), the
 110 imidazole resulting from an oxidation (**7ac**, 7%) and the double addition adduct (**8ac**, 11%)
 111 were also obtained. On the contrary, **8ac** did not yield **6ac** back when it was submitted to the
 112 reaction condition (minus the ynamide) and the direct oxidation of **6ac** into **7ac** was never
 113 observed. Considering all these results a plausible mechanistic proposal was outlined and
 114 verified using DFT calculations (Fig. 3d). Under the strongly basic conditions, and possibly with

115 the assistance of the zinc Lewis acid,⁴⁶ partial decomposition of the DMF to give lithium
 116 dimethylamide would be the trigger to initiate the cleavage of the Boc protecting group of
 117 ynamide **1** giving the semi-stabilized amide **10** that protonates to give ketenimine **2**. The
 118 generation of dimethylamine in the reaction was confirmed by the isolation of amidines **15**,
 119 **15-D₆** (when DMF-D₇ was used) and **16** (Fig. 3e). The latter is rather peculiar and would be
 120 consistent with the formation of cumulenimine **2I'**, rather than the expected ketenimine **2I**
 121 (Fig. 2f), from amide **10I**. Thus its reaction with imine **3c** would give a vinyl-1,5-dihydro-1H-
 122 imidazole which would eventually isomerize to give ethyl-imidazole **9** (Fig. 2b). Deprotonation
 123 of the imine **3** would give the semi-stabilized diaryl azallylanion **5**, which would add onto the
 124 ketenimine to give enamide **11** that would cyclize to give imidazolinide **12**. Overall this process
 125 is nearly ergoneutral ($\Delta G = 1.6 \text{ kcal.mol}^{-1}$), the first step being exergonic by $14.8 \text{ kcal.mol}^{-1}$,
 126 with a rather low activation barrier ($3.1 \text{ kcal.mol}^{-1}$). From this intermediate, successive
 127 protonations and deprotonations as well as tautomerization of the enamide and/or imine
 128 moieties can take place, which would explain the complex deuteration patterns that we
 129 observed (Fig. 2a & 2b). These experiments also indicate that the the imine is the major
 130 purveyor of protons and that the ynamide only contributes to a lesser extent; the protons
 131 being channeled either by direct deprotonation or through the *tert*-butanol generated from
 132 an initial deprotonation with the lithium *tert*-butoxide. By modelling the various anions
 133 resulting from these events (see Supplementary Information) we were able to identify
 134 azallylanion **13** as being the most favored at $-28.1 \text{ kcal.mol}^{-1}$. A final reversible (as evidenced
 135 by the experiment in Fig. 3c) protonation would give **6**, while its reaction with another
 136 equivalent of ketenimine would lead to **8**. Moreover, in the presence of dioxygen, it could be
 137 oxidized to **7**, presumably through an intermediate peroxide anion that would readily
 138 aromatize.

139 **Evaluation of the activity of the different compounds**

140 To evaluate the activity of the compounds, we determined the IC₅₀ of each compound on
 141 purified carbapenemases of OXA-48, KPC-2 and NDM-1 and their effect in combination with
 142 imipenem (IMP) on *E. coli* GUE clinical isolate expressing NDM-1. The minimum inhibitory
 143 concentrations (MICs), for imipenem alone and in combination with the compounds against
 144 the resistant strain were determined (Table 1). It is important to note, that no antibiotic effect

145 was detected for any the compounds tested alone. Overall the tested compounds can be first
146 viewed as a promising novel family of NDM-1 inhibitors. Indeed, most derivatives are active
147 against NDM-1 in the micromolar to submicromolar range and are able to divide by two the
148 MIC of imipenem against clinical isolate GUE-NDM-1 when used at 200 μ M. The simplest
149 example is the triphenyl derivative **6ad** (entry 3, IC_{50} =7.2 μ M against NDM-1). Apparently
150 minimal variations on this basic scaffold can then bring forth significant differences in their
151 activity profile, that allow to draw some general trends for structure-activity relationships
152 (SAR) studies. The introduction of heteroarenes on the imine moiety is highly detrimental and
153 no activity could be measured for **6ak**, **6al** and **6am** (bearing furanes, thiophens and pyridines
154 respectively). However, *para*-substitution of the aryle with a halide (Cl or Br for **6ac** and **6af**)
155 or a methoxy (**6ag**) led to an increase of the anti-NDM-1 activity, both in terms of IC_{50} and of
156 MIC, and to the observation of SBLs inhibition for **6ag** and especially **6af**. The latter's IC_{50} is
157 below 10 μ M for carbapenemases belonging to three distinct molecular classes (NDM-1 is a
158 MBL, while KPC-2 and OXA-48 are class A and D SBLs). Quite interestingly, the *trans* isomer
159 (which is the minor compound in the reaction) exhibit a better inhibition profile than the
160 corresponding *cis* isomer. This is evidenced by *trans*-**6af**, whose IC_{50} are systematically lower
161 than its *cis* isomer **6af** and *trans*-**6af** that, contrary to *cis*-**6af**, has a *pan* inhibitor profile. This
162 is also the case for the tetra-phenyl derivative **6an**. One particular feature of **6ag** is that with
163 a similar *in vitro* potency it appears much better in terms of MIC improvement (from 16mg/L
164 to 2mg/L of imipenem when used at 200 μ M), which could be due to better solubility and
165 membrane-penetration properties compared to the halogenated derivatives. The activity of
166 the 2,5-dihydro-1H-imidazoles derived from the bis *para*-chlorobenzene imine **3c** were then
167 assayed. Most compounds in this sub-series showed a *pan*-inhibitor profile *in vitro*, with the
168 highest activities measured for the more lipophilic derivatives, bearing a substituted
169 methylene at the 5 position, with R being an alkyl (**6ic**), a phenyl (**6jc**) or a silyl group (**6kc**). In
170 the latter case, the *trans* isomer (*trans*-**6kc**) once again showed a slightly better inhibitory
171 profile. The incorporation of a *para*-iodo substituent on the *N*-aryl moiety also led to an
172 increased *in vitro* activity, in particular against NDM-1. Two fully aromatized derivatives **7ac**
173 and **7gc** were evaluated and both showed improved activity compared to the 2,5-dihydro
174 parent compounds **6ac** and **6gc**. Finally, some 4,5-dihydro-1H-imidazole incorporating two
175 ketenimine moieties were also evaluated. All were found to be excellent NDM-1 inhibitors
176 with IC_{50} values between 0.4 μ M and 4.4 μ M, in particular those having two *para*-chlorophenyl

177 substituents at the 2 and 4 positions ((**8ac-8dc**-and **8gc**; $0.4 \mu\text{M} < \text{IC}_{50} < 1.7 \mu\text{M}$) that were as
178 or more potent than their mono-addition counterparts (**6ac-6dc**-and **6gc**). Of particular
179 interest is compound **8cc** that allows for a two-fold decrease of the MIC of imipenem on
180 clinical isolate GUE-NDM-1 at a $50 \mu\text{M}$ dose.

181

182 Conclusions

183 Bu using organic methodology to derive from the β -lactam nucleus we were able to
184 develop a novel [3+2] annulation between ketenimines and azaallyl anions (both generated *in*
185 *situ* from ynamides and benzylarylimines, respectively) to access various five-membered
186 heterocycles. Systematic *in-vitro* evaluation of the compounds thus obtained against three
187 clinically significant carbapenemases – belonging to three distinct β -lactamase classes –
188 showed that they constitute a novel family of *pan* inhibitors. All active compounds were
189 systematically more active against NDM-1 with 8 molecules having IC_{50} s in the submicromolar
190 range and two molecules being able to repotentiate imipenem in a significant manner (the
191 MIC being improved from $16 \mu\text{g}/\text{L}$ to $4 \mu\text{g}/\text{mL}$ and even $2 \mu\text{g}/\text{mL}$ with compounds **8aa** and **6ag**)

192

193 References

- 194 1. Llarrull, L. I., Testero, S. A., Fisher, J. F. & Mobashery, S. The future of the β -lactams. *Current Opinion in*
195 *Microbiology* **13**, 551–557 (2010).
- 196 2. King, D. T., Sobhanifar, S. & Strynadka, N. C. J. One ring to rule them all: Current trends in combating
197 bacterial resistance to the β -lactams. *Protein Sci.* **25**, 787–803 (2016).
- 198 3. O'Neill, J. *Tackling drug-resistant infections globally: final report and recommendations.* (2016).
- 199 4. Hall, B. G. & Barlow, M. Revised Ambler classification of β -lactamases. *J Antimicrob Chemother* **55**, 1050–
200 1051 (2005).
- 201 5. Linciano, P., Cendron, L., Gianquinto, E., Spyrakis, F. & Tondi, D. Ten Years with New Delhi Metallo- β -
202 lactamase-1 (NDM-1): From Structural Insights to Inhibitor Design. *ACS Infect. Dis.* **5**, 9–34 (2019).
- 203 6. Al, P. N. et. Global Spread of Carbapenemase-producing Enterobacteriaceae - Volume 17, Number 10—
204 October 2011 - Emerging Infectious Diseases journal - CDC. doi:10.3201/eid1710.110655
- 205 7. Falagas, M. E., Mavroudis, A. D. & Vardakas, K. Z. The antibiotic pipeline for multi-drug resistant gram
206 negative bacteria: what can we expect? *Expert Rev. Anti Infect. Ther.* **14**, 747–763 (2016).

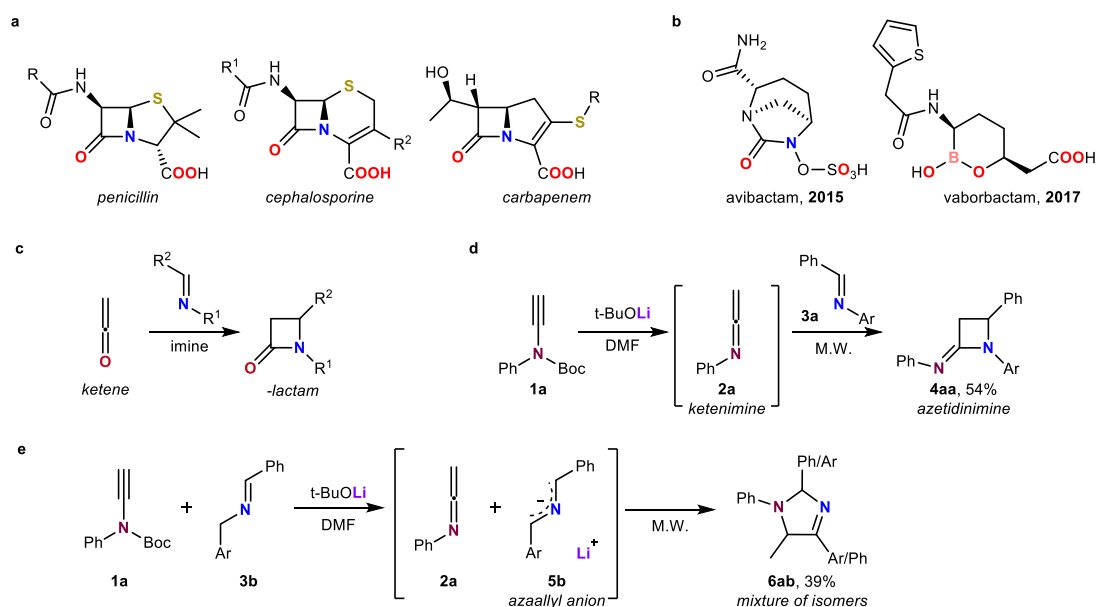
- 207 8. Drawz, S. M., Papp-Wallace, K. M. & Bonomo, R. A. New β -Lactamase Inhibitors: a Therapeutic
208 Renaissance in an MDR World. *Antimicrobial Agents and Chemotherapy* **58**, 1835–1846 (2014).
- 209 9. Chellat, M. F., Raguž, L. & Riedl, R. Targeting Antibiotic Resistance. *Angew. Chem. Int. Ed.* **55**, 6600–6626
210 (2016).
- 211 10. Lakemeyer, M., Zhao, W., Mandl, F. A., Hammann, P. & Sieber, S. A. Thinking Outside the Box—Novel
212 Antibacterials To Tackle the Resistance Crisis. *Angew. Chem. Int. Ed.* **57**, 14440–14475 (2018).
- 213 11. Ehmann, D. E. *et al.* Avibactam is a covalent, reversible, non- β -lactam β -lactamase inhibitor. *Proceedings of*
214 *the National Academy of Sciences* **109**, 11663–11668 (2012).
- 215 12. Hecker, S. J. *et al.* Discovery of a Cyclic Boronic Acid β -Lactamase Inhibitor (RPX7009) with Utility vs
216 Class A Serine Carbapenemases. *J. Med. Chem.* **58**, 3682–3692 (2015).
- 217 13. Hirsch, E. B. *et al.* In Vitro Activity of MK-7655, a Novel β -Lactamase Inhibitor, in Combination with
218 Imipenem against Carbapenem-Resistant Gram-Negative Bacteria. *Antimicrobial Agents and*
219 *Chemotherapy* **56**, 3753–3757 (2012).
- 220 14. Morinaka, A. *et al.* OP0595, a new diazabicyclooctane: mode of action as a serine β -lactamase inhibitor,
221 antibiotic and β -lactam ‘enhancer’. *J. Antimicrob. Chemother.* **70**, 2779–2786 (2015).
- 222 15. Livermore, D. M., Mushtaq, S., Warner, M., Vickers, A. & Woodford, N. In vitro activity of
223 cefepime/zidebactam (WCK 5222) against Gram-negative bacteria. *J. Antimicrob. Chemother.* **72**, 1373–
224 1385 (2017).
- 225 16. Durand-Réville, T. F. *et al.* ETX2514 is a broad-spectrum β -lactamase inhibitor for the treatment of drug-
226 resistant Gram-negative bacteria including *Acinetobacter baumannii*. *Nature Microbiology* **2**, (2017).
- 227 17. Tehrani, K. H. M. E. & Martin, N. I. Thiol-Containing Metallo- β -Lactamase Inhibitors Resensitize Resistant
228 Gram-Negative Bacteria to Meropenem. *ACS Infect. Dis.* **3**, 711–717 (2017).
- 229 18. King, A. M. *et al.* Aspergillomarasmine A overcomes metallo- β -lactamase antibiotic resistance. *Nature*
230 **510**, 503–506 (2014).
- 231 19. Xiang, Y. *et al.* Rhodanine as a Potent Scaffold for the Development of Broad-Spectrum Metallo- β -
232 lactamase Inhibitors. *ACS Med. Chem. Lett.* **9**, 359–364 (2018).
- 233 20. Brem, J. *et al.* Rhodanine hydrolysis leads to potent thioenolate mediated metallo- β -lactamase inhibition.
234 *Nature Chemistry* **6**, 1084–1090 (2014).
- 235 21. Leiris, S. *et al.* SAR Studies Leading to the Identification of a Novel Series of Metallo- β -lactamase
236 Inhibitors for the Treatment of Carbapenem-Resistant Enterobacteriaceae Infections That Display
237 Efficacy in an Animal Infection Model. *ACS Infect. Dis.* **5**, 131–140 (2019).
- 238 22. Brem, J. *et al.* Structural basis of metallo- β -lactamase, serine- β -lactamase and penicillin-binding protein
239 inhibition by cyclic boronates. *Nat. Commun.* **7**, 12406 (2016).
- 240 23. Cahill, S. T. *et al.* Cyclic Boronates Inhibit All Classes of β -Lactamases. *Antimicrob. Agents Chemother.* **61**,
241 e02260-16 (2017).
- 242 24. Brown, D. G. & Boström, J. Analysis of Past and Present Synthetic Methodologies on Medicinal Chemistry:
243 Where Have All the New Reactions Gone? *J. Med. Chem.* **59**, 4443–4458 (2016).
- 244 25. Boström, J., Brown, D. G., Young, R. J. & Keserü, G. M. Expanding the medicinal chemistry synthetic
245 toolbox. *Nat. Rev. Drug Discov.* **17**, 709–727 (2018).

- 246 26. Staudinger, H. Zur Kenntniss der Ketene. Diphenylketen. *Justus Liebigs Annalen der Chemie* **356**, 51–123
 247 (1907).
- 248 27. Pitts, C. R. & Lectka, T. Chemical Synthesis of β -Lactams: Asymmetric Catalysis and Other Recent
 249 Advances. *Chem. Rev.* **114**, 7930–7953 (2014).
- 250 28. Evans, G., Coste, A. & Jouvin, K. Ynamides: Versatile Tools in Organic Synthesis. *Angewandte Chemie*
 251 *International Edition* **49**, 2840–2859 (2010).
- 252 29. DeKorver, K. A. *et al.* Ynamides: A Modern Functional Group for the New Millennium. *Chem. Rev.* **110**,
 253 5064–5106 (2010).
- 254 30. Wang, X.-N. *et al.* Ynamides in Ring Forming Transformations. *Acc. Chem. Res.* **47**, 560–578 (2014).
- 255 31. Hentz, A., Retailleau, P., Gandon, V., Cariou, K. & Dodd, R. H. Transition-Metal-Free Tunable
 256 Chemoselective N Functionalization of Indoles with Ynamides. *Angewandte Chemie International Edition*
 257 **53**, 8333–8337 (2014).
- 258 32. Lu, P. & Wang, Y. The thriving chemistry of ketenimines. *Chem. Soc. Rev.* **41**, 5687–5705 (2012).
- 259 33. Dodd, R. H. & Cariou, K. Ketanimines Generated from Ynamides: Versatile Building Blocks for Nitrogen-
 260 Containing Scaffolds. *Chemistry - A European Journal* (2017). doi:10.1002/chem.201704689
- 261 34. Romero, E. *et al.* Base-Mediated Generation of Ketanimines from Ynamides: Direct Access to
 262 Azetidanimines by an Imino-Staudinger Synthesis. *Chemistry - A European Journal* (2017).
 263 doi:10.1002/chem.201702545
- 264 35. Dodd, R., Cariou, K., Minard, C., Iorga, B. & Naas, T. Azetidanimines as Carbapenemases Inhibitors. (2019).
- 265 36. Li, M. *et al.* Transition-metal-free chemo- and regioselective vinylation of azaallyls. *Nat. Chem.* **9**, 997–
 266 1004 (2017).
- 267 37. Shelp, R. A. & Walsh, P. J. Synthesis of BCP Benzylamines From 2-Azaallyl Anions and [1.1.1]Propellane.
 268 *Angew. Chem. Int. Ed.* **57**, 15857–15861 (2018).
- 269 38. Namitharan, K. & Pitchumani, K. Copper(I)-Catalyzed Three Component Reaction of Sulfonyl Azide,
 270 Alkyne, and Nitrene Cycloaddition/Rearrangement Cascades: A Novel One-Step Synthesis of
 271 Imidazolidin-4-ones. *Org. Lett.* **13**, 5728–5731 (2011).
- 272 39. Li, S., Luo, Y. & Wu, J. Three-Component Reaction of N'-(2-Alkynylbenzylidene)hydrazide, Alkyne, with
 273 Sulfonyl Azide via a Multicatalytic Process: A Novel and Concise Approach to 2-Amino-H-pyrazolo[5,1-
 274 a]isoquinolines. *Org. Lett.* **13**, 4312–4315 (2011).
- 275 40. Alajarin, M., Bonillo, B., Ortin, M.-M., Orenes, R.-A. & Vidal, A. Unprecedented intramolecular [3 + 2]
 276 cycloadditions of azido-ketenimines and azido-carbodiimides. Synthesis of indolo[1,2-a]quinazolines
 277 and tetrazolo[5,1-b]quinazolines. *Org. Biomol. Chem.* **9**, 6741–6749 (2011).
- 278 41. Kauffmann, T., Berg, H., Ludorff, E. & Woltermann, A. Anionic 3 + 2 Cycloaddition of 2-Azaallyllithium
 279 Compounds to CN and NN Double Bonds. *Angewandte Chemie International Edition in English* **9**, 960–961
 280 (1970).
- 281 42. Kauffmann, T., Berg, H. & Köppelmann, E. Anionic 3 + 2 Cycloaddition. *Angewandte Chemie International*
 282 *Edition in English* **9**, 380–381 (1970).
- 283 43. Pearson, W. H. & Stoy, P. Cycloadditions of Nonstabilized 2-Azaallyllithiums (2-Azaallyl Anions) and
 284 Azomethine Ylides with Alkenes: [3+2] Approaches to Pyrrolidines and Application to Alkaloid Total
 285 Synthesis. *Synlett* **2003**, 0903–0921 (2003).

- 286 44.Otero-Fraga, J., Montesinos-Magraner, M. & Mendoza, A. Perspectives on Intermolecular Azomethine
287 Ylide [3+2] Cycloadditions with Non-Electrophilic Olefins. *Synthesis* **49**, 802–809 (2017).
- 288 45.Otero-Fraga, J., Suárez-Pantiga, S., Montesinos-Magraner, M., Rhein, D. & Mendoza, A. Direct and
289 Stereospecific [3+2] Synthesis of Pyrrolidines from Simple Unactivated Alkenes. *Angew. Chem. Int. Ed.*
290 **56**, 12962–12966 (2017).
- 291 46.Yang, L., Lin, J., Kang, L., Zhou, W. & Ma, D.-Y. Lewis Acid-Catalyzed Reductive Amination of Aldehydes
292 and Ketones with N,N-Dimethylformamide as Dimethylamino Source, Reductant and Solvent. *Adv. Synth.*
293 *Catal.* **360**, 485–490 (2018).
- 294 47.Bonnin, R. A., Poirel, L., Carattoli, A. & Nordmann, P. Characterization of an IncFII Plasmid Encoding NDM-
295 1 from Escherichia coli ST131. *PLOS ONE* **7**, e34752 (2012).

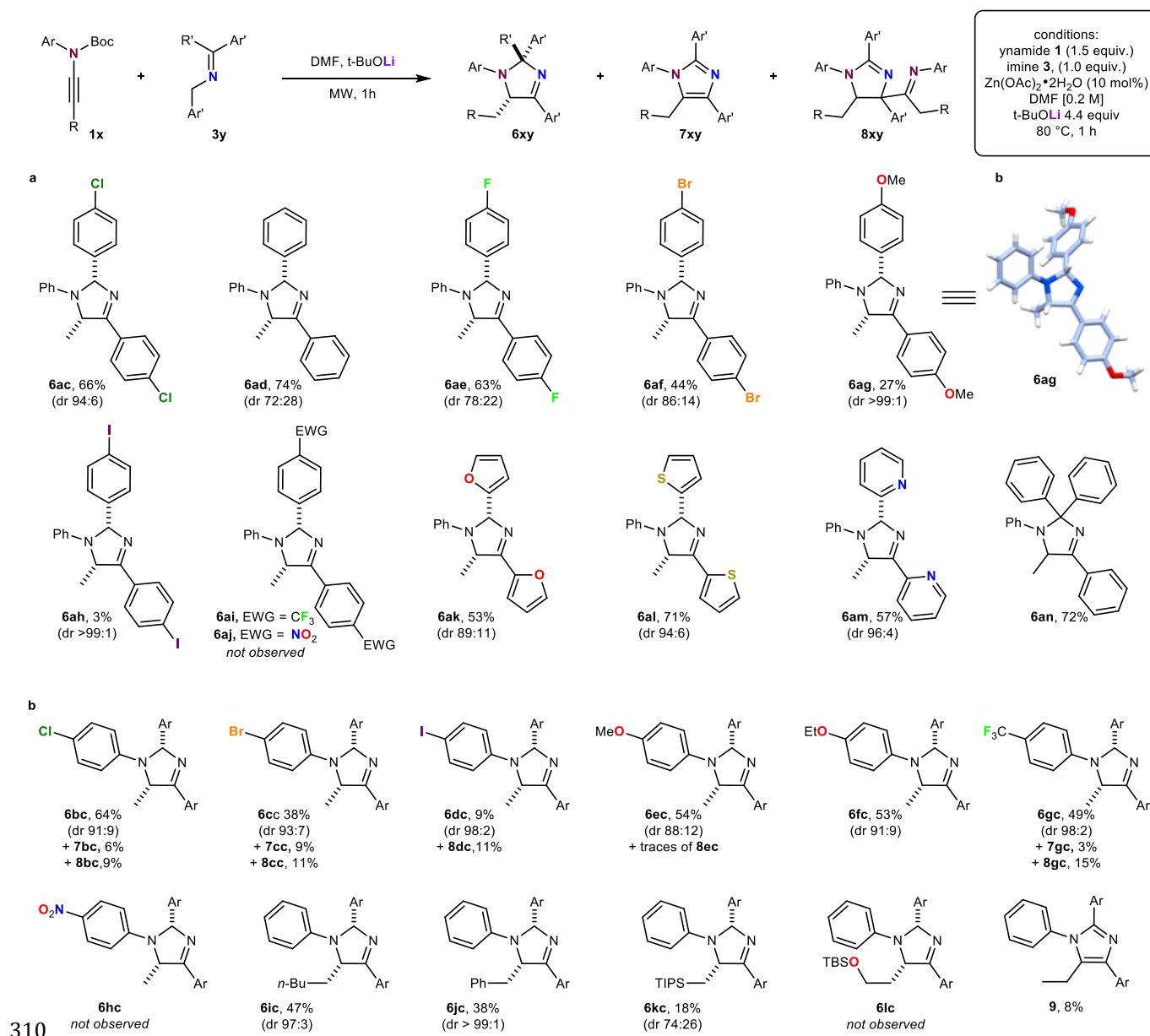
296

297

298 **Figures and Tables**

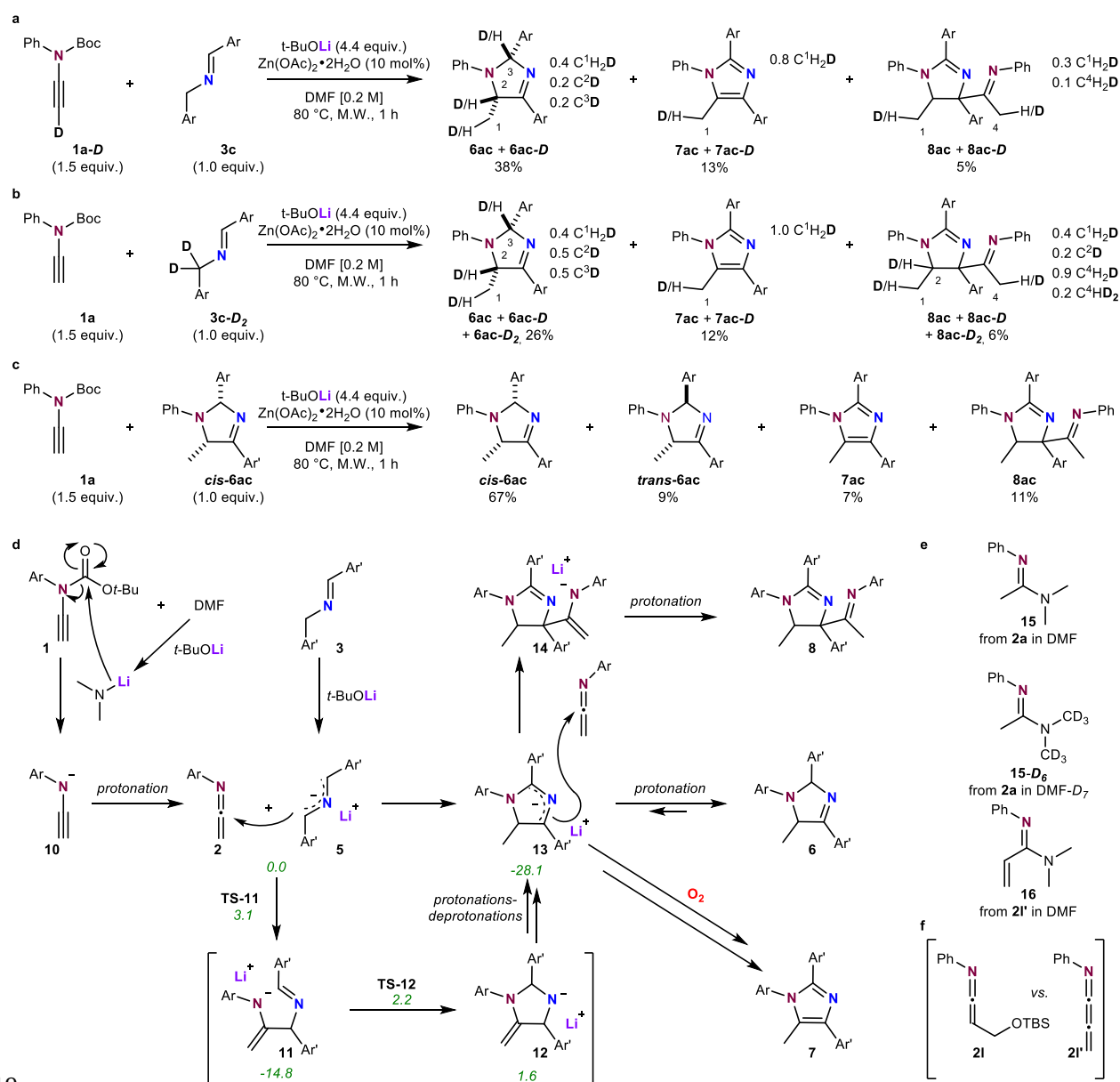
299

300 **Fig. 1 | β -lactamin antibiotics, β -lactamase inhibitors, [2+2] and [3+2] annulations involving ketenes,**
 301 **ketenimines and imines. a**, General structures of penicillin, cephalosporin and carbapenem antibiotics.
 302 **b**, Structure of two β -lactamase inhibitors currently in clinical use (in bold their year of FDA approval).
 303 **c**, The Staudinger Synthesis is a [2+2] cycloaddition between a ketene and an imine to give a β -lactam.
 304 **d**, [2+2] Annulation (imino-Staudinger Synthesis) between *N*-phenyl-ketenimine **2a**, generated *in situ*^a
 305 from ynamide **1a** and imine **3a** (Ar = *p*-OMe-C₆H₄) to give azetidinimine **4aa** in 54% yield.^a **e**, [3+2]
 306 Annulation between ketenimine **2a** and azallyl anion **5b** formed *in situ*^a from ynamide **1a** and imine **3b**
 307 (Ar = *p*-OMe-C₆H₄) to obtain 2,5-dihydro-1H-imidazole **6ab** in 39% yield. ^a Ynamide (2.0 equiv.), imine
 308 (2.0 equiv.), *t*-BuOLi (2.0 equiv.), SiO₂ (1.0 equiv.) in DMF (0.3 M) at 100°C for 1 h. Boc, *tert*-
 309 butoxycarbonyl; *t*-Bu, *tert*-butyl; DMF, dimethylformamide; M.W., microwave irradiation.



311 **Fig. 2 | Scope of the [3+2] annulation. a**, Scope of the imine in the [3+2] annulation using ynamide **1a**.
 312 **b**, ORTEP drawing of the X-ray crystal structure of **6ag**. **c**, Scope of the ynamide in the [3+2] annulation
 313 using imine **5c** (Ar = *p*-Cl-C₆H₄). Reactions were conducted on a 0.2 mmol scale. Isolated yields after
 314 chromatographic purification (sum of the yields for each diastereoisomer). Diastereoisomeric ratios
 315 were evaluated from the analysis of the ¹H NMR spectrum of the crude reaction. *t*-Bu, *tert*-butyl; dr,
 316 diastereoisomeric ratio; DMF, dimethylformamide; M.W., microwave irradiation; TBS, *tert*-
 317 butyldimethylsilyl; TIPS, triisopropylsilyl.

318



319

320 **Fig. 3 | Control experiments and mechanism proposal.** **a**, Deuterium incorporation in the reaction
 321 products starting from using deuterated ynamide **1a-D**. **b** Deuterium incorporation in the reaction
 322 products starting from using deuterated imine **3c-D₂**. **c**, Reaction of 1,5-dihydro-1H-imidazole **cis-6ac**
 323 with ynamide **1a** under the optimized conditions. Reactions were conducted on a 0.2 mmol scale.
 324 Isolated yields after chromatographic purification. Deuterium incorporation positions and
 325 quantification were evaluated from the analysis of the ¹H NMR spectra of the compounds. *t*-Bu, *tert*-
 326 butyl; dr, diastereoisomeric ratio; DMF, dimethylformamide; M.W., microwave irradiation; TBS, *tert*-
 327 butyldimethylsilyl; TIPS, triisopropylsilyl **d**, Mechanism proposal. Gibbs free energies (in green) are in
 328 kcal mol⁻¹ relative to **2** and **5** and were calculated for Ar = Ar' = Ph using. **e**, Isolated amidines from the
 329 addition of dimethylamine to the ketenimines. **f**, Ketenimine vs. cumulenimine intermediates.

Compound	IC ₅₀ (μM)			MIC (mg/L)		
	NDM-1	OXA-48	KPC-2	200 μM compound	100 μM compound	50 μM compound
6ad	7.2	-	-	8	-	-
6ak	-	-	-	-	-	-
6al	-	-	-	-	-	-
6am	-	-	-	-	-	-
6ac	3.9	-	-	-	-	-
Trans-6ac	4.0	7.0	2.5	8	8	-
6af	6.6	9.0	2.0	8	-	-
Trans-6af	3.6	4.0	1.5	8	8	8
6ag	3.8	-	40%	2	4	4
6an	1.3	2.7	2.7	8	8	-
6bc	2.5	10.0	6.0	8	8	-
6cc	10.0	7.0	3.5	8	-	-
6dc	0.5	2.8	4.6	8	8	8
6ec	2.6	-	10.0	NM	8	-
6fc	2.3	9.0	31%	8	8	-
6gc	2.8	3.0	6.1	8	-	-
6ic	0.8	6.0	6.4	8	-	-
6jc	1.1	3.0	4.0	8	8	-
6kc	0.14	2.0	10.0	8	-	-
Trans-6kc	0.15	1.5	4.2	8	8	8
7ac	3.0	6.5	1.5	8	-	-
7gc	0.9	3.0	3.5	8	8	8
8ac	1.7	38%	6.2	8	-	-
8ad	4.4	-	30%	-	-	-
8bc	0.4	31%	3.7	8	8	-
8cc	0.6	36%	4.4	4	4	4
8dc	0.7	4.0	3.0	8	-	-
8gc	1.3	2.2	6.5	8	-	-

MIC without compound =16

330 **Table 1 | *In vitro* activity of the compounds.** IC₅₀ were determined against the panel of purified
331 carbapenemase: OXA-48, KPC-2 and NDM-1 by spectrophotometric assay, using ULTROSPEC 2000 UV
332 spectrophotometer and the SWIFT II software (GE Healthcare, Velizy-Villacoublay, France).
333 Compounds were dissolved in DMSO stock solutions at 10 mM; more dilute stocks were subsequently
334 prepared as necessary by dissolving them also in DMSO. Assay conditions were as follows: 100 mM
335 phosphate buffer, pH 7 (added with 50 μM ZnSO₄ when testing NDM-1, and with 50 mM NaHCO₃ when
336 testing OXA-48), 100 μM imipenem (Tianam). The reaction was monitored at 297 nm, time course 600
337 seconds at 25°C with 3 min of incubation (compound/carbapenemase). Each inhibitor compound was

338 assayed at seven different concentrations, in triplicate for calculating an error value with 95%
339 confidence interval ($p < 0.05$). IC_{50} values were determined using the equation $IC_{50} = ((1/0.5 \times v_0) -$
340 $m)/q$, where v_0 is the rate of hydrolysis of the reporter substrate (v_0 being the rate measured in the
341 absence of inhibitor), q the y axis intercept and m the slope of the resulting linear regression. MIC
342 values were determined by broth microdilution, in triplicate, in cation-adjusted Mueller Hinton broth
343 according to the Clinical Laboratory Standards Institute (CLSI) guidelines. The enterobacterial clinical
344 strains E. coli NDM-1 GUE expressing the carbapenemase NDM-1 was used.⁴⁷ Experiments were
345 performed in microtiter plates containing the medium with imipenem and inhibitors (dissolved in
346 DMSO). Three inhibitor concentrations were tested: 50, 100 and 200 μM . Plates were incubated
347 overnight at 37°C for 18–24 h. DMSO, dimethyl sulfoxide; MIC, Minimum Inhibitory Concentration; ND,
348 Not Determined; UM, Unmeasurable; -, No Activity;

$IC_{50} < 1$

$1 \leq IC_{50} < 5$

$5 < IC_{50}$

349

1 **Article 12: NMR characterization of the Zn(II) ions influence on the**
2 **New-Delhi Metallo- β -lactamase-1 and its interaction with flavonols.**

3
4 Gwladys Rivière^{1§}, Maud Gayral^{2§}, Saoussen Oueslati^{3§}, Jean-Bernard Créchet⁴, Naïma Nhiri¹, Eric Jacquet¹,
5 Ewen Lescop¹, Carine van Heijenoort¹, JC Cintrat⁵, Casimir Blonski², Eric Guittet¹, Thierry Naas³, Bogdan Iorga¹,
6 Nelly Morellet^{1*}

7
8 ¹ Institut de Chimie des Substances Naturelles, CNRS UPR 2301, Université Paris-Sud, Université
9 Paris-Saclay, LabEx LERMIT, 1 avenue de la Terrasse, 91190, Gif-sur-Yvette, France;

10 ² Institut de Chimie Moléculaire et des Matériaux d'Orsay (ICMMO), CNRS, Univ Paris Sud,
11 Université Paris-Saclay, 15 rue Georges Clemenceau, 91405 Orsay Cedex, France.

12 ³ EA7361 'Structure, Dynamic, Function and Expression of Broad Spectrum β -Lactamases', Faculty
13 of Medicine, Université Paris-Sud, LabEx LERMIT, Université Paris-Saclay, Le Kremlin-Bicêtre, France.

14 ⁴ Ecole Polytechnique, Route de Saclay, F-91120 Palaiseau, France;

15 ⁵ Service de Chimie Bio-organique et Marquage (SCBM), CEA, Université Paris-Saclay, 91191
16 Gif/Yvette, France.

17
18 Running title: *NMR characterization of the NDM-1 interaction with flavonols*

19
20 **Keywords:** NDM-1, *Klebsiella pneumoniae*, Flavonols, Nuclear magnetic resonance, Thermal Shift,
21 Molecular modeling

22

23 **ABSTRACT**

24 NDM-1 is a metallo- β -lactamase that has recently emerged as a global threat because of its
25 ability to confer resistance to all common β -lactam antibiotics and of its carriage on multidrug
26 resistant plasmids present in clinically-relevant Gram-negative bacteria (*Enterobacteriales*,
27 *Pseudomonas aeruginosa* and *Acinetobacter baumannii*), responsible of both nosocomial and
28 community-acquired infections. Understanding the molecular basis of β -lactam hydrolysis by NDM
29 is detrimental for designing NDM-inhibitors or β -lactams that are resistant to their hydrolysis. In
30 this study, for the first time NMR was used to investigate the dynamic behaviour of NDM-1 in
31 presence and in absence of Zn(II) ions. Our results highlighted that the binding of Zn(II) in the NDM-
32 1 active site induced several structural and dynamic changes on the ASL2, L9 loops and helix α 2.
33 We subsequently studied the binding of several flavonols: morin, quercetin and myricetin that have
34 been identified as natural and specific NDM-1 inhibitors. The NDM-1/flavonol interactions were
35 investigated by NMR and the results highlighted that residues from the NDM-1 ASL1, ASL2 and ASL4
36 loops are implicated in flavonols binding. Our results provide the first interaction studies by NMR
37 of NDM-1/inhibitors used to generate models, which will be useful for the rational design of
38 inhibitors against NDM-1.

39

40

41 **INTRODUCTION**

42

43 Gram-negative bacteria (GNB), especially *Enterobacteriaceae*, *Pseudomonas aeruginosa*
44 and *Acinetobacter baumannii*, have re-emerged as major players in antimicrobial resistance
45 worldwide (1,2). In these species, resistance may affect all major classes of anti-gram-negative
46 agents, the multidrug resistance (MDR) or even pan drug resistances being relatively common (3).
47 Currently, β -lactamase-mediated resistance does not spare even the newest and most powerful β -
48 lactams (carbapenems), whose activity is challenged by metallo- β -lactamases (MBLs, class B) and
49 by the serine-carbapenemases (classes A and D) (4-6). MBLs are by far the most worrisome β -
50 lactamases since they hydrolyze almost all β -lactam substrates, and because currently no clinically
51 useful inhibitors are available for this class (6). The dissemination of MBL genes among GNB is a

52 matter of great clinical concern, given the importance of these pathogens as causes of nosocomial
53 infections and, for *Enterobacteriaceae*, also of community-acquired infections, and the major role
54 of expanded-spectrum cephalosporins and carbapenems, in the treatment of these infections. β -
55 lactamases catalyzes the opening the β -lactam ring, thus inactivating β -lactam antibiotics (7). Based
56 on their amino acid sequence, the β -lactamases have been grouped into four major classes. Classes
57 A, C and D use an active-site serine to catalyze hydrolysis, while metallo- β -lactamases (MBLs) or
58 class B β -lactamases require one or two Zn(II) ions for their activity (8). Based on structural diversity
59 of the active sites, such as differences in metal content and the residues involved in metal
60 coordination, MBLs have been divided further into three subclasses: B1, B2 and B3 (8). The
61 pandemic New Delhi metallo- β -lactamase-1 (NDM-1) disseminating worldwide in Gram-negative
62 organisms threatens to take medicine back into the pre-antibiotic era since the mortality associated
63 with infections caused by these “superbugs” is very high and the choices of treatment are very
64 limited. NDM-1, a member of subclass B1 MBLs has rapidly spread worldwide located on several
65 MDR plasmids (9-12). Many structures of NDM-1, complexed or not with metal ions and a variety
66 of substrates are available in the Protein Data Bank (PDB). NDM-1 adopts the MBLs general $\alpha\beta/\beta\alpha$
67 fold (13-18), composed of two central β -sheets and five solvent-exposed α -helices. Many
68 experimental and theoretical studies have been carried out to define the catalytic mechanism of
69 NDM-1 (14,18-22). The active site is a hydrophobic cavity, which consists of two Zn(II) atoms (Zn1
70 and Zn2) surrounded by five mobile labelled loops called Active Site Loops (ASL1-5) responsible for
71 substrate binding and specificity (14). Zn1 and Zn2 are coordinated by H120, H122, H189 and D124,
72 C208, H250 respectively, with different affinities (23), and by a water molecule located between
73 these two Zn(II) ions, which acts as a nucleophile during β -lactam hydrolysis. As all MBLs, NDM-1
74 is not sensitive to any serine- β -lactamase inhibitors commercially-available. Development of active
75 inhibitors for the NDM-1 enzyme has been widely undertaken. It has been shown that the metal
76 chelator EDTA inactivates the enzymatic activity of NDM-1 by removing the catalytically-required
77 Zn(II) ions (17,24), but its toxicity hinders its clinical use. It has been shown that the approved drugs
78 that exhibit sulfhydryl moieties such as captopril, captopril derivatives (17,25,26), thiorphan,
79 dimercaprol and tiopronin (27) displayed a high inhibitory effect on NDM-1 enzymatic activity in
80 vitro. Several papers reveal that diaryl-substituted azolythioacetamides (28,29), maleic acid (30),
81 rhodanine (31) bisthiazolidine (32), chromene (33) and chromone (34) derivatives, sulfonamide

82 containing compounds (35) Quinolinium derivatives (36), Diamidine compounds (37), rosmarinic
83 acid and salvianolic acid A (38), dithiocarbamate (39), cationic chalcone derivatives (40),
84 azolylthioacetamides (41), dipicolinic acid derivatives (42) are good starting points for the
85 development of clinically useful MBL inhibitors. Potent NDM-1 inhibitors were identified through
86 virtual screening of natural compounds, such as: i) the natural product aspergillomaramine,
87 analogous to the metal ion chelator EDTA, results also in very potent observed inhibition (43,44),
88 ii) baicalin that has been shown to possess an inhibitory effect on NDM-1 (45), iii) magnolol which
89 has a significant impact on NDM-1 enzyme activity in vitro (46), iv) hesperidin acts directly on key
90 residues near the NDM-1 active site (47). ANT431, a novel pyridine-2-carboxylic acid that was
91 specifically designed to inhibit MBLs, is currently in preclinical development (48,49). ANT431
92 showed sub-micromolar inhibitory activity against purified NDM-1 and VIM-2 in a biochemical
93 assay, with at least 20-fold weaker inhibition of VIM-1 and IMP-1. To gain a more complete
94 understanding of the structural basis for the antibiotic resistance conferred by NDM-1, we have
95 performed NMR assignments and relaxation experiments of NDM-1 in presence and in absence of
96 Zn(II) to better characterize the Zn(II) induced enzymatic activation. The backbone NMR resonance
97 assignments of NDM-1 highlighted the structural and dynamic changes induced by the binding of
98 Zn(II) in the enzyme active site. Moreover, we identified three flavonols (class of flavonoids): morin,
99 quercetin and myricetin as natural and specific inhibitors of NDM-1 activity with a dissociation
100 constant of the order of 300 μ M. The flavonols are polyphenol compounds that are ubiquitously
101 distributed in a wide range of vascular plants (50). The flavonoids are recognized to possess a
102 variety of biological activities and important therapeutic applications (51-59). We used NMR
103 spectroscopy to map the interacting site of NDM-1 upon complexation to the three flavonols. Our
104 results show that the NDM-1 ASL1, ASL2 and ASL4 loops are disturbed by the bindings of flavonols
105 and that the Zn(II) ions are involved in their binding. Our results provide support for models of the
106 NDM-1/flavonol complexes generated using the program HADDOCK, which will be useful for the
107 rational design of ligands with increased activity.

108

109

110

111

112 **RESULTS**

113 ***NDM-1 sample preparation for NMR studies***

114

115 We verified by NMR spectroscopy and Thermal shift experiments that NDM-1 was produced
116 free of Zn(II). No variation of the chemical shifts was observed in the HSQC spectra on one hand
117 and no modification on NDM-1 thermo-stability profiles (data not shown) was noted on the other
118 hand upon addition of EDTA. Addition of increasing amounts of Zn(II) to the metal-free NDM-1
119 followed by thermal shift assay resulted in an increase of the denaturation temperature of the
120 protein (Fig. 1), indicating that Zn(II) strongly stabilizes NDM-1. However, at high concentration of
121 Zn(II) (above 2 molar equivalents of Zn(II)) we observed a noticeable increase in fluorescence
122 background before the denaturation of NDM-1, suggesting the appearance of a hydrophobic region
123 or the formation of oligomers. This effect is slightly observed at a concentration of Zn(II) above 2
124 molar equivalents and is very important around 6 equivalents of Zn(II) relative to the protein
125 concentration. It could be explained by interactions between each His-tag and Zn(II) in excess firstly,
126 and secondly by intermolecular interactions between several NDM-1 proteins, mediated by the His-
127 tag/Zn(II) complexes. These intermolecular interactions seem to destabilize each NDM-1 monomer
128 at low temperature, stability which is recovered with an increasing temperature, resulting in a likely
129 dissociation of the intermolecular NDM-1 interactions, around 42°C and 47°C for Zn(II)
130 concentration of 25 µM and 50 µM respectively. Effect of Zn(II) binding on the structural and
131 dynamic properties of NDM-1 has been followed by NMR. The ¹H-¹⁵N HSQC spectra of ¹⁵N labelled
132 NDM-1, recorded in absence and in presence of 2 molar equivalents of Zn(II), showed well-
133 dispersed cross-peaks characteristic of a well-folded protein, as already mentioned by Zheng *et al.*
134 (60). In presence of 1 equivalent of Zn(II), we observed two NDM-1 states in slow exchange on the
135 NMR chemical shift time scale, as seen for a large number of NDM-1 residues for which the free
136 and bound resonances have different ¹H and ¹⁵N chemical shifts. This indicated slow exchange
137 between free and bound form for NDM-1 at the NMR chemical shift timescale. Upon addition of 2
138 molar equivalents of Zn(II), we only observed resonances of the NDM-1 bound state. The ¹H-¹⁵N
139 HSQC spectrum underwent a drastic change that affected the majority of cross-peaks in the
140 spectrum, demonstrating a high affinity of NDM-1 toward Zn(II). Beyond 2 equivalents of Zn(II),
141 dramatic decrease of all the ¹H-¹⁵N cross-peak intensities was observed together with an intense

142 precipitation, suggesting the formation of NDM-1 oligomers. These NMR data are in agreement
143 with thermal shift experiments (Fig. 1) which show that slight excess of Zn(II) induce an
144 oligomerization of NDM-1 and further demonstrate that NDM-1 binds two Zn(II) ions, in agreement
145 with the crystal structure. Therefore in order to limit protein self -association for the rest of the
146 study we decided to never exceed the 2 molar equivalents of Zn(II).

147

148

149 ***NMR backbone resonance assignment of NDM-1***

150 In order to determine the NDM-1 residues influenced by Zn(II) binding we have undertaken
151 the backbone NMR resonance assignment of NDM-1 alone and complexed with Zn(II), using the
152 classical triple resonance and NOESY correlation experiments. ¹⁵N HSQC and triple resonance
153 spectra were recorded at several temperatures ranging from 20°C to 35°C on ¹³C/¹⁵N-labeled NDM-
154 1 samples. The optimum quality of the spectra, used for assignment was observed at 20°C in
155 absence of Zn(II) and at 27°C in presence of 150 mM NaCl and 2 molar equivalents of Zn(II) relative
156 to the NDM-1 concentration. Amongst the 253 amino acids, 89.7% of metal-free NDM-1 backbone
157 amide protons were assigned. The missing assignments involve residues of the unstructured N-
158 terminus (M28-E30) and the residues located on flexible loops (e.g. V118-D130, Q151-V155, G207
159 and C208. From di-Zn(II) NDM-1 sample, 94% NDM-1 ¹H-¹⁵N cross-peaks were assigned. Only the
160 backbone proton assignments of 14 residues (residues M28-E30, N57, K125, M126, G186, G207,
161 K216, N220, L221, A257, L271 and E272) are missing probably due to intermediate conformational
162 exchange or fast solvent exchange that results into severe line broadening for these amino-acids.
163 Many of these residues play an important role in the enzymatic catalysis. Indeed, the residues N220
164 and L221 are located in the ASL4 loop, which has a direct role in the recognition of substrate (61).
165 10% additional backbone resonances were assigned when compared to the available assignment
166 of NDM-1 in presence of Zn(II) (Yao *et al.*) (62). We used the TALOS-N software (63) to predict the
167 protein backbone torsion angles from NMR chemical shifts and consequently the secondary
168 structure, on the metal-free NDM-1 and di-Zn(II) NDM-1 complex. The predictions were compared
169 to the secondary structure elements present in the X-ray structure of NDM-1 in absence and in
170 presence of Zn(II) (13,64). The secondary structure elements location in the metal-free NDM-1 and
171 di-Zn(II) NDM-1 complex derived from TALOS-N software are in very good agreement with those

172 from crystal NDM-1 structure in absence and in presence of Zn(II), respectively. The results show
173 also that Zn(II) binding does not significantly modify the NDM-1 secondary structures. As already
174 noted by Zheng et al (60) substantial differences were observed between the HSQC spectra
175 recorded on metal-free NDM-1 and di-Zn(II) NDM-1. The analysis of the ^{15}N - ^1H assignment and
176 chemical shift perturbations (CSPs) after addition of increasing concentration of Zn(II) to NDM-1
177 suggests that the protein undergoes local structural changes during the binding of two Zn(II) (Fig.
178 2). The most significant changes are located in the ASL2, ASL3, ASL5 loops, which contain the
179 residues H120, H122, D124, H189, C208 and H250 involved in the two Zn(II) coordination.
180 Interestingly, we also observed that the distant region of the Zn(II) binding site such as the β -sheet
181 which flanked the ASL1 loop, the L5 and L9 loops and the helix α 2 (Fig.2) are also affected by Zn(II)
182 binding. On the contrary the ASL1 and ASL4 loops show smaller chemical shift perturbation upon
183 Zn(II) binding, except the first residues of ASL4 loop (residues 206-209), probably due to the
184 coordination interaction of C208 with Zn(II).

185

186 ***Analysis of ^{15}N relaxation***

187 To gain more insight into the impact of Zn(II) binding on NDM-1 dynamics, we collected ^{15}N
188 R1 and R2 relaxation rates and $\{^1\text{H}\}$ - ^{15}N heteronuclear NOE (hetNOE) values (at 600 MHz and 298
189 K) which provide information about local and global dynamics in the protein. The results show that
190 the overall structure of NDM-1 is relatively rigid in presence or in absence of Zn(II), except the N-
191 terminal extremity, which exhibited the shortest transversal relaxation rates and smallest hetNOE
192 values, as expected for highly mobile regions. The ^{15}N relaxation rates are homogeneous over the
193 folded domains with averaged R1 and R2 values of $0.73 \pm 0.05 \text{ s}^{-1}$ and $24.41 \pm 1.68 \text{ s}^{-1}$ respectively
194 in absence of Zn(II) and $0.63 \pm 0.05 \text{ s}^{-1}$ and $31.48 \pm 1.39 \text{ s}^{-1}$ respectively in presence of Zn(II) (Fig.3).
195 The smaller R1 and higher R2 averaged value calculated in presence of Zn(II) could be explained by
196 the formation of oligomers induced by a slight excess of Zn(II) as already seen using the Thermal
197 shift experiments. In absence of Zn(II), we observed several flexible regions in addition to the N-
198 terminal domain: the ASL1 (residues 65-74), ASL2 (residues 118-124), L9 (residues 150-158), ASL3
199 (residues 184-194), ASL4 (residues 208-226) loops, and the 2 (residues 128-134) and α 3 helices
200 (residues 225-240) (Fig. 3A) that show elevated ^{15}N R1 and decreased ^{15}N R2 and hetNOE values
201 relative to the NDM-1 structured domains. In absence of Zn(II) the three Zn(II) ligands (H120, H122

202 and D124) belonging on the ASL2 loop undergo fluctuations that propagate throughout the ASL2
203 loop and α 2 helix. The ASL2 and L9 loops could influence each other due to their spatial proximities
204 in the 3D structure (Fig. 2B). In absence of Zn(II), the majority of the residues belonging to the ASL2,
205 L9 loops and α 2 helix showed significative line broadening in agreement with intermediate
206 exchange (at the NMR chemical shift timescale), suggesting that the active site is not properly
207 organized. Upon Zn(II) binding, the corresponding cross-peaks reappeared in the NMR spectra,
208 allowing their relaxation parameters to be measured. Only the ASL1 and ASL4 active site loops, the
209 N- and C-termini residues stay flexible in presence of Zn(II) (Fig. 3B). These results suggested that
210 the binding of two Zn(II) induces local structural and dynamical changes on NDM-1 and specific
211 rigidification of the active site loops with potential impact for the correct organization of the active
212 site.

213

214 ***The flavonol molecules inhibit NDM-1 activity***

215

216 NDM-1 uses two Zn(II) ions and a water molecule coordinated in between in its active site
217 for hydrolysis of the β -lactam ring of β -lactam antibiotics, as they stabilize the high-energy
218 intermediate of the hydrolysis reaction (65). Based on this mechanism, we aimed to determine the
219 inhibitory activity of simplified structures, providing an initial structure-activity relationship (SAR)
220 that highlighted a common fragment, which was a phenol, substituted with a keto moiety in the
221 position 2. The second ketone substituent might be aromatic, enolic or aliphatic, the best inhibitory
222 activities being obtained in the first two cases. Based on this minimal structure, a chemoinformatic
223 analysis has identified 222 molecules of this type available within the LabEx LERMIT chemical
224 library. The biological screening of this library using the miniaturized automated assay allowed us
225 to identify three flavonoids (quercetin, myricetin and morin) as the best inhibitors of NDM-1 (Fig.
226 4). Overall the best results have been obtained for myricetin (85 % of inhibition at 50 μ M). Due to
227 solubility problems, the IC50 values for quercetin could only be estimated between 5 and 10 μ M.
228 In order to sort out this problem of solubility, we first synthesized quercetin conjugates that should
229 have better stability, solubility, as well as bioavailability, but none of them gave better result than
230 quercetin. The IC50 for myricetin was determined as 3.3 μ M. Myricetin was also tested at a

231 concentration of 50 μM against other carbapenemases: OXA-48 and KPC-2, with inhibitions of 90%
232 and 78%, respectively.

233

234 ***In vivo activities of flavonol molecules on clinical NDM-1 producing E. coli isolate***

235 Whether these molecules may have a *in vivo* activity on bacteria expressing NDM-1,
236 Minimum inhibitory concentrations for imipemen of *K. pneumoniae* CAG expressing NDM-1 and *E.*
237 *coli* GUE expressing NDM-1 have been determined in presence of increasing amount of myricetin
238 (Table 1). 8 fold drop in MICs was observed with 500 μM myricetin (going from 128, to 16 $\mu\text{g}/\text{ml}$)
239 for *K. pneumoniae* CAG, and a 16 fold drop in MICs for *E. coli* GUE with 500 μM myricetin (128 to 8
240 $\mu\text{g}/\text{ml}$). Thus illustrating that these molecules have an *in vivo* activity. A concentration of 500 μM
241 myricetin has no effect on the growth of the bacteria in absence of imipenem. The values for
242 quercetin could not be determined precisely, due to solubility problems, nevertheless, with 100 μM
243 and 200 μM , two and three dilution drop of MICs was observed respectively with the strain *E.*
244 *coli* GUE NDM-1. No effect has been observed with the strain *K. pneumoniae* CAG (Table 1).

245

246 ***NMR characterization of the binding interface between NDM-1 and the three flavonols: morin,*** 247 ***myricetin and quercetin***

248 The NDM-1/flavonol interactions were investigated by NMR in presence of Zn(II) (Fig. 6 and
249 7). As the ligands (morin, myricetin and quercetin) were sparingly soluble in aqueous solution (these
250 molecules are hydrophobic, and the LogP estimation indicated that the myricetin has the best
251 solubility in water and buffer) they were introduced to the NDM-1 samples from a concentrated
252 stock of a deuterated dimethyl sulfoxide (DMSO). We verified that the addition of low quantities of
253 DMSO (5.36 μL , which corresponds to the quantity added to NDM-1 for 2 equivalents of flavonol)
254 did not induce precipitation of the protein nor chemical shift variations (Fig. 6A1, 6B1, 6C1). We
255 titrated 300 μM of NDM-1 with the flavonols (0 to 4 equivalents) and recorded at each stage of the
256 titration 1D ^1H and 2D ^1H - ^{15}N HSQC spectra (Fig. 6). In all cases we observed a slight precipitation
257 of the ligands probably due to their hydrophobic properties. The flavonol signals were observed in
258 the 1D ^1H NMR spectra only after the addition of 3eq of flavonol, which corresponds to the
259 simultaneous addition of 8 μL of DMSO and therefore to a better dissolution of the molecules. The
260 CSPs of NDM-1 backbone resonances were followed using the ^1H - ^{15}N HSQC spectra as a function of

261 the theoretical calculated flavonol (morin, quercetin, or myricetin) concentrations. The interaction
262 of NDM-1 with flavonols results in significant CSPs of numerous backbone amide protons and
263 nitrogen. The analysis highlighted a specific site for interaction of the three flavonols to NDM-1 (Fig.
264 6 and 7). The NDM-1 residues implicated in the interaction with the three flavonols belong mostly
265 to the flexible loops ASL1, ASL2 and ASL4, and to a lesser extend to ASL3 (Fig.7) with subtle
266 differences between the three flavonols. The residues belonging to the ASL1 and ASL4 loops
267 undergo the largest CSPs in presence of morin, and W93 and H250 show much higher CSP in the
268 presence of morin than in presence of myricetin or quercetin (Fig. 6 and 7). On the contrary the
269 highest CSPs were observed in the ASL2 loop in presence of quercetin by comparison with that
270 observed after addition of morin. Although specific, the disturbances induced by the binding of the
271 flavonols propagate along the flexible domains of NDM-1 as showed by the CSPs of relatively large
272 domains such as: 62-80, 208-223 and 250-254 (Fig. 7). CSPs were used to estimate the dissociation
273 constant, K_d , of morin and myricetin despite the uncertainty about the real concentration of ligands
274 available in solution because of their precipitation. As exchange is fast on the chemical shift
275 timescale, an estimated K_d value around 300 μ M for the two ligands could be calculated using the
276 residues that undergo the highest CSPs (L65 and D66). In order to determine the influence of Zn(II)
277 on the flavonol interaction, CSPs of NDM-1 backbone resonances were followed using the ^1H - ^{15}N
278 HSQC spectra recorded at each increment of morin (0 to 4 eq) in absence of Zn(II). The analysis
279 shows that morin interacts also with NDM-1 in absence of zinc, however the CSPs are of lower
280 intensities at equal concentration of ligand and more dispersed along the sequence of the protein
281 by comparison with that happens in presence of 2 eq of Zn(II). In absence of Zn(II) and in presence
282 of 4 eq of morin the ASL1 and ASL4 loops are the domains of NDM-1 that undergo the major CSPs.
283 However in absence of Zn(II) several other regions are also targeted by the flavonol, including
284 residues 100-111, 135-138, 156-177 by comparison with what happened in presence of Zn(II).
285 Interestingly we noted that the two tryptophan residues (W104 and W168) and the numerous
286 hydrophobic residues localized in these domains could interact with the very hydrophobic flavonol.
287 Thus we conclude that the two Zn(II) ions contribute to increase ligand affinity as well as to direct
288 the flavonol binding to the active site of the NDM-1, which is also consistent with the observed CSPs
289 of several Zn(II) ligands (H122, D124, H250) (Fig. 7). Our results indicate that morin, quercetin and
290 myricetin interact with active site residues of NDM-1 such as D124, H250 and in a lesser extend

291 with C208, and with Zn1 and Zn2 without ejection of Zn(II). Despite some chemical shift variations
292 upon ligand binding, the ^1H - ^{15}N HSQC spectra retain indeed their initial appearance namely the
293 appearance of the spectrum of NDM-1 in presence of 2 equivalents of Zn(II), and not that of NDM-
294 1 recorded in absence of Zn(II). Moreover, hydrophobic residues around the active site L65, F70,
295 and W93 seem also play a significant role in recognizing the substrate. It seems then that the
296 residues L65, M67, F70, W93, H122, Q123, D124, N220, H250 and the two Zn(II) are implicated in
297 the binding of the flavonols.

298

299

300

301 ***Reconstruction of the NDM-1/flavonol binding interfaces by molecular docking simulations.***

302 As no intermolecular NOE was observed in the ^{15}N - ^{13}C filtered ^1H - ^1H NOESYs recorded on
303 ^{13}C - ^{15}N labelled NDM-1/flavonol complexes, structural models of the NDM-1/morin, NDM-
304 1/quercetin and NDM-1/myricetin complexes were constructed using molecular-docking
305 simulations in the NMR data-driven program HADDOCK (High Ambiguity Driven biomolecular
306 DOCKing) on the basis of the experimental CSPs in order to understand the molecular basis for
307 flavonol recognitions by NDM-1. In order to propose relevant models, several series of calculation
308 were undertaken using nineteen crystallographic structures of NDM-1 since the docking can be
309 influenced by the starting protein structure, whether obtained in the presence or absence of ligand.
310 Ten of them were in complex with a ligand and they were used after removing of the complexed
311 ligand. We named them “artificial apo” (art-apo) NDM-1 structures. Five structures were apo NDM-
312 1 crystal structures and four were metal-free apo form of NDM-1. The superimposition of the ten
313 art-apo NDM-1 structures between them or with the five apo NDM-1 structures in one hand and
314 the metal-free apo NDM-1 structures on the other hand, highlights that the major structural
315 differences are located in the ASL1 and ASL4 loops. Moreover the distances between the two Zn(II)
316 (Zn1 and Zn2) fluctuate from one structure to another depending of the presence or not of a ligand
317 and of the type of ligand, with the Zn1-Zn2 distances ranging from 3.1 to 3.8 Å in the apo NDM-1
318 crystal structures, and from 3.6 to 4.6 Å in the art-apo NDM-1 structures as already mentioned by
319 Zhang *et al.* (66). Based on the available experimental NMR CSP values, the residues L65, M67, F70,
320 W93, H122, Q123, D124, N220, H250 were determined as belonging to the interface and used as

321 ambiguous interaction restraints in docking calculation with morin, which induced the largest CSPs
322 (Fig. 7) in NDM-1 spectra. Several of them belong to the flexible loops of NDM-1 (ASL1: L65, M67,
323 F70; L5: W93; ASL4: N220) and several others are implicated in the Zn(II) ions binding (H122, D124,
324 H250). As the NDM-1 CSPs could be the result of direct interaction with the flavonol or/and the
325 result of conformation modifications of the flexible loops, the L65, M67, F70, W93, H122, Q123,
326 D124, N220, H250 NDM-1 residues were defined as “passive” residues and the flavonol as “active”
327 residue (as defined in the HADDOCK software) in a first step. The best generated models, selected
328 on the basis of the HADDOCK score, using four metal-free apo forms of NDM-1 show that the morin
329 is located in the substrate-binding pocket near the Zn(II) ligands. Moreover, the best generated
330 models selected also on the basis of the HADDOCK scores, using either the five apo or the ten art-
331 apo NDM-1 structures show that the morin is located in the substrate-binding pocket and is able to
332 contact the Zn(II) ions through polar contacts. Depending on the NDM-1 crystallographic structures
333 used for the docking, two main orientations are observed for the morin, differing one of the other
334 by a rotation of 180° when the ligand is localized in the active site. The flavonols are recognized to
335 chelate metal ions, forming metal-flavonol complexes (67,68) and a binding association constant of
336 $3.57 \pm 0.1 \times 10^4 \text{ M}^{-1}$ has been found between quercetin and Zn(II) in protein-free solution (69). A
337 flavonol molecule possesses three potential sites for chelating cations: i) the 3', 4' or 2', 4'-
338 dihydroxy group or 3', 4', 5'-trihydroxy group located on the B-ring (depending on the type of
339 flavonol), ii) between the 3-hydroxy and the 4-carbonyl groups in the C-ring, iii) and through the 5-
340 hydroxy and the 4-carbonyl group (Fig. 4). Moreover, we determine by NMR that the Zn(II) ions
341 direct the flavonols binding to the NDM-1 active site. Because of these results and of our first
342 docking simulations, the two NDM-1 Zn(II) ions likely play a role in the coordination of the ligand in
343 the binding site, so they have been defined as “active” residues in addition to the L65, M67, F70,
344 W93, H122, Q123, D124, N220, H250 NDM-1 residues defined as “passive” residues and the morin
345 as “active” residue, in a second step of docking simulations using ten art-apo and five apo NDM-1
346 crystallographic structures. The analysis of the four best structures of each top clusters, shows that
347 as expected the morin targets the Zn(II) ions through polar contacts. The morin orientation in the
348 active site of NDM-1 was again strongly dependent of the crystallographic structure used for the
349 docking. Either the morin adopts almost the same orientation in the NDM-1 active site for all the
350 four structures of each top cluster (art-apo PDB: 4EY2, 4EYB, 4HL2, 4RL2, 4EYF; apo PDB: 4TZF), or

351 none of the orientations are identical (art-apo PDB: 4EXS, 4EYL, 4RAM, 4RBS, 4RL0; apo PDB: 4TYF,
352 3S0Z, 4TZE, 3SPU). Interestingly this difference in behavior seems related to the Zn1-Zn2 distances
353 in the starting structures of NDM-1 used for the docking, since they are ranging from 4.5 to 4.6 Å
354 on one hand and from 3.1 to 4.1 in Å on the other hand. After superposition on the (45-271)
355 backbone atoms of NDM-1, a good quality of superposition is also observed for the ligand, when
356 the starting NDM-1 structure used for the docking possesses the highest Zn1-Zn2 distances (4.5 and
357 4.6 Å) (Fig. 7A). 50 % of the analyzed structures adopt the orientation-1 when using the art-apo
358 NDM-1 structure during the docking simulation (Fig. 8) and 22.5 % of the morin orientations
359 fluctuate around this orientation. In all the other complexes the morin adopts an orientation-2,
360 which differs from orientation-1 by a rotation of approximately 180° (Fig. 8). Fluctuation of the
361 morin orientations and orientation-2 of the ligand in the active site of NDM-1 are only observed for
362 NDM-1 starting structures with the smallest Zn1-Zn2 distances. In orientation-1 and orientation-2
363 electrostatic interactions are observed between Zn2 and O-3 (cycle C), O-4 (cycle C) and O-5 (cycle
364 A). By cons Zn1 is either targeted by 5-O (cycle A) in orientation-1 and by O-3 (cycle C) in orientation-
365 2 (Fig. 8). These Zn(II) interactions are a combination of what is observed in absence of protein, that
366 is to say between the 3-hydroxy and the 4-carbonyl groups in the C-ring on one hand, and through
367 the 5-hydroxy and the 4-carbonyl group on the other hand. In addition, hydrogen bond interactions
368 are also observed between O-7 (cycle A) and amide proton of Q123 and between O-2' (cycle B) and
369 amide proton of N220 in orientation-1 in several complexes (Fig. 8). Morin showed also H-bonding
370 with H189 in orientation-1 (Fig. 8C). In addition, the three rings system forms extensive non-polar
371 interactions with L65, M67, F70 and W93 (Fig. 8). To investigate whether the number and position
372 of the hydroxy groups on B-ring, could influence the flavonol orientations in the active site of NDM-
373 1, docking simulations were also undertaken using quercetin and myricetin using the protocol
374 already described in the paragraph just above: only the two Zn(II) ions and the flavonols were
375 defined as “active” residues and the L65, M67, F70, W93, H122, Q123, D124, N220, H250 NDM-1
376 residues defined as “passive” residues. The molecular docking results show that morin, quercetin
377 and myricetin are located in the same binding site. The number of different orientations for each
378 of the ligands in the active site of NDM-1 is larger for quercetin and myricetin than for morin and
379 the number of rejected structures (generally due to the loss of Zn2 coordination is also greater for
380 quercetin and myricetin than for morin. The loss of Zn2 coordination is only observed for the NDM-

381 1 starting structures with the smallest Zn1-Zn2 distance, again reinforcing that the inter-Zn(II)
382 distance must increase in the complex to accommodate the ligand binding. Quercetin and myricetin
383 predominantly also adopt orientation-1. In orientation-1 and orientation-2 the Zn(II) ions/morin,
384 Zn(II) ions/quercetin and Zn(II) ions/myricetin interactions are quite similar whatever the flavonol.
385 Interestingly, addition of OMe groups at the 3', 5, or 3 positions decrease slightly the inhibition of
386 native quercetin. We verified using molecular-docking simulation, that the three quercetin
387 conjugates are still able to interact with Zn(II) via their C-4 carbonyl group, with approximately the
388 same structure statistics than quercetin wild type. This suggests that the 5-hydroxyl group is not
389 critical for the interaction and that the 3-OMe (quercetin-CH3C) and 3'-OMe groups (quercetin-
390 CH3B) do not prevent the Zn(II) interactions. The slight decreases in inhibition can be explained by
391 the steric hindrance generated by the OMe groups.

392

393 **DISCUSSION**

394

395 The metallo- β -lactamases utilize a metal-dependent pathway to inactivate β -lactam
396 containing antibiotics. Numerous studies have been conducted on the active MBLs forms in the
397 presence of Zn(II), to elucidate the catalytic mechanism of these enzymes (8). The active site of
398 NDM-1 is able to bind with ligands through interaction with Zn1 and Zn2. However crystallographic
399 studies indicated that NDM-1 exists under three forms (13): the metal-free, the mono-Zn(II) and
400 the di-Zn(II)-binding complexes, in complex or not with ligand. In this study we carried out and
401 extended the NMR assignment of metal-free NDM-1 and di-Zn(II) NDM-1 in order to determine the
402 Zn(II) binding influence on the dynamic behavior of NDM-1 and the assembly of the active site. Our
403 Zn(II) titration experiments show that Zn(II) binding induced significant chemical shift
404 perturbation of NDM-1 resonances with the most significant changes located in the ASL2, ASL3, and
405 ASL5 loops, which are directly involved in the di-Zn(II) coordination (Fig. 2). Moreover contrary to
406 what was observed in the crystallographic mono-Zn(II) NDM-1 structure where only one Zn(II) is
407 bound to H120, H122 and H189 (PDB: 3SFP), our Zn(II) titration experiments show that in the
408 presence of 1 equivalent of Zn(II) relative to the protein concentration we did not observe a stable
409 form of NDM-1 with only one Zn(II) bound at a single site, but a slow exchange between the free
410 form of NDM-1 and NDM-1 bound to two Zn(II). As the resonances of the ASL2 and L9 loops, and of

411 helix $\alpha 2$ could not be observed in absence of Zn(II) no information could be obtained on the
412 chemical shift variations for these three domains in presence of Zn(II). By cons these domains
413 undergo the most drastic differences in their dynamic behavior in the presence of Zn(II) compared
414 to what is observed for the free-metal NDM-1 (Fig. 2 and 3). Clearly the binding of the two Zn(II) by
415 their respective ligands in the active site of NDM-1 induces a stiffening of these domains. The same
416 effect of the presence of ions Zn(II) has been observed by Chen *et al.* (22) using molecular dynamics
417 (MD) simulations. In addition the authors also showed that the di-Zn(II) coordination exerts
418 stronger restrictions on the motions of loops ASL1 and ASL4 (noted L3 and L10 respectively in Chen
419 *et al.* (22)). Our relaxation data indicated also a decrease in the ASL4 flexibility except for the
420 residues surrounding N220 upon Zn(II) binding. By cons we do not observe restriction of motion of
421 loop ASL1 in presence of 2 molar equivalent of Zn(II) (Fig. 3) as observed in the MD simulations. The
422 flexibility of ASL1 and to a lesser extent for ASL4 observed by NMR for both metal-free and di-Zn(II)
423 NDM-1 (Fig.3) are in agreement with that observed by comparison of the X-ray crystal structures of
424 NDM-1. Superimposition of several of them highlight a very good tertiary structure preservation
425 with only significant flexibility of ASL1 and ASL4 loops, suggesting that Zn (II) binding does not
426 influence the overall structure of NDM-1. These observations are also in agreement with the results
427 showing that ASL1 and ASL4 are key loops that are able to correctly orient substrate within the
428 active site and therefore must be able, because of their flexibility, to adapt to many types of ligands
429 (13,14,64,70-72). Loop flexibility may therefore be required for ligand recognition and assembly of
430 the Michaelis complex (73,74).

431 From our inhibitor activity assay data, we identified the flavonols as candidate inhibitors of
432 NDM-1 activity. The flavonols occur abundantly in a variety of fruits and vegetables and are
433 recognized to interact with metallo-proteins involved in cancer, cardiovascular and brain diseases
434 (51-59,75,76). The morin, quercetin and myricetin structures are characterized by two aromatic
435 rings (A and B) connected by the γ -pyrone ring C (Fig. 4). Our CSPs experiments highlighted the
436 specific interaction of the three flavonols at the active site of NDM-1. This is in agreement with
437 previous in silico modelling and docking with models of NDM-1 generated, based on alignment with
438 two templates VIM-2 and VIM-4 by Ganugapati *et al.* (77) and crystal structure of NDM-1
439 (PDB:3SPU) by Padmavathi *et al.* (78). In the two studies the results indicated that quercetin could
440 be the best inhibitor among the flavonoids present in green tea (flavan-3-ols, flavones and

441 flavonols) tested during the dockings. Our NMR studies show that the three flavonols are mostly
442 localized at proximity of the Zn(II) binding site and of the ASL1, ASL2, ASL4 and L5 loops (Fig.6). We
443 also show that the Zn(II) improved the binding specificity of morin for NDM-1. This observation is
444 in agreement with the results showing that the flavonols are metal-ion chelators (67-69,79,80). We
445 show that the starting NDM-1 structures used for the docking influence both orientation and the
446 reproducibility of the orientation in the active site of NDM-1. More specifically the Zn1-Zn2 distance
447 is the factor that most strongly affected the positioning of the ligand in the active site during
448 molecular-docking simulations. As already described by Zhang *et al.* (66), although the Zn1-Zn2
449 distances observed in different NDM-1 structures in complex with hydrolyzed antibiotics are longer
450 than that observed for NDM-1 in native form, they fluctuate after all between 3.8 and 4.6 Å and are
451 strongly dependent of the type of ligand. Consequently the choice of NDM-1 starting structures for
452 docking with ligands able to bind Zn(II) strongly influence the final results. On the two orientations
453 observed, orientation-1 is mostly populated and favored by NDM-1 starting structures for which
454 the Zn1-Zn2 distances are around 4.5 Å.

455 The NDM-1 hydrolyzed-antibiotics such as methicillin (PDB: 4EY2), oxacillin (PDB: 4EYB),
456 meropenems (PDB: 4RBS, 4EYL), benzylpenicillin (PDB: 4EYF), cephalosporins (PDB:4RL2, 4RL0),
457 penicillin G (PDB: 4RAM) and ampicillin (PDB:4HL2) bind the two Zn(II) through polar interaction
458 with the carbapenem C3 and C6 carboxylate oxygens. Most of the MBL inhibitors belong to one of
459 the two following categories: either they act via Zn(II) sequestration such as
460 ethylenediaminetetraacetic acid (17,24,81,82) and aspergillomarasmine A (83) with the resulting
461 inactivation of the enzyme, or they possess several electron donor group, such as carboxylate,
462 carboxyl, thiol and/or nitrogen that are able to bind one or the two Zn(II) in the active site (17,25-
463 29,31-42,45,84-87) to act as competitive inhibitors. We show that flavonols belong here to the
464 second category, and that they are able to bind to the two Zn(II) in the NDM-1 active site, without
465 expelling the Zn(II) ions from the protein. There are very few flavonol structures interacting with
466 metal ions on the inside of a protein. Interestingly it has been shown that quercetin possesses
467 strong yeast alcohol dehydrogenase inhibitory activities that has been explained on the basis of
468 formation of a complex between quercetin and the Zn(II) ion which maintains the tertiary structure
469 of the metallo-enzyme (69). Moreover crystal structures of the quercetin 2,3-dioxygenase, a
470 mononuclear copper-dependent dioxygenase (PDB:1H1I, 1H1M) (88) and of the quercetin 2,4-

471 dioxygenases, which uses nickel as the active-site cofactor to catalyze oxidative cleavage,
472 complexed with the substrate quercetin (PDB: 5FLI) (89) show that metal ion coordination implicate
473 in the two cases, the 3-hydroxy and the 4-carbonyl groups in the C-ring of quercetin with distances
474 around 2.3 and 3.5 respectively. We also observed in orientation-1 and orientation-2 of our NDM-
475 1/flavonol models electrostatic interactions between Zn²⁺ and the 3-hydroxy and the 4-carbonyl
476 groups of quercetin.

477 Our inhibitor activities assay and structural characterization of NDM-1/flavonols complexes
478 in presence of Zn(II), highlight that morin, myricetin and quercetin interact in the same binding site
479 as antibiotics, and that these interactions are largely driven by interaction with the two Zn(II) as is
480 the case for substrate recognition in MBLs, which is largely driven by interaction with the metal ions
481 (90,91). Recently a combination of quercetin-meropenem was shown to exert bactericidal activity
482 by disrupting cell-wall/membrane integrity and altering cellular morphology (92). Moreover a
483 quercetin derivative, the quercetin-3-O- β -glucoside was identified to have a potent
484 antimycobacterial activity by glutamine synthetase inhibitory activity in *Mycobacterium*
485 tuberculosis (93). Despite the relatively modest activity of these natural compounds, our models
486 demonstrates that flavonols can provide valuable starting points for broad-spectrum inhibitor
487 discovery against NDM-1.

488

489 **EXPERIMENTAL PROCEDURES**

490

491 ***Protein production and purification***

492 The gene sequence encoding the NDM-1 mature enzyme from G29 to R270 was subcloned
493 into a pET41b vector with a C-terminal His6 tag to facilitate protein purification. For the
494 overexpression of double ¹⁵N/¹³C-labeled NDM-1 sample, the fusion protein was expressed in
495 BL21 *E. coli* cells. A 100 ml LB culture supplemented with 40 μ g ml⁻¹ kanamycin was inoculated with
496 10 ml of a fresh overnight LB preculture and grown at 37°C until OD₆₀₀ = 1.5. After a 10 min
497 centrifugation at 5000 rpm, the bacterial pellet was resuspended in 1 L of M9 minimal medium
498 (Na₂HPO₄, 6 g·l⁻¹; KH₂PO₄, 3 g·l⁻¹; NaCl, 0.5 g·l⁻¹; MgSO₄, 1 mM; CaCl₂, 1.10⁻⁴ M) containing 2.0 g l⁻¹
499 [¹³C]glucose, 1 g·l⁻¹ [¹⁵N]NH₄Cl and 40 μ g ml⁻¹ kanamycin preincubated at 37°C. The culture was

500 maintained in this medium at 37°C until OD₆₀₀ ~ 0.6. Subsequently, induction with 0.4 mM
501 isopropyl-β-D-thiogalacto-pyranoside took place for 20 hours at 28°C.

502 The bacteria were spun down at 5000 rpm for 10 min and the pellet (3.5g) was washed in
503 PBS buffer (phosphate buffered saline), sonicated for 15 times with 10s pulses at 4°C in 30 ml buffer
504 A (20 mM sodium phosphate pH7.5, 0.5 M NaCl, 10 mM imidazole, 1 mM β-ME) containing 0.5 mg
505 ml⁻¹ lysosyme, 100 µg ml⁻¹ DNase, one tablet of complete mini EDTA free protease inhibitor cocktail
506 (Roche Diagnostics) and centrifuged (100, 000 g for 30 minutes). Supernatant was applied two
507 times on a 1 ml His GraviTrap affinity column (GE Healthcare) equilibrated with buffer A and the
508 column was washed with 20 ml buffer A containing 20 mM imidazole. Then elution of the protein
509 was carried out in buffer A containing 0.3 M imidazole. The eluted fraction containing pure NDM-1
510 (about 50 mg) were brought to a concentration of 500 µM by ultrafiltration and dialysis against
511 0.1M Bis-Tris-HCl pH 7.0.

512

513 ***Thermal Shift Assay***

514 The thermal shift assay was performed using the ABI7900HT Real-Time PCR system (Applied
515 Biosystems). The assay quantifies binding of the Sypro Orange probe to exposed hydrophobic
516 regions of proteins challenged to a temperature gradient (94). The dye becomes highly fluorescent
517 when bound to protein hydrophobic sites. NDM-1 samples (9 µM) were incubated in buffer 100
518 mM Bis-Tris pH-7 containing different ZnCl₂ concentrations and Sypro Orange (650-fold diluted
519 from stock solution; Invitrogen). Reactions were carried out in duplicate in a 96-well fast PCR plate
520 at a final volume of 20 µl. The samples were submitted to a denaturation from 15 to 95°C at a rate
521 of 3°C/min and fluorescence of Sypro Orange dye was recorded in real time (excitation 488 nm and
522 emission spectra 500-650 nm). The protein denaturation temperature was calculated using the
523 software SDS2.4.1 as the maximum of the derivative of the resulting fluorescence curves.

524

525

526 ***Enzyme activity assay screening library***

527 All the compounds tested as potential inhibitors of NDM-1 were either purchased from
528 Sigma-Aldrich Corporation, or available from the Labex LERMIT libraries. The CAS numbers are for
529 quercetin (CAS 117-39-5), myricetin (CAS 529-44-2) and morin (CAS 654055-01-3), rutin (CAS

530 207671-50-9), eriodictyol (CAS 4049-38-1), taxifolin (CAS 480-18-2), naringenin (CAS 67604-48-2)
531 and dihydromyricetin (CAS 27200-12-0). They were dissolved in 100% DMSO as 5 or 10 mM stock
532 solutions. The imipenem antibiotic was purchased from Ranbaxy and dissolved in Milli-Q water as
533 10 mM stock solution. The screening assay conditions were as follows: 100 mM phosphate buffer,
534 pH 7.0 (Na₂HPO₄/ NaH₂PO₄) added with 50 μM ZnSO₄; 100 μM imipenem and 50 μM of compound
535 (dissolved in DMSO) monitored by a Varian Cary 300 Bio UV-Visible spectrophotometer at 297 nm,
536 time course 600 seconds 25 °C. Imipenem was added into the reaction, after 5 min of incubation.
537 In parallel, Two control was performed: positive control was performed with DMSO instead of
538 compound and the negative control with 1mM EDTA. The equation for the calculation of the
539 percentage of inhibition is defined as following: Percentage inhibition = (1- (I₀ – I_{EDTA}) / (I_{DMSO} -
540 I_{EDTA})) x 100%, where I₀ is the intensity of the product signal in each well, I_{EDTA} is the intensity in
541 the presence of EDTA and I_{DMSO} is the intensity in the presence of DMSO.

542

543

544

545 **IC₅₀ determination**

546 IC₅₀ of the inhibitors was determined in 100 mM phosphate buffer, pH 7.0 (Na₂HPO₄/
547 NaH₂PO₄) added with 50 μM ZnSO₄, with 100 μM imipenem and an incubation of 3 min. The assay
548 was performed with an ULTROSPEC 2000 UV spectrophotometer and the SWIFT II software (GE
549 Healthcare, Velizy-Villacoublay, France). IC₅₀ values were obtained using the equation IC₅₀ =
550 ((1/0.5 x v₀) – m)/q, where v₀ is the rate of hydrolysis of the reporter substrate (v₀ being the rate
551 measured in the absence of inhibitor), q the y axis intercept and m the slope of the resulting linear
552 regression.

553

554 **Minimum Inhibitory Concentration (MIC) Determination.**

555 MIC values were determined by broth microdilution, in triplicate, in cation-adjusted Mueller
556 Hinton broth according to the Clinical Laboratory Standards Institute (CLSI) guidelines. Two
557 enterobacterial clinical strains expressing the carbapenemase NDM-1 were used : *E. coli* NDM-1
558 GUE and *K. pneumoniae* NDM-1 CAG. Experiments were performed in microtiter plates containing
559 the medium with imipenem and inhibitors (myricetin and quercetin) dissolved (DMSO) at different

560 concentrations (0,5; 5; 50; 500 and 1000 μ M) . Plates were incubated overnight at 37°C for 18–24
561 h.

562

563 ***NMR backbone resonance assignment***

564 Samples for NMR spectroscopy are composed either of 0.1M Bis-Tris-HCl pH 7.0 buffer,
565 supplemented by 150 mM NaCl or 50mM phosphate sodium pH 6.5 depending respectively of the
566 absence or the presence of ZnCl₂ in the solutions, and 95%/5% H₂O/D₂O. Protein concentration was
567 set from 100 μ M to 1 mM. The NMR spectra were recorded on 600 and 800 MHz Bruker Avance III
568 spectrometers at different temperatures ranging from 293K to 308K depending of the presence or
569 not of ZnCl₂. The two spectrometers are equipped with a 5mm z-gradient TCI (H/C/N) cryoprobe.
570 The backbone resonance assignments were performed in absence or in presence of ZnCl₂ using the
571 standard triple resonance experiments: HNCA, HN(CO)CA, HNCO, HN(CA)CO, HNCACB and HN
572 (CO)CACB. 3D NOESY-15N edited spectra (mixing times 100 and 200 ms) were also collected to help
573 the assignment. NMR data were processed using TOPSPIN 3.5 software (Bruker) and analyzed using
574 CcpNmr 2.4.2 software (<http://www.ccpn.ac.uk>). NDM-1 resonance assignments in absence and in
575 presence of Zn were deposited in BMRB with entry codes 26950 and 26952 respectively.

576

577 ***¹⁵N relaxation measurements***

578 The ¹⁵N R₁ and R₂ relaxation rates and {¹H}-¹⁵N heteronuclear NOE were measured at 298K
579 and 600 MHz ¹H frequency on the metal-free NDM-1 and NDM-1:Zn(II) complex. The experiments
580 were based on the TROSY-based relaxation experiments (95) and recorded in an interleaved
581 pseudo-3D method. For the determination of R₁ relaxation constants 13 total data set were
582 collected at relaxation delay times of 20 (duplicated), 200, 300, 500, 600, 750, 1000, 1200, 1500
583 and 1900 ms. For the determination of R₂ relaxation constants, 13 data set were collected at delay
584 times of 33.92 (duplicated), 50.88, 67.84, 101.76, 118.72, 135.68, 169.60, 186.56, 220.48, 271.36
585 and 339.20 ms. In the case of the {¹H}-¹⁵N heteronuclear NOE experiment, two 2D ¹H-¹⁵N planes
586 were collected in presence or absence of a 3s ¹H saturation sequence (120° ¹H pulses train) during
587 relaxation delay. Spectral widths were 1.630 and 4.208 kHz along the ¹⁵N and ¹H dimension
588 respectively, and the interscan delay was set to 5s.

589

590 ***NMR HSQC titration experiments***

591 The NDM-1:Zn(II) interaction was characterized by means of chemical shift perturbations
592 (CSPs), using a series of ¹H-¹⁵N HSQC experiments recorded upon addition of increasing
593 concentration of ZnCl₂. The protein, concentrated to 200 -250 μM, was solubilized in 0.1 mM Bis-
594 Tris buffer pH 7, supplemented by 150 mM NaCl. ZnCl₂ was dissolved in 0.1 mM Bis-tris buffer pH 7
595 to a concentration of 20 mM.

596 The flavonols (morin, quercetin and myricetin) interaction surfaces on NDM-1 were
597 characterized in presence of 2 equivalents of Zn(II). The flavonols were dissolved in 100% DMSO at
598 a concentration of 20 mM. The concentration of DMSO-d₆ did not exceed 5% in the NMR tube.

599 For chemical shift perturbations experiments, NMR spectra were acquired at 293K on
600 samples containing 300 μM NDM-1 on which increasing amounts of flavonols (0 to 4 molar
601 equivalents relative to the NDM-1 concentration, which corresponds to approximately 2.7 μL of
602 DMSO added by equivalent of flavonol), were titrated, in 0.1M Bis-Tris-HCl, 150 mM NaCl (pH 7.0).
603 For each titration point a ¹H-¹⁵N HSQC experiment and 1D ¹³C-¹⁵N-filtered spectra were performed.
604 In the 1D ¹³C-¹⁵N-filtered experiment, the ¹H signals originating from the ¹⁵N-¹³C labeled protein
605 were filtered out and only ¹H signals from the small molecules were observed. Each HSQC spectrum
606 was collected with 8 scans per increment with spectral widths of 9.6 kHz for ¹H and 3.2 kHz for ¹⁵N
607 as well as 256 data points in the indirect dimension. The experiments used the 3-9-19 watergate
608 sequence (96) for water suppression. The weighted chemical shift change of each NH signal was
609 calculated according to:

610
$$\Delta\delta (^1\text{H}, ^{15}\text{N}) = [((\Delta\delta_{\text{H}})^2 + (\Delta\delta_{\text{N}})^2 * 0.14) * 0.5]^{1/2}.$$

611 where δ_{H} and δ_{N} are the modifications of the chemical shift in the ¹H and ¹⁵N dimensions,
612 respectively (97).

613

614 ***NDM-1/flavonol dockings using HADDOCK***

615 Ambiguous distance restraints based on chemical shift perturbations were used to drive the
616 docking between NDM-1 and the three flavonols: morin, quercetin and myricetin. Nineteen
617 crystallographic structures of NDM-1 were used: i) ten of them were in complex with a ligand:
618 hydrolyzed methicillin (PDB: 4EY2), hydrolyzed oxacillin (PDB: 4EYB), L-captopril (PDB: 4EXS);
619 hydrolyzed meropenems (PDB: 4EYL, 4RBS); hydrolyzed benzylpenicillin (PDB: 4EYF); hydrolyzed

620 cephalosporins (PDB: 4RL0, 4RL2), hydrolyzed penicillin G (PDB: 4RAM), hydrolyzed ampicillin (PDB:
621 4HL2), these structures were used after removing of the ligand localized in the active site of the
622 NDM-1 crystallographic structures, and named “artificial apo” (art-apo) NDM-1 structures; ii) five
623 of them were apo NDM-1 crystal structures (PDB: 4TYF, 3S0Z, 4TZF, 4TZE, 3SPU); iii) four were
624 metal-free apo form of NDM-1 (PDB: 3RKJ, 3RKK, 3SBL, 3PG4). The three flavonols structures were
625 extracted from crystal structures: morin PDB: 6AE3, 5AUY; quercetin PDB:2UXH; myricetin PDB:
626 2O63 where they were in complex with proteins. The L65, M67, F70, W93, H122, Q123, D124, N220,
627 H250 residues were defined as belonging to the NDM-1 interaction surface with the flavonols. In a
628 first series of calculations they were defined as passive residues, in a second series the two Zn(II)
629 were also added as passive residues, and in a third series the two Zn(II) were defined as active
630 residues and L65, M67, F70, W93, Q123, N220, D124, H250 as passive residues. In addition, a
631 restraint file (unambiguous restraints), that imposed the distances between Zn1 and Zn2 on one
632 hand and between each Zn1 and Zn2, and their respective ligands His120, His122, His189 and
633 Asp124, Cys208, His250, was supplied to HADDOCK in order to maintain the geometry around each
634 Zn(II). In all the steps, the residues belonging to the segments 65, 92-94, 123, 218-222 were defined
635 as fully flexible segments, and those belonging to 66-73 as semi-flexible segments. During the rigid-
636 body docking, 2000 structures were calculated, and 400 during both simulated annealing and water
637 refinement. All 400 water-refined structures were analyzed, and cut-off for clustering was 7.5 Å or
638 0.6 (interface RMSD or Fraction of Common Contacts (FCC) respectively) with four structures per
639 cluster. The ranking of the clusters is based on the average score of the top 4 members of each
640 cluster. The HADDOCK score is calculated as function of the intermolecular van der Waals energy,
641 the intermolecular electrostatic energy, the empirical desolvation energy term and the Ambiguous
642 Interaction Restraints (AIRs) energy. The cluster numbering reflects the size of the cluster, with
643 cluster 1 being the most populated cluster. After successful docking, the best complex models were
644 selected on the basis of the HADDOCK score.

645 The same protocol was used for the docking of NDM-1 (PDB:4EY2) and three quercetin
646 conjugates : quercetin-CH3A (quercetin with OMe in position 5); quercetin-CH3B (quercetin with
647 OMe in position 3’); quercetin-CH3C (quercetin with OMe in position 3).

648

649

650 **Acknowledgments:**

651 This work was supported by the Assistance Publique –Yes Hôpitaux de Paris (AP-HP), the University
652 Paris-Sud, the Laboratory of Excellence in Research on Medication and Innovative Therapeutics
653 (LERMIT) supported by a grant from the French National Research Agency [ANR-10-LABX-33] and
654 by the Joint Programming Initiative on Antimicrobial Resistance (JPIAMR) DesInMBL [ANR-14-
655 JAMR-002].

656

657 **Conflict of interest:** The authors declare that they have no conflicts of interests with the contents of
658 this article.

659

660 **Author contributions:** GR, MG, EJ, CB, TN, BI, EG, NM designed the experiments. GR, MG, JBC, SO,
661 NN, JCC, EJ, EL, and NM conducted experiments and analyzed data. GR, MG, CvH, EL, TN and NM
662 wrote the paper.

663

664

665

666

667

668

669

670

671

672

673

674

675

676

677

678

679

680 **REFERENCES**

681

- 682 1. Oliveira, J., and Reygaert, W. C. (2019) Gram Negative Bacteria. in *StatPearls*, Treasure Island
 683 (FL). pp
- 684 2. Ruppe, E., Woerther, P. L., and Barbier, F. (2015) Mechanisms of antimicrobial resistance in
 685 Gram-negative bacilli. *Ann Intensive Care* **5**, 61
- 686 3. Vasoo, S., Barreto, J. N., and Tosh, P. K. (2015) Emerging issues in gram-negative bacterial
 687 resistance: an update for the practicing clinician. *Mayo Clin Proc* **90**, 395-403
- 688 4. Ambler, R. P. (1980) The structure of beta-lactamases. *Philos Trans R Soc Lond B Biol Sci* **289**,
 689 321-331
- 690 5. Naas, T., Oueslati, S., Bonnin, R. A., Dabos, M. L., Zavala, A., Dortet, L., Retailleau, P., and
 691 Iorga, B. I. (2017) Beta-lactamase database (BLDB) - structure and function. *J Enzyme Inhib*
 692 *Med Chem* **32**, 917-919
- 693 6. Nordmann, P., Naas, T., and Poirel, L. (2011) Global spread of Carbapenemase-producing
 694 Enterobacteriaceae. *Emerg Infect Dis* **17**, 1791-1798
- 695 7. Page, M. I. (1999) The reactivity of beta-lactams, the mechanism of catalysis and the
 696 inhibition of beta-lactamases. *Current Pharmaceutical Design* **5**, 895-913
- 697 8. Bebrone, C. (2007) Metallo-beta-lactamases (classification, activity, genetic organization,
 698 structure, zinc coordination) and their superfamily. *Biochemical Pharmacology* **74**, 1686-
 699 1701
- 700 9. Bonomo, R. A. (2011) New Delhi Metallo-beta-Lactamase and Multidrug Resistance: A
 701 Global SOS? (vol 52, pg 485, 2011). *Clinical Infectious Diseases* **52**
- 702 10. Kumarasamy, K. K., Toleman, M. A., Walsh, T. R., Bagaria, J., Butt, F., Balakrishnan, R.,
 703 Chaudhary, U., Doumith, M., Giske, C. G., Irfan, S., Krishnan, P., Kumar, A. V., Maharjan, S.,
 704 Mushtaq, S., Noorie, T., Paterson, D. L., Pearson, A., Perry, C., Pike, R., Rao, B., Ray, U.,
 705 Sarma, J. B., Sharma, M., Sheridan, E., Thirunarayan, M. A., Turton, J., Upadhyay, S., Warner,
 706 M., Welfare, W., Livermore, D. M., and Woodford, N. (2010) Emergence of a new antibiotic
 707 resistance mechanism in India, Pakistan, and the UK: a molecular, biological, and
 708 epidemiological study. *Lancet Infectious Diseases* **10**, 597-602
- 709 11. Koh, T. H., Khoo, C. T., Wijaya, L., Leong, H. N., Lo, Y. L., Lim, L. C., and Koh, T. Y. (2010) Global
 710 spread of New Delhi metallo-beta-lactamase 1. *Lancet Infectious Diseases* **10**, 828-828
- 711 12. Nordmann, P., Poirel, L., Walsh, T. R., and Livermore, D. M. (2011) The emerging NDM
 712 carbapenemases. *Trends in Microbiology* **19**, 588-595
- 713 13. Kim, Y., Tesar, C., Mire, J., Jedrzejczak, R., Binkowski, A., Babnigg, G., Sacchettini, J., and
 714 Joachimiak, A. (2011) Structure of apo- and monometalated forms of NDM-1--a highly
 715 potent carbapenem-hydrolyzing metallo-beta-lactamase. *PLoS One* **6**, e24621
- 716 14. Zhang, H., and Hao, Q. (2011) Crystal structure of NDM-1 reveals a common beta-lactam
 717 hydrolysis mechanism. *FASEB J* **25**, 2574-2582
- 718 15. King, D., and Strynadka, N. (2011) Crystal structure of New Delhi metallo-beta-lactamase
 719 reveals molecular basis for antibiotic resistance. *Protein Sci* **20**, 1484-1491
- 720 16. King, D. T., Worrall, L. J., Gruninger, R., and Strynadka, N. C. (2012) New Delhi metallo-beta-
 721 lactamase: structural insights into beta-lactam recognition and inhibition. *J Am Chem Soc*
 722 **134**, 11362-11365

- 723 17. Guo, Y., Wang, J., Niu, G., Shui, W., Sun, Y., Zhou, H., Zhang, Y., Yang, C., Lou, Z., and Rao, Z.
 724 (2011) A structural view of the antibiotic degradation enzyme NDM-1 from a superbug.
 725 *Protein Cell* **2**, 384-394
- 726 18. Kim, Y., Cunningham, M. A., Mire, J., Tesar, C., Sacchettini, J., and Joachimiak, A. (2013)
 727 NDM-1, the ultimate promiscuous enzyme: substrate recognition and catalytic mechanism.
 728 *FASEB J* **27**, 1917-1927
- 729 19. Liang, Z., Li, L., Wang, Y., Chen, L., Kong, X., Hong, Y., Lan, L., Zheng, M., Guang-Yang, C., Liu,
 730 H., Shen, X., Luo, C., Li, K. K., Chen, K., and Jiang, H. (2011) Molecular basis of NDM-1, a new
 731 antibiotic resistance determinant. *PLoS One* **6**, e23606
- 732 20. Feng, H., Ding, J., Zhu, D., Liu, X., Xu, X., Zhang, Y., Zang, S., Wang, D. C., and Liu, W. (2014)
 733 Structural and mechanistic insights into NDM-1 catalyzed hydrolysis of cephalosporins. *J Am*
 734 *Chem Soc* **136**, 14694-14697
- 735 21. Zhu, K., Lu, J., Ye, F., Jin, L., Kong, X., Liang, Z., Chen, Y., Yu, K., Jiang, H., Li, J. Q., and Luo, C.
 736 (2013) Structure-based computational study of the hydrolysis of New Delhi metallo-beta-
 737 lactamase-1. *Biochem Biophys Res Commun* **431**, 2-7
- 738 22. Chen, J., Wang, J., and Zhu, W. (2017) Zinc ion-induced conformational changes in new
 739 Delhi metallo-beta-lactamase 1 probed by molecular dynamics simulations and umbrella
 740 sampling. *Phys Chem Chem Phys* **19**, 3067-3075
- 741 23. Thomas, P. W., Zheng, M., Wu, S., Guo, H., Liu, D., Xu, D., and Fast, W. (2011)
 742 Characterization of purified New Delhi metallo-beta-lactamase-1. *Biochemistry* **50**, 10102-
 743 10113
- 744 24. Li, T., Wang, Q., Chen, F., Li, X., Luo, S., Fang, H., Wang, D., Li, Z., Hou, X., and Wang, H. (2013)
 745 Biochemical characteristics of New Delhi metallo-beta-lactamase-1 show unexpected
 746 difference to other MBLs. *PLoS One* **8**, e61914
- 747 25. Li, N., Xu, Y., Xia, Q., Bai, C., Wang, T., Wang, L., He, D., Xie, N., Li, L., Wang, J., Zhou, H. G.,
 748 Xu, F., Yang, C., Zhang, Q., Yin, Z., Guo, Y., and Chen, Y. (2014) Simplified captopril analogues
 749 as NDM-1 inhibitors. *Bioorg Med Chem Lett* **24**, 386-389
- 750 26. Liu, S., Jing, L., Yu, Z. J., Wu, C., Zheng, Y., Zhang, E., Chen, Q., Yu, Y., Guo, L., Wu, Y., and Li,
 751 G. B. (2018) ((S)-3-Mercapto-2-methylpropanamido)acetic acid derivatives as metallo-beta-
 752 lactamase inhibitors: Synthesis, kinetic and crystallographic studies. *Eur J Med Chem* **145**,
 753 649-660
- 754 27. Klingler, F. M., Wichelhaus, T. A., Frank, D., Cuesta-Bernal, J., El-Delik, J., Muller, H. F., Sjuts,
 755 H., Gottig, S., Koenigs, A., Pos, K. M., Pogoryelov, D., and Proschak, E. (2015) Approved Drugs
 756 Containing Thiols as Inhibitors of Metallo-beta-lactamases: Strategy To Combat Multidrug-
 757 Resistant Bacteria. *J Med Chem* **58**, 3626-3630
- 758 28. Zhang, Y. L., Yang, K. W., Zhou, Y. J., LaCuran, A. E., Oelschlaeger, P., and Crowder, M. W.
 759 (2014) Diaryl-substituted azolythioacetamides: Inhibitor discovery of New Delhi metallo-
 760 beta-lactamase-1 (NDM-1). *ChemMedChem* **9**, 2445-2448
- 761 29. Zhai, L., Zhang, Y. L., Kang, J. S., Oelschlaeger, P., Xiao, L., Nie, S. S., and Yang, K. W. (2016)
 762 Triazolylthioacetamide: A Valid Scaffold for the Development of New Delhi Metallo-beta-
 763 Lactmase-1 (NDM-1) Inhibitors. *ACS Med Chem Lett* **7**, 413-417
- 764 30. Livermore, D. M., Mushtaq, S., Morinaka, A., Ida, T., Maebashi, K., and Hope, R. (2013)
 765 Activity of carbapenems with ME1071 (disodium 2,3-diethylmaleate) against
 766 Enterobacteriaceae and Acinetobacter spp. with carbapenemases, including NDM enzymes.
 767 *J Antimicrob Chemother* **68**, 153-158

- 768 31. Brem, J., van Berkel, S. S., Aik, W., Rydzik, A. M., Avison, M. B., Pettinati, I., Umland, K. D.,
 769 Kawamura, A., Spencer, J., Claridge, T. D., McDonough, M. A., and Schofield, C. J. (2014)
 770 Rhodanine hydrolysis leads to potent thioenolate mediated metallo-beta-lactamase
 771 inhibition. *Nat Chem* **6**, 1084-1090
- 772 32. Gonzalez, M. M., Kosmopoulou, M., Mojica, M. F., Castillo, V., Hinchliffe, P., Pettinati, I.,
 773 Brem, J., Schofield, C. J., Mahler, G., Bonomo, R. A., Llarrull, L. I., Spencer, J., and Vila, A. J.
 774 (2015) Bisthiazolidines: A Substrate-Mimicking Scaffold as an Inhibitor of the NDM-1
 775 Carbapenemase. *ACS Infect Dis* **1**, 544-554
- 776 33. Klingler, F. M., Moser, D., Buttner, D., Wichelhaus, T. A., Lohr, F., Dotsch, V., and Proschak,
 777 E. (2015) Probing metallo-beta-lactamases with molecular fragments identified by
 778 consensus docking. *Bioorg Med Chem Lett* **25**, 5243-5246
- 779 34. Christopheit, T., and Leiros, H. K. (2016) Fragment-based discovery of inhibitor scaffolds
 780 targeting the metallo-beta-lactamases NDM-1 and VIM-2. *Bioorg Med Chem Lett* **26**, 1973-
 781 1977
- 782 35. Wang, X., Lu, M., Shi, Y., Ou, Y., and Cheng, X. (2015) Discovery of novel new Delhi metallo-
 783 beta-lactamases-1 inhibitors by multistep virtual screening. *PLoS One* **10**, e0118290
- 784 36. Sun, N., Du, R. L., Zheng, Y. Y., Guo, Q., Cai, S. Y., Liu, Z. H., Fang, Z. Y., Yuan, W. C., Liu, T., Li,
 785 X. M., Lu, Y. J., and Wong, K. Y. (2018) Antibacterial activity of 3-methylbenzo[d]thiazol-
 786 methylquinolinium derivatives and study of their action mechanism. *J Enzyme Inhib Med*
 787 *Chem* **33**, 879-889
- 788 37. Liu, Y., Hu, X., Wu, Y., Zhang, W., Chen, X., You, X., and Hu, L. (2018) Synthesis and structure-
 789 activity relationship of novel bisindole amidines active against MDR Gram-positive and
 790 Gram-negative bacteria. *Eur J Med Chem* **150**, 771-782
- 791 38. Yu, Z. J., Liu, S., Zhou, S., Li, H., Yang, F., Yang, L. L., Wu, Y., Guo, L., and Li, G. B. (2018) Virtual
 792 target screening reveals rosmarinic acid and salvianolic acid A inhibiting metallo- and serine-
 793 beta-lactamases. *Bioorg Med Chem Lett* **28**, 1037-1042
- 794 39. Zhang, E., Wang, M. M., Huang, S. C., Xu, S. M., Cui, D. Y., Bo, Y. L., Bai, P. Y., Hua, Y. G., Xiao,
 795 C. L., and Qin, S. (2018) NOTA analogue: A first dithiocarbamate inhibitor of metallo-beta-
 796 lactamases. *Bioorg Med Chem Lett* **28**, 214-221
- 797 40. Chu, W. C., Bai, P. Y., Yang, Z. Q., Cui, D. Y., Hua, Y. G., Yang, Y., Yang, Q. Q., Zhang, E., and
 798 Qin, S. (2018) Synthesis and antibacterial evaluation of novel cationic chalcone derivatives
 799 possessing broad spectrum antibacterial activity. *Eur J Med Chem* **143**, 905-921
- 800 41. Xiang, Y., Chang, Y. N., Ge, Y., Kang, J. S., Zhang, Y. L., Liu, X. L., Oelschlaeger, P., and Yang,
 801 K. W. (2017) Azolythioacetamides as a potent scaffold for the development of metallo-beta-
 802 lactamase inhibitors. *Bioorg Med Chem Lett* **27**, 5225-5229
- 803 42. Chen, A. Y., Thomas, P. W., Stewart, A. C., Bergstrom, A., Cheng, Z., Miller, C., Bethel, C. R.,
 804 Marshall, S. H., Credille, C. V., Riley, C. L., Page, R. C., Bonomo, R. A., Crowder, M. W.,
 805 Tierney, D. L., Fast, W., and Cohen, S. M. (2017) Dipicolinic Acid Derivatives as Inhibitors of
 806 New Delhi Metallo-beta-lactamase-1. *J Med Chem* **60**, 7267-7283
- 807 43. King, A. M., Reid-Yu, S. A., Wang, W., King, D. T., De Pascale, G., Strynadka, N. C., Walsh, T.
 808 R., Coombes, B. K., and Wright, G. D. (2014) Aspergillomarasmine A overcomes metallo-
 809 beta-lactamase antibiotic resistance. *Nature* **510**, 503-506
- 810 44. Zhang, J., Wang, S., Wei, Q., Guo, Q., Bai, Y., Yang, S., Song, F., Zhang, L., and Lei, X. (2017)
 811 Synthesis and biological evaluation of Aspergillomarasmine A derivatives as novel NDM-1
 812 inhibitor to overcome antibiotics resistance. *Bioorg Med Chem* **25**, 5133-5141

- 813 45. Shi, C., Bao, J., Sun, Y., Kang, X., Lao, X., and Zheng, H. (2019) Discovery of Baicalin as NDM-
814 1 inhibitor: Virtual screening, biological evaluation and molecular simulation. *Bioorg Chem*
815 **88**, 102953
- 816 46. Liu, S., Zhou, Y., Niu, X., Wang, T., Li, J., Liu, Z., Wang, J., Tang, S., Wang, Y., and Deng, X.
817 (2018) Magnolol restores the activity of meropenem against NDM-1-producing *Escherichia*
818 *coli* by inhibiting the activity of metallo-beta-lactamase. *Cell Death Discov* **4**, 28
- 819 47. Shi, C., Chen, J., Xiao, B., Kang, X., Lao, X., and Zheng, H. (2019) Discovery of NDM-1 inhibitors
820 from natural products. *J Glob Antimicrob Resist* **18**, 80-87
- 821 48. Bush, K., and Bradford, P. A. (2019) Interplay between beta-lactamases and new beta-
822 lactamase inhibitors. *Nat Rev Microbiol* **17**, 295-306
- 823 49. Everett, M., Sprynski, N., Coelho, A., Castandet, J., Bayet, M., Bougnon, J., Lozano, C., Davies,
824 D. T., Leiris, S., Zalacain, M., Morrissey, I., Magnet, S., Holden, K., Warn, P., De Luca, F.,
825 Docquier, J. D., and Lemonnier, M. (2018) Discovery of a Novel Metallo-beta-Lactamase
826 Inhibitor That Potentiates Meropenem Activity against Carbapenem-Resistant
827 Enterobacteriaceae. *Antimicrob Agents Chemother* **62**
- 828 50. , and (1986) *Plant Flavonoids in Biology and Medicine*, Alan. R. Liss ed., New York
- 829 51. Cao, S., Jiang, X., and Chen, J. (2010) Effect of Zinc (II) on the interactions of bovine serum
830 albumin with flavonols bearing different number of hydroxyl substituent on B-ring. *Journal*
831 *of Inorganic Biochemistry* **104**, 146-152
- 832 52. Guerrero, L., Castillo, J., Quinones, M., Garcia-Vallve, S., Arola, L., Pujadas, G., and
833 Muguerza, B. (2012) Inhibition of Angiotensin-Converting Enzyme Activity by Flavonoids:
834 Structure-Activity Relationship Studies. *Plos One* **7**
- 835 53. Tolomeo, M., Grimaudo, S., Di Cristina, A., Pipitone, R. M., Dusonchet, L., Meli, M., Crosta,
836 L., Gebbia, N., Invidiata, F. P., Titone, L., and Simoni, D. (2008) Galangin increases the
837 cytotoxic activity of imatinib mesylate in imatinib-sensitive and imatinib-resistant Bcr-Abl
838 expressing leukemia cells. *Cancer Letters* **265**, 289-297
- 839 54. Grundmann, O., Nakajima, J.-I., Kamata, K., Seo, S., and Butterweck, V. (2009) Kaempferol
840 from the leaves of *Apocynum venetum* possesses anxiolytic activities in the elevated plus
841 maze test in mice. *Phytomedicine* **16**, 295-302
- 842 55. Chimenti, F., Cottiglia, F., Bonsignore, L., Casu, L., Casu, M., Floris, C., Secci, D., Bolasco, A.,
843 Chimenti, P., Granese, A., Befani, O., Turini, P., Alcaro, S., Ortuso, F., Trombetta, G., Loizzo,
844 A., and Guarino, I. (2006) Quercetin as the active principle of *Hypericum hircinum* exerts a
845 selective inhibitory activity against MAO-A: Extraction, biological analysis, and
846 computational study. *Journal of Natural Products* **69**, 945-949
- 847 56. Fahlman, B. M., and Krol, E. S. (2009) Inhibition of UVA and UVB Radiation-Induced Lipid
848 Oxidation by Quercetin. *Journal of Agricultural and Food Chemistry* **57**, 5301-5305
- 849 57. Lu, J., Papp, L. V., Fang, J. G., Rodriguez-Nieto, S., Zhivotovsky, B., and Holmgren, A. (2006)
850 Inhibition of mammalian thioredoxin reductase by some flavonoids: Implications for
851 myricetin and quercetin anticancer activity. *Cancer Research* **66**, 4410-4418
- 852 58. Hsu, Y.-L., Chang, J.-K., Tsai, C.-H., Chien, T.-T. C., and Kuo, P.-L. (2007) Myricetin induces
853 human osteoblast differentiation through bone morphogenetic protein-2/p38 mitogen-
854 activated protein kinase pathway. *Biochemical Pharmacology* **73**, 504-514
- 855 59. Kwon, O., Eck, P., Chen, S., Corpe, C. P., Lee, J.-H., Kruhlak, M., and Levine, M. (2007)
856 Inhibition of the intestinal glucose transporter GLUT2 by flavonoids. *Faseb Journal* **21**, 366-
857 377

- 858 60. Zheng, B., Tan, S., Gao, J., Han, H., Liu, J., Lu, G., Liu, D., Yi, Y., Zhu, B., and Gao, G. F. (2011)
859 An unexpected similarity between antibiotic-resistant NDM-1 and beta-lactamase II from
860 *Erythrobacter litoralis*. *Protein Cell* **2**, 250-258
- 861 61. Materon, I. C., Beharry, Z., Huang, W. Z., Perez, C., and Palzkill, T. (2004) Analysis of the
862 context dependent sequence requirements of active site residues in the metallo-beta-
863 lactamase IMP-1. *Journal of Molecular Biology* **344**, 653-663
- 864 62. Yao, C., Wu, Q., Xu, G., and Li, C. (2017) NMR backbone resonance assignment of New Delhi
865 metallo-beta-lactamase. *Biomol NMR Assign* **11**, 239-242
- 866 63. Shen, Y., and Bax, A. (2013) Protein backbone and sidechain torsion angles predicted from
867 NMR chemical shifts using artificial neural networks. *Journal of Biomolecular Nmr* **56**, 227-
868 241
- 869 64. King, D., and Strynadka, N. (2011) Crystal structure of New Delhi metallo-beta-lactamase
870 reveals molecular basis for antibiotic resistance. *Protein Science* **20**, 1484-1491
- 871 65. Bebrone, C. (2007) Metallo-beta-lactamases (classification, activity, genetic organization,
872 structure, zinc coordination) and their superfamily. *Biochem Pharmacol* **74**, 1686-1701
- 873 66. Zhang, H., Ma, G., Zhu, Y., Zeng, L., Ahmad, A., Wang, C., Pang, B., Fang, H., Zhao, L., and
874 Hao, Q. (2018) Active-Site Conformational Fluctuations Promote the Enzymatic Activity of
875 NDM-1. *Antimicrob Agents Chemother* **62**
- 876 67. Mira, L., Fernandez, M. T., Santos, M., Rocha, R., Florencio, M. H., and Jennings, K. R. (2002)
877 Interactions of flavonoids with iron and copper ions: A mechanism for their antioxidant
878 activity. *Free Radical Research* **36**, 1199-1208
- 879 68. Grazul, M., and Budzisz, E. (2009) Biological activity of metal ions complexes of chromones,
880 coumarins and flavones. *Coordination Chemistry Reviews* **253**, 2588-2598
- 881 69. Bhuiya, S., Haque, L., Pradhan, A. B., and Das, S. (2017) Inhibitory effects of the dietary
882 flavonoid quercetin on the enzyme activity of zinc(II)-dependent yeast alcohol
883 dehydrogenase: Spectroscopic and molecular docking studies. *Int J Biol Macromol* **95**, 177-
884 184
- 885 70. Guo, Y., Wang, J., Niu, G., Shui, W., Sun, Y., Zhou, H., Zhang, Y., Yang, C., Lou, Z., and Rao, Z.
886 (2011) A structural view of the antibiotic degradation enzyme NDM-1 from a superbug.
887 *Protein & Cell* **2**, 384-394
- 888 71. Green VL, V. A., Owens RJ, Phillips SE, Carr SB. (2011) Structure of New Delhi metallo-β-
889 lactamase 1 (NDM-1). *Acta Crystallogr Sect F Struct Biol Cryst Commun.* **67**, 1160–1164
- 890 72. Chen, J., Chen, H., Shi, Y., Hu, F., Lao, X., Gao, X., Zheng, H., and Yao, W. (2013) Probing the
891 effect of the non-active-site mutation Y229W in New Delhi metallo-beta-lactamase-1 by
892 site-directed mutagenesis, kinetic studies, and molecular dynamics simulations. *PLoS One* **8**,
893 e82080
- 894 73. Lescop, E., Lu, Z., Liu, Q., Xu, H., Li, G., Xia, B., Yan, H., and Jin, C. (2009) Dynamics of the
895 conformational transitions in the assembling of the Michaelis complex of a bisubstrate
896 enzyme: a (15)N relaxation study of *Escherichia coli* 6-hydroxymethyl-7,8-dihydropterin
897 pyrophosphokinase. *Biochemistry* **48**, 302-312
- 898 74. Yan, H., and Ji, X. (2011) Role of protein conformational dynamics in the catalysis by 6-
899 hydroxymethyl-7,8-dihydropterin pyrophosphokinase. *Protein Pept Lett* **18**, 328-335
- 900 75. Dajas, F., Andres Abin-Carriquiry, J., Arredondo, F., Blasina, F., Echeverry, C., Martinez, M.,
901 Rivera, F., and Vaamonde, L. (2015) Quercetin in brain diseases: Potential and limits.
902 *Neurochemistry International* **89**, 140-148

- 903 76. Brito, A. F., Ribeiro, M., Abrantes, A. M., Pires, A. S., Teixo, R. J., Tralhao, J. G., and Botelho,
904 M. F. (2015) Quercetin in Cancer Treatment, Alone or in Combination with Conventional
905 Therapeutics? *Current Medicinal Chemistry* **22**, 3025-3039
- 906 77. Ganugapati, M., Sirisha, V., Mukkavalli, S., Atimamula, S., and Sai, S. (2011) Insilico modeling
907 and docking studies of new delhi metallo Beta lactamase-1 (super bug). *International*
908 *Journal of Engineering Science and Technology* **3**, 2427-2434
- 909 78. Padmavathi, M., Prasanth Reddy, V., and Rao, R. (2012) Inhibition of NDM-1 in superbugs
910 by flavonoids- an insilico approach. *Journal of Advanced Bioinformatics Applications and*
911 *Research* **3**, 328-332
- 912 79. Liu, Y., and Guo, M. (2015) Studies on transition metal-quercetin complexes using
913 electrospray ionization tandem mass spectrometry. *Molecules* **20**, 8583-8594
- 914 80. Dolatabadi, J. E. (2011) Molecular aspects on the interaction of quercetin and its metal
915 complexes with DNA. *Int J Biol Macromol* **48**, 227-233
- 916 81. Aoki, N., Ishii, Y., Tateda, K., Saga, T., Kimura, S., Kikuchi, Y., Kobayashi, T., Tanabe, Y.,
917 Tsukada, H., Gejyo, F., and Yamaguchi, K. (2010) Efficacy of calcium-EDTA as an inhibitor for
918 metallo-beta-lactamase in a mouse model of Pseudomonas aeruginosa pneumonia.
919 *Antimicrob Agents Chemother* **54**, 4582-4588
- 920 82. Ma, J., McLeod, S., MacCormack, K., Sriram, S., Gao, N., Breeze, A. L., and Hu, J. (2014) Real-
921 time monitoring of New Delhi metallo-beta-lactamase activity in living bacterial cells by 1H
922 NMR spectroscopy. *Angew Chem Int Ed Engl* **53**, 2130-2133
- 923 83. Bergstrom, A., Katko, A., Adkins, Z., Hill, J., Cheng, Z., Burnett, M., Yang, H., Aitha, M.,
924 Mehaffey, M. R., Brodbelt, J. S., Tehrani, K., Martin, N. I., Bonomo, R. A., Page, R. C., Tierney,
925 D. L., Fast, W., Wright, G. D., and Crowder, M. W. (2018) Probing the Interaction of
926 Aspergillomarasmine A with Metallo-beta-lactamases NDM-1, VIM-2, and IMP-7. *ACS Infect*
927 *Dis* **4**, 135-145
- 928 84. Hinchliffe, P., Gonzalez, M. M., Mojica, M. F., Gonzalez, J. M., Castillo, V., Saiz, C.,
929 Kosmopoulou, M., Tooke, C. L., Llarrull, L. I., Mahler, G., Bonomo, R. A., Vila, A. J., and
930 Spencer, J. (2016) Cross-class metallo-beta-lactamase inhibition by bisthiazolidines reveals
931 multiple binding modes. *Proc Natl Acad Sci U S A* **113**, E3745-3754
- 932 85. Spyraakis, F., Celenza, G., Marcoccia, F., Santucci, M., Cross, S., Bellio, P., Cendron, L., Perilli,
933 M., and Tondi, D. (2018) Structure-Based Virtual Screening for the Discovery of Novel
934 Inhibitors of New Delhi Metallo-beta-lactamase-1. *ACS Med Chem Lett* **9**, 45-50
- 935 86. Khan, A. U., Ali, A., Danishuddin, Srivastava, G., and Sharma, A. (2017) Potential inhibitors
936 designed against NDM-1 type metallo-beta-lactamases: an attempt to enhance efficacies of
937 antibiotics against multi-drug-resistant bacteria. *Sci Rep* **7**, 9207
- 938 87. Chiou, J., Wan, S., Chan, K. F., So, P. K., He, D., Chan, E. W., Chan, T. H., Wong, K. Y., Tao, J.,
939 and Chen, S. (2015) Ebselen as a potent covalent inhibitor of New Delhi metallo-beta-
940 lactamase (NDM-1). *Chem Commun (Camb)* **51**, 9543-9546
- 941 88. Steiner, R. A., Kalk, K. H., and Dijkstra, B. W. (2002) Anaerobic enzyme-substrate structures
942 provide insight into the reaction mechanism of the copper-dependent quercetin 2,3-
943 dioxygenase. *Proc Natl Acad Sci U S A* **99**, 16625-16630
- 944 89. Jeoung, J. H., Nianios, D., Fetzner, S., and Dobbek, H. (2016) Quercetin 2,4-Dioxygenase
945 Activates Dioxygen in a Side-On O₂-Ni Complex. *Angew Chem Int Ed Engl* **55**, 3281-3284
- 946 90. Rasia, R. M., and Vila, A. J. (2004) Structural determinants of substrate binding to Bacillus
947 cereus metallo-beta-lactamase. *J Biol Chem* **279**, 26046-26051

- 948 91. Meini, M. R., Gonzalez, L. J., and Vila, A. J. (2013) Antibiotic resistance in Zn(II)-deficient
949 environments: metallo-beta-lactamase activation in the periplasm. *Future Microbiol* **8**, 947-
950 979
- 951 92. Pal, A., and Tripathi, A. (2019) Quercetin potentiates meropenem activity among pathogenic
952 carbapenem resistant *Pseudomonas aeruginosa* and *Acinetobacter baumannii*. *J Appl*
953 *Microbiol*
- 954 93. Safwat, N. A., Kashef, M. T., Aziz, R. K., Amer, K. F., and Ramadan, M. A. (2018) Quercetin 3-
955 O-glucoside recovered from the wild Egyptian Sahara plant, *Euphorbia paralias* L., inhibits
956 glutamine synthetase and has antimycobacterial activity. *Tuberculosis (Edinb)* **108**, 106-113
- 957 94. Lo, M. C., Aulabaugh, A., Jin, G., Cowling, R., Bard, J., Malamas, M., and Ellestad, G. (2004)
958 Evaluation of fluorescence-based thermal shift assays for hit identification in drug discovery.
959 *Anal Biochem* **332**, 153-159
- 960 95. Zhu, G., Xia, Y. L., Nicholson, L. K., and Sze, K. H. (2000) Protein dynamics measurements by
961 TROSY-based NMR experiments. *Journal of Magnetic Resonance* **143**, 423-426
- 962 96. Piotto, M., Saudek, V., and Sklenar, V. (1992) Gradient-tailored excitation for single-
963 quantum NMR spectroscopy of aqueous solutions. *J Biomol NMR* **2**, 661-665
- 964 97. Williamson, M. P. (2013) Using chemical shift perturbation to characterise ligand binding.
965 *Prog Nucl Magn Reson Spectrosc* **73**, 1-16
966

967 **TABLE**

968 **Table 1.** Minimum inhibitory concentrations of imipenem in presence of myricetin and quercetin for *E. coli*
 969 GUE NDM-1 and *K. pneumoniae* CAG NDM-1

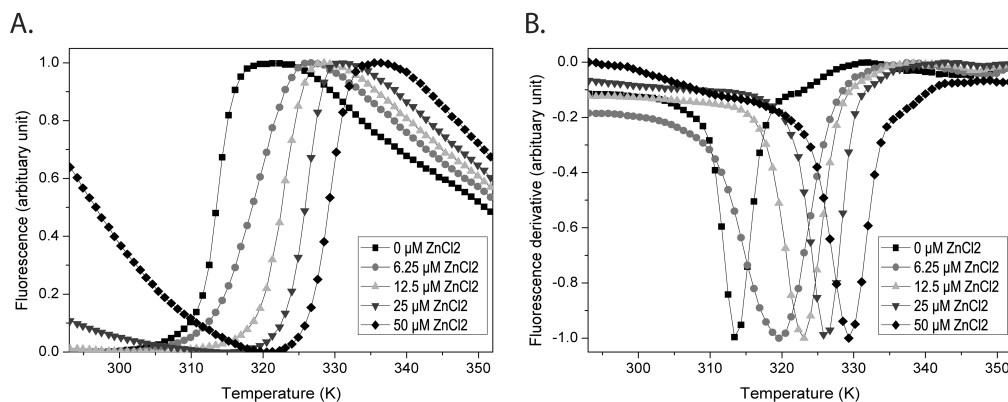
	MICs (mg/L)					
	Myricetin concentration			Quercetin concentration		
	0 μ M	50 μ M	100 μ M	0 μ M	100 μ M	200 μ M
<i>E. coli</i> NDM-1 GUE	128	32	8	128	32	16
<i>K. pneumoniae</i> NDM-1 CAG	128	64	16	128	128	128

970

971

972 **FIGURES**

973

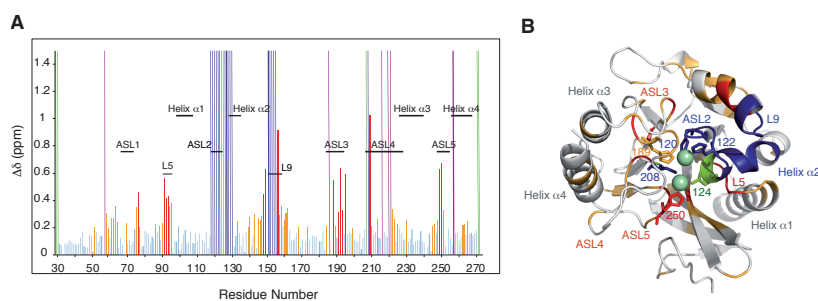


974

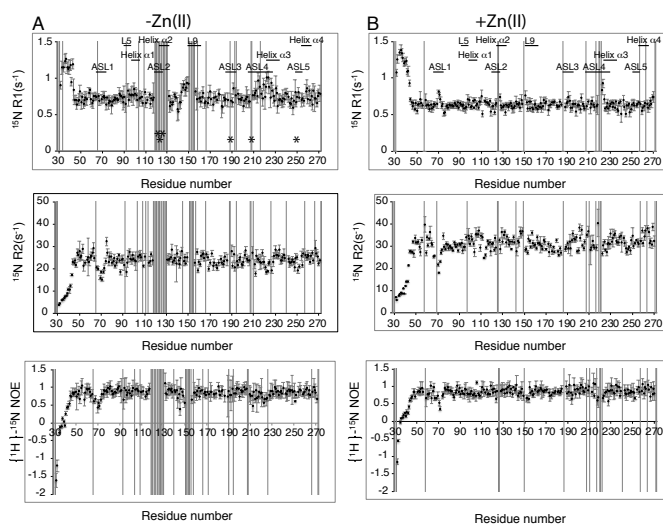
976 **FIGURE 1.** Effect of Zn(II) ions on NDM-1 denaturation followed by Thermal shift assay. The
 977 thermal denaturation profiles of NDM-1 were performed in the presence of various concentrations
 978 of ZnCl₂ (0 to 50 μ M) and 9 μ M of NDM-1. (A) Fluorescence profiles of denaturation curves and
 979 (B) opposite of the derivative of the fluorescence curves.

980

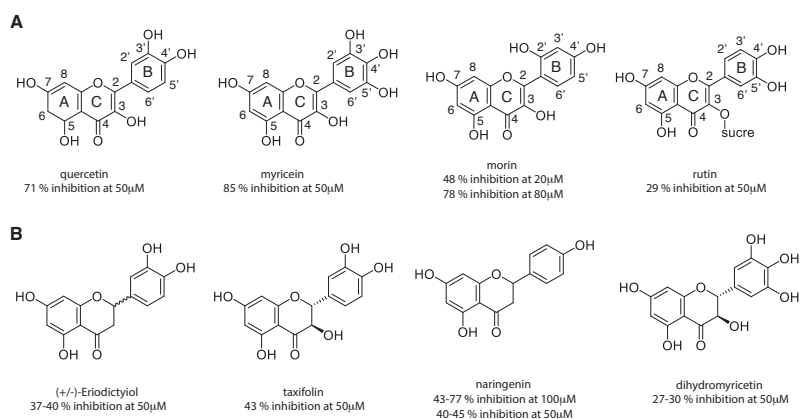
981



982
 983
 984 **FIGURE 2. Specific interactions between NDM-1 and Zn(II).** (A) Chemical shift perturbations
 985 of the amide protons and nitrogen between the metal-free NDM-1 and di-Zn(II) NDM-1. The ^1H and
 986 ^{15}N chemical shifts were extracted from NDM-1 spectra recorded in absence of Zn(II) at 293K and
 987 800 MHz ^1H frequency, on a sample containing a phosphate buffer 50 mM (pH 7.0 and 150 mM
 988 NaCl) and in presence of 2 eq of Zn(II) at 308K and 800MHz ^1H frequency on a sample buffer
 989 containing 0.1 mM bis tris (pH 7.0, 150 mM NaCl). (B) Location of residues with significantly
 990 perturbed amide proton and nitrogen resonances upon binding of Zn(II), mapped onto the X-ray
 991 structure of metallo- β -lactamase (PDB: 3S0Z). In red and orange are represented the residues with
 992 $\Delta\delta > 0.4$ ppm and $0.2 > \Delta\delta > 0.4$ ppm, respectively. The unassigned residues of NDM-1 are
 993 represented with dark blue lines in absence of Zn(II) and with green lines in absence and in presence
 994 of Zn(II). Zn(II) are represented by green spheres.
 995
 996

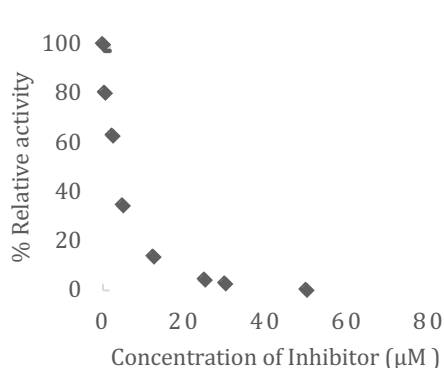


997
 998 **FIGURE 3. NMR relaxation parameters of NDM-1.** ^{15}N R1, R2 relaxation and heteronuclear $\{^1\text{H}\}$
 999 ^{-15}N NOE parameters obtained for NDM-1 (A) in absence of Zn(II) (phosphate buffer 50 mM (pH
 1000 7.0 and 150 mM NaCl), (B) in presence of 2 equivalents of Zn(II) (0.1 mM bis tris (pH 7.0, 150 mM
 1001 NaCl), at 600 MHz ^1H and 298K. The light grey bars represent either the unassigned residues or the
 1002 residues for which the R1, R2 and NOE values could not be obtained because of superimposition of
 1003 several cross-peaks. The residues in direct interaction with Zn(II) in the crystal structure are
 1004 represented by stick.
 1005



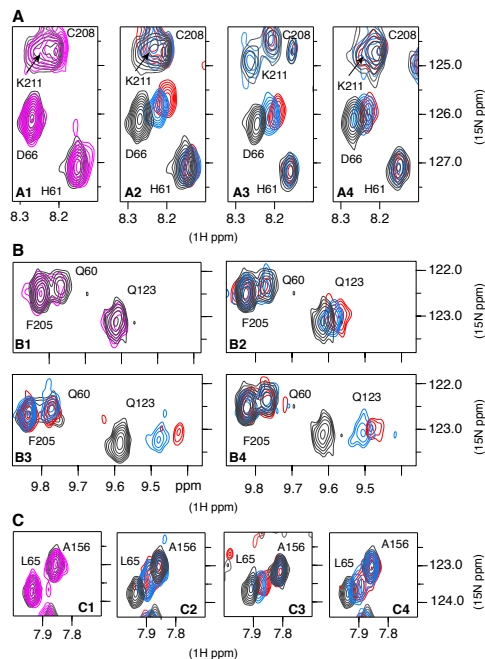
1006
1007
1008
1009
1010
1011
1012
1013
1014
1015
1016
1017

FIGURE 4. Summary of the inhibitory activity of flavonoids. All these molecules have the general structure of the flavonoids, a 15-carbon skeleton, which consists of two phenyl rings (A and B) and a heterocyclic ring (C). **A)** The four molecules differ from each other by the number and the position of the hydroxy groups: quercetin, myricetin and morin. In rutin the hydroxy group at position C-3 is substituted with glucose and rhamnose sugar groups. **B)** These molecules have two stereocenters on the C-ring, as opposed to the previous ones which have none. They differ also from each other by the number and the position of the hydroxy groups: eriodictyol, taxifolin, naringenin and dihydromyricetin.

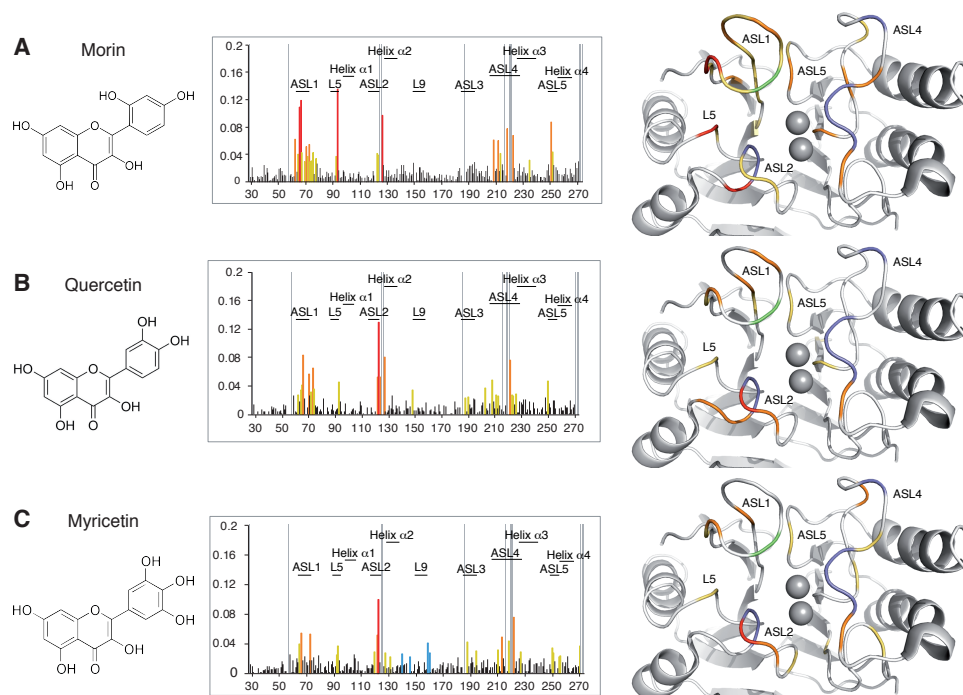


1018
1019
1020
1021
1022
1023
1024
1025
1026

FIGURE 5. IC₅₀ Determination for myricetin on purified NDM-1. Representation of IC₅₀ curve for myricetin with residual activity of NDM-1 as monitored by the hydrolysis of different concentration of inhibitor with constant concentration of imipenem (100 μ M).

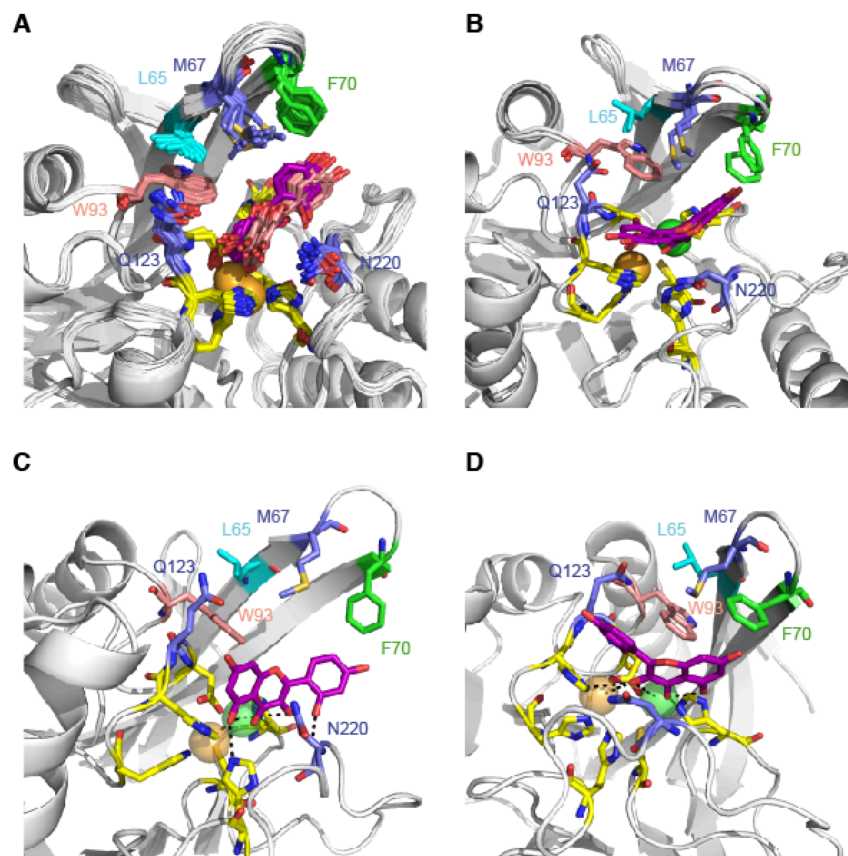


1027
 1028 **FIGURE 6. Selected regions of the ^1H - ^{15}N HSQC spectra probing the NDM-1:flavonol**
 1029 **interactions.** Panels A1, B1 and C1 show that addition of DMSO (black in absence of DMSO and
 1030 pink in presence of the quantity of DMSO corresponding to that is added to have 2 equivalents of
 1031 flavonol relative to the NDM-1 concentration: 5.36 μl DMSO) do not induce significant chemical
 1032 shift variations of the NDM-1 resonances. Titrations of NDM-1 (in black in absence of flavonol) by
 1033 1eq (in blue) and 2eq (in red) of morin (A2, B2 and C2), quercetin (A3, B3 and C3) and myricetin
 1034 (A4, B4 and C4) show the influence of the flavonols on several NDM-1 resonances. The spectra
 1035 were recorded in presence of 2 equivalents Zn(II) at 293K and 800 MHz ^1H frequency on a sample
 1036 buffer containing 0.1 mM bis tris (pH 7.0) and 150 mM NaCl with increasing concentrations of
 1037 DMSO as the ligand is incremented.
 1038



1039
 1040
 1041
 1042
 1043
 1044
 1045
 1046
 1047
 1048
 1049
 1050
 1051
 1052

FIGURE 7. Specific interaction between NDM-1 and flavonols. Plots of measured chemical shift perturbations of the amide protons and nitrogen of NDM-1 upon addition of 2 molar equivalents of flavonols: **A**) morin, **B**) quercetin, **C**) myricetin as function of NDM-1 residues. The ^1H and ^{15}N chemical shifts were extracted from NDM-1 spectra recorded in presence of Zn(II) at 293K and 800MHz ^1H frequency on a sample buffer containing 0.1 mM bis tris (pH 7.0) and 150 mM NaCl and 2.6% of DMSO. In red, orange and yellow are represented the residues with a $\Delta\delta > 0.09$ ppm, $0.09 > \Delta\delta > 0.05$ ppm, and $\Delta\delta > 0.02$ ppm respectively. The unassigned residues of NDM-1 are represented with grey lines. The same code of colour is used to highlight residues undergoing significant chemical shifts variations upon binding of flavonols onto the X-ray structure of metallo- β -lactamase (PDB:3S0Z). The unassigned residues are in blue and P68 in green.



1053
 1054
 1055
 1056
 1057
 1058
 1059
 1060
 1061
 1062
 1063
 1064
 1065
 1066

FIGURE 8. Models of the NDM-1/morin complexes generated using HADDOCK. A) Superimposition of 20 structures over the 40 structures clustered in the top clusters generated using the ten NDM-1 crystallographic structures (PDB: 4EXS, 4EY2, 4EYB, 4EYF, 4EYL, 4HL2, 4RAM, 4RBS, 4RL2, 4RL0) showing the majority orientation of the morin in the active site of NDM-1 (orientation-1). These 20 structures adopt two different orientations in the active site, in 13 dark pink and 7 in light pink. B). A minority orientation is also observed in the docking generated structures (orientation-2). C) Zoom on one of the 20 structures in which the morin adopts the orientation-1 showing the polar contacts between the ligand and the Zn(II) ions (PDB: 4HL2 (cluster 1: structure 2)). D) Zoom on one of the structures in which the morin adopts the orientation-2 showing the polar contacts between the ligand and the Zn(II) ions (PDB: 4RBS (cluster 1: structures 1)).

Discussion

L'objectif initial de mon projet était de combiner différentes approches complémentaires (microbiologie, biochimie, biologie structurale, modélisation moléculaire et synthèse chimique) pour mieux comprendre le fonctionnement des carbapénèmases les plus répandues dans le monde : OXA-48, KPC-2 et NDM-1 ; dont la prévalence ne cesse d'augmenter, constituant un problème mondial de santé publique.

Dans un premier temps, l'étude de variants naturels a permis de mettre en lien les relations structure-activité de ces carbapénèmases avec les spécificités de substrats. L'objectif était alors de déterminer les résidus clés impliqués dans la reconnaissance et l'hydrolyse des carbapénèmes. Ainsi, nous avons pu caractériser ces enzymes d'un point de vue moléculaire et biochimique. En parallèle, nous avons déterminé leurs structures par cristallographie et identifié précisément les interactions avec leurs substrats. Ce travail a permis de fournir des informations essentielles pour la compréhension du mode d'action des carbapénèmases, étape cruciale pour le développement d'inhibiteurs efficaces.

Les carbapénèmases de type OXA-48 constituent une famille hétérogène. La caractérisation des différents variants a contribué à mettre en lien le profil hydrolytique et la structure de l'enzyme. La comparaison structurale entre des oxacillinasés non-carbapénèmases (OXA-10) et carbapénèmases (OXA-48, OXA-23) menée par De Luca *et al*³⁹² avait montré une différence majeure au niveau de la structure de la boucle β 5- β 6. Ainsi, ils ont supposé qu'il existait un lien entre l'activité carbapénémase et la boucle β 5- β 6. Enfin, l'analyse structurale a suggéré que l'arginine 214 (R214) pourrait être impliquée dans l'hydrolyse des carbapénèmes.¹⁹² Nos premiers travaux, qui visaient à caractériser les variants naturels d'OXA-48 en 2012, ont souligné l'impact de la substitution R214S chez le variant OXA-232 et la délétion de la boucle β 5- β 6 chez les variants naturels dépourvus d'activité carbapénémase, OXA-163 et OXA-405. En effet, nous avons pu montrer que la substitution du résidu 214 et que la perte de la boucle β 5- β 6 ont pour conséquence une diminution significative voire même une perte quasi totale de l'activité carbapénémase ainsi qu'une augmentation de l'hydrolyse des céphalosporines pour les variants OXA-163 et OXA-405. Docquier *et al* proposaient que le résidu R214 établisse une interaction avec l'acide aspartique en position 159 (D159). Ainsi,

cette interaction, permettrait de délimiter au niveau du site actif une poche hydrophile. Ainsi, des molécules d'eau viendraient se loger dans cette cavité située à proximité de la serine 70 (S70), favorisant ainsi l'étape de catalyse. L'étude des mutants de la carbapénèmase OXA-232, dont R214 a été substituée par des résidus possédant une chaîne latérale ne permettant plus d'interaction avec l'acide aspartique D159 (Glycine et l'acide glutamique), montre que de façon globale, la perte de l'activité enzymatique est due à une diminution des k_{cat} . Ainsi, il y aurait bien un lien étroit entre l'interaction R214/D159 et la réaction catalytique de l'enzyme. On peut supposer, que la perte de cette interaction ne permette plus d'avoir des molécules d'eau à proximité du site actif, ce qui diminue donc l'activité hydrolytique. Pour pouvoir confirmer cette hypothèse, il pourrait être envisagé de réaliser des substitutions du résidu D159 d'OXA-48 et d'observer *via* une étude enzymatique si une diminution des k_{cat} est bien détectée. La perte d'affinité de l'imipénème, ainsi que la perte d'hydrolyse de la témocilline pour le mutant OXA-232 R214E, pourrait s'expliquer par la charge négative de l'acide glutamique. En effet, notre étude de modélisation propose une autre conformation de liaison de l'imipénème incompatible avec une attaque nucléophile de la Ser70. Dans ce cas, l'imipénème agirait comme un inhibiteur, ce qui explique les valeurs de K_m significativement plus élevées. Nous avons également montré que, dans le même mutant 214E, l'interaction défavorable entre le substituant R1 chargé négativement de la témocilline et le résidu Glu214 muté exclut la liaison de cet antibiotique, révélant ainsi les détails structuraux responsables de l'absence d'hydrolyse pour ce substrat. L'étude enzymatique des variants OXA-163 et OXA-405 a permis de montrer que le changement du profil hydrolytique pourrait être la conséquence de plusieurs phénomènes. En effet, les faibles valeurs de k_{cat} pour ces mutants, indiquent une perte totale de l'activité catalytique, confirmant l'hypothèse suggérée ci-dessus que la poche hydrophile est cruciale pour l'activité enzymatique. En revanche, en l'absence de cette boucle, on constate une meilleure affinité pour les céphalosporines ainsi qu'une hydrolyse de la ceftazidime. On peut donc supposer que l'accès au niveau du site actif à des substrats de grandes tailles est favorisé. Enfin, il a pu être montré une diminution de l'affinité de l'imipénème et du méropénème. L'absence de la boucle ne permettrait plus d'avoir un site actif structuré et dans ce cas, les résidus impliqués dans la reconnaissance et la fixation des carbapénèmes ne pourraient plus assurer leurs rôles.

Tout comme les enzymes de type OXA-48, les carbapénèmases de type KPC représentent un groupe hétérogène avec des profils hydrolytiques très variés. Au cours des

travaux menés, nous avons pu montrer que contrairement à OXA-48, une simple substitution pouvait modifier le spectre d'hydrolyse passant d'un profil carbapénèmase à un profil BLSE. L'analyse des variants naturels et des mutants générés a permis de mettre en exergue le rôle de certains acides aminés. Ainsi, nous avons montré que les résidus P104, W105 et L168, situés au niveau du site actif, serraient impliqués dans la reconnaissance et/ou dans la fixation des carbapénèmes. La substitution des résidus C238 et D179 a conduit à une perte quasi totale de l'activité carbapénèmase. Ces deux résidus ont une fonction structurale. La cystéine 238 assure un pont disulfure avec la cystéine 68,⁹⁶ qui est adjacente à la serine active S70, permettant ainsi le maintien de la structure du site actif. Nous avons montré qu'une substitution à cette position conduit à une perte de l'activité enzymatique globale. Le résidu D179 possède un rôle clé au niveau de la boucle oméga Ω , il interagit avec plusieurs acides aminés (P67, L68 et R161) via des liaisons hydrogène mais également avec R164 via un pont salin.³⁹³ Toutes ces interactions permettent le maintien de cette boucle, qui est cruciale pour l'activité enzymatique. En effet, cette boucle contient l'un des 3 motifs très conservés chez les SBLs : ¹⁶⁶EXXXN¹⁷⁰, où le résidu E166 jouerait un rôle crucial dans l'étape de déacylation. Néanmoins, la déstructuration de la boucle oméga favorise l'hydrolyse de la ceftazidime. Il semblerait que tout comme la boucle β 5- β 6, la boucle oméga Ω empêcherait l'accès de cette grande molécule au site actif. Les résidus V240 et P104 ont également un impact sur l'hydrolyse de la ceftazidime. Cette observation n'est pas spécifique à KPC-2. En effet, il s'agit d'une stratégie commune à toutes les β -lactamases de classe A. Par exemple, il a été montré qu'une mutation du résidu E104K chez TEM-1 entraîne une multiplication par 4 de la CMI pour la ceftazidime et une multiplication par 50 de l'efficacité catalytique vis-à-vis de cette molécule.³⁹⁴ De même, dans le cas des β -lactamases de type CTX-M, une substitution D240G augmente la CMI de la ceftazidime de 8 fois en raison d'une augmentation de 10 fois en efficacité catalytique.³⁹⁵ L'étude des variants KPC-14 et KPC-28, tous deux délétés des 2AA Δ 242-GT-243, a révélé que cette délétion n'était pas la cause directe de la modification du spectre d'hydrolyse (perte de l'activité carbapénèmase et gain de l'hydrolyse des C3G), mais qu'il s'agissait d'un événement indirect. Cette délétion a conduit à un décalage de 2,4 Å du résidu A244, provoquant une répulsion avec le résidu 274 situé au niveau du site actif. Ainsi, nous avons confirmé le rôle de ce résidu dans la reconnaissance des substrats. En effet, il avait déjà été montré, *via* l'étude du variant KPC-3,³⁹⁶ que la substitution H274Y modifiait le profil d'hydrolyse de KPC *via* l'augmentation de l'hydrolyse des C3G mais n'avait aucun impact sur l'hydrolyse des carbapénèmes. Cette répulsion n'aurait pas d'impact sur la fixation des C3G, mais, en revanche

ne permettrait plus celle des carbapénèmes. Depuis l'utilisation en clinique de l'inhibiteur avibactam associé à la ceftazidime, des cas de plus en plus nombreux de résistance sont rapportés dans la littérature.³⁹⁷⁻⁴⁰¹ Il est maintenant établi qu'il existe deux principaux mécanismes conduisant à cette résistance : (i) La première serait causée par une forte augmentation de l'efficacité catalytique pour la ceftazidime dépassant les capacités inhibitrices de l'avibactam, alors que la deuxième (ii) s'expliquerait par une perte de l'affinité de KPC vis-à-vis de l'avibactam. Nous avons pu observer ces deux phénomènes. Avec les variants KPC-14 et KPC-28, l'IC50 de l'avibactam reste inchangé mais l'activité catalytique de l'enzyme vis-à-vis de la ceftazidime est fortement augmentée. A l'inverse, pour les variants KPC-31 et KPC-33, nous avons pu identifier une augmentation d'environ 100 fois de l'IC50.

Les mécanismes d'action de ces différentes enzymes sont de plus en plus étudiés. Ainsi, on comprend de mieux en mieux l'importance des interactions entre résidus-substrats et résidus-inhibiteurs. Cependant ces études sont basées sur des techniques de cristallographie qui ne tiennent pas compte de la dynamique de la protéine et surtout de la dynamique des molécules d'eau présentes au niveau du site actif et indispensables à la réaction enzymatique. Il serait donc intéressant d'étudier les résidus qui pourraient permettre le recrutement des molécules d'eau, avec pour but final le développement de nouveaux composés thérapeutiques.

Nos travaux ont permis de révéler la formidable plasticité structurale et hydrolytique des carbapénémases de type OXA-48 et KPC. Cependant, la question sur le coût de tous ces changements reste en suspens. Il a été montré que l'augmentation de l'hydrolyse de la ceftazidime avait directement un impact sur la stabilité de l'enzyme.⁹³ Enfin, la question de la genèse de l'activité carbapénémase reste en suspens. S'agit-il tout simplement de l'émergence vis-à-vis d'une pression de sélection due à l'utilisation des carbapénèmes ou s'agit-il d'enzymes qui ont été optimisées dans la nature par des expositions avec des streptomyces ? En fait, cela dépend de la référence que l'on utilise comme point de comparaison. Si l'on compare la structure d'OXA-48 à celle de l'oxacillinase OXA-10 (qui est la plus proche d'OXA-48 avec 45% d'identité)³⁹², on peut dire que la boucle β 5- β 6 et la présence du R214 seraient à l'origine de l'acquisition de l'activité carbapénémase. Cependant, il semblerait que le genre que *Shewanella* sp. soit le progéniteur des oxacillinasés capable d'hydrolyser les carbapénèmes. Une étude récente a identifié la présence d'un gène chromosomique, chez la souche *Shewanella oneidensis* MR-1, *bla*_{OXA-54} qui présente 88% d'identité avec le gène *bla*_{OXA-48}.¹⁷⁷ La comparaison de la structure primaire indique une bonne conservation en acides aminés dans la

boucle β 5- β 6 dont le résidu R214. Ces bactéries sont largement répandues dans les milieux marins et d'eau douce et sont faiblement pathogènes pour l'homme.⁴⁰² L'expression de ce type d'enzyme par des souches environnementales pourrait correspondre à un mécanisme de défense envers d'autres micro-organismes tels que *Streptomyces cattleya* capable de produire la thiénamycine (un dérivé de l'imipénème).

Contrairement à OXA-48, le progéniteur de KPC-2 n'est toujours pas connu. Nous ne pouvons donc pas réellement parler d'acquisition. Par comparaison des séquences d'acides aminés, il a été reconnu que KPC-2 se distingue des autres β -lactamases de classe A par la présence d'un pont disulfure entre les résidus 69 et 238. L'étude de SME-1,⁶⁰ ainsi que celle de notre mutant C238S, montre que la rupture du pont disulfure est structurellement importante. Cependant, il ne s'agirait pas d'un élément essentiel et déterminant pour l'activité carbapénémase car sa perte conduit à une perte totale de l'activité enzymatique. Il semblerait que cette activité résulte de plusieurs événements, contrairement aux carbapénémases de type GES. En effet, GES-1 qui présente également un pont disulfure, ne possède pas d'activité carbapénémase mais une activité de type BLSE. Cependant, une simple substitution du résidu en position 170 conduit à l'acquisition de l'activité carbapénémase.^{68,403} Dans le cas de KPC-2, on peut supposer que l'activité hydrolytique vis-à-vis des carbapénèmes résulte d'un ensemble de facteurs qui pourrait être, (i) le positionnement de la boucle oméga Ω , (ii) la formation du pont disulfure favorisant le rapprochement de résidus au niveau du site actif et bien évidemment (iii) la présence de résidus critiques (D92, P104, W105, L168, D179, C238), tel que nous avons pu le montrer dans nos travaux.

Contrairement aux SBLs, les MBLs font partie de la superfamille des métallohydrolases.⁴⁰⁴ Ces enzymes se trouvent principalement chez les procaryotes et ont des fonctions biologiques très variées avec une gamme de substrats très diverse, allant de certaines petites molécules (thioesters, phosphonates) jusqu'aux acides nucléiques.^{354,405} Chez les eucaryotes supérieurs ces enzymes sont impliquées dans la réparation de l'ADN et dans les voies de maturation des ARNs.⁴⁰⁶ Les MBLs de type NDM-1 présentent un centre de zinc binucléaire, comprenant 3-His (Zn1) et les sites métalliques Cys-His-Asp (Zn2) qui sont à la base du mécanisme d'action de ces enzymes. En plus, NDM-1 se distingue des autres carbapénémases de type SBLs par son spectre d'activité exceptionnellement large qui englobe les pénicillines, les céphalosporines et les carbapénèmes. En revanche elle ne présente pas

d'activité vis-à-vis de l'aztréonam. Les études menées sur les différents variants de NDM-1 ont tenté d'identifier les acides aminés impliqués dans la reconnaissance des substrats et donc dans le profil hydrolytique de l'enzyme. Cependant, il faut rester prudent quant à l'interprétation de l'impact des substitutions sur l'activité carbapénémase de ces variants. En effet, il existe des incohérences de résultats de sensibilité phénotypique dues aux méthodologies expérimentales utilisées (différents promoteurs, vecteurs...). Plusieurs résidus ont notamment été proposés comme permettant l'augmentation de l'hydrolyse des carbapénèmes tels que la V88 (NDM-5, -17, -20 et 21)⁴⁰⁷⁻⁴⁰⁹, M154L (NDM-4 et 8)^{391,410}, D130G (NDM-14).⁴¹¹ Cependant, il semblerait qu'il n'y ait pas d'impact réellement significatif de toutes ces mutations. Le variant NDM-9 (E152K), qui est considéré comme le plus actif vis-à-vis de l'imipénème, présente une efficacité catalytique augmentée de 9-fois par rapport à celle de NDM-1.³⁹⁰ Parmi la banque de mutants que nous avons générée, nous n'avons pas obtenu de mutants présentant un phénotype plus résistant. Bien au contraire nous avons observé des augmentations de sensibilité, ce qui nous a permis d'identifier un certain nombre de résidus impliqués dans la reconnaissance et l'activité catalytique de l'enzyme. Il est intéressant de noter que nous n'avons pas observé de modulation du phénotype comme c'est le cas chez les variants de KPC-2. Les substitutions obtenues ont toujours conduit à une diminution de l'hydrolyse de toutes les β -lactamines, à l'exception du mutant N142T. Dans ce dernier cas, le résidu N142 est substitué par une thréonine, résidu de même nature polaire et non chargé. Cette substitution a conduit à une diminution de la résistance des carbapénèmes et des céphalosporines mais confère toujours une résistance à l'amoxicilline. Notre étude a également confirmé le rôle de certains résidus F218, K121, D199 et S262 considérés comme clés pour les autres MBLs tel que VIM et IMP.⁴¹²

La caractérisation des nouveaux variants, ainsi que celle des mutants générés *in vivo*, ne tient très rarement (voire pas du tout) compte de la disponibilité en ion zinc dans le milieu. Il serait intéressant de voir si ces enzymes se comportent de la même manière dans des conditions riches et pauvres en ion zinc. Pourrait-on observer l'émergence de nouveaux variants par une pression de sélection dans des conditions appauvries en zinc et contenant des carbapénèmes ? Au sein du labo, nous avons pu constater que la protéine NDM-1 était beaucoup moins stable que OXA-48 et KPC-2. Or, Bahr *et al.* suggèrent que la substitution M154, largement présente chez les variants de NDM-1 (12/28)¹⁹⁰, serait responsable de l'amélioration de la fixation des ions zinc, permettant d'accroître la stabilité.⁴¹³ Leurs résultats suggèrent aussi que la privation en ion zinc impose une contrainte stricte à l'évolution de cette MBL. Une étude menée par Gonzalez *et al.*⁴¹⁴ a révélé que l'ancrage membranaire serait l'un des mécanismes évolutifs permettant d'améliorer considérablement la stabilité de NDM dans des conditions de carence

en zinc, ce qui a lieu sur le site d'infection où de grandes quantités de calprotectine, une protéine chélatant les métaux, sont libérées suite à la réponse immunitaire de l'hôte. Cette carence pourrait donc interférer avec la fonction enzymatique de NDM-1.

Ainsi, les β -lactamases ont évolué au fil du temps en accumulant des mutations en réponse à la pression environnementale leur permettant de modifier leur profil d'hydrolyse avec, dans certains cas, une modification de leurs stabilités. Face à cette évolution rapide, les options thérapeutiques disponibles ont gravement été compromises. De plus, le développement de médicament de substitution a très peu progressé. De nos jours, il n'est disponible en clinique, qu'un seul inhibiteur efficace sur des carbapénèmases à sérine active (Classes A, C et certaines D), l'avibactam. Malheureusement, depuis la première utilisation de cet inhibiteur en association avec la ceftazidime en 2016, on dénombre l'apparition croissante de carbapénèmases de type KPC résistantes à cette association. De plus, cet inhibiteur n'a aucun effet sur les carbapénèmases de type MBLs. C'est pour cela qu'il est indispensable de continuer à développer de nouvelles classes d'inhibiteurs qui soient capables d'inhiber les 3 classes de carbapénèmases. Ainsi, nous avons entrepris, avec de nombreux collaborateurs, le développement de pan-inhibiteurs selon plusieurs stratégies faisant intervenir la synthèse de composés de natures différentes : chélateurs de métaux, azetidimines et imizadolines, des dérivés de flavonoïdes, des monobactames fluorés. Ces composés ont été sélectionnés soit (i) par un criblage *in silico* (« docking ») utilisant les données structure/activité obtenues précédemment (cas des chélateurs de métaux), soit par (ii) criblage d'une chimiothèque (cas des dérivés de flavonoïdes), ou (iii) simplement parce que la structure des composés était similaire aux β -lactamines substrat naturel des β -lactamases (analogue de substrat : monobactames fluorés et azetidimines). Le criblage de composés flavonoïdes a montré l'efficacité de 3 composés : la quercétine, la myricétine et le morin. Parmi ces 3 molécules, la myricétine était la plus active avec un pourcentage d'inhibition de 85% pour NDM-1, mais aussi de 90% pour OXA-48 et 78% pour KPC-2. De plus, une activité inhibitrice a été observée, en synergie avec l'imipénème, sur une souche clinique productrice de NDM-1. Ces composés étant relativement hydrophobes, il avait été entrepris de synthétiser des dérivés plus solubles mais, malheureusement, cela n'a pas pu se faire du fait d'une chimie trop compliquée. L'étude dynamique de RMN a permis de mettre en lumière les résidus impliqués dans la fixation entre NDM-1 et les flavonoïdes (présents sur les boucles L1, L2 et L4 et au niveau des sites impliqués dans la coordination des ions zinc). Le « docking » a révélé que ces 3 composés s'orienteraient

et se fixeraient de la même manière et formeraient un complexe avec les ions zinc ce qui inhiberait NDM-1.

L'autre approche a été de développer deux séries de molécules : les azetimidines (analogues de β -lactamines)⁴¹⁵ et les imidazolines, obtenues par une nouvelle voie de synthèse chimique basée sur la synthèse de Staudinger. Ces deux séries de molécules ont montré des propriétés inhibitrices extrêmement intéressantes, elles sont efficaces sur les 3 carbapénèmes purifiées et même sur CMY-2, une β -lactamase de classe C. La modification de certains groupements a permis de gagner en solubilité mais aussi en efficacité. Ainsi, nous avons pu identifier plusieurs inhibiteurs actifs avec des valeurs de CI50 sub-micromolaire. En raison de problème de solubilité l'effet sur la souche *E. coli* productrice de NDM-1 reste cependant faible. L'amélioration de la solubilité de cette série de molécule est en cours. En outre, des études cristallographiques ainsi que de « docking » permettraient de mieux comprendre le mode d'action de ces inhibiteurs.

Au cours de cette dernière décennie, les EPCs sont devenues une menace réelle, et risquent de compromettre les avancées de la Médecine moderne, due à leur propagation rapide dans les établissements de santé du monde entier. Les infections liées aux EPC sont difficiles à traiter et associées à une mortalité élevée en raison des options de traitement limitées. La détection rapide et précise des EPC est donc d'une importance capitale pour guider les cliniciens et limiter leur dissémination. Au début de mes travaux, il existait quelques outils de diagnostic basés principalement sur des approches phénotypiques (long et peu spécifique) et moléculaires (souvent des PCRs maisons). Les tests de type Carba NP⁴¹⁶ ont apporté une réelle amélioration du fait d'une excellente spécificité et sensibilité tout en étant très rapide (<2h). Les tests moléculaires, plus ou moins rapides, reposent sur la détection et l'amplification des 4, voire 5 carbapénèmes les plus fréquentes. Nous avons contribué à l'évaluation de nouvelles trousse de diagnostic moléculaire ciblant d'autres gènes de résistance d'intérêt clinique (VanA/VanB, MCR, OXA-Acinetobacter, et GES) : Amplidiag® CarbaR+VRE, Amplidiag® CarbaR+MCR et Novodiag Carba (Mobidiag). Ce test est basé sur une PCR multiplex qualitative en temps réel permettant l'identification d'un large panel de carbapénèmes exprimées aussi bien chez les entérobactéries que chez *Acinetobacter* sp. Ce test, réalisé à partir d'échantillons rectaux ou de colonies pures, a permis l'identification des carbapénèmes les plus répandues tel que KPC, NDM, VIM, IMP et OXA-48-like mais aussi OXA-23, OXA-24/-40, OXA-58 et OXA-51 (lorsqu'elle est surexprimée). Cependant, ces trousse ne permettent pas de détecter les carbapénèmes les moins répandues telles que les GES-like (GES-2, GES-

5, et GES-14), GIM-1, AIM-1, SPM-1, DIM-1, OXA-198 chez *P. aeruginosa*, ou encore OXA-143-like chez *A. baumannii*.

Un autre type de test de diagnostic a pu être expertisé le BYG Carba v2.0. Il repose sur un test électrochimique capable de détecter, en temps réel, les variations de la conductivité résultant de la dégradation de l'imipénème par les carbapénèmases. Cette étude européenne, menée sur plus de 1000 souches cliniques, a montré que ce test présentait une sensibilité de 96,3% et une spécificité de 99,7% pour la détection des EPC parmi les souches d'entérobactéries de sensibilité diminuée aux carbapénèmes.

Enfin, l'optimisation du protocole, visant à la surexpression et à la purification de carbapénèmases, a contribué au développement d'un nouveau type de test de diagnostic basé sur une méthode immuno-chromatographique capable de détecter les 5 principales familles de carbapénémase (KPC, NDM, VIM, IMP, OXA-48-like) en moins de 15 minutes. La première étude s'est focalisée sur la détection des carbapénèmases de type NDM, pour cela 175 souches cliniques de référence avaient été testées et les résultats furent très encourageants avec 100% de sensibilité et de spécificité. Une seconde étude a permis de proposer un nouveau kit permettant l'identification d'autres types de carbapénèmases : KPC, IMP, VIM et OXA-48 avec une sensibilité de 100% et une spécificité de 95,3% (rétrospectivement) et de 100% (de manière prospective).

Les différentes méthodes de détection des EPC deviennent de plus en plus efficaces avec l'obtention de résultats très rapides et une utilisation de plus en plus simplifiée. Cependant comme toutes techniques, elles ont toutes leurs limites. Par exemple, les tests moléculaires détectent uniquement la présence du gène d'intérêt mais n'apportent aucune information sur l'expression de la protéine, ni même sur son activité carbapénémase cela qui peut conduire à la validation de faux positif et donc à une mauvaise prise en charge du patient. L'autre limite, est l'incapacité à détecter de nouveaux variants. Ceci n'est pas réservé aux tests moléculaires. En effet, le même problème est observé avec les tests immunochromatographiques. C'est pour cela que pour une détection efficace des EPC, il est crucial de combiner un test biochimique qui révélera la présence d'une activité carbapénémase à des tests moléculaires ou immunochromatographiques qui permettront d'identifier le type de carbapénémase.

Conclusion

En conclusion, au cours de cette thèse, nous avons participé à (i) la compréhension des mécanismes d'action des carbapénèmases les plus fréquentes, (ii) au développement de nouvelles molécules thérapeutiques ainsi qu'au (iii) développement de nouveaux outils de diagnostics. Ces travaux peuvent donc s'inscrire dans le cadre des études participant à la lutte contre l'antibiorésistance. En France, ce phénomène est la cause de plus de 5 000 décès par an, selon une étude du Centre Européen de Prévention et Contrôle des Maladies.⁴¹⁷ A l'échelle mondiale, les résistances microbiennes seraient la cause de 700 000 morts par an. Si aucune mesure n'est entreprise, les maladies liées aux infectieuses bactériennes graves pourraient redevenir, en 2050, une des premières causes de mortalité dans le monde, en provoquant jusqu'à 10 millions de morts.⁴¹⁸ En plus des pertes humaines, ce phénomène est onéreux pour la société. Le coût financier est estimé à plus de 1,5 milliards d'euros en Europe et plus de 55 milliards de dollars aux Etats-Unis.⁴¹⁷ Il a été estimé que l'antibiorésistance pourrait coûter plus de 100 000 milliards de dollars d'ici 2050.⁴¹⁷ En 2015, l'OMS a mis en place le concept « *One Health* » permettant le regroupement de différents secteurs tels que la santé publique, la santé animale, et l'environnement pour lutter contre l'antibiorésistance. Ainsi, des mesures de surveillance et de contrôle des infections ont vu le jour. Cependant, la vigilance reste de rigueur car les gènes codant pour les carbapénèmases, situés principalement sur des éléments génétiques mobiles, ont démontré un potentiel exceptionnel de dissémination inter et intra-espèce.^{72,75,131,183,419} Nos résultats démontrent des capacités d'évolution importantes des enzymes en fonction des pressions de sélection antibiotique. De plus l'évolution constante des mouvements de population liée à la démocratisation des voyages mais aussi aux conflits politiques, et dans un futur plus ou moins proche au réchauffement climatique, conduisent à l'accentuation du phénomène de dissémination.

Références bibliographiques

1. Anon. Nauciel C, Vildé J-L. Bactériologie médicale. 2e édition. Masson; 2005. 272 p. Available at: <https://www.elsevier-masson.fr/bacteriologie-medicale-9782294018589.html>. Accessed April 19, 2018.
2. François D, Marie-Cécile P, biologiste MC, et al. Denis François et al. *Bactériologie médicale : techniques usuelles. 2e édition largement revue et actualisée. Issy-les-Moulineaux Elsevier Masson DL 2011; 2e édition largement revue et actualisée. Issy-les-Moulineaux: Elsevier Masson; 2011.*
3. Petruzzello-Pellegrini TN, Moslemi-Naeini M, Marsden PA. New insights into Shiga toxin-mediated endothelial dysfunction in hemolytic uremic syndrome. *Virulence* 2013; **4**: 556–63.
4. Wiles TJ, Kulesus RR, Mulvey MA. Origins and virulence mechanisms of uropathogenic *Escherichia coli*. *Experimental and Molecular Pathology* 2008; **85**: 11–9.
5. Tommasi R, Brown DG, Walkup GK, Manchester JI, Miller AA. ESKAPEing the labyrinth of antibacterial discovery. *Nat Rev Drug Discov* 2015; **14**: 529–42.
6. Nikaido H. Outer membrane barrier as a mechanism of antimicrobial resistance. *Antimicrobial Agents and Chemotherapy* 1989; **33**: 1831–6.
7. Nikaido H, Nikaido K, Harayama S. Identification and characterization of porins in *Pseudomonas aeruginosa*. *J Biol Chem* 1991; **266**: 770–9.
8. Goffin C, Ghuyssen J-M. Multimodular Penicillin-Binding Proteins: An Enigmatic Family of Orthologs and Paralogs. *MICROBIOL MOL BIOL REV* 1998; **62**: 15.
9. Frère J-M. Beta-lactamases and bacterial resistance to antibiotics. *Molecular Microbiology* 1995; **16**: 385–95.
10. Cava F, Lam H, de Pedro MA, Waldor MK. Emerging knowledge of regulatory roles of D-amino acids in bacteria. *Cell Mol Life Sci* 2011; **68**: 817–31.
11. Massova I, Mobashery S. Kinship and Diversification of Bacterial Penicillin-Binding Proteins and β -Lactamases. *ANTIMICROB AGENTS CHEMOTHER* 1998; **42**: 17.
12. Matagne A, Dubus A, Galleni M, Frère J-M. The β -lactamase cycle: a tale of selective pressure and bacterial ingenuity. : 19.
13. Procópio RE de L, Silva IR da, Martins MK, Azevedo JL de, Araújo JM de. Antibiotics produced by *Streptomyces*. *Braz J Infect Dis* 2012; **16**: 466–71.
14. Kardos N, Demain AL. Penicillin: the medicine with the greatest impact on therapeutic outcomes. *Applied Microbiology and Biotechnology* 2011; **92**: 677–87.
15. Mascaretti OA. Bacteria versus antibacterial agents : an integrated approach /. 2003.
16. Birnbaum J, Kahan FM, Kropp H, MacDonald JS. Carbapenems, a new class of beta-lactam antibiotics. Discovery and development of imipenem/cilastatin. *Am J Med* 1985; **78**: 3–21.
17. Zhanel GG, Wiebe R, Dilay L, et al. Comparative review of the carbapenems. *Drugs* 2007; **67**: 1027–52.
18. Papp-Wallace KM, Endimiani A, Taracila MA, Bonomo RA. Carbapenems: Past, Present, and Future. *Antimicrobial Agents and Chemotherapy* 2011; **55**: 4943–60.
19. Patel G, Bonomo RA. ‘Stormy waters ahead’: global emergence of carbapenemases. *Front Microbiol* 2013; **4**: 48.
20. Barber M. The present position of penicillin. *St Thomas Hosp Gaz* 1948; **46**: 162.
21. Zorzi W, Zhou XY, Dardenne O, et al. Structure of the low-affinity penicillin-binding protein 5 PBP5_{fm} in wild-type and highly penicillin-resistant strains of *Enterococcus faecium*. *Journal of Bacteriology* 1996; **178**: 4948–57.
22. Amin NE, Lund B, Tjernlund A, Lundberg C, Jalakas K, Wretling B. Mechanisms of resistance to imipenem in imipenem-resistant, ampicillin-sensitive *Enterococcus faecium*.

APMIS 2001; **109**: 791–7.

23. Sauvage E, Kerff F, Fonzé E, *et al.* The 2.4-Å crystal structure of the penicillin-resistant penicillin-binding protein PBP5fm from *Enterococcus faecium* in complex with benzylpenicillin. *Cellular and Molecular Life Sciences (CMLS)* 2002; **59**: 1223–32.

24. Lim D, Strynadka NCJ. Structural basis for the β lactam resistance of PBP2a from methicillin-resistant *Staphylococcus aureus*. *Nature Structural Biology* 2002. Available at: <http://www.nature.com/doi/10.1038/nsb858>. Accessed May 13, 2019.

25. Neuwirth C, Siébor E, Duez JM, Péchinot A, Kazmierczak A. Imipenem resistance in clinical isolates of *Proteus mirabilis* associated with alterations in penicillin-binding proteins. *J Antimicrob Chemother* 1995; **36**: 335–42.

26. García-Sureda L, Doménech-Sánchez A, Barbier M, Juan C, Gascó J, Albertí S. OmpK26, a Novel Porin Associated with Carbapenem Resistance in *Klebsiella pneumoniae*. *Antimicrobial Agents and Chemotherapy* 2011; **55**: 4742–7.

27. Wong JLC, Romano M, Kerry LE, *et al.* OmpK36-mediated Carbapenem resistance attenuates ST258 *Klebsiella pneumoniae* in vivo. *Nat Commun* 2019; **10**: 3957.

28. Li X-Z, Nikaido H. Efflux-mediated drug resistance in bacteria: an update. *Drugs* 2009; **69**: 1555–623.

29. Yılmaz Ç, Özcengiz G. Antibiotics: Pharmacokinetics, toxicity, resistance and multidrug efflux pumps. *Biochem Pharmacol* 2017; **133**: 43–62.

30. Wang Z, Fast W, Valentine AM, Benkovic SJ. Metallo-beta-lactamase: structure and mechanism. *Curr Opin Chem Biol* 1999; **3**: 614–22.

31. Suvorov M, Vakulenko SB, Mobashery S. Cytoplasmic-Membrane Anchoring of a Class A -Lactamase and Its Capacity in Manifesting Antibiotic Resistance. *Antimicrobial Agents and Chemotherapy* 2007; **51**: 2937–42.

32. Ghuyssen JM. Membrane topology, structure, and functions of the penicillin-interactive proteins. *Biotechnol Appl Biochem* 1990; **12**: 468–72.

33. Abraham EP, Chain E. An enzyme from bacteria able to destroy penicillin. 1940. *Rev Infect Dis* 1988; **10**: 677–8.

34. Ambler RP, Coulson AFW, Frère JM, *et al.* A standard numbering scheme for the class A β -lactamases. *Biochemical Journal* 1991; **276**: 269–70.

35. Cornaglia G, Giamarellou H, Rossolini GM. Metallo- β -lactamases: a last frontier for β -lactams? *Lancet Infect Dis* 2011; **11**: 381–93.

36. Poirel L, Naas T, Nordmann P. Diversity, epidemiology, and genetics of class D beta-lactamases. *Antimicrob Agents Chemother* 2010; **54**: 24–38.

37. Joris B, Ledent P, Fonzé E, *et al.* Comparison of the Sequences of Class A 1-Lactamases and of the Secondary Structure Elements of Penicillin-Recognizing Proteins. *ANTIMICROB AGENTS CHEMOTHER* 1991; **35**: 8.

38. Szarecka A, Lesnock KR, Ramirez-Mondragon CA, Nicholas HB, Wymore T. The Class D β -lactamase family: residues governing the maintenance and diversity of function. *Protein Eng Des Sel* 2011; **24**: 801–9.

39. Wommer S, Rival S, Heinz U, *et al.* Substrate-activated Zinc Binding of Metallo- β -lactamases: PHYSIOLOGICAL IMPORTANCE OF THE MONONUCLEAR ENZYMES. *Journal of Biological Chemistry* 2002; **277**: 24142–7.

40. Massidda O, Rossolini GM, SATTAt G. The *Aeromonas hydrophila* cphA Gene: Molecular Heterogeneity among Class B Metallo-3-Lactamases. *J BACTERIOL*: 7.

41. Bebrone C, Anne C, De Vriendt K, *et al.* Dramatic broadening of the substrate profile of the *Aeromonas hydrophila* CphA metallo-beta-lactamase by site-directed mutagenesis. *J Biol Chem* 2005; **280**: 28195–202.

42. Bellais S, Aubert D, Naas T, Nordmann P. *Chryseobacterium meningosepticum*. 2000; **44**: 9.

43. Boschi L, Mercuri PS, Riccio ML, *et al.* The Legionella (Fluoribacter) gormanii Metallo- β -Lactamase: a New Member of the Highly Divergent Lineage of Molecular-Subclass B3 β -Lactamases. *ANTIMICROB AGENTS CHEMOTHER* 2000; **44**: 6.
44. Lisa M-N, Palacios AR, Aitha M, *et al.* A general reaction mechanism for carbapenem hydrolysis by mononuclear and binuclear metallo- β -lactamases. *Nature Communications* 2017; **8**. Available at: <http://www.nature.com/articles/s41467-017-00601-9>. Accessed February 25, 2019.
45. Meini M-R, Llarrull LI, Vila AJ. Overcoming differences: The catalytic mechanism of metallo- β -lactamases. *FEBS Letters* 2015; **589**: 3419–32.
46. Grall N, Andremont A, Armand-Lefèvre L. Résistance aux carbapénèmes: vers une nouvelle impasse? */data/revues/22106545/v13i2/S2210654511000299/* 2011. Available at: <https://www.em-consulte.com/en/article/293790>. Accessed August 11, 2019.
47. Felici A, Amicosante G, Oratore A, *et al.* An overview of the kinetic parameters of class B beta-lactamases. *Biochem J* 1993; **291**: 151–5.
48. Yang YJ, Wu PJ, Livermore DM. Biochemical characterization of a beta-lactamase that hydrolyzes penems and carbapenems from two Serratia marcescens isolates. *Antimicrob Agents Chemother* 1990; **34**: 755–8.
49. Naas T, Vandell L, Sougakoff W, Livermore DM, Nordmann P. Cloning and sequence analysis of the gene for a carbapenem-hydrolyzing class A beta-lactamase, Sme-1, from Serratia marcescens S6. *Antimicrob Agents Chemother* 1994; **38**: 1262–70.
50. Rasmussen BA, Bush K, Keeney D, *et al.* Characterization of IMI-1 beta-lactamase, a class A carbapenem-hydrolyzing enzyme from Enterobacter cloacae. *Antimicrob Agents Chemother* 1996; **40**: 2080–6.
51. Poirel L, Pitout JD, Nordmann P. Carbapenemases: molecular diversity and clinical consequences. <http://dx.doi.org/10.2217/1746091325501> 2007. Available at: <https://www.futuremedicine.com/doi/abs/10.2217/17460913.2.5.501>. Accessed May 13, 2019.
52. Yu Y-S, Du X-X, Zhou Z-H, Chen Y-G, Li L-J. First Isolation of bla_{IMI-2} in an Enterobacter cloacae Clinical Isolate from China. *Antimicrobial Agents and Chemotherapy* 2006; **50**: 1610–1.
53. Rojo-Bezares B, Martín C, López M, Torres C, Sáenz Y. First Detection of bla_{IMI-2} Gene in a Clinical Escherichia coli Strain. *Antimicrobial Agents and Chemotherapy* 2012; **56**: 1146–7.
54. Nordmann P, Nicolas M-H. Biochemical Properties of a Carbapenem-Hydrolyzing β -Lactamase from Enterobacter cloacae and Cloning of the Gene into Escherichia coli. 1993; **37**: 8.
55. Rasmussen BA, Bush K, Keeney D, *et al.* Characterization of IMI-1 β -Lactamase, a Class A Carbapenem- Hydrolyzing Enzyme from Enterobacter cloacae. *ANTIMICROB AGENTS CHEMOTHER* 1996; **40**: 7.
56. Yang Y. Biochemical Characterization of a β -Lactamase That Hydrolyzes Penems and Carbapenems from Two Serratia marcescens Isolates. *ANTIMICROB AGENTS CHEMOTHER*: 4.
57. Henriques I, Moura A, Alves A, Saavedra MJ, Correia A. Molecular Characterization of a Carbapenem-Hydrolyzing Class A β -Lactamase, SFC-1, from Serratia fonticola UTAD54. *Antimicrobial Agents and Chemotherapy* 2004; **48**: 2321–4.
58. Mariotte-Boyer S, Nicolas-Chanoine MH, Labia R. A kinetic study of NMC-A β -lactamase, an Ambler class A carbapenemase also hydrolyzing cephamycins. *FEMS Microbiology Letters* 1996; **143**: 29–33.
59. Sougakoff W, L'Hermite G, Pernot L, *et al.* Structure of the imipenem-hydrolyzing class A β -lactamase SME-1 from Serratia marcescens. *Acta Cryst D* 2002; **58**: 267–74.
60. Majiduddin FK, Palzkill T. Amino Acid Sequence Requirements at Residues 69 and 238

- for the SME-1 β -Lactamase To Confer Resistance to β -Lactam Antibiotics. *Antimicrobial Agents and Chemotherapy* 2003; **47**: 1062–7.
61. Swarén P, Maveyraud L, Raquet X, *et al.* X-ray Analysis of the NMC-A β -Lactamase at 1.64-Å Resolution, a Class A Carbapenemase with Broad Substrate Specificity. *J Biol Chem* 1998; **273**: 26714–21.
62. Queenan AM, Bush K. Carbapenemases: the Versatile β -Lactamases. *Clin Microbiol Rev* 2007; **20**: 440–58.
63. Nordmann P, Carrer A. Les carbapénèmases des entérobactéries. *Archives de Pédiatrie* 2010; **17**: S154–62.
64. Poirel L, Weldhagen GF, Naas T, De Champs C, Dove MG, Nordmann P. GES-2, a class A beta-lactamase from *Pseudomonas aeruginosa* with increased hydrolysis of imipenem. *Antimicrob Agents Chemother* 2001; **45**: 2598–603.
65. Kotsakis SD, Miriagou V, Tzelepi E, Tzouveleki LS. Comparative biochemical and computational study of the role of naturally occurring mutations at Ambler positions 104 and 170 in GES β -lactamases. *Antimicrob Agents Chemother* 2010; **54**: 4864–71.
66. Moubareck C, Brémont S, Conroy M-C, Courvalin P, Lambert T. GES-11, a novel integron-associated GES variant in *Acinetobacter baumannii*. *Antimicrob Agents Chemother* 2009; **53**: 3579–81.
67. Poirel L, Brinas L, Verlinde A, Ide L, Nordmann P. BEL-1, a novel clavulanic acid-inhibited extended-spectrum beta-lactamase, and the class 1 integron In120 in *Pseudomonas aeruginosa*. *Antimicrob Agents Chemother* 2005; **49**: 3743–8.
68. Bonnin RA, Nordmann P, Potron A, Lecuyer H, Zahar J-R, Poirel L. Carbapenem-hydrolyzing GES-type extended-spectrum beta-lactamase in *Acinetobacter baumannii*. *Antimicrob Agents Chemother* 2011; **55**: 349–54.
69. Zhang F, Wang X, Xie L, *et al.* A novel transposon, Tn6306, mediates the spread of bla_{IMI} in Enterobacteriaceae in hospitals. *Int J Infect Dis* 2017; **65**: 22–6.
70. Naas T, Poirel L, Nordmann P. Minor extended-spectrum beta-lactamases. *Clin Microbiol Infect* 2008; **14 Suppl 1**: 42–52.
71. Nordmann P, Poirel L. Emerging carbapenemases in Gram-negative aerobes. *Clinical Microbiology and Infection* 2002; **8**: 321–31.
72. Nordmann P, Cuzon G, Naas T. The real threat of *Klebsiella pneumoniae* carbapenemase-producing bacteria. *The Lancet Infectious Diseases* 2009; **9**: 228–36.
73. Yigit H, Queenan AM, Anderson GJ, *et al.* Novel Carbapenem-Hydrolyzing β -Lactamase, KPC-1, from a Carbapenem-Resistant Strain of *Klebsiella pneumoniae*. *Antimicrob Agents Chemother* 2001; **45**: 1151–61.
74. Cuzon G, Naas T, Nordmann P. Carbapénèmases de type KPC : quel enjeu en microbiologie clinique ? *Pathologie Biologie* 2010; **58**: 39–45.
75. Naas T, Cuzon G, Villegas M-V, Lartigue M-F, Quinn JP, Nordmann P. Genetic Structures at the Origin of Acquisition of the β -Lactamase bla_{KPC} Gene. *Antimicrobial Agents and Chemotherapy* 2008; **52**: 1257–63.
76. Cuzon G, Naas T, Truong H, *et al.* Worldwide Diversity of *Klebsiella pneumoniae* That Produce β -Lactamase bla_{KPC-2} Gene1. *Emerging Infectious Diseases* 2010; **16**: 1349–56.
77. Bratu S, Landman D, Haag R, *et al.* Rapid Spread of Carbapenem-Resistant *Klebsiella pneumoniae* in New York City: A New Threat to Our Antibiotic Armamentarium. *Arch Intern Med* 2005; **165**: 1430–5.
78. Woodford N, Tierno PM, Young K, *et al.* Outbreak of *Klebsiella pneumoniae* producing a new carbapenem-hydrolyzing class A beta-lactamase, KPC-3, in a New York Medical Center. *Antimicrob Agents Chemother* 2004; **48**: 4793–9.
79. Bratu S, Landman D, Alam M, Tolentino E, Quale J. Detection of KPC carbapenem-hydrolyzing enzymes in *Enterobacter* spp. from Brooklyn, New York. *Antimicrob Agents*

Chemother 2005; **49**: 776–8.

80. Giakkoupi P, Papagiannitsis CC, Miriagou V, *et al.* An update of the evolving epidemic of blaKPC-2-carrying *Klebsiella pneumoniae* in Greece (2009-10). *J Antimicrob Chemother* 2011; **66**: 1510–3.

81. Chen L, Mathema B, Chavda KD, DeLeo FR, Bonomo RA, Kreiswirth BN. Carbapenemase-producing *Klebsiella pneumoniae*: molecular and genetic decoding. *Trends in Microbiology* 2014; **22**: 686–96.

82. Lee C-R, Lee JH, Park KS, Kim YB, Jeong BC, Lee SH. Global Dissemination of Carbapenemase-Producing *Klebsiella pneumoniae*: Epidemiology, Genetic Context, Treatment Options, and Detection Methods. *Front Microbiol* 2016; **7**. Available at: <http://www.frontiersin.org/articles/10.3389/fmicb.2016.00895/full>. Accessed January 11, 2019.

83. Mathers AJ, Peirano G, Pitout JDD. The role of epidemic resistance plasmids and international high-risk clones in the spread of multidrug-resistant Enterobacteriaceae. *Clin Microbiol Rev* 2015; **28**: 565–91.

84. García-Fernández A, Villa L, Carta C, *et al.* *Klebsiella pneumoniae* ST258 producing KPC-3 identified in Italy carries novel plasmids and OmpK36/OmpK35 porin variants. *Antimicrob Agents Chemother* 2012; **56**: 2143–5.

85. Chen L, Chavda KD, Melano RG, *et al.* Comparative genomic analysis of KPC-encoding pKpQIL-like plasmids and their distribution in New Jersey and New York Hospitals. *Antimicrob Agents Chemother* 2014; **58**: 2871–7.

86. Pitout JDD, Nordmann P, Poirel L. Carbapenemase-Producing *Klebsiella pneumoniae*, a Key Pathogen Set for Global Nosocomial Dominance. *Antimicrob Agents Chemother* 2015; **59**: 5873–84.

87. Leavitt A, Chmelnitsky I, Carmeli Y, Navon-Venezia S. Complete nucleotide sequence of KPC-3-encoding plasmid pKpQIL in the epidemic *Klebsiella pneumoniae* sequence type 258. *Antimicrob Agents Chemother* 2010; **54**: 4493–6.

88. Roth AL, Kurpiel PM, Lister PD, Hanson ND. bla(KPC) RNA expression correlates with two transcriptional start sites but not always with gene copy number in four genera of Gram-negative pathogens. *Antimicrob Agents Chemother* 2011; **55**: 3936–8.

89. Munoz-Price LS, Poirel L, Bonomo RA, *et al.* Clinical epidemiology of the global expansion of *Klebsiella pneumoniae* carbapenemases. *Lancet Infect Dis* 2013; **13**: 785–96.

90. Palzkill T. Structural and Mechanistic Basis for Extended-Spectrum Drug-Resistance Mutations in Altering the Specificity of TEM, CTX-M, and KPC β -lactamases. *Front Mol Biosci* 2018; **5**: 16.

91. Naas T, Dortet L, Iorga BI. Structural and Functional Aspects of Class A Carbapenemases. *Curr Drug Targets* 2016; **17**: 1006–28.

92. Levitt PS, Papp-Wallace KM, Taracila MA, *et al.* Exploring the Role of a Conserved Class A Residue in the Ω -Loop of KPC-2 β -Lactamase: A MECHANISM FOR CEFTAZIDIME HYDROLYSIS. *Journal of Biological Chemistry* 2012; **287**: 31783–93.

93. Mehta SC, Rice K, Palzkill T. Natural Variants of the KPC-2 Carbapenemase have Evolved Increased Catalytic Efficiency for Ceftazidime Hydrolysis at the Cost of Enzyme Stability Bonomo R, ed. *PLOS Pathogens* 2015; **11**: e1004949.

94. Ke W, Bethel CR, Thomson JM, Bonomo RA, van den Akker F. Crystal Structure of KPC-2: Insights into Carbapenemase Activity in Class A β -Lactamases. *Biochemistry* 2007; **46**: 5732–40.

95. Papp-Wallace KM, Taracila M, Hornick JM, *et al.* Substrate Selectivity and a Novel Role in Inhibitor Discrimination by Residue 237 in the KPC-2 β -Lactamase. *Antimicrob Agents Chemother* 2010; **54**: 2867–77.

96. Levitt PS, Papp-Wallace KM, Taracila MA, *et al.* Exploring the Role of a Conserved Class

- A Residue in the Ω -Loop of KPC-2 β -Lactamase: A MECHANISM FOR CEFTAZIDIME HYDROLYSIS. *Journal of Biological Chemistry* 2012; **287**: 31783–93.
97. Hussein K, Sprecher H, Mashiach T, Oren I, Kassis I, Finkelstein R. Carbapenem resistance among *Klebsiella pneumoniae* isolates: risk factors, molecular characteristics, and susceptibility patterns. *Infect Control Hosp Epidemiol* 2009; **30**: 666–71.
98. Urban C, Bradford PA, Tuckman M, *et al.* Carbapenem-resistant *Escherichia coli* harboring *Klebsiella pneumoniae* carbapenemase beta-lactamases associated with long-term care facilities. *Clin Infect Dis* 2008; **46**: e127-130.
99. Endimiani A, Depasquale JM, Forero S, *et al.* Emergence of blaKPC-containing *Klebsiella pneumoniae* in a long-term acute care hospital: a new challenge to our healthcare system. *J Antimicrob Chemother* 2009; **64**: 1102–10.
100. Patel G, Huprikar S, Factor SH, Jenkins SG, Calfee DP. Outcomes of Carbapenem-Resistant *Klebsiella pneumoniae* Infection and the Impact of Antimicrobial and Adjunctive Therapies. *Infection Control & Hospital Epidemiology* 2008; **29**: 1099–106.
101. Daly MW, Riddle DJ, Ledebner NA, Dunne WM, Ritchie DJ. Tigecycline for treatment of pneumonia and empyema caused by carbapenemase-producing *Klebsiella pneumoniae*. *Pharmacotherapy* 2007; **27**: 1052–7.
102. Watanabe M, Iyobe S, Inoue M, Mitsuhashi S. Transferable imipenem resistance in *Pseudomonas aeruginosa*. *Antimicrob Agents Chemother* 1991; **35**: 147–51.
103. Osano E, Arakawa Y, Wacharotayankun R, *et al.* Molecular characterization of an enterobacterial metallo beta-lactamase found in a clinical isolate of *Serratia marcescens* that shows imipenem resistance. *Antimicrob Agents Chemother* 1994; **38**: 71–8.
104. Hirakata Y, Izumikawa K, Yamaguchi T, *et al.* Rapid detection and evaluation of clinical characteristics of emerging multiple-drug-resistant gram-negative rods carrying the metallo-beta-lactamase gene blaIMP. *Antimicrob Agents Chemother* 1998; **42**: 2006–11.
105. Lincopan N, McCulloch JA, Reinert C, Cassettari VC, Gales AC, Mamizuka EM. First isolation of metallo-beta-lactamase-producing multiresistant *Klebsiella pneumoniae* from a patient in Brazil. *J Clin Microbiol* 2005; **43**: 516–9.
106. Muratani T, Kobayashi T, Matsumoto T. Emergence and prevalence of beta-lactamase-producing *Klebsiella pneumoniae* resistant to cepheims in Japan. *Int J Antimicrob Agents* 2006; **27**: 491–9.
107. Shiroto K, Ishii Y, Kimura S, *et al.* Metallo-beta-lactamase IMP-1 in *Providencia rettgeri* from two different hospitals in Japan. *J Med Microbiol* 2005; **54**: 1065–70.
108. Biendo M, Canarelli B, Thomas D, *et al.* Successive emergence of extended-spectrum beta-lactamase-producing and carbapenemase-producing *Enterobacter aerogenes* isolates in a university hospital. *J Clin Microbiol* 2008; **46**: 1037–44.
109. Riccio ML, Franceschini N, Boschi L, *et al.* Characterization of the metallo-beta-lactamase determinant of *Acinetobacter baumannii* AC-54/97 reveals the existence of bla(IMP) allelic variants carried by gene cassettes of different phylogeny. *Antimicrob Agents Chemother* 2000; **44**: 1229–35.
110. Tysall L, Stockdale MW, Chadwick PR, *et al.* IMP-1 carbapenemase detected in an *Acinetobacter* clinical isolate from the UK. *J Antimicrob Chemother* 2002; **49**: 217–8.
111. Yamamoto M, Nagao M, Hotta G, *et al.* Molecular characterization of IMP-type metallo- β -lactamases among multidrug-resistant *Achromobacter xylosoxidans*. *J Antimicrob Chemother* 2012; **67**: 2110–3.
112. Chen L-R, Zhou H-W, Cai J-C, Zhang R, Chen G-X. Combination of IMP-4 metallo-beta-lactamase production and porin deficiency causes carbapenem resistance in a *Klebsiella oxytoca* clinical isolate. *Diagn Microbiol Infect Dis* 2009; **65**: 163–7.
113. Bonomo RA, Burd EM, Conly J, *et al.* Carbapenemase-Producing Organisms: A Global Scourge. *Clin Infect Dis* 2018; **66**: 1290–7.

114. Pournaras S, Köck R, Mossialos D, *et al.* Detection of a phylogenetically distinct IMP-type metallo- β -lactamase, IMP-35, in a CC235 *Pseudomonas aeruginosa* from the Dutch-German border region (Euregio). *J Antimicrob Chemother* 2013; **68**: 1271–6.
115. Shet V, Gouliouris T, Brown NM, Turton JF, Zhang J, Woodford N. IMP metallo- β -lactamase-producing clinical isolates of *Enterobacter cloacae* in the UK. *J Antimicrob Chemother* 2011; **66**: 1408–9.
116. Jeannot K, Poirel L, Robert-Nicoud M, Cholley P, Nordmann P, Plésiat P. IMP-29, a novel IMP-type metallo- β -lactamase in *Pseudomonas aeruginosa*. *Antimicrob Agents Chemother* 2012; **56**: 2187–90.
117. Polotto M, Casella T, de Lucca Oliveira MG, *et al.* Detection of *P. aeruginosa* harboring bla CTX-M-2, bla GES-1 and bla GES-5, bla IMP-1 and bla SPM-1 causing infections in Brazilian tertiary-care hospital. *BMC Infect Dis* 2012; **12**: 176.
118. Gibb AP, Tribuddharat C, Moore RA, *et al.* Nosocomial outbreak of carbapenem-resistant *Pseudomonas aeruginosa* with a new bla(IMP) allele, bla(IMP-7). *Antimicrob Agents Chemother* 2002; **46**: 255–8.
119. Limbago BM, Rasheed JK, Anderson KF, *et al.* IMP-producing carbapenem-resistant *Klebsiella pneumoniae* in the United States. *J Clin Microbiol* 2011; **49**: 4239–45.
120. Peleg AY, Franklin C, Bell JM, Spelman DW. Dissemination of the metallo-beta-lactamase gene blaIMP-4 among gram-negative pathogens in a clinical setting in Australia. *Clin Infect Dis* 2005; **41**: 1549–56.
121. Sekyere JO, Govinden U, Essack S. The Molecular Epidemiology and Genetic Environment of Carbapenemases Detected in Africa. *Microb Drug Resist* 2016; **22**: 59–68.
122. Pagani L, Colinin C, Migliavacca R, *et al.* Nosocomial outbreak caused by multidrug-resistant *Pseudomonas aeruginosa* producing IMP-13 metallo-beta-lactamase. *J Clin Microbiol* 2005; **43**: 3824–8.
123. Lauretti L, Riccio ML, Mazzariol A, *et al.* Cloning and characterization of blaVIM, a new integron-borne metallo-beta-lactamase gene from a *Pseudomonas aeruginosa* clinical isolate. *Antimicrob Agents Chemother* 1999; **43**: 1584–90.
124. Poirel L, Naas T, Nicolas D, *et al.* Characterization of VIM-2, a carbapenem-hydrolyzing metallo-beta-lactamase and its plasmid- and integron-borne gene from a *Pseudomonas aeruginosa* clinical isolate in France. *Antimicrob Agents Chemother* 2000; **44**: 891–7.
125. Yum JH, Yi K, Lee H, *et al.* Molecular characterization of metallo-beta-lactamase-producing *Acinetobacter baumannii* and *Acinetobacter* genomospecies 3 from Korea: identification of two new integrons carrying the bla(VIM-2) gene cassettes. *J Antimicrob Chemother* 2002; **49**: 837–40.
126. Tsakris A, Poulou A, Markou F, *et al.* Dissemination of clinical isolates of *Klebsiella oxytoca* harboring CMY-31, VIM-1, and a New OXY-2-type variant in the community. *Antimicrob Agents Chemother* 2011; **55**: 3164–8.
127. Sianou E, Kristo I, Petridis M, *et al.* A cautionary case of microbial solidarity: concurrent isolation of VIM-1-producing *Klebsiella pneumoniae*, *Escherichia coli* and *Enterobacter cloacae* from an infected wound. *J Antimicrob Chemother* 2012; **67**: 244–6.
128. Galani I, Souli M, Koratzanis E, Koratzanis G, Chryssouli Z, Giamarellou H. Emerging bacterial pathogens: *Escherichia coli*, *Enterobacter aerogenes* and *Proteus mirabilis* clinical isolates harbouring the same transferable plasmid coding for metallo-beta-lactamase VIM-1 in Greece. *J Antimicrob Chemother* 2007; **59**: 578–9.
129. Miriagou V, Tzouvelekis LS, Flevari K, Tsakiri M, Douzinas EE. *Providencia stuartii* with VIM-1 metallo-beta-lactamase. *J Antimicrob Chemother* 2007; **60**: 183–4.
130. Nastro M, Monge R, Zintgraff J, *et al.* First nosocomial outbreak of VIM-16-producing *Serratia marcescens* in Argentina. *Clin Microbiol Infect* 2013; **19**: 617–9.
131. Nordmann P, Dortet L, Poirel L. Carbapenem resistance in Enterobacteriaceae: here is the

- storm! *Trends in Molecular Medicine* 2012; **18**: 263–72.
132. Loli A, Tzouveleki LS, Gianneli D, Tzelepi E, Miriagou V. Outbreak of *Acinetobacter baumannii* with chromosomally encoded VIM-1 undetectable by imipenem-EDTA synergy tests. *Antimicrob Agents Chemother* 2008; **52**: 1894–6.
133. Zioga A, Miriagou V, Tzelepi E, *et al.* The ongoing challenge of acquired carbapenemases: a hospital outbreak of *Klebsiella pneumoniae* simultaneously producing VIM-1 and KPC-2. *Int J Antimicrob Agents* 2010; **36**: 190–1.
134. Sánchez-Romero I, Asensio A, Oteo J, *et al.* Nosocomial outbreak of VIM-1-producing *Klebsiella pneumoniae* isolates of multilocus sequence type 15: molecular basis, clinical risk factors, and outcome. *Antimicrob Agents Chemother* 2012; **56**: 420–7.
135. Toleman MA, Simm AM, Murphy TA, *et al.* Molecular characterization of SPM-1, a novel metallo-beta-lactamase isolated in Latin America: report from the SENTRY antimicrobial surveillance programme. *J Antimicrob Chemother* 2002; **50**: 673–9.
136. Zavascki AP, Gaspareto PB, Martins AF, Gonçalves AL, Barth AL. Outbreak of carbapenem-resistant *Pseudomonas aeruginosa* producing SPM-1 metallo- β -lactamase in a teaching hospital in southern Brazil. *J Antimicrob Chemother* 2005; **56**: 1148–51.
137. Gales AC, Menezes LC, Silbert S, Sader HS. Dissemination in distinct Brazilian regions of an epidemic carbapenem-resistant *Pseudomonas aeruginosa* producing SPM metallo-beta-lactamase. *J Antimicrob Chemother* 2003; **52**: 699–702.
138. Castanheira M, Toleman MA, Jones RN, Schmidt FJ, Walsh TR. Molecular characterization of a beta-lactamase gene, blaGIM-1, encoding a new subclass of metallo-beta-lactamase. *Antimicrob Agents Chemother* 2004; **48**: 4654–61.
139. Yong D, Toleman MA, Bell J, *et al.* Genetic and biochemical characterization of an acquired subgroup B3 metallo- β -lactamase gene, blaAIM-1, and its unique genetic context in *Pseudomonas aeruginosa* from Australia. *Antimicrob Agents Chemother* 2012; **56**: 6154–9.
140. Poirel L, Rodríguez-Martínez J-M, Al Naiemi N, Debets-Ossenkopp YJ, Nordmann P. Characterization of DIM-1, an integron-encoded metallo-beta-lactamase from a *Pseudomonas stutzeri* clinical isolate in the Netherlands. *Antimicrob Agents Chemother* 2010; **54**: 2420–4.
141. Wachino J, Yoshida H, Yamane K, *et al.* SMB-1, a novel subclass B3 metallo-beta-lactamase, associated with ISCR1 and a class 1 integron, from a carbapenem-resistant *Serratia marcescens* clinical isolate. *Antimicrob Agents Chemother* 2011; **55**: 5143–9.
142. Pollini S, Maradei S, Pecile P, *et al.* FIM-1, a new acquired metallo- β -lactamase from a *Pseudomonas aeruginosa* clinical isolate from Italy. *Antimicrob Agents Chemother* 2013; **57**: 410–6.
143. Lange F, Pfennigwerth N, Hartl R, *et al.* LMB-1, a novel family of class B3 MBLs from an isolate of *Enterobacter cloacae*. *J Antimicrob Chemother* 2018; **73**: 2331–5.
144. Dabos ML, Rodriguez CH, Nastro M, Famiglietti A, Iorga BI, Naas T. Lmb-1, a novel B3 MBL and CMY-150, a novel CMY-2 variant from *Citrobacter freundii* from Argentina-ECCMID Congress. In: , 2018.
145. El Salabi A, Borra PS, Toleman MA, Samuelsen Ø, Walsh TR. Genetic and biochemical characterization of a novel metallo- β -lactamase, TMB-1, from an *Achromobacter xylosoxidans* strain isolated in Tripoli, Libya. *Antimicrob Agents Chemother* 2012; **56**: 2241–5.
146. Sekiguchi J, Morita K, Kitao T, *et al.* KHM-1, a novel plasmid-mediated metallo-beta-lactamase from a *Citrobacter freundii* clinical isolate. *Antimicrob Agents Chemother* 2008; **52**: 4194–7.
147. Boyd DA, Lisboa LF, Rennie R, Zhanel GG, Dingle TC, Mulvey MR. Identification of a novel metallo- β -lactamase, CAM-1, in clinical *Pseudomonas aeruginosa* isolates from Canada. *J Antimicrob Chemother* 2019; **74**: 1563–7.
148. Mojica MF, Bonomo RA, Fast W. B1-Metallo-beta-Lactamases: Where do we stand? *Curr Drug Targets* 2016; **17**: 1029–50.

149. Yong D, Toleman MA, Giske CG, *et al.* Characterization of a New Metallo-β-Lactamase Gene, blaNDM-1, and a Novel Erythromycin Esterase Gene Carried on a Unique Genetic Structure in *Klebsiella pneumoniae* Sequence Type 14 from India. *Antimicrobial Agents and Chemotherapy* 2009; **53**: 5046–54.
150. Kumarasamy KK, Toleman MA, Walsh TR, *et al.* Emergence of a new antibiotic resistance mechanism in India, Pakistan, and the UK: a molecular, biological, and epidemiological study. *Lancet Infect Dis* 2010; **10**: 597–602.
151. Walsh TR, Weeks J, Livermore DM, Toleman MA. Dissemination of NDM-1 positive bacteria in the New Delhi environment and its implications for human health: an environmental point prevalence study. *The Lancet Infectious Diseases* 2011; **11**: 355–62.
152. Savard P, Gopinath R, Zhu W, *et al.* First NDM-positive *Salmonella* sp. strain identified in the United States. *Antimicrob Agents Chemother* 2011; **55**: 5957–8.
153. Darley E, Weeks J, Jones L, *et al.* NDM-1 polymicrobial infections including *Vibrio cholerae*. *Lancet* 2012; **380**: 1358.
154. Livermore DM, Walsh TR, Toleman M, Woodford N. Balkan NDM-1: escape or transplant? *Lancet Infect Dis* 2011; **11**: 164.
155. Khan AU, Maryam L, Zarrilli R. Structure, Genetics and Worldwide Spread of New Delhi Metallo-β-lactamase (NDM): a threat to public health. *BMC Microbiology* 2017; **17**: 101.
156. Bonnin RA, Poirel L, Nordmann P. New Delhi metallo-β-lactamase-producing *Acinetobacter baumannii*: a novel paradigm for spreading antibiotic resistance genes. *Future Microbiol* 2014; **9**: 33–41.
157. Dortet L, Nordmann P, Poirel L. Association of the emerging carbapenemase NDM-1 with a bleomycin resistance protein in Enterobacteriaceae and *Acinetobacter baumannii*. *Antimicrob Agents Chemother* 2012; **56**: 1693–7.
158. Nordmann P, Poirel L, Walsh TR, Livermore DM. The emerging NDM carbapenemases. *Trends in Microbiology* 2011; **19**: 588–95.
159. Cheng Z, Thomas PW, Ju L, *et al.* Evolution of New Delhi metallo-β-lactamase (NDM) in the clinic: Effects of NDM mutations on stability, zinc affinity, and mono-zinc activity. *J Biol Chem* 2018; **293**: 12606–18.
160. Zhang H, Hao Q. Crystal structure of NDM-1 reveals a common β-lactam hydrolysis mechanism. *FASEB J* 2011; **25**: 2574–82.
161. Chiou J, Leung TY-C, Chen S. Molecular mechanisms of substrate recognition and specificity of New Delhi metallo-β-lactamase. *Antimicrob Agents Chemother* 2014; **58**: 5372–8.
162. Oelschlaeger P, Pleiss J. Hydroxyl groups in the betabeta sandwich of metallo-beta-lactamases favor enzyme activity: Tyr218 and Ser262 pull down the lid. *J Mol Biol* 2007; **366**: 316–29.
163. Barguigua A, El Otmani F, Lakbakbi El Yaagoubi F, Talmi M, Zerouali K, Timinouni M. First report of a *Klebsiella pneumoniae* strain coproducing NDM-1, VIM-1 and OXA-48 carbapenemases isolated in Morocco. *APMIS* 2013; **121**: 675–7.
164. Dolejska M, Villa L, Poirel L, Nordmann P, Carattoli A. Complete sequencing of an IncHI1 plasmid encoding the carbapenemase NDM-1, the ArmA 16S RNA methylase and a resistance-nodulation-cell division/multidrug efflux pump. *Journal of Antimicrobial Chemotherapy* 2013; **68**: 34–9.
165. Poirel L, Ros A, Carricajo A, *et al.* Extremely drug-resistant *Citrobacter freundii* isolate producing NDM-1 and other carbapenemases identified in a patient returning from India. *Antimicrob Agents Chemother* 2011; **55**: 447–8.
166. Samuelsen Ø, Naseer U, Karah N, *et al.* Identification of Enterobacteriaceae isolates with OXA-48 and coproduction of OXA-181 and NDM-1 in Norway. *J Antimicrob Chemother* 2013; **68**: 1682–5.

167. Berçot B, Poirel L, Dortet L, Nordmann P. In vitro evaluation of antibiotic synergy for NDM-1-producing Enterobacteriaceae. *J Antimicrob Chemother* 2011; **66**: 2295–7.
168. Bush K, Jacoby GA. Updated functional classification of beta-lactamases. *Antimicrob Agents Chemother* 2010; **54**: 969–76.
169. Afzal-Shah M, Villar HE, Livermore DM. Biochemical characteristics of a carbapenemase from an *Acinetobacter baumannii* isolate collected in Buenos Aires, Argentina. *J Antimicrob Chemother* 1999; **43**: 127–31.
170. Mugnier PD, Poirel L, Naas T, Nordmann P. Worldwide dissemination of the blaOXA-23 carbapenemase gene of *Acinetobacter baumannii*. *Emerging Infect Dis* 2010; **16**: 35–40.
171. Wang XD, Cai JC, Zhou HW, Zhang R, Chen G-X. Reduced susceptibility to carbapenems in *Klebsiella pneumoniae* clinical isolates associated with plasmid-mediated beta-lactamase production and OmpK36 porin deficiency. *J Med Microbiol* 2009; **58**: 1196–202.
172. Saule M, Samuelsen Ø, Dumpis U, *et al.* Dissemination of a carbapenem-resistant *Acinetobacter baumannii* strain belonging to international clone II/sequence type 2 and harboring a novel AbaR4-like resistance island in Latvia. *Antimicrob Agents Chemother* 2013; **57**: 1069–72.
173. Zarrilli R, Di Popolo A, Bagattini M, *et al.* Clonal spread and patient risk factors for acquisition of extensively drug-resistant *Acinetobacter baumannii* in a neonatal intensive care unit in Italy. *J Hosp Infect* 2012; **82**: 260–5.
174. Bonnet R, Marchandin H, Chanal C, *et al.* Chromosome-encoded class D beta-lactamase OXA-23 in *Proteus mirabilis*. *Antimicrob Agents Chemother* 2002; **46**: 2004–6.
175. Poirel L, Héritier C, Tolün V, Nordmann P. Emergence of oxacillinase-mediated resistance to imipenem in *Klebsiella pneumoniae*. *Antimicrob Agents Chemother* 2004; **48**: 15–22.
176. Potron A, Poirel L, Nordmann P. Origin of OXA-181, an emerging carbapenem-hydrolyzing oxacillinase, as a chromosomal gene in *Shewanella xiamenensis*. *Antimicrob Agents Chemother* 2011; **55**: 4405–7.
177. Poirel L, Héritier C, Nordmann P. Chromosome-encoded ambler class D beta-lactamase of *Shewanella oneidensis* as a progenitor of carbapenem-hydrolyzing oxacillinase. *Antimicrob Agents Chemother* 2004; **48**: 348–51.
178. Jousset AB, Dabos L, Bonnin RA, *et al.* CTX-M-15-Producing *Shewanella* Species Clinical Isolate Expressing OXA-535, a Chromosome-Encoded OXA-48 Variant, Putative Progenitor of the Plasmid-Encoded OXA-436. *Antimicrob Agents Chemother* 2018; **62**.
179. Aktaş Z, Kayacan CB, Schneider I, Can B, Midilli K, Bauernfeind A. Carbapenem-hydrolyzing oxacillinase, OXA-48, persists in *Klebsiella pneumoniae* in Istanbul, Turkey. *Chemotherapy* 2008; **54**: 101–6.
180. Cuzon G, Naas T, Bogaerts P, Glupczynski Y, Huang T-D, Nordmann P. Plasmid-encoded carbapenem-hydrolyzing beta-lactamase OXA-48 in an imipenem-susceptible *Klebsiella pneumoniae* strain from Belgium. *Antimicrob Agents Chemother* 2008; **52**: 3463–4.
181. Cuzon G, Naas T, Lesenne A, Benhamou M, Nordmann P. Plasmid-mediated carbapenem-hydrolysing OXA-48 beta-lactamase in *Klebsiella pneumoniae* from Tunisia. *Int J Antimicrob Agents* 2010; **36**: 91–3.
182. Carrër A, Poirel L, Eraksoy H, Cagatay AA, Badur S, Nordmann P. Spread of OXA-48-positive carbapenem-resistant *Klebsiella pneumoniae* isolates in Istanbul, Turkey. *Antimicrob Agents Chemother* 2008; **52**: 2950–4.
183. Poirel L, Potron A, Nordmann P. OXA-48-like carbapenemases: the phantom menace. *J Antimicrob Chemother* 2012; **67**: 1597–606.
184. Nordmann P, Poirel L. The difficult-to-control spread of carbapenemase producers among Enterobacteriaceae worldwide. *Clin Microbiol Infect* 2014; **20**: 821–30.
185. Lixandru BE, Cotar AI, Straut M, *et al.* Carbapenemase-Producing *Klebsiella pneumoniae* in Romania: A Six-Month Survey. *PLoS ONE* 2015; **10**: e0143214.

186. Fursova NK, Astashkin EI, Knyazeva AI, *et al.* The spread of bla OXA-48 and bla OXA-244 carbapenemase genes among Klebsiella pneumoniae, Proteus mirabilis and Enterobacter spp. isolated in Moscow, Russia. *Ann Clin Microbiol Antimicrob* 2015; **14**: 46.
187. Potron A, Poirel L, Nordmann P. Derepressed transfer properties leading to the efficient spread of the plasmid encoding carbapenemase OXA-48. *Antimicrob Agents Chemother* 2014; **58**: 467–71.
188. Kumar S, Stecher G, Tamura K. MEGA7: Molecular Evolutionary Genetics Analysis Version 7.0 for Bigger Datasets. *Mol Biol Evol* 2016; **33**: 1870–4.
189. Dabos L, Bogaerts P, Peyrat A, *et al.* OXA-517, an extended-spectrum cephalosporin- and carbapenem-hydrolysing OXA-48-like variant - ECCMID congress. In: Vol P0234., 2017.
190. Naas T, Oueslati S, Bonnin RA, *et al.* Beta-lactamase database (BLDB) – structure and function. *Journal of Enzyme Inhibition and Medicinal Chemistry* 2017; **32**: 917–9.
191. Potron A, Nordmann P, Lafeuille E, Al Maskari Z, Al Rashdi F, Poirel L. Characterization of OXA-181, a carbapenem-hydrolyzing class D beta-lactamase from Klebsiella pneumoniae. *Antimicrob Agents Chemother* 2011; **55**: 4896–9.
192. Docquier J-D, Calderone V, De Luca F, *et al.* Crystal structure of the OXA-48 beta-lactamase reveals mechanistic diversity among class D carbapenemases. *Chem Biol* 2009; **16**: 540–7.
193. Dabos L, Bogaerts P, Bonnin RA, *et al.* Genetic and Biochemical Characterization of OXA-519, a Novel OXA-48-Like β -Lactamase. *Antimicrob Agents Chemother* 2018; **62**.
194. Potron A, Rondinaud E, Poirel L, *et al.* Genetic and biochemical characterisation of OXA-232, a carbapenem-hydrolysing class D β -lactamase from Enterobacteriaceae. *Int J Antimicrob Agents* 2013; **41**: 325–9.
195. Kasap M, Torol S, Kolayli F, Dundar D, Vahaboglu H. OXA-162, a novel variant of OXA-48 displays extended hydrolytic activity towards imipenem, meropenem and doripenem. *J Enzyme Inhib Med Chem* 2013; **28**: 990–6.
196. Oteo J, Hernández JM, Espasa M, *et al.* Emergence of OXA-48-producing Klebsiella pneumoniae and the novel carbapenemases OXA-244 and OXA-245 in Spain. *J Antimicrob Chemother* 2013; **68**: 317–21.
197. Dortet L, Oueslati S, Jeannot K, Tandé D, Naas T, Nordmann P. Genetic and Biochemical Characterization of OXA-405, an OXA-48-Type Extended-Spectrum β -Lactamase without Significant Carbapenemase Activity. *Antimicrob Agents Chemother* 2015; **59**: 3823–8.
198. Gomez S, Pasteran F, Faccone D, *et al.* Inpatient emergence of OXA-247: a novel carbapenemase found in a patient previously infected with OXA-163-producing Klebsiella pneumoniae. *Clin Microbiol Infect* 2013; **19**: E233–235.
199. Dabos L, Jousset AB, Bonnin RA, *et al.* Genetic and Biochemical Characterization of OXA-535, a Distantly Related OXA-48-Like β -Lactamase. *Antimicrob Agents Chemother* 2018; **62**.
200. Gülmez D, Woodford N, Palepou M-FI, *et al.* Carbapenem-resistant Escherichia coli and Klebsiella pneumoniae isolates from Turkey with OXA-48-like carbapenemases and outer membrane protein loss. *Int J Antimicrob Agents* 2008; **31**: 523–6.
201. Carrër A, Poirel L, Yilmaz M, *et al.* Spread of OXA-48-encoding plasmid in Turkey and beyond. *Antimicrob Agents Chemother* 2010; **54**: 1369–73.
202. Poirel L, Bonnin RA, Nordmann P. Genetic features of the widespread plasmid coding for the carbapenemase OXA-48. *Antimicrob Agents Chemother* 2012; **56**: 559–62.
203. Potel C, Ortega A, Martínez-Lamas L, Bautista V, Regueiro B, Oteo J. Interspecies Transmission of the blaOXA-48 Gene from a Klebsiella pneumoniae High-Risk Clone of Sequence Type 147 to Different Escherichia coli Clones in the Gut Microbiota. *Antimicrob Agents Chemother* 2018; **62**.
204. Aubert D, Naas T, Héritier C, Poirel L, Nordmann P. Functional characterization of

- IS1999, an IS4 family element involved in mobilization and expression of beta-lactam resistance genes. *J Bacteriol* 2006; **188**: 6506–14.
205. Giani T, Conte V, Di Pilato V, *et al.* Escherichia coli from Italy producing OXA-48 carbapenemase encoded by a novel Tn1999 transposon derivative. *Antimicrob Agents Chemother* 2012; **56**: 2211–3.
206. Potron A, Nordmann P, Rondinaud E, Jauregui F, Poirel L. A mosaic transposon encoding OXA-48 and CTX-M-15: towards pan-resistance. *J Antimicrob Chemother* 2013; **68**: 476–7.
207. Skalova A, Chudejova K, Rotova V, *et al.* Molecular Characterization of OXA-48-Like-Producing Enterobacteriaceae in the Czech Republic and Evidence for Horizontal Transfer of pOXA-48-Like Plasmids. *Antimicrob Agents Chemother* 2017; **61**.
208. Mairi A, Pantel A, Sotto A, Lavigne J-P, Touati A. OXA-48-like carbapenemases producing Enterobacteriaceae in different niches. *Eur J Clin Microbiol Infect Dis* 2018; **37**: 587–604.
209. Turton JF, Doumith M, Hopkins KL, Perry C, Meunier D, Woodford N. Clonal expansion of Escherichia coli ST38 carrying a chromosomally integrated OXA-48 carbapenemase gene. *J Med Microbiol* 2016; **65**: 538–46.
210. Beyrouthy R, Robin F, Delmas J, *et al.* IS1R-mediated plasticity of IncL/M plasmids leads to the insertion of bla OXA-48 into the Escherichia coli Chromosome. *Antimicrob Agents Chemother* 2014; **58**: 3785–90.
211. Sampaio JLM, Ribeiro VB, Campos JC, *et al.* Detection of OXA-370, an OXA-48-related class D β -lactamase, in Enterobacter hormaechei from Brazil. *Antimicrob Agents Chemother* 2014; **58**: 3566–7.
212. Nakano R, Okamoto R, Nagano N, Inoue M. Resistance to gram-negative organisms due to high-level expression of plasmid-encoded ampC beta-lactamase blaCMY-4 promoted by insertion sequence ISEcp1. *J Infect Chemother* 2007; **13**: 18–23.
213. Poirel L, Decousser J-W, Nordmann P. Insertion sequence ISEcp1B is involved in expression and mobilization of a bla(CTX-M) beta-lactamase gene. *Antimicrob Agents Chemother* 2003; **47**: 2938–45.
214. Doi Y, Paterson DL. Carbapenemase-producing Enterobacteriaceae. *Semin Respir Crit Care Med* 2015; **36**: 74–84.
215. Huang T-D, Poirel L, Bogaerts P, Berhin C, Nordmann P, Glupczynski Y. Temocillin and piperacillin/tazobactam resistance by disc diffusion as antimicrobial surrogate markers for the detection of carbapenemase-producing Enterobacteriaceae in geographical areas with a high prevalence of OXA-48 producers. *J Antimicrob Chemother* 2014; **69**: 445–50.
216. Pasteran F, Gonzalez LJ, Albornoz E, Bahr G, Vila AJ, Corso A. Triton Hodge Test: Improved Protocol for Modified Hodge Test for Enhanced Detection of NDM and Other Carbapenemase Producers. *J Clin Microbiol* 2016; **54**: 640–9.
217. Asthana S, Mathur P, Tak V. Detection of Carbapenemase Production in Gram-negative Bacteria. *J Lab Physicians* 2014; **6**: 69–75.
218. van der Zwaluw K, de Haan A, Pluister GN, Bootsma HJ, de Neeling AJ, Schouls LM. The carbapenem inactivation method (CIM), a simple and low-cost alternative for the Carba NP test to assess phenotypic carbapenemase activity in gram-negative rods. *PLoS ONE* 2015; **10**: e0123690.
219. Pierce VM, Simner PJ, Lonsway DR, *et al.* Modified Carbapenem Inactivation Method for Phenotypic Detection of Carbapenemase Production among Enterobacteriaceae. *J Clin Microbiol* 2017; **55**: 2321–33.
220. Muntean M-M, Muntean A-A, Gauthier L, *et al.* Evaluation of the rapid carbapenem inactivation method (rCIM): a phenotypic screening test for carbapenemase-producing Enterobacteriaceae. *J Antimicrob Chemother* 2018; **73**: 900–8.
221. Bernabeu S, Poirel L, Nordmann P. Spectrophotometry-based detection of carbapenemase

- producers among Enterobacteriaceae. *Diagn Microbiol Infect Dis* 2012; **74**: 88–90.
222. Hrabák J, Walková R, Studentová V, Chudácková E, Bergerová T. Carbapenemase activity detection by matrix-assisted laser desorption ionization-time of flight mass spectrometry. *J Clin Microbiol* 2011; **49**: 3222–7.
223. Lasserre C, De Saint Martin L, Cuzon G, *et al.* Efficient Detection of Carbapenemase Activity in Enterobacteriaceae by Matrix-Assisted Laser Desorption Ionization-Time of Flight Mass Spectrometry in Less Than 30 Minutes. *J Clin Microbiol* 2015; **53**: 2163–71.
224. Kohlmann R, Hoffmann A, Geis G, Gatermann S. MALDI-TOF mass spectrometry following short incubation on a solid medium is a valuable tool for rapid pathogen identification from positive blood cultures. *Int J Med Microbiol* 2015; **305**: 469–79.
225. Papagiannitsis CC, Študentová V, Izdebski R, *et al.* Matrix-assisted laser desorption ionization-time of flight mass spectrometry meropenem hydrolysis assay with NH₄HCO₃, a reliable tool for direct detection of carbapenemase activity. *J Clin Microbiol* 2015; **53**: 1731–5.
226. Hrabák J, Studentová V, Walková R, *et al.* Detection of NDM-1, VIM-1, KPC, OXA-48, and OXA-162 carbapenemases by matrix-assisted laser desorption ionization-time of flight mass spectrometry. *J Clin Microbiol* 2012; **50**: 2441–3.
227. Kempf M, Bakour S, Flaudrops C, *et al.* Rapid detection of carbapenem resistance in *Acinetobacter baumannii* using matrix-assisted laser desorption ionization-time of flight mass spectrometry. *PLoS ONE* 2012; **7**: e31676.
228. Dortet L, Tandé D, de Briel D, *et al.* MALDI-TOF for the rapid detection of carbapenemase-producing Enterobacteriaceae: comparison of the commercialized MBT STAR®-Carba IVD Kit with two in-house MALDI-TOF techniques and the RAPIDEC® CARBA NP. *J Antimicrob Chemother* 2018; **73**: 2352–9.
229. Nordmann P, Poirel L, Dortet L. Rapid Detection of Carbapenemase-producing Enterobacteriaceae. *Emerg Infect Dis* 2012; **18**: 1503–7.
230. Glupczynski Y, Evrard S, Ote I, *et al.* Evaluation of two new commercial immunochromatographic assays for the rapid detection of OXA-48 and KPC carbapenemases from cultured bacteria. *J Antimicrob Chemother* 2016; **71**: 1217–22.
231. Bernabeu S, Dortet L, Naas T. Evaluation of the β -CARBATM test, a colorimetric test for the rapid detection of carbapenemase activity in Gram-negative bacilli. *J Antimicrob Chemother* 2017; **72**: 1646–58.
232. Tijet N, Boyd D, Patel SN, Mulvey MR, Melano RG. Evaluation of the Carba NP test for rapid detection of carbapenemase-producing Enterobacteriaceae and *Pseudomonas aeruginosa*. *Antimicrob Agents Chemother* 2013; **57**: 4578–80.
233. Pires J, Novais A, Peixe L. Blue-carba, an easy biochemical test for detection of diverse carbapenemase producers directly from bacterial cultures. *J Clin Microbiol* 2013; **51**: 4281–3.
234. Markoulatos P, Siafakas N, Moncany M. Multiplex polymerase chain reaction: a practical approach. *J Clin Lab Anal* 2002; **16**: 47–51.
235. Singh P, Pfeifer Y, Mustapha A. Multiplex real-time PCR assay for the detection of extended-spectrum β -lactamase and carbapenemase genes using melting curve analysis. *J Microbiol Methods* 2016; **124**: 72–8.
236. Findlay J, Hopkins KL, Meunier D, Woodford N. Evaluation of three commercial assays for rapid detection of genes encoding clinically relevant carbapenemases in cultured bacteria. *J Antimicrob Chemother* 2015; **70**: 1338–42.
237. Cuzon G, Naas T, Bogaerts P, Glupczynski Y, Nordmann P. Evaluation of a DNA microarray for the rapid detection of extended-spectrum β -lactamases (TEM, SHV and CTX-M), plasmid-mediated cephalosporinases (CMY-2-like, DHA, FOX, ACC-1, ACT/MIR and CMY-1-like/MOX) and carbapenemases (KPC, OXA-48, VIM, IMP and NDM). *J Antimicrob Chemother* 2012; **67**: 1865–9.

238. Smiljanic M, Kaase M, Ahmad-Nejad P, Ghebremedhin B. Comparison of in-house and commercial real time-PCR based carbapenemase gene detection methods in Enterobacteriaceae and non-fermenting gram-negative bacterial isolates. *Ann Clin Microbiol Antimicrob* 2017; **16**: 48.
239. Lutgring JD, Limbago BM. The Problem of Carbapenemase-Producing-Carbapenem-Resistant-Enterobacteriaceae Detection. *J Clin Microbiol* 2016; **54**: 529–34.
240. Wareham DW, Shah R, Betts JW, Phee LM, Momin MHFA. Evaluation of an Immunochromatographic Lateral Flow Assay (OXA-48 K-SeT) for Rapid Detection of OXA-48-Like Carbapenemases in Enterobacteriaceae. *J Clin Microbiol* 2016; **54**: 471–3.
241. Glupczynski Y, Jousset A, Evrard S, *et al.* Prospective evaluation of the OKN K-SeT assay, a new multiplex immunochromatographic test for the rapid detection of OXA-48-like, KPC and NDM carbapenemases. *J Antimicrob Chemother* 2017; **72**: 1955–60.
242. Boutal H, Vogel A, Bernabeu S, *et al.* A multiplex lateral flow immunoassay for the rapid identification of NDM-, KPC-, IMP- and VIM-type and OXA-48-like carbapenemase-producing Enterobacteriaceae. *J Antimicrob Chemother* 2018; **73**: 909–15.
243. Hopkins KL, Meunier D, Naas T, Volland H, Woodford N. Evaluation of the NG-Test CARBA 5 multiplex immunochromatographic assay for the detection of KPC, OXA-48-like, NDM, VIM and IMP carbapenemases. *J Antimicrob Chemother* 2018; **73**: 3523–6.
244. Lau AF, Wang H, Weingarten RA, *et al.* A rapid matrix-assisted laser desorption ionization-time of flight mass spectrometry-based method for single-plasmid tracking in an outbreak of carbapenem-resistant Enterobacteriaceae. *J Clin Microbiol* 2014; **52**: 2804–12.
245. Gaibani P, Galea A, Fagioni M, Ambretti S, Sambri V, Landini MP. Evaluation of Matrix-Assisted Laser Desorption Ionization-Time of Flight Mass Spectrometry for Identification of KPC-Producing *Klebsiella pneumoniae*. *J Clin Microbiol* 2016; **54**: 2609–13.
246. Partridge SR. Tn4401 carrying blaKPC is inserted within another insertion in pKpQIL and related plasmids. *J Clin Microbiol* 2014; **52**: 4448–9.
247. Tischendorf J, de Avila RA, Safdar N. Risk of infection following colonization with carbapenem-resistant Enterobacteriaceae: A systematic review. *Am J Infect Control* 2016; **44**: 539–43.
248. van Duin D, Doi Y. The global epidemiology of carbapenemase-producing Enterobacteriaceae. *Virulence* 2017; **8**: 460–9.
249. Dautzenberg MJD, Ossewaarde JM, de Greeff SC, Troelstra A, Bonten MJM. Risk factors for the acquisition of OXA-48-producing Enterobacteriaceae in a hospital outbreak setting: a matched case-control study. *J Antimicrob Chemother* 2016; **71**: 2273–9.
250. van der Bij AK, Pitout JDD. The role of international travel in the worldwide spread of multiresistant Enterobacteriaceae. *J Antimicrob Chemother* 2012; **67**: 2090–100.
251. Ruppé E, Armand-Lefèvre L, Estellat C, *et al.* High Rate of Acquisition but Short Duration of Carriage of Multidrug-Resistant Enterobacteriaceae After Travel to the Tropics. *Clin Infect Dis* 2015; **61**: 593–600.
252. Ruppé E, Armand-Lefèvre L, Estellat C, *et al.* Acquisition of carbapenemase-producing Enterobacteriaceae by healthy travellers to India, France, February 2012 to March 2013. *Euro Surveill* 2014; **19**.
253. Falagas ME, Tansarli GS, Karageorgopoulos DE, Vardakas KZ. Deaths attributable to carbapenem-resistant Enterobacteriaceae infections. *Emerging Infect Dis* 2014; **20**: 1170–5.
254. Temkin E, Adler A, Lerner A, Carmeli Y. Carbapenem-resistant Enterobacteriaceae: biology, epidemiology, and management. *Ann N Y Acad Sci* 2014; **1323**: 22–42.
255. Nordmann P, Naas T, Poirel L. Global spread of Carbapenemase-producing Enterobacteriaceae. *Emerging Infect Dis* 2011; **17**: 1791–8.
256. Tamma PD, Goodman KE, Harris AD, *et al.* Comparing the Outcomes of Patients With Carbapenemase-Producing and Non-Carbapenemase-Producing Carbapenem-Resistant

- Enterobacteriaceae Bacteremia. *Clin Infect Dis* 2017; **64**: 257–64.
257. Falagas ME, Lourida P, Poulidakos P, Rafailidis PI, Tansarli GS. Antibiotic treatment of infections due to carbapenem-resistant Enterobacteriaceae: systematic evaluation of the available evidence. *Antimicrob Agents Chemother* 2014; **58**: 654–63.
258. Markogiannakis A, Tzouvelekis LS, Psychogiou M, Petinaki E, Daikos GL. Confronting carbapenemase-producing *Klebsiella pneumoniae*. *Future Microbiol* 2013; **8**: 1147–61.
259. Qureshi ZA, Paterson DL, Potoski BA, *et al.* Treatment outcome of bacteremia due to KPC-producing *Klebsiella pneumoniae*: superiority of combination antimicrobial regimens. *Antimicrob Agents Chemother* 2012; **56**: 2108–13.
260. Yamamoto M, Pop-Vicas AE. Treatment for infections with carbapenem-resistant Enterobacteriaceae: what options do we still have? *Crit Care* 2014; **18**: 229.
261. Tzouvelekis LS, Markogiannakis A, Piperaki E, Souli M, Daikos GL. Treating infections caused by carbapenemase-producing Enterobacteriaceae. *Clin Microbiol Infect* 2014; **20**: 862–72.
262. Oliva A, Scorzolini L, Castaldi D, *et al.* Double-carbapenem regimen, alone or in combination with colistin, in the treatment of infections caused by carbapenem-resistant *Klebsiella pneumoniae* (CR-Kp). *J Infect* 2017; **74**: 103–6.
263. De Pascale G, Martucci G, Montini L, *et al.* Double carbapenem as a rescue strategy for the treatment of severe carbapenemase-producing *Klebsiella pneumoniae* infections: a two-center, matched case-control study. *Crit Care* 2017; **21**: 173.
264. Cprek JB, Gallagher JC. Ertapenem-Containing Double-Carbapenem Therapy for Treatment of Infections Caused by Carbapenem-Resistant *Klebsiella pneumoniae*. *Antimicrob Agents Chemother* 2016; **60**: 669–73.
265. Krishnappa LG, Marie MAM, Al Sheikh YA. Characterization of carbapenem resistance mechanisms in *Klebsiella pneumoniae* and in vitro synergy of the colistin-meropenem combination. *J Chemother* 2015; **27**: 277–82.
266. Mavroidi A, Katsiari M, Likousi S, *et al.* Characterization of ST258 Colistin-Resistant, blaKPC-Producing *Klebsiella pneumoniae* in a Greek Hospital. *Microb Drug Resist* 2016; **22**: 392–8.
267. Maherault A-C, Nordmann P, Therby A, Pangon B. Efficacy of imipenem for the treatment of bacteremia due to an OXA-48-producing *Klebsiella pneumoniae* isolate. *Clin Infect Dis* 2012; **54**: 577–8.
268. Mimos O, Grégoire N, Poirel L, Marliat M, Couet W, Nordmann P. Broad-spectrum β -lactam antibiotics for treating experimental peritonitis in mice due to *Klebsiella pneumoniae* producing the carbapenemase OXA-48. *Antimicrob Agents Chemother* 2012; **56**: 2759–60.
269. Tacconelli E, Cataldo MA, Dancer SJ, *et al.* ESCMID guidelines for the management of the infection control measures to reduce transmission of multidrug-resistant Gram-negative bacteria in hospitalized patients. *Clin Microbiol Infect* 2014; **20 Suppl 1**: 1–55.
270. Copeland RA. Evaluation of enzyme inhibitors in drug discovery. A guide for medicinal chemists and pharmacologists. *Methods Biochem Anal* 2005; **46**: 1–265.
271. Bush K. Evaluation of enzyme inhibition data in screening for new drugs. *Drugs Exp Clin Res* 1986; **12**: 565–76.
272. Moussard C. *Biochimie structurale et métabolique*. De Boeck Supérieur; 2006.
273. Bush K. Beta-lactamase inhibitors from laboratory to clinic. *Clin Microbiol Rev* 1988; **1**: 109–23.
274. Williams JD. beta-Lactamase inhibition and in vitro activity of sulbactam and sulbactam/cefoperazone. *Clin Infect Dis* 1997; **24**: 494–7.
275. Helfand MS, Totir MA, Carey MP, Hujer AM, Bonomo RA, Carey PR. Following the reactions of mechanism-based inhibitors with beta-lactamase by Raman crystallography. *Biochemistry* 2003; **42**: 13386–92.

276. Buynak JD. Understanding the longevity of the beta-lactam antibiotics and of antibiotic/beta-lactamase inhibitor combinations. *Biochem Pharmacol* 2006; **71**: 930–40.
277. Cantón R, Coque TM. The CTX-M beta-lactamase pandemic. *Curr Opin Microbiol* 2006; **9**: 466–75.
278. Philippon A, Labia R, Jacoby G. Extended-spectrum beta-lactamases. *Antimicrob Agents Chemother* 1989; **33**: 1131–6.
279. Urban C, Rahal JJ, Luft B. Effect of a beta-lactamase inhibitor, tazobactam, on growth and penicillin-binding proteins of *Borrelia burgdorferi*. *FEMS Microbiol Lett* 1991; **66**: 113–6.
280. Urban C, Go E, Mariano N, *et al.* Effect of sulbactam on infections caused by imipenem-resistant *Acinetobacter calcoaceticus* biotype *anitratus*. *J Infect Dis* 1993; **167**: 448–51.
281. Miller JM, Baker CN, Thornsberry C. Inhibition of beta-lactamase in *Neisseria gonorrhoeae* by sodium clavulanate. *Antimicrob Agents Chemother* 1978; **14**: 794–6.
282. Higgins PG, Wisplinghoff H, Stefanik D, Seifert H. In vitro activities of the beta-lactamase inhibitors clavulanic acid, sulbactam, and tazobactam alone or in combination with beta-lactams against epidemiologically characterized multidrug-resistant *Acinetobacter baumannii* strains. *Antimicrob Agents Chemother* 2004; **48**: 1586–92.
283. Levin AS. Multiresistant *Acinetobacter* infections: a role for sulbactam combinations in overcoming an emerging worldwide problem. *Clin Microbiol Infect* 2002; **8**: 144–53.
284. Neu HC, Fu KP. Clavulanic acid, a novel inhibitor of beta-lactamases. *Antimicrob Agents Chemother* 1978; **14**: 650–5.
285. Reading C, Cole M. Clavulanic acid: a beta-lactamase-inhibiting beta-lactam from *Streptomyces clavuligerus*. *Antimicrob Agents Chemother* 1977; **11**: 852–7.
286. White AR, Kaye C, Poupard J, Pypstra R, Woodnutt G, Wynne B. Augmentin (amoxicillin/clavulanate) in the treatment of community-acquired respiratory tract infection: a review of the continuing development of an innovative antimicrobial agent. *J Antimicrob Chemother* 2004; **53 Suppl 1**: i3-20.
287. Drawz SM, Bonomo RA. Three decades of beta-lactamase inhibitors. *Clin Microbiol Rev* 2010; **23**: 160–201.
288. Cartwright SJ, Coulson AF. A semi-synthetic penicillinase inactivator. *Nature* 1979; **278**: 360–1.
289. Charnas RL, Fisher J, Knowles JR. Chemical studies on the inactivation of *Escherichia coli* RTEM beta-lactamase by clavulanic acid. *Biochemistry* 1978; **17**: 2185–9.
290. Fisher J, Charnas RL, Knowles JR. Kinetic studies on the inactivation of *Escherichia coli* RTEM beta-lactamase by clavulanic acid. *Biochemistry* 1978; **17**: 2180–4.
291. Durkin JP, Viswanatha T. Clavulanic acid inhibition of beta-lactamase I from *Bacillus cereus* 569/H. *J Antibiot* 1978; **31**: 1162–9.
292. Chen CC, Herzberg O. Inhibition of beta-lactamase by clavulanate. Trapped intermediates in cryocrystallographic studies. *J Mol Biol* 1992; **224**: 1103–13.
293. Anon. Inactivation of class A beta-lactamases by clavulanic acid: the role of arginine-244 in a proposed nonconcerted sequence of events. Available at: <https://pubs.acs.org/doi/pdf/10.1021/ja00064a003>. Accessed August 17, 2019.
294. Imtiaz U, Manavathu EK, Mobashery S, Lerner SA. Reversal of clavulanate resistance conferred by a Ser-244 mutant of TEM-1 beta-lactamase as a result of a second mutation (Arg to Ser at position 164) that enhances activity against ceftazidime. *Antimicrob Agents Chemother* 1994; **38**: 1134–9.
295. Brenner DG, Knowles JR. Penicillanic acid sulfone: an unexpected isotope effect in the interaction of 6 alpha- and 6 beta-monodeuterio and of 6,6-dideuterio derivatives with RTEM beta-lactamase from *Escherichia coli*. *Biochemistry* 1981; **20**: 3680–7.
296. Shapiro AB. Kinetics of Sulbactam Hydrolysis by β -Lactamases, and Kinetics of β -Lactamase Inhibition by Sulbactam. *Antimicrob Agents Chemother* 2017; **61**.

297. Toomer CA, Schwalbe CH, Ringan NS, Lambert PA, Lowe PR, Lee VJ. Structural studies on tazobactam. *J Med Chem* 1991; **34**: 1944–7.
298. Bonomo RA, Rudin SA, Shlaes DM. Tazobactam is a potent inactivator of selected inhibitor-resistant class A beta-lactamases. *FEMS Microbiol Lett* 1997; **148**: 59–62.
299. Bush K, Macalintal C, Rasmussen BA, Lee VJ, Yang Y. Kinetic interactions of tazobactam with beta-lactamases from all major structural classes. *Antimicrob Agents Chemother* 1993; **37**: 851–8.
300. Cluck D, Lewis P, Stayer B, Spivey J, Moorman J. Ceftolozane–tazobactam: A new-generation cephalosporin. *Am J Health Syst Pharm* 2015; **72**: 2135–46.
301. Bulik CC, Tessier PR, Keel RA, Sutherland CA, Nicolau DP. In Vivo Comparison of CXA-101 (FR264205) with and without Tazobactam versus Piperacillin-Tazobactam Using Human Simulated Exposures against Phenotypically Diverse Gram-Negative Organisms. *Antimicrobial Agents and Chemotherapy* 2012; **56**: 544–9.
302. Zhanel GG, Chung P, Adam H, *et al.* Ceftolozane/tazobactam: a novel cephalosporin/ β -lactamase inhibitor combination with activity against multidrug-resistant gram-negative bacilli. *Drugs* 2014; **74**: 31–51.
303. Payne DJ, Cramp R, Winstanley DJ, Knowles DJ. Comparative activities of clavulanic acid, sulbactam, and tazobactam against clinically important beta-lactamases. *Antimicrob Agents Chemother* 1994; **38**: 767–72.
304. Thomson JM, Distler AM, Prati F, Bonomo RA. Probing active site chemistry in SHV beta-lactamase variants at Ambler position 244. Understanding unique properties of inhibitor resistance. *J Biol Chem* 2006; **281**: 26734–44.
305. Thomson JM, Distler AM, Bonomo RA. Overcoming resistance to beta-lactamase inhibitors: comparing sulbactam to novel inhibitors against clavulanate resistant SHV enzymes with substitutions at Ambler position 244. *Biochemistry* 2007; **46**: 11361–8.
306. Bonnefoy A, Dupuis-Hamelin C, Steier V, *et al.* In vitro activity of AVE1330A, an innovative broad-spectrum non-beta-lactam beta-lactamase inhibitor. *J Antimicrob Chemother* 2004; **54**: 410–7.
307. Docquier J-D, Mangani S. An update on β -lactamase inhibitor discovery and development. *Drug Resist Updat* 2018; **36**: 13–29.
308. Ehmann DE, Jahić H, Ross PL, *et al.* Kinetics of Avibactam Inhibition against Class A, C, and D β -Lactamases. *Journal of Biological Chemistry* 2013; **288**: 27960–71.
309. Ehmann DE, Jahić H, Ross PL, *et al.* Avibactam is a covalent, reversible, non- β -lactam β -lactamase inhibitor. *PNAS* 2012; **109**: 11663–8.
310. Stachyra T, Levasseur P, Pechereau M-C, *et al.* In vitro activity of the -lactamase inhibitor NXL104 against KPC-2 carbapenemase and Enterobacteriaceae expressing KPC carbapenemases. *Journal of Antimicrobial Chemotherapy* 2009; **64**: 326–9.
311. Livermore DM, Mushtaq S, Warner M, Miossec C, Woodford N. NXL104 combinations versus Enterobacteriaceae with CTX-M extended-spectrum beta-lactamases and carbapenemases. *J Antimicrob Chemother* 2008; **62**: 1053–6.
312. Mushtaq S, Warner M, Williams G, Critchley I, Livermore DM. Activity of chequerboard combinations of ceftaroline and NXL104 versus beta-lactamase-producing Enterobacteriaceae. *J Antimicrob Chemother* 2010; **65**: 1428–32.
313. van Duin D, Bonomo RA. Ceftazidime/Avibactam and Ceftolozane/Tazobactam: Second-generation β -Lactam/ β -Lactamase Inhibitor Combinations. *Clin Infect Dis* 2016; **63**: 234–41.
314. Marshall S, Hujer AM, Rojas LJ, *et al.* Can Ceftazidime-Avibactam and Aztreonam Overcome β -Lactam Resistance Conferred by Metallo- β -Lactamases in Enterobacteriaceae? *Antimicrob Agents Chemother* 2017; **61**.
315. Davido B, Fellous L, Lawrence C, Maxime V, Rottman M, Dinh A. Ceftazidime-Avibactam and Aztreonam, an Interesting Strategy To Overcome β -Lactam Resistance

Conferred by Metallo- β -Lactamases in Enterobacteriaceae and *Pseudomonas aeruginosa*. *Antimicrob Agents Chemother* 2017; **61**.

316. Shaw E, Rombauts A, Tubau F, *et al*. Clinical outcomes after combination treatment with ceftazidime/avibactam and aztreonam for NDM-1/OXA-48/CTX-M-15-producing *Klebsiella pneumoniae* infection. *J Antimicrob Chemother* 2018; **73**: 1104–6.

317. Testa R, Cantón R, Giani T, *et al*. In vitro activity of ceftazidime, ceftaroline and aztreonam alone and in combination with avibactam against European Gram-negative and Gram-positive clinical isolates. *Int J Antimicrob Agents* 2015; **45**: 641–6.

318. Papp-Wallace KM, Bajaksouzian S, Abdelhamed AM, *et al*. Activities of ceftazidime, ceftaroline, and aztreonam alone and combined with avibactam against isogenic *Escherichia coli* strains expressing selected single β -lactamases. *Diagn Microbiol Infect Dis* 2015; **82**: 65–9.

319. Karaiskos I, Galani I, Souli M, Giamarellou H. Novel β -lactam- β -lactamase inhibitor combinations: expectations for the treatment of carbapenem-resistant Gram-negative pathogens. *Expert Opin Drug Metab Toxicol* 2019; **15**: 133–49.

320. Stachyra T, Péchereau M-C, Bruneau J-M, *et al*. Mechanistic studies of the inactivation of TEM-1 and P99 by NXL104, a novel non-beta-lactam beta-lactamase inhibitor. *Antimicrob Agents Chemother* 2010; **54**: 5132–8.

321. Zhanel GG, Lawson CD, Adam H, *et al*. Ceftazidime-avibactam: a novel cephalosporin/ β -lactamase inhibitor combination. *Drugs* 2013; **73**: 159–77.

322. Lahiri SD, Johnstone MR, Ross PL, McLaughlin RE, Olivier NB, Alm RA. Avibactam and class C β -lactamases: mechanism of inhibition, conservation of the binding pocket, and implications for resistance. *Antimicrob Agents Chemother* 2014; **58**: 5704–13.

323. Lahiri SD, Mangani S, Jahić H, *et al*. Molecular basis of selective inhibition and slow reversibility of avibactam against class D carbapenemases: a structure-guided study of OXA-24 and OXA-48. *ACS Chem Biol* 2015; **10**: 591–600.

324. Papp-Wallace KM, Winkler ML, Taracila MA, Bonomo RA. Variants of β -Lactamase KPC-2 That Are Resistant to Inhibition by Avibactam. *Antimicrobial Agents and Chemotherapy* 2015; **59**: 3710–7.

325. Winkler ML, Papp-Wallace KM, Taracila MA, Bonomo RA. Avibactam and inhibitor-resistant SHV β -lactamases. *Antimicrob Agents Chemother* 2015; **59**: 3700–9.

326. Winkler ML, Papp-Wallace KM, Bonomo RA. Activity of ceftazidime/avibactam against isogenic strains of *Escherichia coli* containing KPC and SHV β -lactamases with single amino acid substitutions in the Ω -loop. *J Antimicrob Chemother* 2015; **70**: 2279–86.

327. Blizzard TA, Chen H, Kim S, *et al*. Discovery of MK-7655, a β -lactamase inhibitor for combination with Primaxin®. *Bioorg Med Chem Lett* 2014; **24**: 780–5.

328. Olsen I. New promising β -lactamase inhibitors for clinical use. *Eur J Clin Microbiol Infect Dis* 2015; **34**: 1303–8.

329. Zhanel GG, Lawrence CK, Adam H, *et al*. Imipenem-Relebactam and Meropenem-Vaborbactam: Two Novel Carbapenem- β -Lactamase Inhibitor Combinations. *Drugs* 2018; **78**: 65–98.

330. Livermore DM, Warner M, Mushtaq S. Activity of MK-7655 combined with imipenem against Enterobacteriaceae and *Pseudomonas aeruginosa*. *J Antimicrob Chemother* 2013; **68**: 2286–90.

331. Lapuebla A, Abdallah M, Olafisoye O, *et al*. Activity of Imipenem with Relebactam against Gram-Negative Pathogens from New York City. *Antimicrob Agents Chemother* 2015; **59**: 5029–31.

332. Mavridou E, Melchers RJB, van Mil ACHAM, Mangin E, Motyl MR, Mouton JW. Pharmacodynamics of imipenem in combination with β -lactamase inhibitor MK7655 in a murine thigh model. *Antimicrob Agents Chemother* 2015; **59**: 790–5.

333. Karlowsky JA, Lob SH, Kazmierczak KM, *et al.* In vitro activity of imipenem/relebactam against Gram-negative ESKAPE pathogens isolated in 17 European countries: 2015 SMART surveillance programme. *J Antimicrob Chemother* 2018; **73**: 1872–9.
334. Lob SH, Hackel MA, Kazmierczak KM, *et al.* In Vitro Activity of Imipenem-Relebactam against Gram-Negative ESKAPE Pathogens Isolated by Clinical Laboratories in the United States in 2015 (Results from the SMART Global Surveillance Program). *Antimicrob Agents Chemother* 2017; **61**.
335. Morinaka A, Tsutsumi Y, Yamada M, *et al.* OP0595, a new diazabicyclooctane: mode of action as a serine β -lactamase inhibitor, antibiotic and β -lactam ‘enhancer’. *J Antimicrob Chemother* 2015; **70**: 2779–86.
336. Livermore DM, Mushtaq S, Warner M, Woodford N. Activity of OP0595/ β -lactam combinations against Gram-negative bacteria with extended-spectrum, AmpC and carbapenem-hydrolysing β -lactamases. *J Antimicrob Chemother* 2015; **70**: 3032–41.
337. Moya B, Barcelo IM, Bhagwat S, *et al.* WCK 5107 (Zidebactam) and WCK 5153 Are Novel Inhibitors of PBP2 Showing Potent ‘ β -Lactam Enhancer’ Activity against *Pseudomonas aeruginosa*, Including Multidrug-Resistant Metallo- β -Lactamase-Producing High-Risk Clones. *Antimicrob Agents Chemother* 2017; **61**.
338. Sader HS, Rhomberg PR, Flamm RK, Jones RN, Castanheira M. WCK 5222 (cefepime/zidebactam) antimicrobial activity tested against Gram-negative organisms producing clinically relevant β -lactamases. *J Antimicrob Chemother* 2017; **72**: 1696–703.
339. Durand-Réville TF, Guler S, Comita-Prevoir J, *et al.* ETX2514 is a broad-spectrum β -lactamase inhibitor for the treatment of drug-resistant Gram-negative bacteria including *Acinetobacter baumannii*. *Nat Microbiol* 2017; **2**: 17104.
340. Tommasi R, Iyer R, Miller AA. Antibacterial Drug Discovery: Some Assembly Required. *ACS Infect Dis* 2018; **4**: 686–95.
341. Shapiro AB, Gao N, Jahić H, Carter NM, Chen A, Miller AA. Reversibility of Covalent, Broad-Spectrum Serine β -Lactamase Inhibition by the Diazabicyclooctenone ETX2514. *ACS Infect Dis* 2017; **3**: 833–44.
342. Bush K. Game Changers: New β -Lactamase Inhibitor Combinations Targeting Antibiotic Resistance in Gram-Negative Bacteria. *ACS Infect Dis* 2018; **4**: 84–7.
343. Bone R, Shenvi AB, Kettner CA, Agard DA. Serine protease mechanism: structure of an inhibitory complex of alpha-lytic protease and a tightly bound peptide boronic acid. *Biochemistry* 1987; **26**: 7609–14.
344. Lindquist RN, Terry C. Inhibition of subtilisin by boronic acids, potential analogs of tetrahedral reaction intermediates. *Arch Biochem Biophys* 1974; **160**: 135–44.
345. Hecker SJ, Reddy KR, Totrov M, *et al.* Discovery of a Cyclic Boronic Acid β -Lactamase Inhibitor (RPX7009) with Utility vs Class A Serine Carbapenemases. *J Med Chem* 2015; **58**: 3682–92.
346. Castanheira M, Rhomberg PR, Flamm RK, Jones RN. Effect of the β -Lactamase Inhibitor Vaborbactam Combined with Meropenem against Serine Carbapenemase-Producing Enterobacteriaceae. *Antimicrob Agents Chemother* 2016; **60**: 5454–8.
347. Castanheira M, Huband MD, Mendes RE, Flamm RK. Meropenem-Vaborbactam Tested against Contemporary Gram-Negative Isolates Collected Worldwide during 2014, Including Carbapenem-Resistant, KPC-Producing, Multidrug-Resistant, and Extensively Drug-Resistant Enterobacteriaceae. *Antimicrob Agents Chemother* 2017; **61**.
348. Lapuebla A, Abdallah M, Olafisoye O, *et al.* Activity of Meropenem Combined with RPX7009, a Novel β -Lactamase Inhibitor, against Gram-Negative Clinical Isolates in New York City. *Antimicrob Agents Chemother* 2015; **59**: 4856–60.
349. Brem J, Cain R, Cahill S, *et al.* Structural basis of metallo- β -lactamase, serine- β -lactamase and penicillin-binding protein inhibition by cyclic boronates. *Nat Commun* 2016; **7**: 12406.

350. J BC, Rajesh G, W JR, *et al.* Beta-lactamase Inhibitors. 2010. Available at: <https://lens.org/194-514-452-545-153>.
351. Cahill ST, Cain R, Wang DY, *et al.* Cyclic Boronates Inhibit All Classes of β -Lactamases. *Antimicrob Agents Chemother* 2017; **61**.
352. Ke W, Sampson JM, Ori C, *et al.* Novel insights into the mode of inhibition of class A SHV-1 beta-lactamases revealed by boronic acid transition state inhibitors. *Antimicrob Agents Chemother* 2011; **55**: 174–83.
353. Walsh TR, Toleman MA, Poirel L, Nordmann P. Metallo-beta-lactamases: the quiet before the storm? *Clin Microbiol Rev* 2005; **18**: 306–25.
354. Bebrone C. Metallo-beta-lactamases (classification, activity, genetic organization, structure, zinc coordination) and their superfamily. *Biochem Pharmacol* 2007; **74**: 1686–701.
355. Garau G, García-Sáez I, Bebrone C, *et al.* Update of the standard numbering scheme for class B beta-lactamases. *Antimicrob Agents Chemother* 2004; **48**: 2347–9.
356. Ju L-C, Cheng Z, Fast W, Bonomo RA, Crowder MW. The Continuing Challenge of Metallo- β -Lactamase Inhibition: Mechanism Matters. *Trends Pharmacol Sci* 2018; **39**: 635–47.
357. Fast W, Sutton LD. Metallo- β -lactamase: inhibitors and reporter substrates. *Biochim Biophys Acta* 2013; **1834**: 1648–59.
358. García-Saez I, Hopkins J, Papamicael C, *et al.* The 1.5-Å structure of *Chryseobacterium meningosepticum* zinc beta-lactamase in complex with the inhibitor, D-captopril. *J Biol Chem* 2003; **278**: 23868–73.
359. García-Sáez I, Mercuri PS, Papamicael C, *et al.* Three-dimensional structure of FEZ-1, a monomeric subclass B3 metallo-beta-lactamase from *Fluoribacter gormanii*, in native form and in complex with D-captopril. *J Mol Biol* 2003; **325**: 651–60.
360. King DT, Worrall LJ, Gruninger R, Strynadka NCJ. New Delhi metallo- β -lactamase: structural insights into β -lactam recognition and inhibition. *J Am Chem Soc* 2012; **134**: 11362–5.
361. Nauton L, Kahn R, Garau G, Hernandez JF, Dideberg O. Structural insights into the design of inhibitors for the L1 metallo-beta-lactamase from *Stenotrophomonas maltophilia*. *J Mol Biol* 2008; **375**: 257–69.
362. Li N, Xu Y, Xia Q, *et al.* Simplified captopril analogues as NDM-1 inhibitors. *Bioorg Med Chem Lett* 2014; **24**: 386–9.
363. Klingler F-M, Wichelhaus TA, Frank D, *et al.* Approved Drugs Containing Thiols as Inhibitors of Metallo- β -lactamases: Strategy To Combat Multidrug-Resistant Bacteria. *J Med Chem* 2015; **58**: 3626–30.
364. Liu X-L, Shi Y, Kang JS, Oelschlaeger P, Yang K-W. Amino Acid Thioester Derivatives: A Highly Promising Scaffold for the Development of Metallo- β -lactamase L1 Inhibitors. *ACS Med Chem Lett* 2015; **6**: 660–4.
365. Liu X-L, Yang K-W, Zhang Y-J, *et al.* Optimization of amino acid thioesters as inhibitors of metallo- β -lactamase L1. *Bioorg Med Chem Lett* 2016; **26**: 4698–701.
366. Arjomandi OK, Hussein WM, Vella P, *et al.* Design, synthesis, and in vitro and biological evaluation of potent amino acid-derived thiol inhibitors of the metallo- β -lactamase IMP-1. *Eur J Med Chem* 2016; **114**: 318–27.
367. Cain R, Brem J, Zollman D, *et al.* In Silico Fragment-Based Design Identifies Subfamily B1 Metallo- β -lactamase Inhibitors. *J Med Chem* 2018; **61**: 1255–60.
368. Hinchliffe P, González MM, Mojica MF, *et al.* Cross-class metallo- β -lactamase inhibition by bisthiazolidines reveals multiple binding modes. *Proc Natl Acad Sci USA* 2016; **113**: E3745-3754.
369. Hinchliffe P, Tanner CA, Krismanich AP, *et al.* Structural and Kinetic Studies of the Potent Inhibition of Metallo- β -lactamases by 6-Phosphonomethylpyridine-2-carboxylates.

Biochemistry 2018; **57**: 1880–92.

370. Chen C, Xiang Y, Yang K-W, *et al.* A protein structure-guided covalent scaffold selectively targets the B1 and B2 subclass metallo- β -lactamases. *Chem Commun (Camb)* 2018; **54**: 4802–5.

371. Wang R, Lai T-P, Gao P, *et al.* Bismuth antimicrobial drugs serve as broad-spectrum metallo- β -lactamase inhibitors. *Nat Commun* 2018; **9**: 439.

372. Horsfall LE, Garau G, Liénard BMR, *et al.* Competitive inhibitors of the CphA metallo-beta-lactamase from *Aeromonas hydrophila*. *Antimicrob Agents Chemother* 2007; **51**: 2136–42.

373. Chen AY, Thomas PW, Stewart AC, *et al.* Dipicolinic Acid Derivatives as Inhibitors of New Delhi Metallo- β -lactamase-1. *J Med Chem* 2017; **60**: 7267–83.

374. King AM, Reid-Yu SA, Wang W, *et al.* Aspergillomarasmine A overcomes metallo- β -lactamase antibiotic resistance. *Nature* 2014; **510**: 503–6.

375. Somboro AM, Tiwari D, Bester LA, *et al.* NOTA: a potent metallo- β -lactamase inhibitor. *J Antimicrob Chemother* 2015; **70**: 1594–6.

376. Zhang E, Wang M-M, Huang S-C, *et al.* NOTA analogue: A first dithiocarbamate inhibitor of metallo- β -lactamases. *Bioorg Med Chem Lett* 2018; **28**: 214–21.

377. Kurosaki H, Yamaguchi Y, Higashi T, *et al.* Irreversible inhibition of metallo-beta-lactamase (IMP-1) by 3-(3-mercaptopropionylsulfanyl)propionic acid pentafluorophenyl ester. *Angew Chem Int Ed Engl* 2005; **44**: 3861–4.

378. Chiou J, Wan S, Chan K-F, *et al.* Ebselen as a potent covalent inhibitor of New Delhi metallo- β -lactamase (NDM-1). *Chem Commun (Camb)* 2015; **51**: 9543–6.

379. Dobias J, Dénervaud-Tendon V, Poirel L, Nordmann P. Activity of the novel siderophore cephalosporin cefiderocol against multidrug-resistant Gram-negative pathogens. *Eur J Clin Microbiol Infect Dis* 2017; **36**: 2319–27.

380. Ito-Horiyama T, Ishii Y, Ito A, *et al.* Stability of Novel Siderophore Cephalosporin S-649266 against Clinically Relevant Carbapenemases. *Antimicrob Agents Chemother* 2016; **60**: 4384–6.

381. Ito A, Kohira N, Bouchillon SK, *et al.* In vitro antimicrobial activity of S-649266, a catechol-substituted siderophore cephalosporin, when tested against non-fermenting Gram-negative bacteria. *J Antimicrob Chemother* 2016; **71**: 670–7.

382. Ito A, Nishikawa T, Matsumoto S, *et al.* Siderophore Cephalosporin Cefiderocol Utilizes Ferric Iron Transporter Systems for Antibacterial Activity against *Pseudomonas aeruginosa*. *Antimicrob Agents Chemother* 2016; **60**: 7396–401.

383. Kohira N, West J, Ito A, *et al.* In Vitro Antimicrobial Activity of a Siderophore Cephalosporin, S-649266, against Enterobacteriaceae Clinical Isolates, Including Carbapenem-Resistant Strains. *Antimicrob Agents Chemother* 2016; **60**: 729–34.

384. Livermore DM. Interplay of impermeability and chromosomal beta-lactamase activity in imipenem-resistant *Pseudomonas aeruginosa*. *Antimicrob Agents Chemother* 1992; **36**: 2046–8.

385. Falagas ME, Skolidis T, Vardakas KZ, Legakis NJ, Hellenic Cefiderocol Study Group. Activity of cefiderocol (S-649266) against carbapenem-resistant Gram-negative bacteria collected from inpatients in Greek hospitals. *J Antimicrob Chemother* 2017; **72**: 1704–8.

386. Tsuji M, Hackel M, Echols R, Yamano Y, Sahn D. In vitro Activity of Cefiderocol against Globally Collected Carbapenem-Resistant Gram-Negative Bacteria Isolated from Urinary Track Source: SIDERO-CR-2014/2016. *Open Forum Infect Dis* 2017; **4**: S366.

387. Portsmouth S, van Veenhuizen D, Echols R, *et al.* Cefiderocol versus imipenem-cilastatin for the treatment of complicated urinary tract infections caused by Gram-negative uropathogens: a phase 2, randomised, double-blind, non-inferiority trial. *Lancet Infect Dis* 2018; **18**: 1319–28.

388. Materon IC, Beharry Z, Huang W, Perez C, Palzkill T. Analysis of the context dependent sequence requirements of active site residues in the metallo-beta-lactamase IMP-1. *J Mol Biol* 2004; **344**: 653–63.
389. Borra PS, Leiros H-KS, Ahmad R, *et al.* Structural and computational investigations of VIM-7: insights into the substrate specificity of vim metallo- β -lactamases. *J Mol Biol* 2011; **411**: 174–89.
390. Wang X, Li H, Zhao C, *et al.* Novel NDM-9 metallo- β -lactamase identified from a ST107 *Klebsiella pneumoniae* strain isolated in China. *International Journal of Antimicrobial Agents* 2014; **44**: 90–1.
391. Nordmann P, Boulanger AE, Poirel L. NDM-4 Metallo- β -Lactamase with Increased Carbapenemase Activity from *Escherichia coli*. *Antimicrobial Agents and Chemotherapy* 2012; **56**: 2184–6.
392. De Luca F, Benvenuti M, Carboni F, *et al.* Evolution to carbapenem-hydrolyzing activity in noncarbapenemase class D -lactamase OXA-10 by rational protein design. *Proceedings of the National Academy of Sciences* 2011; **108**: 18424–9.
393. Barnes MD, Winkler ML, Taracila MA, *et al.* *Klebsiella pneumoniae* Carbapenemase-2 (KPC-2), Substitutions at Ambler Position Asp179, and Resistance to Ceftazidime-Avibactam: Unique Antibiotic-Resistant Phenotypes Emerge from β -Lactamase Protein Engineering Bush K, ed. *mBio* 2017; **8**. Available at: <http://mbio.asm.org/lookup/doi/10.1128/mBio.00528-17>. Accessed February 4, 2019.
394. Petit A, Maveyraud L, Lenfant F, Samama JP, Labia R, Masson JM. Multiple substitutions at position 104 of beta-lactamase TEM-1: assessing the role of this residue in substrate specificity. *Biochem J* 1995; **305 (Pt 1)**: 33–40.
395. Bonnet R. Effect of D240G substitution in a novel ESBL CTX-M-27. *Journal of Antimicrobial Chemotherapy* 2003; **52**: 29–35.
396. Alba J, Ishii Y, Thomson K, Moland ES, Yamaguchi K. Kinetics Study of KPC-3, a Plasmid-Encoded Class A Carbapenem-Hydrolyzing β -Lactamase. *Antimicrob Agents Chemother* 2005; **49**: 4760–2.
397. Humphries RM, Yang S, Hemarajata P, *et al.* First Report of Ceftazidime-Avibactam Resistance in a KPC-3-Expressing *Klebsiella pneumoniae* Isolate. *Antimicrob Agents Chemother* 2015; **59**: 6605–7.
398. Shields RK, Potoski BA, Haidar G, *et al.* Clinical Outcomes, Drug Toxicity, and Emergence of Ceftazidime-Avibactam Resistance Among Patients Treated for Carbapenem-Resistant Enterobacteriaceae Infections. *Clin Infect Dis* 2016; **63**: 1615–8.
399. Giddins MJ, Macesic N, Annavajhala MK, *et al.* Successive Emergence of Ceftazidime-Avibactam Resistance through Distinct Genomic Adaptations in blaKPC-2-Harboring *Klebsiella pneumoniae* Sequence Type 307 Isolates. *Antimicrob Agents Chemother* 2018; **62**: e02101-17.
400. Both A, Büttner H, Huang J, *et al.* Emergence of ceftazidime/avibactam non-susceptibility in an MDR *Klebsiella pneumoniae* isolate. *J Antimicrob Chemother* 2017; **72**: 2483–8.
401. Gaibani P, Campoli C, Lewis RE, *et al.* In vivo evolution of resistant subpopulations of KPC-producing *Klebsiella pneumoniae* during ceftazidime/avibactam treatment. *J Antimicrob Chemother* 2018; **73**: 1525–9.
402. Holt HM, Gahrn-Hansen B, Bruun B. *Shewanella* algae and *Shewanella putrefaciens*: clinical and microbiological characteristics. *Clin Microbiol Infect* 2005; **11**: 347–52.
403. Naas T, Dortet L, Iorga B. Structural and Functional Aspects of Class A Carbapenemases. *Current Drug Targets* 2016; **17**: 1006–28.
404. Daiyasu H, Osaka K, Ishino Y, Toh H. Expansion of the zinc metallo-hydrolase family of the β -lactamase fold. *FEBS Letters* 2001; **503**: 1–6.
405. Baier F, Tokuriki N. Connectivity between catalytic landscapes of the metallo- β -lactamase

- superfamily. *J Mol Biol* 2014; **426**: 2442–56.
406. Pettinati I, Brem J, Lee SY, McHugh PJ, Schofield CJ. The Chemical Biology of Human Metallo- β -Lactamase Fold Proteins. *Trends in Biochemical Sciences* 2016; **41**: 338–55.
407. Hornsey M, Phee L, Wareham DW. A novel variant, NDM-5, of the New Delhi metallo- β -lactamase in a multidrug-resistant *Escherichia coli* ST648 isolate recovered from a patient in the United Kingdom. *Antimicrob Agents Chemother* 2011; **55**: 5952–4.
408. Liu Z, Li J, Wang X, *et al.* Novel Variant of New Delhi Metallo- β -lactamase, NDM-20, in *Escherichia coli*. *Front Microbiol* 2018; **9**: 248.
409. Liu L, Feng Y, McNally A, Zong Z. blaNDM-21, a new variant of blaNDM in an *Escherichia coli* clinical isolate carrying blaCTX-M-55 and rmtB. *J Antimicrob Chemother.* Available at: <https://academic-oup-com.gate2.inist.fr/jac/advance-article/doi/10.1093/jac/dky226/5038110>. Accessed June 25, 2018.
410. Tada T, Miyoshi-Akiyama T, Dahal RK, *et al.* NDM-8 metallo- β -lactamase in a multidrug-resistant *Escherichia coli* strain isolated in Nepal. *Antimicrob Agents Chemother* 2013; **57**: 2394–6.
411. Zou D, Huang Y, Zhao X, *et al.* A novel New Delhi metallo- β -lactamase variant, NDM-14, isolated in a Chinese Hospital possesses increased enzymatic activity against carbapenems. *Antimicrob Agents Chemother* 2015; **59**: 2450–3.
412. Oelschlaeger P, Pleiss J. Hydroxyl Groups in the $\beta\beta$ Sandwich of Metallo- β -lactamases Favor Enzyme Activity: Tyr218 and Ser262 Pull Down the Lid. *Journal of Molecular Biology* 2007; **366**: 316–29.
413. Bahr G, Vitor-Horen L, Bethel CR, Bonomo RA, González LJ, Vila AJ. Clinical Evolution of New Delhi Metallo- β -Lactamase (NDM) Optimizes Resistance under Zn(II) Deprivation. *Antimicrobial Agents and Chemotherapy* 2018; **62**: 10.
414. González LJ, Bahr G, Nakashige TG, Nolan EM, Bonomo RA, Vila AJ. Membrane anchoring stabilizes and favors secretion of New Delhi metallo- β -lactamase. *Nat Chem Biol* 2016; **12**: 516–22.
415. Romero E, Minard C, Benchekroun M, *et al.* Base-Mediated Generation of Ketenimines from Ynamides: Direct Access to Azetidinemines by an Imino-Staudinger Synthesis. *Chemistry – A European Journal* 2017; **23**: 12991–4.
416. Dortet L, Agathine A, Naas T, Cuzon G, Poirel L, Nordmann P. Evaluation of the RAPIDEC® CARBA NP, the Rapid CARB Screen® and the Carba NP test for biochemical detection of carbapenemase-producing Enterobacteriaceae. *J Antimicrob Chemother* 2015; **70**: 3014–22.
417. o'neill J. *TACKLING DRUG-RESISTANT INFECTIONS GLOBALLY: FINAL REPORT AND RECOMMENDATIONS, THE REVIEW ON ANTIMICROBIAL RESISTANCE.* 2016. Available at: https://solidarites-sante.gouv.fr/IMG/pdf/o_neill_3_final_report_.pdf.
418. Cassini A, Högberg LD, Plachouras D, *et al.* Attributable deaths and disability-adjusted life-years caused by infections with antibiotic-resistant bacteria in the EU and the European Economic Area in 2015: a population-level modelling analysis. *The Lancet Infectious Diseases* 2019; **19**: 56–66.
419. Cornaglia G, Rossolini GM. The emerging threat of acquired carbapenemases in Gram-negative bacteria. *Clin Microbiol Infect* 2010; **16**: 99–101.

Annexes

A GREATER THAN EXPECTED VARIABILITY AMONG OXA-48-LIKE CARBAPENEMASES

Saoussen Oueslati^{1,2,3}, Maria-Laura Dabos^{1,2,4}, Agustin Zavala^{1,2,4}, Bogdan I. Iorga^{4*}, Thierry Naas^{1,2,3*}

¹EA7361, Université Paris-Sud, Université Paris-Saclay, LabEx Lermite, Bacteriology-Hygiene Unit,
APHP, Hôpital Bicêtre, Le Kremlin-Bicêtre, France

²EERA "Evolution and Ecology of Resistance to Antibiotics" Unit, Institut Pasteur-APHP-Université Paris Sud, Paris, France

³Associated French National Reference Center for Antibiotic Resistance "Carbapenemase-producing Enterobacteriaceae"

⁴Institut de Chimie des Substances Naturelles, CNRS UPR 2301, Université Paris-Saclay, LabEx LERMIT, Gif-sur-Yvette, France

ABSTRACT

Background: OXA-48-like carbapenemases represent a major health concern given their difficult detection, their epidemic behavior and their propensity to modify their spectrum of hydrolysis through point mutations.

Objective: To get an extensive view on the current variability among OXA-48-like enzymes, we have retrieved all the sequences available from NCBI (National Center for Biotechnology Information).

Method: We carried out several BLAST (Basic Local Alignment Search Tool) searches in the NCBI's "nr" and "nr_env" databases (downloaded on December 20th, 2016) using known members of OXA-48-like subfamily as query.

Results: While 23 variants have assigned OXA-numbers, 62 novel alleles have been identified. They correspond to novel enzymes with mutations located in some cases within the conserved active site motives. The important number of novel variants identified by this study is of great interest, since it provides a more realistic assessment of OXA-48-like variants.

Conclusion: A large variety of OXA-48-like enzymes has been unraveled through our bioinformatic search for variants. The finding of OXA-48-like enzymes in environmental isolates may reflect the contamination by Enterobacteriaceae producing OXA-48-like enzymes and/or the presence of *Shewanella* spp. isolates.

Keywords: OXA-48, variability, variants.

REZUMAT

Introducere: Carbapenemazele OXA-48-like reprezintă o problemă majoră pentru sănătate, având în vedere detectarea lor dificilă, comportamentul epidemic și tendința lor de a-și modifica spectrul de hidroliză prin mutații punctiforme.

Obiectiv: Pentru a obține o imagine amplă asupra variabilității actuale a enzimelor OXA-48-like, am recuperat toate secvențele disponibile de la NCBI (National Center for Biotechnology Information).

Metodă: Am efectuat mai multe căutări BLAST (Basic Local Alignment Search Tool) în bazele de date „nr” și „nr_env” ale NCBI (descărcate pe 20 decembrie 2016), utilizând ca interogare membrii cunoscuți ai sub-familiei OXA-48.

Rezultate: În timp ce unui număr de 23 de variante li s-au atribuit numere OXA, au fost identificate 62 de alele noi. Acestea corespund noilor enzime cu mutații localizate în unele cazuri în cadrul motivelor conservate ale site-ului activ. Numărul important de variante noi identificate în acest studiu este de mare interes, deoarece oferă o evaluare mai realistă a variantelor de tip OXA-48-like.

Concluzie: O mare varietate de enzime OXA-48-like a fost descoperită în urma căutării bioinformatică a variantelor. Detectarea enzimelor OXA-48-like în izolate din mediu poate reflecta contaminarea cu Enterobacteriaceae producătoare de enzime OXA-48-like și/sau prezența de izolate *Shewanella* spp.

Cuvinte-cheie: OXA-48, variabilitate, variante.

*Corresponding author's:

Thierry Naas, Service de Bactériologie-Hygiène, Hôpital de Bicêtre, 78 rue du Général Leclerc, 94275 Le Kremlin-Bicêtre Cedex, France.

Tel: + 33 1 45 21 20 19. E-mail : thierry.naas@bct.aphp.fr;

Bogdan Iorga, Institut de Chimie des Substances Naturelles, CNRS UPR 2301, 1 avenue de la Terrasse, Bât. 27, 91198 Gif-sur-Yvette,

France. Tel : + 33 1 69 82 30 94. E-mail : bogdan.iorga@cnrs.fr

INTRODUCTION

In the last decade, the emergence of carbapenem-resistance in Gram-negatives has been observed worldwide, both in non-fermenters and in *Enterobacteriaceae* [1, 2]. The emergence of carbapenemase-producing *Enterobacteriaceae* (CPE) has become a major public health concern [1, 3]. Among these CPEs, OXA-48-producing *Enterobacteriaceae* have now widely disseminated throughout European countries and are identified on all continents [3, 4]. OXA-48 confers high-level resistance to penicillins, including temocillin, and hydrolyzes carbapenems at a low level, but spares extended-spectrum cephalosporins [5, 6]. OXA-48-like enzymes are Ambler class D enzymes, that belong to active-serine β -lactamases. According to the DBL (class D β -lactamase numbering scheme), oxacillinases possess a serine residue at position DBL 70 and a carbamoylated lysine at position DBL 73 [5, 7, 8]. The YGN (positions 144 to 146) and KTG (positions 216 to 218) motives are mostly conserved in oxacillinase sequences, the YGN motif being replaced by a FGN motif in several cases [5, 9]. The omega loop plays an interesting role in the function of the beta-lactamases: mutations in the “omega loop region” of a beta-lactamase can change its specific function and substrate profile, perhaps due to an important functional role of the correlated dynamics of the region [5]. A sign of the current spread of OXA-48-like enzymes is the identification of point mutant derivatives, differing by few amino acid substitutions or deletions. Most of these differences are located within the β 5- β 6 loop, which is important in the substrate specificity of OXA-48 [9-11].

Whereas some OXA-48-variants (mostly point mutant derivatives) have similar hydrolytic activities as compared to OXA-48 (OXA-181, OXA-204), others have slightly increased carbapenem-hydrolyzing activities (OXA-162) or slightly reduced carbapenem and temocillin hydrolyzing activities (OXA-232, OXA-244) [11, 12]. In contrast, variants presenting a four amino acid deletion within the β 5- β 6 loop (Table 1) such as OXA-163, OXA-247, OXA-405 have lost their carbapenem-hydrolytic activity but gained instead the capacity to hydrolyze expanded-

spectrum cephalosporins (Fig. 1, Table S1) [11, 13]. A comprehensive list of variants identified in clinical isolates can be found in the Beta-Lactamase DataBase (<http://bldb.eu/alignment.php?align=D:OXA-48-like>).

Twenty-two OXA-48 variants have been described, most of them from enterobacterial isolates, and have been assigned an OXA-number initially by Lahey Clinic (<http://www.lahey.org/Studies/other.asp>), and now by the Bacterial Antimicrobial Resistance Reference Gene Database at NCBI (<https://www.ncbi.nlm.nih.gov/bioproject/313047>). *Shewanella* species have been suggested as the reservoir of *bla*_{OXA-48} type oxacillinase genes [14]. This is the case for OXA-54 from *S. oneidensis* as it shares significant amino acid sequence identity with OXA-48. *Shewanella xianemensis* has recently been identified as the progenitor of OXA-181, OXA-48, and OXA-204 [15, 16]. However, this is not the case for all *Shewanella* species, since *S. algae* produces OXA-55, which has only 57% sequence identity with OXA-48 [14]. Several natural variants (7/23) have been described in *Shewanella* sp. isolates and have been assigned an OXA number. For these variants, kinetic data are not always available [7].

With the high throughput sequencing of many bacterial genomes, and the tremendous amount of metagenomic sequencing data, the available bacterial DNA sequences increase exponentially in the databases. In many cases, these sequence entries have not been carefully analyzed in respect to β -lactamase gene content. In this study, we have searched for the presence of OXA-48-like enzymes in these genomic and metagenomic sequence databases.

MATERIAL AND METHODS

We carried out several BLAST searches in the NCBI’s “nr” and “nr_env” databases (downloaded on December 20th, 2016) using known members of OXA-48-like subfamily as query.

ClustalW was used to align the protein sequences of the identified novel chromosomally- and plasmid-encoded OXA-48-like β -lactamases with those already published, and Dendroscope was used to construct a phylogram [17, 18]. The references of all these enzymes can be found in the Beta-

Table 1. Sequence alignment for the OXA-48-like subfamily of class D β -lactamases. Only the sequences and the positions with mutations or deletions from loop β 5- β 6 are shown. The complete alignment can be found in the Beta-Lactamase DataBase at <http://bldb.eu/alignment.php?align=D:OXA-48-like> [7]

DBL ^a AA numbering scheme	219 ^c	220	224	225	226	227	228	229	230
OXA-48 AA numbering ^b	211	212	213	214	215	216	217	218	219
OXA-48	Y	S	T	R	I	E	P	K	I
OXA-54								Q	
OXA-162			A						
OXA-163, OXA-439		- ^d	-	-	-	D	T		
OXA-232				S					
OXA-244, OXA-484				G					
OXA-247	S	-	-	-	-	N	T		
OXA-370		E							
OXA-405		-	-	-	-	S			
OXA-436			V						
OXA-438		G	Y	-	-	D	T		
OXA-538			G						F
OXA-D281, OXA-D282, OXA-D284			V						
OXA-D303	C								
OXA-D312		P							
OXA-D340					V				

^a Class D β -lactamase numbering scheme [5, 8];

^b OXA-48 specific numbers. Numbers in bold correspond to residues of the β 5- β 6 loop ;

^c Only the sequences and the positions with mutations or deletions from loop β 5- β 6 are shown. The complete alignment can be found in the Beta-Lactamase DataBase at <http://bldb.eu/alignment.php?align=D:OXA-48-like>

^d - indicates a deletion.

Lactamase DataBase at <http://bldb.eu/BLDB.php?class=D#OXA> [7]; (b) Sequence of OXA-48; (c) Three-dimensional structure of OXA-48 (PDB 3HBR). Active site serine 70 is colored in green, and the residues from loop β 5- β 6 are colored with different shades of blue.

RESULTS-DISCUSSION

In this way, we could identify, along with the known 23 members of the OXA-48-like subfamily (enzymes with an assigned OXA-name), 62 novel OXA-48-like variants (displaying at least one point mutation to any of the 23 known variants) belonging to the OXA-48-like subfamily, and thus that are not present in the Bacterial Antimicrobial Resistance Reference Gene Database (<https://www.ncbi.nlm.nih.gov/bioproject/313047>).

No OXA-number has been assigned to these variants, since most of them were not isolated in clinical settings and their identification was primarily based on *in silico* analysis. These variants have been added to the BLDB database, as OXA-D type enzymes followed by a number, while waiting for a definitive assignment by NCBI. These novel variants show >90% sequence identity as compared with OXA-48. The nucleotide and protein sequences along with their GenBank accession numbers can be found in the Beta-Lactamase DataBase (<http://bldb.eu/BLDB.php?class=D#OXA>) [7].

Among the sequences presented in Table S1, 2 were retrieved from dye-degrading bacteria [17, 18], 7 from *Shewanella* sp., and 43 from uncultured bacteria.

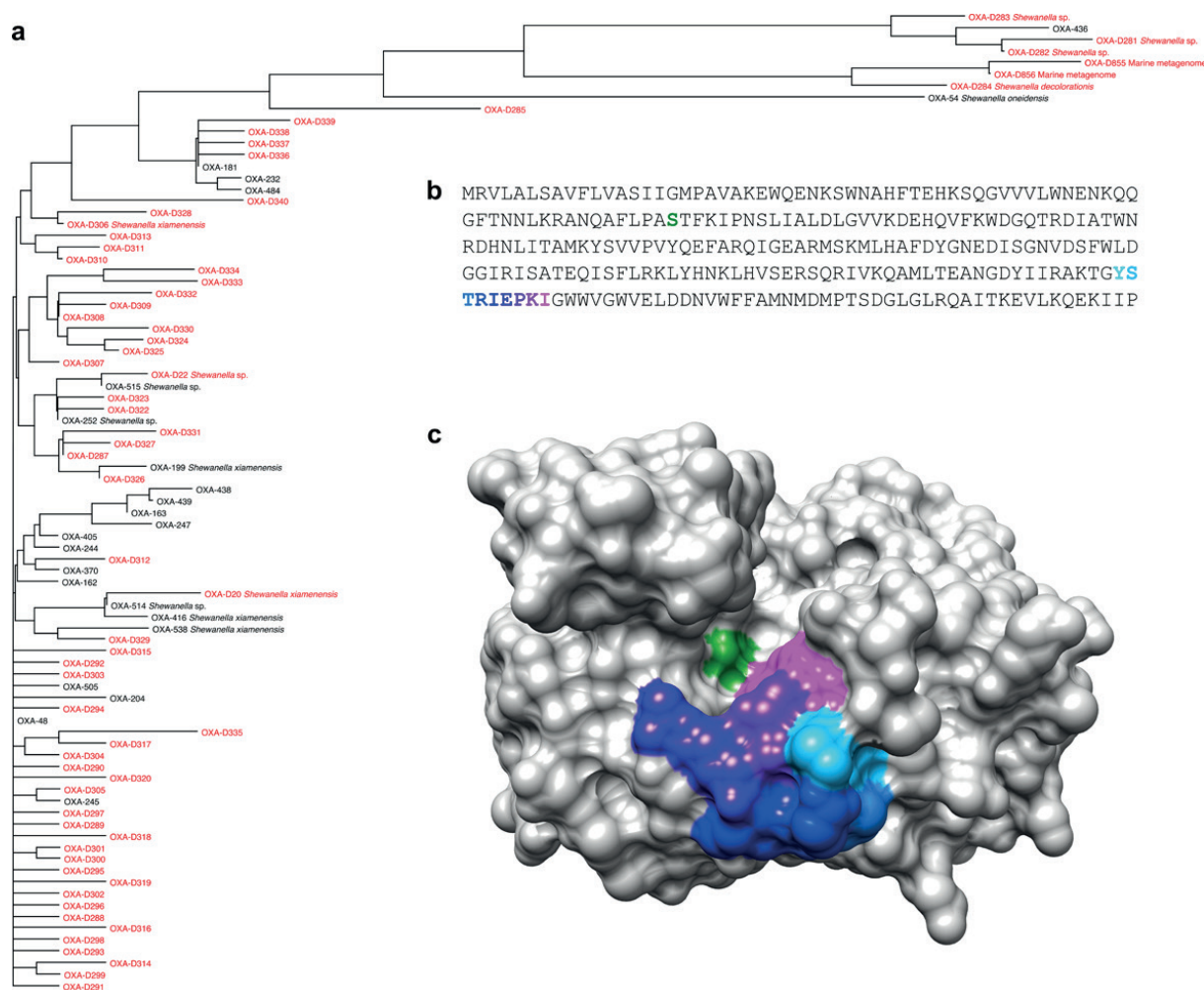


Fig. 1. (a) Phylogeny of the chromosomally- and plasmid-encoded class D β -lactamases belonging to the OXA-48-like subfamily. For naturally-occurring enzymes, the bacterial host name is indicated. The alleles identified in this study are colored in red. The phylogram was constructed with Dendroscope using ClustalW aligned protein sequences [19, 20]. The references of all these enzymes can be found in the Beta-Lactamase DataBase at <http://bldb.eu/BLDB.php?class=D#OXA> [7]; (b) Sequence of OXA-48; (c) Three-dimensional structure of OXA-48 (PDB 3HBR). Active site serine 70 is colored in green, and the residues from loop β 5- β 6 are colored with different shades of blue.

Among the 62 novel variants a great variability has been observed differing by one up to 24 amino-acids (Fig. 1). The most distantly related variants are close to OXA-436, a carbapenemase responsible of an outbreak in Denmark. The amino acid changes are scattered all over the sequence, but some are located within the conserved regions of class D enzymes (represented as boxes in the Supplementary Information file), and thus are likely to generate altered phenotypes. For instance, the F72I change in OXA-D320, which is located next to the S70 and the K73 may impact the activity of the enzyme. Similarly, Y144C and N146S, found in OXA-D319 and

D338, respectively, are located within the YGN motif. A Y to F change is responsible of NaCl resistance of oxacillinases, as shown for OXA-40 [9].

The T217A change is located within the highly conserved KTG box. This threonine has been replaced by serine in OXA-40 without effect on hydrolysis, but the effect of an alanine in this position has not been addressed [9].

Finally, three novel variants were found with changes in the β 5- β 6 loop. The T221V as found in OXA-D281, -D282, and -D284 may have increased hydrolysis as shown for OXA-162, even though in the latter the T was replaced by A [11]. The S220P (OXA-D312)

may alter significantly the loop conformation, which would likely induce a drastic effect on the activity of the enzyme. The I226V is likely silent in terms of activity, as we have recently shown that I226A replacement does not alter the activity of the enzyme (T. Naas, personal communication).

CONCLUSION

Genomic and metagenomics data turn to be an inestimable source for discovering novel resistance gene or derivatives of known genes. In most cases, the reasons these genomic or metagenomics data were generated were not linked to antibiotic resistance studies. A large variety of OXA-48-like enzymes has been unraveled through our bioinformatic search for variants. The finding of OXA-48-like enzymes in environmental isolates may reflect the contamination by Enterobacteriaceae producing OXA-48-like enzymes and/or the presence of *Shewanella spp.* isolates. The important number of novel variants identified by this study is of great interest, since it provides a more realistic assessment of OXA-48-like variants. The finding of some amino-acid changes in the key boxes or the β 5- β 6 loop, suggests likely changes in hydrolysis profile. Further work will be necessary to address these issues.

Acknowledgements

This work was funded by a grant from the Ministère de l'Éducation Nationale et de la Recherche (EA7361), Université Paris Sud, by the Région Ile-de-France (DIM Malinf) and by the Laboratory of Excellence LERMIT supported by a grant from ANR (ANR-10-LABX-33).






Conflict of interests: None to declare.

REFERENCES

- Logan LK, Weinstein RA. The Epidemiology of Carbapenem-Resistant Enterobacteriaceae: The Impact and Evolution of a Global Menace. *J Infect Dis.* 2017;215:S28-S36.
- Gniadek TJ, Carroll KC, Simner PJ. Carbapenem-Resistant Non-Glucose-Fermenting Gram-Negative Bacilli: the Missing Piece to the Puzzle. *J Clin Microbiol.* 2016;54:1700-10.
- Albiger B, Glasner C, Struelens MJ, Grundmann H, Monnet DL; European Survey of Carbapenemase-Producing Enterobacteriaceae (EuSCAPE) working group. Carbapenemase-producing Enterobacteriaceae in Europe: assessment by national experts from 38 countries. *Euro Surveill.* 2015;20 (45).
- Dortet L, Cuzon G, Ponties V, Nordmann P. Trends in carbapenemase-producing Enterobacteriaceae, France, 2012 to 2014. *Euro Surveill.* 2017;22(6). pii:30461.
- Poirel L, Naas T, Nordmann P. Diversity, epidemiology, and genetics of class D β -lactamases. *Antimicrob. Agents Chemother.* 2010;54:24-38.
- Aubert D, Naas T, Héritier C, Poirel L, Nordmann P. Functional characterization of IS1999, an IS4 family element involved in mobilization and expression of beta-lactam resistance genes. *J Bacteriol.* 2006;188:6506-14.
- Naas T, Oueslati S, Bonnin RA, Dabos ML, Zavala A, Dortet L et al. Beta-lactamase database (BLDB) - structure and function. *J Enzyme Inhib Med Chem.* 2017;32:917-919.
- Couture F, Lachapelle J, Levesque RC. Phylogeny of LCR-1 and OXA-5 with class A and class D beta-lactamases. *Mol Microbiol* 1992;6:1693-1705.
- Heritier C, Poirel L, Aubert D, Nordmann P. Genetic and functional analysis of the chromosome-encoded carbapenem-hydrolyzing oxacillinase OXA-40 of *Acinetobacter baumannii*. *Antimicrob Agents Chemother* 2003; 47:268-273.
- Docquier JD, Calderone V, De Luca F, Benvenuti M, Giuliani F, Bellucci L, et al. Crystal structure of the OXA-48 beta-lactamase reveals mechanistic diversity among class D carbapenemases. *Chem Biol.* 2009;16:540-547.
- Oueslati S, Nordmann P, Poirel L. Heterogeneous hydrolytic features for OXA-48-like β -lactamases. *J Antimicrob Chemother.* 2015;70:1059-63.
- Hoyos-Mallecot Y, Naas T, Bonnin RA, Patino R, Glaser P, Fortineau N, et al. OXA-244-Producing *Escherichia coli* Isolates, a Challenge for Clinical Microbiology Laboratories. *Antimicrob Agents Chemother.* 2017;61. pii:e00818-17.
- Dortet L, Oueslati S, Jeannot K, Tandé D, Naas T, Nordmann P. Genetic and biochemical characterization of OXA-405, an OXA-48-type extended-spectrum β -lactamase without significant carbapenemase activity. *Antimicrob Agents Chemother.* 2015;59:3823-8.
- Poirel L, Potron A, Nordmann P. OXA-48-

- like carbapenemases: the phantom menace. *J. Antimicrob. Chemother.* 2012;67:1597–1606
15. Potron A, Poirel L, Nordmann P. Origin of OXA-181, an emerging carbapenem-hydrolyzing oxacillinase, as a chromosomal gene in *Shewanella xiamenensis*. *Antimicrob Agents Chemother.* 2011;55:4405-7.
 16. Tacão M, Correia A, Henriques I. Environmental *Shewanella xiamenensis* strains that carry blaOXA-48 or blaOXA-204 genes: additional proof for blaOXA-48-like gene origin. *Antimicrob Agents Chemother.* 2013;57:6399-400.
 17. Xu M, Fang Y, Liu J, Chen X, Sun G, Guo J, et al. Draft genome sequence of *Shewanella decolorationis* S12, a dye-degrading bacterium isolated from a wastewater treatment plant. *Genome Announc.* 2013;1:e00993-00913.
 18. Li Y, Ng IS, Zhang X, Wang N. Draft genome sequence of the dye-decolorizing and nanowire-producing bacterium *Shewanella xiamenensis* BC01. *Genome Announc.* 2014;2:e00721-00714.
 19. Huson DH, Scornavacca C. Dendroscope 3: An interactive tool for rooted phylogenetic trees and networks. *Syst. Biol.* 2012;6:1061-1067.
 20. Larkin MA, Blackshields G, Brown NP, Chenna R, McGettigan PA, McWilliam H, et al. Clustal W and Clustal X version 2.0. *Bioinformatics* 2007;23:2947-2948

Beta-lactamase database (BLDB) – structure and function

Thierry Naas^a , Saoussen Oueslati^a, Rémy A. Bonnin^a , Maria Laura Dabos^{a,b}, Agustin Zavala^{a,b}, Laurent Dortet^a , Pascal Retailleau^b  and Bogdan I. Iorga^b 

^aService de Bactériologie-Hygiène, Hôpital de Bicêtre, AP-HP, EA7361, Université et Faculté de Médecine Paris-Sud, LabEx LERMIT, Le Kremlin-Bicêtre, France; ^bInstitut de Chimie des Substances Naturelles, CNRS UPR 2301, Université Paris-Saclay, LabEx LERMIT, Gif-sur-Yvette, France

ABSTRACT

Beta-Lactamase Database (BLDB) is a comprehensive, manually curated public resource providing up-to-date structural and functional information focused on this superfamily of enzymes with a great impact on antibiotic resistance. All the enzymes reported and characterised in the literature are presented according to the class (A, B, C and D), family and subfamily to which they belong. All three-dimensional structures of β -lactamases present in the Protein Data Bank are also shown. The characterisation of representative mutants and hydrolytic profiles (kinetics) completes the picture and altogether these four elements constitute the essential foundation for a better understanding of the structure-function relationship within this enzymes family. BLDB can be queried using different protein- and nucleotide-based BLAST searches, which represents a key feature of particular importance in the context of the surveillance of the evolution of the antibiotic resistance. BLDB is available online at <http://blldb.eu> without any registration and supports all modern browsers.

ARTICLE HISTORY

Received 2 May 2017
Revised 8 June 2017
Accepted 11 June 2017

KEYWORDS

Database; beta-lactamase; antibiotic resistance; hydrolytic profile; mutant

Introduction

β -Lactams, due to their safety, reliable killing properties and clinical efficacy, are among the most frequently prescribed antibiotics used to treat bacterial infections. However, their utility is being threatened by the worldwide proliferation of β -lactamases (BLs) with broad hydrolytic capabilities, especially in multi-drug-resistant gram-negative bacteria. These BLs are divided into four classes based on their sequence identities¹. While a handful of BLs were known in the early 1970s, their number has ever since been growing rapidly, especially with the description in clinical isolates of novel enzymes being capable of hydrolysing carbapenems, last resort antibiotics². A representative example is the class A KPC-2 that in a few years became one of the most menacing BL currently spreading worldwide³.

Historically, the principal resource of BLs was maintained from 2001 at the Lahey Clinic (<http://www.lahey.org/Studies/>) by George Jacoby and Karen Bush, by assigning new enzyme numbers for a number of representative BL families. From July 2015, this resource was transferred into the Bacterial Antimicrobial Resistance Reference Gene Database (<https://www.ncbi.nlm.nih.gov/bioproject/313047/>) maintained at the NCBI. Other resources are the Institute Pasteur MLST Database (<http://bigsdbs.pasteur.fr/klebsiella/klebsiella.html>), the Antibiotic Resistance Genes Database⁴, the Lactamase Engineering Database^{5,6}, the Metallo- β -Lactamase Engineering Database⁷, the Comprehensive Antibiotic Resistance Database⁸, the β -Lactamase Database⁹, the Comprehensive β -Lactamase Molecular Annotation Resource¹⁰. However, most of these databases are either not maintained

anymore, have a very broad scope or are focused on a few BL families.

The aim of our *Beta-Lactamase Database (BLDB)* is to compile sequence information as well as biochemical and structural data on all the currently known BLs. This comprehensive web-based database, which is updated on a weekly basis, may provide at a glance useful insights in the structure-function relationships of BLs, allowing a better understanding of substrate specificities and key residues involved in substrate recognition and hydrolysis. Altogether, the information provided by BLDB may help to foresee the impact of future mutations on the evolution of BLs.





Implementation details


The database is hosted on a dedicated virtual server in the cloud, which allows easy adjustments and evolution of computing resources according to the needs.

The core pages are implemented in PHP on a Linux Server under the CentOS 7.2 operating system, whereas the raw data is stored as tabulated files in order to facilitate the updates.

The interactive images showing the list of BL families that are present in the BLDB are generated dynamically in SVG format from the raw data, thus ensuring an updated display at any time. The corresponding URL links are directly embedded in the SVG images.

Multiple sequence alignments are automatically generated with Clustal Omega¹¹ using the default parameters. Phylogenetic trees are processed using Phylip version 3.695

CONTACT Thierry Naas  thierry.naas@aphp.fr  Service de Bactériologie-Hygiène, Hôpital de Bicêtre, AP-HP, EA7361, Université et Faculté de Médecine Paris-Sud, LabEx LERMIT, Le Kremlin-Bicêtre, France; Bogdan I. Iorga  bogdan.iorga@cnrs.fr  Institut de Chimie des Substances Naturelles, CNRS UPR 2301, Université Paris-Saclay, LabEx LERMIT, Gif-sur-Yvette, France

 Supplemental data for this article can be accessed [here](#).

© 2017 The Author(s). Published by Informa UK Limited, trading as Taylor & Francis Group.

This is an Open Access article distributed under the terms of the Creative Commons Attribution License (<http://creativecommons.org/licenses/by/4.0/>), which permits unrestricted use, distribution, and reproduction in any medium, provided the original work is properly cited.

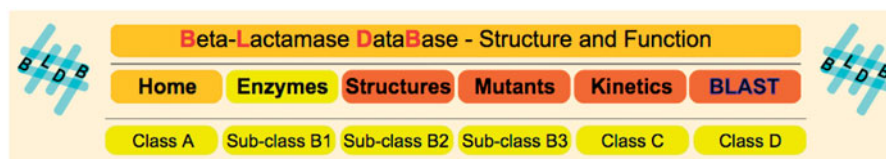


Figure 1. Global architecture of the Beta-Lactamase Database. In addition to the *Home page*, there are five main sections, dedicated to *Enzymes* (classified into the four classes A, B, C and D, and further into the three sub-classes of class B), three-dimensional *Structures* available in the Protein Data Bank, synthetic *Mutants* and hydrolytic profiles (*Kinetics*) described in the literature, and a graphical interface for *BLAST* queries.

(<http://evolution.genetics.washington.edu/phylip/>) using Clustal Omega's *DND* output files and represented as *SVG* images to provide the best quality and minimal file size.

The radar charts representing hydrolytic profiles are dynamically built using a modified and personalised version of the *D3.js* JavaScript library (<https://gist.github.com/nbremer/6506614>).

The BLAST interface is provided by SequenceServer¹² and the BLAST+ binaries are downloaded from NCBI¹³.

Input data is downloaded from NCBI using the "Entrez Direct: E-utilities on the UNIX Command Line"¹³ and from the PDB with personalised scripts.

Structures are updated semi-automatically on a weekly basis, after each PDB update. New enzymes are added following every update of the Bacterial Antimicrobial Resistance Reference Gene Database. Constant literature survey also provides newly described BLs and synthetic mutants, as well as their hydrolytic profiles. The long-term maintenance of the BLDB is ensured by the collaboration between two academic teams with active interest and experience in the field of BL-mediated antibiotic resistance.

Database architecture

BLDB is designed around five main sections, which are strongly interconnected and gathered around the main home page (Figure 1). All pages contain (i) a header showing the overall structure of the BLDB, with links for an easy access to all sections at any moment, and (ii) a footer with acknowledgments to funding bodies that have contributed to this project and with contact details.

Home page

A short introduction to the present challenges associated with the antibiotic resistance is presented, highlighting the important contribution provided by the BLDB in this field.

Real-time statistics with the number of entries for each type of data present in the BLDB (*Enzymes*, *Structures*, *Mutants* and *Kinetics*) and for each one of the four classes of BL are also provided. The entries corresponding to the subclasses B1, B2 and B3 of class B are further detailed, for a better presentation of their similarities and differences (Figure S1).

Enzymes

The *Enzymes* tab of the main menu gives access to a list of classes and sub-classes of BLs, together with their corresponding BL families (Figure S3). This is represented as an *SVG* image that is dynamically generated from the raw data, which always ensures up-to-date information.

Each entry of a given BL family contains the class, protein name and eventually alternative names. When the family features several clearly defined sub-families, this information is also present. GenPeptID and GenBankID (with a RefSeq number when provided by NCBI) are also provided, with the corresponding links on the NCBI's website for more detailed information. Bibliographic

data (PubMedID, DOI), functional (phenotype, hydrolytic profile) and genetic (natural or acquired type) information and links to the other sections are also provided (Figure S2).

Sequence alignments are provided for each class, subclass, family and subfamily (Figure S4), together with the corresponding phylogenetic tree (Figure S5).

Structures

The *Structures* tab gives access to a table containing all three-dimensional structures of BLs reported in the Protein Data Bank¹⁴. Each entry contains the name of BL, together with the class or sub-class to which it belongs, followed by the PDB code and resolution (if applicable). The protein sequence is linked to the corresponding UniProt entry and, if appropriate, the existing mutations (extracted from the PDB file content) are shown. Bibliographic data (PubMedID, DOI) allows an easy retrieval of the original articles associated with the structure through links to PubMed and to the journal website. All ligands, buffer molecules and ions present in the structures are highlighted, together with their interaction mode with the protein (non-covalent, covalent, metal coordination). For all these molecules, links to their corresponding dedicated page on the PDB website are provided. Crystallographic details (space group, unit cell parameters, Z-value) are also presented, in order to facilitate the resolution of new structures and to allow an easy comparison of the existing ones (Figure S6).

Mutants

The synthetic mutants that were described for each enzyme in the literature are presented, together with bibliographical information (PubMedID, DOI) and links to PDB structures and hydrolytic profiles when appropriate (Figure S7). Given the very important number of synthetic mutants described to date, the present version of the BLDB is not complete. More mutants will be added in the near future.

Kinetics (hydrolytic profiles)

This section is organised in two parts: (i) a table containing the hydrolytic profiles on different β -lactam antibiotics, with values for the turnover number (k_{cat}), the Michaelis constant (K_m) and the catalytic efficiency (k_{cat}/K_m) (Figure S8); (ii) a radar chart representing a superposition of hydrolytic profiles selected for easier comparison (Figure S9). The number of hydrolytic profiles currently available in the BLDB is relatively modest, and more entries are scheduled to be added in the near future.

BLAST

Protein- and nucleotide-based BLAST search capabilities of BLDB are implemented using a personalised version of the SequenceServer graphical interface¹². The input sequence type (protein or nucleotide) is automatically detected, and the BLAST search type is adapted accordingly. Advanced parameters can be

used for the BLAST search in order to obtain more refined results (Figure S10).

The BLAST search is executed using the default parameters and the results are shown using a personalised interface, with the name of BL highlighted in red and links to the corresponding entries on the NCBI's website. The number of identical residues between the query and each sequence producing a significant alignment is provided, together with the percentage of identity (Figure S11). Together with the E-value, this represents useful information for a quick assessment of the BLAST results. A percentage of 100.00% means that the input sequence is already present in the BLDB, whereas a high sequence identity points out towards the BL class and/or family to which the input sequence might belong.

In the lower part of the results page, the alignments between the query and sequences producing significant alignments are provided (Figure S12).

Initial content

As of 25 April 2017, BLDB contains 2666 unique enzymes from all four classes of BLs, as well as 810 three-dimensional structures of BLs that are currently available in the Protein Data Bank (PDB)¹⁴. BLDB also contains 167 mutants and 47 hydrolytic profiles.

Conclusion

BLDB is developed and maintained by two well-established research groups that are active in the field of BL-mediated antibiotic resistance. This resource is designed to provide appropriate answers to the needs of the research and clinical communities working on antimicrobial resistance.

Acknowledgements

The technical support provided by Olivia Inocénté and Gatien Tafforeau is gratefully acknowledged.

Disclosure statement

No potential conflict of interest was reported by the authors.

Funding

This work was supported by the Laboratory of Excellence in Research on Medication and Innovative Therapeutics (LERMIT) [grant number ANR-10-LABX-33], by the JPIAMR transnational project DesInMBL [grant number ANR-14-JAMR-0002] and by the Région Ile-de-France (DIM Malinf).

ORCID

Thierry Naas  <http://orcid.org/0000-0001-9937-9572>
 Rémy A. Bonnin  <http://orcid.org/0000-0002-2307-3232>
 Laurent Dortet  <http://orcid.org/0000-0001-6596-7384>
 Pascal Retailleau  <http://orcid.org/0000-0003-3995-519X>
 Bogdan I. Iorga  <http://orcid.org/0000-0003-0392-1350>

References

1. Bonomo RA. β -Lactamases: a focus on current challenges. *Cold Spring Harb Perspect Med* 2017;7:a025239.
2. Nordmann P, Naas T, Poirel L. Global spread of Carbapenemase-producing Enterobacteriaceae. *Emerg Infect Dis* 2011;17:1791–8.
3. Naas T, Dortet L, Iorga BI. Structural and functional aspects of class A carbapenemases. *Curr Drug Targets* 2016;17:1006–28.
4. Liu B, Pop M. ARDB – Antibiotic Resistance Genes Database. *Nucleic Acids Res* 2009;37:D443–7.
5. Thai QK, Bös F, Pleiss J. The Lactamase Engineering Database: a critical survey of TEM sequences in public databases. *BMC Genomics* 2009;10:390.
6. Thai QK, Pleiss J. SHV Lactamase Engineering Database: a reconciliation tool for SHV β -lactamases in public databases. *BMC Genomics* 2010;11:563.
7. Widmann M, Pleiss J, Oelschlaeger P. Systematic analysis of metallo- β -lactamases using an automated database. *Antimicrob Agents Chemother* 2012;56:3481–91.
8. McArthur AG, Waglechner N, Nizam F, et al. The comprehensive antibiotic resistance database. *Antimicrob Agents Chemother* 2013;57:3348–57.
9. Danishuddin M, Hassan Baig M, Kaushal L, Khan AU. BLAD: a comprehensive database of widely circulated β -lactamases. *Bioinformatics* 2013;29:2515–16.
10. Srivastava A, Singhal N, Goel M, et al. CBMAR: a comprehensive β -lactamase molecular annotation resource. *Database (Oxford)* 2014;2014:bau111.
11. Sievers F, Wilm A, Dineen D, et al. Fast, scalable generation of high-quality protein multiple sequence alignments using Clustal Omega. *Mol Syst Biol* 2011;7:539.
12. Priyam A, Woodcroft BJ, Rai V, et al. Sequenceserver: a modern graphical user interface for custom BLAST databases. 2015:bioRxiv 033142. doi: <https://doi.org/10.1101/033142>
13. Agarwala R, Barrett T, Beck J, et al. Database resources of the National Center for Biotechnology Information. *Nucleic Acids Res* 2016;44:D7–19.
14. Berman HM, Westbrook J, Feng Z, et al. The Protein Data Bank. *Nucleic Acids Res* 2000;28:235–42.



False-Positive Carbapenem-Hydrolyzing Confirmatory Tests Due to ACT-28, a Chromosomally Encoded AmpC with Weak Carbapenemase Activity from *Enterobacter kobei*

Agnès B. Jousset,^{a,b,c,d} Saoussen Oueslati,^{b,d} Sandrine Bernabeu,^{a,b,c,d} Julie Takissian,^b Elodie Creton,^c Anaïs Vogel,^c Aimie Sauvadet,^c Garance Cotellon,^c Lauraine Gauthier,^{a,b,c,d} Rémy A. Bonnin,^{b,c,d} Laurent Dortet,^{a,b,c,d}  Thierry Naas^{a,b,c,d}

^aBacteriology-Hygiene Unit, Assistance Publique/Hôpitaux de Paris, Bicêtre Hospital, Le Kremlin-Bicêtre, France

^bEA 7361 (Structure, dynamic, function and expression of broad spectrum β -lactamases), Faculty of Medicine University Paris-Sud, University Paris-Saclay, Le Kremlin-Bicêtre, France

^cFrench National Reference Center for Antibiotic Resistance: Carbapenemase Producing Enterobacteriaceae, Le Kremlin-Bicêtre, France

^dJoint Research Unit EERA (Evolution and Ecology of Resistance to Antibiotics), Institut Pasteur-APHP-University Paris Sud, Paris, France

ABSTRACT In *Enterobacter cloacae* complex (ECC), the overproduction of the chromosome-encoded cephalosporinase (cAmpC) associated with decreased outer membrane permeability may result in carbapenem resistance. In this study, we have characterized ACT-28, a cAmpC with weak carbapenemase activity, from a single *Enterobacter kobei* lineage. ECC clinical isolates were characterized by whole-genome sequencing (WGS), susceptibility testing, and MIC, and carbapenemase activity was monitored using diverse carbapenem hydrolysis methods. ACT-28 steady-state kinetic parameters were determined. Among 1,039 non-carbapenemase-producing ECC isolates with decreased susceptibility to carbapenems received in 2016-2017 at the French National Reference Center for antibiotic resistance, only 8 had a positive carbapenemase detection test (Carba NP). These eight ECC isolates were resistant to broad-spectrum cephalosporins due to AmpC derepression, showed decreased susceptibility to carbapenems, and were categorized as carbapenemase-producing *Enterobacteriaceae* (CPE) according to several carbapenemase detection assays. WGS identified a single clone of *E. kobei* ST125 expressing only its cAmpC, ACT-28. The *bla*_{ACT-28} gene was expressed in a wild-type and in a porin-deficient *Escherichia coli* background and compared to the *bla*_{ACT-1} gene. Detection of carbapenemase activity was positive only for *E. coli* expressing the *bla*_{ACT-28} gene. Kinetic parameters of purified ACT-28 revealed a slightly increased imipenem hydrolysis compared to that of ACT-1. *In silico* porin analysis revealed the presence of a peculiar AmpC-like protein specific to *E. kobei* ST125 that could impair carbapenem influx into the periplasm and thus enhance carbapenem-resistance caused by ACT-28. We described a widespread lineage of *E. kobei* ST125 producing ACT-28, with weak carbapenemase activity that can lead to false-positive detection by several biochemical and phenotypic diagnostic tests.

KEYWORDS AmpC, carbapenem hydrolysis, cephalosporinase, dissemination

Enterobacter cloacae complex (ECC) organisms are highly adapted to the hospital environment and are mostly responsible for hospital-acquired infections such as intravenous-catheter-related bacteremia, urinary tract infections (UTIs), and pulmonary infections (1). The ECC shows a genomic heterogeneity with 13 clusters based on their *hsp60* sequences (2) and currently comprises seven different species (3): *Enterobacter asburiae*, *E. cloacae*, *Enterobacter hormaechei*, *Enterobacter kobei*, *Enterobacter ludwigii*, *Enterobacter mori*, and *Enterobacter xiangfangensis*.

Enterobacter spp. naturally exhibit resistance to aminopenicillins, first- and second-

Citation Jousset AB, Oueslati S, Bernabeu S, Takissian J, Creton E, Vogel A, Sauvadet A, Cotellon G, Gauthier L, Bonnin RA, Dortet L, Naas T. 2019. False-positive carbapenem-hydrolyzing confirmatory tests due to ACT-28, a chromosomally encoded AmpC with weak carbapenemase activity from *Enterobacter kobei*. *Antimicrob Agents Chemother* 63:e02388-18. <https://doi.org/10.1128/AAC.02388-18>.

Copyright © 2019 American Society for Microbiology. All Rights Reserved.

Address correspondence to Thierry Naas, thierry.naas@aphp.fr.

Received 9 November 2018

Returned for modification 6 December 2018

Accepted 12 February 2019

Accepted manuscript posted online 19 February 2019

Published 25 April 2019

TABLE 1 MICs of β -lactams for *E. kobei* ST125 and transformants^a

Drug	MIC ($\mu\text{g/ml}$)						
	<i>E. kobei</i> (ACT-28 chr)	<i>E. coli</i> TOP10 (pTOPO-ACT-28)	<i>E. coli</i> TOP10 (pTOPO-ACT-1)	<i>E. coli</i> TOP10	<i>E. coli</i> HB4- (pTOPO-ACT-28)	<i>E. coli</i> HB4- (pTOPO-ACT-1)	<i>E. coli</i> HB4
Ticarcillin	>256	>256	>256	2	>256	>256	4
Cefoxitin	>256	>256	>256	2	>256	>256	256
Cefotaxime	>32	>32	>32	0.06	>32	>32	0.38
Ceftazidime	>256	>256	>256	0.12	>256	>256	4
Cefepime	0.5	0.25	0.25	0.06	6	2	0.75
Ertapenem	0.5	0.125	0.125	0.003	>32	>32	1
Meropenem	0.25	0.047	0.06	0.016	>32	>32	0.25
Imipenem (Etest)	0.75	0.5	0.5	0.25	>32	12	0.25
Imipenem (BMD)	ND	ND	ND	ND	>128	64	ND

^aBMD, broth microdilution; ND, not determined.

generation cephalosporins, by the production of an inducible chromosomally encoded Ambler class C β -lactamase (cAmpC) characterized by its ability to hydrolyze cephalosporins without being inhibited by clavulanic acid or tazobactam (4). In *Enterobacter* spp., resistance to broad-spectrum cephalosporins can occur through acquisition of an extended-spectrum β -lactamase (ESBL) or by chromosomal mutations, mostly in *ampD* or in *ampR*, that lead to cAmpC derepression (5). Resistance to carbapenems in *Enterobacter* spp. can arise by acquisition of carbapenemases (mostly KPC, NDM, VIM, IMP, or OXA-48-like). However, alteration or loss of nonspecific porins, leading to outer membrane permeability defect, associated with overproduction of the natural AmpC and/or production of an ESBL is the most common mechanism (6).

cAmpC β -lactamases, through different genetic elements, may be mobilized on plasmids that may be acquired by *Enterobacteriaceae* that are not expected to produce an AmpC β -lactamase (7). Some of these plasmid-encoded AmpC (pAmpC) β -lactamases displayed a slight carbapenemase activity, such as CMY-10, CMY-2, and, to a lesser extent, ACT-1, as revealed by kinetic studies (8, 9). To date, no cAmpC has been proved to hydrolyze carbapenems in *Enterobacteriaceae*.

Here we describe a single *E. kobei* lineage capable of hydrolyzing imipenem, only due to the expression of a novel cAmpC β -lactamase called ACT-28. Whole-genome sequencing (WGS), cloning experiments, specific activity determination, and enzymatic purification were performed to characterize this clone and this enzyme. Comparative genomic approaches revealed that *E. kobei* producing ACT-28 formed a distinct lineage.

RESULTS AND DISCUSSION

Eight ECC isolates with AmpC derepressed and carbapenemase activity. From January 2016 to December 2017, 1,465 ECC isolates with decreased susceptibility to carbapenems were received at the French National Reference Center for Antibiotic Resistance (F-NRC) for expertise. A total of 426 produced a carbapenemase of the OXA-48-like, KPC, NDM, and/or VIM type (data not shown), and among the 1,039 that were negative for these carbapenemases, only 8 isolates had a positive Carba NP test. These isolates were resistant or intermediate to penicillins, β -lactamase inhibitor-penicillin combinations, expanded-spectrum cephalosporins, and aztreonam but remained susceptible to cefepime, imipenem, and meropenem (Table 1). No synergy image was observed on disk diffusion antibiogram between of expanded-spectrum cephalosporins and clavulanic acid disks, suggesting AmpC overexpression rather than ESBL acquisition. This was confirmed by determining specific activity with cephalothin as a substrate. The activity was 2,000 to 5,000 times higher than the activity of the wild-type *E. cloacae* CIP79.33 used as a reference (see Table S2 in the supplemental material). This confirmed the derepressed status of the AmpC in the eight ECC isolates. Furthermore, there was no associated resistance to other antimicrobial agents, such as aminoglycosides or fluoroquinolones (data not shown).

Disk diffusion susceptibility testing revealed zone inhibition diameters for ertapenem at 20 mm and imipenem at 26 mm, which were below the epidemiological

TABLE 2 Results of carbapenemase detection tests^a

Test	Detection of carbapenem-hydrolytic activity						
	<i>E. kobei</i> (ACT-28 chr)	<i>E. coli</i> TOP10(pTOPO- ACT-28)	<i>E. coli</i> TOP10(pTOPO- ACT-1)	<i>E. coli</i> TOP10	<i>E. coli</i> HB4(pTOPO- ACT-28)	<i>E. coli</i> HB4(pTOPO- ACT-1)	<i>E. coli</i> HB4
In-house Carba NP test	+	+	–	–	ND	ND	ND
RAPIDEC CARBA NP	Doubtful	Doubtful	Doubtful	–	ND	ND	ND
β-CARBA test	–	–	–	–	ND	ND	ND
MALDI-TOF MBT STAR-Carba IVD Kit	+	+	–	–	ND	ND	ND
rCIM test	+	+	–	–	ND	ND	ND

^a+, positive result; –, negative result; ND, not determined.

cutoffs (ECOFFs) fixed by EUCAST (<25 for ertapenem and <28 mm for imipenem). Accordingly, several complementary tests were performed to detect the presence of a carbapenemase (Table 2). Five tests based on carbapenem hydrolysis were performed. Three of them gave a positive result: the Carba NP test (10), the MBT STAR-Carba IVD kit, a commercially available matrix-assisted laser desorption ionization–time of flight (MALDI-TOF)-based technique (11), and the rapid CIM (rCIM) (12), while the RAPIDEC CARBA NP was doubtful and the β-CARBA test remained negative (Table 2). Complementary tests based on the detection of the main 5 carbapenemases either by immunochromatographic assays (RESIST-4 O.K.N.V. kit [CORIS BioConcept] or NG-CARBA 5 test [NG Biotech]) or by molecular tests (in-house PCR or Xpert Carba-R test [Cepheid]) provided negative results (13–16). Antimicrobial susceptibility testing was also performed on Mueller-Hinton agar supplemented with cloxacillin. On this medium, the susceptibility of carbapenems and broad-spectrum cephalosporins was fully restored, suggesting that the observed phenotype might have been due to the overexpression of the cephalosporinase. To determine whether a pAmpC was present in these isolates, plasmid extractions and subsequent electroporation into *Escherichia coli* Top10 were performed. Despite repeated attempts, no plasmid could be evidenced by electrophoresis on a 0.7% agarose gel and no transfer of cephalosporin resistance could be evidenced.

Characterization of ACT-28. Whole-genome sequencing (WGS) was performed to identify the resistome of the eight ECC isolates and to investigate the molecular determinant of the imipenem hydrolysis. Genome annotation indicated that the unique β-lactamase-encoding gene was *bla*_{ACT-28}, a natural variant of the gene encoding cAmpC of ECC (GenBank accession number [NG_048614](#)). In addition, no antimicrobial resistance genes were found using Resfinder server, except a chromosomal allele of *fosA* (91% of nucleotide identity with *fosA2*) known to confer resistance to fosfomycin. Of note, the *fosA* gene is known to be widespread in ECC organisms, with a distribution in 82.4% in their genomes (17).

To determine whether the ACT-28 cephalosporinase possesses a carbapenemase activity, cloning experiments were performed. To date, 54 ACT variants have been described, and among them, no single amino acid mutant of ACT-28 has been found (18). Thus, we decided to compare the activity of ACT-28 to that of the well-characterized ACT-1, a pAmpC recovered from ertapenem-resistant *Klebsiella pneumoniae* with porin deficiency (8, 19).

To compare the β-lactam hydrolytic properties of ACT-28 and ACT-1, the two corresponding genes were cloned into pTOPO plasmid under the control of *Plac* promoter and expressed in *E. coli* TOP10. As expected, expression of the *bla*_{ACT-1} and *bla*_{ACT-28} genes conferred resistance to penicillins and to expanded-spectrum cephalosporins (Table 1). Surprisingly, despite the same MICs for imipenem (0.5 mg/liter) with both *bla*_{ACT-1}- and *bla*_{ACT-28}-expressing *E. coli* TOP10 clones, carbapenemase activities monitored by the Carba NP test, MALDI-TOF technique (MBT STAR-Carba IVD kit) and the rCIM test were positive only for *bla*_{ACT-28}-expressing clones (Table 2). To characterize more precisely whether ACT-28 possesses specific carbapenem hydrolytic properties, a steady-state kinetic parameters were determined. As expected, benzylpenicillin and cephalothin

TABLE 3 Kinetic parameter values for ACT-28 and ACT-1^a

Drug	K_m (μM)		k_{cat} (s^{-1})		k_{cat}/K_m ($\text{mM}^{-1}/\text{s}^{-1}$)	
	ACT-28	ACT-1	ACT-28	ACT-1	ACT-28	ACT-1
Penicillin G	36	45	70	49	1,944	1,090
Cephalothin	138	110	384	325	2,783	2,955
Cefotaxime	3.8	4.3	0.07	0.05	18	12
Ceftazidime	306	32	0.10	0.03	0.33	0.94
Imipenem	1.9	4.6	0.025	0.041	13.3	8.8

^aMeasurements were done in triplicates, and the error rates were below 10%.

were excellent substrates for ACT-28 and ACT-1, whereas these two enzymes exhibited a lower catalytic activity toward cefotaxime and ceftazidime (Table 3) (5). Regarding imipenem, ACT-28 showed a 2-fold increase in imipenem affinity (K_m at $1.9 \pm 0.4 \mu\text{M}$) compared to ACT-1 ($4.6 \pm 0.4 \mu\text{M}$) ($P < 0.01$, Student *t* test) (Table 3). The catalytic efficiency of ACT-28 ($13.3 \pm 2.0 \text{ mM}^{-1}/\text{s}^{-1}$) was 1.5 times higher than that of ACT-1 ($8.8 \pm 0.02 \text{ mM}^{-1}/\text{s}^{-1}$). This significant difference ($P < 0.05$, Student *t* test) in catalytic efficiency toward imipenem was confirmed on several independent measurements.

Identification of a single *E. kobei* ST125 subgroup. To date, MALDI-TOF mass spectrometry (MS)-based identification and biochemical tests (e.g., API galleries) are not able to distinguish the different species within the ECC (2, 20, 21). As proposed by Hoffman et al. (2), the construction of the *hsp60*-based maximum likelihood tree revealed that all ACT-28 producers clustered within *hsp60* cluster II, i.e., *E. kobei* with 100% identity (data not shown). Recently, Chavda et al. extended the number of clusters in the ECC to 18 phylogenomic groups (A to R) by analyzing core single nucleotide polymorphisms (SNPs) in 390 whole genomes (3). Using the WGS data, the phylogenomic analysis confirmed that the 8 genomes of the ACT-28 producers were distributed within the Q-like group comprising *E. kobei* (Fig. 1A). Average nucleotide identity (ANI) between ECC 99G2 as a representative and *E. kobei* DSM 13645 as a reference was 99.21% (22).

Multilocus sequence typing (MLST) analysis revealed that all ACT-28 producers belonged to sequence type 125 (ST125). This ST is not particularly known as a high-risk clone in the hospital environment (23). To evaluate the genetic diversity among non-carbapenemase ECC isolates with decreased susceptibility to carbapenems and negative by the Carba NP test, we analyzed the genomes of 19 randomly chosen ECC isolates addressed to the F-NRC between 2016 and 2017. Most of them were identified as *E. hormaechei* and *E. xiangfangensis* (Fig. 2). We observed a diversity of natural cAmpC and sequence types, but none was of ST125 (Fig. 2).

Phylogenetic analysis of the 19 natural cAmpCs revealed that the AmpC of the isolate 131G4 was closely related to ACT-28 (Fig. 2). Indeed, AmpC of isolate 131G4, ACT-64 newly described here, shared 97% amino acid identity with ACT-28 (371/381). Of note isolate, 131G4 was identified as *E. kobei*, but the Carba NP test was negative, suggesting that ACT-64 lacked detectable carbapenemase activity with this test. Residues conserved between ACT-1 and ACT-64 but mutated in ACT-28 might be involved in the increased carbapenemase activity of ACT-28. Alignment of ACT-28, ACT-64, and ACT-1 revealed the presence of unique residues in ACT-28—His157, Ala166, Ile229 (Ω loop), Ile247 (Ω loop), and Leu254—that could be responsible for its carbapenemase activity (Fig. 3).

ACT-28-producing *E. kobei* ST125 forms a distinct subspecies of *E. kobei*. All ACT-28-producing isolates addressed to the F-RNC were isolated from patients with no known travel history. To determine whether *E. kobei* ST125 was frequently observed around the world, we searched for other genomes in the NCBI database. To date, 8 genomes with their shotgun contigs are deposited in the GenBank database and are from different countries (United States, Brazil, and United Kingdom), suggesting that *E. kobei* ST125 organisms are present at least in three distantly located geographical areas (Fig. 2). These 8 isolates were all ACT-28 producers.

To evaluate the genetic diversity between the 16 ACT-28-producing *E. kobei* ST125 isolates, phylogeny based on SNP calling in the core genome was performed using CSI

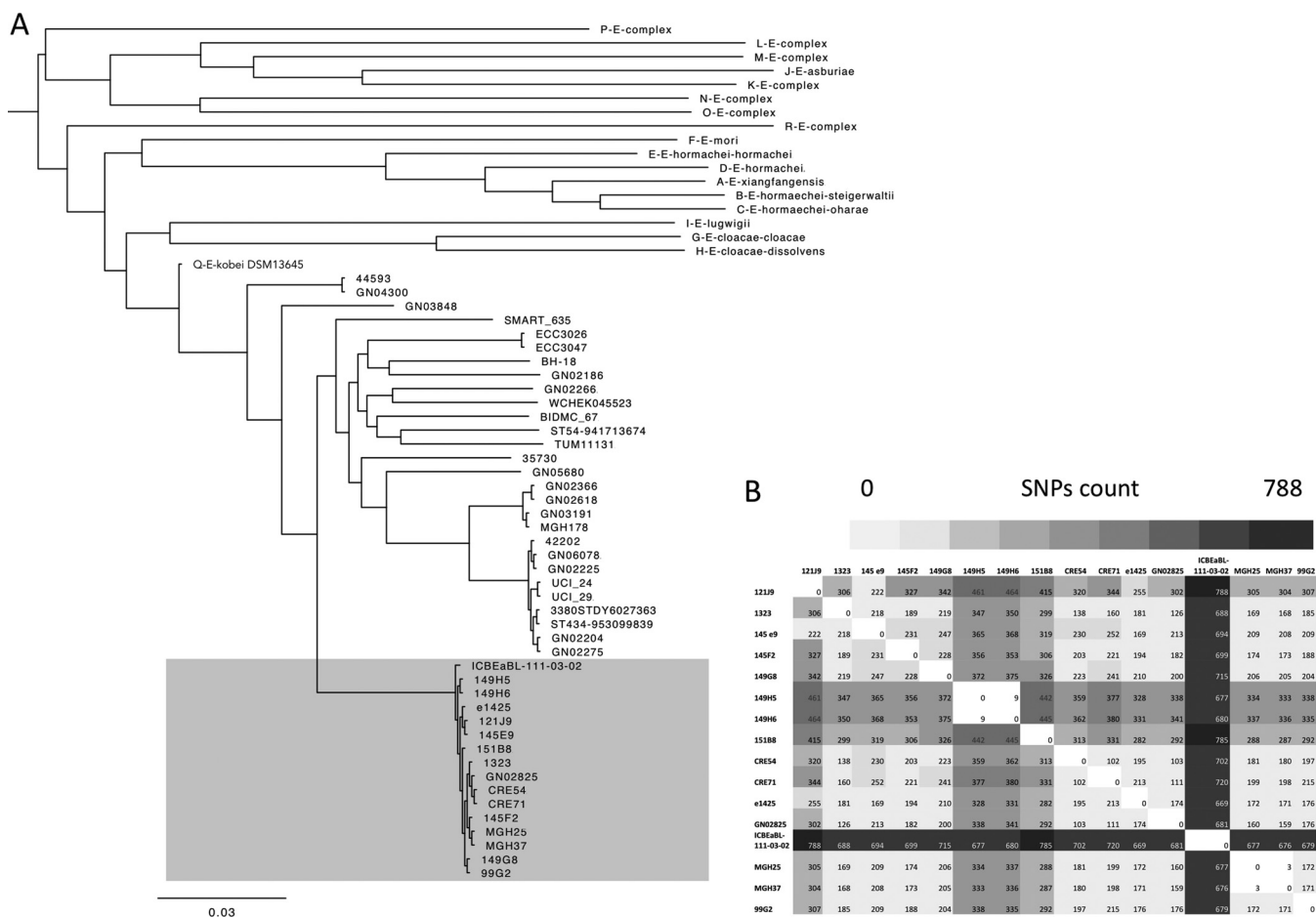
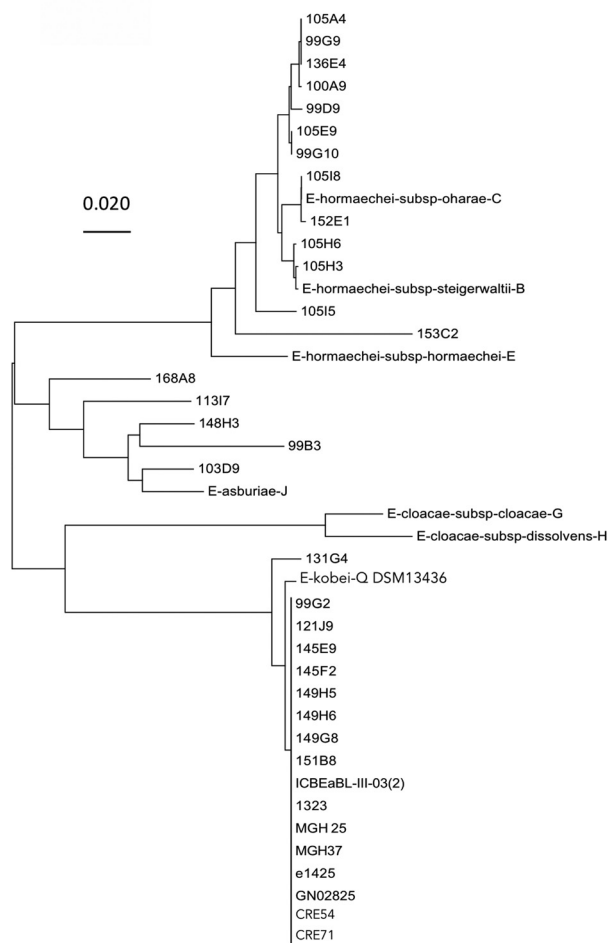


FIG 1 ECC ACT-28 producers belong to *E. kobei*. (A) Phylogeny based on SNP calling among the core genomes of ECC isolates. All ACT-28 producers ($n = 16$) belonged to Chavda’s phylogenomic group Q (23), as well as other *E. kobei* genomes publicly available online ($n = 29$). Among *E. kobei* isolates, ACT-28 producers form a single subgroup we propose to name *E. kobei* subsp. *bicestrii*, indicated by shading. (B) Heat map representing SNP counts among the core genomes of ACT-28-producing isolates: 8 strains were addressed to the F-NRC and 8 genomes were downloaded from the NCBI database (1323, e1425, MGH25, MGH37, ICBEaBL-111-03-02, CRE54, CRE71, and GN02825). Analysis was performed using CSI Phylogeny (27).

Phylogeny (24). These strains differed by 102 to 788 SNPs (Fig. 1B). Only 3 SNPs were detected between MGH25 and MGH37 and 9 SNPs between 149H5 and 149H6, suggesting that in both cases, isolates came from related patients. Of note, the 149H5 and 149H6 ACT-28-producing *E. kobei* strains were isolated from two patients hospitalized in the same ward, suggesting a cross-transmission. ACT-28 producers were mostly identified as an agent of UTI ($n = 8$) and of bloodstream infection ($n = 3$). Phylogenomic comparison with *E. kobei* genomes available on the NCBI database ($n = 24$) revealed that ACT-28-producing isolates formed a single lineage (Fig. 1A and Fig. 2). A total of 11,720 to 13,617 SNPs were detected between *E. kobei* ST125 and other *E. kobei* isolates (Table S1). Thus, we propose to define ACT-28 producers as a single subspecies that we name *Enterobacter kobei* subsp. *bicestrii*.

ACT-28 in strains with decreased outer membrane permeability. Previous studies indicated that AmpC β -lactamases could weakly hydrolyze some substrates (e.g., carbapenems) despite a low k_{cat} as long as they possess concomitantly a high affinity (low K_m) for the substrate (5, 25). The concentration of β -lactams in the periplasm is therefore a crucial issue and depends on the number of porin entry channels or the efflux pump overexpression that can extrude molecules and therefore increase enzyme efficacy.

To study the impact of ACT-1 and ACT-28 expression in a porin-deficient strain, pTOPO-ACT-1 and pTOPO-ACT-28 were electroporated into *E. coli* HB4 lacking porins



Name	Carba NP test	AmpC-Variant	Identification	Chavda's phylogenomic group	Sequence-type	Source	Location
105A4	-	ACT-45	<i>E. xiangfangensis</i>		ST66	urine	France
99G9	-	ACT-45	<i>E. xiangfangensis</i>	A	ST66	urine	France
136E4	-	ACT-45	<i>E. xiangfangensis</i>	A	ST66	blood	France
100A9	-	ACT-61	<i>E. xiangfangensis</i>	A	ST1069	urine	France
99D9	-	ACT-16	<i>E. xiangfangensis</i>	A	ST114	lung	France
105E9	-	ACT-16	<i>E. xiangfangensis</i>	A	ST136	urine	France
99G10	-	ACT-16	<i>E. xiangfangensis</i>	A	ST136	blood	France
105I8	-	ACT-55	<i>E. hormaechei</i> subsp. <i>oharae</i>	C	ST108	urine	France
C	NR	ACT-55	<i>E. hormaechei</i> subsp. <i>oharae</i>	C	ST108	unknown	Germany
152E1	-	ACT-60	<i>E. hormaechei</i> subsp. <i>oharae</i>	C	ST1067	urine	France
105H6	-	ACT-27	<i>E. hormaechei</i> subsp. <i>steigerwaltii</i>	B	ST-110	unknown	France
105H3	-	ACT-15	<i>E. hormaechei</i> subsp. <i>steigerwaltii</i>	B	ST-153	urine	France
B	NR	ACT-56	<i>E. hormaechei</i> subsp. <i>steigerwaltii</i>	B	ST906	wound	Belgium
105I5	-	ACT-15	<i>E. hormaechei</i>	D	ST153	urine	France
153C2	-	ACT-59	<i>E. hormaechei</i>	D	ST487	blood	France
E	NR	ACT-37	<i>E. hormaechei</i> subsp. <i>hormaechei</i>	E	ST269	lung	USA
168A8	-	MIR-20	<i>E. cloacae</i> complex	M	ST595	rectal swab	France
113I7	-	ACT-62	<i>E. cloacae</i> complex	M	ST1066	rectal swab	France
148H3	-	ACT-58	<i>E. cloacae</i> complex	M	ST1067	rectal swab	France
99B3	-	ACT-63	<i>E. cloacae</i> complex	L	ST1065	rectal swab	France
103D9	-	ACT-57	<i>E. asburiae</i>	J	ST-25	rectal swab	France
J	NR	ACT-4	<i>E. asburiae</i>	J	ST807	unknown	unknown
G	NR	CMH-4	<i>E. cloacae</i> subsp. <i>cloacae</i>	G	ST1	unknown	unknown
H	NR	CMH-5	<i>E. cloacae</i> subsp. <i>dissolvens</i>	H	ST674	cutaneous	Malaysia
131G4	-	ACT-64	<i>E. kobei</i>	Q	ST-54	rectal swab	France
Q	NR	ACT-9	<i>E. kobei</i>	Q	ST806	blood	Japan
99G2	+	ACT-28	<i>E. kobei</i>	Q	ST-125	unknown	France
121J9	+	ACT-28	<i>E. kobei</i>	Q	ST-125	urine	France
145E9	+	ACT-28	<i>E. kobei</i>	Q	ST-125	rectal swab	France
145F2	+	ACT-28	<i>E. kobei</i>	Q	ST-125	urine	France
149H5	+	ACT-28	<i>E. kobei</i>	Q	ST-125	urine	France
149H6	+	ACT-28	<i>E. kobei</i>	Q	ST-125	urine	France
149G8	+	ACT-28	<i>E. kobei</i>	Q	ST-125	urine	France
151B8	+	ACT-28	<i>E. kobei</i>	Q	ST-125	urine	France
ICBEaBL	NR	ACT-28	<i>E. kobei</i>	Q	ST-125	Stool	Brazil
1323	NR	ACT-28	<i>E. kobei</i>	Q	ST-125	unknown	USA
MGH25	NR	ACT-28	<i>E. kobei</i>	Q	ST-125	urine	USA
MGH37	NR	ACT-28	<i>E. kobei</i>	Q	ST-125	blood	UK
e1425	NR	ACT-28	<i>E. kobei</i>	Q	ST-125	Urine	unknown
GN02825	NR	ACT-28	<i>E. kobei</i>	Q	ST-125	unknown	USA
CRE54	NR	ACT-28	<i>E. kobei</i>	Q	ST-125	blood	USA
CRE71	NR	ACT-28	<i>E. kobei</i>	Q	ST-125	blood	USA

FIG 2 Phylogenetic analysis of AmpC β -lactamases of ECC isolates addressed to the French National Reference Center for carbapenemase detection. This unrooted tree was constructed based on *ampC* genes using the maximum likelihood method with the Tamura-Nei model using the MEGA program (7.0). The tree is drawn to scale, with branch lengths representing the evolutionary distances. ACT-28-producing ECC isolates from the NCBI database (1323, e1425, MGH25, MGH37, ICBEaBL-111-03-02, CRE54, CRE71, and GN02825) and *ampC* of ECC genomes of Chavda's phylogenomic groups B, C, E, J, G, H, and Q were added to the analysis (23). NR, not realized.

OmpF and OmpC (26). Expression of the *bla*_{ACT-1} and *bla*_{ACT-28} genes conferred high-level resistance to all β -lactams, including carbapenems, with MICs of 12 μ g/ml and >32 μ g/ml, respectively (Table 1). The higher MICs for imipenem conferred by ACT-28 compared to ACT-1 are in agreement with our biochemical results (steady-state kinetic and Carba NP test results).

To evaluate the role of membrane permeability defect in the global resistance phenotype of ACT-28-producing *E. kobei*, *in silico* analysis of porins was performed. Using WGS data, outer membrane protein sequences of the *ompF* and *ompC* types were compared to that of the *E. kobei* DSM 13645 reference strain. These porins are homologs of *K. pneumoniae ompK35* and *ompK36* porins, respectively. In both species, alterations of these porins are known to be involved in decreased susceptibility to carbapenems and notably ertapenem (6). *ompF* shared 100% nucleotide identity to the corresponding gene in *E. kobei* DSM 13645. Surprisingly, analysis of *ompC* revealed an allelic replacement of 967 bp that occurred within the gene in all ACT-28-producing *E. kobei* ST125 isolates (Fig. 4A). Intriguingly, this allelic replacement was in phase with the identical 5' end of *ompC* and led to a complete coding sequence. This *ompC* chimera, likely the result of homologous recombination, was 1,077 bp instead of 1,143 bp for *ompC* from DSM 13645. All ACT-28 producers possessed this peculiar modified OmpC,



FIG 3 Amino acid alignment of ACT-28, ACT-1, and ACT-64. To highlight the differences, amino acids in common with ACT-28 have been replaced by dashes. Amino acids conserved within serine β -lactamases are in bold. The two loops (Ω and R2) are shaded. Helices H-9, H-10, and H-11 are boxed.

and BLAST analysis revealed that this genetic event was specific to ACT-28-producing *E. kobei* ST125. This in-phase allelic replacement, resulting in OmpC from ACT-28 producers sharing only 53% amino acid sequence identity with OmpC from DSM 13645, might modify the functionality of the porin (Fig. 4B).

WGS data were also used to investigate the molecular mechanism that led to AmpC derepression in ACT-28-producing *E. kobei* ST125 isolates. Most ECC clinical isolates with AmpC derepressed have mutations in AmpD, a cytosolic amidase involved in cell wall recycling, and less commonly in AmpR (27). Alignment of AmpD proteins of the 8 ACT-28 producers and *E. kobei* 131G4 (AmpC not derepressed [data not shown]) to *E. kobei* DSM 13645 as a reference revealed mutations that led to truncated proteins due to early stop codons in 3 isolates (99G2, 145H5, and 154H6) (Fig. S1). Only the 48 final amino acids of AmpD were present in isolate 145F2, whereas the gene was totally absent in 121J9. In 149G8, the initial Met codon was absent; hence, AmpD expression could be decreased. In 145E9 and 151B8, AmpD is strictly identical to the sequence of DSM 13645 (Fig. S1). Otherwise, alignment of *ampR* of all ACT-28 producers revealed the presence of 7 SNPs in comparison to *ampR* of 131G4, but they do not impact amino acid sequence (data not shown). Therefore, it is unlikely that AmpR might be involved in AmpC derepression. At last, no mutations in *ampC* and *ampD* promoters were observed. Overall, mutations in AmpD were present in the majority of isolates but we cannot exclude that mutations in partners of the AmpC derepression pathway other than AmpD and AmpR might be implicated in the phenotype of ACT-28 producers (27).

Conclusions. We have described a novel lineage of *E. kobei* ST125 that can be falsely identified as a member of the carbapenemase-producing *Enterobacteriaceae* (CPE) by several diagnostic tests. ACT-28, a specific chromosome-encoded cephalosporinase, was the only β -lactamase detected in this lineage. Kinetic study revealed its high affinity for

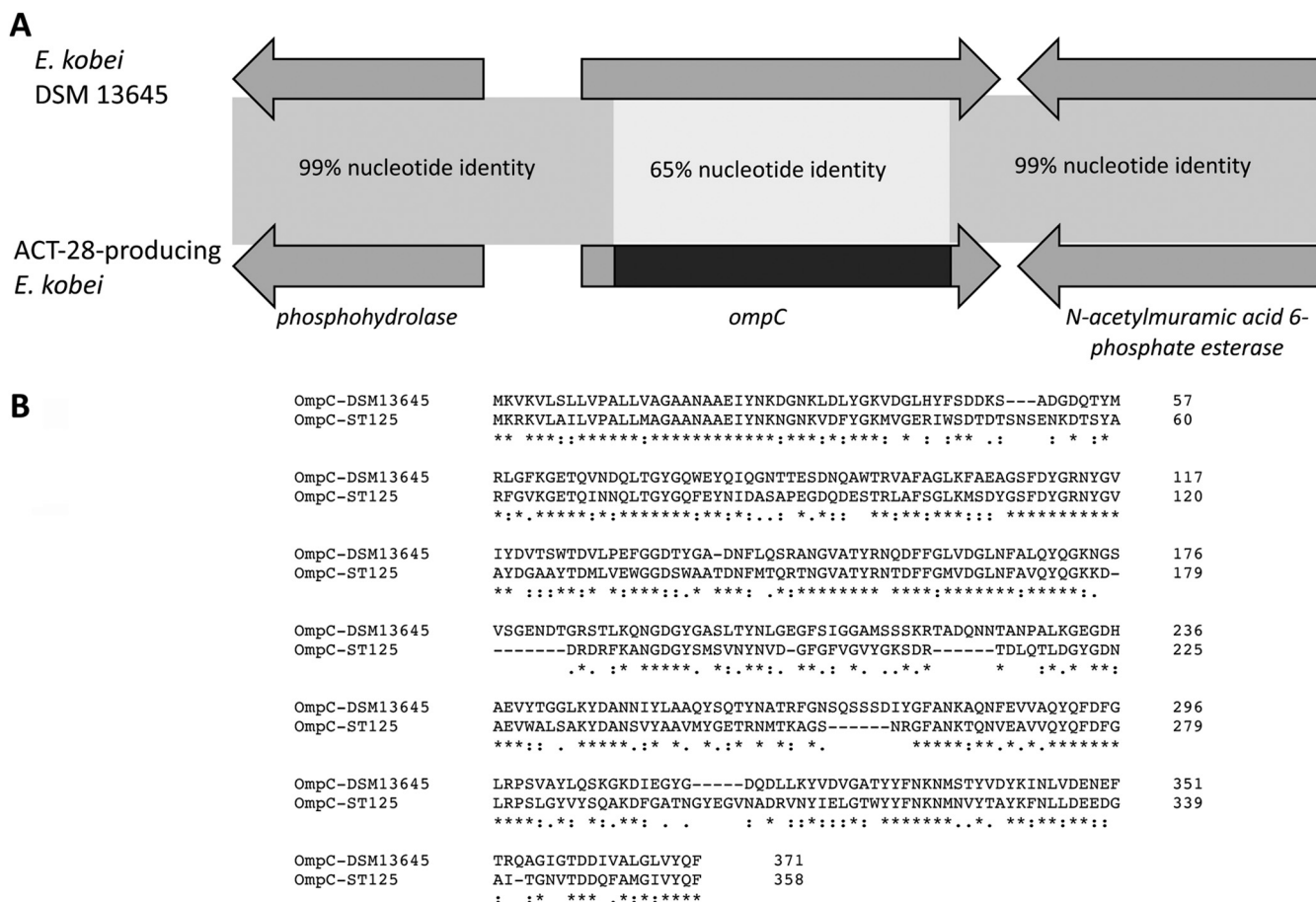


FIG 4 An allelic replacement of *ompC* occurred in *E. kobei* ST125. (A) Schematic representation of the *ompC* region found in all ACT-28-producing *E. kobei* isolates and *E. kobei* DSM 13645, used as reference. (B) Amino acid alignment of OmpC of *E. kobei* ST125 and *E. kobei* DSM 13456. The two proteins shared only 53% amino acid identity.

imipenem, which might result in carbapenem resistance when associated with outer membrane permeability defect. We showed that ACT-28 led to a weak but significant carbapenemase activity as revealed with imipenem hydrolysis-based diagnostic tests (Carba NP test, MALDI-TOF-based assay, and rCIM test). As a consequence, patients carrying these isolates may be mistakenly categorized as CPE carriers and isolated with dedicated staff or even cohorted with true CPE carriers. With cAmpC-producing bacteria, biochemical tests have to be interpreted with susceptibility testing on a cloxacillin-containing plate. Indeed, in a strain with a cephalosporinase overproduced and impaired permeability, diameters around the β -lactam disks increase, whereas with true carbapenemase producers, diameters around imipenem change only slightly, if at all (28).

MATERIALS AND METHODS

Bacterial strains. Eight ACT-28-producing *E. kobei* isolates (99G2, 121J9, 145E9, 145F2, 149H5, 149H6, 149G8, and 151B8) were addressed to the French National Reference Center for Antibiotic Resistance (F-NRC) between 2016 and 2017 for carbapenemase detection. Nineteen other ECC clinical isolates addressed to the F-NRC over the same period were used as controls (99B3, 99D9, 99G9, 99G10, 100A9, 103D9, 105A4, 105E9, 105H3, 105H6, 105I5, 105I8, 113I7, 131G4, 136E4, 148H3, 152E1, 153C2, and 168A8). These isolates were randomly picked among the 1,039 ECC collection isolates with reduced susceptibility to carbapenems but lacking main carbapenemases (OXA-48-like, KPC, NDM, VIM, and IMP enzymes) and lacking carbapenemase activity (negative Carba NP test).

Identification of ECC was performed using MALDI-TOF MS using the Bruker MS system (Bruker Daltonics, Bremen, Germany), according to the manufacturer’s instructions. In addition, analysis of the *hsp60* sequences was performed to distinguish species among the *Enterobacter cloacae* complex (ECC) (2). ACT-1-producing *K. pneumoniae* was used as source of the *bla*_{ACT-1} gene for PCR amplification prior to cloning experiments (19). Electrocompetent *E. coli* TOP10 and *E. coli* HB4 (a strain with permeability

defect due to OmpC and OmpF major porin deficiency) were used as recipients for electroporation experiments, and *E. coli* BL21(DE3) (Invitrogen, Eragny, France) was used for overexpressing ACT-28 (29).

Susceptibility testing and MIC determinations. Susceptibility testing was performed by the disk diffusion method on Mueller-Hinton agar plates (Bio-Rad, Marnes la Coquette, France) with or without cloxacillin (bioMérieux, La Balmes les Grottes, France) incubated for 18 h at 37°C and interpreted according to the EUCAST breakpoints, updated in 2018 (<http://www.eucast.org>). MICs for ticarcillin, cefoxitin, ceftazidime, cefotaxime, cefepime, imipenem, meropenem, and ertapenem were determined by Etest (bioMérieux). For *E. coli* HB4(pTOPO-ACT-1) and *E. coli* HB4(pTOPO-ACT-28), imipenem MICs were also determined using commercially available dry-form broth microdilution technique (Sensititre; Thermo Fisher Scientific, Courtaboeuf, France).

Plasmid extraction. Natural plasmid extraction was attempted using the Kieser extraction method and subsequently analyzed by electrophoresis on a 0.7% agarose gel as previously described (30).

Biochemical, immunological, and molecular carbapenemase confirmatory tests. Bacterial colonies of ECC isolates were recovered from Trypticase soy agar to perform the in-house Carba NP test as previously described (10) and the β -CARBA test (Bio-Rad) and RAPIDEC CARBA NP (bioMérieux) according to the manufacturer's recommendations. The rapid CIM (rCIM) test was performed as previously described (12). Imipenem hydrolysis monitored by MALDI-TOF MS was done using the MBT STAR-Carba IVD kit (Bruker Daltonics, Bremen, Germany) according to the manufacturer's recommendations (11). Briefly, 50 μ l of MBT STAR-BL incubation buffer was added to a ready-to-use tube containing MBT STAR-BL antibiotic reagent. One to five individual bacterial colonies were resuspended in the tube by vortexing. Samples were incubated at 37°C for 30 min under agitation (900 rpm). The bacteria were pelleted by centrifugation for 2 min at 16,000 \times g. One microliter of the supernatant was loaded on the MALDI target, dried under a stream of air (1 min), and overlaid with the MBT STAR-BL matrix solution. The spots were dried gently under a stream of air (less than 1 min). MALDI-TOF MS analysis was performed on a Microflex LT mass spectrometer (Bruker Daltonics). Final spectra were automatically interpreted using the MBT STAR-BL IVD software.

Carbapenemase production was investigated by lateral flow immunoassays using the RESIST-4 O.K.N.V. kit (CORIS BioConcept, Gembloux, Belgium) for the detection of KPC, NDM, VIM, and OXA-48-like enzymes and the NG-CARBA 5 test (NG Biotech, Guipry, France) for the detection of KPC, NDM, VIM, OXA-48-like, and IMP enzymes (13–15). Finally, genes for KPC, NDM, VIM, OXA-48-like, and IMP enzymes were sought using the Xpert Carba-R kit (Cepheid, Sunnyvale, CA) (16).

Sequencing, whole-genome sequencing, and bioinformatic analysis. Recombinant plasmids pTOPO-ACT-28, pTOPO-ACT-1, pET41b-ACT1, and pET41b-ACT28 were purified using a QIAprep spin miniprep kit (Qiagen, Courtaboeuf, France) and were sequenced using an ABI3130 automated sequencer (Applied Biosystems Thermo Fisher, Courtaboeuf, France). The nucleotide and the deduced protein sequences were analyzed using software from the National Center for Biotechnology Information (www.ncbi.nlm.nih.gov) and the BLDB (www.bldb.eu) (18).

The DNA libraries were prepared using the NexteraXT v3 kit (Illumina, San Diego, CA), according to the manufacturer's instructions, and then run on the HiSeq system (Illumina) for generating paired-end 150-bp reads. Illumina read *de novo* assembly was performed using CLC genomic workbench 10.0 according to the manufacturer's recommendations (Qiagen). The genome was annotated using the RAST tool (<http://rast.nmpdr.org/rast.cgi>) (29).

Resfinder online software (<https://cge.cbs.dtu.dk/services/ResFinder/>) was used for the detection of resistance determinants other than β -lactamase (31). Sequence type determination was performed using the *Enterobacter cloacae* MSLT scheme available online at <https://pubmlst.org/ecloacae/>. Average nucleotide identity (ANI) was calculated with the online tool <http://enve-omics.ce.gatech.edu/ani/> (22). Phylogenetic trees based on *hsp60* or *ampC* sequences were drawn with MEGA7 software using the maximum likelihood method based on the Tamura-Nei model.

Multiple-sequence alignment of ACT variants, AmpD, and OmpC was done online using the Clustal Omega program (<https://www.ebi.ac.uk/Tools/msa/clustalo/>). Sequences of AmpD from wild-type *E. kobei* 131G4 and *E. kobei* DSM 13645 (GenBank accession number CP017181.1) were used as references for molecular analysis of AmpC derepression. Sequences of OmpC and OmpF from *E. kobei* DSM 13645 were used as references for porin analysis.

The draft genomes of eight ACT-28-producing ECC isolates available online were included in bioinformatic analyses: *E. kobei* ICBEaBL-III-03(2) (NIHL01000275.1), *E. kobei* GN02825 (LEDC01000001.1), *E. cloacae* 1323 (JVTR01000062.1), *E. cloacae* e1425 (FJYX01000004.1), *Enterobacter* sp. strain MGH 37 (JCLI01000015.1), *Enterobacter* sp. MGH 25 (AYJF01000016.1), *Enterobacter kobei* CRE54 (PXKD01000001.1), and *Enterobacter kobei* CRE71 (PXKA01000001.1) (all accession numbers from GenBank). Identification of *E. kobei* was confirmed after *hsp60* and phylogenomic analyses.

CSI Phylogeny 1.4 was used for phylogenomic analysis based on SNP calling among the core genomes of the 16 ACT-28-producing *E. kobei* isolates (24). The 18 reference genomes of Chavda's classification (A to R) and 28 non-ACT-28-producing *E. kobei* genomes available in NCBI database were added to the analysis (<https://cge.cbs.dtu.dk/services/CSIPhylogeny/>) (3, 24). All accession numbers of genomes used in the study are listed in Table S3.

Enzymatic activities. AmpC expression in ACT-28-producing *E. kobei* and in wild-type ECC isolate CIP79.33, used as a reference, was studied using specific activity. This was determined using the supernatant of a whole-cell crude extract obtained from an overnight culture with an Ultrospec 2000 UV spectrophotometer (Amersham Pharmacia Biotech), as previously described (32). Cephalothin was used as a substrate at a concentration of 100 μ M.

Cloning experiments. The *bla*_{ACT-28} and *bla*_{ACT-1} genes were amplified using ACT-28F (5'-ATGAAGACAAAATCCCTTTGC-3') and ACT-28R (5'-CAGGCAACCA-CTAAAAACGC-3') primers and using ACT-1F (5'-ATGATGATGACTAAATCCCTTTGC-3') and ACT-1R (5'-CTACAGCGCGCTCAAATACG-3') primers, respectively, and were subsequently cloned into pTOPO (Zero Blunt TOPO PCR cloning kit; Invitrogen, Courtaboeuf, France), resulting in plasmids pTOPO-ACT-28 and pTOPO-ACT-1, respectively. These plasmids were electroporated into *E. coli* TOP10 and *E. coli* HB4.

For β -lactamase production and purification, the *bla*_{ACT-28} and *bla*_{ACT-1} genes corresponding to the mature β -lactamase were PCR amplified using the primers ACT28-cloningpET41-For (5'-CTTTAAGAAGGAGATATACATATGGCGCGATGTCAGAGAACAGC-3') and ACT28-cloningpET41-Rev (5'-GTGGTGGTGGTG GTGCTCGAGCTGCAGAGCGCTCAGAATACG) and primers ACT1-cloningpET41-For (5'-CTTTAAGAAGGAGATATACATATGGCTACCCCGATGTCAGAAAAACAGC-3') and ACT1-cloningpET41-Rev (5'-GGTGGTGGTGGTG GTGCTCGAGCAGCGCTCAAATACGGTATGC-3'), respectively, and cloned into the expression vector pET-41b(+) (Novagen, VWR International, Fontenay-sous-Bois, France) using the NEBuilder HiFiDNA assembly cloning kit (New England BioLabs Inc., United Kingdom), following the manufacturer's instructions. Recombinant plasmids pET41b-ACT1 and pET41b-ACT28 were transformed into electrocompetent *E. coli* BL21(DE3) (32).

β -Lactamase purification and steady-state kinetics. An overnight culture of *E. coli* strain BL21(DE3) harboring pET41b-ACT-28 or pET41b-ACT-1 recombinant plasmid was used to inoculate 2 liters of brain heart infusion (BHI) broth supplemented with kanamycin at 50 mg/liter. Bacteria were cultured at 37°C until reaching an optical density at 600 nm (OD_{600}) of 0.6. Then expression of the β -lactamase genes was carried out overnight at 25°C with 0.2 mM isopropyl- β -D-thiogalactopyranoside (IPTG) as an inducer. Cultures were centrifuged at $6,000 \times g$ for 15 min, and then the pellets were resuspended with 10 ml of buffer A (20 mM phosphate-buffered saline [PBS], 175 mM K_2SO_4 , 40 mM imidazole [pH 7.4]) (32). Bacterial cells were disrupted by sonication; the bacterial pellet was removed by two consecutive centrifugation steps at $10,000 \times g$ for 1 h at 4°C. The supernatant was further centrifuged at $48,000 \times g$ for 1 h at 4°C. β -Lactamases were purified using a one-step pseudoaffinity chromatography nitrilotriacetic acid (NTA)-nickel column (GE Healthcare, Freiburg, Germany). Protein purity was estimated by SDS-PAGE, and pure fractions were pooled and dialyzed against 20 mM HEPES–50 mM K_2SO_4 (pH 7) and concentrated by using Vivaspin columns (GE Healthcare). Protein concentration was determined using the Bradford protein assay (Bio-Rad) (32).

Purified β -lactamases were used to determine the kinetic parameters (K_m and k_{cat}) of benzylpenicillin, cephalothin, cefotaxime, ceftazidime, and imipenem in 100 mM sodium phosphate (pH 7.4). Experiments were performed three times. The rates of hydrolysis were determined with an Ultrospec 2100 spectrophotometer and were analyzed using SWIFT II software (GE Healthcare, Velizy-Villacoublay, France). K_m and k_{cat} values were determined by analyzing the β -lactam hydrolysis under initial rate conditions using the Eadie-Hofstee linearization of the Michaelis-Menten equation as previously described (33).

Accession number(s). All of the genomes determined in this study are available at NCBI under BioProject no. PRJNA472443. All genomes used in this study are listed in Table S3. New ACT and CMH alleles described in this study, listed as follows, have been deposited in GenBank (accession numbers in parentheses): ACT-55 (MH469274), ACT-56 (MH469275), ACT-57 (MH469278), ACT-58 (MH469279), ACT-59 (MH469280), ACT-60 (MH469281), ACT-61 (MH469283), ACT-62 (MH469270), ACT-63 (MH469271), ACT-64 (MH469272), CMH-4 (MH469276), and CMH-5 (MH469277).

SUPPLEMENTAL MATERIAL

Supplemental material for this article may be found at <https://doi.org/10.1128/AAC.02388-18>.

SUPPLEMENTAL FILE 1, PDF file, 3.3 MB.

SUPPLEMENTAL FILE 2, XLSX file, 0.02 MB.

SUPPLEMENTAL FILE 3, XLSX file, 0.01 MB.

SUPPLEMENTAL FILE 4, XLSX file, 0.01 MB.

ACKNOWLEDGMENTS

This work was supported by the Assistance Publique-Hôpitaux de Paris, by a grant from the Université Paris-Sud (EA 7361), and by the LabEx LERMIT, supported by a grant from the French National Research Agency (ANR-10-LABX-33). This work was also funded in part by a grant from Joint Programming Initiative on Antimicrobial Resistance (ANR-14-JAMR-0002).

L.D. is a coinventor of the Carba NP test, the patent for which has been licensed to bioMérieux (La Balmes les Grottes, France).

REFERENCES

- Sanders WE, Sanders CC. 1997. Enterobacter spp.: pathogens poised to flourish at the turn of the century. *Clin Microbiol Rev* 10:220–241. <https://doi.org/10.1128/CMR.10.2.220>.
- Hoffmann H, Roggenkamp A. 2003. Population genetics of the nomenclature species *Enterobacter cloacae*. *Appl Environ Microbiol* 69:5306–5318. <https://doi.org/10.1128/AEM.69.9.5306-5318.2003>.
- Chavda KD, Chen L, Fouts DE, Sutton G, Brinkac L, Jenkins SG, Bonomo RA, Adams MD, Kreiswirth BN. 2016. Comprehensive genome analysis of

- carbapenemase-producing Enterobacter spp.: new insights into phylogeny, population structure, and resistance mechanisms. *mBio* 7:e02093-16. <https://doi.org/10.1128/mBio.02093-16>.
4. Bush K, Jacoby GA. 2010. Updated functional classification of beta-lactamases. *Antimicrob Agents Chemother* 54:969–976. <https://doi.org/10.1128/AAC.01009-09>.
 5. Jacoby GA. 2009. AmpC β -lactamases. *Clin Microbiol Rev* 22:161–182. <https://doi.org/10.1128/CMR.00036-08>.
 6. Doumith M, Ellington MJ, Livermore DM, Woodford N. 2009. Molecular mechanisms disrupting porin expression in ertapenem-resistant *Klebsiella* and Enterobacter spp. clinical isolates from the UK. *J Antimicrob Chemother* 63:659–667. <https://doi.org/10.1093/jac/dkp029>.
 7. Philippon A, Arlet G, Jacoby GA. 2002. Plasmid-determined AmpC-type β -lactamases. *Antimicrob Agents Chemother* 46:1–11. <https://doi.org/10.1128/AAC.46.1.1-11.2002>.
 8. Mammeri H, Guillon H, Eb F, Nordmann P. 2010. Phenotypic and biochemical comparison of the carbapenem-hydrolyzing activities of five plasmid-borne AmpC β -lactamases. *Antimicrob Agents Chemother* 54:4556–4560. <https://doi.org/10.1128/AAC.01762-09>.
 9. Kim JY, Jung HI, An YJ, Lee JH, Kim SJ, Jeong SH, Lee KJ, Suh P-G, Lee H-S, Lee SH, Cha S-S. 2006. Structural basis for the extended substrate spectrum of CMY-10, a plasmid-encoded class C β -lactamase. *Mol Microbiol* 60:907–916. <https://doi.org/10.1111/j.1365-2958.2006.05146.x>.
 10. Dortet L, Agathine A, Naas T, Cuzon G, Poirel L, Nordmann P. 2015. Evaluation of the RAPIDEC CARBA NP, the Rapid CARB Screen and the Carba NP test for biochemical detection of carbapenemase-producing Enterobacteriaceae. *J Antimicrob Chemother* 70:3014–3022. <https://doi.org/10.1093/jac/dkv213>.
 11. Dortet L, Tandé D, de Briel D, Bernabeu S, Lasserre C, Gregorowicz G, Jousset AB, Naas T. 2018. MALDI-TOF for the rapid detection of carbapenemase-producing Enterobacteriaceae: comparison of the commercialized MBT STAR-Carba IVD kit with two in-house MALDI-TOF techniques and the RAPIDEC CARBA NP. *J Antimicrob Chemother* 73:2352–2359. <https://doi.org/10.1093/jac/dky209>.
 12. Muntean M-M, Muntean A-A, Gauthier L, Creton E, Cotellon G, Popa MI, Bonnin RA, Naas T. 2018. Evaluation of the rapid carbapenem inactivation method (rCIM): a phenotypic screening test for carbapenemase-producing Enterobacteriaceae. *J Antimicrob Chemother* 73:900–908. <https://doi.org/10.1093/jac/dkx519>.
 13. Sağıroğlu P, Hasdemir U, Altinkanat Gelmez G, Aksu B, Karatuna O, Söyletir G. 2018. Performance of “RESIST-3 O.K.N. K-SeT” immunochromatographic assay for the detection of OXA-48 like, KPC, and NDM carbapenemases in *Klebsiella pneumoniae* in Turkey. *Braz J Microbiol Publ Braz Soc Microbiol* 49:885–890. <https://doi.org/10.1016/j.bjm.2018.02.002>.
 14. Glupczynski Y, Jousset A, Evrard S, Bonnin RA, Huang T-D, Dortet L, Bogaerts P, Naas T. 2017. Prospective evaluation of the OKN K-SeT assay, a new multiplex immunochromatographic test for the rapid detection of OXA-48-like, KPC and NDM carbapenemases. *J Antimicrob Chemother* 72:1955–1960. <https://doi.org/10.1093/jac/dkx089>.
 15. Boutal H, Vogel A, Bernabeu S, Devilliers K, Creton E, Cotellon G, Plaisance M, Oueslati S, Dortet L, Jousset A, Simon S, Naas T, Volland H. 2018. A multiplex lateral flow immunoassay for the rapid identification of NDM-, KPC-, IMP- and VIM-type and OXA-48-like carbapenemase-producing Enterobacteriaceae. *J Antimicrob Chemother* 73:909–915. <https://doi.org/10.1093/jac/dkx521>.
 16. Dortet L, Fusaro M, Naas T. 2016. Improvement of the Xpert Carba-R kit for the detection of carbapenemase-producing Enterobacteriaceae. *Antimicrob Agents Chemother* 60:3832–3837. <https://doi.org/10.1128/AAC.00517-16>.
 17. Ito R, Mustapha MM, Tomich AD, Callaghan JD, McElheny CL, Mettus RT, Shanks RMQ, Sluis-Cremer N, Doi Y. 2017. Widespread fosfomycin resistance in Gram-negative bacteria attributable to the chromosomal *fosA* gene. *mBio* 8:e00749-17. <https://doi.org/10.1128/mBio.00749-17>.
 18. Naas T, Oueslati S, Bonnin RA, Dabos ML, Zavala A, Dortet L, Retailleau P, Iorga BI. 2017. Beta-lactamase database (BLDB)—structure and function. *J Enzyme Inhib Med Chem* 32:917–919. <https://doi.org/10.1080/14756366.2017.1344235>.
 19. Bradford PA, Urban C, Mariano N, Projan SJ, Rahal JJ, Bush K. 1997. Imipenem resistance in *Klebsiella pneumoniae* is associated with the combination of ACT-1, a plasmid-mediated AmpC beta-lactamase, and the foss [sic] of an outer membrane protein. *Antimicrob Agents Chemother* 41:563–569. <https://doi.org/10.1128/AAC.41.3.563>.
 20. Paauw A, Caspers MPM, Schuren FHJ, Leverstein-van Hall MA, Delétoile A, Montijn RC, Verhoef J, Fluit AC. 2008. Genomic diversity within the Enterobacter cloacae complex. *PLoS One* 3:e3018. <https://doi.org/10.1371/journal.pone.0003018>.
 21. Jamal W, Albert MJ, Rotimi VO. 2014. Real-time comparative evaluation of bioMérieux VITEK MS versus Bruker Microflex MS, two matrix-assisted laser desorption-ionization time-of-flight mass spectrometry systems, for identification of clinically significant bacteria. *BMC Microbiol* 14:289. <https://doi.org/10.1186/s12866-014-0289-0>.
 22. Goris J, Konstantinidis KT, Klappenbach JA, Coenye T, Vandamme P, Tiedje JM. 2007. DNA-DNA hybridization values and their relationship to whole-genome sequence similarities. *Int J Syst Evol Microbiol* 57:81–91. <https://doi.org/10.1099/ijs.0.64483-0>.
 23. Izdebski R, Baraniak A, Herda M, Fiett J, Bonten MJM, Carmeli Y, Goossens H, Hryniewicz W, Brun-Buisson C, Gniadkowski M, Grabowska A, Nikonow E, Derde LPG, Dautzenberg MJ, Adler A, Kazma M, Navon-Venezia S, Malhotra-Kumar S, Lammens C, Dumpis U, Giamarellou H, Muzlovic I, Nardi G, Petrikos GL, Stammet P, Salomon J, Lawrence C, Legrand P, Rossini A, Salvia A, Samsó JV, Fierro J, Paul M, Lerman Y. 2015. MLST reveals potentially high-risk international clones of Enterobacter cloacae. *J Antimicrob Chemother* 70:48–56. <https://doi.org/10.1093/jac/dku359>.
 24. Kaas RS, Leekitcharoenphon P, Aarestrup FM, Lund O. 2014. Solving the problem of comparing whole bacterial genomes across different sequencing platforms. *PLoS One* 9:e104984. <https://doi.org/10.1371/journal.pone.0104984>.
 25. Vu H, Nikaido H. 1985. Role of beta-lactam hydrolysis in the mechanism of resistance of a beta-lactamase-constitutive Enterobacter cloacae strain to expanded-spectrum beta-lactams. *Antimicrob Agents Chemother* 27:393–398. <https://doi.org/10.1128/AAC.27.3.393>.
 26. Mammeri H, Nordmann P, Berkani A, Eb F. 2008. Contribution of extended-spectrum AmpC (ESAC) beta-lactamases to carbapenem resistance in *Escherichia coli*. *FEMS Microbiol Lett* 282:238–240. <https://doi.org/10.1111/j.1574-6968.2008.01126.x>.
 27. Guérin F, Isnard C, Cattoir V, Giard JC. 2015. Complex regulation pathways of AmpC-mediated β -lactam resistance in Enterobacter cloacae complex. *Antimicrob Agents Chemother* 59:7753–7761. <https://doi.org/10.1128/AAC.01729-15>.
 28. Dortet L, Cuzon G, Plésiat P, Naas T. 2016. Prospective evaluation of an algorithm for the phenotypic screening of carbapenemase-producing Enterobacteriaceae. *J Antimicrob Chemother* 71:135–140. <https://doi.org/10.1093/jac/dkv308>.
 29. Dabos L, Bogaerts P, Bonnin RA, Zavala A, Sacré P, Iorga BI, Huang DT, Glupczynski Y, Naas T. 2018. Genetic and biochemical characterization of OXA-519, a novel OXA-48-like β -lactamase. *Antimicrob Agents Chemother* 62:e00469-18. <https://doi.org/10.1128/AAC.00469-18>.
 30. Kieser T. 1984. Factors affecting the isolation of CCC DNA from *Streptomyces lividans* and *Escherichia coli*. *Plasmid* 12:19–36. [https://doi.org/10.1016/0147-619X\(84\)90063-5](https://doi.org/10.1016/0147-619X(84)90063-5).
 31. Zankari E, Hasman H, Cosentino S, Vestergaard M, Rasmussen S, Lund O, Aarestrup FM, Larsen MV. 2012. Identification of acquired antimicrobial resistance genes. *J Antimicrob Chemother* 67:2640–2644. <https://doi.org/10.1093/jac/dks261>.
 32. Dortet L, Oueslati S, Jeannot K, Tandé D, Naas T, Nordmann P. 2015. Genetic and biochemical characterization of oxa-405, an oxa-48-type extended-spectrum β -lactamase without significant carbapenemase activity. *Antimicrob Agents Chemother* 59:3823–3828. <https://doi.org/10.1128/AAC.05058-14>.
 33. Cornish-Bowden A. 1995. Fundamentals of enzyme kinetics. Portland Press, Seattle, WA.

OXY-2-15, a novel variant showing increased ceftazidime hydrolytic activity

R. H. T. Nijhuis^{1*}, S. Oueslati², K. Zhou³, R. W. Bosboom¹, J. W. A. Rossen³ and T. Naas²

¹Laboratory for Medical Microbiology and Immunology, Rijnsland, Velp, The Netherlands; ²Bactériologie-Virologie, AP-HP, LabEx LERMIT, Univ. Paris-Sud, Paris, France; ³Molecular Unit, Department of Medical Microbiology, University of Groningen, University Medical Center Groningen, Groningen, The Netherlands

*Corresponding author. Tel: +31-88-0055455; E-mail: rht.nijhuis@outlook.com

Received 6 October 2014; returned 17 December 2014; revised 29 December 2014; accepted 31 December 2014

Objectives: *Klebsiella oxytoca* is a member of the family of Enterobacteriaceae and often contains the β -lactamase *bla*_{OXY} gene. Although this β -lactamase does not naturally hydrolyse ceftazidime, this study describes possible *in vivo* selection of a clinical *K. oxytoca* isolate showing increased MICs of ceftazidime.

Methods: To reveal the molecular mechanism underlying this unusual resistance phenotype, WGS, cloning, over-expression, MIC and steady-state kinetic studies were performed.

Results: A patient was treated for a septic episode with ceftazidime (4 g/day). This therapy was based on earlier culture results in which, amongst others, a *K. oxytoca* (Velp-1) isolate was identified. After 11 days of treatment, *K. oxytoca* Velp-2 was isolated from a pus sample drained from the wound. The isolate showed increased resistance to ceftazidime (MIC \geq 64 mg/L) compared with the original *K. oxytoca* isolate (Velp-1). WGS revealed the presence of a novel *bla*_{OXY-2} allele, designated *bla*_{OXY-2-15}, with a two amino acid deletion at Ambler positions 168 and 169 compared with OXY-2-2. Cloning *bla*_{OXY-2-15} into *Escherichia coli* TOP10 resulted in increased MICs of ceftazidime, but reduced MICs of most other β -lactams compared with OXY-2-2. Steady-state kinetics confirmed the results of the MIC data, showing clearly significant ceftazidime hydrolysis.

Conclusions: This report shows the risk of *in vivo* selection of ceftazidime-resistant *K. oxytoca* isolates after prolonged ceftazidime treatment. Furthermore, it is the first known report of a *K. oxytoca* isolate conferring resistance to ceftazidime by a two amino acid deletion in the omega loop of OXY-2-2.

Keywords: antimicrobial resistance mechanisms, *bla* genes, Enterobacteriaceae, Gram-negative, K1, KOXY, ESBLs

Introduction

Klebsiella oxytoca is a Gram-negative bacillus of the family of Enterobacteriaceae involved in nosocomial infections. The main mechanisms of resistance to expanded-spectrum cephalosporins in this species are related to overproduction of a chromosomally encoded penicillinase (Ambler class A β -lactamase) due to mutations in the promoter region of the gene^{1,2} or to production of a plasmid-mediated ESBL.³ The naturally occurring chromosomal β -lactamase gene of *K. oxytoca* is called OXY and can be divided into six main groups, *bla*_{OXY-1} to *bla*_{OXY-6}, of which OXY-1 and OXY-2 are the clinically most prevalent.^{4,5}

OXY β -lactamases share ~80%–85% amino acid identity and confer a similar phenotype of resistance to many β -lactams, including aztreonam but not ceftazidime. A few OXY-2 derivatives with peculiar properties have been described. OXY-2-5 and OXY-2-6 confer a significant degree of resistance to ceftazidime as a result of a proline-to-serine substitution at Ambler position

167 compared with OXY-2.^{6,7} More recently, Younes *et al.*⁸ described an alanine-to-threonine change at position 237 in OXY-2, enhancing resistance to both cefotaxime and ceftazidime. Here, we present the first known report of a clinical isolate of *K. oxytoca* expressing an OXY-2-2 variant with a two amino acid deletion in the omega loop, resulting in increased hydrolysis of ceftazidime but decreased hydrolysis to most other β -lactams.

Materials and methods

Bacterial strains and plasmids

Clinical *K. oxytoca* Velp-1 and Velp-2 isolates were identified by MALDI-TOF MS, Maldi Biotyper v3.1 and FlexControl v3.3 (Bruker Daltonik GmbH, Bremen, Germany). *K. oxytoca* A producing OXY-2-2 and *K. oxytoca* B producing OXY-2-5 were used as controls for subcloning of *bla*_{OXY} alleles.^{5,6} *Escherichia coli* TOP10 (Life Technologies, Eragny, France) was used as the host strain for electroporation and cloning experiments and *E. coli*

BL21 for overexpression experiments.⁹ The plasmid vector pPCRBluntII-TOPO plasmid (Life Technologies) was used for subcloning PCR products and pET-9a (Stratagene, Amsterdam, the Netherlands) for overexpression experiments.

Antimicrobial agents, susceptibility testing and ESBL confirmation

Antibiotic susceptibility patterns were determined and interpreted by the Vitek 2 expert system (bioMérieux, Marcy-l'Étoile, France) according to EUCAST criteria.

The antibiogram of the recombinant *E. coli* clones was determined using disc diffusion on Mueller–Hinton agar (Bio-Rad, Marnes-La-Coquette, France) and the susceptibility breakpoints were determined as previously described.⁹ MICs of β -lactam antibiotics were determined using Etest or the microbroth dilution technique as previously described and interpreted as recommended by EUCAST.^{9,10}

Phenotypical ESBL confirmation was performed by using the combination disc diffusion test as recommended by the Dutch guideline.¹¹ The genotypic confirmation method was performed using the Check-MDR ESBL assay (Check-Points, Wageningen, the Netherlands).^{12,13}

WGS and nucleotide sequence accession number

Total DNA was extracted from colonies using the Ultraclean Microbial DNA Isolation Kit (MO BIO Laboratories, Carlsbad, CA, USA) following the manufacturer's instructions. The DNA concentration and purity were controlled by a Qubit[®] 2.0 Fluorometer using the dsDNA HS and/or BR Assay Kit (Life Technologies, Carlsbad, CA, USA). The DNA library was prepared using the Nextera XT-v3 Kit (Illumina, San Diego, CA, USA) according to the manufacturer's instructions and then run on Miseq (Illumina) for generating paired-end 300 bp reads. *De novo* assembly was performed by CLC Genomics Workbench v7.0.4 (Qiagen, Hilden, Germany) after quality trimming (Qs \geq 20) with word size 34. The acquired antimicrobial resistance genes were identified by uploading assembled genomes to Resfinder server v2.1 (<http://cge.cbs.dtu.dk/services/ResFinder-2.1/>).¹⁴

The *bla*_{OXY-2-15} nucleotide and deduced protein sequences have been deposited in the *Klebsiella* sequence typing database (Pasteur Institute, <http://bigsdw.web.pasteur.fr/klebsiella/klebsiella.html>) and in the GenBank nucleotide database (KM382431).

PCR, cloning and Sanger sequencing

Total DNA was extracted using the Qiagen DNA Kit. Recombinant plasmids, pOXY-2-2, pOXY-2-5 and pOXY-2-15, were constructed according to the manufacturer's instruction by cloning the PCR-generated fragments using primers NdeI-ATG (5'-AAAAACATATGATAAAAAGTTCGTGGCGTA-3') and BamHI-STOP (5'-AAAAAGGATCCTTAAAGCCCTTCGGTCACGA-3') into pPCRBluntII-TOPO plasmid from *K. oxytoca* A, *K. oxytoca* B and *K. oxytoca* Velp-2, respectively. Recombinant plasmids were electroporated into *E. coli* TOP10 using a GenePulser II as recommended by the manufacturer (Bio-Rad).

The PCR fragment of the *bla*_{OXY-2-15} gene using primers NdeI-ATG and BamHI-STOP was also restricted using NdeI and BamHI restriction enzymes and cloned directly into an NdeI/BamHI-restricted pET-9a expression vector, resulting in recombinant plasmid pET-OXY-2-15 that was electroporated into *E. coli* BL21.

Recombinant plasmid DNAs were extracted with the Qiagen Plasmid DNA Midi Kit and both strands of the inserts were sequenced with an Applied Biosystems sequencer (ABI PRISM 3100).

Purification and steady-state kinetics

E. coli BL21 (pET-OXY-2-15) with an OD₆₀₀ of 0.6 was induced with IPTG (0.2 mM) overnight at 24°C in 2 L of trypticase soy (TS) broth containing

kanamycin (50 mg/L), as previously described.⁹ The culture was centrifuged at 6000 g for 15 min, after which the pellet was resuspended with 10 mL of 20 mM Bis-Tris propane H₂SO₄ (pH 7.3) and treated with lysozyme. After two subsequent centrifugations (14 000 rpm for 1 h at 4°C and 48 000 rpm for an additional 1 h at 4°C), the supernatant was loaded onto a Q-Sepharose column (GE Healthcare, Courtaboeuf, France) that was pre-equilibrated with 20 mM Tris H₂SO₄ (pH 8) and eluted using a linear NaCl gradient (0–1 M) in the same buffer. The fractions containing the highest β -lactamase activity as revealed with nitrocefin (Calbiochem, Paris, France) were pooled and dialysed overnight against 50 mM sodium phosphate buffer (pH 7.0)/150 mM NaCl. The β -lactamase extract was concentrated using a Vivaspin[®] 10 000 MWCO PES column (Sartorius, Paris, France) before loading onto a Sephadex 75 gel filtration column (GE Healthcare). Peaks containing β -lactamase activity were concentrated and dialysed against 100 mM sodium phosphate buffer (pH 7.0). The protein content was measured using the Bio-Rad DC protein assay. The purity of the enzyme was estimated by SDS–PAGE.

The purified β -lactamase OXY-2-15 was used for kinetic parameter (k_{cat} and K_m) determination as previously described using the Eadie–Hofstee linearization $\{V = (V_{max} - V)K_m/[S]\}$ of the Michaelis–Menten equation $\{V = V_{max}[S]/(K_m + [S])\}$.¹⁰

Ethics

No ethics approval was required for this study.

Results

Clinical case

In November 2013, a patient with Crohn's disease was admitted for subtotal colectomy at Rijnstate Hospital, Arnhem, the Netherlands. During his stay on the ICU, he developed a bowel perforation and was treated with cefuroxime and metronidazole. Bacterial culturing revealed, amongst two others, *K. oxytoca* Velp-1 that was shown to be resistant to the prescribed cefuroxime but susceptible to ceftazidime. Hence, treatment was changed to ceftazidime (4 g/day). In early December, a new septic episode occurred, for which the treatment with ceftazidime was restarted and continued for 11 days. At the end of December 2013, a pus specimen coming from the abdominal wound revealed the presence of a ceftazidime-resistant *K. oxytoca* Velp-2 that showed resistance to ceftazidime (MIC \geq 64 mg/L) and was suspected to be an ESBL producer according to the Vitek 2 expert system.

ESBL confirmation and WGS analysis

Antibiotic susceptibility testing of *K. oxytoca* Velp-2 using Vitek 2 displayed high-level resistance to most β -lactams except carbapenems and presented an unusual resistance to ceftazidime. ESBL confirmation using the combination disc diffusion suggested the production of an acquired ESBL (data not shown), while the Check-MDR ESBL assay, which detects *bla*_{TEM}, *bla*_{SHV} and *bla*_{CTX-M} genes, remained negative.

WGS revealed a novel *bla*_{OXY-2-2}-type β -lactamase gene: *bla*_{OXY-2-15}. This gene differed from the reference *bla*_{OXY-2-2} gene (AJ871867.1)⁵ by a six nucleotide in-frame deletion resulting in a two amino acid deletion, threonine168 and leucine169 according to Ambler numbering (Figure 1).¹⁵ No additional resistance genes were found in the *in silico* analysis.

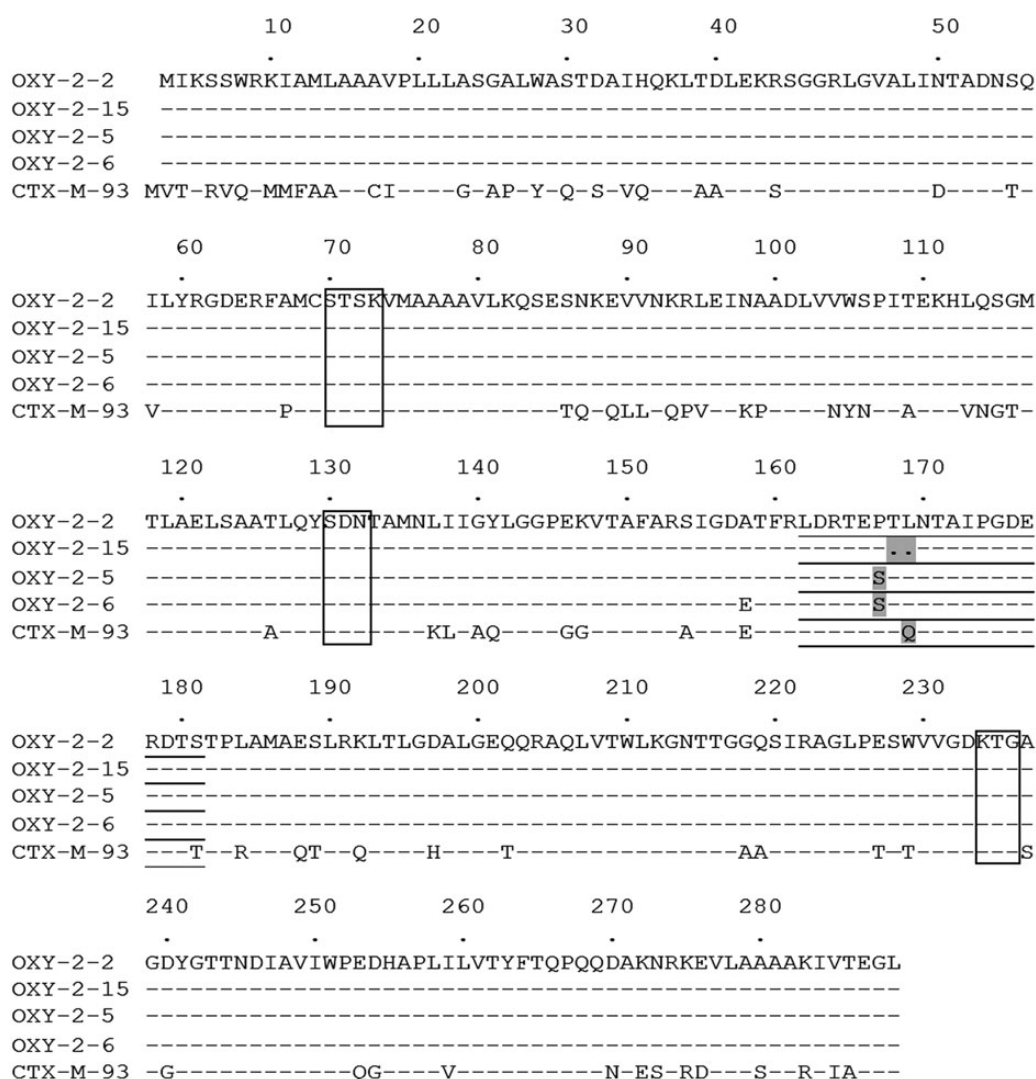


Figure 1. Alignment of the amino acid sequence of β-lactamase OXY-2-15 with those of the parental enzyme OXY-2-2 and three enzymes with increased ceftazidime hydrolysis [two OXY-2-2 variants (OXY-2-5 and OXY-2-6) and CTX-M-93].¹⁷ Numbering is according to the previous description.¹⁵ Dashes represent identical amino acid residues. Dots indicate gaps introduced to optimize the alignment. Differences in the omega loop (underlined amino acids) are indicated with grey highlighting. Structural elements characteristic of class A β-lactamases are boxed.

Cloning of *bla*_{OXY-2-15} gene

By cloning the different *bla*_{OXY} alleles into an isogenic background (pPCRBluntII-TOPO plasmid and *E. coli* TOP10), we were able to observe differences in MICs as the result of amino acid differences between the enzymes. The MIC of ceftazidime for OXY-2-15 (64 mg/L) showed a major increase compared with its parental type OXY-2-2 and even OXY-2-5, a variant with increased ceftazidime hydrolysis, with MICs of 0.5 and 16 mg/L, respectively (Table 1). In comparison with OXY-2-2 and OXY-2-5, OXY-2-15 showed reduced MICs of all substrates other than ceftazidime.

Steady-state kinetic parameters

The purity of the OXY-2-15 was estimated to be >99% according to SDS-PAGE analysis and its apparent molecular mass was ~27 kDa.

The kinetic parameters of purified OXY-2-15 β-lactamase revealed activity against restricted and expanded-spectrum cephalosporins (Table 1). The enzyme showed high affinities (K_m) for cephalosporins including ceftazidime and the highest level of activity (k_{cat}) against cefaloridine, aztreonam and ceftazidime. Interestingly, catalytic efficiency (k_{cat}/K_m) for ceftazidime is higher than for cefotaxime. As expected from MIC data, there was no or only very weak hydrolysis of penicillins. The OXY-2-15 β-lactamase remained unable to hydrolyse carbapenems or cephamycins.

Discussion

A novel OXY variant, OXY-2-15, has been identified in a clinical strain of *K. oxytoca* Velp-2 isolated from a pus specimen coming from an abdominal wound. Based on the susceptibility patterns of both

Table 1. Kinetic parameters of purified β -lactamase OXY-2-15 and MICs for clinical strain *K. oxytoca* Velp-2 and *E. coli* TOP10 recombinant clones expressing OXY-2-15, OXY-2-2 and OXY-2-5

	Kinetic parameters of purified β -lactamase OXY-2-15			MIC (mg/L)				
	K_m (μ M)	k_{cat} (s^{-1})	k_{cat}/K_m ($mM^{-1}\cdot s^{-1}$)	<i>K. oxytoca</i> Velp-2 ^a	<i>E. coli</i> TOP10 (pTOPO-OXY-2-15) ^b	<i>E. coli</i> TOP10 (pTOPO-OXY-2-2) ^b	<i>E. coli</i> TOP10 (pTOPO-OXY-2-5) ^b	<i>E. coli</i> TOP10
Benzylpenicillin	ND ^c	ND	ND	— ^d	—	—	—	—
Amoxicillin	280 ^e	0.05	0.2	12	6	>256	>256	3
Amoxicillin+CLA ^f	—	—	—	4	6	24	12	3
Piperacillin	43	0.05	1.3	64	16	>256	>256	1.5
Piperacillin+TZB ^f	—	—	—	6	2	12	1.5	1.5
Ticarcillin ^g	ND	ND	ND	64	32	>256	>256	2
Temocillin	—	—	—	8	8	8	12	4
Cefalotin	6	0.03	5	8	8	>256	>256	4
Cefaloridine	10	0.2	22	—	—	—	—	—
Cefoxitin	—	—	—	8	8	16	2	2
Cefuroxime	—	—	—	32	16	>256	>256	4
Ceftriaxone	ND	ND	ND	—	—	—	—	—
Cefepime	11	0.007	0.6	3	1	0.38	0.38	0.023
Cefotaxime	69	0.006	0.1	3	1	1	1.5	0.06
Ceftazidime	47	0.1	2	>256	64	0.5	16	0.25
Imipenem	ND	ND	ND	0.19	0.19	0.25	0.25	0.19
Aztreonam	18	0.2	11	8	2	6	3	0.047

^aClinical *K. oxytoca* Velp-2 isolate producing OXY-2-15.

^b*E. coli* TOP10 (pTOPO-OXY-2-15), *E. coli* TOP10 (pTOPO-OXY-2-2) and *E. coli* TOP10 (pTOPO-OXY-2-5), expression of OXY-2-15, OXY-2-2 and OXY-2-5, respectively.

^cND, not detectable (the initial rate of hydrolysis was $<0.001 \mu$ M/s).

^d—, not included in the experiments.

^eData are means from three independent experiments. Standard deviations were within 15%.

^fCLA, clavulanic acid at a fixed concentration of 2 mg/L; TZB, tazobactam at a fixed concentration of 4 mg/L.

^g k_{cat} (s^{-1}) value for ticarcillin was very low, even though the K_m (μ M) value was $<1 \mu$ M.

K. oxytoca Velp-2 and the earlier identified *K. oxytoca* Velp-1, it is likely that *K. oxytoca* Velp-2 and Velp-1 are related and that OXY-2-15 is the result of *in vivo* selection. Unfortunately, since Velp-1 has not been stored, typing to confirm the relatedness of the two isolates is not possible.

Nevertheless, WGS analysis of *K. oxytoca* Velp-2 revealed the presence of a novel bla_{OXY-2} allele that differed from the $bla_{OXY-2-2}$ gene by a six nucleotide in-frame deletion resulting in a deletion of threonine168 and leucine169 according to Ambler numbering. Amino acid substitutions in the omega loop of class A β -lactamases (e.g. proline-to-serine substitutions at Ambler position 167 in CTX-M-19, OXY-2-5 and OXY-2-6 β -lactamases¹⁶) have previously been shown to result in a higher level of catalytic activity against ceftazidime with slightly reduced activity against other β -lactams. Position 169 is well conserved among ESBLs, most of them showing a leucine or methionine residue.¹⁷ In CTX-M-93, the Leu169Gln replacement was responsible for increased activity against ceftazidime with a concomitant decreased activity against penicillins.¹⁷ Interestingly, Leu169Cys substitution found in TLA-2 ESBL conferred similar activities.¹⁷ Moreover, *in vitro* mutagenesis experiments with TEM-1 enzyme showed similar behaviour against ceftazidime in mutants with Leu169Pro substitution.¹⁸ Therefore, the deletion of threonine168

and leucine169 may be responsible for the ceftazidime resistance in *K. oxytoca* Velp-2. This hypothesis was confirmed by cloning OXY-2-15 into *E. coli* TOP10, which showed a major increase in the MIC of ceftazidime compared with its parental type OXY-2-2 and by steady-state kinetic parameters, revealing high activity against ceftazidime.

This is the first known report of a ceftazidime-resistant *K. oxytoca* isolate that is the consequence of a two amino acid deletion in the natural OXY-2 β -lactamase. This work indicates the possible risk of *in vivo* selection of ceftazidime resistance subsequent to prolonged use of this antibiotic and that ceftazidime resistance in *K. oxytoca* may not always be related to plasmid-mediated ESBL production. Thus, in contrast to plasmid-mediated ESBL-producing strains, isolation of ceftazidime-resistant *K. oxytoca* isolates will not always require isolation measures. Moreover, although ceftazidime has been suggested for treating infections caused by β -lactamase-overproducing *K. oxytoca* strains, our study suggests that it might be safer to use other antibiotics.

Acknowledgements

This work was done in collaboration with the ESCMID Study Group on Molecular Diagnostics (ESGMD), Basel, Switzerland.

Funding

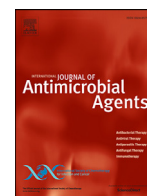
This study was partly supported by the Interreg Iva-funded projects EurSafety Heath-net (III-1-02=73) and SafeGuard (III-2-03=025) and by a grant from the Université Paris Sud, France. T. N. and S. O. are members of the Laboratory of Excellence LERMIT supported by a grant from ANR (ANR-10-LABX-33).

Transparency declarations

None to declare.

References

- 1 Fournier B, Lu CY, Lagrange PH *et al.* Point mutation in the pnbw box, the molecular basis of β -lactamase overproduction in *Klebsiella oxytoca*. *Antimicrob Agents Chemother* 1995; **39**: 1365–8.
- 2 Fournier B, Gravel A, Hooper DC *et al.* Strength and regulation of the different promoters for chromosomal β -lactamases of *Klebsiella oxytoca*. *Antimicrob Agents Chemother* 1999; **43**: 850–5.
- 3 Bush K, Jacoby GA, Medeiros AA. A functional classification scheme for β -lactamases and its correlation with molecular structure. *Antimicrob Agents Chemother* 1995; **39**: 1211–33.
- 4 Fournier B, Roy PH, Lagrange PH *et al.* Chromosomal β -lactamase genes of *Klebsiella oxytoca* are divided into two main groups, *bla*_{OXY-1} and *bla*_{OXY-2}. *Antimicrob Agents Chemother* 1996; **40**: 454–9.
- 5 Fevre C, Jbel M, Passet V *et al.* Six groups of the OXY β -lactamase evolved over millions of years in *Klebsiella oxytoca*. *Antimicrob Agents Chemother* 2005; **49**: 3453–62.
- 6 Mammeri H, Poirel L, Nordmann P. In vivo selection of a chromosomally encoded β -lactamase variant conferring ceftazidime resistance in *Klebsiella oxytoca*. *Antimicrob Agents Chemother* 2003; **47**: 3739–42.
- 7 Rodríguez-Martínez J-M, Poirel L, Nordmann P *et al.* Ceftazidime-resistant *Klebsiella oxytoca* producing an OXY-2-type variant from Switzerland. *Int J Antimicrob Agents* 2008; **32**: 278–9.
- 8 Younes A, Hamouda A, Amyes SGB. First report of a novel extended-spectrum β -lactamase KOXY-2 producing *Klebsiella oxytoca* that hydrolyses cefotaxime and ceftazidime. *J Chemother* 2011; **23**: 127–30.
- 9 Naas T, Aubert D, Özcan A *et al.* Chromosome-encoded narrow-spectrum Ambler class A β -lactamase GIL-1 from *Citrobacter gillenii*. *Antimicrob Agents Chemother* 2007; **51**: 1365–72.
- 10 Philippon LN, Naas T, Bouthors AT *et al.* OXA-18, a class D clavulanic acid-inhibited extended-spectrum β -lactamase from *Pseudomonas aeruginosa*. *Antimicrob Agents Chemother* 1997; **41**: 2188–95.
- 11 Nederlandse Vereniging voor Medische Microbiologie (NVMM). *Guideline: Laboratory Detection of Highly Resistant Microorganisms (HRMO)*. 2012. <http://www.nvmm.nl/richtlijnen/hrmo-laboratory-detection-highly-resistant-microorganisms>.
- 12 Nijhuis R, van Zwet A, Stuart JC *et al.* Rapid molecular detection of extended-spectrum β -lactamase gene variants with a novel ligation-mediated real-time PCR. *J Med Microbiol* 2012; **61**: 1563–7.
- 13 Willemsen I, Hille L, Vrolijk A *et al.* Evaluation of a commercial real-time PCR for the detection of extended spectrum β -lactamase genes. *J Med Microbiol* 2014; **63**: 540–3.
- 14 Zankari E, Hasman H, Cosentino S *et al.* Identification of acquired antimicrobial resistance genes. *J Antimicrob Chemother* 2012; **67**: 2640–4.
- 15 Ambler RP, Coulson AF, Frere JM *et al.* A standard numbering scheme for the class A β -lactamases. *Biochem J* 1991; **276**: 269–70.
- 16 Poirel L, Naas T, Le Thomas I *et al.* CTX-M-type extended-spectrum β -lactamase that hydrolyzes ceftazidime through a single amino acid substitution in the omega loop. *Antimicrob Agents Chemother* 2001; **45**: 3355–61.
- 17 Djamdjian L, Naas T, Tande D *et al.* CTX-M-93, a CTX-M variant lacking penicillin hydrolytic activity. *Antimicrob Agents Chemother* 2011; **55**: 1861–6.
- 18 Vakulenko S, Golemi D. Mutant TEM β -lactamase producing resistance to ceftazidime, ampicillins, and β -lactamase inhibitors. *Antimicrob Agents Chemother* 2002; **46**: 646–53.



Whole-genome sequencing of NDM-1-producing ST85 *Acinetobacter baumannii* isolates from Tunisia

Nadia Jaidane^{a,b,c,f}, Thierry Naas^{c,d,e}, Saoussen Oueslati^{c,e}, Sandrine Bernabeu^{c,e},
Noureddine Boujaafar^{a,b,f}, Olfa Bouallegue^{a,b,g}, Rémy A. Bonnin^{c,d,e,*}

^aUR 12 SP 37, Emerging Bacterial Resistance and Safety of Care, Department of Clinical Microbiology, University Hospital of Sahloul, Sousse, Tunisia

^bClinical Microbiology Laboratory, University Hospital of Sahloul, Sousse, Tunisia

^cEA7361, Université Paris-Sud, Université Paris-Saclay, LabEx Lermite, Bacteriology-Hygiene Unit, APHP, Hôpital Bicêtre, Le Kremlin-Bicêtre, France

^dEERA 'Evolution and Ecology of Resistance to Antibiotics' Unit, Institut Pasteur-APHP-Université Paris Sud, Paris, France

^eAssociated French National Reference Centre for Antibiotic Resistance 'Carbapenemase-producing Enterobacteriaceae', Le Kremlin-Bicêtre, France

^fFaculty of Pharmacy, University of Monastir, Monastir, Tunisia

^gFaculty of Medicine Ibn El Jazzar, University of Sousse, Sousse, Tunisia

ARTICLE INFO

Article history:

Received 6 February 2018

Accepted 23 May 2018

Keywords:

Acinetobacter baumannii

Carbapenemase

Resistome

OXA-23

Tn2008

*bla*_{NDM-1}

ABSTRACT

Background: New Delhi metallo- β -lactamase (NDM)-producing *Acinetobacter baumannii* have been described in several countries worldwide, and studies have suggested that *Acinetobacter* spp. could play the role of intermediate progenitor of the *bla*_{NDM-1} gene between environmental progenitor and Enterobacteriaceae.

Materials and methods: In total, 246 carbapenem-resistant *A. baumannii* isolates from a teaching hospital in Sousse, Tunisia were investigated between 1st June 2013 and 31st December 2015 to detect metallo- β -lactamase (MBL) production. Polymerase chain reaction (PCR), antibiotic susceptibility testing, and genetic and whole-genome sequencing tools were used to study the underlying carbapenem resistance mechanisms.

Results: PCR screening of the 246 carbapenem-resistant *A. baumannii* isolates revealed that 242 of 246 isolates harboured carbapenemase genes (seven of 246 positive for *bla*_{NDM-1}, four of 246 positive for *bla*_{NDM-1} and *bla*_{OXA-23}, 231 positive for *bla*_{OXA-23}). Conjugation and electroporation experiments suggested that the *bla*_{NDM-1} gene is likely to be chromosomally located. All the NDM-1-producing *A. baumannii* isolates were clonally related, and belonged to ST85 according to the Pasteur Institute's multi-locus sequence typing scheme. Analysis of the immediate genetic environment of the *bla*_{NDM-1} gene revealed that the gene was located within a truncated isoform of Tn125 transposon (Δ Tn125). The *bla*_{OXA-23} gene was located within transposon Tn2008.

Conclusion: This study showed the dissemination of a single clone of NDM-1-producing *A. baumannii* in a Tunisian hospital. Countries in north Africa may constitute a significant reservoir for NDM-1-producing *A. baumannii*. The spread of the *bla*_{NDM-1} gene in *A. baumannii* was linked to clonal spread in this study.

© 2018 Elsevier B.V. and International Society of Chemotherapy. All rights reserved.

1. Introduction

Over the last decade, *Acinetobacter baumannii* has become the most threatening of the ESKAPE pathogens in hospital settings [1]. The high level of carbapenem-resistant *A. baumannii* is more commonly mediated by production of acquired class D carbapenem-

hydrolysing β -lactamases and, to a lesser extent, class A and B carbapenemases [2,3].

Since its first description in 2009 in *Klebsiella pneumoniae* clinical isolates from a Swedish patient who had previously been hospitalized in India, New Delhi metallo- β -lactamase 1 (NDM-1) is spreading worldwide among Gram-negative bacteria [4,5]. Cases of NDM-producing *A. baumannii* have been described in several countries [6,7]. Rapid dissemination of this gene within Enterobacteriaceae and *Acinetobacter* species and across genera can be explained by the variability of the location and the genetic environment of *bla*_{NDM-1} [7,8]. *bla*_{NDM-1} is carried by a class I composite transposon bracketed by two copies of ISAb125 [8]. This transposon has been

* Corresponding author: Service de Bactériologie-Hygiène, Hôpital de Bicêtre, 78 rue du Général Leclerc, 94275 Le Kremlin-Bicêtre Cedex, France.

E-mail address: remy.bonnin@u-psud.fr (R.A. Bonnin).

identified on plasmids and chromosomes [7]. The present study reports the genomic characterization of 11 *bla*_{NDM-1}-positive *A. baumannii* strains recovered from patients hospitalized in a Tunisian hospital.

2. Materials and methods

2.1. Clinical data and susceptibility testing

In total, 408 non-duplicate clinical isolates of *A. baumannii* were collected from June 2013 to December 2015 at the University Hospital of Sahloul, Sousse, Tunisia. Of these, 376 isolates were resistant to carbapenem, and it was possible to reculture 246 isolates for further study. Species identification was initially performed using a VITEK 2 fluorescent card (bioMérieux, La Balme Les Grottes, France), and was confirmed by matrix-assisted laser desorption/ionization time-of-flight mass spectrometry (Microflex, Bruker Daltonics, Bremen, Germany), as described previously.

Routine antibiograms were determined by disk diffusion on Mueller-Hinton agar plates at 37°C. The minimum inhibitory concentrations (MICs) of β -lactams, including ceftazidime, cefotaxime, imipenem, meropenem and doripenem, were determined by Etest (bioMérieux). The MICs for colistin were determined by broth microdilution in cation-adjusted Mueller-Hinton broth, according to the recommendations of the Clinical and Laboratory Standards Institute [9]. All results were interpreted in accordance with the updated EUCAST breakpoint tables for interpretation of MICs and zone diameters (www.eucast.org/fileadmin/src/media/PDFs/EUCAST_files/Breakpoint_tables/v_5.0_Breakpoint_Table_01.pdf) [10]. Carbapenemase activity was investigated using the CarbAcineto NP test, as described previously [11]. As there is no breakpoint for tigecycline for *Acinetobacter* spp., the breakpoint for Enterobacteriaceae was used.

Metallo- β -lactamase (MBL) production was assessed by the inhibition of carbapenemase activity by EDTA. Briefly, two 10 μ g disks of imipenem were placed 25 mm apart on Mueller-Hinton plates, and 10 μ L of MBL inhibitor solution (0.5 M EDTA) was added to one disk. After 24 h of incubation at 35°C, the inhibition zone diameter for each disk was measured and compared. If the difference in the inhibition zone between the carbapenem disk and the carbapenem-EDTA disk was ≥ 7 mm, the isolate was considered to be MBL positive [10].

The MBL phenotype was confirmed with MBL Etest for the positive strains ($n=11$), in accordance with the manufacturer's instructions (bioMérieux). MBL Etest (imipenem 4–256 μ g/mL and imipenem/EDTA 1–64 μ g/mL) (Liöfilchem, Roseto degli Abruzzi, Italy) was performed according to the manufacturer's recommendations.

2.2. Carbapenemase gene detection

Real-time polymerase chain reaction (PCR) and conventional PCR were performed to screen for the presence of *bla*_{OXA-58}, *bla*_{OXA-23}, *bla*_{OXA-24}, *bla*_{NDM-1}, *bla*_{IMP}, *bla*_{VIM}, *bla*_{SIM} and *bla*_{GIM} genes using primers described previously [2].

2.3. Plasmid identification and transformation

Plasmid DNA of MBL-positive isolates of *A. baumannii* were extracted using the Kieser method, as described previously [13]. Plasmids of ca. 154, 66, 48 and 7 kb of *Escherichia coli* NCTC 50192 were used as plasmid size markers. Plasmid DNA of MBL-positive *A. baumannii* was analysed by agarose gel electrophoresis. Conjugation and electroporation experiments were performed using MBL-positive *A. baumannii* as the donor and rifampin-resistant *A. baumannii* BM4547 as the recipient, as described elsewhere [14].

2.4. Whole-genome sequencing

Genomic DNA was extracted using an UltraClean microbial DNA isolation kit (MO BIO Laboratories, Mo-Bio, Sait-Quentin en Yvelines, France) from overnight cultures in LB agar (Bio-Rad, Marnes-la-Coquette, France). Genomic DNA quantification was performed using a Qubit fluorometer (Life Technologies, Carlsbad, CA, USA) and adjusted to 0.2 ng/ μ L. Library preparation was performed using a Nextera XT DNA sample preparation kit (Illumina, San Diego, CA, USA), and an Illumina MiSeq 2000 sequencer with v3 chemistry with 2 \times 150-bp paired-end reads was used for sequencing. The 150-bp paired-end reads were assembled de novo using CLC Genomics Workbench with a minimum contig length of 500 bp.

2.5. Identification of antibiotic resistance genes

Antibiotic-resistance-related genes were predicted using ResFinder Version 2.1 with the following parameters: 'all databases' were used for antimicrobial configuration, type of reads as 'assembled genomes/contigs', and thresholds of 98% identity and 80% coverage between sequences.

2.6. Phylogenetic classification and multi-locus sequence typing

Whole-genome sequences were submitted to the CSI phylogeny server to construct a single nucleotide polymorphism (SNP)-based phylogenetic tree (<http://www.genomicepidemiology.org/>). The parameters used to construct the tree were as follows: minimum depth at SNP position 10X, minimum distance between SNPs 10 bp and minimum read mapping quality at 25. FigTree v1.4.3 was used to represent the tree. The reference genome used was *A. baumannii* AYE (Genbank Accession Number CT025791).

MLST was performed using the MLST 1.8 server (<http://www.genomicepidemiology.org/>). The two MLST schemes (Oxford and Pasteur) available for *A. baumannii* were tested (<http://pubmlst.org/abaumannii/>) [15,16].

2.7. Nucleotide sequence accession numbers

The Whole Genome Shotgun project has been deposited at DDBJ/ENA/GenBank under accession numbers MWTR00000000 to MWTZ00000000 and MWUB00000000 to MWUB00000000.

3. Results and discussion

3.1. Demographic, clinical microbiological and molecular data

In total, 246 *A. baumannii* isolated from 1st June 2013 to 31st December 2015 were investigated at a teaching hospital in Sousse, Tunisia. The majority [196 of 246 (79.7%)] of isolates were recovered from patients hospitalized in the intensive care unit. The predominant sites of infection were blood [94 of 246 (38.2%)], urine cultures [50 of 246 (20.3%)], respiratory specimens [29 of 246 (11.8%)] and other specimens [73 of 246 (29.7%)].

The results of antibiotic susceptibility testing for the 246 *A. baumannii* isolates showed high-level resistance to all β -lactams (>90%), aminoglycosides (92% to gentamicin, 90% to amikacin) and fluoroquinolones (>95%). Isolates remained susceptible to tigecycline, rifampin and colistin, with resistance rates of 55.6%, 36% and 0.4%, respectively.

The EDTA double-disk test revealed 11 MBL-positive carbapenem-resistant *A. baumannii* (MBL_{Ab}) confirmed by an MBL Etest (bioMérieux), which revealed a several-fold reduction in the imipenem MIC when combined with EDTA, which suggested production of an MBL. The presence of carbapenemase responsible

for carbapenem hydrolysis was detected in the 11 MBLAb with the CarbAcineto NP test [9].

PCR screening of the 246 carbapenem-resistant *A. baumannii* isolates revealed 242 isolates harbouring carbapenemase genes (seven positive for *bla*_{NDM}, four positive for *bla*_{NDM-1} and *bla*_{OXA-23}, 231 positive for *bla*_{OXA-23} with-specific primers) [12]. Sequencing of the NDM amplicons using Sanger's sequencing method revealed the presence of NDM-1.

The 11 MBLAb were isolated from different patients of different ages (between 2 and 74 years old) admitted to different wards, presented different co-morbidities, and were empirically treated with different antimicrobial treatments before isolation of the MBL-positive strain (Table 1).

3.2. Sequencing data

The draft genome of the 11 MBLAb isolates resulted in a mean of 1 474 352 reads, with an average length of 15 032 bp. The mean number of contigs was 735 with a N50 of 15 963 bp (Table 2). Genomic GC content showed little variation around an average value of 38.92%, which is in accordance with the genome of *A. baumannii* species. The genomes ranged in size between 3 718 150 and 4 007 735 bp (average size 3 863 250 bp).

A mean total of 3612 protein-coding sequences involved in essential metabolism of the bacteria was predicted, and 44 RNAs were predicted by the RAST server [17]. Accessory features were also present, such as those conferring resistance to antibiotics and toxic compounds (e.g. β -lactam, fosfomycin and aminoglycoside resistance genes; arsenic, copper and mercury resistance genes).

3.3. Resistome: β -lactamases

*bla*_{OXA-94}, belonging to the OXA-51-type enzymes, was detected in all strains (Table 2). The *bla*_{OXA-51}-like gene is the naturally occurring β -lactamase in *A. baumannii*. This gene can be used as a rapid method for *A. baumannii* identification [18]. Moreover, *ISAb1* was found to be inserted 7 bp upstream of *bla*_{OXA-94}, providing a promoter that significantly increases its expression and contributes to carbapenem resistance [19]. Also, chromosomally-encoded ADC-like cephalosporinases were identified with 99% amino acid identity with the closest ADC-79. This gene was overexpressed by *ISAb1* in all the strains, leading to cephalosporinase overexpression and resistance to broad-spectrum cephalosporins. *ISAb1* was inserted 7 bp upstream of the *bla*_{ADC} gene, providing promoter sequences. *ISAb1* was inserted exactly 7 bp upstream of *bla*_{OXA-94} and *bla*_{ADC-79}-like. The terminal bases of the inverted repeat associated with the bp at the vicinity also provide a potential ribosome-binding site (RBS): AGAGGC and GAGAAG for *bla*_{ADC-79}-like and *bla*_{OXA-94} respectively. *ISAb1* is the most common insertion sequence (IS), responsible for the overexpression of antimicrobial resistance genes such as *bla*_{OXA-23}-like, *bla*_{OXA-51}-like and *bla*_{ADC}-like in *A. baumannii* [20].

All the MBLAb sequences harboured a chromosomally located *bla*_{NDM-1} gene. Four isolates co-expressed the *bla*_{OXA-23} carbapenemase gene.

Further analysis of the immediate genetic environment of *bla*_{NDM-1} revealed the location of the gene within an isoform of Tn125 transposon (Δ Tn125). This transposon is the result of a truncation in the right-hand extremity of Tn125 by insertion sequence *ISAb14* (Fig. 1A). This structure starts with one copy of *ISAb125* at the 5' end of the *bla*_{NDM-1} gene, followed by *ble*_{MBL} encoding a 121-amino-acid-long protein conferring resistance to bleomycin as described previously and *ISAb14* at the 3' end as described previously [21].

Dissemination of the NDM gene within Enterobacteriaceae and *Acinetobacter* species and across genera can be explained by the

Table 1
Clinical features for 11 *Acinetobacter baumannii* isolates harbouring *bla*_{NDM-1}.

Isolates	Date of isolation	Age range (years)	Sex	Date of admission	Ward	Sample	MIC (mg/L)						Previous treatment	Outcome				
							CTX ^a	CAZ ^a	IP ^a	MP ^a	DP ^a	COL ^b			IP/IP1 ^a	CIP ^a	L VX ^a	RA ^a
M1	13.06.13	20–30	M	2013–05	PMR	Urine	>32	>256	>32	>32	>32	0.5	192/<1	>32	8	5	Discharge on 15-08-2013	
M2	22.06.14	40–50	M	2014–06	Surgical ICU	Urine	>32	>256	>32	>32	>32	0.5	96/<1	>32	12	4	Discharge on 08-07-2014	
M3	16.09.14	>70	M	2014–09	Medical ICU	Blood	>32	>256	>32	>32	>32	0.5	96/<1	8	1.5	2	Dead on 19-09-2014	
M4	23.03.15	20–30	M	2015–03	Surgical ICU	Blood	>32	>256	>32	>32	>32	0.5	96/6	>32	12	4	Discharge on 11-04-2015	
M5	28.03.15	>10	M	2015–03	Paediatric unit	urinary tract catheter	>32	>256	>32	>32	>32	0.5	128/6	>32	>32	3	3	Discharge on 21-04-2015
M6	15.04.15	NA	M	NA	Urology ext	Urine	>32	>256	>32	>32	>32	0.5	96/1	>32	8	4	Not available	
M7	25.04.15	20–30	M	2015–04	Surgical ICU	Blood	>32	>256	>32	>32	>32	1	96/4	>32	8	4	Discharge on 07-05-2015	
M8	15.05.15	50–60	M	2015–05	Nephrology	Urine	>32	>256	>32	>32	>32	1	96/12	>32	8	4	Discharge on 11-05-2015	
M9	23.05.15	50–60	M	2015–05	Medical ICU	urinary tract catheter	>32	>256	>32	>32	>32	1	192/1	>32	7	6	Discharge on 25-05-2015	
M10	01.09.15	30–40	M	2015–08	Burn unit	Blood	>32	>256	>32	>32	>32	1	24/8	>32	>32	4	4	Dead on 21-09-2015
M11	01.10.15	>70	F	2015–09	Surgical ICU	Urine	>32	>256	>32	>32	>32	0.5	24/8	>32	24	4	Dead on 19-02-2015	

N/A, not available; MIC, minimum inhibitory concentration; ICU, intensive care unit; AMC, amoxicillin/clavulanate; CTX, cefotaxim; CAZ, ceftazidim; DP, doripenem; IP, imipenem; IP/1, imipenem+inhibitor; COL, colistin; CIP, ciprofloxacin; LVX, levofloxacin; OFX, ofloxacin; RA, rifampin; GEN, gentamicin; VM, vancomycin.
^a MIC was determined using Etest (bioMérieux, France) and interpreted according to the EUCAST guidelines.
^b MIC for colistin were determined by broth microdilution in cation-adjusted Mueller-Hinton broth according to the guidelines of the Clinical and Laboratory Standards Institute [33,34].

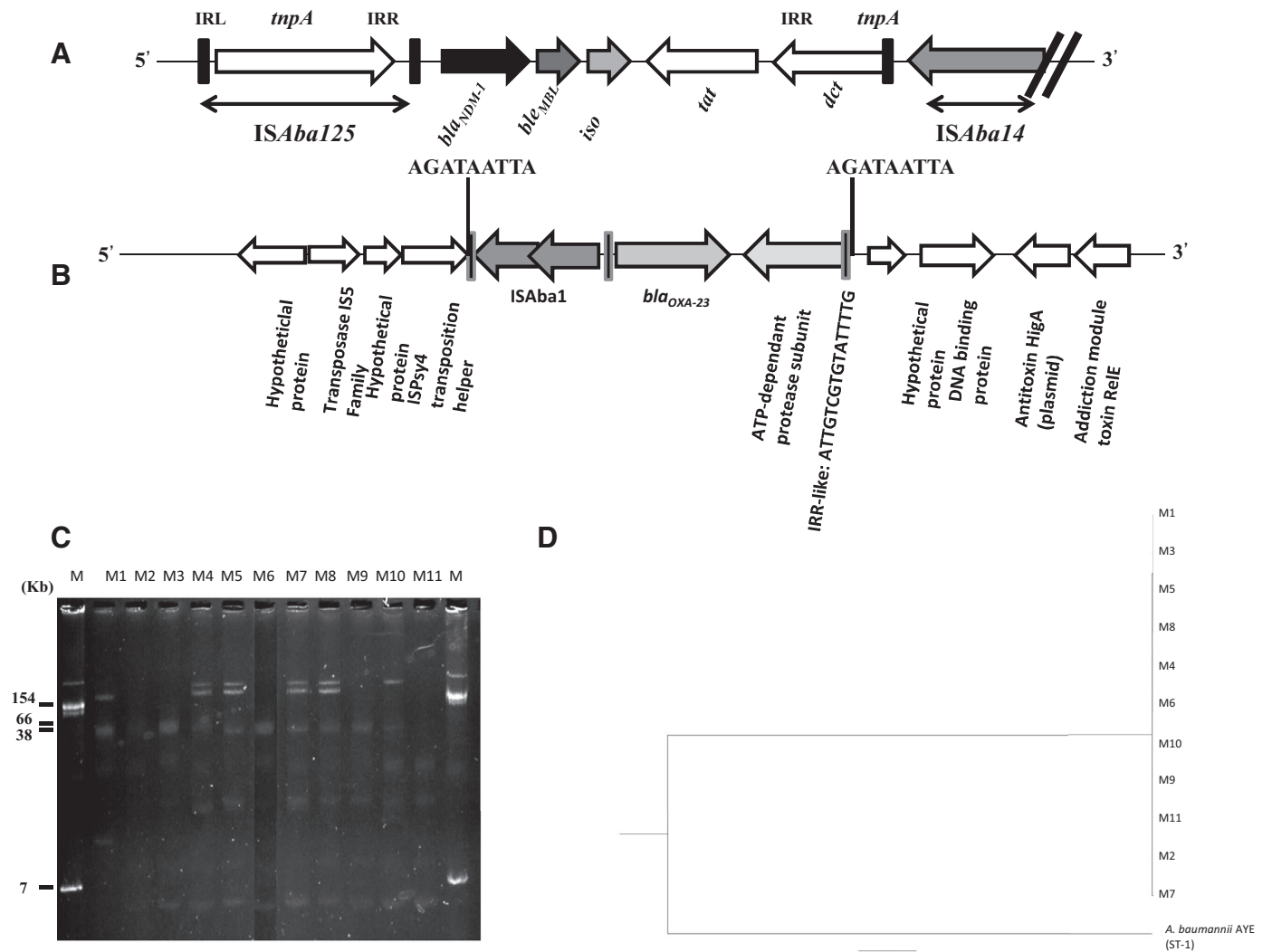


Fig. 1. (A) Features of Tn125 isoform transposon (Δ Tn125) carrying the *bla*_{NDM-1} gene. Genes and their transcription orientations are indicated by arrows. Gene names are abbreviated according to their corresponding proteins: *iso*, phosphoribosylanthranilate isomerase (212 amino acids long); *tat*, twin-arginine translocation pathway signal sequence protein (343 amino acids long); *dcr*, divalent cation tolerance protein (135 amino acids long). IRL, inverted repeat left; IRR, inverted repeat right. The lengths of the target genes and the exact location of the target site are not to scale. (B) Features of Tn2008 transposon carrying the *bla*_{OXA-23} gene. Genes and their transcription orientations are indicated by arrows. The lengths of the target genes and the exact location of the target site are not to scale. IRR-like corresponds to the imperfect inverted repeat of ISAbA1 (ATTGTCGTGATTTTG). (C) Gel electrophoresis of plasmid extraction by Kieser's method. *Escherichia coli* 50192 reference strain (lane M), *Acinetobacter baumannii* M1 (lane M1), M2 (lane M2), M3 (lane M3), M4 (lane M4), M5 (lane M5), M6 (lane M6), M7 (lane M7), M8 (lane M8), M9 (lane M9), M10 (lane M10) and M11 (lane M11). (D) Single nucleotide polymorphism (SNP)-based phylogenetic tree. Analysis of the SNPs was performed using CSI phylogeny and visualized by FigTree. The reference strain corresponds to *A. baumannii* AYE (GenBank Accession No. CT025791) belonging to ST1 according to the Pasteur Institute's multi-locus sequence typing scheme.

variability of the location and the genetic environment of *bla*_{NDM-1}. Tn125 transposon was suggested to be responsible for dissemination of the *bla*_{NDM-1} gene in *Acinetobacter* spp. and subsequently among *Enterobacteriaceae* [7,22].

This study also found wide dissemination of *bla*_{OXA-23}, and the co-occurrence of this gene with *bla*_{NDM-1} in four strains. In fact, the most common molecular mechanism leading to resistance to carbapenems in *Acinetobacter* spp. is acquisition of the *bla*_{OXA-23} gene.

The genetic environment surrounding the *bla*_{OXA-23} gene was analysed further. Using the entire 23.9 kb contig from strain M4 containing the *bla*_{OXA-23} gene as a reference sequence and mapping it with all the reads of the four MBLab harbouring both *bla*_{NDM-1} and *bla*_{OXA-23} genes, 100% sequence identity was observed, suggesting the same genetic environment in all strains. The *bla*_{OXA-23} gene was located within a transposon flanked upstream by a single copy of ISAbA1 located 27 bp upstream of the *bla*_{OXA-23} gene. ISAbA1 was preceded by a 9 bp direct repeat. This structure was bounded by *bla*_{OXA-23}- Δ ATPase gene downstream. An imperfect inverted re-

peat (ATTGTCGTGATTTTG) at the right-hand end of the transposon was identified (Fig. 1B). This imperfect inverted repeat might allow Tn2008 to move. It is well documented that all of the structures that contain *bla*_{OXA-23} are class I transposon structures (e.g. Tn2006, Tn2007 or Tn2008) [23,24].

3.4. Resistome: additional resistance mechanisms

Genes encoding aminoglycoside resistance determinants were identified as *aph*(3')-VIa and *aadB*, and were documented to be associated with high resistance to kanamycin, gentamicin, tobramycin, streptomycin and spectinomycin.

Although resistance to macrolides was mediated by the impermeability of Gram-negative membrane, two macrolide resistance genes were identified, namely *mph*(E) and *msr*(E). The products of *sul2* caused resistance to sulfamethoxazole-trimethoprim and were identified in all strains, as well as tetracycline resistance *tet*(39).

Table 2
Genetic features of metallo-beta-lactamase-producing *Acinetobacter baumannii*.

Strains	Reads	Nucleotides	Contigs	N50	Total nucleotide (contigs)	GC%	ST ⁰	ST ^R	Resistome	β -lactamases	Other
M1	829 640	124 712 161	286	34 016	3 854 369	38.8%	ST-1089	ST-85	aphI(3')-Vtar; aadB	bla _{NDM-1} ; bla _{OXA-94} ; bla _{ADC-79} -like	mphI(E); msr(E); sul2; tet(39)
M2	1 474 352	221 964 691	1202	5109	3 718 150	38.8%	ST-1089	ST-85	aphI(3')-Vtar; aadB	bla _{NDM-1} ; bla _{OXA-94} ; bla _{ADC-79} -like	mphI(E); msr(E); sul2
M3	1 457 758	219 502 249	864	6947	3 760 132	38.9%	ST-1089	ST-85	aphI(3')-Vtar; aadB	bla _{NDM-1} ; bla _{OXA-94} ; bla _{ADC-79} -like	mphI(E); msr(E); sul2; tet(39)
M4	1 618 590	243 610 505	359	20 204	4 000 414	39%	ST-1089	ST-85	aphI(3')-Vtar; aadB	bla _{NDM-1} ; bla _{OXA-94} ; bla _{ADC-79} -like; bla _{OXA-23}	mphI(E); msr(E); sul2; tet(39)
M5	1 425 272	214 633 794	1032	6209	3 868 322	39%	ST-1089	ST-85	aphI(3')-Vtar; aadB	bla _{NDM-1} ; bla _{OXA-94} ; bla _{ADC-79} -like; bla _{OXA-23}	mphI(E); msr(E); sul2; tet(39)
M6	1 324 940	199 312 720	530	12 736	3 859 629	39.2%	ST-1089	ST-85	aphI(3')-Vtar; aadB	bla _{NDM-1} ; bla _{OXA-94} ; bla _{ADC-79} -like	mphI(E); msr(E); sul2
M7	2 305 900	347 237 008	882	8377	3 958 661	38.9%	ST-1089	ST-85	aphI(3')-Vtar; aadB	bla _{NDM-1} ; bla _{OXA-94} ; bla _{ADC-79} -like; bla _{OXA-23}	mphI(E); msr(E); sul2; tet(39)
M8	1 087 542	163 778 264	1180	5356	3 877 908	38.9%	ST-1089	ST-85	aphI(3')-Vtar; aadB	bla _{NDM-1} ; bla _{OXA-94} ; bla _{ADC-79} -like; bla _{OXA-23}	mphI(E); msr(E); sul2; tet(39)
M9	1 478 890	222 725 964	488	12 842	3 860 077	38.8%	ST-1089	ST-85	aphI(3')-Vtar; aadB	bla _{NDM-1} ; bla _{OXA-94} ; bla _{ADC-79} -like	mphI(E); msr(E); sul2; tet(39)
M10	1 818 740	273 770 240	247	31 902	4 007 735	38.9%	ST-1089	ST-85	aphI(3')-Vtar; aadB	bla _{NDM-1} ; bla _{OXA-94} ; bla _{ADC-79} -like	mphI(E); msr(E); sul2; tet(39)
M11	1 218 000	183 384 839	849	7659	3 812 526	38.8%	ST-1089	ST-85	aphI(3')-Vtar; aadB	bla _{NDM-1} ; bla _{OXA-94} ; bla _{ADC-79} -like	msr(E); sul2

ST⁰ and ST^R correspond to Oxford and Pasteur's MLST schemes respectively.

No acquired quinolone resistance genes (*qnr*) were found in MBLAb. However, after comparison of the sequence of MBLAb with the *A. baumannii* ATCC 19606 reference strain, missense mutations in GyrA (S81L), GyrB (A264T), ParC (S84L/G569S) and ParE (V237A) genes were identified. Mutations in GyrA and ParC were known to be involved in high-level resistance to fluoroquinolones in *Acinetobacter* spp. [25].

It is known that low permeability of the porins, together with the presence of constitutive β -lactamases and multi-drug efflux pumps, is involved in intrinsic resistance to a number of antibiotics in *A. baumannii*. Thus, to give a deeper insight into non-enzymatic resistance mechanisms, the sequences of different porins of MBLAb were compared with those of reference strain *A. baumannii* ATCC19606. A *carO* porin was analysed and showed a perfect identity with that of *A. baumannii* ATCC19606. In addition, the *OmpA* porin, the roles of which in *A. baumannii* virulence and drug resistance have been well investigated, shows high identity (99%) with the reference strain protein, with only two substitutions (G30S, T122N). Some mutations were identified within the *OprD* protein, with 99% identity with the reference strain ATCC19606 (two to three substitutions S14G, G193S, V372I and insertion of two AA in six strains in position 85). The impact of such substitution in the functionality of these proteins remains to be determined.

The regulatory efflux pumps involved in the increase in carbapenem MICs were compared with those of *A. baumannii* ATCC 19606. The *AdeR* and *AdeS* of MBLAb showed 99% (two substitutions) and 97% (seven substitutions) identity, respectively. *AdeN* (*tetR* type regulator) and *AdeB* of MBLAb showed 97% and 99% amino acid sequence identity, respectively, without any interruption in the *tetR* type regulator *adeN* by an IS; a phenomenon known to increase the level of resistance in *A. baumannii* [26].

The drug resistance genes of *A. baumannii* isolates are often clustered into antibiotic resistance islands (AbaRs) that interrupt the *ATPase* gene (*comM*), recognized as a hot spot for the integration of AbaRs [27]. The presence of the *comM* gene and the boundary junctions (J1 and J2) of AbaRs were investigated. The *comM* gene was intact and no integrase of AbaR was found in silico, suggesting the absence of this structure.

3.5. Transfer of resistance gene

Conjugation and electroporation experiments failed to transfer the *bla*_{NDM-1} gene (data not shown). Plasmid extractions revealed the presence of one or two plasmids of >150 kb in seven strains (Fig. 1C) that did not hybridize with a *bla*_{NDM-1}-specific probe. This result suggests that the *bla*_{NDM-1} gene is likely to be chromosomal, as described for other NDM-producing *A. baumannii* isolates [7]. However, the *bla*_{OXA-23} gene was carried by a plasmid and can be transferred by conjugation in *A. baumannii* BM 4547. This resistance gene was carried by a conjugative repAci6-family plasmid, as reported previously. This result is in accordance with the genetic structure identified in the contig, revealing a plasmid structure carrying the *bla*_{OXA-23} gene (Fig. 1B). In addition, the *bla*_{OXA-23} gene is carried by transposon Tn2008 with a single copy of *ISAbal*. Analysis of the region surrounding the Tn2008 revealed direct repeats, indicating acquisition by a transposition process (Fig. 1B).

3.6. Genetic relatedness of MBLAb isolates and phylogeny

The MLST 1.8 server showed that all the isolates were clonally related and belonged to the same sequence type: ST1085 according to the Oxford database and ST85 according to the Pasteur scheme. This sequence type has been described previously in sporadic cases in France associated with repatriated patients from North Africa

[28,29]. Other carbapenem-resistant *A. baumannii* isolates belonging to ST-85 have been reported in Spain, Lebanon, Turkey and Algeria [30–32].

Analysis of the relationship was also performed using an SNP-related phylogenetic tree (Fig. 1D). All these isolates were almost identical, with fewer than 50 SNPs between these isolates over a 2-year period. SNP comparison with NDM-producing *A. baumannii* recovered from France in 2012 revealed that these isolates were closely related with very few differences, ranging from 39 to 60 SNPs, with French isolates. It should be noted that the main difference between these isolates was the acquisition of the *bla*_{OXA-23}-carrying plasmid in four isolates. This sequence was not included in the SNP-based tree as it does not correspond to a shared sequence between all isolates.

4. Conclusion

This paper reports the genome analysis of NDM-1-producing *A. baumannii* clinical isolates in a teaching hospital in Tunisia. Interestingly, the study identified a single clone spreading the *bla*_{NDM-1} gene in Tunisia. The clone ST-85 was previously identified in NDM-1-producing *A. baumannii* recovered from France [29]. This clone, circulating for at least 5 years in Tunisia, is well conserved.

Acknowledgements

The authors wish to thank the many dedicated staff who helped with data collection and technical issues: the members of the French National Reference Centre for Antibiotic Resistance 'Carbapenemase-producing Enterobacteriaceae' and the staff of the Laboratory of Clinical Microbiology, University Hospital of Sahloul, Sousse, Tunisia.

Declarations

Funding

This work was funded by a grant from the *Ministère de l'Éducation Nationale et de la Recherche* (EA7361), Université Paris Sud. RAB and TN are members of the Laboratory of Excellence LERMIT, supported by a grant from ANR (ANR-10-LABX-33). In addition, this study was partially supported by the University Hospital of Sahloul, Sousse, Tunisia.

Competing interests

None declared.

Ethical approval

Not required.

References

- [1] Boucher HW, Talbot GH, Bradley JS, Edwards JE, Gilbert D, Rice LB, et al. Bad bugs, no drugs: no ESKAPE! An update from the Infectious Diseases Society of America. *Clin Infect Dis Off Publ Infect Dis Soc Am* 2009;48:1–12.
- [2] Bonnin RA, Nordmann P, Poirel L. Screening and deciphering antibiotic resistance in *Acinetobacter baumannii*: a state of the art. *Expert Rev Anti Infect Ther* 2013;11:571–83.
- [3] Peleg AY, Seifert H, Paterson DL. *Acinetobacter baumannii*: emergence of a successful pathogen. *Clin Microbiol Rev* 2008;21:538–82.
- [4] Yong D, Toleman MA, Giske CG, Cho HS, Sundman K, Lee K, et al. Characterization of a new metallo-beta-lactamase gene, *bla*(NDM-1), and a novel erythromycin esterase gene carried on a unique genetic structure in *Klebsiella pneumoniae* sequence type 14 from India. *Antimicrob Agents Chemother* 2009;53:5046–54.
- [5] Rolain JM, Parola P, Cornaglia G. New Delhi metallo-beta-lactamase (NDM-1): towards a new pandemic? *Clin Microbiol Infect Off Publ Eur Soc Clin Microbiol Infect Dis* 2010;16:1699–701.
- [6] Karthikeyan K, Thirunarayan MA, Krishnan P. Coexistence of *bla*OXA-23 with *bla*NDM-1 and *armA* in clinical isolates of *Acinetobacter baumannii* from India. *J Antimicrob Chemother* 2010;65:2253–4.
- [7] Bonnin RA, Poirel L, Nordmann P. New Delhi metallo-β-lactamase-producing *Acinetobacter baumannii*: a novel paradigm for spreading antibiotic resistance genes. *Future Microbiol* 2014;9:33–41.
- [8] Poirel L, Bonnin RA, Boulanger A, Schrenzel J, Kaase M, Nordmann P. Tn125-related acquisition of *bla*NDM-Like genes in *Acinetobacter baumannii*. *Antimicrob Agents Chemother* 2012;56:1087–9.
- [9] Clinical and Laboratory Standards Institute. CLSI publishes new antimicrobial susceptibility testing standards (<https://clsi.org>).
- [10] Clinical and Laboratory Standards Institute. New editions of M100-S24 and eM100 - CLSI (<https://clsi.org>).
- [11] Dortet L, Poirel L, Errera C, Nordmann P. CarbAcineto NP test for rapid detection of carbapenemase-producing *Acinetobacter* spp. *J Clin Microbiol* 2014;52:2359–64.
- [12] Bonnin RA, Naas T, Poirel L, Nordmann P. Phenotypic, biochemical, and molecular techniques for detection of metallo-β-lactamase NDM in *Acinetobacter baumannii*. *J Clin Microbiol* 2012;50:1419–21.
- [13] Kieser T. Factors affecting the isolation of CCC DNA from *Streptomyces lividans* and *Escherichia coli*. *Plasmid* 1984;12:19–36.
- [14] Bonnin RA, Nordmann P, Potron A, Lecuyer H, Zahar J-R, Poirel L. Carbapenem-hydrolyzing GES-type extended-spectrum beta-lactamase in *Acinetobacter baumannii*. *Antimicrob Agents Chemother* 2011;55:349–54.
- [15] Diancourt L, Passet V, Nemeč A, Dijkshoorn L, Brisse S. The population structure of *Acinetobacter baumannii*: expanding multiresistant clones from an ancestral susceptible genetic pool. *PLoS One* 2010;5:e10034.
- [16] Bartual SG, Seifert H, Hippler C, Luzon MAD, Wisplinghoff H, Rodríguez-Valera F. Development of a multilocus sequence typing scheme for characterization of clinical isolates of *Acinetobacter baumannii*. *J Clin Microbiol* 2005;43:4382–90.
- [17] Aziz RK, Bartels D, Best AA, DeJongh M, Disz T, Edwards RA, et al. The RAST Server: rapid annotations using subsystems technology. *BMC Genomics* 2008;9:75.
- [18] Poirel L, Naas T, Nordmann P. Diversity, epidemiology, and genetics of class D beta-lactamases. *Antimicrob Agents Chemother* 2010;54:24–38.
- [19] Figueiredo S, Poirel L, Croize J, Recule C, Nordmann P. In vivo selection of reduced susceptibility to carbapenems in *Acinetobacter baumannii* related to IS-Aba1-mediated overexpression of the natural *bla*(OXA-66) oxacillinase gene. *Antimicrob Agents Chemother* 2009;53:2657–9.
- [20] Pagano M, Martins AF, Barth AL. Mobile genetic elements related to carbapenem resistance in *Acinetobacter baumannii*. *Braz J Microbiol* 2016;47:785–92.
- [21] Bonnin RA, Poirel L, Naas T, Pirs M, Seme K, Schrenzel J, Nordmann P. Dissemination of New Delhi metallo-β-lactamase-1-producing *Acinetobacter baumannii* in Europe. *Clin Microbiol Infect Off Publ Eur Soc Clin Microbiol Infect Dis* 2012;18:E362–5.
- [22] Bontron S, Nordmann P, Poirel L. Transposition of Tn125 Encoding the NDM-1 Carbapenemase in *Acinetobacter baumannii*. *Antimicrob Agents Chemother* 2016;60:7245–51.
- [23] Corvec S, Poirel L, Naas T, Drugeon H, Nordmann P. Genetics and expression of the carbapenem-hydrolyzing oxacillinase gene *bla*OXA-23 in *Acinetobacter baumannii*. *Antimicrob Agents Chemother* 2007;51:1530–3.
- [24] Guerrero-Lozano I, Fernández-Cuenca F, Galán-Sánchez F, Egea P, Rodríguez-Iglesias M, Pascual Á. Description of the OXA-23 β-lactamase gene located within Tn2007 in a clinical isolate of *Acinetobacter baumannii* from Spain. *Microb Drug Resist Larchmt N* 2015;21:215–17.
- [25] Hooper DC, Jacoby GA. Mechanisms of drug resistance: quinolone resistance. *Ann N Y Acad Sci* 2015;1354:12–31.
- [26] Saranathan R, Pagal S, Sawant AR, Tomar A, Madhangi M, Sah S, et al. Disruption of tetR type regulator *adeN* by mobile genetic element confers elevated virulence in *Acinetobacter baumannii*. *Virulence* 2017;8:1316–34.
- [27] Bonnin RA, Poirel L, Nordmann P. AbaR-type transposon structures in *Acinetobacter baumannii*. *J Antimicrob Chemother* 2012;67:234–6.
- [28] Decousser JW, Jansen C, Nordmann P, Emirian A, Bonnin RA, Anais L, et al. Outbreak of NDM-1-producing *Acinetobacter baumannii* in France, January to May 2013. *Euro Surveill* 2013;18:31.
- [29] Bonnin RA, Cuzon G, Poirel L, Nordmann P. Multidrug-resistant *Acinetobacter baumannii* clone. France. *Emerg Infect Dis* 2013;19:822–3.
- [30] Mosqueda N, Espinal P, Cosgaya C, Viota S, Plasencia V, Alvarez-Lerma F, et al. Globally expanding carbapenemase finally appears in Spain: nosocomial outbreak of *Acinetobacter baumannii* producing plasmid-encoded OXA-23 in Barcelona. *Antimicrob Agents Chemother* 2013;57:5155–5157.
- [31] Rafei R, Dabboussi F, Hamze M, Eveillard M, Lemarié C, Mallat H, et al. First report of *bla*NDM-1-producing *Acinetobacter baumannii* isolated in Lebanon from civilians wounded during the Syrian war. *Int J Infect Dis IJID Off Publ Int Soc Infect Dis* 2014;21:21–3.
- [32] Zenati K, Touati A, Bakour S, Sahli F, Rolain JM. Characterization of NDM-1 and OXA-23-producing *Acinetobacter baumannii* isolates from inanimate surfaces in a hospital environment in Algeria. *J Hosp Infect* 2016;92:19–26.
- [33] EUCAST: Clinical breakpoints (www.eucast.org/clinical_breakpoints/).
- [34] Hindler JA, Humphries RM. Colistin MIC variability by method for contemporary clinical isolates of multidrug-resistant Gram-negative bacilli. *J Clin Microbiol* 2013;51:1678–84.

Genetic and Biochemical Characterization of FRI-1, a Carbapenem-Hydrolyzing Class A β -Lactamase from *Enterobacter cloacae*

Laurent Dortet,^{a,b,c} Laurent Poirel,^{a,b,c,d} Samia Abbas,^b Saoussen Oueslati,^b Patrice Nordmann^{a,b,c,d,e}

Associated National Reference Center for Antibiotic Resistance, Le Kremlin-Bicêtre, France^a; Faculty of Medicine, South Paris University, Le Kremlin-Bicêtre, France^b; Bacteriology-Hygiene Unit, Hospital Bicêtre, Assistance Publique/Hôpitaux de Paris, and INSERM U914, Le Kremlin-Bicêtre, France^c; Emerging Antibiotic Resistance Unit, Medical and Molecular Microbiology, Department of Medicine, University of Fribourg, Fribourg, Switzerland^d; HFR-Hôpital Cantonal, Fribourg, Switzerland^e

An *Enterobacter cloacae* isolate was recovered from a rectal swab from a patient hospitalized in France with previous travel to Switzerland. It was resistant to penicillins, narrow- and broad-spectrum cephalosporins, aztreonam, and carbapenems but remained susceptible to expanded-spectrum cephalosporins. Whereas PCR-based identification of the most common carbapenemase genes failed, the biochemical Carba NP test II identified an Ambler class A carbapenemase. Cloning experiments followed by sequencing identified a gene encoding a totally novel class A carbapenemase, FRI-1, sharing 51 to 55% amino acid sequence identity with the closest carbapenemase sequences. However, it shared conserved residues as a source of carbapenemase activity. Purified β -lactamase FRI-1 hydrolyzed penicillins, aztreonam, and carbapenems but spared expanded-spectrum cephalosporins. The 50% inhibitory concentrations (IC₅₀s) of clavulanic acid and tazobactam were 10-fold higher than those found for *Klebsiella pneumoniae* carbapenemase (KPC), IMI, and SME, leading to lower sensitivity of FRI-1 activity to β -lactamase inhibitors. The *bla*_{FRI-1} gene was located on a ca. 110-kb untypeable, transferable, and non-self-conjugative plasmid. A putative LysR family regulator-encoding gene at the 5' end of the β -lactamase gene was identified, leading to inducible expression of the *bla*_{FRI-1} gene.

Carbapenem resistance in *Enterobacteriaceae* may be related to two mechanisms: (i) overexpression of a β -lactamases possessing no (or weak) activity against carbapenems (e.g., extended-spectrum beta-lactamase [ESBL] and cephalosporinases) combined with decreased outer membrane permeability and (ii) expression of enzymes able to hydrolyze carbapenems, namely, the carbapenemases (1). The most clinically relevant carbapenemases are classified into three groups according to protein sequence identity: (i) the *Klebsiella pneumoniae* carbapenemase (KPC)-type enzymes (Ambler class A), first described in the United States but now found worldwide (2, 3); (ii) the VIM, IMP, and NDM metallo- β -lactamases (Ambler class B) (1, 4); and (iii) the OXA-48-type enzymes (Ambler class D), widespread among Mediterranean countries and progressively disseminating to other geographical areas (5).

Ambler class A carbapenemases hydrolyze a large variety of β -lactams, including penicillins, cephalosporins, carbapenems, and aztreonam (6). Their hydrolytic activity is *in vitro* inhibited by clavulanic acid and tazobactam. Four main types of class A carbapenemases are known: Nmca/IMI, SME, KPC, and several variants of the GES type (GES-2, -4, -5, -6, and -11) (7).

The SME family includes three variants (SME-1 to -3). These enzymes have all been chromosome encoded in *S. marcescens* isolates (8–11). The chromosome-encoded Nmca and IMI enzymes have been detected in rare isolates of *Enterobacter* spp. (12, 13). The gene encoding the IMI-2 variant has been identified sporadically as plasmid located in environmental strains of *Enterobacter* spp. (14). The GES-type family includes 27 variants, only a few of which possess carbapenemase activity (7). All the GES variants possess the ability to hydrolyze broad-spectrum cephalosporins, but only some variants (mainly GES-2, GES-4, and GES-5 in *Enterobacteriaceae*) possess amino acid substitutions within their active sites (positions 104 and 170 according to the Ambler classification) that enlarge their spectra of activity against carbapenems (7, 15). Although still rare, GES enzymes have been identified

worldwide. The most prevalent Ambler class A carbapenemase is KPC. This plasmid-encoded enzyme was first identified in 2001 in the United States (16). Since then, KPC-producing *Enterobacteriaceae* have spread worldwide, mostly due to the clonal dissemination of KPC-producing *K. pneumoniae* isolates of sequence type 258 (ST258) (2, 3). While this study was being completed, another class A carbapenemase, BKC-1, was identified from *K. pneumoniae* in Brazil (17).

The aim of this study was to characterize at the genetic and biochemical levels the molecular mechanisms of resistance to carbapenems from an *Enterobacter cloacae* isolate.

MATERIALS AND METHODS

Bacterial strains and plasmids. The *E. cloacae* isolate DUB was recovered from a urine sample from a patient, hospitalized in a suburb of Paris, with a previous history of travel (without hospitalization) in Switzerland. Identification of the clinical isolate was done by matrix-assisted laser desorption/ionization–time of flight (MALDI-TOF) mass spectrometry (MALDI Biotyper CA system; Bruker Daltonics, Billerica, MA, USA). *Escherichia coli* TOP10 (Invitrogen, Saint-Aubin, France) was used for cloning experiments and azide-resistant *E. coli* J53 for conjugation assays. The kanamycin-resistant pBK-CMV (Invitrogen, Saint-Aubin, France) was used as the cloning vector. Bacterial cultures were grown in Trypticase soy (TS) broth at 37°C for 18 h unless otherwise indicated.

Received 15 July 2015 Returned for modification 1 August 2015

Accepted 8 September 2015

Accepted manuscript posted online 21 September 2015

Citation Dortet L, Poirel L, Abbas S, Oueslati S, Nordmann P. 2015. Genetic and biochemical characterization of FRI-1, a carbapenem-hydrolyzing class A β -lactamase from *Enterobacter cloacae*. Antimicrob Agents Chemother 59:7420–7425. doi:10.1128/AAC.01636-15.

Address correspondence to Patrice Nordmann, patrice.nordmann@unifr.ch.

Copyright © 2015, American Society for Microbiology. All Rights Reserved.

TABLE 1 MICs of β -lactams for *E. cloacae* DUB, *E. coli* TOP10 transformed with the natural *bla*_{FRI-1}-bearing plasmid (pDUB), *E. coli* TOP10 harboring a recombinant plasmid (pFRI), and the *E. coli* TOP10 reference strain

β -Lactam(s)	MIC (μ g/ml)			
	<i>E. cloacae</i> DUB	<i>E. coli</i> TOP10(pDUB) ^a	<i>E. coli</i> TOP10(pFRI) ^b	<i>E. coli</i> TOP10
Amoxicillin	>256	128	>256	2
Amoxicillin + CLA ^c	>256	64	96	2
Ticarcillin	>256	>256	>256	2
Ticarcillin + CLA	256	96	96	2
Piperacillin	128	12	24	1
Piperacillin + TZB ^d	96	8	12	1
Cefalotin	>256	256	>256	4
Cefoxitin	>256	2	2	2
Ceftazidime	4	2	2	0.12
Ceftazidime + CLA	0.78	0.5	0.75	0.12
Ceftazidime + TZB	4	1.5	1.5	0.12
Cefotaxime	1	0.38	0.5	0.06
Cefotaxime + CLA	0.5	0.12	0.19	0.06
Cefotaxime + TZB	1	0.09	0.5	0.06
Cefepime	0.5	0.19	0.19	0.02
Cefepime + CLA	0.06	0.06	0.06	0.02
Cefepime + TZB	0.25	0.06	0.06	0.02
Cefpirome	1.5	0.25	0.38	0.02
Cefpirome + CLA	1	0.06	0.09	0.02
Cefpirome + TZB	0.75	0.06	0.38	0.02
Aztreonam	256	256	256	0.09
Aztreonam + CLA	256	8	32	0.09
Aztreonam + TZB	256	64	256	0.09
Imipenem	8	0.75	4	0.06
Imipenem + CLA	4	0.38	2	0.06
Imipenem + TZB	4	0.5	1.5	0.06
Meropenem	3	0.12	0.38	0.02
Meropenem + CLA	2	0.03	0.12	0.02
Meropenem +TZB	4	0.09	0.25	0.02
Ertapenem	24	0.12	0.75	0.06
Ertapenem + CLA	8	0.03	0.12	0.06
Ertapenem + TZB	4	0.06	0.38	0.06

^a pDUB, natural plasmid carrying the *bla*_{FRI-1} gene.

^b pFRI, the *bla*_{FRI-1} gene cloned in the pBK-CMV plasmid.

^c CLA, clavulanic acid at a fixed concentration of 4 μ g/ml.

^d TZB, tazobactam at a fixed concentration of 4 μ g/ml.

Susceptibility testing. Antimicrobial susceptibilities were determined by the disc diffusion technique on Mueller-Hinton agar (Bio-Rad, Marnes-La-Coquette, France) and interpreted according to the EUCAST breakpoints as updated in 2015 (<http://www.eucast.org>). MICs were determined using the Etest technique (bioMérieux, La Balme-Les-Grottes, France).

Detection of carbapenemase activity. Carbapenemase activity was analyzed by using two techniques, namely, the biochemical Carba NP test (18) and UV spectrophotometry, as previously described (19). Discrimination between Ambler class A, B, and non-A non-B carbapenemases was assessed using the Carba NP test II results, as previously described (20).

Molecular detection of carbapenemase-encoding genes. PCR screening for the most common class A carbapenemase genes (*bla*_{KPC}, *bla*_{IMP}, *bla*_{VIM}, *bla*_{NDM}, *bla*_{OXA-48}, *bla*_{GES}, *bla*_{SFC-1}, and *bla*_{IMI/NMC-A}) was done as previously described (21).

Plasmid extraction and conjugation assays. Plasmid DNA of *E. cloacae* DUB was extracted and analyzed using the Kieser method, as described previously (22). Recombinant plasmid DNA was prepared using Qiagen maxi columns (Qiagen, Courtaboeuf, France). Transfer of the imipenem resistance marker into *E. coli* TOP10 was attempted by electroporation. Transformants were selected on ticarcillin (100 μ g/ml)-con-

taining TS agar plates (Oxoid, Dardilly, France). Transfer of the β -lactam resistance marker into azide-resistant *E. coli* J53 was also attempted by liquid mating-out assays at 37°C. Transformants were selected on azide (100 μ g/ml)- and ticarcillin (100 μ g/ml)-containing TS agar plates. Plasmid typing was performed on electrotransformant strains by using the PCR-based replicon-typing (PBRT) method, as described previously (23).

Cloning experiments, recombinant plasmid analysis, and DNA sequencing. PCR amplification of the identified *bla*_{FRI-1} gene was performed by using the internal primers FRI-1A (5'-TGAACATTCGCC TCTCAG-3') and FRI-1B (5'-CTGCTTCGTCATGTTTGTTCG-3'). Whole-cell DNA of the *E. cloacae* isolate was extracted using a QIAamp DNA minikit (Qiagen, Courtaboeuf, France). Partially Sau3AI-restricted DNA was ligated into the BamHI-restricted pBK-CMV plasmid and introduced into *E. coli* TOP10 by electroporation. Recombinant plasmids were selected on ticarcillin (100 μ g/ml)- and kanamycin (50 μ g/ml)-containing Trypticase soy agar plates. The recombinant plasmid possessing the shortest insert, namely, pFRI, was retained for further analysis. Both strands of the cloned DNA inserts of recombinant plasmids were sequenced by using an Applied Biosystems sequencer (ABI 377). The nucleotide and deduced protein sequences were analyzed with software avail-

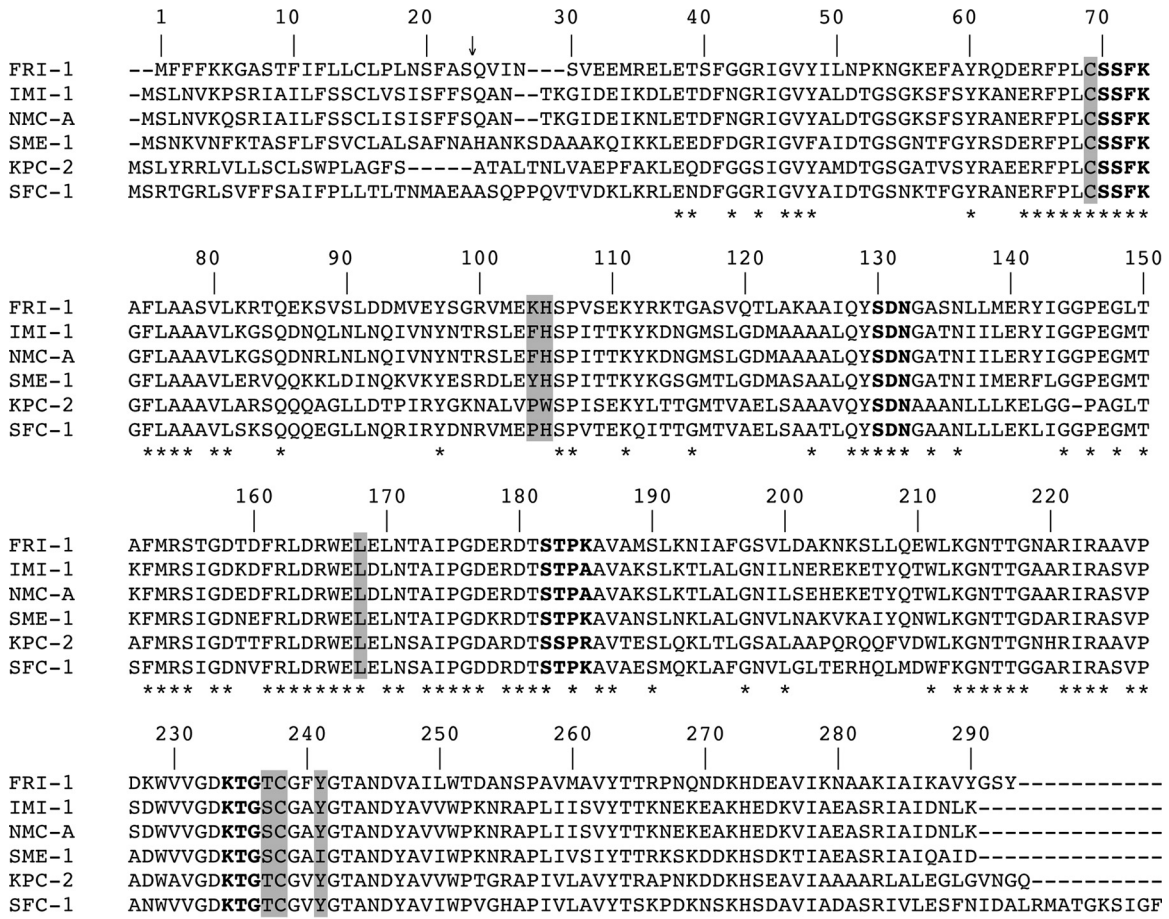


FIG 1 Comparison of the amino acid sequence of FRI-1 with those of IMI-1, NMC-A, SME-1, KPC-2, and SFC-1. Dashes indicate the gaps that were inserted to optimize the alignment, and dashes indicate residues identical to those of BIC-1. The numbering is according to the method described by Ambler et al (33). The conserved domains of class A β -lactamases are in boldface. The residues shaded in gray are conserved among class A carbapenemases. The conserved residues are marked by asterisks. The arrow indicates the cleavage site for the leader peptide of FRI-1.

able on the Internet from the National Center for Biotechnology Information website (<http://www.ncbi.nlm.nih.gov/BLAST/>).

Protein analysis. β -Lactamase extracts from cultures of *E. cloacae* DUB and the *E. coli* TOP10 strain harboring the recombinant plasmid pFRI were subjected to analytical isoelectric focusing (IEF) analysis. Multiple nucleotide and protein sequence alignments were carried out online using the program ClustalW (<http://www.ebi.ac.uk/Tools/clustalW2/index.html>).

β -Lactamase purification. Purification of the β -lactamase FRI-1 was carried out by ion-exchange chromatography. *E. coli* TOP10(pFRI) was grown overnight at 37°C in 2 liters of TS broth containing ticarcillin (100 μ g/ml) and kanamycin (50 μ g/ml). The bacterial suspension was resuspended and disrupted by sonication in 10 ml of 20 mM triethanolamine buffer (pH 7.2) (Sigma-Aldrich, Saint Quentin Fallavier, France) and cleared by ultracentrifugation. The protein extracts obtained were loaded onto a preequilibrated S-Sepharose column (Amersham Pharmacia Biotech) in the same buffer. The β -lactamase recovered in the flow-through was subsequently dialyzed against triethanolamine buffer (pH 9.5), loaded onto a Q-Sepharose column preequilibrated with the same buffer, and eluted with a linear NaCl gradient (0 to 500 mM). The fractions containing the highest β -lactamase activity, as determined qualitatively using nitrocefin hydrolysis (Oxoid, Dardilly, France), were pooled and dialyzed overnight against 50 mM sodium phosphate buffer (pH 7). The protein content was measured by the Bio-Rad DC protein assay. The

protein purification rate and the relative molecular mass of the FRI-1 β -lactamase were estimated by sodium dodecyl sulfate-polyacrylamide gel electrophoresis (SDS-PAGE) analysis.

Kinetic studies. Kinetic measurements (k_{cat} and K_m) of purified β -lactamase FRI-1 were performed as described previously (24). The 50% inhibitory concentration (IC_{50}) for FRI-1 was determined as the concentration of clavulanate or tazobactam that reduced the hydrolysis rate of 100 μ M benzylpenicillin by 50% under conditions in which FRI-1 was preincubated with various concentrations of inhibitor for 3 min at 30°C before the substrate was added.

Nucleotide sequence accession number. The nucleotide sequence data reported in this paper have been submitted to the GenBank nucleotide database under accession no. [KT192551](https://www.ncbi.nlm.nih.gov/nuclot/KT192551).

RESULTS

Susceptibility testing, carbapenemase detection, and IEF analysis. *E. cloacae* DUB was resistant to amino-, carboxy-, and ureidopenicillins; narrow-spectrum cephalosporins; aztreonam; and carbapenems (Table 1). It remained susceptible to broad-spectrum cephalosporins (cefotaxime, cefepime, and cefpirome), except for ceftazidime (MIC, 4 μ g/ml). *E. cloacae* DUB was susceptible to non- β -lactam antibiotics, except for rifampin. Addition of tazobactam or clavulanic acid partially restored susceptibility to

ceftazidime and carbapenems (Table 1). The positivity of the Carba NP test identified the expression of carbapenemase. PCR experiments carried out on purified DNA of whole-cell *E. cloacae* DUB with primers specific for the most common carbapenemase genes (bla_{KPC} , bla_{IMP} , bla_{VIM} , bla_{NDM} , and bla_{OXA-48}) remained negative. The Carba NP test II was therefore performed to identify the type of carbapenemase. The inhibition of carbapenemase activity by tazobactam suggested that this carbapenemase belonged to the Ambler class A group. Accordingly, additional PCR experiments were performed using primers specific for rarer Ambler class A carbapenemase genes (bla_{GES} , bla_{SFC-1} , and $bla_{IMI/NMC-A}$), but they also remained negative. IEF analysis revealed that strain DUB produced an acquired β -lactamase with a pI value of ca. 8.4.

Cloning, conjugation, and transformation of the β -lactamase gene. Shotgun cloning resulted in the selection of an *E. coli* TOP10(pFRI) recombinant strain that expressed a clavulanic acid-inhibited carbapenemase phenotype with resistance or reduced susceptibility to penicillins, ceftazidime, aztreonam, and carbapenems. The addition of clavulanic acid partially restored the activities of the β -lactams (Table 1). IEF analysis showed that *E. coli* TOP10(pFRI) produced a β -lactamase with a pI value of 8.4, identical to that identified in *E. cloacae* DUB (data not shown). Analysis of the plasmid DNA extract of the *E. cloacae* DUB isolate revealed a ca. 110-kb plasmid. Transfer of the imipenem resistance marker into *E. coli* TOP10 by electroporation was successful. In contrast, mating-out assays failed to give any transconjugant. PBRT analysis performed using a DNA extract of an *E. coli* TOP10 transformant (pDUB) (23) failed to identify a plasmid of any known incompatibility group.

Identification of β -lactamase FRI-1. DNA sequence analysis of the 2,863-bp insert of pFRI revealed an open reading frame (ORF) of 885 bp encoding a 295-amino-acid preprotein, FRI-1 (French imipenemase), with a relative molecular mass of 32.5 kDa. The G+C content of this ORF was 39%. The signal peptide cleavage site was identified between the alanine and serine residues at positions 23 and 24 (AS-QV) of FRI-1 (Fig. 1). The β -lactamase FRI-1 contained four conserved motifs of class A serine β -lactamases, namely, $^{70}SSFK^{73}$, $^{130}SDN^{132}$, $^{166}EXXXN^{170}$, and $^{234}KTG^{236}$ (25) (Fig. 1). Interestingly, FRI-1 contains the amino acid residues that, associated, have been identified as a source of carbapenemase activity in class A β -lactamases; ^{69}C , ^{105}H , ^{167}L , ^{237}S , ^{238}C , and ^{241}Y (25–27). The β -lactamase FRI-1 shares 55%, 54%, 53%, 53%, and 51% amino acid identity with the class A carbapenemases NMC-A, IMI-1, SME-1, SFC-1, and KPC-2, respectively (Fig. 1). It shares 42% amino acid identity with the recently identified β -lactamase BKC-1 (data not shown). A dendrogram was generated from the amino acid sequence alignment of FRI-1 with main class A β -lactamases. It showed that FRI-1 is more closely related to the subgroup that includes SME-1, IMI-1, and NMC-A than to that of KPC-2, SFC-1, and BIC-1 (Fig. 2).

Biochemical features of β -lactamase FRI-1. The purification state of FRI-1 was estimated to be >95% by SDS-PAGE analysis (data not shown). Kinetic parameters of the purified β -lactamase FRI-1 showed that it possessed quite significant carbapenemase activity (Table 2). The highest k_{cat} value for carbapenems was obtained with imipenem and was approximately 39- and 12-fold higher than those for meropenem and ertapenem, respectively (Table 2). The k_{cat}/K_m values obtained for FRI-1 were close to

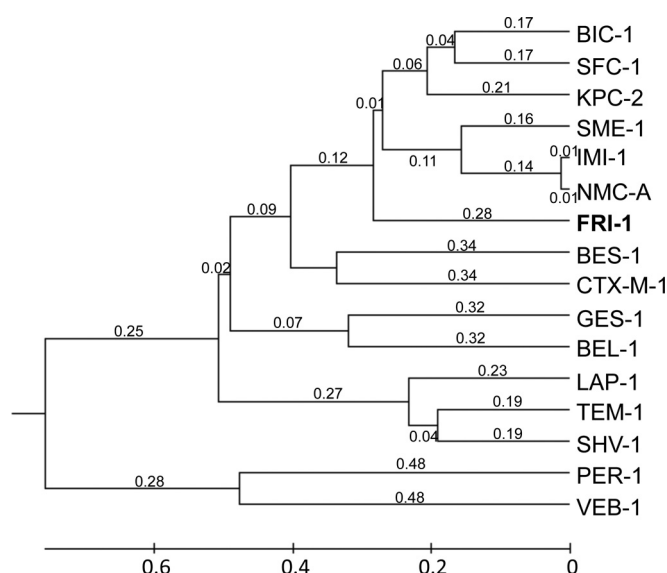


FIG 2 Dendrogram obtained for 16 representative class A β -lactamases by neighbor-joining analysis. The alignment used for the tree calculation was performed with the ClustalW program. Branch lengths are drawn to scale and are proportional to the number of amino acid changes. The distance along the vertical axis has no significance. The β -lactamases (GenBank accession numbers) are BIC-1 (GQ260093), SFC-1 (AY354402), KPC-2 (AY034847), SME-1 (Z28968), IMI-1 (U50278), NMC-A (Z21956), BES-1 (AF234999), CTX-M-1 (X92506), GES-1 (AF156486), BEL-1 (DQ089809), LAP-1 (EF026092), TEM-1 (AY458016), SHV-1 (AF148850), PER-1 (Z21957), and VEB-1 (AF010416).

those obtained for NMC-A and IMI-1 (Table 2). Notably, the k_{cat} value for aztreonam was very high (Table 2), which correlates with the high MIC values obtained with the *E. coli* TOP10 transformant and the *E. coli* TOP10(pFRI) recombinant strain (Table 1). Inhibition studies, as measured by IC_{50} s, showed that the activity of FRI was weakly inhibited by clavulanic acid (IC_{50} , 90 μ M) and tazobactam (IC_{50} , 15 μ M). These values are in the same range as those found for SFC-1, 72.8 and 6.9 μ M for clavulanic acid and tazobactam, respectively (28, 29). In addition, we observed that bla_{FRI-1} expression was inducible (\sim 8- to 10-fold) by imipenem (5 μ g/ml) or by ceftazidime (50 μ g/ml and 200 μ g/ml).

Genetic environment of the bla_{FRI-1} gene. Part of the 5,750-bp insert of the recombinant plasmid pFRI was sequenced to identify the flanking sequences of the bla_{FRI-1} gene (Fig. 3). The bla_{FRI-1} gene was bracketed by two insertion sequences (IS). The closest IS shared 93% identity with IS $Raq1$ (GenBank accession no. AY528232), identified in *Rahnella aquatilis*. This IS $Raq1$ -like IS was truncated by the insertion of another IS belonging to the IS66 family, sharing 87% identity with IS $Kpn24$ (GenBank accession no. NC_014312). Upstream of bla_{FRI-1} , a gene encoding FRI-R, a LysR transcriptional regulator sharing 63% amino acid identity with SmeR, the regulator of SME-1, was identified. The *friR* gene possessed a G+C content similar to that of the bla_{FRI-1} gene (39%).

DISCUSSION

Our study identified a novel plasmid-encoded class A carbapenemase from the urine of a French patient who had traveled in Switzerland. The β -lactamase FRI-1 shares the highest amino acid identity with the chromosome-encoded Ambler class A carbapen-

TABLE 2 Steady-state kinetic parameters of the β -lactamase FRI-1 and comparison of parameters obtained for the β -lactamases NMC-A (24), IMI-1 (13), SME-1 (11), KPC-2 (16), SFC-1 (28), and GES-4 (15)

Parameter	β -Lactam	Value ^a						
		FRI-1	NMC-A	IMI-1	SME-1	KPC-2	SFC-1	GES-4
k_{cat} (s^{-1})	Benzylpenicillin	1,060	260	36	19.3	63	NA	130
	Amoxicillin	>17,000	816	190	181	NA	NA	19
	Ticarcillin	120	81	NA	NA	NA	NA	NA
	Piperacillin	>2,600	NA	6.1	NA	NA	NA	NA
	Cefotaxime	>220	286	3.4	<0.98	17	8.3	17
	Cefepime	28	NA	NA	NA	12	NA	NA
	Ceftazidime	—	—	<0.01	NA	0.5	2.1	2.5
	Aztreonam	>8,300	707	51	108	66	162	NA
	Imipenem	1,790	1,040	89	104	31	54	7.7
	Ertapenem	150	NA	NA	NA	NA	NA	NA
	Meropenem	46	12	10	8.9	3.6	6.5	NA
	K_m (μM)	Benzylpenicillin	567	28	64	16.7	30	NA
Amoxicillin		>5,000	90	780	488	NA	NA	62
Ticarcillin		393	152	NA	NA	NA	NA	NA
Piperacillin		>3,000	NA	13	NA	NA	NA	NA
Cefotaxime		>5,000	956	190	—	100	89	700
Cefepime		3,400	NA	NA	NA	540	NA	NA
Ceftazidime		—	—	270	—	230	52	1,500
Aztreonam		>5,000	125	93	259	420	484	—
Imipenem		1,614	92	170	202	90	82	4.7
Ertapenem		98	NA	NA	NA	NA	NA	NA
Meropenem		70	4.35	26	13.4	13	26	NA
k_{cat}/K_m (mM^{-1}/s)		Benzylpenicillin	1,870	9,300	560	1,160	2,100	NA
	Amoxicillin	3,400	9,060	240	370	NA	NA	310
	Ticarcillin	305	530	NA	NA	NA	NA	NA
	Piperacillin	867	NA	470	NA	NA	NA	NA
	Cefotaxime	44	300	18	—	170	93	24
	Cefepime	8	NA	NA	NA	22	NA	NA
	Ceftazidime	—	52	0.02	—	2.1	40	1.7
	Aztreonam	1,660	5,600	550	420	160	3.5	—
	Imipenem	1,109	11,000	520	520	340	660	81
	Ertapenem	1,531	NA	NA	NA	280	250	NA
	Meropenem	657	2,700	380	660	NA	NA	NA

^a —, no detectable hydrolysis; NA, no data available.

emases NMC-A from *E. cloacae* (12) and IMI-1 (13). Biochemical characterization of FRI-1 showed significant hydrolysis of carbapenemase, and its protein structure analysis identified conserved amino acid residues as a source of its carbapenemase activity. As observed for other class A β -lactamases, such as NMC-A (12), IMI-1 (13), and SFC-1 (30), FRI-1 confers a high level of resistance to aztreonam but does not confer significant resistance to broad-spectrum cephalosporins, such as ceftazidime, cefotaxime, and cefepime (Table 1). Therefore, its resistance profile differs

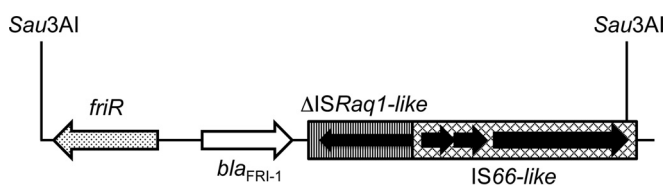


FIG 3 Schematic map of the structures surrounding $bla_{\text{FRI-1}}$ identified in the *E. cloacae* DUB isolate. The genes and their corresponding transcriptional orientations are indicated by horizontal arrows. Sau3AI restriction sites that allowed cloning in the pBK-CMV plasmid (pFRI) are indicated.

from that of KPCs that hydrolyze all extended-spectrum β -lactams.

Analysis of the immediate upstream genetic environment of the $bla_{\text{FRI-1}}$ gene identified a LysR-type transcriptional regulator, FriR, as previously observed for other class A carbapenemases, such as NMC-A, IMI-1, and SME (13, 31, 32). Notably, the G+C content of the $bla_{\text{FRI-1}}$ gene and its regulator *friR* (39%) differed from that of *E. cloacae* genes (ca. 55%), suggesting the acquisition of the *friR*- $bla_{\text{FRI-1}}$ locus through a horizontal gene transfer process. These results further emphasize that acquisition of carbapenemase genes by a group of *Enterobacteriaceae* results from acquisition “in block” of the β -lactamase gene and its regulator from a nonenterobacterial species acting as the reservoir. The presence of IS upstream and downstream of the DNA fragment *friR*- $bla_{\text{FRI-1}}$ suggested that those elements might have been involved in the mobilization process. The plasmid location of the $bla_{\text{FRI-1}}$ gene identified in an enterobacterial species adds to the list of carbapenemase genes able to disseminate worldwide.

Finally, this work highlights the need to use, not only molecular-based techniques, but also biochemical methods for the screening

of carbapenemase-producing strains due to the growing diversity of carbapenemases.

ACKNOWLEDGMENTS

This work was financed by INSERM U914, Paris, France, and the University of Fribourg, Fribourg, Switzerland.

REFERENCES

- Nordmann P, Dortet L, Poirel L. 2012. Carbapenem resistance in Enterobacteriaceae: here is the storm! *Trends Mol Med* 18:263–272. <http://dx.doi.org/10.1016/j.molmed.2012.03.003>.
- Cuzon G, Naas T, Truong H, Villegas MV, Wisell KT, Carmeli Y, Gales AC, Venezia SN, Quinn JP, Nordmann P. 2010. Worldwide diversity of *Klebsiella pneumoniae* that produce β -lactamase *bla*_{KPC-2} gene. *Emerg Infect Dis* 16:1349–1356. <http://dx.doi.org/10.3201/eid1609.091389>.
- Munoz-Price LS, Poirel L, Bonomo RA, Schwaber MJ, Daikos GL, Cormican M, Cornaglia G, Garau J, Gniadkowski M, Hayden MK, Kumarasamy K, Livermore DM, Maya JJ, Nordmann P, Patel JB, Paterson DL, Pitout J, Villegas MV, Wang H, Woodford N, Quinn JP. 2013. Clinical epidemiology of the global expansion of *Klebsiella pneumoniae* carbapenemases. *Lancet Infect Dis* 13:785–796. [http://dx.doi.org/10.1016/S1473-3099\(13\)70190-7](http://dx.doi.org/10.1016/S1473-3099(13)70190-7).
- Dortet L, Poirel L, Nordmann P. 2014. Worldwide dissemination of the NDM-type carbapenemases in Gram-negative bacteria. *Biomed Res Int* 2014:249856. <http://dx.doi.org/10.1155/2014/249856>.
- Poirel L, Potron A, Nordmann P. 2012. OXA-48-like carbapenemases: the phantom menace. *J Antimicrob Chemother* 67:1597–1606. <http://dx.doi.org/10.1093/jac/dks121>.
- Bush K. 2013. The ABCD's of β -lactamase nomenclature. *J Infect Chemother* 19:549–559. <http://dx.doi.org/10.1007/s10156-013-0640-7>.
- Kotsakis SD, Miriagou V, Tzelepi E, Tzouveleki LS. 2010. Comparative biochemical and computational study of the role of naturally occurring mutations at Ambler positions 104 and 170 in GES β -lactamases. *Antimicrob Agents Chemother* 54:4864–4871. <http://dx.doi.org/10.1128/AAC.00771-10>.
- Naas T, Vandel L, Sougakoff W, Livermore DM, Nordmann P. 1994. Cloning and sequence analysis of the gene for a carbapenem-hydrolyzing class A β -lactamase, SME-1, from *Serratia marcescens* S6. *Antimicrob Agents Chemother* 38:1262–1270. <http://dx.doi.org/10.1128/AAC.38.6.1262>.
- Poirel L, Wenger A, Bille J, Bernabeu S, Naas T, Nordmann P. 2007. SME-2-producing *Serratia marcescens* isolate from Switzerland. *Antimicrob Agents Chemother* 51:2282–2283. <http://dx.doi.org/10.1128/AAC.00309-07>.
- Queenan AM, Shang W, Schreckenberger P, Lolans K, Bush K, Quinn J. 2006. SME-3, a novel member of the *Serratia marcescens* SME family of carbapenem-hydrolyzing β -lactamases. *Antimicrob Agents Chemother* 50:3485–3487. <http://dx.doi.org/10.1128/AAC.00363-06>.
- Queenan AM, Torres-Viera C, Gold HS, Carmeli Y, Eliopoulos GM, Moellering RC, Jr, Quinn JP, Hindler J, Medeiros AA, Bush K. 2000. SME-type carbapenem-hydrolyzing class A β -lactamases from geographically diverse *Serratia marcescens* strains. *Antimicrob Agents Chemother* 44:3035–3039. <http://dx.doi.org/10.1128/AAC.44.11.3035-3039.2000>.
- Nordmann P, Mariotte S, Naas T, Labia R, Nicolas MH. 1993. Biochemical properties of a carbapenem-hydrolyzing β -lactamase from *Enterobacter cloacae* and cloning of the gene into *Escherichia coli*. *Antimicrob Agents Chemother* 37:939–946. <http://dx.doi.org/10.1128/AAC.37.5.939>.
- Rasmussen BA, Bush K, Keeney D, Yang Y, Hare R, O'Gara C, Medeiros AA. 1996. Characterization of IMI-1 β -lactamase, a class A carbapenem-hydrolyzing enzyme from *Enterobacter cloacae*. *Antimicrob Agents Chemother* 40:2080–2086.
- Aubron C, Poirel L, Ash RJ, Nordmann P. 2005. Carbapenemase-producing *Enterobacteriaceae*, U.S. rivers. *Emerg Infect Dis* 11:260–264. <http://dx.doi.org/10.3201/eid1102.030684>.
- Wachino J, Doi Y, Yamane K, Shibata N, Yagi T, Kubota T, Arakawa Y. 2004. Molecular characterization of a cephalosporin-hydrolyzing and inhibitor-resistant class A β -lactamase, GES-4, possessing a single G170S substitution in the omega-loop. *Antimicrob Agents Chemother* 48:2905–2910. <http://dx.doi.org/10.1128/AAC.48.8.2905-2910.2004>.
- Yigit H, Queenan AM, Anderson GJ, Domenech-Sanchez A, Biddle JW, Steward CD, Alberti S, Bush K, Tenover FC. 2001. Novel carbapenem-hydrolyzing β -lactamase, KPC-1, from a carbapenem-resistant strain of *Klebsiella pneumoniae*. *Antimicrob Agents Chemother* 45:1151–1161. <http://dx.doi.org/10.1128/AAC.45.4.1151-1161.2001>.
- Nicoletti AG, Marcondes MF, Martins WM, Almeida LG, Nicolas MF, Vasconcelos AT, Oliveira V, Gales AC. 2015. Characterization of BKC-1 class A carbapenemase from *Klebsiella pneumoniae* clinical isolates in Brazil. *Antimicrob Agents Chemother* 59:5159–5164. <http://dx.doi.org/10.1128/AAC.00158-15>.
- Dortet L, Brechard L, Poirel L, Nordmann P. 2014. Impact of the isolation medium for detection of carbapenemase-producing *Enterobacteriaceae* using an updated version of the Carba NP test. *J Med Microbiol* 63:772–776. <http://dx.doi.org/10.1099/jmm.0.071340-0>.
- Bernabeu S, Poirel L, Nordmann P. 2012. Spectrophotometry-based detection of carbapenemase producers among *Enterobacteriaceae*. *Diagn Microbiol Infect Dis* 74:88–90. <http://dx.doi.org/10.1016/j.diagmicrobio.2012.05.021>.
- Dortet L, Poirel L, Nordmann P. 2012. Rapid identification of carbapenemase types in *Enterobacteriaceae* and *Pseudomonas* spp. by using a biochemical test. *Antimicrob Agents Chemother* 56:6437–6440. <http://dx.doi.org/10.1128/AAC.01395-12>.
- Dortet L, Brechard L, Cuzon G, Poirel L, Nordmann P. 2014. Strategy for rapid detection of carbapenemase-producing *Enterobacteriaceae*. *Antimicrob Agents Chemother* 58:2441–2445. <http://dx.doi.org/10.1128/AAC.01239-13>.
- Kieser T. 1984. Factors affecting the isolation of CCC DNA from *Streptomyces lividans* and *Escherichia coli*. *Plasmid* 12:19–36. [http://dx.doi.org/10.1016/0147-619X\(84\)90063-5](http://dx.doi.org/10.1016/0147-619X(84)90063-5).
- Carattoli A, Bertini A, Villa L, Falbo V, Hopkins KL, Threlfall EJ. 2005. Identification of plasmids by PCR-based replicon typing. *J Microbiol Methods* 63:219–228. <http://dx.doi.org/10.1016/j.mimet.2005.03.018>.
- Mariotte-Boyer S, Nicolas-Chanoine MH, Labia R. 1996. A kinetic study of NMC-A β -lactamase, an Ambler class A carbapenemase also hydrolyzing cephalosporins. *FEMS Microbiol Lett* 143:29–33.
- Majiduddin FK, Palzkill T. 2005. Amino acid residues that contribute to substrate specificity of class A β -lactamase SME-1. *Antimicrob Agents Chemother* 49:3421–3427. <http://dx.doi.org/10.1128/AAC.49.8.3421-3427.2005>.
- Majiduddin FK, Palzkill T. 2003. Amino acid sequence requirements at residues 69 and 238 for the SME-1 β -lactamase to confer resistance to β -lactam antibiotics. *Antimicrob Agents Chemother* 47:1062–1067. <http://dx.doi.org/10.1128/AAC.47.3.1062-1067.2003>.
- Papp-Wallace KM, Taracila M, Hornick JM, Hujer AM, Hujer KM, Distler AM, Endimiani A, Bonomo RA. 2010. Substrate selectivity and a novel role in inhibitor discrimination by residue 237 in the KPC-2 β -lactamase. *Antimicrob Agents Chemother* 54:2867–2877. <http://dx.doi.org/10.1128/AAC.00197-10>.
- Fonseca F, Sarmento AC, Henriques I, Samyn B, van Beeumen J, Domingues P, Domingues MR, Saavedra MJ, Correia A. 2007. Biochemical characterization of SFC-1, a class A carbapenem-hydrolyzing β -lactamase. *Antimicrob Agents Chemother* 51:4512–4514. <http://dx.doi.org/10.1128/AAC.00491-07>.
- Naas T, Dortet L, Iorga BI. Structural and functional aspects of class A carbapenemases. *Curr Drug Targets*, in press.
- Henriques I, Moura A, Alves A, Saavedra MJ, Correia A. 2004. Molecular characterization of a carbapenem-hydrolyzing class A β -lactamase, SFC-1, from *Serratia fonticola* UTAD54. *Antimicrob Agents Chemother* 48:2321–2324. <http://dx.doi.org/10.1128/AAC.48.6.2321-2324.2004>.
- Naas T, Livermore DM, Nordmann P. 1995. Characterization of an LysR family protein, SmeR from *Serratia marcescens* S6, its effect on expression of the carbapenem-hydrolyzing β -lactamase SME-1, and comparison of this regulator with other β -lactamase regulators. *Antimicrob Agents Chemother* 39:629–637. <http://dx.doi.org/10.1128/AAC.39.3.629>.
- Naas T, Nordmann P. 1994. Analysis of a carbapenem-hydrolyzing class A β -lactamase from *Enterobacter cloacae* and of its LysR-type regulatory protein. *Proc Natl Acad Sci USA* 91:7693–7697. <http://dx.doi.org/10.1073/pnas.91.16.7693>.
- Ambler RP, Coulson AF, Frère JM, Ghuyssen JM, Joris B, Forsman M, Levesque RC, Tiraby G, Waley SG. 1991. A standard numbering scheme for the class A beta-lactamases. *Biochem J* 276:269–270.



A 2.5-Year Within-Patient Evolution of *Pseudomonas aeruginosa* Isolates with *In Vivo* Acquisition of Ceftolozane-Tazobactam and Ceftazidime-Avibactam Resistance upon Treatment

Thibaud Boulant,^{a,b} Agnès B. Jousset,^{a,b,c} Rémy A. Bonnin,^{a,b} Aurélie Barrail-Tran,^d Adrien Borgel,^{a,b,c} Saoussen Oueslati,^{a,b}  Thierry Naas,^{a,b,c}  Laurent Dortet^{a,b,c}

^aEA7361 Structure, dynamic, function and expression of broad spectrum β -lactamases, Paris-Sud University, Paris Saclay University, Le Kremlin-Bicêtre, France

^bFaculty of Medicine, Paris-Sud University, Paris Saclay University, Le Kremlin-Bicêtre, France

^cDepartment of Bacteriology-Hygiene, Bicêtre Hospital, Assistance Publique-Hôpitaux de Paris, Le Kremlin-Bicêtre, France

^dDepartment of Pharmacy, Bicêtre Hospital, Assistance Publique-Hôpitaux de Paris, Le Kremlin-Bicêtre, France

ABSTRACT Ceftolozane-tazobactam is considered to be a last-resort treatment for infections caused by multidrug-resistant (MDR) *Pseudomonas aeruginosa*. Although resistance to this antimicrobial has been described *in vitro*, the development of resistance *in vivo* has rarely been reported. Here, we describe the evolution of resistance to ceftolozane-tazobactam of *P. aeruginosa* isolates recovered from the same patient during recurrent infections over 2.5 years. Antimicrobial susceptibility testing results showed that 24 of the 27 *P. aeruginosa* isolates recovered from blood ($n = 18$), wound ($n = 2$), pulmonary ($n = 1$), bile ($n = 2$), and stool ($n = 4$) samples from the same patient were susceptible to ceftolozane-tazobactam and ceftazidime-avibactam but resistant to ceftazidime, piperacillin-tazobactam, imipenem, and meropenem. Three clinical isolates acquired resistance to ceftolozane-tazobactam and ceftazidime-avibactam along with a partial restoration of piperacillin-tazobactam and carbapenem susceptibilities. Whole-genome sequencing analysis reveals that all isolates were clonally related (sequence type 111 [ST-111]), with a median of 24.9 single nucleotide polymorphisms (SNPs) (range, 8 to 48 SNPs). The ceftolozane-tazobactam and ceftazidime-avibactam resistance was likely linked to the same G183D substitution in the chromosome-encoded cephalosporinase. Our results suggest that resistance to ceftolozane-tazobactam in *P. aeruginosa* might occur *in vivo* upon treatment through an amino acid substitution in the intrinsic AmpC leading to ceftolozane-tazobactam and ceftazidime-avibactam resistance, accompanied by re-sensitization to piperacillin-tazobactam and carbapenems.

KEYWORDS AmpC, G183D, *Pseudomonas aeruginosa*, ceftolozane-tazobactam, ceftazidime-avibactam

Pseudomonas aeruginosa causes more than 51,000 health care-associated infections per year in the United States, as reported by the Centers for Disease Control and Prevention (1). This Gram-negative extracellular pathogen is mostly reported in health care-associated infections in immunocompromised patients. These infections are diverse, ranging from urinary tract infections, acute pulmonary infections, wound infections, acute otitis, and septicemia (2). *P. aeruginosa* is also the major cause of chronic infection in cystic fibrosis patients (3). In 2017, the World Health Organization included *P. aeruginosa* in its list of pathogens of global concern, mostly due to the dissemination of multidrug-resistant isolates in this species (4). Although extended-spectrum β -lactamases (ESBLs) and carbapenemases (mostly VIM and IMP) are increasingly reported

Citation Boulant T, Jousset AB, Bonnin RA, Barrail-Tran A, Borgel A, Oueslati S, Naas T, Dortet L. 2019. A 2.5-year within-patient evolution of *Pseudomonas aeruginosa* isolates with *in vivo* acquisition of ceftolozane-tazobactam and ceftazidime-avibactam resistance upon treatment. *Antimicrob Agents Chemother* 63:e01637-19. <https://doi.org/10.1128/AAC.01637-19>.

Copyright © 2019 American Society for Microbiology. All Rights Reserved.

Address correspondence to Laurent Dortet, laurent.dortet@aphp.fr.

Received 13 August 2019

Returned for modification 30 August 2019

Accepted 25 September 2019

Accepted manuscript posted online 21 October 2019

Published 21 November 2019

worldwide (5, 6), multidrug resistance (MDR) in *P. aeruginosa* often involves an association of intrinsic mechanisms. Indeed, *P. aeruginosa* is intrinsically resistant to many antimicrobials through the constitutive expression of several efflux pumps, low permeability of the outer membrane, and (over)production of the chromosome-encoded cephalosporinase (PDC) (7). Recently, ceftolozane was commercialized in association with tazobactam for the treatment of urinary tract and intra-abdominal severe infections. This association is particularly efficient in *P. aeruginosa* MDR isolates (8–10). Indeed, ceftolozane is not affected by decreased outer membrane permeability that results in carbapenem resistance (OprD mutations and MexAB-OprM efflux), and it possesses improved stability toward the intrinsic AmpC compared to the other β -lactams (e.g., ceftazidime) (11).

Although resistance to ceftolozane-tazobactam (C-T) has been described *in vitro* (12–14), the development of resistance *in vivo* has been rarely reported (10, 15–18).

Here, we describe the evolution of resistance to ceftolozane-tazobactam, ceftazidime-avibactam, piperacillin-tazobactam, and carbapenems of *P. aeruginosa* isolates recovered from the same patient during recurrent infections over 2.5 years.

RESULTS AND DISCUSSION

A 3-year-old patient with biliary atresia was liver transplanted twice. Following the second surgery, the patient was treated by colistin (intravenous [i.v.] for 7 days plus aerosol for 14 days) for a ventilator-acquired pneumonia caused by an extremely drug-resistant (XDR) *P. aeruginosa* isolate susceptible to polymyxins only (MIC, 1 mg/liter). During the next 6 months, four episodes of catheter-related bacteremia caused by ESBL-producing *Klebsiella pneumoniae* were efficiently treated by imipenem and amikacin and catheter ablation. During the same time, the patient remained colonized with the XDR *P. aeruginosa* isolate which was cultivated from bile (strains 1 and 5), stool (strain 2), and wound (strains 3 and 4) samples (Fig. 1A). In March 2016, C-T (400 mg/kg of body weight, 3 times per day) was introduced for the treatment of a bacteremia caused by the XDR *P. aeruginosa* (strains 7 to 11) (Fig. 1A), related to the Gore-Tex graft infection used for replacement of the vena cava. This uncommon dosage corresponds to an adaptation to the patient weight compared to that with adults. After 22 days of therapy with C-T, the first C-T-resistant isolate was recovered from blood culture (strain 17). During the following year, two other bacteremias caused by the XDR *P. aeruginosa* isolate were successfully treated by C-T (500 mg/kg, 3 times per day). Among these 53 *P. aeruginosa* clinical isolates recovered over a 2.5-year period, three were found to be resistant to C-T, ceftazidime-avibactam (CZA), and ceftazidime (CAZ) (Fig. 1). Intriguingly, partial restoration of piperacillin-tazobactam (TZP) and carbapenem (imipenem and meropenem) susceptibilities was observed in these C-T- and CZA-resistant isolates (Fig. 1B). To decipher if the three C-T-resistant isolates derived from a previously C-T-susceptible *P. aeruginosa* isolate and to potentially identify the resistance mechanism involved in this phenotype, 27 *P. aeruginosa* clinical isolates (including the 3 C-T-resistant isolates) recovered from diverse samples ($n = 4$ from stool, $n = 2$ from wound, $n = 2$ from bile, $n = 1$ from bronchial aspirate fluid, and $n = 18$ from positive blood cultures) covering the 2.5-year period were randomly selected and whole-genome sequenced using Illumina technology. *De novo* assembly and read mappings were performed using CLC Genomics Workbench v10.1 (Qiagen, Les Ulis, France). Multilocus sequence typing derived from whole-genome sequencing (WGS) data demonstrated that all of the 27 XDR *P. aeruginosa* isolates were from the same sequence type (ST), ST-111 (Fig. 2A). The phylogenetic tree and single nucleotide polymorphism (SNP) count demonstrated that all of these 27 isolates belonged to the same clone, with a median of 24.9 SNPs (range, 8 to 48 SNPs) based on whole-genome SNP analysis (Fig. 1B). Overall, the evolution scale of this clone is of 7.04 SNPs per year (Fig. 2B). In all of the 27 *P. aeruginosa* isolates (resistant and susceptible isolates), *bla*_{OXA-9} and *bla*_{OXA-395} genes were identified as acquired resistance genes. Accordingly, the production of OXA-9 and OXA-395 is not supposed to play a role in C-T resistance. Of note, only OXA-539 and GES-6 were previously described to be involved in resistance to C-T (15,

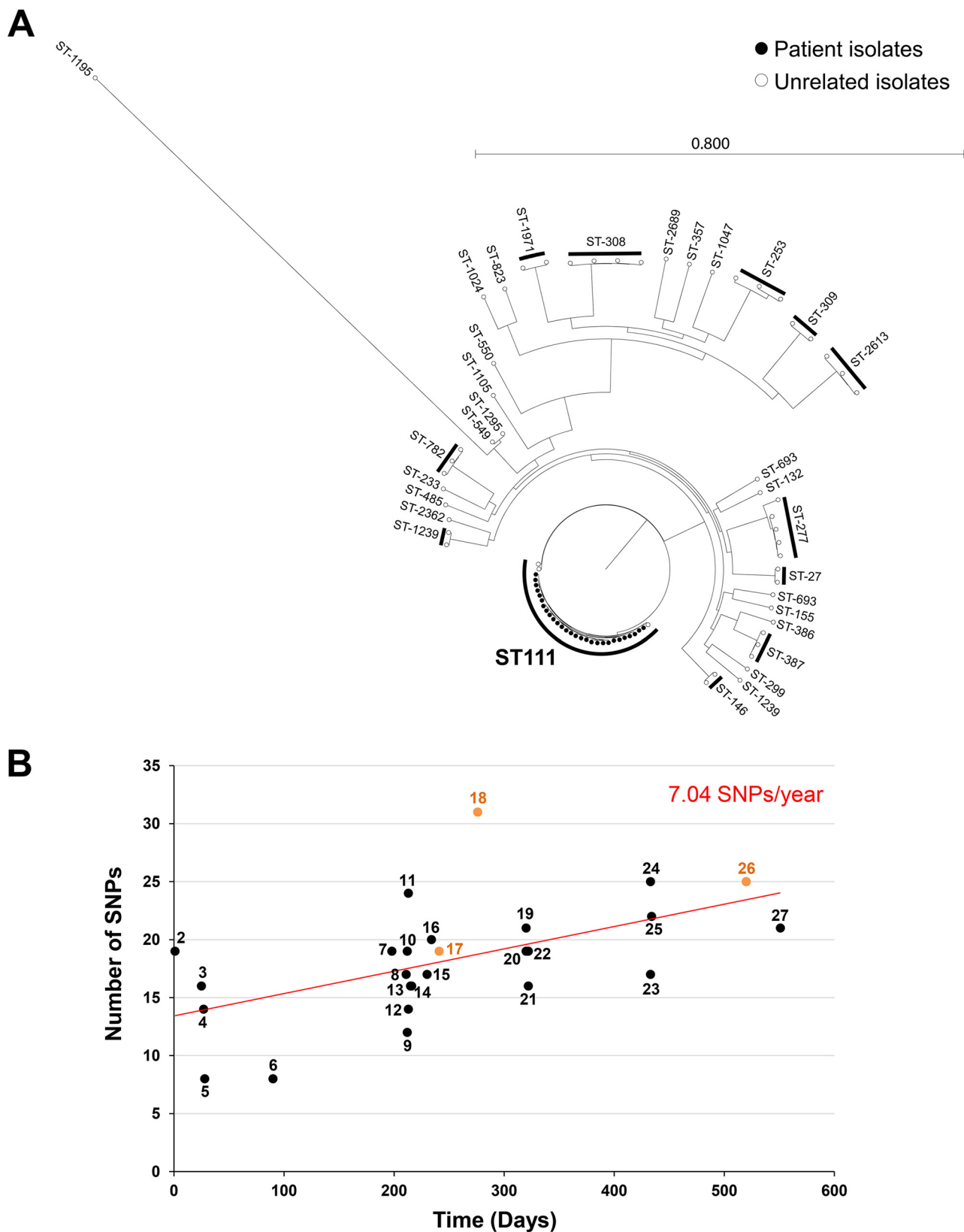


FIG 2 (A) Phylogenetic relationships and sequence types of the 27 clinical *P. aeruginosa* isolates with *P. aeruginosa* genomes from the GenBank database. (B) Evolution rates of the ST-111 *P. aeruginosa* clone (27 clinical *P. aeruginosa* isolates). Each point corresponds to one *P. aeruginosa* clinical isolate. The first isolate was used as a reference. The numbers correspond to the isolate number indicated in Fig. 1. Ceftolozane-tazobactam-resistant isolates are indicated in orange. The red curve corresponds to the tendency curve. The evolution rate (indicated in red) corresponds to the slope of the tendency curve.

detectable hydrolysis activity for the three C-T-resistant isolates. This phenomenon has been previously identified for CMY-2 and ADC-7 (21, 22). Of note, resistance to CZA (caused by increased hydrolytic activity toward CAZ) accompanied by resensitization to carbapenems was recently reported with two variants of KPC carbapenemases. Indeed, it was demonstrated that the catalytic efficiencies of KPC-28 and KPC-14 were 10-fold lower for carbapenems and 10- to 30-fold higher for CAZ than those obtained for wild-type enzymes KPC-2 and KPC-3, respectively (23). Accordingly, a comparison of the wild-type (24) with G183D mutant PDC of *Pseudomonas aeruginosa* indicates a conformational change of the catalytic pocket that likely is involved in the observed phenotype (Fig. 3). Indeed, we could observe an opening of the catalytic cavity which might help better accommodate large molecules such as ceftolozane and ceftazidime. In the same time, we observed the appearance of a negative charge in the catalytic site (Fig. 3D and E), along with clashes between D183 and N179 (Fig. 3C) that are involved in stabilization of the substrate in the binding pocket of the enzyme.

In addition, our evolutionary analysis showed that this particular substitution occurred three times independently (Fig. 1B). These results might indicate that the G183 position of the *P. aeruginosa* PDC might be a preferential hot spot mutation site under C-T-selective pressure. Accordingly, the emergence of the same substitution in two C-T-resistant *P. aeruginosa* isolates recovered from a patient who was treated for 42 days with this antimicrobial agent for a recurrent wound infection corroborates our hypothesis (17). In our case, C-T resistance occurred more rapidly (22 days versus 42 days).

Globally, our results suggest that C-T therapy might result in the development of resistance by a single mutation in the intrinsic cephalosporinase PDC within 3 weeks. This single G183D mutation is responsible for resistance to C-T but also to CZA. This substitution seems to result in decreased hydrolytic activity toward TZP but also to carbapenems, thus restoring a potential alternative therapy in the absence of other carbapenem resistance mechanisms (here, deficiency of the OprD porin). It also paves the way for a potential benefit of C-T and carbapenem association for the treatment of difficult-to-treat infection caused by XDR *P. aeruginosa* that required prolonged therapy. Indeed, this kind of unusual association might prevent the development of resistance to C-T upon treatment. However, in endovascular graft infection, biofilm formation might also play a significant role that should be considered (25). Finally, we should also acknowledge that the low C-T dosage, which was empirically adapted to the weight of the patient, might have been not effective enough to clear the infection and prevent mutant formation. However, no blood dosage was available at the time of this clinical case.

MATERIALS AND METHODS

***P. aeruginosa* clinical isolates.** Over 2.5 years, 53 *P. aeruginosa* clinical isolates were collected from stools ($n = 10$), positive blood cultures ($n = 23$), bronchial aspirate fluid ($n = 5$), wounds ($n = 5$), ascites ($n = 1$), bile ($n = 8$), and urine ($n = 1$).

Antimicrobial susceptibility testing. Antimicrobial susceptibility testing was performed by the disk diffusion method on Mueller-Hinton (MH) agar (Bio-Rad, Marnes-La-Coquette, France) and interpreted according to EUCAST guidelines updated in 2019 (<http://www.eucast.org/>). MICs to ceftolozane-tazobactam (C-T), ceftazidime (CAZ), ceftazidime-avibactam (CZA), and piperacillin-tazobactam (TZP) were determined using the Etest (bioMérieux, Marcy l'Etoile, France) and interpreted according to EUCAST breakpoints updated in 2019 (<http://www.eucast.org/>). MICs to colistin were determined by broth microdilution (Sensititre/Thermo Fisher), as recommended by EUCAST guidelines.

DNA extraction and sequencing. Total DNA was extracted from colonies using the UltraClean microbial DNA isolation kit (Mo Bio Laboratories, Ozyme, Saint-Quentin, France), following the manufacturer's instructions. The DNA concentrations and purity assessments were determined using a Qubit 2.0 fluorometer using the double-stranded DNA (dsDNA) HS and/or BR assay kit and NanoDrop 2000 spectrophotometer (Thermo Fisher, Saint-Herblain, France). The DNA library was prepared using the Nextera XT v2 kit (Illumina, Paris, France) and then run on NextSeq 500 automated system (Illumina), using a 2×100 -bp paired-end approach.

Bioinformatic analysis. *De novo* assembly and read mappings were performed using CLC Genomics Workbench v10.1 (Qiagen, Les Ulis, France). The acquired antimicrobial resistance genes were identified using the ResFinder server v3.1 (<https://cge.cbs.dtu.dk/services/ResFinder/>). MLST was performed using the MLST 1.8 server (<https://cge.cbs.dtu.dk/services/pMLST/>). Phylogeny was performed using the CSI

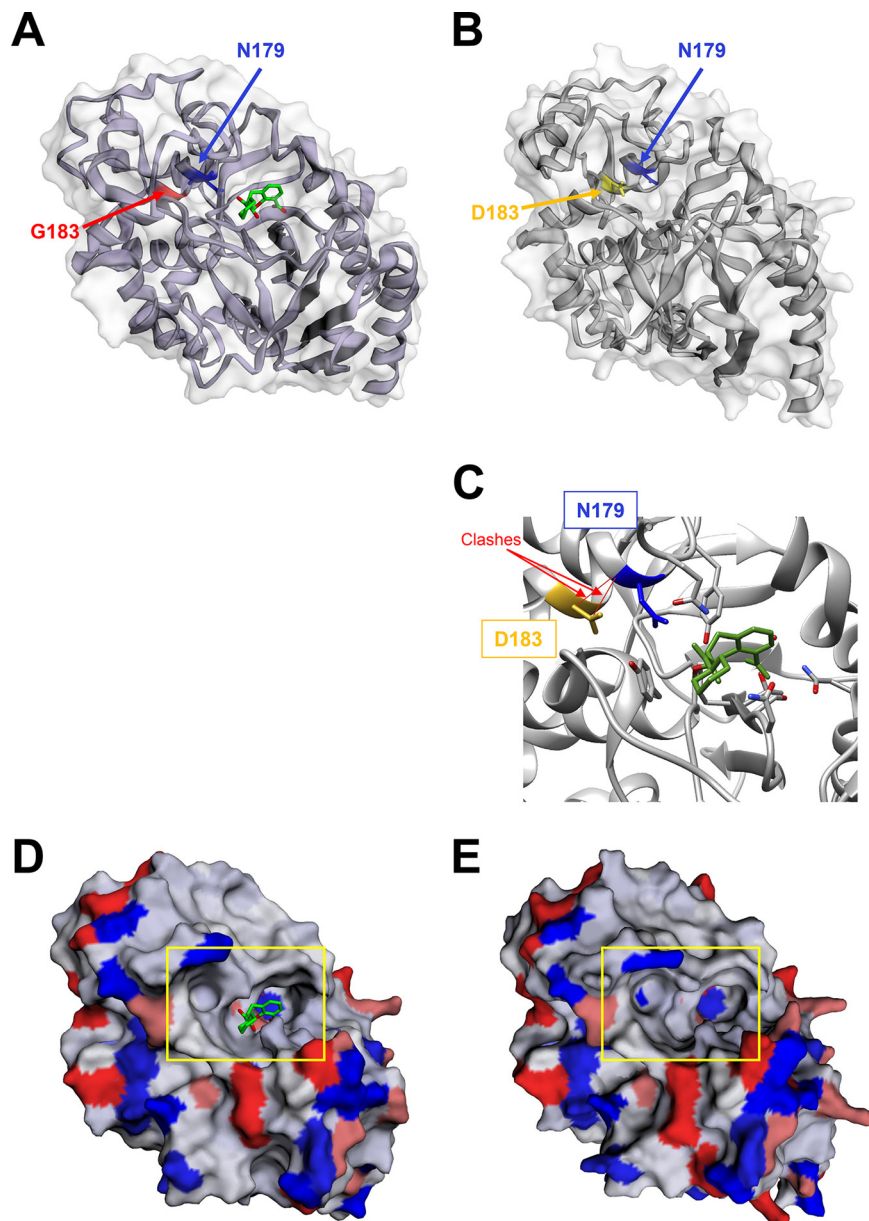


FIG 3 (A to E) Comparison of three-dimensional (3D) structures of the wild-type (A and D) and G183D mutant (B, C, and E) PDC β -lactamase. The wild-type PDC corresponds to the 6I30 PDB crystal structure of the AmpC from *Pseudomonas aeruginosa* in complex with bicyclic boronate, as described by Cahill et al. (24). (C) The clashes between D183 and N179 in the mutated PDC are indicated in red. (D and E) Surface charges of the wild-type (D) and G183D mutant (E) PDC β -lactamase. The 3D structure of G183D mutant PDC was modeled using the Phyre² software (<http://www.sbg.bio.ic.ac.uk/~phyre2/html/page.cgi?id=index>). Both 3D structure visualizations were performed using the EzMol 2.1 software (<http://www.sbg.bio.ic.ac.uk/>).

Phylogeny v1.4 server (<https://cge.cbs.dtu.dk/services/CSIPhylogeny/>) set with default parameters (10 \times coverage at SNP position, 10% relative depth at SNP position, and 10-bp distance between SNPs) and visualized using the FigTree software v1.4.3 (<http://tree.bio.ed.ac.uk/software/figtree/>).

Hydrolysis analysis. The specific activities toward piperacillin of the wild-type and the G183D mutated PDC were determined using the supernatant of a whole-cell crude extract obtained from an overnight culture of C-T-resistant and C-T-susceptible *P. aeruginosa* clinical isolates with the UV spectrophotometer Ultrospec 2000 (Amersham Pharmacia Biotech), as previously described (26).

Data availability. The whole-genome sequences generated in the study have been submitted to the GenBank nucleotide sequence database under the accession numbers detailed in Table S2.

SUPPLEMENTAL MATERIAL

Supplemental material for this article may be found at <https://doi.org/10.1128/AAC.01637-19>.

SUPPLEMENTAL FILE 1, PDF file, 0.8 MB.

ACKNOWLEDGMENTS

We thank Pasteur International Bioresources Networking (PibNet, Paris, France) for providing whole-genome sequencing facilities.

This work was partially funded by the University Paris-Sud, France. L.D. and T.N. are members of the Laboratory of Excellence in Research on Medication and Innovative Therapeutics (LERMIT) supported by a grant from the French National Research Agency (ANR-10-LABX-33).

We declare no competing interests.

T.B. and L.D. had full access to all of the data in the study and take responsibility for the integrity of the data and the accuracy of the data analysis. L.D. and T.N. developed the study concept and design. All authors were involved in the acquisition, analysis, and/or interpretation of the data. T.B. and L.D. drafted the manuscript. L.D. and T.N. critically revised the manuscript for important intellectual content.

REFERENCES

- Centers for Disease Control and Prevention. 2013. Antibiotic resistance threats in the United States, 2013. Centers for Disease Control and Prevention, Atlanta, GA. <https://www.cdc.gov/drugresistance/pdf/ar-threats-2013-508.pdf>.
- Stryjewski M, Sexton D. 2003. *Pseudomonas aeruginosa* infections in specific types of patients and clinical settings, p 1–15. In Hauser AR, Rello J (ed), *Severe infections caused by Pseudomonas aeruginosa. Perspectives on critical care infectious diseases*. Springer US, New York, NY.
- Lund-Palau H, Turnbull AR, Bush A, Bardin E, Cameron L, Soren O, Wierre-Gore N, Alton EW, Bundy JG, Connett G, Faust SN, Filloux A, Freemont P, Jones A, Khoo V, Morales S, Murphy R, Pabary R, Simbo A, Schelenz S, Takats Z, Webb J, Williams HD, Davies JC. 2016. *Pseudomonas aeruginosa* infection in cystic fibrosis: pathophysiological mechanisms and therapeutic approaches. *Expert Rev Respir Med* 10:685–697. <https://doi.org/10.1080/17476348.2016.1177460>.
- World Health Organization. 2017. Guidelines for the prevention and control of carbapenem-resistant *Enterobacteriaceae*, *Acinetobacter baumannii* and *Pseudomonas aeruginosa* in health care facilities. World Health Organization, Geneva, Switzerland. <https://apps.who.int/iris/bitstream/handle/10665/259462/9789241550178-eng.pdf?sequence=1>.
- Gupta V. 2008. Metallo- β -lactamases in *Pseudomonas aeruginosa* and *Acinetobacter* species. *Expert Opin Invest Drugs* 17:131–143. <https://doi.org/10.1517/13543784.17.2.131>.
- Mesaros N, Nordmann P, Plesiat P, Roussel-Delvallez M, Van Eldere J, Glupczynski Y, Van Laethem Y, Jacobs F, Lebecque P, Malfroot A, Tulkens PM, Van Bambeke F. 2007. *Pseudomonas aeruginosa*: resistance and therapeutic options at the turn of the new millennium. *Clin Microbiol Infect* 13:560–578. <https://doi.org/10.1111/j.1469-0691.2007.01681.x>.
- El Zowalaty ME, Al Thani AA, Webster TJ, El Zowalaty AE, Schweizer HP, Nasrallah GK, Marei HE, Ashour HM. 2015. *Pseudomonas aeruginosa*: arsenal of resistance mechanisms, decades of changing resistance profiles, and future antimicrobial therapies. *Future Microbiol* 10:1683–1706. <https://doi.org/10.2217/fmb.15.48>.
- Bassetti M, Castaldo N, Cattelan A, Mussini C, Righi E, Tascini C, Menichetti F, Mastroianni CM, Tumbarello M, Grossi P, Artioli S, Caranante N, Cipriani L, Coletto D, Russo A, Digaetano M, Losito AR, Peghin M, Capone A, Nicole S, Vena A, CEFTABUSE Study Group. 2019. Ceftolozane/tazobactam for the treatment of serious *Pseudomonas aeruginosa* infections: a multicentre nationwide clinical experience. *Int J Antimicrob Agents* 53:408–415. <https://doi.org/10.1016/j.ijantimicag.2018.11.001>.
- Shorridge D, Duncan LR, Pfaller MA, Flamm RK. 2019. Activity of ceftolozane-tazobactam and comparators when tested against Gram-negative isolates collected from paediatric patients in the USA and Europe between 2012 and 2016 as part of a global surveillance programme. *Int J Antimicrob Agents* 53:637–643. <https://doi.org/10.1016/j.ijantimicag.2019.01.015>.
- Haidar G, Philips NJ, Shields RK, Snyder D, Cheng S, Potoski BA, Doi Y, Hao B, Press EG, Cooper VS, Clancy CJ, Nguyen MH. 2017. Ceftolozane-tazobactam for the treatment of multidrug-resistant *Pseudomonas aeruginosa* infections: clinical effectiveness and evolution of resistance. *Clin Infect Dis* 65:110–120. <https://doi.org/10.1093/cid/cix182>.
- Takeda S, Ishii Y, Hatano K, Tateda K, Yamaguchi K. 2007. Stability of FR264205 against AmpC β -lactamase of *Pseudomonas aeruginosa*. *Int J Antimicrob Agents* 30:443–445. <https://doi.org/10.1016/j.ijantimicag.2007.05.019>.
- Barnes MD, Taracila MA, Rutter JD, Bethel CR, Galdadas I, Hujer AM, Caselli E, Prati F, Dekker JP, Papp-Wallace KM, Haider S, Bonomo RA. 2018. Deciphering the evolution of cephalosporin resistance to ceftolozane-tazobactam in *Pseudomonas aeruginosa*. *mBio* 9:e02085-18. <https://doi.org/10.1128/mBio.02085-18>.
- Berrazeg M, Jeannot K, Ntsogo Enguéné VY, Broutin I, Loeffert S, Fournier D, Plésiat P. 2015. Mutations in β -lactamase AmpC increase resistance of *Pseudomonas aeruginosa* isolates to antipseudomonal cephalosporins. *Antimicrob Agents Chemother* 59:6248–6255. <https://doi.org/10.1128/AAC.00825-15>.
- Cabot G, Bruchmann S, Mulet X, Zamorano L, Moya B, Juan C, Haussler S, Oliver A. 2014. *Pseudomonas aeruginosa* ceftolozane-tazobactam resistance development requires multiple mutations leading to overexpression and structural modification of AmpC. *Antimicrob Agents Chemother* 58:3091–3099. <https://doi.org/10.1128/AAC.02462-13>.
- Fraille-Ribot PA, Mulet X, Cabot G, Del Barrio-Tofino E, Juan C, Perez JL, Oliver A. 2017. *In vivo* emergence of resistance to novel cephalosporin- β -lactamase inhibitor combinations through the duplication of amino acid D149 from OXA-2 β -lactamase (OXA-539) in sequence type 235 *Pseudomonas aeruginosa*. *Antimicrob Agents Chemother* 61:e01117-17. <https://doi.org/10.1128/AAC.01117-17>.
- Ganguangco LM, Clark P, Stewart C, Miljkovic G, Saul ZK. 2016. Persistent bacteremia from *Pseudomonas aeruginosa* with *in vitro* resistance to the novel antibiotics ceftolozane-tazobactam and ceftazidime-avibactam. *Case Rep Infect Dis* 2016:1520404. <https://doi.org/10.1155/2016/1520404>.
- MacVane SH, Pandey R, Steed LL, Kreiswirth BN, Chen L. 2017. Emergence of ceftolozane-tazobactam-resistant *Pseudomonas aeruginosa* during treatment is mediated by a single AmpC structural mutation. *Antimicrob Agents Chemother* 61:e01183-17. <https://doi.org/10.1128/AAC.01183-17>.
- Munita JM, Aitken SL, Miller WR, Perez F, Rosa R, Shimose LA, Lichtenberger PN, Abbo LM, Jain R, Nigo M, Wanger A, Araos R, Tran TT, Adachi J, Rakita R, Shelburne S, Bonomo RA, Arias CA. 2017. Multicenter evaluation of ceftolozane/tazobactam for serious infections caused by carbapenem-resistant *Pseudomonas aeruginosa*. *Clin Infect Dis* 65:158–161. <https://doi.org/10.1093/cid/cix014>.

19. Poirel L, Ortiz De La Rosa JM, Kieffer N, Dubois V, Jayol A, Nordmann P. 2019. Acquisition of extended-spectrum β -lactamase GES-6 leading to resistance to ceftolozane-tazobactam combination in *Pseudomonas aeruginosa*. *Antimicrob Agents Chemother* 63:e01809-18. <https://doi.org/10.1128/AAC.01809-18>.
20. Lahiri SD, Walkup GK, Whiteaker JD, Palmer T, McCormack K, Tanudra MA, Nash TJ, Thresher J, Johnstone MR, Hajec L, Livchak S, McLaughlin RE, Alm RA. 2015. Selection and molecular characterization of ceftazidime/avibactam-resistant mutants in *Pseudomonas aeruginosa* strains containing derepressed AmpC. *J Antimicrob Chemother* 70: 1650–1658. <https://doi.org/10.1093/jac/dkv004>.
21. Skalweit MJ, Li M, Conklin BC, Taracila MA, Hutton RA. 2013. N152G, -S, and -T substitutions in CMY-2 β -lactamase increase catalytic efficiency for cefoxitin and inactivation rates for tazobactam. *Antimicrob Agents Chemother* 57:1596–1602. <https://doi.org/10.1128/AAC.01334-12>.
22. Skalweit MJ, Li M, Taracila MA. 2015. Effect of asparagine substitutions in the YXN loop of a class C β -lactamase of *Acinetobacter baumannii* on substrate and inhibitor kinetics. *Antimicrob Agents Chemother* 59: 1472–1477. <https://doi.org/10.1128/AAC.03537-14>.
23. Oueslati S, Iorga BI, Tlili L, Exilie C, Zavala A, Dortet L, Jousset AB, Bernabeu S, Bonnin RA, Naas T. 2019. Unravelling ceftazidime/avibactam resistance of KPC-28, a KPC-2 variant lacking carbapenemase activity. *J Antimicrob Chemother* 74:2239–2246. <https://doi.org/10.1093/jac/dkz209>.
24. Cahill ST, Tyrrell JM, Navratilova IH, Calvopina K, Robinson SW, Lohans CT, McDonough MA, Cain R, Fishwick CWG, Avison MB, Walsh TR, Schofield CJ, Brem J. 2019. Studies on the inhibition of AmpC and other β -lactamases by cyclic boronates. *Biochim Biophys Acta Gen Subj* 1863: 742–748. <https://doi.org/10.1016/j.bbagen.2019.02.004>.
25. Domitrovic TN, Hujer AM, Perez F, Marshall SH, Hujer KM, Woc-Colburn LE, Parta M, Bonomo RA. 2016. Multidrug resistant *Pseudomonas aeruginosa* causing prosthetic valve endocarditis: a genetic-based chronicle of evolving antibiotic resistance. *Open Forum Infect Dis* 3:ofw188. <https://doi.org/10.1093/ofid/ofw188>.
26. Dortet L, Oueslati S, Jeannot K, Tande D, Naas T, Nordmann P. 2015. Genetic and biochemical characterization of OXA-405, an OXA-48-type extended-spectrum β -lactamase without significant carbapenemase activity. *Antimicrob Agents Chemother* 59:3823–3828. <https://doi.org/10.1128/AAC.05058-14>.

Titre : Caractérisation moléculaire et biochimique des carbapénèmases les plus répandues chez les Entérobactéries associées à des infections sévères en vue de développer de nouveaux inhibiteurs

Mots clés : β -lactamines, carbapénèmases, inhibiteurs

Résumé : Les antibiotiques, et plus particulièrement les β -lactamines, furent pendant longtemps considérés comme l'arme absolue pour le traitement des infections bactériennes, du fait de leur efficacité, leur bonne tolérance et de leur faible coût. Cependant, les bactéries ont développé des mécanismes de résistance, y compris vis-à-vis des β -lactamines possédant le spectre d'activité le plus large, les carbapénèmes. Ces derniers sont considérés comme les antibiotiques de derniers recours pour le traitement des infections sévères à bacilles à Gram négatif en milieu hospitalier. Chez les entérobactéries, cette résistance émergente aux carbapénèmes est principalement due à l'expression d'enzymes appelées les carbapénèmases capables d'inactiver les carbapénèmes. L'émergence exponentielle à l'échelle mondiale de ces entérobactéries productrices de carbapénèmases (EPC) constitue un problème majeur de santé publique. Actuellement, les carbapénèmases les plus répandues dans le monde sont les KPC (*Klebsiella pneumoniae* carbapenemase), NDM-1 (New Delhi metallo- β -lactamase) et OXA-48 (Oxacillinase). La première KPC a été identifiée en 1996 aux Etats-Unis, NDM-1 en 2009 en Suède chez une patiente en provenance d'Inde et OXA-48 en 2003 en Turquie. En France, les carbapénèmases de type OXA-48 sont largement majoritaires et représentent près de 70% des EPC. Ainsi, le retentissement de leur dissémination et le besoin de développer de nouveaux inhibiteurs capables d'inactiver les carbapénèmases se fait de plus en plus pressante.

Cette thèse a pour objectif de mieux comprendre le mode d'action de ces 3 carbapénèmases d'un point de vue moléculaire et biochimique, afin d'identifier les éléments structuraux nécessaires à leur fonctionnement, mais aussi de poser les bases du développement de « pan-inhibiteurs » et de nouveaux outils de diagnostics. Pour cela, la caractérisation biochimique des carbapénèmases de type KPC, NDM et OXA-48, de leurs variants naturels et de mutants générés *in vitro* a été entreprise. Il a pu être mis en exergue l'implication de résidus spécifiques et d'éléments structuraux nécessaires à l'hydrolyse des carbapénèmes. L'étude cristallographique et RMN ainsi que l'étude *in silico* (modélisation) de ces enzymes et de leurs mutants respectifs, nous a permis de mieux comprendre le mode d'interaction enzyme-substrat. Nous avons ainsi pu comprendre les bases de la capacité impressionnante de ces carbapénèmases à s'adapter et à évoluer en fonction des pressions de sélections exercées.

En collaborations avec différentes équipes de chimistes nous avons développés différentes séries de molécules « pan-inhibiteurs » capables d'inhiber les 3 classes de carbapénèmases. Ainsi nous avons montré un effet inhibiteur de certains composés de la famille des flavonoïdes dont la myrécétine, molécule la plus active. Nous avons également identifié une série de composés, les imidazolines, possédant un effet pan-inhibiteur avec des valeurs de CI50 sub-micromolaires et donc compatible avec une utilisation *in vivo*.

Enfin, nous avons participé au développement (en collaboration avec le CEA) d'un outil de diagnostic rapide basé sur l'immunochromatographie, permettant la détection des EPC en moins de 15 minutes.

Title : Molecular and biochemical characterization of the most common carbapenemases in Enterobacteriaceae associated with severe infections in order to develop new inhibitors

Keywords : β -lactams, carbapenemases, inhibitors

Abstract : Antibiotics, and particularly β -lactams, have long been considered the ultimate weapon for the treatment of bacterial infections, because of their effectiveness, good tolerance and low cost. However, bacteria have developed mechanisms of resistance, including against β -lactams with the broadest spectrum of activity, carbapenems. The latter are considered as last resort antibiotics for the treatment of severe infections due to Gram negative bacilli in hospital. This emerging resistance to carbapenems in Enterobacteriaceae is mainly due to the expression of enzymes called carbapenemases capable of inactivating carbapenems. The worldwide exponential spread of these carbapenemase-producing enterobacteria (CPE) represents a major public health issue. Currently, the most common carbapenemases in the world are KPC (*Klebsiella pneumoniae* carbapenemase), NDM-1 (New Delhi metallo- β -lactamase) and OXA-48 (Oxacillinase). The first KPC was identified in 1996 in the United States, NDM-1 in 2009 in Sweden in a patient from India and OXA-48 in 2003 in Turkey. In France, OXA-48-type are the most abundant carbapenemases with nearly 70% of the EPCs. Thus, the repercussion of their dissemination and the development of new inhibitors capable of inactivating carbapenemases is becoming more and more urgent.

The aims of this thesis were to better understand the mode of action of the 3 main carbapenemases from a molecular and biochemical point of view, in order to identify the structural elements necessary for their functioning, but also to lay the basis for the development of "pan-inhibitors" and novel

diagnostic tools. For this purpose, the biochemical characterization of carbapenemases of the KPC, NDM and OXA-48 type, their natural variants and mutants generated *in vitro* has been undertaken.

We could highlight the involvement of specific residues and structural elements necessary for the hydrolysis of carbapenems. The crystallographic and NMR study as well as the *in silico* (modeling) studies of these enzymes and their respective mutants, allowed us to better understand the enzyme-substrate interaction mode. We could thus understand the basis of the impressive capacity of these carbapenemases to adapt and therefore to evolve according to the selection pressures exerted.

In collaboration with several chemists we participated in the development of different series of "pan-inhibitors" that were able to inhibit the 3 classes of carbapenemases. Thus we could show the inhibitory properties of some compounds of the family of flavonoids including myricetin, the most active molecule. We have also been able to identify a series of compounds, imidazolines, possessing a pan-inhibitory effect with sub-micromolar IC50 values and therefore compatible with *in vivo* use. Finally, we participated in the development (in collaboration with the CEA) of a rapid diagnostic tool based on the immunochromatographic, allowing the detection of EPCs in less than 15 minutes.